FCT
Fundação para a Ciência e a Tecnologia
MINISTÉRIO DA EDUCAÇÃO E CIÊNCIA
POPH PROGRAMA OPERACIONAL POTENCIAL HUMANO
QREN QUADRO DE REFERÊNCIA ESTRATÉGICO NACIONAL PORTUGAL 2007.2013
Governo da República Portuguesa
UNIÃO EUROPEIA Fundo Europeu de Desenvolvimento Regional

Algae-origin Fucoidan on development of therapeutic approaches for Diabetes Mellitus
Lara Priscila Lopes Reys
UMinho | 2021

Universidade do Minho
I3Bs - Instituto de Investigação em Biomateriais, Biodegradáveis e Biomiméticos

Lara Priscila Lopes Reys

Algae-origin Fucoidan on development of therapeutic approaches for Diabetes Mellitus

Abril de 2021

Universidade do Minho

I3Bs - Instituto de Investigação em Biomateriais, Biodegradáveis e Biomiméticos

Lara Priscila Lopes Reys

Algae-origin Fucoidan on development of therapeutic approaches for Diabetes Mellitus

Tese de Doutoramento

Doutoramento em Engenharia de Tecidos, Medicina Regenerativa e Células Estaminais

Trabalho efetuado sob a orientação do

Professor Doutor Rui Luís Gonçalves dos Reis

Doutor Tiago José Quinteiros Lopes Henriques da Silva

Abril de 2021

DIREITOS DE AUTOR E CONDIÇÕES DE UTILIZAÇÃO DO TRABALHO POR TERCEIROS

Este é um trabalho académico que pode ser utilizado por terceiros desde que respeitadas as regras e boas práticas internacionalmente aceites, no que concerne aos direitos de autor e direitos conexos.

Assim, o presente trabalho pode ser utilizado nos termos previstos na licença abaixo indicada.

Caso o utilizador necessite de permissão para poder fazer um uso do trabalho em condições não previstas no licenciamento indicado, deverá contactar o autor, através do RepositóriUM da Universidade do Minho.

Licença concedida aos utilizadores deste trabalho



Atribuição
CC BY

https://creativecommons.org/licenses/by/4.0/

ACKNOWLEDGMENTS

Last words to be written... the most difficult for me!

Actually, my name would not appear in the front cover of this thesis without the important contribution of several people to which I am and always be profoundly grateful.

First, I would like to express my gratitude to my supervisor and director of the 3B's Research Group, Professor Rui Reis, for giving me the opportunity to be part of his multidisciplinary and internationally recognized lab. His accomplishments are an inspiration for any student and an example, that great things can be achieved with hard work and dedication. I would like to express my admiration and gratitude to my co-supervisors, Dr. Tiago Silva and Dr. Simone Silva, for their advice, stimulating discussions, encouragement, patience and friendship. Thanks for all the opportunities that have been given to me over all these years. A big thank you to Dr. Aart van Apeldoorn and Dr. Pamela Habibovic for giving me the opportunity to work at Merln Institute, at Maastricht University. This institute provided me everything I needed to do an excellent job. Special thanks to my friends of Islets group and also to Mireille and Eduardo, who made my life richer, both professionally and personally. I am also grateful to all my colleagues and friends of 3B´s research group, for supporting me in the good and less good moments. I would like to acknowledge the Foundation for Science and Technology (FCT) for my personal doctoral grant (SFRH/BD/112139/2015) and all projects that support this thesis. I also thanks to my co-authors, who directly contribute with their expertise to the work in this thesis.

I also would like to thank all my friends for your support, especially those who helped me with this thesis. I also want to thank to my second family, Fernandes family, for affection and encouragement.

I want to express how much I am grateful to my family for their love, invaluable support and encouragement. Special thanks to my mother and sister who I adore, for supporting and accepting my choices.

I am grateful to my beloved companion, Rui Fernandes (Ruizinho), for this love, tolerance, optimism and invaluable support and encouragement. For all the time that he spent helping me, supporting every decision that I made, and for all his patience that contributed positively to my work. Even in a big distance you were always there. Thanks for being my soul made, my sun in raining days!!!!!

Finally, I would like to acknowledge my father, for everything that he did in my life, because I know the pride that he would have to see me here.

STATEMENT OF INTEGRITY

I hereby declare having conducted this academic work with integrity. I confirm that I have not used plagiarism or any form of undue use of information or falsification of results along the process leading to its elaboration.

I further declare that I have fully acknowledged the Code of Ethical Conduct of the University of Minho.

ABSTRACT

Alga-origin Fucoidan on development of therapeutic approaches for diabetes mellitus

Diabetes mellitus (DM) is a metabolic disorder that affects 450 million people worldwide, being the sixth most common cause of death. Therefore, it is crucial to develop new therapeutic strategies and relevant models for diabetes in order to accelerate the discovery of new treatments. In this perspective, marine origin polymers represent a relatively untapped source that can be used in the creation of platforms/models to attend these needs. Algae, for instance, synthesize sulfated polysaccharides with several bioactivity properties, which added to their structural role, open new avenues in biomaterials research.

The main focus of this thesis consists in the demonstration of the potential of fucoidan on the development of therapeutic approaches for diabetes mellitus treatment. Fucoidan (Fu) is an underexploited sulfated polysaccharide extracted from brown algae, which has interesting chemical and biological properties. The major obstacle for using fucoidan on polymeric devices for biomedical applications is the higher solubility in water. In order to control the solubility of fucoidan in water and increase its processability, a chemical modification was studied, a methacrylation reaction, enabling its further gelation by photocrosslinking. Quasi-spherical hydrogel particles were thus prepared, supporting the culture of human pancreatic cells (1.1B4HP), as well as the sustained delivery of insulin. Moreover, alternative methodologies based in blends of fucoidan with other natural/synthetic polymers were also explored. In particular, attention was given to agarose, with attractive gelling properties mediated by temperature. The properties of the resulting hydrogel were assessed, envisaging its use on the encapsulation of pancreatic cells (1.1B4HP cells) as a system to protect those cells from the host immune system. As pancreatic cells and islets are highly vascularized, a platform device was developed based on fibrous meshes of PCL/fucoidan using airbrush technique, with capacity to promote angiogenesis. Additionally, the anti-oxidant effect of fucoidan on beta cells was also assessed, enabling to protect those cells from oxidative stress. This fucoidan was combined with alginate, developing hydrogels capable to support the encapsulation of pancreatic cells and islets with insulin secretion responsive to glucose concentration in medium.

Altogether the results obtained under the scope of this thesis gave interesting insights on the use of the new fucoidan-based structures as functional biomaterials with a potential pivotal role for diabetes treatment.

Keywords: Brown Algae; Diabetes Mellitus; Fucoidan; Hydrogels; Marine Biomaterials.

RESUMO

Fucoidan de algas marinhas usado no desenvolvimento de abordagens terapêuticas para diabetes mellitus

A diabetes mellitus (DM) é um distúrbio metabólico que afeta cerca de 450 milhões de pessoas em todo o mundo, sendo a sexta causa de morte. Por conseguinte, é crucial desenvolver novas estratégias/modelos terapêuticos para a diabetes levando à descoberta de novos tratamentos. Nesta perspetiva, os polímeros de origem marinha representam uma fonte relativamente inexplorada que pode ser usada na criação de plataformas/modelos para atender a essas necessidades. As algas, são um exemplo, porque sintetizam uma grande variedade de polímeros e compostos mais pequenos com várias propriedades bioativas. O foco principal desta tese consiste na demonstração do potencial do fucoidan no desenvolvimento de novas abordagens terapêuticas desenvolvidas para o tratamento da diabetes mellitus. Fucoidan (Fu) é um polissacarídeo sulfatado extraído de algas castanhas, com propriedades químicas e biológicas interessantes sendo pouco explorado. O principal obstáculo para o uso de fucoidan em dispositivos poliméricos para aplicações biomédicas é ser bastante solúvel em água. Para controlar a solubilidade do Fu na água e aumentar sua processabilidade, foi estudada uma modificação química, uma reação de metacrilação, permitindo a sua gelificação através da foto reticulação. Desta forma, foram preparadas partículas quase-esféricas, permitindo o contacto direto com células pancreáticas humanas (1.1B4HPcélulas) bem como o encapsulamento/libertação de insulina foram abordados. Além disso, metodologias alternativas baseadas em misturas do Fu com outros polímeros naturais/sintéticos também foram exploradas. A agarose teve uma atenção particular, com propriedades gelificantes atrativas dependentes da temperatura. As propriedades do hidrogel resultante foram avaliadas, antevendo a sua utilização no encapsulamento de 1.1B4HP células, para proteger essas células do sistema imunitário do hospedeiro. Como as células pancreáticas e as ilhotas Langerhans são altamente vascularizadas, foi desenvolvido um bicomposito de nanofibras PCL/Fu usando uma técnica de aerografia, esse dispositivo/plataforma tinha a capacidade de promover a angiogênese. O efeito antioxidante do fucoidan nas células beta também foi avaliado, permitindo proteger as células do stress oxidativo. Hidrogéis de fucoidan e alginato foram desenvolvidos, sendo capazes de suportar o encapsulamento das ilhotas Langerhans e promover a secreção à insulina em resposta à concentração de glucose presente no meio. Em conclusão, os resultados obtidos no âmbito desta tese foram interessantes e promissores, demonstraram a capacidade do fucoidan a ser usado como base em estruturas e mecanismos que poderão ser fundamentais para o tratamento da diabetes.

Palavras-chave: Algas castanhas, Biomateriais Marinhos; Diabetes Mellitus; Fucoidan; Hidrogéis.

TABLE OF CONTENTS

ACKNOWLEDGMENTS III

STATEMENT OF INTEGRITY IV

ABSTRACT V

RESUMO VI

TABLE OF CONTENTS VII

LIST OF ABBREVIATIONS XI

LIST OF EQUATIONS XIV

LIST OF FIGURES XV

LIST OF SUPPLEMENTARY FIGURES XIX

LIST OF TABLES XX

SHORT *CURRICULUM VITAE* XXI

LIST OF PUBLICATIONS XXIII

INTRODUCTION TO THE THESIS FORMAT XXIX

SECTION 1 1

GENERAL INTRODUCTION 1

CHAPTER I - FUCOIDAN: A SEAWEED SULFATED POLYSACCHARIDE ON CURRENT AND STRATEGIES FOR BIOMEDICAL APPLICATIONS 3

Abstract 3

I-1. Graphical abstract 4

I-2. Introduction 4

I-3. Methodologies of extraction 6

I-4. Chemical composition and physicochemical properties 9

I-5. Biological properties 11

I-6. Complexes, Composites, and blends of fucoidan 15

I-7. Fucoidan applications 24

I-8. Industrial property 29

I-9. Final Remarks 33

I-10. Acknowledgments 34

I-11. References 34

CHAPTER II - BIOMATERIALS-BASED THERAPIES AGAINST DIABETES 48
Abstract 48
General Introduction 49
II-1. Diabetes Mellitus 49
II-2. Complications of diabetes 50
II-3. Current treatments 52
II-4. Biomaterials based matrix architectures for diabetes treatment 54
II-5. Future perspectives 66
II-6. References 66
SECTION 2 74
DETAILED DESCRIPTION OF EXPERIMENTAL MATERIALS AND METHODOLOGIES 74
CHAPTER III - MATERIALS AND METHODS 76
Overview 76
III-1. Materials 78
III-2. Methodologies for processing of biomaterials 86
III-3. Techniques used for characterizing the developed materials/structures 96
III-4. Biological evaluation of the developed materials/structures 120
III-5. Statistical Analysis 148
III-6. References 149
SECTION 3 163
EXPERIMENTAL SECTION 163
CHAPTER IV - FUCOIDAN HYDROGELS PHOTO-CROSS-LINKED WITH VISIBLE RADIATION AS MATRICES FOR CELL CULTURE 165
Abstract 165
IV-1. Graphical Abstract 166
IV-2. Introduction 166
IV-3. Materials and Methods 168
IV-4. Results 173
IV-5. Discussion 181
IV-6. Conclusion 184
IV-7. Acknowledgements 185

IV-8. Abbreviations 185
IV-9. References 186
IV-10. Supplementary part 191
CHAPTER V - FUCOIDAN-BASED HYDROGEL PARTICLES AS BIOMATERIALS FOR DIABETES TREATMENT STRATEGIES 194
Abstract 194
V-1. Graphical Abstract 195
V-2. Introduction 195
V-3. Experimental 197
V-4. Results and Discussion 202
V-5. Conclusions 208
V-6. Acknowledgements 208
V-7. References 208
CHAPTER VI - BUILDING FUCOIDAN/AGAROSE-BASED HYDROGELS AS A PLATFORM FOR THE DEVELOPMENT OF THERAPEUTIC APPROACHES DIABETES 213
Abstract 213
VI-1. Graphical Abstract 214
VI-2. Introduction 214
VI-3. Experimental 216
VI-4. Results and Discussion 225
VI-5. Conclusions 243
VI-6. Acknowledgments 243
VI-7. References 244
VI-8. Supplementary part 249
CHAPTER VII - ANGIOGENIC POTENTIAL OF AIRBRUSH FUCOIDAN/POLYCAPROLACTONE NANOFIBROUS MESHES 253
Abstract 253
VII-1. Graphical Abstract 254
VII-2. Introduction 254
VII-3. Materials and Methods 256
- Cell culture 260

- Cell morphology 261
VII-4. Results and Discussion 263
VII-5. Conclusion 276
VII-6. Acknowledgements 276
VII-7. References 277
CHAPTER VIII - FUCOIDAN HYDROGELS SIGNIFICANTLY ALLEVIATE OXIDATIVE STRESS AND ENHANCE THE ENDOCRINE FUNCTION OF ENCAPSULATED BETA CELLS 284
Abstract 284
VIII-1. Graphical Abstract 285
VIII-2. Introduction 285
VIII-3. Materials and Methods 288
VIII-4. Results & Discussion 300
VIII-5. Conclusion 317
VIII-6. Acknowledgments 318
VIII-7. References 318
VIII-8. Supplementary Part 323
SECTION 4 326
CONCLUSIONS AND FUTURE PERSPECTIVES 326
CHAPTER IX - GENERAL CONCLUSIONS AND FUTURE PERSPECTIVES 328
IX-1. General conclusions and future perspectives 328

LIST OF ABBREVIATIONS

A

AFM - atomic force microscopy

Aga - Agarose

AgaFu - Blend of Agarose and Fucoidan

ALG - Alginate

AlgFA - Blend of alginate and fucoidan from Ascophylum nodosum

AlgFF - Blend of alginate and fucoidan from Fucus vesiculosus

AlgFu - Blend of Alginate and fucoidan

ANOVA - analysis of variance

ATR - attenuated total reflectance

B

β - beta

BDDE - 1,4-butanediol diglycidyl ether

BSA - bone serum albumin

C

C - carbon

Calcein-AM - Calcein acetomethoxy

CAM - Chick embryo chorioallantoic membrane

CLSM - confocal laser scanning microscopy

cm - centimeter (unit)

°C - degree Celsius (unit)

D

DA – Dalton (unit)

DAPI - 4',6-diamidino-2-phenylindole

DPBS - Dulbecco´s Phosphate Buffer Saline

DM - diabetes mellitus

DMA - dynamic mechanical analysis

DMEM - Dulbecco´s modified Eagle´s medium

DMSO - dimethyl sulfoxide

DNA - deoxyribonucleic acid

dsDNA - double stranded DNA

2D - two dimensional

3D - three dimensional

E

E´- storage modulus

E" - loss modulus

ECM - extracellular matrix

EDS - Energy dispersive X-ray spectroscopy

ELISA - Enzyme-linked immunosorbent assay

F

FA - Fucoidan from Ascophylum nodosum

FBS - fetal bovine serum

FF- Fucoidan from Fucus vesiculosus

FTIR - Fourier transform infrared spectroscopy

Fu - Fucoidan

Fucogel - Alginate/fucoidan hydrogels

Fucocaps - Alginate/fucoidan capsules

G

G` - elastic modulus

G´´ - viscous modulus

H

h - hours (unit)

H - hydrogen

^{1}H-NMR – hydrogen -1 nuclear magnetic resonance

HEPES - 4-(2-hydroxyethyl)-1-piperazinesulfonic acid

H&E - Hematoxilin and eosin

I

IR - infrared

ISO - International Organization for Standardization

K

kDa – kilodalton (unit)

kg - kilogram (unit)

L

L - liter (unit)

L929 - Mouse fibroblast-like cells

M

µm - micrometer (unit)

µL - microliter (unit)

M - molar (unit)

mg - milligram(unit)

min - minute (unit)

mL - milliliter (unit)

mm - millimeter (unit)

MA - Methacrylic anhydride

MFu - methacrylated fucoidan

MTS - 3 - (4,5-dimethylthiazol-2-yl)-5(3-carboxymethoxyphenyl)- 2 (4-sulfofenyl)-2H-tetrazolium

M_w - Molecular weight

M199 - Medium 199

N

η´ - dynamic viscosity

N_2 – nitrogen

n - number of the samples

NMR - nuclear magnetic resonance

O

OD - optical density

P

PBS - phosphate buffered saline

PCL - Poly (E- caprolactone)

PCLFA - Poly (E- caprolactone) with fucoidan from *Ascophylum nodosum* algae (FA)

PCLFA - Poly (E- caprolactone) with fucoidan from *Fucus vesiculosus* algae (FF)

PCLFu - Poly (E- caprolactone) with fucoidan (Fu)

PDMS - polydimethylsiloxane

PI - propidium iodide

pH - Measure of the acidity or basicity of an aqueous solution

R

ROS - reactive oxygen species

rpm - revolution per minute (unit)

RT - room temperature

S

sec – seconds (unit)

SEM - scanning electron microscopy

SD or S.D. or s. d. - standard deviation

SH - Superhydrophobic

T

t - time (unit)

T - temperature (unit)

TCPS - Tissue Culture Polystyrene

TE - Tissue engineering

TERM - Tissue Engineering and Regenerative Medicine

T1D - Type I diabetes

T2D - Type II diabetes

U

UV - Vis - ultraviolet-visible spectrophotometry

UVO - ultraviolet/ozone

V

Vol. - volume (unit)

v/v - volume in volume (unit)

W

w/w – weight in weight (unit)

w/v - weight in volume (unit)

WCA - water contact angle

Wt - weight

X

XPS - X-ray photoelectron spectroscopy

Z

ζ – zeta

LIST OF EQUATIONS

Equation III-1- Methacrylation degree 98

Equation III-2- Henry equation 99

Equation III-3 - Antioxidant activity 105

Equation III-4 - Percentage of radical scavenging activity 106

Equation III-5 - Frequency dependence of the complex modulus 110

Equation III-6 - Loss factor 111

Equation III-7- Loss tangent 111

Equation III-8 - Mesh size of hydrogels 113

Equation III-9- Shear modulus G´ 113

Equation III-10- Water uptake 115

Equation III-11 - Weight loss 116

Equation III-12 - Weight loss 116

Equation III-13 - Permeability (P) of glucose 119

Equation III-14- Determination of the diffusion coefficient 119

Equation III-15 - Determination of partition coefficient 119

Equation IV-1. Methacrylation degree 169

Equation VI-1. Mesh size Dmesh 219

Equation VI-2. Permeability (P) of glucose 222

Equation VI-3. Diffusion coefficient of glucose across the membrane. 222

Equation VI-4. Partition coefficient 223

Equation VI-5. Viability of cells 224

Equation VII-1. Degree of swelling 260

Equation VIII-1. The percentage of radical scavenging: 293

Equation VIII-2. The hydrogel mesh size 295

LIST OF FIGURES

Figure I-1. Schematic illustration of fucoidan applications and biological properties. 6

Figure I-2. General procedure for the extraction of fucoidan from brown seaweed 9

Figure I-3. Model of the chemical structure of fucoidan 11

Figure I-4. Schematic illustration of fucoidan-based biomaterials 18

Figure I-5. Scheme of photo-crosslinked methacrylated fucoidan particles with mouse fibroblast-like cells (L929) 19

Figure I-6. Analysis of the distribution of the fucoidan in different application areas based on a literature survey 25

Figure II-1. Representative scheme of the insulin and glucose function mechanism 50

Figure II-2. Micro/macro vascular complications of diabetes mellitus. 51

Figure II-3. Schematic illustration of clinical islet transplantation 54

Figure II-4. Extrahepatic beta-cell delivery strategies 62

Figure III-1. Schematics overview of the materials studied and respective processing and characterization techniques. 77

Figure III-2.Schematic representation of brown algae as well as the cell wall where fucoidan is present. 79

Figure III-3. Chemical structure of Fucoidan from species *Fucus vesiculosus and Ascophyllum nodosum*. 81

Figure III-4. Scheme-of the possible reaction mechanism of fucoidan and methacrylated anhydride and further crosslinking mediated by visible radiation 83

Figure III-5.Chemical structure of agarose 84

Figure III-6. Chemical structure of alginate (M-(1-4)-β-D-mannuronic acid and G-α-(1-4)-L-guluronic acid residues). 85

Figure III-7. Chemical structure of poly (ε- caprolactone) (PCL). 86

Figure III-8. Scheme representative of glass superhydrophobic surface (G-SHS) 87

Figure III-9. Scheme depicting the methodology for the production of modified fucoidan particles (MFu). 89

Figure III-10. Schematic representation for the production of agarose-fucoidan hydrogels (AgaFu)..... 90

Figure III-11. Schematic representation of the methodology used for the production of alginate/fucoidan microcapsules (ALG or Fucocaps). 92

Figure III-12. Schematic overview of the experimental steps required to fabricate airbrushed nanofibrous of PCL and PCLFu. 95

Figure III-13. Scheme of repeating units A) fucoidan, B) methacrylated fucoidan. 98

Figure III-14. Representative scheme of the principle of total antioxidant capacity. 105

Figure III-15. Schematic representation of the principal of DPPH radical scavenging capacity assay. . 107

Figure III-16. Varying a water contact angle. 108

Figure III-17. Schematic representation of a compression-stress-strain curve for a polymer. 109

Figure III-18. Schematic representation of a hydrogel network 114

Figure III-19. Schematic representation of the experimental glucose diffusion systems used during the assay 120

Figure III-20. Schematic representation of rat islet isolation. 125

Figure III-21. Scheme representative of protocol for the isolation of neonatal porcine islets and islet progenitor cells. 127

Figure III-22. Scheme depicting of modified fucoidan particles (MFu) and direct contact with cells (L929 and 1.1B4 cells). 130

Figure III-23. Schematic representation for production of agarose-fucoidan hydrogels (AgaFu). 131

Figure III-24. Schematic representation of agarose microwell fabrication and cell aggregation. 132

Figure III-25. Schematic illustration of the mitochondrial ROS sensor mt-roGFP2-Orp1 135

Figure III-26. Schematic representation of cell encapsulation in ALG or ALGFu. 135

Figure IV-1. ^{1}H-NMR spectra (T=50°C) 174

Figure IV-2. FTIR spectra of fucoidan and modified fucoidan 175

Figure IV-3. SEM images of methacrylated fucoidan photocrosslinked particles after freeze-drying 177

Figure IV-4. Metabolic activity (MTS) of L929 cells cultured in the presence of fucoidan (Fu) and methacrylated fucoidan (MFu). 178

Figure IV-5. Metabolic activity (MTS) results, B) dsDNA content and C) total protein quantified by MicroBCA, of L929-cells seeded and cultured up to 14 days on MFu1 particles.**Erro! Marcador não definido.**

Figure IV-6. Confocal laser micrographs of L929 cells cultured on MFu1 particles during 7 days. 181

Figure V-1. Scheme to illustrate the formation of the fucoidan-based hydrogels particles using visible light and superamphiphobic surface 199

Figure V-2. Characterization of fucoidan (Fu) and modified fucoidan (MFu). 203

Figure V-3. SEM images of MFu microparticles 204

Figure V-4. Insulin release from MFu1 and MFu2 hydrogel particles in PBS 206

Figure V-5. Biological performance of 1.1B4HP cells in MFu microparticles. 207

Figure VI-1.Schematic representation for production of agarose-fucoidan hydrogels (AgaFu). 226

Figure VI-2. Rheological characterization of Aga, Fu and AgaFu hydrogels 229

Figure VI-3.Chemical characterization of Aga, Fu and AgaFu hydrogels 231

Figure VI-4.Characterization of fucoidan powder, Aga and AgaFu hydrogels by XPS analysis 233

Figure VI-5. Schematic representation of a hydrogel network consist of a) cross-links connecting and b) polymer chains with molecule junction diameter (D) and average mesh width (M), as adapted from Schurz et al. [43] B) Mesh size of Aga and AgaFu hydrogels. C) Young Modulus of Aga and AgaFu hydrogels 235

Figure VI-6. Diffusion of glucose across A) AgaFu 3 and B) AgaFu 5 hydrogels 237

Figure VI-7. A) MTS results, B) dsDNA content of 1.1B4 human pancreatic cells encapsulated in Aga 3, 5 and AgaFu 3 and AgaFu 5 at different proportions (a (4/10), b (5/10) and c (7/10)) hydrogels 240

Figure VI-8. Live/dead microscopy images of 1.1B4 HP cells encapsulated into A) Aga and AgaFu 3 and B) Aga and AgaFu 5 hydrogels after 1, 3 and 7 days in culture. 241

Figure VI-9. Confocal images of 1.1B4HP cells encapsulated in A1) Aga3 and AgaFu 3 and A2) Aga5, AgaFu 5 hydrogels for 1, 3 and 7 days in culture. 243

Figure VII-1. Schematic overview of the experimental steps required to fabricate ANFM of PCL and PCL/Fu 257

Figure VII-2. Schematic representation of the optimized chick chorioallantoic membrane (CAM) assay. 263

Figure VII-3. Toluidine blue (TBO) assay in ANFM 264

Figure VII-4. Morphology and composition of PCL and PCLFu ANFM 266

Figure VII-5. Characterization of PCL and PCLFu ANFM by XPS analysis 267

Figure VII-6. Contact angle measurements of A) PCL, B) PCLFA, and C) PCLFF ANFM. 269

Figure VII-7. Swelling of ANFMs after immersion in PBS under stirring at 37°C. 270

Figure VII-8. Mechanical properties 271

Figure VII-9. Cell viability and morphology of PCL and PCLFu ANFM 273

Figure VII-10. Characterization of angiogenic potential of ANFM using CAM assay 275

Figure VIII-1. Chemical characterization and antioxidant properties of purified fucoidans. 302

Figure VIII-2. Cytotoxicity and free radical scavenging properties of fucoidan and its ability to alleviate oxidative stress. 304

Figure VIII-3. Effect of fucoidan on beta cell viability and function. 306

Figure VIII-4. Characterization of fucogels. 308

Figure VIII-5. Characterization of fucocaps. 311

Figure VIII-6. Encapsulation of rat islets in fucocaps. 313

Figure VIII-7. Encapsulation of neonatal pig islets in fucocaps. 315

Figure VIII-8. Gene expression clustering in INS1E cells. 317

LIST OF SUPPLEMENTARY FIGURES

Supplementary Figure IV-1. Immersion of fucoidan cross-linked with epichlorohydrin.....191

Supplementary Figure IV- 2. Immersion of fucoidan based particles in DPBS in different time point´s.192

Supplementary Figure VI-1. Images of Agarose (Aga) and Agarose/fucoidan (AgaFu) hydrogels (3% A) and (5% B) evidencing the diffusion of methylene blue for different time points 249

Supplementary Figure VI-2. Diffusion of methylene blue through the different hydrogels formulations A) Aga3 and Aga5 hydrogels B1) Aga3 and AgaFu 3 a, b,c hydrogels (b1a) and B2) Aga5 and AgaFu 5 a,b,c hydrogels (b1a).....250

Supplementary Figure VI-3. MTS/dsDNA as indication of normalized metabolic activity of 1.1B4 human pancreatic cells encapsulated in Aga 3, 5, and AgaFu 3 and AgaFu 5 at different proportions (a (4/10), b (5/10) and c (7/10)) hyrogels.....251

Supplementary Figure VIII-1. NMR spectra of purified fucoidans.....323

Supplementary Figure VIII-2. Encapsulation of pseudo-islets in fucocaps.....324

Supplementary Figure VIII-3. Differential expression analysis of the RNA-seq data.....325

LIST OF TABLES

Table I-1.Summary of relevant biological activities associated with fucoidan and its potential biomedical applications. 14

Table I-2.Fucoidan-based structures produced by combination with other polymers or ceramics and respective potential application in biomedicine. 20

Table II-1. Microencapsulation systems based on natural/synthetic polymers or a combination thereof used in diabetes treatment. 57

Table II-2. Macroencapsulation systems based on natural/synthetic polymers or combination thereof used in diabetes treatment 63

Table V-1. Methacrylation degree (MD) and zeta potential of bare and modified fucoidan, as determined by ^{1}HNMR and laser Doppler anemometry, respectively. 203

Table VI-1. Summary of formulations used in the preparation of Aga and AgaFu hydrogels. 218

Table VI-2. Relative atomic composition (O, C and S) of the samples obtained by XPS data quantification and their ratio as a function of Carbon. 232

Table VI-3. Permeability (P), Partition (Kd) and diffusion (D) Coefficients of glucose on AgaFu hydrogels. 237

Table VII-1. XPS surface atomic ratios of the main components (O1s, C1s, and S2p) and the respective ratio of O/C and S/C of the controls (fucoidan FA, FF, PCL, PCLFA, and PCLFF) and ANFM. ... 268

Table VII-2. Contact angle in water for the ANFM nanofibrous 269

Table VII-3. Viscoelastic properties of ANFM at a physiological frequency (1Hz). 271

SHORT *CURRICULUM VITAE*

Lara Priscila Lopes Reys, was born on the 24th of May 1982, in Braga, Portugal. She is currently a PhD student at 3B's Research Group (Biomaterials, Biodegradables and Biomimetics), at University of Minho, Headquarters of the European Institute of Excellence on Tissue Engineering and Regenerative Medicine at Avepark, Barco, Guimarães, Portugal. This is a research unit that has been classified by the Foundation of Science and Technology (FCT) as excellent and is part of the Portuguese Associate Laboratory ICVs/3B's. Her work is supervised by Prof. Rui L. Reis, also the Director of the 3B´s Research Group, and co-supervised by Dr. Tiago H. Silva, senior researcher at the 3B´s Research Group.

She received her degree in 2006 in Chemistry- Branch of Quality Control of Plastic Materials, at University of Minho, Braga, Portugal with a final grade of 13 (0-20). In her thesis, she spends six months at BRAVAL- Valorização e Tratamento de Resíduos Sólidos S.A., working under the supervision of Doctor Pedro Machado and Dr. Ana Vera Machado, where developed an alternative environmentally friendly process for recycling car bumpers for her degree thesis obtaining a score in thesis of 18/20.

Her work in different types of polymers in PIEP, Guimarães, Portugal, where she collaborated on the study of recycling polymers, new synthetic polymers in different applications under supervision of Prof. Júlio Viana and Prof. José António Covas.

She received her MSc degree in 2010 in Properties and technology of polymers, at University of Minho, Braga, Portugal with a final grade of 15 (0-20). In her master thesis at the 3B's Research Group working under the supervision of Professor Rui L. Reis and Dr. Tiago H. Silva. The work was performed in her master thesis entitled "Preparation of Squid Chitosan porous structures for Tissue Engineering applications, obtaining a final classification of 15/20 (0-20 scale).

Later on, she formally started her PhD at 3B's Research Group, at University of Minho, Portugal, with a main focus on fucoidan and its applicability on biomedical area, which was further supported by a grant received from the Portuguese Foundation for Science and Technology (FCT) in November of 2015. During eleven months, she was a visiting student at MERLN - Institute for Technology-Inspired Regenerative Medicine under supervision of Prof. Aart van Apeldoorn, studying and developing systems based on fucoidan for diabetes type I treatment.

As a researcher in the 3B´s Research Group, she has been involved in the writing, preparation, and execution of several grant proposals both at National and European levels. As a result of her research work, she attended several important international meetings in her field of research mostly with oral

communications. Presently, she is author of 8 research papers (5 as first author and 3 as co-author), 2 reviews papers as co-author, 3 book chapter, and 20 communications (oral and poster).

LIST OF PUBLICATIONS

Papers in international scientific journals with referees performed under the scope of this PhD thesis

1. **Reys L.L.,** Silva S.S., Reis R.L., and Silva T.H.," Fucoidan: a seaweed sulfated polysaccharide on current and future strategies for biomedical applications", review paper, submitted 2020, 2020.
2. **Reys L.L.,** Silva S.S., Oliveira C., Neves N.M., Martins A., Reis R.L., and Silva T.H., "Angiogenic potential of airbrushed fucoidan/polycaprolactone nanofibrous meshes", submitted 2020, 2020.
3. **Reys L.L.,** Silva S.S., Soares da Costa D., Rodrigues L.C. Reis R.L., and Silva T.H.," Building fucoidan/agarose-based hydrogels as a platform for the development of therapeutic approaches against diabetes", submitted 2020, 2020.
4. **Reys L.L.,** Silva S.S., Soares da Costa D., Reis R.L., and Silva T.H.," Fucoidan-based hydrogels particles as biomaterials for diabetes treatment strategies", submitted 2020, 2020.
5. **Reys. L. L.**, Vaithilingam V., Sthijns M.M.J.P.E. , Soares E., de Vries R. , Mohammed S., de Bont D., Jetten M., Hermanns C., Paulino da Silva Filho O., Stell A. , Mourad NI, Gianello P, LaPointe V. L.S., Silva S. S., Reis R. L., Silva T.H. and van Apeldoorn A. A., *"Fucoidan hydrogels significantly alleviate oxidative stress and enhance the endocrine function of encapsulated beta cells", accepted for publication on Advanced Functional Materials*, 2021.
6. **Reys L.L.,** Silva S.S., Soares da Costa D., Oliveira N.M., Mano J.F., Reis R.L., and Silva T.H., "Fucoidan hydrogels photo-cross-linked with visible radiation as matrices for cell culture", ACS Biomaterials Science & Engineering, vol.2, issue 7, pp.1151-1161, doi:10.1021/acsbiomaterials.6b00180, 2016.

Others papers in international scientific journals with referees

1. Carvalho D. N., López- Cebral R., Sousa R.O., Alves A. L., **Reys L. L.,** Silva S. S., Oliveira J.M., Reis R. L. and Silva T.H.,"Marine collagen-chitosan-fucoidan cryogels as cell-laden biocomposites envisaging tissue engineering", Biomedical Materials,doi:10.1088/1748-605X/ab9f04, 2020.
2. López- Cebral R., Peng G., **Reys L.L.**, Silva S. S., Oliveira J.M., Chen J., Silva T.H., and Reis R. L., "Dual delivery of hydrophilic and hydrophobic drugs from chitosan/diatomaceous earth composite membranes", Journal of Materials Science: Materials in Medicine, vol.29, issue 3, pp. 21-23, doi: 10.1007/s10856-018-6025-9, 2018.

3. **Reys L.L.**, Silva S.S., Pirraco R.P., Marques A.P., Mano J.F., Silva T.H., and Reis R.L., "Influence of freezing temperature and deacetylation degree on the performance of freeze-dried chitosan scaffolds towards cartilage tissue engineering", European Polymer Journal, vol,95, issue C, pp 232 – 240, doi:10.1016/j.eurpolymj.2017.08.017, 2017.
4. Silva S.S., Santos T.C, Cerqueira M.T., Marques A.P., **Reys L.L.**, Silva T.H., Caridade S. G., Mano J.F. and Reis R.L., "The use of ionic liquids in the processing of chitosan/silk hydrogels for biomedical applications", Green Chemistry, vol 14, pp. 1463-1470, doi: 101039/C2GC16535J,2012.
5. Silva T.H., Alves A., Popa E. G., **Reys L. L.**, Gomes M. E., Sousa R. A., Silva S.S., Mano J. F., and Reis R.L., "Marine Algae Sulfated Polysaccharides for Tissue Engineering and Drug Delivery Approaches", BioMatter, vol2, issue 4, pp 278-289, doi:doi.org/10.4161/biom.22947, 2012.

Invited Review Paper (as a co-author)

1. Silva T.H., Alves A., Ferreira B.M., Oliveira J.M., **Reys L. L.**, Ferreira R.F., Sousa R. A., Silva S.S., Mano J.F., and Reis R.L., "Materials of marine origin: a review on polymers and ceramics of biomedical interest", International Materials Reviews, vol.57, issue 5, pp. 276-306, doi: doi.org/10.1179/1743280412Y.0000000002, 2012.

Book Chapters

1. Inácio A.R., Carvalho A.C., Oliveira C., **Reys L. L.**, Silva S. S., Neve N.M., Martins A., Reis R.L. and Silva T.H.,"Chapter XVI: Sulphated Seaweed Polysaccharides", Polysaccharides of Microbial Origin for Biomedical Applications, Eds. Joaquim M. Oliveira, Hajer Radhouani and Rui L. Reis, submitted 2020, 2020.
2. **Reys L. L.,** Silva S.S., Oliveira C., Lopez-Cebral, Neves N.M., Martins A., Oliveira J.M., Silva T.H. and Reis R.L., "Marine-Origin Polysaccharides for Tissue Engineering and Regenerative Medicine", Encyclopedia of Marine Biotechnology, Eds. Se-Kwon Kim, Volume IV, Chapter 118, ISBN: 978-1-119-14377-2, 2020.
3. **Reys L. L.,** Oliveira C., Oliveira J. M., López- Cebral R., Silva S. S., Silva T. H., and Reis R. L., "Polissacarídeos de origem marinha para aplicação em estratégias de engenharia de tecidos", *Valorização dos Recursos Marinhos: Biomateriais em Regeneração de Tecidos e Libertação de*

Fármacos, Eds. Carmen G. S., Pilar S. P., Julio M. L., José V. A., Ricardo P. M. I., Tiago S. H., and Reis R. L., IIM-CSIC, Vigo, Espanha, pp. 107-145, doi:D.L: C2166-2015, 2015.

Conference Abstracts - Isi Web of Science Indexed

1- Silva T.H., Oliveira C., **Reys L.L.**, Soares da Costa D., Nova-Caballal R., Oliveira N.M., Ferreira A.S., Nunes C., Silva S.S., Martins A., Coimbra M.A., Mano J.F., Neves N.M., and Reis R.L., "Biomedical potential of fucoidan, a seaweed sulfated polysaccharide: from an anticancer agent to a building block of cell encapsulating systems for regenerative medicine", Front. Bioeng. Biotechnol, pp.221, doi:10.3389/conf. FBIOE.2016.01.00221, 2016.

2- **Reys L.L.**, Silva S.S., Soares da Costa D., Oliveira N.M., Mano J.F., Reis R.L., and Silva T.H., "Evaluation of the potential of fucoidan-based microparticles for diabetes treatment", European Cells & Materials,1, vol.1, issue 1, P349, 2016.

3- **Reys L. L.,** Silva S. S., Soares da Costa D., Oliveira N. M., Mano J. F., Silva T. H., and Reis R. L., "Fucoidan-based Particles for Diabetes Mellitus Treatment.", *Tissue Engineering Part A*, vol. 21, issue S1, pp. A204, doi:10.1089/ten.tea.2015.5000.abstracts, 2015.

Conference oral presentations

1- Silva T.H., **Reys L. L.**, Silva S.S., Oliveira N.M., Soares da Costa D., Mano J.F., Oliveira C., Martins A., Neves N.M., and Reis R. L.," Marine macroalgae, sulfated polysaccharide resembling GAGs in Biomedical applications: using fucoidan on the development of biomaterials", Advanced Functional Polymers for Medicine 2015, Galway, Ireland, 23rd to 25th March, 2015.

2- **Reys L. L**., Silva S. S., Soares da Costa D., Oliveira N. M., Mano J. F., Silva T. H., and Reis R. L., "Assessing the potential of fucoidan-based microparticles for biomedical applications", European Society of Biomaterials 2015 (ESB 2015), Kraków, Poland, 30th August to 3rd September, 2015.

3- **Reys L**. L., Vaithilingam V., Sthijns M.M.J.P.E., Soares E., Silva S.S., Silva T.H., Reis R.L. and Apeldoorn A.A.V, "Incorporation of fucoidan in algae microcapsules leads to reduction of oxidative stress and enhances glucose responsiveness in pseudo-islets", 11th World Biomaterials Congress (WBC2020), Glasgow, Scotland, 11-16th of December, 2020 (accepted for oral presentation).

Conference posters

1- Vaithilingam V., **Reys L. L.**, Silva T.H., Silva S.S., Reis R.L., van Apeldoorn A.A. "Fucoidan hydrogels significantly alleviate oxidative stress and enhance the function of encapsulated beta cells and islets", 10th EPITA symposium & 39th AIDPIT workshop 2020, Innsbruck, Austria, 26th to 28th January, 2020.

2- **Reys L. L.,** Silva S. S., Soares da Costa D., Reis R. L and Silva T. H." Construction of fucoidan-based hydrogels as pancreatic beta cells encapsulating system for diabetes treatment", TERMSTEM 2019, Braga, Portugal, 6th to 8th November, 2019.

3- **Reys L. L.,** Silva S. S., Soares da Costa D., Reis R. L and Silva T. H." Fucoidan-based hydrogels as pancreatic beta cells encapsulating system", 1st Discoveries Forum on Regenerative and Precision Medicine, Porto, Portugal, 25th to 27th September, 2019.

4- Carvalho D.N., Lopez-Cebral R., Sousa R.O., **Reys L. L.**, Oliveira J.M., Reis R.L. and Silva T.H., "Marine origin biopolymers on the development of cryo-system gels envisaging cartilage tissue engineering and regenerative medicine". 30th Annual Conference of the European Society of Biomaterials (ESB 2019), Dresden, Germany, 9th to 13th September, 2019.

5- Carvalho D.N., Lopez-Cebral R., Sousa R.O., **Reys L. L.**, Oliveira J.M., Reis R.L. and Silva T.H., "Marine origin biopolymers on the development of innovative scaffolds envisaging cartilage tissue engineering and regenerative medicine", 1st Conference of Achilles, Porto, Portugal, 8th to 10th July, 2019.

6- **Reys L. L.,** Silva S. S., Soares da Costa D., Pirraco R.P., Silva T. H and Reis R. L." Assessing the potential of fucoidan-based hydrogels for pancreatic cells encapsulation" 29th Annual Conference of the European Society of Biomaterials (ESB 2018), Maastricht, Netherlands, 9th to 13th of September, 2018.

7- **Reys L. L.,** Silva S. S., Soares da Costa D., Pirraco R.P., Reis R. L and Silva T. H., "Design of fucoidan-agarose hydrogels as a platform for encapsulation of pancreatic cells towards an advanced therapy for diabetes mellitus", Summer School Gene2Skin/Summer School Chem2Nature 2018,Porto, Portugal, 3rd to 8th June, 2018.

8- **Reys L. L.,** Silva S. S., Soares da Costa D., Reis R. L and Silva T. H., "Fucoidan-based hydrogels for pancreatic beta cells encapsulating system", Gene2Skin Winter School/Forecast 2017,Porto, Portugal, 13th to 17th November, 2017.

9- **Reys L. L.,** Silva S. S., Soares da Costa D., Reis R. L and Silva T. H., "Design of agarose-fucoidan hydrogels for Diabetes Treatment", Chem2Nature Second School,5th to 9th June, Porto, Portugal, 2017.

10- **Reys L. L.,** Silva S. S., Oliveira N. M., Soares da Costa D., Mano J. F., Reis R. L and Silva T. H." Construction of fucoidan microparticles as an insulin delivery system for diabetes treatment", Chem2Nature First School, Guimarães, Portugal, 21th to 25th November, 2016.

11- **Reys L. L.,** Silva S. S., Oliveira N. M., Soares da Costa D., Mano J. F., Reis R. L and Silva T. H." Construction of fucoidan microparticles as an insulin delivery system for diabetes treatment", TERM STEM 2016, Guimarães, Portugal, 24th to 28th October, 2016.

12- Silva T.H., Oliveira C., **Reys L. L.,** Soares da Costa D, Novoa-Carballal R., Oliveira N. M., Ferreira A. S., Nunes C., Silva S. S., Martins A., Coimbra M. A., Mano J. F., Neves N.M. and Reis R.L., "Biomedical potential of fucoidan, a seaweed sulfated polysaccharide: from an anticancer agent to a building block of cell encapsulating system for regenerative medicine", 10th *World Congress Biomaterials Congress* (WBC),Montreal, Canada, 17th to 22th May, 2016.

13- **Reys L. L.,** Silva S. S., Oliveira N. M., Soares da Costa D., Mano J. F., Reis R. L and Silva T. H.," Evaluation of the potential of fucoidan-based microparticles for diabetes treatment", *TERMIS EU Congress*, Uppsala, Sweden, 28th June to 1st July, 2016

14- **Reys L. L.,** Silva S. S., Soares da Costa D., Oliveira N. M., Mano J. F., Silva T. H., and Reis R. L., "Fucoidan-based particles for Diabetes Mellitus treatment", 4th *TERMIS World Congress*, Boston, Massachusetts, 8th to 11th September, 2015.

15- **Reys L. L**., Silva S. S., Soares da Costa D., Oliveira N. M., Mano J. F., Silva T. H., and Reis R. L., "Fucoidan-based Microparticles for Biomedical Applications.", *5th* ICVS/3B´s Meeting, Braga, Portugal, 2015.

16- **Reys L. L.**, Silva S. S., Oliveira N.M., Mano J. F., Silva T.H., Reis R.L., "Methacrylated fucoidan as photocrosslinkable biopolymer for Tissue Engineering applications, in 3th ICV´s/3B´s- Associated Laboratory meeting, Braga, Portugal, 2014.

17- **Reys L. L.**, Silva S. S., Oliveira N.M., Mano J.F., Silva T.H., Reis R. L., "Methacrylated fucoidan as photocrosslinkable biopolymer for Tissue Engineering applications, *TERM STEM* 2014, Porto, Portugal, 23th to 24th October, 2014.

18- Silva T. H., Barros, A. A., Marques A. L. P., Duarte A. R. C., Diogo G. S., Moreira-Silva J., **Reys L. L.**, Silva S. S., and Reis R. L., "The Oceans as a Source and as an Inspiration for Biomaterials

Development: Some key examples", 26th Annual Conference – European Society for Biomaterials (ESB2014), Liverpool, UK, 31th August to 3rd September, 2014.

Patents

1- Carvalho D.N., Lopez-Cebral R., Sousa R.O., **Reys L. L.**, Oliveira J.M., Reis R.L. and Silva T.H. "Eco-friendly gels from marine-biopolymers, products and uses thereof", (Submitted 2019).

Awarded grant

1- Fundação para a Ciência e Tecnologia (FCT) – PhD scholarship (SFRH/BD/1121139/2015).

INTRODUCTION TO THE THESIS FORMAT

The present thesis is divided into four main sections (1 to 4) containing nine chapters (I to IX). This structure was adopted to allow a proper organization of the data presented in the various chapters. An introduction (Section 1) can be found divided in two Chapters: **Chapter I and II**. An overall materials and methods section (Section 2). The Section 3 shows the experimental results obtained in the context of this thesis and their discussion, focusing on use of sulphate polysaccharide-fucoidan in the production of architectures, which can be useful in the development of therapeutic strategies for diabetes mellitus. The Section 4 finalizes this thesis with general conclusions and final remarks.

The main body of the thesis is based on a series of publications published in international journals or submitted for publication. Each chapter is presented in a manuscript form, i.e., abstract, introduction, experimental section, discussion (or in two separate sections, i.e., results plus discussion), conclusion, and acknowledgements. A list of relevant references is also provided as a subsection within each chapter. **Figure 1** shows the structure of the thesis divided in the 4 main sections. The contents of each part and chapter are described below in more detail.

Section 1 – General introduction - Background

This chapter is divided in two chapters, the first is a brief literature review about fucoidan the marine biomaterial selected for this thesis, the second is more about general concepts about diabetes and currently strategies used for treatment of this disease.

Chapter I - Fucoidan: a seaweed sulfated polysaccharide on current and future strategies for biomedical applications: This chapter provides an introduction to fucoidan a marine biopolymer and its applications in the biomedical field. This marine biopolymer was used along the entire thesis.

Chapter II – Biomaterials - based therapies against diabetes: This chapter provides background information about diabetes mellitus. Its complications and the currently available methods using biomaterials.

Section 2 - Detailed description of experimental materials and methodologies

Chapter III - Materials and Methods: A list of the materials used, and methods applied to obtain the results described further on is provided, being the basis to the whole work described in this thesis.

Section 3 - Experimental work regarding the development of therapeutic approaches for diabetes mellitus based on fucoidan.

Chapter IV - Fucoidan hydrogels photo-cross-linked with visible radiation as matrices for cell culture: This chapter studied the modification of fucoidan with methacrylation reaction in order to control its water-solubility and consequently to improve its processability.

Chapter V – Fucoidan - based hydrogel particles as biomaterials for diabetes treatment strategies**:** Similarly, to **Chapter IV**, modified fucoidan (MFu) were cross-linked with visible light, using the reaction conditions previous optimized. In this case, besides the chemical characterization, the insulin diffusion and the direct contact with1.1B4 human pancreatic cells (1.1B4HPcells) were also evaluated.

Chapter VI - Building fucoidan/agarose-based hydrogels as a platform for development of therapeutic approaches against diabetes: This chapter describes the combination of agarose (Aga), a gelling polymer with fucoidan (Fu), a non-gelling one, as an alternative pathway to prepare hydrogels for diabetes treatment. The influence of different concentrations of fucoidan and agarose on the overall properties of the hydrogels was evaluated in terms of physicochemical and biological properties.

Chapter VII - Angiogenic potential of airbrushed fucoidan/polycaprolactone nanofibers meshes: This chapter aims to show the production of poly(ε-caprolactone) and fucoidan (PCLFu) airbrush nanofibers mesh, that could be used as platform device for support therapeutic approaches for biomedical applications in special for vascularization field.

Chapter VIII - Fucoidan hydrogels significantly alleviated oxidative stress and enhance the endocrine function of encapsulated beta cells: In this Chapter, the incorporation of two polysaccharides from brown algae - namely fucoidan (Fu) and alginate (ALG) - in encapsulating materials was studied. In this work, the anti-diabetic potential of fucoidan was assessed by studying its oxidative stress relying properties on beta cells and further using them on the development of functional microparticles for the encapsulation of rat insulinoma cells (INS1E).

Section 4 - Conclusions and final remarks

Chapter IX - General conclusions and final remarks: The final section of the thesis presents the general conclusions and implications, current limitations and potential of the work described for biomedical applications.

This thesis is based on six manuscripts that were submitted or accepted for publication, as referenced in the chapters of section III of the thesis.

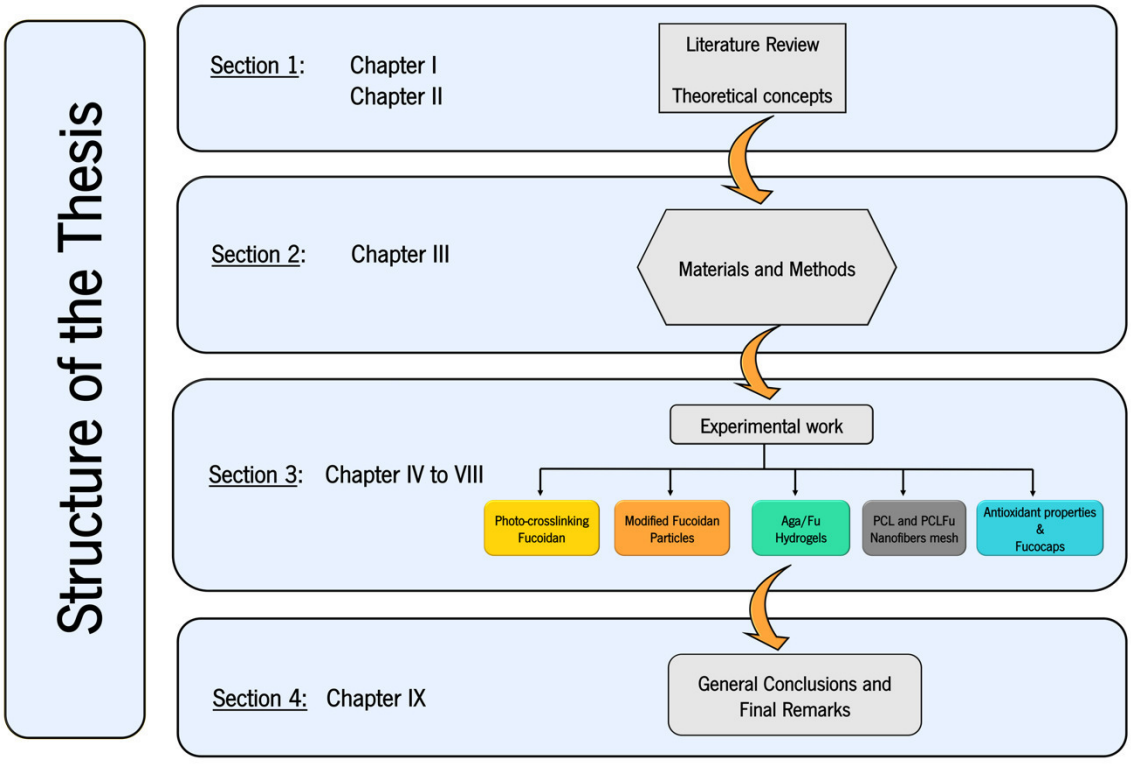


Figure 1. Scheme representing the structure of the thesis.

"It always seems Impossible until it´s Done"

—Nelson Mandela (1918-2013)

SECTION 1

GENERAL INTRODUCTION

CHAPTER I

FUCOIDAN: A SEAWEED SULFATED POLYSACCHARIDE ON CURRENT AND FUTURE STRATEGIES FOR BIOMEDICAL APPLICATIONS

Chapter I

Fucoidan: a seaweed sulfated polysaccharide on current and strategies for biomedical applications[1]

ABSTRACT

Brown seaweeds are rich sources of bioactive compounds, including polysaccharides, carotenoids, peptides, omega-3, pigments, vitamins and minerals. Fucoidan is a sulfated polysaccharide and bioactive compound present in the cell wall of brown seaweed. Structurally, fucoidan is formed by different amounts of L-fucose, sulfate groups, glucuronic acid and xylose, with other sugars being present depending on the origin. Fucoidan is promising worldwide, as a result of its good therapeutic effects, especially among the biomedical and pharmaceutical industry. Classical biological properties associated with fucoidan include antitumor, antioxidant, and anti-inflammatory action, but despite intensive research, the correlation between the various bioactive properties and the molecular and structural features of fucoidan still has to be clarified. Deeply studying the structure of fucoidan and exploring the relationship between activity and structure are useful tools for developing and utilizing this brown seaweed asset in a sustainable way, tackling the variability found in natural origin products. Besides the bioactive features, fucoidan´s performance as support polymer is also playing a relevant role in research and innovation, from drug delivery devices to cell culture matrices and biomaterials for tissue engineering and regenerative medicine. This review starts by addressing the extraction procedures/techniques to produce fucoidan from brown seaweeds, and further discuss the recent findings on the applicability of fucoidan in the biomedical field and how fucoidan´s chemical versatility is affecting its performance. The present review thus aims to shed some light on the contribution of fucoidan

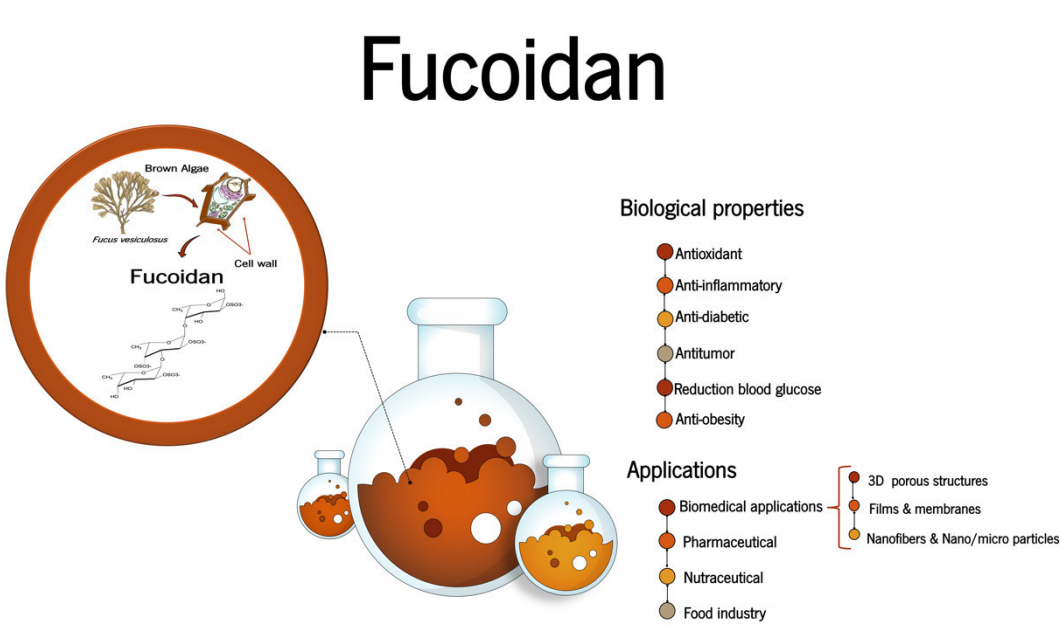
[1] This chapter is based on the following publication:

Reys L. L., Silva S. S., Reis R. L. and Silva T. H., *"Fucoidan: a seaweed sulfated polysaccharide on current and future strategies for biomedical applications"*, (submitted for publication)

for scientific and technological development in biomedicine, stressing the opportunities and the challenges it is and will be facing to assume a key role in this highly demanding sector.

Keywords: Fucoidan; brown seaweed; biomedical application; sulfated polysaccharide; anti-diabetic, antioxidant, anti-obesity, antitumoral, marine biomaterial.

I-1. GRAPHICAL ABSTRACT



I-2. INTRODUCTION

During the past decades, marine organisms have been the focus of considerable and growing attention as potential sources of valuable materials [1–3]. Valorization of by-products derived from those marine organisms, as well as underexploited species, as natural renewable resources for obtaining relevant bioactive compounds, could have both economic and environmental positive impacts [3,4]. Nevertheless, they remain

largely unexploited on what concerns it´s biotechnological applications. Marine algae possess a special group of polysaccharides, sulfated polysaccharides, which face no similar in terrestrial plants but resemble the glycosaminoglycans found in the extracellular matrix of mammals. Recently, increasing attention has been paid to brown algae, known to contain in the cell walls a range of different polysaccharides including alginate, laminarin and fucoidan [5]. Fucoidan is an anionic and sulfated polysaccharide, containing a substantial amount of L-fucose often functionalized with sulfate groups, together with other sugars, as glucuronic acid and xylose, which can be extracted by water [4–7]. This polysaccharide can be isolated from different species of brown algae such as *Fucus vesiculosus* [8], *Undaria pinnatifida* [9]*, Ascophyllum nodosum* [8]*,* and Bifurcaria bifurcata [8,10]. The interest in fucoidan comes from its intrinsic properties namely anti-tumoral [6,11], anti-coagulant [6,11,12], anti-viral [6,13], anti-inflammatory [6,14], blood glucose reducer [6,15–17] and antioxidant activities [6,8,18,19]. For this reason, is also playing a relevant role in research and innovation, from drug delivery and cell culture 3D matrices to cosmetic and food additives [20,21]. Nevertheless, the exploitation of fucoidan for tissue engineering (TE) has been scarcely addressed, despite its good bioactive properties that could act strongly in the search for novel functional applications in pharmaceutical and biomedical areas [22], including in regenerative medicine and advanced therapies [23,24].

An overview of the current and potential applications of fucoidan in the food, cosmeceutical pharmaceutical, and biomedical areas will be addressed, including in particular, the research relevant for tissue engineering and biomedical field **(Figure I - 1)**. Foundational information about bioactive properties, extraction methods, and structure will also be reported. This review intends thus to show significant scientific/industry applications that fucoidan can have in the biomedical field.

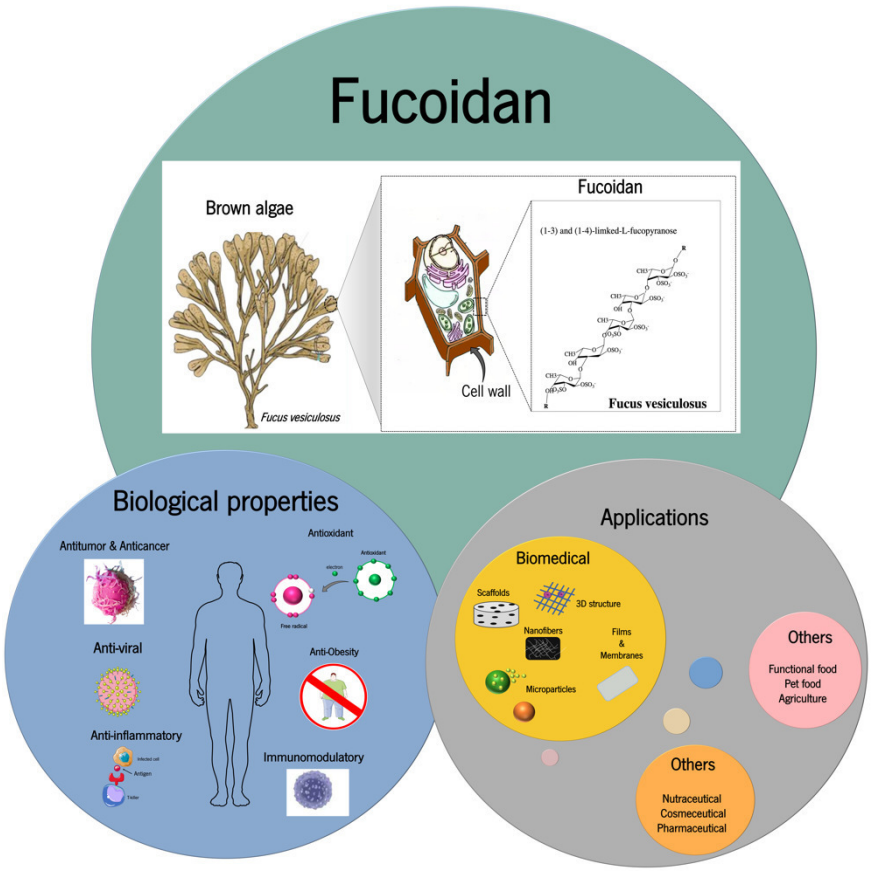


Figure I-1. Schematic illustration of fucoidan applications and biological properties.

I-3. METHODOLOGIES OF EXTRACTION

Various extraction methods have been studied and employed in research laboratories and in the industry to produce high-quality fucoidan. It can be extracted using hot acid/salt ($CaCl_2$) [7,21,25,26] or ethanol/water solutions [26–28] further assisted by ultrasound and microwave radiation [29] or enzymes [30], as well as using acidic extraction [26]. The latter method is the most common one used in the industry, as this method produces fucoidan with the highest yield, higher purity, and better quality [20,29,31–34]. In all those methods, the correct adjustment of parameters such as temperature, extraction time, concentration/pH, and species of algae should be controlled in order to avoid large variability among fucoidan extracts, the

degradation of fucose chains or the removal of undesirable components [29]. The minimum change in these parameters can affect the composition, chemical structure, molecular weight, size of fucoidan fractions, and yields of resulting fucoidan and subsequently influencing the bioactivity of the produced extracts [35]. A fucoidan production process **(Figure I - 2)** can be described in three steps: i) mill seaweed, ii) extraction and purification of the extracts, iii) drying, and careful storage [23]. In the first step, the seaweed can be collected *in loco*, cultured, or obtained through specialized enterprises and then grounded. Subsequently, the fucoidan is extracted from brown algae using hot acid (hydrochloric acid (HCl) or sulphuric acid (H_2SO_4)) or ethanol/aqueous solutions [32,36], together with calcium addition to promote precipitation of alginates normally co-extracted with fucoidan [7,20,25,29]. The ethanol used in the process of extraction is used to remove the salts and small molecules from the target polysaccharides. Extraction with acidic solutions gives higher yields of crude fucoidan [37], but care is needed as it could result in undesirable products such as alginic acids and metals and may cause degradation on fucose chains [7,38]. Then, the material is centrifuged to remove the alginate previously precipitated with calcium and obtain the crude fucoidan extract is obtained after filtration to remove insoluble components [7,36–38]. Finally, the crude extract is purified through different methods namely: i) in the form of lead hydroxide complex the fucoidan is extracted with hot water, the extracted is lead with acetate and barium hydroxide), ii) formaldehyde/alcohol, the fucoidan is extracted with dilute acid, then is precipitated by treating with ethanol and iii) cetylpyridinium chloride, the fucoidan extracted is dialyzed with water and precipitated with calcium chloride and supernatant are treated with cetylpyridinium chloride [20,32,39–42]. Fucoidan is normally obtained after dialysis and freeze-drying in a powder form with yellow-brown color. The color of fucoidan powder is directly related to the amount of fucoidan in the powder [36,37,39,43]. If the powder contained very small quantities of fucoidan, it would be very white or creamy color. The powder containing large concentrations of fucoidan will be close to a dark brown color [36]. An advantage of extraction with hot acid solutions, give higher yields of crude fucoidan but could result in the extraction of undesirable products such as alginic acids and metals [36–38]. However, the application of diluted acid at ambient temperature may result in partial cleavage of sulfate ester (SO_4^{2-}) and degradation of fucose chain, which can influence the bioactive properties, these groups are normally associated with fucoidan bioactive properties [7,36] Ultrasound, and microwave-assisted extraction consist of the penetration of radiation (energy) into the material structure, promoting the extraction of the compounds

selectively. It is faster as compared to the classical process of extraction [44–48]. In the process of microwave-assisted extraction, microwaves induce the vibrations of water molecules in the algae. Because of these vibrations, the temperature of intracellular liquids increases, and water evaporates and exerts pressure on the cell walls. As the cell walls break, the intracellular contents where fucoidans are present are released into the medium [29,49,50]. This method requires short extraction time, use of non-corrosive solvents, requires lower energy consumption and generates fewer wastes, when compared with other techniques [21]. The principal disadvantage of this process is the energy input in the process that can exceed the energy level required for the cleavage of sulfate esters (SO_4^{2-}); thus, it is highly recommended that the necessary energy input is carefully exerted during the extraction process to avoid any structural alteration of the sulfated polysaccharides [29]. The enzyme-assisted extraction of fucoidan is still being studied. This process consists in the isolation of fucoidan from algae by enzyme degradation of the cell wall. The extraction with enzymes is performed under moderate conditions that conserve the bioactivity of fucoidan. For the extraction it is necessary an enzyme mixture because the algae cell wall is chemically and structurally heterogeneous [29,51]: alginate lyase [29], cellulose and laminarinase [52], are some of the used ones because these enzymes do not hydrolyze fucoidan, as demonstrated by *Athukorola et al* [53]. Another advantage of this process is the simple separation of fucoidan from other products only using crossflow filtration or membrane with an adequate cut off, where sulfated polysaccharides are retained on the membrane.

Furthermore, there is an urgent need for more well-defined, gentle extraction methods, using shorter extraction times, lower temperatures, and lower acid levels, to help ensure the removal of distinct fucoidan structures. In addition, the extraction method must be cost-effective and environmentally sustainable for industrial production, and of course, a bid for acceptable legal standards concerning solvent use.

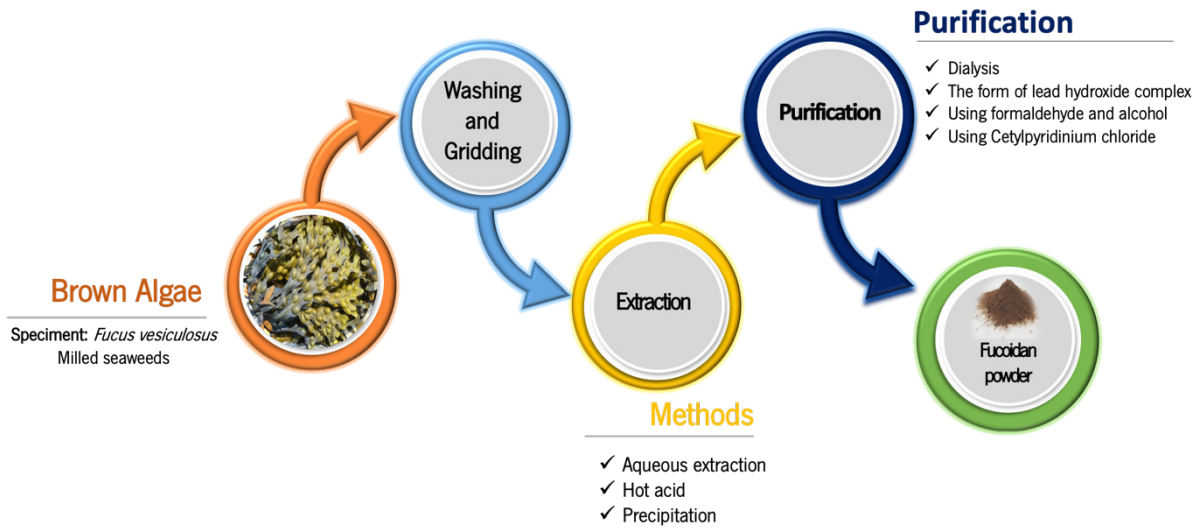


Figure I-2. General procedure for the extraction of fucoidan from brown seaweed (adapted from [4,31,39]).

I-4. CHEMICAL COMPOSITION AND PHYSICOCHEMICAL PROPERTIES

Despite many studies on the chemical composition and structure of fucoidan, the uncertain remains due to the large variability that can be observed between different extracts [36,54]. Fucoidan is composed mainly of L-fucose or L-fucopyranose and sulfate groups substituting on hydroxyl groups. Besides, other monosaccharides are also present, such as mannose [42,55], galactose [47], glucose [46], xylose [47,56], uronic acids [23,46], as well as acetyl groups [38,40,57] **(Figure I - 3)** Moreover, the backbone of fucoidan polymers from *Laminaria, Analipus japonius, Cladosiphom okamurans and Chorda filum* species have the L-fucopyranose residues substituted with sulfate (SO_3) on the C-2 position. Other fucoidan polymers such as the ones from *Ascophyllum and Fucus* species have substitutions at C-2 or C-4 (rarely on C3). *Li et al* [6] reported that the structure of fucoidan of various brown algae differs from one species to another. Generally, fucoidan has a backbone of (1→3)-linked-α-L-fucopyranose or alternating (1→3) and (1→4)-linked-α-L-fucopyranose residues. The type of glycosidic linkage of fucoidan monosaccharides in the backbone is closely related to the species of seaweed [58–61]. In general, fucoidan is branched in various ways, whereas some sulfated fucan polymers have been detected in invertebrates, classified as well as fucoidans, but having a linear backbone [6,60,62]. Fucoidan can differ in structure among seaweed species and can vary even within

the same species [63]. The chemical composition, namely monosaccharide composition, sulfation patterns, fine structure, and differences in the bioactivity of fucoidan varies according to the season, geographic location, the maturity of the specimen, among others [5,31,36,48]. Until today, different chemical structures of the fucoidan extracted from different seaweed have been proposed. Thus, fucoidan should be understood as a family of polymers (sulfated fucans) and not only one polymer with different molecular weight (Mw) or sulfate contents. The molecular weight of fucoidan varies between 20-300 kDa for low molecular weights fractions and 200-800 kDa for high molecular weight exhibiting significant variations [44,46,47]. The differences in molecular weight can be influenced as well by algae species, sugar variations, and sulfate groups distribution, but also to the conditions used on the extraction, which may cause partial hydrolysis of the polymer and the lower Mw [39,64–66]. The difficulty in measure of molecular weight (Mw) can be related to the presence of some contaminants and the heterogeneity of components. Furthermore, the molecular weight of fucoidan can influence other physicochemical properties of fucoidan, namely the hydrocolloids properties (a colloid system where the colloid particles are hydrophilic and diffused in water), related with intermolecular associations, as well as capability to form gel network [48]. Nevertheless, this bottleneck in fucoidan characterization can also be related to glycosidic linkage angles, negative charges originating from sulfate groups, which tend to expand the polysaccharides in water through mutual electrostatic repulsion and by hydroxyl groups involved in intra-molecular or intermolecular hydrogen bonds [67].

Regarding processability, fucoidan is a water-soluble polymer, but it is not able to form gels alone but only viscous solutions [48]. The processability/viscosity of fucoidan is influenced by molecular weight, sulfation degree, and pattern, as well as polymer branching, besides experimental factors such as polymer concentrations temperature, ionic strength, and pH [11,32,39,48,68]. In some areas like the biomedical area, the solubility in water of fucoidan can be a limitation because pure structures cannot be obtained, requiring modifications of the polymer or combination with other compounds, challenging its bioactive performance [69,70].

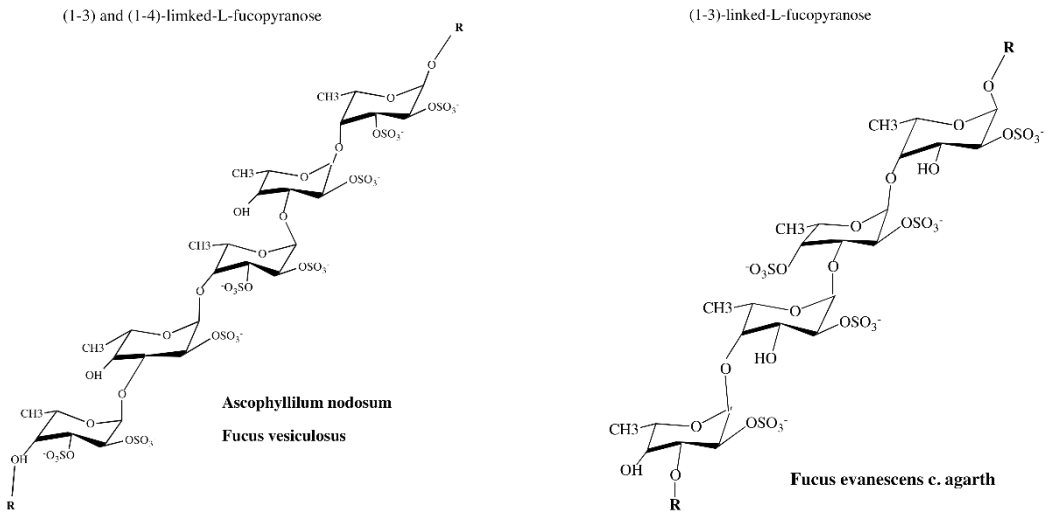


Figure I-3. Model of the chemical structure of fucoidan (adapted from [7,71]).

I-5. BIOLOGICAL PROPERTIES

The chemical structure of fucoidan, namely molecular weight, number, and position of sulfate groups and amount of L-fucose and other sugar residues, influences most biological activities exhibited by this biopolymer, although the structure-activity relationships are not yet well established [31,36,62,72]. Fucose, the major constituent of fucoidan is a useful indicator of important biological activities, namely antioxidant and antitumor effect: in general, higher content of fucose, the higher are the biological activities [39]. Sulfate groups also form a large component of fucoidan, and fucoidan´s biological activities are closely related to its sulfate content [36,73], as well as position and pattern [6]. Another important parameter that influences the bioactivity of fucoidan is the molecular weight [6]. For these reasons, each type of fucoidan may have unique structural features and possess (or not) several biological activities. Fucoidan is known to exhibit a wide variety of biological activities, namely antioxidant [6,39,74], antitumor [6,11,75], anti-inflammatory [6,14], anticoagulant [6,12,39] and reducing blood glucose [76,77]. In **Table I - 1,** it is possible to find summarized information on the main biological properties of fucoidan and their applications. The biological activities must always be confirmed in the laboratory, at least when extracts are obtained by different methodologies or using different species (ideally, specimens) for comparison. For instance, our group has recently shown that extracts

from the same algae species like *Fucus vesiculosus* can show very different activity with some having antitumor activity, while others are not showing any toxicity or being toxic to all cells [78].

Antioxidants can prolong or prevent the oxidative stresses applied in organs. In fucoidan, the antioxidant activity is related to the molecular weight and fucoidan sulfate content [6]. Fucoidan, in recent years, demonstrated to have a better total antioxidant capacity (TAC) compared with synthetic antioxidants [36,79]. Some authors reported that fucoidan was a natural antioxidant because the sulfate group present in the structure has particular involvement in antioxidant activity and has a significant potential for avoiding or delaying free radical-mediated illnesses [36,39,79]. In the literature, it is also suggested that the sulfate groups of fucoidan would be present in the reaction with oxygen radicals and prevent oxidative stress [36,39,74,80]. However, the scavenging effects are related to a lower amount of sulfate in the polymer backbone. Therefore, the lower the molecular weight, the stronger is the effects of scavenging. *Ruperez et al* [80] demonstrated that fucose could be the key to the radical scavenging ability of fucoidan that could be potentially used as an antioxidant for the food industry [7,36,80]. For comparison, this polymer has shown a much higher scavenging activity than vitamin C and K-carrageenan [7].

Furthermore, the antitumoral activity of fucoidan has been discussed as a strategy for the treatment of cancer [6,11,81,82]. In fact, the sulfate groups present in fucoidan could be responsible for this property. Some authors reported that oversulfation influence the anticancer activity [83–85] through higher angiogenic activity, thus more effectively inhibiting the growth of tumor [83]. The role of sulfate groups in cancer treatment has been described by Belting *et. al*, reporting that the negative charge of sulfate groups can interact with a positive charge of natural polyamines with equal or even higher affinity than DNA [56,86–88]. Natural polyamines (putrescine, supermidine and spermine) are present in all mammalian cells, binding the nucleic acids and play an important role in DNA conformation, replication, transcription, and translation. Because cellular proliferation depends on an adequate supply of polyamines, the polyamines biosynthetic pathway has been an attractive target for the proliferation disorders, such as cancer [86,89,90]. It was also reported that fucoidan from *Fucus vesiculosus* inhibited the proliferation and induced apoptosis in human lymphoma HS-sultan cell lines [6,11,75]. By its turn, *Alekseyenko et al* [85] studied the activity of fucoidan isolated from *Fucus evanescens* in C57B1/6 mice with transplanted Lewis lung adenocarcinoma, with injections of 10mg/kg to 25mg/kg potentiating the antimetastatic and anti-tumor activities of

cyclophosphamide [6,11,85]. Molecular weight is another crucial factor for anti-cancer fucoidan activity. *Cho et al* produced three fucoidan fractions with molecular weights of < 5, 5-30, and > 30 kDa and reported that the $F_{5\text{-}30K}$ show most tumor growth inhibitory effect, despite the sulfate amount in $F_{<5K}$ being higher than in the two other fractions [91,92]. *Yang et al* realized a study that suggested that anticancer activity of fucoidan could be significantly improved by lowering their molecular weight when they are depolymerized by mild hydrolysis conditions without causing desulfation [44]. Other studies identified the antitumoral potential on fucoidan in different perspectives: inhibiting proliferation of tumor cells, stimulating the apoptosis of tumor cells, blocking tumor cells metastasis, or enhancing immune response [83].

Studies also suggested that fucoidan could be used for the treatment of inflammatory pathologies, namely chronic wound (chronic leg ulcers) and rheumatoid arthritis, because fucoidan can significantly inhibit the release of nitric oxide (NO) induced by bacterial lipopolysaccharide and reduce inflammation [93]. *Li Fan et al* [94] studied that fucoidan isolated from *Laminaria japonica* can regulate the inflammation response via genes (HM6B1 and NF-K3) inactivation in induced myocardial damage on mice. *Medeiros et al* and *Cumashi et al* [56,69] reported that sulfated fucans from brown seaweed possess anti-inflammatory potential because inhibited phagocyte migration to the inflammation site. Additionally, a *Laminaria saccharina* fucoidan extract was shown to interact with L- and P-selectins and reduce the escape of neutrophils polymorphonuclear leucocytes (PMNs) to the abdominal cavity and the induction of acute peritonitis [69].

According to the literature, the anticoagulant activity exhibited by several fucoidan extracts may have some relation with molecular weight, sugar composition, sulfate content and position in fucose [6,35,39]. Regarding molecular weight, it was found that a sugar chain long enough to bind the thrombin is required. Thus, only fucoidan with Mw above 45 kDa would be capable of hindering blood coagulation. The anticoagulant activities of fucoidan, isolated from nine species, were tested by different authors that found that fucoidan from *Ecklonia kurome and Hijikia fusiform* exhibited the highest activity of activated partial thromboplastin time (APTT) and thromboplastin time (TT) [6,20]. Some studies reported that anticoagulant activity may be related to sugar composition [36,55]. However, uronic acid composition is not necessary for this activity but could improve the anticoagulant action by enhancing the sugar chain´s flexibility [36,95]. The position of sulfated groups on fucose residues is also important for anti-coagulation effects [6,42] . Duarte *et al.* studied that anticoagulant activity of fucoidan was mainly determined by the fucose sulfated chains, in

particular by the disulfated fucosyl units [6,42].

In the literature, *in vitro,* and *in vivo* studies propose the application of fucoidan in reducing blood glucose [76,96]. In fact, some studies shown the anti-diabetic potential of extracts and components of brown algae [96]. *Kim et al.* [76] have shown that a low molecular weight fucoidan prevented hyperglycemia in diabetic rats [97]. Furthermore, it has been referred that the lowering of blood glucose is related to inhibition of enzymes α-amylase and α-glycosidase during the digestion of carbohydrates [97,98]. In the process of digestion of a diet rich in carbohydrates, enzymes α-glycosidase and α-amylase play a vital role, and the inhibition of these enzymes would reduce the digestion of oligosaccharides and disaccharides, leading to a delay in the production of glucose. The action of fucoidan on the cited enzymes, when fully understood, can play a major role in the treatment of diabetes mellitus type I and II.

Table I-1.Summary of relevant biological activities associated with fucoidan and its potential biomedical applications.

Biological activities	Brown algae	Possible biomedical applications	Reference
Antioxidant	*E. cava* *F. evanescens* *P. gymnospora* *A. nodosum* *S. fulvellum*	Prevention of antioxidant activity, great potential for preventing free radical-mediated diseases (i.e. diabetes mellitus)	[6]
Antitumor	*U. pinnatifida* *E. cava* *F. evanescens* *L. guryanovae*	Agent for inhibition of cancer cells proliferation	[4,6]
Anti-Inflammatory	*L. japonica* *E. cava*	Inhibited leucocyte recruitment in an inflammation model	[6,11,14]
Anticoagulant	*E. cava* *F. evanescens*	Potent anticoagulant activity, mediated by antithrombin and/or heparin cofactor II	[4,6,12]

	H. fusiforme		
Anti-viral	*L. Japonica* *A. utricularis* *U. pinnatifida* *Stochoplimum*	Inhibit viral sortation so as to inhibit viral induced syncytium formation	[6,13]
Reducing blood lipids	*L. japonica* *E. stolonifera* *S. robusta* *F. vesiculosus* *E. cottonii*	Reduction of cholesterol serum	[99,100]
Anti-hyperglycemic	*E. stolonifera* *P. bagingtoni* *A. nodosum*	Help in type II diabetes mellitus	[101,102]
Antimicrobial (bacterial and fungal)	*D. humifusa* *A. orientalis* *G. acerosa* *H. species* *S. robusta*	Inhibitory and bactericidal effect against some bacterial/ fungal pathogens	[45]

I-6. COMPLEXES, COMPOSITES, AND BLENDS OF FUCOIDAN

As remarked before, the high water solubility of fucoidan hinders its processability into pure fucoidan systems [48,70,103]. In a recent study, we have demonstrated that it was possible to obtain structures of fucoidan alone using methacrylation reaction to modify the fucoidan backbone and further obtain structures using photocrosslinking technique with visible light. The study demonstrated that photocrosslinked fucoidan structures were stable in Dulbecco´s Phosphate - Buffered Saline (DPBS) until 28 days, and they were not cytotoxic for fibroblast-like cells (L929). The direct contact with L929 cells demonstrated that cells had a spindle-like shape and tended to migrate into particle core [70] **(Figure I - 5)**.

Nevertheless, in most approaches, fucoidan was combined with natural/synthetic polymers and inorganic materials, such as chitosan, polycaprolactone (PCL) or even ceramics to produce blended films [104], hydrogels [105], microparticles [70] in gels [106], microspheres [70], fibers [107], polyelectrolytes complexes, and 3D porous structures **(Figure I - 4)**. For instance, chitosan/fucoidan-based structures have been reported for use as a wound dressing and second degree-dermal burn treatments. *Sezer et al* [106] prepared a blend of fucoidan and chitosan in acidic medium yielding a hydrogel to be applied as burn injuries healing accelerator, with interesting performance demonstrated on rabbits. These researchers also studied the coating of chitosan films with fucoidan for wound dressing for dermal burn healing. The fucoidan-chitosan films caused major contraction of wounds and accelerated the closure and healing process of wounds. Nanoparticles of chitosan/fucoidan with a pH-sensitive feature to protect the drug from deterioration were investigated by *Huang et al* [108]. The authors verified that it was possible to obtain particles with a diameter of 200-300 nm at a pH 1.2, from which they proposed that it would be possible to overcome the major barriers in oral delivery, such as the low pH of the gastric medium in the stomach [105,108].

In addition to chitosan, other natural materials, namely silk fibroin, collagen, gelatin, and hyaluronic acid, have been blended with fucoidan for the production of different structures such as films and hydrogels for biomedical applications [109–111]. *Zhen Gao et al* reported a study of the incorporation of fucoidan to silk fibroin films to be used as blood-contacting biomaterials. Fucoidan incorporation increased the roughness, hydrophilicity and did not prevent the formation of beta-sheet conformation in silk. The incorporation of this sulfated polysaccharide brought excellent anticoagulant activity for silk films. These films hold the potential to be used as blood-contacting biomaterial [111]. Another natural polymer blended with fucoidan was collagen, as reported by Ramesh Perumal *et al.* The authors showed that fucoidan protected collagen against enzymatic degradation, increased the structural stability of collagen, and facilitated the proliferation of cells. The collagen-fucoidan blend films would thus allow their safe and more efficient use for various tissue regenerative applications [110]. A blend of fucoidan hyaluronic acid and gelatin was studied by H-Tsung Lu *et al* to be used as injectable hybrid hydrogels for intra-articular delivery of platelet-rich plasma. This blend shows that the addition of fucoidan and hyaluronic acid to gelatin enabled high strength, high solubility, and strong adhesive ability to the final structure. These hydrogels are also a promising biomaterial to be used in the treatment of cartilage injury [109].

In the literature, is also described the combination of fucoidan with synthetic polymers such as PCL and polyethylene oxide (PEO). PCL was blended with fucoidan using the rapid-prototyping methodology in order to provide a system with an appropriate pore structure for bone tissue regeneration. Fucoidan was used to induce not only cell proliferation but additionally influence osteoconductive properties, including alkaline phosphatase activity, collagen type I expression, and mineral deposition [112]. Instead, micro/ nanofibrous scaffolds of PCL and fucoidan have been produced by using an electrospinning process, aimed for application in bone regenerative medicine [103]. Biocomposite formed by a layer of PCL/PEO nanofibers and fucoidan for vascular grafts was also reported. This study demonstrated the nanofibers with fucoidan had a decrease in proinflammatory cytokine and chemokine production as well as inhibition of proliferation [113,114]. The physical/biological results of these studies demonstrate that the incorporation of fucoidan increased the hemocompatibility and the potential for bone regeneration [112,115,116].

A blend of fucoidan and ceramics (nano-hydroxyapatite) for bone regeneration was investigated by *Jeong et al* [105]. Hydroxyapatite-fucoidan nanocomposite was prepared by using *in situ* chemical method. The authors analyzing the bioactivity, chemical, and biological properties and concluded that nanocomposites, with fucoidan, promoted two times higher mineralization than scaffolds only with nano-hydroxyapatite, which could be promising biomaterials for bone tissue engineering.

These systems presented interesting results regarding their effectiveness in different diseases and pathological situations. As a result, different polymeric matrices such as nanoparticles/microparticles, membranes, and hydrogels have been produced for use as drug delivery devices or tissue engineering scaffolds **(Table I - 2)** [7,48,106,108,110,112,115,117–121].

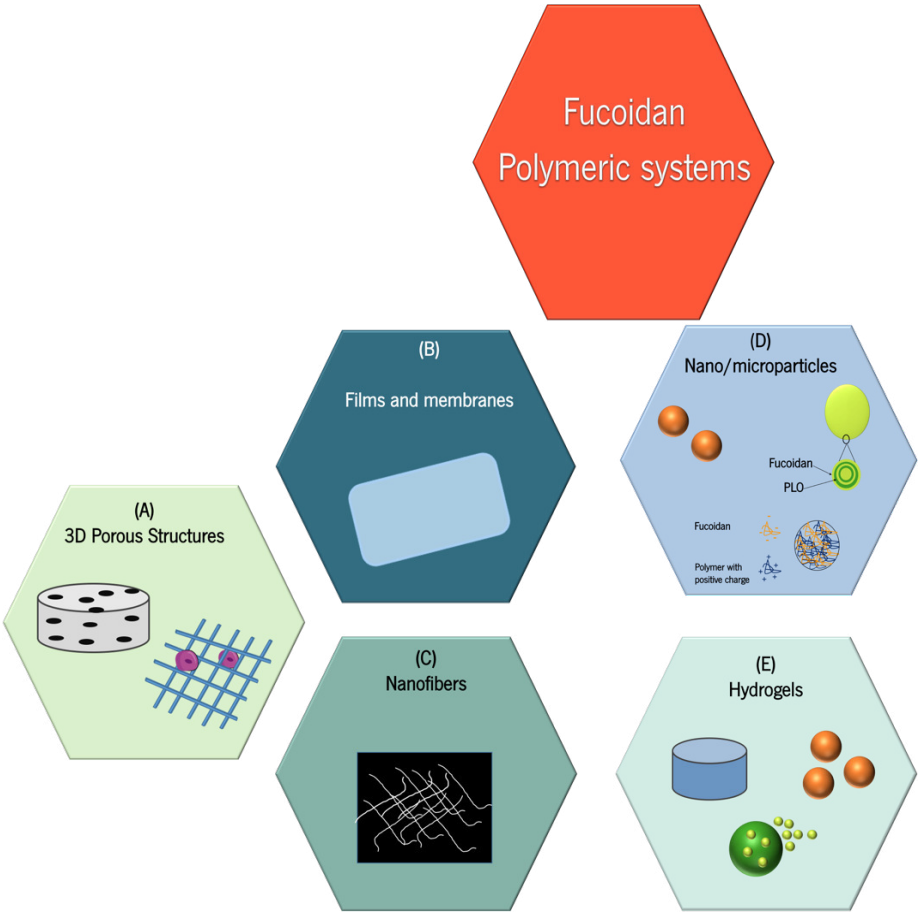


Figure I-4. Schematic illustration of fucoidan-based biomaterials : A) 3D porous structures [105,106,121–123], B) Films [108,111,115], C) Nanofibers [103] D) Nano/microparticles [70,124–127] and E) Hydrogels [70,106,109,128].

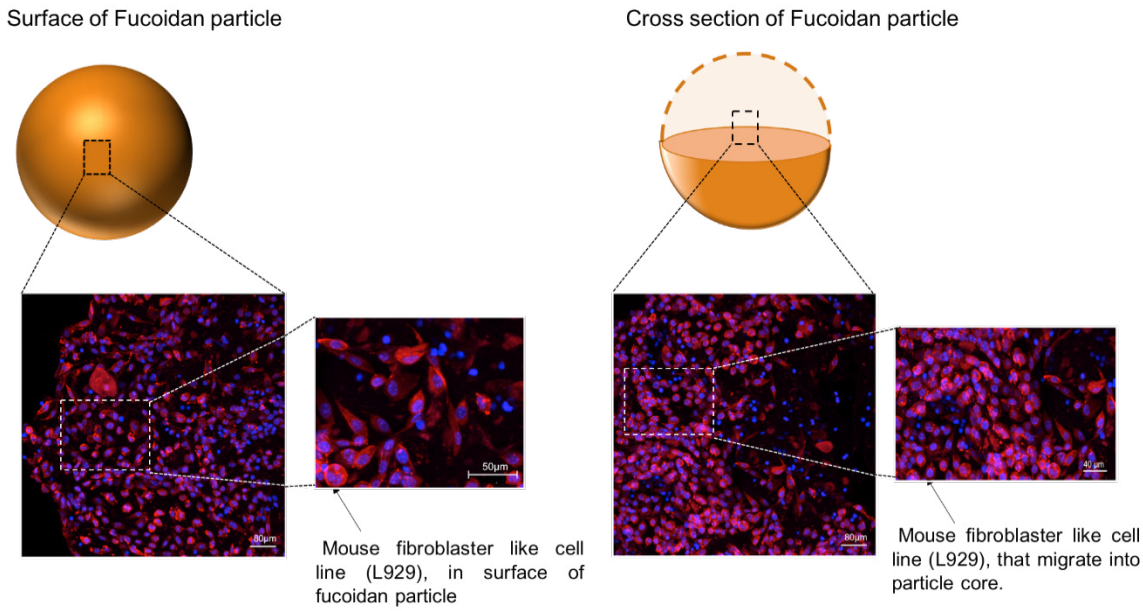


Figure I-5. Scheme of photo-crosslinked methacrylated fucoidan particles with mouse fibroblast-like cells (L929).

Table I-2.Fucoidan-based structures produced by combination with other polymers or ceramics and respective potential application in biomedicine.

Composition	Matrix type	Cell type (source/line)	Potential application	Reference
ALG/CH/CHT/Fu **ALG/CHT and Fu**	Hydrogel sheet Sponges	Human dermal fibroblast cells (DFCs) Primary human gingival fibroblast (hGFs)	Wound healing	[123,129]
CM - curdlan and FU	Nanoparticles	———	Pharmaceutical and biomedical applications	[127]
Fu/CHT	Nanoparticles	———	Oral drug delivery system	[108,130]
		Human umbilical vein endothelial (EA, Hy926) Breast cancer (MDA-MB-231)	Nanosystems for drug delivery and regenerative medicine	[124]
		Human prostate cancer cells Human dermal fibroblast cells (hDFB)	Anticancer therapy	[131]
	Hydrogel	Fibroblast	Dermal wounds	[106]

	Porous Fibers	Fibroblast	Wound Dressing	[132,133]
	Microspheres	_____	Drug release	[107]
		Fibroblast	Dermal burns	[134]
HApFu	Composites	Osteoblast cells (MG63)	Bone tissue regeneration	[135]
PCL/Fu	Micro/nanofibrous scaffolds	Osteoblast cells (MG63)	Bone tissue regeneration	[136]
	3D porous structure	Osteoblast cells (MG63)	Bone tissue regeneration	[112]
Fu/PET	Surface functionalization (Immobilization of fucoidan on surface of PET)	_____	Vascular implants with improved adhesion	[115]
		Human blood plasma	To avoid blood clot formation	[116]
Fu/PHEMA	Hydrogel	_____	Optical biofilm	[128,137]

Fu/MAA				
Fu/SF	Films	Human umbilical vein endothelial cells (HUVEC) Human endothelial cells (ECV-304)	Blood-contacting	[111]
Fu-Gel-peptide	Scaffold	Mouse pre-osteoblasts (MC3T-E1)	Bone Tissue Engineering	[138]
PVA/CHT/Fu	Bioartificial polymeric materials (BAPMs): Hydrogels, Films and scaffolds	Primary mouse embryonic fibroblast cells (NIH/3T3)	Cell regeneration	[121]
Fu/HA/Gel	Hydrogels	Human chondrocyte primary cells	Cartilage Injury: hybrid hydrogel for intra articular delivery of platelet rich plasma	[109]

Col/Fu	films	Fibroblast cell line (NiH3T3)	Tissue regenerative applications	[110]

Abbreviations: Fu (Fucoidan); **CHT** (chitosan); **Alg** (alginate), **CH** (chitin); **CM** (Carboxymethylated); **SF** (Silk fibroin); **HA** (hyaluronic acid); **PET** (Polyethylene terephalate); **Gel** (gelatin); **PCL** (polycaprolactone); **PHEMA** (Poly(2-hydroxyethyl methacrylated); **PVA** (Poly (vinyl alcohol)); HAp (Hydroxyapatite); **Col** (Collagen).

I-7. FUCOIDAN APPLICATIONS

Investigation on fucoidan has been carried out more intensively in Japan, Australia, China, and United States of America, inspired by the very significant consumption of brown algae patterns in East Asia and North America for thousands of years in different areas of application [139]. Fucoidan from different species has been used in various applications, namely on the food industry (dietetic fibers, cholesterol reducer and sports beverage), cosmetic industry (skin exfoliation, acne treatment, hair hydration, and toothpaste), agriculture (fertilizer for plants), water treatment (removal of metal ions), biofuel (using in some fuels) and biopharmaceutical (immunologic, antiviral and anticoagulant), oral health care, and animal/human biomedicine [22,93,140]. The use of fucoidan in nutraceutical and food supplements has been known since long data without known adverse effects [141]. Moreover, new formulations for health care, food supplements, and medical devices based on fucoidan have also been developed, with attention being attributed to its good biological properties and applicability in different areas. **Figure I - 6** depicts the percentages of different applications of fucoidan being proposed in the literature (according to Scopus in early 2020).

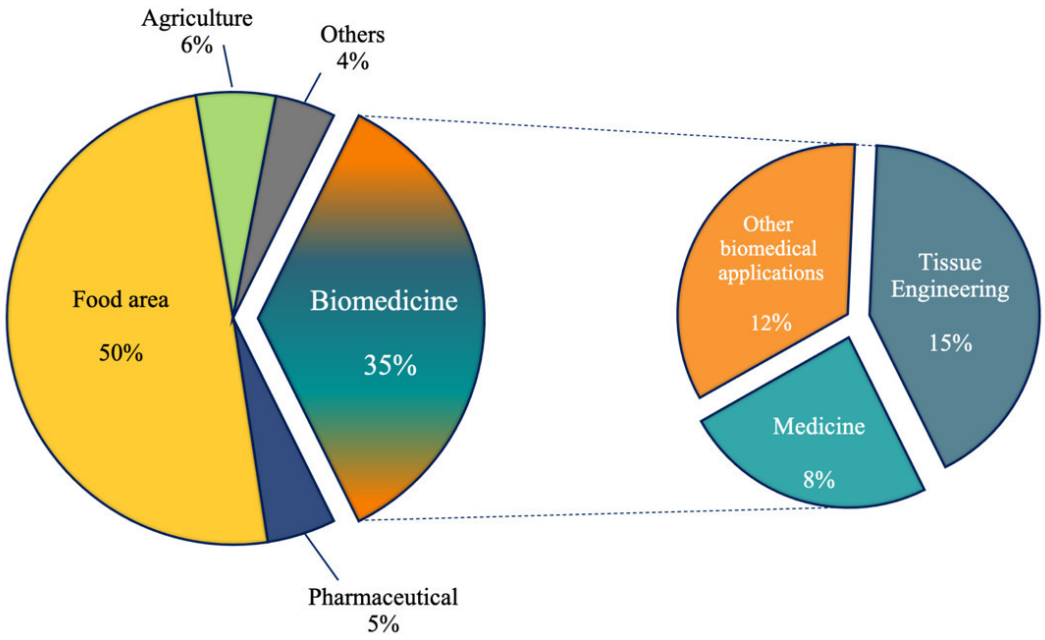


Figure I-6. Analysis of the distribution of the fucoidan in different application areas based on a literature survey (engine Scopus in early 2020). Some of the keywords used in search fucoidan: in the biomedical area, for agriculture, pharmaceutical area, and medicine/tissue engineering.

I-7.1. Biomedical/Pharmaceutical applications

The use of fucoidan in medicine as support material present advantages due to its biological and structural properties (i.e., with support role), in areas as demanding as tissue engineering and regenerative medicine [24]. In this sense, its anti-coagulant [122], anti-inflammatory [69], anti-oxidant [93,142] and antitumoral [78,93] effects, as well as potential against bacterial infections [6], has been investigated. Additionally, fucoidan has recently been shown to reduce cholesterol [100,143] and reducing blood glucose [76,144] by inhibiting α-amylase and α-glycosidase [98,145]. Thus, focus on fucoidan bioactive properties in the literature is highlighting its benefits in the treatment of some human diseases, namely: Parkinson's disease [146], tumor [124,147,148]; renal diseases [149], bone/cartilage defects [150], inflammatory pathologies [93,151] and diabetes [152,153]. Herein, the action of fucoidan over diabetes, cancer treatment, and medical devices will be discussed.

- *Diabetes treatment*

Recently, some studies focus on the use of fucoidan for the treatment of diabetes mellitus. The mechanism of fucoidan action in the treatment of diabetes disease is not well known. In the literature is reported that some chemical characteristics such as sulfate groups, the molecular weight of fucoidan, and few bioactive properties namely the antioxidant property, anti-obesity effects and inhibition of α-amylase and α-glycosidase enzymes could be the responsible for the possible use of fucoidan in diabetes treatment [6,145,153–158]. *Kim et al* demonstrated that fucoidan prevents hyperglycemia in diabetic rats, noting that glucose reduction depended on the molecular weight (Mw) of fucoidan [76]. *Sung* Sim *et al.* studied the hypothesis that fucoidan (from *Undaria pinnatifida*) could exert and anti-diabetic function by stimulating glucose uptake and decreasing basal lipolysis in adipocytes without inducing obesity [77]. The authors associated these results with the high molecular weight of fucoidan. In addition, it has also been proposed that the reduction of blood glucose is related to inhibition of enzymes α-amylase and α-glycosidase during carbohydrate digestion [98]. The action of fucoidan as an inhibitor of the mentioned enzymes can play an important role in the treatment of type I and II diabetes. In the literature, it is also published that fucoidan can help in diabetic retinopathy, a relatively common complication of diabetes [154,159]. The authors studied the effects of fucoidan in the protection of retina cells (ARPE-19 cells) damage by hyperglycemia. They concluding that fucoidan protects ARPE-19 cells against high-glucose induce oxidative damage via normalization of ROS through the Ca^{2+} - dependent ERK signaling pathway, which is associated with the antioxidant property of fucoidan [154].

- *Cancer treatment*

Over the past few years, fucoidan´s antitumoral properties have gained considerable interest. They have been tested on different cancers, such as the ability to suppress the growth of Ehrlich ascites carcinoma [160], Lewis lung adenocarcinoma [147,161,162], mammary adenocarcinoma [124,147,148] in human lymphoma [92,163], human colon cancer cells [147,164–167] and breast cancer [147,168–170]. Fucoidan´s mechanism of action in tumor therapies is still not well known. Some authors reported that

oversulfation and sulfate groups present in fucoidan could be responsible for this property [83,85,91]. In literature, it is also reported that molecular weight of fucoidan is relevant in anticancer effects, a high molecular weight is often more effective than low molecular weight [171]. However, a recent study from our group has shown the relevance of the other factors, as polymer branching and sulfation pattern [78]. According to the literature, the antitumoral potential of fucoidan revealed this inhibits tumor growth and the antimetastatic process by enhancing the immune response [172,173]. It has thus been identified antitumoral potential on fucoidan in different perspectives: inhibiting proliferation of tumor cells, stimulating the apoptosis of tumor cells, blocking tumor cells metastasis, and prevention angiogenesis, which cuts off the nutrient supply to the tumor cells [36]. In all these cases, fucoidan is being regarded as a bioactive compound or drug.

- *Medical devices and advanced therapies*

Fucoidan can also play a pivotal role in medical devices and advanced therapy medicinal products (ATMPs). In this regard, fucoidan-based structures, namely: 3D porous systems, fibers, and films based on fucoidan have been developed for cell support [103,106,112,123]. The mentioned structures can be obtained using a wide range of methodologies, such as electrospinning, rapid prototyping, and solvent casting [103,112,118]. These matrixes can be applied in bone regeneration and drug delivery [103,112]. An overview of these structures with possible applications, including drug delivery wound dressing or bone regeneration is present in **Table I - 2.** From those, we can highlight the work developed by *Jin et al* where they studied 3D porous structures of PCL/fucoidan produced using rapid prototyping technique for bone regeneration. The authors concluded that PCL/fucoidan composite scaffolds were a potential biomaterial for bone regeneration because fucoidan increased the mechanical properties and mineralization as compared with pure PCL [112]. Other authors developed 3D micro/nanofibrous structure of PCL/fucoidan or PEO/PCL fucoidan using the electrospinning process [112,114,136]. PCL/fucoidan study reported that the electrospinability can vary with the molecular weight (Mw) fraction of fucoidan. At the same time, better mechanical properties and cellular behavior of electrospun biocomposites was observed when low molecular weight fucoidan fraction was used [103]. A study of a vascular graft where fucoidan was loaded as an intermediate layer, like a sandwich

between two layers of PEO/PCL nanofibers meshes, was reported by *S. U. Kumar et al* [113,114]. Fucoidan was used as a prospective drug to overcome intimal hyperplasia *in vitro* and *in vivo*, with its use being related to stronger antithrombotic activity. The authors concluded that these grafts could be a potential solution for long term patency of small-diameter vascular graft (SDVG) with controlled and extended drug delivery. The immobilization of fucoidan in the surface of different synthetic polymers has also been proposed for different biomedical applications [113,114]. *Ozaltin et al* [116], reported the immobilization of fucoidan in PET substracts to avoid blood clot formation. The authors concluded that fucoidan was successfully immobilized and all samples presented anticoagulant activity. The interest in fucoidan has also been extended in areas such as nanomedicine [108,127] and tissue engineering [150] by combination with other polymers, as already mentioned, but also taking advantage of their biological properties, the sulfate content and the anionic character.

I-7.2. Other applications

Although biomedical applications have been elected as the focus of this review, we find appropriate to include also other applications associated with human health and well-being, ranging from food to cosmeceutical. Fucoidan is applied in the food industry due to their bioactive properties, namely: anti-obesity [174,175], anti-allergy [14], antioxidant [6,36] and anti-inflammatory [176], being thus an attractive food additive or supplement. This sulfated polysaccharide present in brown algae is widely used in Asian cuisine, is also approved by the European Medicines Agency (EMA) and the United States of America Food and Drug Administration (FDA) [177,178]. Fucoidan based products are rich in calcium, iodine, zinc, iron, selenium, and vitamin A, and these nutrients are essential for the functional properties of some systems, namely: immune, circulatory, and neurological. Some research is advancing into using fucoidan for the production of functional foods for disease prevention and health promotion, such as health beverages and processed meat products. Examples of commercial food include *Limu Seaweed blend* an energetic drink [179]; *Seaherb a* snack health food [179], and *Mekabu Wakame*, a sea vegetable [180].

In the cosmeceutical area, fucoidan is used as a natural ingredient in the development of novel cosmetic formulations as emollients and skin conditioning agents attracting increasing attention because of its reported

beneficial effects on human health [181,182]. Furthermore, some crude extracts of fucoidan also contain proteins, vitamins, and other carbohydrates. Among others, these components can regulate sebaceous gland activity, anti-inflammatory, and cicatrization properties [182,183]. Epidemiological and experimental studies have suggested that fucoidan has some important bioactive properties on skin protection, namely anti-oxidation and anti-aging, that can be applied in the cosmeceutical industry [182]. On the market, fucoidan has been used namely in some soap (*Tirzah,* a Korean fucoidan soap; *Seaza Sun Clear Essence,* a facial cleansing soap containing fucoidan) and shampoo (*RaKuten,* non-silicone fucoidan shampoo, and conditioner; *Haetobi Shampoo)*, where fucoidan increases physiological activation and strengthens hair roots and preventing alopecia.

I-8. INDUSTRIAL PROPERTY

There is an increasing number of patents focused on the different possibilities of use of fucoidan in medical, pharmaceutical, cosmetics, food, and agricultural context, as demonstrated in **Table I - 3.** The table **Table I – 3** presents an overview of the rapidly expanding areas of fucoidan research/patents including 1) extraction, identification of sugars, purification/degradation methods; 2) used as part of the composition or food supplement in the food field, and 3) absorption and bioavailability, as well as the potential of fucoidan for treatment of some diseases. Examples of successful companies which explore the potential of fucoidan include Marinova in Australia (development and production of seaweed extracts), Haerim Fucoidan in Korea (production and sales of fucoidan and other supplement materials), BioTechMarine in France (development of products for use in cosmetic and haircare with seaweed) and Irish Seaweed in Ireland (development and production of seaweed), among others.

In the coming years, is expected an increase in the number of companies and industrial property due to the large increase in the scientific activity of this polymer, fucoidan, particularly in the biomedical area.

Table I - 1.Summary of patents and patent applications related to fucoidan and its uses.

Area	Product based on/including	Application	Year	Patent/patent application number	Ref.
Methods	Fucoidan	Sulfated saccharides	2003	*US20030176395*	[183]
		Degradation of brown algae-derived fucoidan	2009	*US20090270607A1*	[184]
			2012		
		Methods for extracting fucoidan	2010	*US20100056473A1*	[38]
		Methods for fucoidan purification	2010	*US20100144667A1*	[185]
			2012	*EP253268A1*	[186]
			2014	*US20140328827A1*	[185]
				US8748595B2	
			2018	*EP3409694A1*	[187]
Cosmeceutical		Skin care	2006	*US20060210524A1*	[188]
		Hair growth/restoring agent	2000	*EP1234568B1*	[189]

		2019	*EP343173A1*	[190]
	Skin aging antipruritic agent and hair-care product	2006	*US200606093566A1*	[191]
Pharmaceutical	Agent for the treatment, prevention, inhibition of inflammatory diseases.	2011	*CN10329472A*	[192]
	Drug for preventing and/or treating diabetic cardiomyopathy	2013	*CN103288978A*	[193]
	Anti-aging formulations		*US201301151951A1*	[194]
	Anti-tumor activity	2012	*US201206515851A1*	[195]
Medicine	Preventing and treating retinopathy.	2013	*CN103239472A*	[192]
	Method and application of antidiabetic alpha-glycosidase inhibitor		*CN103288978A*	[193]
	Method for treating Thrombotic disorders.	2007	*W0200802841 0A1*	[196]
	Preparation of medicament for the treatment of cardiovascular and cerebrovascular diseases			
	Multi-particulate drug carrier systems	2005	*W0200609118 0A2*	[132]
	Enhance stem cell mobilization	2013	*US201301085871*	

			2018	*US10159705B2*	[197]
		Nanostructures for improving cell adhesion ability	2019	*US20190270883A1*	[198]
Food	Hydrolyzed fucoidan	Sport drinks	2006	*US20060210688A1*	[199]
		Baby food composition for prepared food or drink		*US20060210692A1*	[200]
		Dietary and nutritional supplements in the form of beverages, tablets, capsules and powders	2010	*US20100330211A1*	[201]

I-9. FINAL REMARKS

Fucoidan is a relatively new marine-derived polysaccharide in the context of biomedicine, mainly when compared with agar, chitosan, or even carrageenan. However, its wide range of biological activities together with chemical features make it highly promising. The source of fucoidan can be easily obtained, identified, and advantageously comparing with other molecules. However, this polysaccharide has some particular shortcomings regarding its chemical structure, purification, and biological activities. In this perspective, the time and place to collect and process brown algae and design of a novel extraction of fucoidan focused on target applications become crucial. For instance, the use of algae from aquaculture, with controlled production conditions, may reduce the batch-to-batch variability, commonly hindering the industrial exploitation of natural origin compounds. This certainly opens the way to the possibility of different areas of application, but it is also known that aquaculture conditions may result in less biologically active biomaterials. In this review, the applicability of fucoidan was discussed, bearing in mind that fucoidan demonstrates interesting properties that may justify additional research and technological developments, opening the door for future applications, particularly those related to human health. Literature is rich in reports that highlight the nature and bioactive properties of fucoidan. However, since most of the studies reported the use of fucoidan extracts, it is quite challenging to determine the relationships between structure and activity. Future studies based on the clarification of fucoidan structure should help establish a better understanding of the relation in chemical characteristics and its bioactive properties. In addition, there is relatively little information about the absorption, distribution excretion, and available regarding the chemical/biological reaction mechanisms of fucoidan. Further studies are needed to take advantage of the good properties of fucoidan for the treatment of some diseases and pathologies. Despite numerous studies on fucoidan so far, there a still few *in vivo* or trials planned or completed. However, further in-depth research is needed to understand the action mechanism for a specific type of fucoidan.

Nevertheless, the practical understanding of fucoidan is still an open field of research. if we consider fucoidan in the biomedical area, research strategies may be focused on fucoidan modified for obtaining structures of fucoidan alone, processing and material design, and cell interactions with the material to achieve successful development. It is expected a growing interest in the development of fucoidan-based structures that target the biomedical field. The positive results obtained within the academic activity with

the proposed strategies to enhance the performance of the fucoidan-structures will contribute sustaining these developments towards the establishment of new functional biomaterials.

I-10. ACKNOWLEDGMENTS

The authors especially acknowledge financial support from the Portuguese Foundation for Science FCT (Grant SFRH/BD/112139/2015), PTDC/CTM-CTM//29813/2017 with support from Fundo Social Europeu and the Programa Operacional de Potencial Humano and the research project EXPL/MAR-BIO/0165/2013, from European Union with co-funding of INTERREG POCTEP projects 0330-IBEROMARE_1_P and 0687_NOVOMAR_1_P INTERREG Espanha Portugal 2014-2020 project 0302_CVMAR_I_1_P and Atlantic Area project 2011/1/164 MARMED, through ERDF as well as from Northern Portugal Regional Operational Programme (NORTE 2020), under the Portugal 2020 Partnership Agreement, through Structured projects NORTE-01-0145-FEDER-000021 and NORTE-01-0145-FEDER-000023.

I-11. REFERENCES

[1] Blanco Sotelo, C.G. M. *Trends in food and science and technology*.Elsevier 2006. 18:19–36.

[2] Venkatesan J, Anil S, Kim S-K. *Chapter 1 - Introduction to Seaweed Polysaccharides*.In: Venkatesan J, Anil S, Kim S-KBT-SP, editors. 2017. Elsevier; 2017. p. 1–9.

[3] Silva TH, Alves A, Ferreira BM, Oliveira JM, Reys LL, Ferreira RJF, et al. *Materials of marine origin: a review on polymers and ceramics of biomedical interest*.Int Mater Rev 2012. 57(5):276–306.

[4] Silva TH, Alves A, Popa EG, Reys LL, Gomes ME, Sousa RA, et al. *Marine algae sulfated polysaccharides for tissue engineering and drug delivery approaches*.Biomatter 2012. 2(4):278–89.

[5] Hennequart Franck; Elaine O´Connell Tuohy G.Maria SJ, FranK Hennequart Jonh Spence and Maria G. Tuohy EO, Hennequart Franck; Elaine O´Connell John; Tuohy G.Maria S. *Brown Macro-algae*.Aqua Feed Beyond 2004. 1(4):14–8.

[6] Li B, Lu F, Wei X, Zhao R. *Fucoidan: Structure and bioactivity*.Molecules 2008. 13:1671–95.

[7] Ale MT, Mikkelsen JD, Meyer AS. *Important determinants for fucoidan bioactivity: A critical review of structure-function relations and extraction methods for fucose-containing sulfated polysaccharides from brown seaweeds*.Mar Drugs 2011. 9(10):2106–30.

[8] Agregán R, Munekata PES, Franco D, Carballo J, Barba FJ, Lorenzo JM. *Antioxidant Potential of*

Extracts Obtained from Macro- (Ascophyllum nodosum, Fucus vesiculosus and Bifurcaria bifurcata) and Micro-Algae (Chlorella vulgaris and Spirulina platensis) Assisted by Ultrasound.Med (Basel, Switzerland) 2018. 5(2):33.

[9] Fletcher HR, Biller P, Ross AB, Adams JMM. *The seasonal variation of fucoidan within three species of brown macroalgae*.Algal Res 2017. 22:79–86.

[10] Inácio ARM. *Fucoidan extracted from brown seaweed Bifurcaria bifurcata: seasonal variations on physicochemical features and anti-tumor activity against breast cancer cell line*.Masther Thesis, Instituto Politécnico de Leiria, Portugal; 2019.

[11] Gupta S, Abu-Ghannam N. *Bioactive potential and possible health effects of edible brown seaweeds*.Vol. 22, Trends in Food Science and Technology. 2011. p. 315–26.

[12] Mourão A., S. P. *Use of sulfated fucans as anticoagulant and antithrombotic agents: future perspectives*.Curr Pharm Des 2004. (10):967–81.

[13] Mandal P, Mateu CG, Chattopadhyay K, Pujol CA, Damonte EB, Ray B. *Structural features and antiviral activity of sulphated fucans from the brown seaweed Cystoseira indica*.Antivir Chem Chemother 2007. 18:153–62.

[14] Maruyama H, Tamauchi H, Hashimoto M, Nakano T. *Suppression of Th2 immune responses by mekabu fucoidan from Undaria pinnatifida sporophylls*.Int Arch Allergy Immunol 2005. 137:289–94.

[15] Wang A.F., SZB. *Clinic observation of fucoidan on patients with hyperlipidemia*.MedJQilu 1994. :173–4.

[16] Li Zhang,S.H. DYX. *Prevention and cure of fucoidan of L.Japonica on mice with hypercholestrolemia*.Food Sci Biotechnol 1999. 20:45–6.

[17] li Huang, L.M. ,Wang, H.B.Zhasng, S.H. DYX. *Effect of fucoidan of L.Japonica on rats with hiperlipidemia*.Food Sci 2001. 22:92–5.

[18] Jiang X, Yu J, Ma Z, Zhang H, Xie F. *Effects of fucoidan on insulin stimulation and pancreatic protection via the cAMP signaling pathway in vivo and in vitro*.Mol Med Rep 2015. 12(3):4501–7.

[19] Li Bo Wei X. and Zhao R. LF. *Fucoidan: Structure and Biactivity*.Molecules 2008. 13:1671–95.

[20] Kitamura K, Matsuo M, Yasui T. *Fucoidan from Brown Seaweed Laminaria angustata var. longissima*.Agric Biol Chem 1991. 55(2):615–6.

[21] Rodriguez-Jasso RM, Mussatto SI, Pastrana L, Aguilar CN, Teixeira JA. *Microwave-assisted extraction of sulfated polysaccharides (fucoidan) from brown seaweed*.Carbohydr Polym 2011. 86:1137–44.

[22] Fitton HJ, Stringer DS, Park AY, Karpiniec SN. *Therapies from Fucoidan: New Developments*.Mar Drugs 2019. 17(10):571.

[23] Ponce NMA, Pujol CA, Damonte EB, Flores ML, Stortz CA. *Fucoidans from the brown seaweed Adenocystis utricularis: Extraction methods, antiviral activity and structural studies*.Carbohydr Res 2003. 338:153–65.

[24] Senthilkumar K, Ramajayam G, Venkatesan J, Kim S-K, Ahn B-C. *Chapter 14 - Biomedical Applications of Fucoidan, Seaweed Polysaccharides*.In: Venkatesan J, Anil S, Kim S-KBT-SP, editors. 2017. Elsevier; 2017. p. 269–81.

[25] January GG, Naidoo RK, Kirby-McCullough B, Bauer R. *Assessing methodologies for fucoidan extraction from South African brown algae*.Algal Res 2019. 40:101517.

[26] Dobrincic A, Balbino S, Zorić Z, Sandra P, Bursać Kovačević D, Garofulić I, et al. *Advanced Technologies for the Extraction of Marine Brown Algal Polysaccharides*.Mar Drugs 2020. 18:168.

[27] Pomin VH, Valente AP, Pereira MS, Mourão PAS. *Mild acid hydrolysis of sulfated fucans: A selective 2-desulfation reaction and an alternative approach for preparing tailored sulfated oligosaccharides*.Glycobiology 2005. 15:1376–85.

[28] Balboa EM, Rivas S, Moure A, Dominguez H, Parajo JC. *Simultaneous extraction and depolymerization of fucoidan from Sargassum muticum in aqueous media*.Mar Drugs 2013. 11(11):4612–27.

[29] Hahn T, Lang S, Ulber R, Muffler K. *Novel procedures for the extraction of fucoidan from brown algae*.Vol. 47, Process Biochemistry. 2012. p. 1691–8.

[30] Ale MT, Maruyama H, Tamauchi H, Mikkelsen JD, Meyer AS. *Fucoidan from Sargassum sp. and Fucus vesiculosus reduces cell viability of lung carcinoma and melanoma cells in vitro and activates natural killer cells in mice in vivo*.Int J Biol Macromol 2011. 49:331–6.

[31] Foley SA, Szegezdi E, Mulloy B, Samali A, Tuohy MG, Foley Eva; Mulloy, Barbara; Samali, Afshin; Tuohy, Maria G. SA. S. *An Unfractionated Fucoidan from Ascophyllum nodosum: Extraction, Characterization, and Apoptotic Effects in Vitro*.J Nat Prod 2011. 74(9):1851–61.

[32] D'Ayala GG, Malinconico M, Laurienzo P. *Marine derived polysaccharides for biomedical applications: chemical modification approaches*.Molecules 2008. 13(9):2069–106.

[33] Black DEwar, E.T. Woodward, F.N. WAP. *Manuifacturing of algal chemicals 4: Laboratory scale isolation of fucoidan from brown marine algae*.J Sci Food Agric 1952. 3:122–9.

[34] Xing R, Liu S, Yu H, Chen X, Qin Y, Li K, et al. *Extraction and Separation of Fucoidan from Laminaria japonica with Chitosan as Extractant*.Biomed Res Int 2013.

[35] Ale MT, Mikkelsen JD, Meyer AS. *Designed optimization of a single-step extraction of fucose-containing sulfated polysaccharides from Sargassum sp.*J Appl Phycol 2012. 24:715–23.

[36] Wilfred Fung, Mak W, White Nazimah LH, Mak WWF, White Nazimah LH, Wilfred Fung, Mak W, White Nazimah LH. *Extraction, Characterization and Antioxidant Activity of Fucoidan from New Zealand Undaria pinnatifida (Harvey) Suringar.*Auckland University; 2012.

[37] Kawamoto H, Miki Y, Kimura T, Tanaka K, Nakagawa T, Kawamukai M, et al. *Effects of Fucoidan from Mozuku on Human Stomach Cell Lines*.Vol. 12, Food Science and Technology Research. 2006. p. 218–22.

[38] Hagiwara H, Giwara. H. *Method of extracting fucoidan*.Vol. US2010/005, Hihimsa Fondation, La Jolla, CA. United States; US20100056473A1, Publish patent, 2010.

[39] Sezer A, Cevher E. *Fucoidan: A Versatile Biopolymer for Biomedical Applications*.In: Zilberman M, editor. 2011. Springer Berlin Heidelberg; 2011. p. 377–406.

[40] Jiao GL, Yu GL, Zhang JZ, Ewart HS, Guangling Jiao Junzeng Zhang and H. Stephen Ewart GY. *Chemical Structures and Bioactivities of Sulfated Polysaccharides from Marine Algae*.Mar Drugs 2011. 9(2):196–223.

[41] Passaquet C, Thomas JC, Caron L, Hauswirth N, Puel F, Berkaloff C. *Light-harvesting complexes of brown algae. Biochemical characterization and immunological*

relationships.FEBS Lett 1991. 280:21–6.

[42] Duarte MER, Cardoso MA, Noseda MD, Cerezo AS. *Structural studies on fucoidans from the brown seaweed Sargassum stenophyllum*.Carbohydr Res 2001. 333:281–93.

[43] Tachikawa D. *Immune system Booster with Fucoidan, what is this really?*2010.

[44] Yang C, Chung D, You S. *Determination of physicochemical properties of sulphated fucans from sporophyll of Undaria pinnatifida using light scattering technique*.Food Chem 2008. 111(2):503–7.

[45] Mohamed S, Hashim SN, Rahman HA. *Seaweeds: A sustainable functional food for complementary and alternative therapy*.Trends Food Sci Technol 2012. 23(2):83–96.

[46] Nagaoka M, Shibata H, Kimura-Takagi I, Hashimoto S, Kimura K, Makino T, et al. *Structural study of fucoidan from Cladosiphon okamuranus TOKIDA*.Glycoconj J 1999. 16:19–26.

[47] Rocha HAO, Moraes FA, Trindade ES, Franco CRC, Torquato RJS, Veiga SS, et al. *Structural and hemostatic activities of a sulfated galactofucan from the brown alga Spagtoglossum schroederi: An ideal antithrombotic agent?*J Biol Chem 2005. 280:41278–88.

[48] Rioux LE, Turgeon SL, Beaulieu M. *Rheological characterisation of polysaccharides extracted from brown seaweeds*.J Sci Food Agric 2007. 87:1630–8.

[49] Zeng C, Liu Z. *Microwave extraction of polysaccharides from the traditional Chinese medicinal plant, sterculia lychnophora*.In: 2011. 2011. p. 6931–4.

[50] Ru QM, Zhang LR, Chen JD, Pei ZM, Zheng HL. *Microwave–assisted extraction and identification of polysaccharide from Lycoris aurea*.Chem Nat Compd 2009. 45(4):474.

[51] Jeon Y-J, Wijesinghe WAJP, Kim S-K. *Enzyme-assisted Extraction and Recovery of Bioactive Components from Seaweeds*.In: 2011. John Wiley & Sons, Ltd; 2011. p. 221–8.

[52] Heo S-J, Park E-J, Lee K-W, Jeon Y-J. *Antioxidant activities of enzymatic extracts from brown seaweeds*.Bioresour Technol 2005. 96(14):1613–23.

[53] Athukorala Y, Jung WK, Vasanthan T, Jeon YJ. *An anticoagulative polysaccharide from an enzymatic hydrolysate of Ecklonia cava*.Carbohydr Polym 2006. 66:184–91.

[54] Zvyagintseva TN, Shevchenko NM, Chizhov AO, Krupnova TN, Sundukova E V., Isakov V V. *Water-soluble polysaccharides of some far-eastern brown seaweeds. Distribution, structure, and their dependence on the developmental conditions*.J Exp Mar Bio Ecol 2003. 294:1–13.

[55] Nishino T, Yokoyama G, Dobashi K, Fujihara M, Nagumo T. *Isolation, purification, and characterization of fucose-containing sulfated polysaccharides from the brown seaweed Ecklonia kurome and their blood-anticoagulant activities.*Carbohydr Res 1989. 186:119–29.

[56] Leite EL, Medeiros MGL, Rocha HAO, Farias GGM, Da Silva LF, Chavante SF, et al. *Structure and pharmacological activities of a sulfated xylofucoglucuronan from the alga Spatoglossum schroederi*.Plant Sci 1998. 132:215–28.

[57] Teruya K, Kawagoe K, Kimura T, Chen CJ, Sakasegawa Y, Doh-ura K. *Amyloidophilic compounds for prion diseases*.Infect Disord Drug Targets 2009. 9(1):15–22.

[58] Yang M, Ma C, Sun J, Shao Q, Gao W, Zhang Y, et al. *Fucoidan stimulation induces a functional maturation of human monocyte-derived dendritic cells*.Int Immunopharmacol 2008. 8:1754–60.

[59] Bilan MI, Kusaykin MI, Grachev AA, Tsvetkova EA, Zvyagintseva TN, Nifantiev NE, et al. *Effect of*

enzyme preparation from the marine mollusk Littorina kurila on fucoidan from the brown alga Fucus distichus.Biochem 2005. 70:1321–6.

[60] Chizhov AO, Dell A, Morris HR, Haslam SM, McDowell RA, Shashkov AS, et al. *A study of fucoidan from the brown seaweed Chorda filum*.Carbohydr Res 1999. 320:108–19.

[61] Patankar MS, Oehninger S, Barnett T, Williams RL, Clark GF. *A revised structure for fucoidan may explain some of its biological activities*.J Biol Chem 1993. 268:21770–6.

[62] Bilan MI, Grachev AA, Ustuzhanina NE, Shashkov AS, Nifantiev NE, Usov AI. *Structure of a fucoidan from the brown seaweed Fucus evanescens C.Ag.*Carbohydr Res 2002. 337(8):719–30.

[63] Senni K, Pereira J, Gueniche F, Delbarre-Ladrat C, Sinquin C, Ratiskol J, et al. *Marine Polysaccharides: A Source of Bioactive Molecules for Cell Therapy and Tissue Engineering*.Mar Drugs 2011. 9(9):1664–81.

[64] Durig J, Bruhn T, Zurborn KH, Gutensohn K, Bruhn HD, Beress L, et al. *Anticoagulant fucoidan fractions from Fucus vesiculosus induce platelet activation in vitro*.Thromb Res 1997. 85(6):479–91.

[65] Mabeau S, Kloareg B, Joseleau J-P. *Fractionation and analysis of fucans from brown algae*.Phytochemistry 1990. 29(8):2441–5.

[66] Andrea Holtkamp D, von Andrea Désirée Holtkamp M an der R, Holtkamp AD, von Andrea Désirée Holtkamp M an der R. *Isolation, Characterisation, Modification and Application of Fucoidan from Fucus vesiculosus*.Doctoral Thesis, Universität Carolo Wilhelmina zu Braunschweig, Germany; 2009.

[67] Lahaye M. *Chemistry and physico-chemistry of phycocolloids*.Cahuers Biol Mar 2001. 42(1–2):137–57.

[68] Cosway. *SupaFuco from Cosway Malaysia*.2012 [cited 2014 Dec].

[69] Cumashi Ushakova, N. A.; Preobrazhenskaya, M. E.; D'Incecco, A.; Piccoli, A.; Totani, L.; Tinari, N.; Morozevich, G. E.; Berman, A. E.; Bilan, M. I.; Usov, A. I.; Ustyuzhanina, N. E.; Grachev, A. A.; Sanderson, C. J.; Kelly, M.; Rabinovich, G. A.; Iacobe A, Cumashi A, Ushakova NA, Preobrazhenskaya ME, D'Incecco A, Piccoli A, et al. *A comparative study of the anti-inflammatory, anticoagulant, antiangiogenic, and antiadhesive activities of nine different fucoidans from brown seaweeds*.Glycobiology 2007. 17(5):541–52.

[70] Reys LL, Silva SS, Soares da Costa D, Oliveira NM, Mano JF, Reis RL, et al. *Fucoidan Hydrogels Photo-Cross-Linked with Visible Radiation As Matrices for Cell Culture*.ACS Biomater Sci Eng 2016. 2(7):1151–61.

[71] Lim SJ, Wan Aida WM, Maskat MY, Latip J, Badri KH, Hassan O, et al. *Characterisation of fucoidan extracted from Malaysian Sargassum binderi*.Food Chem 2016. 209:267–73.

[72] Eluvakkal T, Sivakumar SR, Arunkumar K, T. Eluvakkal SRS. ALA. *Fucoidan in some indian brown seaweeds found along the coast Gulf of Mannar.*Int J Bot 2010. 78(1):7–14.

[73] Yang C, Chung D, Shin I-S, Lee H, Kim J, Lee Y, et al. *Effects of molecular weight and hydrolysis conditions on anticancer activity of fucoidans from sporophyll of Undaria pinnatifida*.Int J Biol Macromol 2008. 43(5):433–7.

[74] de Souza Marques, C.T., Dore, C.M.G., da Silva, F.R.F., Rocha, H.A. O. E.L. MCR, Rocha De Souza MC, Marques CT, Guerra Dore CM, Ferreira Da Silva FR, Oliveira Rocha HA, et al. *Antioxidant*

activities of sulfated polysaccharides from brown and red seaweeds.J Appl Phycol 2007. 19:153–60.

[75] Aisa Y, Miyakawa Y, Nakazato T, Shibata H, Saito K, Ikeda Y, et al. *Fucoidan induces apoptosis of human HS-Sultan cells accompanied by activation of caspase-3 and down-regulation of ERK pathways*.Am J Hematol 2005. 78:7–14.

[76] Kim KJ, Yoon KY, Lee BY. *Fucoidan regulate blood glucose homeostasis in C57BL/KSJ m+/+db and C57BL/KSJ db/db mice*.Fitoterapia 2012. 83:1105–9.

[77] Sim S-Y, Shin Y-E, Kim H-K. *Fucoidan from Undaria pinnatifida has anti-diabetic effects by stimulation of glucose uptake and reduction of basal lipolysis in 3T3-L1 adipocytes*.Nutr Res 2019. 65:54–62.

[78] Oliveira C, Ferreira AS, Novoa-Carballal R, Nunes C, Pashkuleva I, Neves NM, et al. *The Key Role of Sulfation and Branching on Fucoidan Antitumor Activity*.Macromol Biosci 2017. 17(5):1600340-n/a.

[79] Wang J, Zhang Q, Zhang Z, Li Z. *Antioxidant activity of sulfated polysaccharide fractions extracted from Laminaria japonica*.Int J Biol Macromol 2008. 42(2):127–32.

[80] Ruperez P, Ahrazem O, Leal JA. *Potential antioxidant capacity of sulfated polysaccharides from the edible marine brown seaweed Fucus vesiculosus*.J Agric Food Chem 2002. 50(4):840–5.

[81] Funahashi H, Imai T, Mase T, Sekiya M, Yokoi K, Hayashi H, et al. *Seaweed prevents breast cancer?*Jpn J Cancer Res 2001. 92(5):483–7.

[82] Dias PF, Siqueira JM, Vendruscolo LF, Neiva TD, Gagliardi AR, Maraschin M, et al. *Antiangiogenic and antitumoral properties of a polysaccharide isolated from the seaweed Sargassum stenophyllum*.Cancer Chemother Pharmacol 2005. 56(4):436–46.

[83] Cho ML, Lee BY, You SG. *Relationship between oversulfation and conformation of low and high molecular weight fucoidans and evaluation of their in vitro anticancer activity*.Molecules 2010. 16(1):291–7.

[84] Schepetkin IA, Quinn MT. *Botanical polysaccharides: Macrophage immunomodulation and therapeutic potential*.Vol. 6, International Immunopharmacology. 2006. p. 317–33.

[85] Alekeseyenko Zhanaayeva, S.Y., Venediktova, A.A., Zvyagintseva, T.N., Kuznetsova, T.A. Besednova, N.N. & Korolenko, T.A. T V, Alekseyenko T V., Zhanayeva SY, Venediktova AA, Zvyagintseva TN, Kuznetsova TA, et al. *Antitumor and antimetastatic activity of fucoidan, a sulfated polysaccharide isolated from the Okhotsk sea Fucus evanescens brown alga*.Bull Exp Biol Med 2007. 143(216–225):730–2.

[86] Belting M, Borsig L, Fuster MM, Brown JR, Persson L, Fransson LA, et al. *Tumor attenuation by combined heparan sulfate and polyamine depletion*.Proc Natl Acad Sci U S A 2002. 99(1):371–6.

[87] Pegg AE. *Polyamine metabolism and its importance in neoplastic growth and a target for chemotherapy*.Cancer Res 1988. 48(4):759–74.

[88] Belting M, Havsmark B, Jonsson M, Persson S, Fransson LA. *Heparan sulphate/heparin glycosaminoglycans with strong affinity for the growth-promoter spermine have high antiproliferative activity*.Glycobiology 1996. 6(2):121–9.

[89] Da, Dara AA, Walter RD. *Molecular and biochemical characterization of S-adenosylmethionine*

decarboxylase from the free-living nematode Caenorhabditis elegans.Biochem J 1998. 336(3):545.

[90] Thomas T, Thomas TJ. *Polyamines in cell growth and cell death: molecular mechanisms and therapeutic applications*.Cell Mol Life Sci 2001. 58(2):244–58.

[91] Morya VK, Kim J, Kim EK. *Algal fucoidan: Structural and size-dependent bioactivities and their perspectives*.Vol. 93, Applied Microbiology and Biotechnology. 2012. p. 71–82.

[92] Atashrazm F, Lowenthal RM, Woods GM, Holloway AF, Dickinson JL. *Fucoidan and cancer: a multifunctional molecule with anti-tumor potential*.Mar Drugs 2015. 13(4):2327–46.

[93] Wang Y, Xing M, Cao Q, Ji A, Liang H, Song S. *Biological Activities of Fucoidan and the Factors Mediating Its Therapeutic Effects: A Review of Recent Studies*.Mar Drugs 2019. 17(3):183.

[94] Li F, Tian T, Shi Y, Liu Y, Zhang S, Fan L, et al. *Study on anti-virus effect of fucoidan in vitro*.Baiqiuen Yike Daxue Xuebao 1995. 21(3):255–7.

[95] Li B, Zhao R-X, Wei X-J. *Anticoagulant activity of fucoidan from Hizikia fusiforme*.Agro Food Ind Hi Tech 2008. 19:22–4.

[96] Hang Wang ZF and CH, Wang H, Fu Z, Han C. *The Potential Applications of Marine Bioactives Against Diabetes and Obesity*.Am J Mar Sci 2014. 2(1):1–8.

[97] Kim KT, Rioux LE, Turgeon SL. *Alpha-amylase and alpha-glucosidase inhibition is differentially modulated by fucoidan obtained from Fucus vesiculosus and Ascophyllum nodosum*.Phytochemistry 2014. 98:27–33.

[98] Ali H, Houghton PJ, Soumyanath A. *α-Amylase inhibitory activity of some Malaysian plants used to treat diabetes; with particular reference to Phyllanthus amarus*.J Ethnopharmacol 2006. 107(3):449–55.

[99] Li Bo Wei X. and Zhao R. LF, Li Lu, F.; Wei X., and Zhao, R. B, Li Bo Wei X. and Zhao R. LF, Li B, Lu F., Wei X., et al. *Fucoidan: Structure and Biactivity*.Molecules 2008. 13:1671–95.

[100] Huang L, Wen K, Gao X, Liu Y. *Hypolipidemic effect of fucoidan from Laminaria japonica in hyperlipidemic rats*.Pharm Biol 2010. 48(4):422–6.

[101] Shan X, Liu X, Hao J, Cai C, Fan F, Dun Y, et al. *In vitro and in vivo hypoglycemic effects of brown algal fucoidans*.Int J Biol Macromol 2016. 82:249–55.

[102] Pozharitskaya ON, Obluchinskaya ED, Shikov AN. *Mechanisms of Bioactivities of Fucoidan from the Brown Seaweed Fucus vesiculosus L. of the Barents Sea*.Mar Drugs 2020. 18(5).

[103] Ji Seok Lee Myung Gu Yeo, Chul Ho Jang, Haeongnam Lee, Geun Hyung Kim GHJ, Lee JS, Jin GH, Yeo MG, Jang CH, Lee H, et al. *Fabrication of electrospun biocomposites comprising polycaprolactone/fucoidan for tissue regeneration*.Carbohydr Polym 2012. 90:181–8.

[104] Liu H, Li X, Zhou G, Fan H, Fan Y. *Electrospun sulfated silk fibroin nanofibrous scaffolds for vascular tissue engineering*.Biomaterials 2011. 32:3784–93.

[105] Jeong H-SS, Venkatesan J, Kim S-K, Jeong Venkatesan; Jayachandran; Kim, Se-Kwon H-S, Jeong H-SS, Venkatesan J, et al. *Hydroxyapatite-fucoidan nanocomposites for bone tissue engineering*.Int J Biol Macromol 2013. 57(0):138–41.

[106] Sezer AD, Cevher E, Hatıpoğlu F, Oğurtan Z, Baş AL, Akbuğa J, et al. *Preparation of Fucoidan-Chitosan Hydrogel and Its Application as Burn Healing Accelerator on Rabbits*.Biol Pharm Bull

2008. 31(12):2326–33.

[107] SEZER AD& JA, Akbuga J. *Fucosphere—New microsphere carriers for peptide and protein delivery: Preparation and in vitro characterization*.J Microencapsul 2006. 23(5):513–22.

[108] Huang Lam, U. Ian, Y-C, Huang Y-C, Lam UI. *Chitosan/Fucoidan pH Sensitive Nanoparticles for Oral Delivery System*.J Chinese Chem Soc 2011. 58(6):779–85.

[109] Lu, Chang, Tsai, Chen Q, Mi. *Development of Injectable Fucoidan and Biological Macromolecules Hybrid Hydrogels for Intra-Articular Delivery of Platelet-Rich Plasma*.Mar Drugs 2019. 17:236.

[110] Perumal RK, Perumal S, Thangam R, Gopinath A, Ramadass satiesh kumar, Madhan B, et al. *Collagen-fucoidan blend film with the potential to induce fibroblast proliferation for regenerative applications*.Int J Biol Macromol 2018. 106:1032–40.

[111] Gao Z, Wang S, Zhu H, Zhao D, Xu J. *Improvements of anticoagulant activities of silk fibroin films with fucoidan*.Front Mater Sci China 2008. 2(2):221–7.

[112] Kim GJ and GH, Gyuhyun Hyung, Kim; JG. *Rapid-prototyped PCL/fucoidan composite scaffolds for bone tissue regeneration: design, fabrication, and physical/biological properties*.J Mater Chem 2011. 21(1):17710–8.

[113] Mishra NC, Kumar SU, Jayaganthan R. *Fucoidan Loaded PCL-PEO Nanofibrous Scaffold for Small Diameter Vascular Graft - a Solution to Intimal Hyperplasia*.In: 2012. 2012.

[114] S. Uday Kumar, Kumar U. *Electrospun fucoidan loaded PCL/PEO nanofiber scaffolds for small diameter vascular grafts*.Masther Thesis, Indian Institute of Technology Roorkee, India; 2012.

[115] Vesel A, Mozetic M, Strnad S. *Improvement of adhesion of fucoidan on polyethylene terephthalate surface using gas plasma treatments*.In: 2011. 2011. p. 1083–6.

[116] Ozaltin K, Lehocký M, Humpolíček P, Pelkova J, Di martino A, Karakurt I, et al. *Anticoagulant Polyethylene Terephthalate Surface by Plasma-Mediated Fucoidan Immobilization*.Polymers (Basel) 2019. 11:750.

[117] Huang GY, Zhou LH, Zhang QC, Chen YM, Sun W, Xu F, et al. *Microfluidic hydrogels for tissue engineering*.Biofabrication 2011. 3:012001.

[118] Cheng Z, Wang S, Zhu H, Cheng S.; Zhu, H. Z. W, Cheng Z, Wang S, et al. *Structural and thermal characteristics of silk fibroin/fucoidan blend films*.Acta Polym Sin 2004. (3):446–9.

[119] Holtkamp AD, Kelly S, Ulber R, Lang S. *Fucoidans and fucoidanases–focus on techniques for molecular structure elucidation and modification of marine polysaccharides*.Appl Microbiol Biotechnol 2009. 82(1):1–11.

[120] Nakamura S, Nambu M, Ishizuka T, Hattori H, Kanatani Y, Takase B, et al. *Effect of controlled release of fibroblast growth factor-2 from chitosan/fucoidan micro complex-hydrogel on in vitro and in vivo vascularization*.J Biomed Mater Res - Part A 2008. 85:619–27.

[121] Bernal-Ballen A, Lopez-Garcia J-A, Ozaltin K. *(PVA/Chitosan/Fucoidan)-Ampicillin: A Bioartificial Polymeric Material with Combined Properties in Cell Regeneration and Potential Antibacterial Features*.Polymers (Basel) 2019. 11(8):1325.

[122] Kuznetsova TA, Besednova NN, Mamaev AN, Momot AP, Shevchenko NM, Zvyagintseva TN. *Anticoagulant activity of fucoidan from brown algae Fucus evanescens of the Okhotsk Sea*.Bull Exp Biol Med 2003. 136:471–3.

[123] Murakami K, Aoki H, Nakamura S ichiro, Nakamura S ichiro, Takikawa M, Hanzawa M, et al. *Hydrogel blends of chitin/chitosan, fucoidan and alginate as healing-impaired wound dressings*.Biomaterials 2010. 31(1):83–90.

[124] Oliveira C, Neves NM, Reis RL, Martins A, Silva TH. *Gemcitabine delivered by fucoidan/chitosan nanoparticles presents increased toxicity over human breast cancer cells*.Nanomedicine 2018. 13(16):2037–50.

[125] Fan J, Liu Y, Wang S, Liu Y, Li S, Long R, et al. *Synthesis and characterization of innovative poly(lactide-co-glycolide)-(poly-L-ornithine/fucoidan) core–shell nanocarriers by layer-by-layer self-assembly*.RSC Adv 2017. 7:32786.

[126] Nindo C, Powers J, Tang J. *Thermal properties of Aloe vera powder and rheology of reconstituted gels*.Trans ASABE 2011. 53:1193–200.

[127] Leung TCY, Wong CK, Xie Y. *Green synthesis of silver nanoparticles using biopolymers, carboxymethylated-curdlan and fucoidan*.Mater Chem Phys 2010. 121(3):402–5.

[128] Lee HM, Kim J-K, Cho T-S. *Applications of ophthalmic biomaterials embedded with fucoidan*.J Ind Eng Chem 2012. 18(4):1197–201.

[129] Hao Y, Zhao W, Zhang L, Zeng X, Sun Z, Zhang D, et al. *Bio-multifunctional alginate/chitosan/fucoidan sponges with enhanced angiogenesis and hair follicle regeneration for promoting full-thickness wound healing*.Mater Des 2020. 193:108863.

[130] Eun Ju Lee SAK and AKHL. *Chitosan-Nanoparticle preparation polyelectrilyte complexation*.Vol. 2017. wjoe.hebeu.edu.cn.; 2012.

[131] Choi DG, Venkatesan J, Shim MS. *Selective Anticancer Therapy Using Pro-Oxidant Drug-Loaded Chitosan-Fucoidan Nanoparticles*.Int J Mol Sci 2019. 20(13):3220.

[132] Sezer AD. *Fucoidan multiparticulate drug carrier systems*.Vol. WO20060911. WIPO; WO2006091180A2, 2006.

[133] Sezer AD, Hatipoğlu F, Cevher E, Oğurtan Z, Baş AL, Akbuğa J. *Chitosan film containing fucoidan as a wound dressing for dermal burn healing: preparation and in vitro/in vivo evaluation*.AAPS PharmSciTech 2007. 8:Article 39.

[134] Sezer AD, Cevher E, Hatipoğlu F, Oğurtan Z, Baş AL, Akbuğa J. *The use of fucosphere in the treatment of dermal burns in rabbits*.Eur J Pharm Biopharm 2008. 69(1):189–98.

[135] Jeong HS, Venkatesan J, Kim S-K. *Hydroxyapatite-fucoidan nanocomposites for bone tissue engineering*.Int J Biol Macromol 2013. 57(0):138–41.

[136] Lee JS, Jin GH, Yeo MG, Jang CH, Lee H, Kim GH. *Fabrication of electrospun biocomposites comprising polycaprolactone/ fucoidan for tissue regeneration*.Carbohydr Polym 2012. 90:181–8.

[137] Lira MCB, Santos-Magalhães NS, Nicolas V, Marsaud V, Silva MPC, Ponchel G, et al. *Cytotoxicity and cellular uptake of newly synthesized fucoidan-coated nanoparticles*.Eur J Pharm Biopharm 2011. 79:162–70.

[138] Pajovich HT, Banerjee IA. *Biomineralization of Fucoidan-Peptide Blends and Their Potential Applications in Bone Tissue Regeneration*.J Funct Biomater 2017. 8(3):41.

[139] Wells ML, Potin P, Craigie JS, Raven JA, Merchant SS, Helliwell KE, et al. *Algae as nutritional and functional food sources: revisiting our understanding*.J Appl Phycol 2017. 29(2):949–82.

[140] Courtois J. *Oligosaccharides from land plants and algae: production and applications in therapeutics and biotechnology*.Vol. 12, Current Opinion in Microbiology. 2009. p. 261–73.

[141] Choi J il, Raghavendran HRB, Sung NY, Kim JH, Chun BS, Ahn DH, et al. *Effect of fucoidan on aspirin-induced stomach ulceration in rats*.Chem Biol Interact 2010. 183:249–54.

[142] Magalhaes KD, Costa LS, Fidelis GP, Oliveira RM, Nobre LTDB, Dantas-Santos N, et al. *Anticoagulant, antioxidant and antitumor activities of heterofucans from the seaweed dictyopteris delicatula*.Int J Mol Sci 2011. 12:3352–65.

[143] Yang Z, Liu G, Wang Y, Yin J, Wang J, Xia B, et al. *Fucoidan A2 from the Brown Seaweed Ascophyllum nodosum Lowers Lipid by Improving Reverse Cholesterol Transport in C57BL/6J Mice Fed a High-Fat Diet*.J Agric Food Chem 2019. 67(20):5782–91.

[144] Vinoth Kumar T, Lakshmanasenthil S, Geetharamani D, Marudhupandi T, Suja G, Suganya P. *Fucoidan – A α-d-glucosidase inhibitor from Sargassum wightii with relevance to type 2 diabetes mellitus therapy*.Int J Biol Macromol 2015. 72:1044–7.

[145] Kim K-T, Rioux L-E, Turgeon SL. *Alpha-amylase and alpha-glucosidase inhibition is differentially modulated by fucoidan obtained from Fucus vesiculosus and Ascophyllum nodosum*.Phytochemistry 2014. 98:27–33.

[146] Zhang L, Hao J, Zheng Y, Su R, Liao Y, Gong X, et al. *Fucoidan Protects Dopaminergic Neurons by Enhancing the Mitochondrial Function in a Rotenone-induced Rat Model of Parkinson's Disease*.Aging Dis 2018. 9(4):590–604.

[147] Oliveira C, Neves NM, Reis RL, Martins A, Silva TH. *A review on fucoidan antitumor strategies: from a biological active agent to a structural component of fucoidan-based systems*.Carbohydr Polym 2020. :116131.

[148] Oliveira C, Granja S, Neves NM, Reis RL, Baltazar F, Silva TH, et al. *Fucoidan from Fucus vesiculosus inhibits new blood vessel formation and breast tumor growth in vivo*.Carbohydr Polym 2019. 223:115034.

[149] Wang J, Geng L, Yue Y, Zhang Q. *Chapter Six - Use of fucoidan to treat renal diseases: A review of 15 years of clinic studies*.In: Zhang LBT-P in MB and TS, editor. 2019. Academic Press; 2019. p. 95–111.

[150] Venkatesan J, Anil S, Rao S, Kim S-K. *Macroalgal Fucoidan for biomedical applications*.In: Ravishankar CA, Rao AR, editors. 2019. 2019. p. 13–24.

[151] Lean QY, Eri RD, Fitton JH, Patel RP, Gueven N. *Fucoidan Extracts Ameliorate Acute Colitis*.PLoS One 2015. 10(6):e0128453–e0128453.

[152] Kim K-J, Lee O-H, Lee H-C, Kim Y-C, Lee B-Y. *Effect of fucoidan on expression of diabetes mellitus related genes in mouse adipocytes*.Food Sci Biotechnol 2007. 16:212–7.

[153] Mukhamejanov E, Kon G, Erjanova S, Kirgizbaeva A, Muhamadieva E. *Fucoidan—New Principle Prevention and Treatment of Diabetes*.J Pharm Pharmacol 2019. 7.

[154] Li X, Zhao H, Wang Q, Liang H, Jiang X. *Fucoidan protects ARPE-19 cells from oxidative stress via normalization of reactive oxygen species generation through the Ca(2)(+)-dependent ERK signaling pathway*.Mol Med Rep 2015. 11(5):3746–52.

[155] Kim K-T, Rioux L-E, Turgeon SL. *Molecular weight and sulfate content modulate the inhibition of α-amylase by fucoidan relevant for type 2 diabetes management*.PharmaNutrition 2015.

3(3):108–14.

[156] Kim KJ, Lee OH, Lee BY. *Fucoidan, a sulfated polysaccharide, inhibits adipogenesis through the mitogen-activated protein kinase pathway in 3T3-L1 preadipocytes*.Life Sci 2010. 86:791–7.

[157] Kim MJ, Jeon J, Lee JS. *Fucoidan prevents high-fat diet-induced obesity in animals by suppression of fat accumulation*.Phyther Res 2014. 28:137–43.

[158] Han YR, Ali MY, Woo M-H, Jung HA, Choi JS. *Anti-Diabetic and Anti-Inflammatory Potential of the Edible Brown Alga Hizikia Fusiformis*.J Food Biochem 2015. 39(4):417–28.

[159] Klettner A. *Fucoidan as a Potential Therapeutic for Major Blinding Diseases–A Hypothesis*.Mar Drugs 2016. 14(2):31.

[160] Itoh H Amano H, Zhuaug C, Mizuno T, Ito H NH. *Antitumor activity and immunological properties of marine algal polysaccharides, especially fucoidan, prepared from Sargassum thunbergii of Phaeophyceae.*Anticancer Res 1993. 13(6A):2045-2052.

[161] Marudhupandi T, Kumar TTA, Lakshmanasenthil S, Suja G, Vinothkumar T. *In vitro anticancer activity of fucoidan from Turbinaria conoides against A549 cell lines*.Int J Biol Macromol 2015. 72:919–23.

[162] Lee H, Kim J-SS, Kim E. *Fucoidan from Seaweed Fucus vesiculosus Inhibits Migration and Invasion of Human Lung Cancer Cell via PI3K-Akt-mTOR Pathways*.PLoS One 2012. 7(11):1–10.

[163] Yang G, Zhang Q, Kong Y, Xie B, Gao M, Tao Y, et al. *Antitumor activity of fucoidan against diffuse large B cell lymphoma in vitro and in vivo*.Acta Biochim Biophys Sin (Shanghai) 2015. 47(11):925–31.

[164] Azuma K, Ishihara T, Nakamoto H, Amaha T, Osaki T, Tsuka T, et al. *Effects of oral administration of fucoidan extracted from Cladosiphon okamuranus on tumor growth and survival time in a tumor-bearing mouse model*.Mar Drugs 2012. 10(10):2337–48.

[165] Usoltseva R V, Anastyuk SD, Surits V V, Shevchenko NM, Thinh PD, Zadorozhny PA, et al. *Comparison of structure and in vitro anticancer activity of native and modified fucoidans from Sargassum feldmannii and S. duplicatum*.Int J Biol Macromol 2019. 124:220–8.

[166] Han Y-S, Lee JH, Lee SH. *Antitumor Effects of Fucoidan on Human Colon Cancer Cells via Activation of Akt Signaling*.Biomol Ther (Seoul) 2015. 23(3):225–32.

[167] Han Y-S, Lee JH, Lee SH. *Fucoidan inhibits the migration and proliferation of HT-29 human colon cancer cells via the phosphoinositide-3 kinase/Akt/mechanistic target of rapamycin pathways*.Mol Med Rep 2015. 12(3):3446–52.

[168] ZHANG Z, TERUYA K, ETO H, SHIRAHATA S. *Induction of Apoptosis by Low-Molecular-Weight Fucoidan through Calcium- and Caspase-Dependent Mitochondrial Pathways in MDA-MB-231 Breast Cancer Cells*.Biosci Biotechnol Biochem 2013. 77(2):235–42.

[169] Lu J, Shi KK, Chen S, Wang J, Hassouna A, White LN, et al. *Fucoidan Extracted from the New Zealand Undaria pinnatifida-Physicochemical Comparison against Five Other Fucoidans: Unique Low Molecular Weight Fraction Bioactivity in Breast Cancer Cell Lines*.Mar Drugs 2018. 16(12):461.

[170] He X, Xue M, Jiang S, Li W, Yu J, Xiang S. *Fucoidan Promotes Apoptosis and Inhibits EMT of Breast Cancer Cells*.Biol Pharm Bull 2019. 42:442–7.

[171] van Weelden G, Bobiński M, Okła K, van Weelden WJ, Romano A, Pijnenborg JMA. *Fucoidan*

Structure and Activity in Relation to Anti-Cancer Mechanisms.Mar Drugs 2019. 17(1):32.

[172] Zorofchian Moghadamtousi S, Karimian H, Khanabdali R, Razavi M, Firoozinia M, Zandi K, et al. *Anticancer and antitumor potential of fucoidan and fucoxanthin, two main metabolites isolated from brown algae*.Vol. 2014, The Scientific World Journal. 2014.

[173] Oh B, Kim J, Lu W, Rosenthal D. *Anticancer Effect of Fucoidan in Combination with Tyrosine Kinase Inhibitor Lapatinib*.Tian M, editor. Evidence-Based Complement Altern Med 2014. 2014:865375.

[174] Park MK, Jung U, Roh C. *Fucoidan from marine brown algae inhibits lipid accumulation*.Mar Drugs 2011. 9(8):1359–67.

[175] Kim M-J, Park M, Jeong MK, Yeo J, Cho W-I, Chang P-S, et al. *Radical scavenging activity and anti-obesity effects in 3T3-L1 preadipocyte differentiation of Ssuk (Artemisia princeps Pamp.) extract*.Food Sci Biotechnol 2010. 19(2):535–40.

[176] Li B, Wei XJ, Sun JL, Xu SY. *Structural investigation of a fucoidan containing a fucose-free core from the brown seaweed, Hizikia fusiforme*.Carbohydr Res 2006. 341:1135–46.

[177] *European Medicine agency*.(www.ema.europa.eu). [cited 2020 May].

[178] *FDA U.S. Food & Drug administration*.(www.fda.gov). [cited 2020 May].

[179] *Seaherb fucoidan and pure skin*.(www.seaherb.com). [cited 2016 Aug].

[180] *Mekabu, Wakame Spotophyll, food*.(www.muso-intl.com). [cited 2019 Nov].

[181] Witvrouw M, De Clercq E. *Sulfated polysaccharides extracted from sea algae as potential antiviral drugs*.Gen Pharmacol 1997. 29(4):497–511.

[182] Kim S-K, Ravichandran YD, Khan SB, Kim YT. *Prospective of the cosmeceuticals derived from marine organisms*.Biotechnol Bioprocess Eng 2008. 13(5):511–23.

[183] Katsushige Ikai Ikunoshin Kato, Hitomi Kimura, Takeshi Sakai, Kazuo Shimanaka. KK. *Sulfated saccharides*.Vol. CA2307868A. United States; US20030176395 A1, Published patent (status: Abandoned), 2003.

[184] Oh KD. *Degradation of brown algae-derived fucoidan*.United States; US20090270607A1, Published patent, (status: Active), 2009.

[185] Shaklee PN, Bahr-Davidson J, Prasad S, Johnson K. *Methods for fucoidan purification from sea weed extracts*.United States; US8748595B2, 2014.

[186] Shaklee PN, Bahr-Davidson J, Prasad S, Johnson K. *Process methods for fucoidan purification from seaweed extracts*.PCT Int. Appl. European Patent; EP2532686A1, Published patent (status:active), 2012. p. 45pp.

[187] Springate CMK. *Pharmaceutical compositions comprising modified fucans for use in the treatment of fibrous adhesions and other disorders*.European patent; EP2459200A1, Published patent , (satus:Ceased), 2018.

[188] Mower TE. *Skin care composition*.United States; US20060210524A1, Published patent, (status: Abandoned), 2006.

[189] Shigetoshi Mizutani Eiji Kobayashi, Edishiyama, Hiroaki Sagawa, Ikunoshin Kato SD. *Use of fucoidan as effective hair restoring ingredient*.Vol. CN1433295A. European Patent; EP1234568B1, Published patent, (status: Expired-Fee Related), 2008.

[190] Quan Y, Yamashita H, Kamiyama F, Yamamoto A. *Fucoidan hair growth agent*.European Patent; EP3431073, Published patent (satus:pending), 2019.

[191] Shigetoshi Mizutani Eiji Kobayashi, Edishiyama, Hiroaki Sagawa, Ikunoshin Kato SD. *Fucoidan-conating cosmetics*.United States; US20060093566A1, Published patent, (status:Expired-Fee Related), 2006.

[192] Dali L, Wenzhe Y, Wentong C, Quanbin Z. *Novel medicianl application of fucoidan polysaccharide sulfate*.Vol. CN10320947. China; CN103239472A, Publish patent, (status: active), 2013.

[193] Guangli Y, Jiejie H, Xin L, Xiaoliang Z, Guangling J. *Fucosan sulphate and preparation method and application there of in preparation of antidiabetic alpha-glycosidase inhibitor*.Vol. CN10328897. China; CN103288978A, Published patent (status:active), 2013.

[194] Cappello J V. *Anti-aging Formulations*.Vol. W201300115. United States; US20130115195A1, Published patent, (status: active), 2013.

[195] Okamoto Y, Minami S, Tsuka T, Miki Y. *Fucoidan having antitumor activity*.United States; US20120065158A1, Published patent, (status:Abandoned), 2012.

[196] Hao S. *Use of low moleculaer weight fucoidan in the preparation of medicament for the treatment of cardiovascular and cerbrovascular diseases*.Vol. WO20080284. WIPO; WO2008028410A1, Published patent, (status: Active), 2008.

[197] Drapeau C, Jensen GS. *Methods and compositions for enhancing stem cell mobilization*.United State; US20130108587A1, Published patent, (status:active), 2018.

[198] KWAK JY, Kim JM, Park YJ, Park DB, Jeong YH, Kim JH. *Method of manufacturing nanostructure with improved cell adhesive ability containing fucoidan and nanostructure with improved cell adhesive ability containing fucoidan manufactured thereby*.United State; US20190270883A1, Published patent, (status:pending), 2019.

[199] Mower TE. *Dehydratation sports drink power*.United States; US20060210688A1, Published patent, (status:Abandoned), 2006.

[200] Mower TE. *Baby food composition*.United States: Google Patents; US2006210692A1, 2006.

[201] Mower TE. *Fucoidan compositions and methods for dietary and nutritional supplements*.United States; US20100330211A1, Published patent, (status: Abandoned), 2010.

Chapter II

Biomaterials - based therapies against Diabetes

Chapter II

Biomaterials-based therapies against diabetes

ABSTRACT

Worldwide, chronic diseases such as diabetes mellitus have become a major public health problem. Diabetes mellitus (DM) is a metabolic disorder caused by inherited and/or acquired deficiency in the production of insulin by the pancreas. There are mainly two types: Type I - insulin-dependent, in which pancreatic insulin-producing β-cells are destroyed by an autoimmune reaction, and Type II - non-insulin-dependent, in which although the patients have a functional pancreas capable of producing insulin, their cells are resistant to this hormone. Different therapeutic strategies have been designed, from insulin injection,β-cells replacement therapies, including whole pancreas transplantation and islet cell transplantation, delivery systems (polymeric, lipid and porous based), including their clinically for such patients. Biomaterials can give a valuable contribute to the research, aiming to develop new therapeutic strategies and models to drive developments in drug discovery and to diminish reliance on cadaveric islets. Herein, a panoply of materials and current strategies that have been used in diabetes mellitus treatment are overviewed.

Keywords: Diabetes mellitus, type I diabetes, type II diabetes, islet of Langerhans, islet transplantation, insulin, micro/macro complications, biomaterials.

GENERAL INTRODUCTION

II-1. DIABETES MELLITUS

Diabetes mellitus (DM) is a chronic disease with a dramatic consequence in patients' life, being the sixth most common cause of death worldwide and one of the most critical healthcare emergencies of the 21th century. The number of people affected by diabetes went from 108 million in 1980 to 422 million adults in 2014 and may reach 642 million in 2040 [1,2], with approximately 5% accounting for type 1 diabetes, and 95% for type 2 diabetes [3,4]. The problem is also increased by the progressive aging of the worldwide population, which will be responsible for a further increase in the diabetes prevalence in the coming years.

The term diabetes mellitus (DM) is derived from the Greek word *diabetes*, meaning 'to pass through a siphon' and the Latin word *Mellitus*, meaning 'honeyed' or 'sweet', referring to the abnormally high levels of glucose in the blood and urine of diabetes patients. DM is a metabolic disorder characterized by high levels of glucose in the blood caused by insufficient production of or resistance to, insulin which is produced by beta cells (β cells) within the pancreatic islets **(Figure II-1)** [5–7]. Patients who suffer from DM have symptoms like excessive thirst, frequent urination, malnourishment, weight loss, and fatigue [8,9]. Aetiologically, diabetes can be subdivided into different types: type I, type II, and gestational diabetes [10,11]. Type I DM (T1D) is characterized by an absolute deficiency in the production of insulin by the pancreas, which is the result of autoimmune destruction of the insulin-producing cells (β cells) in most cases. As insulin is the hormone promoting the uptake of glucose by cells, when the β-cells are destroyed, the blood glucose levels cannot be lowered, resulting in hyperglycemia. This condition can become very dangerous when glucose accumulates and damages small vessels like capillaries in the eyes, nerves, and kidneys. It could also lead to strokes and heart attacks, making T1D a deadly disease if not treated properly [4,12]. People who suffer from this autoimmunity are genetically predisposed to the disease, which may be caused by environmental factors (i.e., microbial, chemical, dietary). Without insulin treatment, T1D patients are exposed to the risk of death from acute ketoacidosis [8]. Type II DM (T2D) is characterized by the ineffectiveness of the insulin produced or insulin resistance, which is caused by several factors. The risk for the development of T2D is strongly familial, but the pathogenesis is mainly associated with increasing age, unhealthy diets, obesity, and a sedentary lifestyle, which explains why the mainstay of both treatment and prevention of T2D is dieting and physical activity. T1D is much less abundant than T2D, and accounts for approximately 5% of all diabetes cases worldwide. The higher

morbidity, the severity of the symptoms, and the drastic impact on the life quality of the patients are the main reasons for the research increases on diabetes type I (T1D) instead of diabetes type II (T2D). Besides, there is also gestational diabetes, characterized by an elevated blood glucose level during pregnancy, with onset between the 24th and 28th weeks of pregnancy [10,13]. A woman affected by gestational diabetes have a higher risk of high blood pressure and fetal macrosomia, moreover babies born to mother with gestational diabetes show a higher risk to be affected by T2D in their adulthood [10,13]. Diabetes poses a higher risk for affected people to develop a variety of systemic, health-threatening complications, mainly caused by a sustained high blood glucose level.

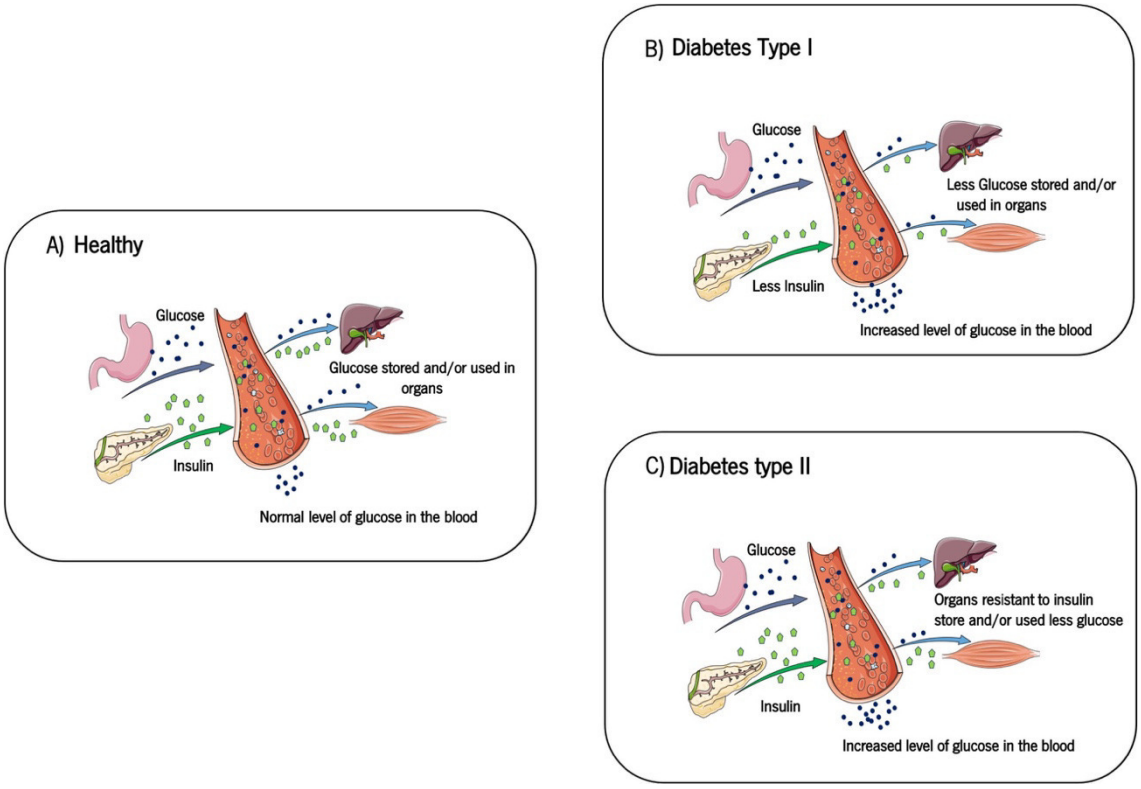


Figure II-1. Representative scheme of the insulin and glucose function mechanism in A) healthy person, B) diabetes type I, and C) diabetes type II.

II-2. COMPLICATIONS OF DIABETES

Diabetes-related complications, including cardiovascular disease, kidney disease, neuropathy, blindness, chronic wounds and ulcers and ultimately lower extremity amputation, are the causes of increased morbidity and mortality among people with diabetes. These complications are broadly divided

into microvascular, including neuropathy, nephropathy, and retinopathy; and macrovascular complications as e.g., cardiovascular disease, stroke, and peripheral artery disease (PAD) [14] (see **Figure II – 2)**.

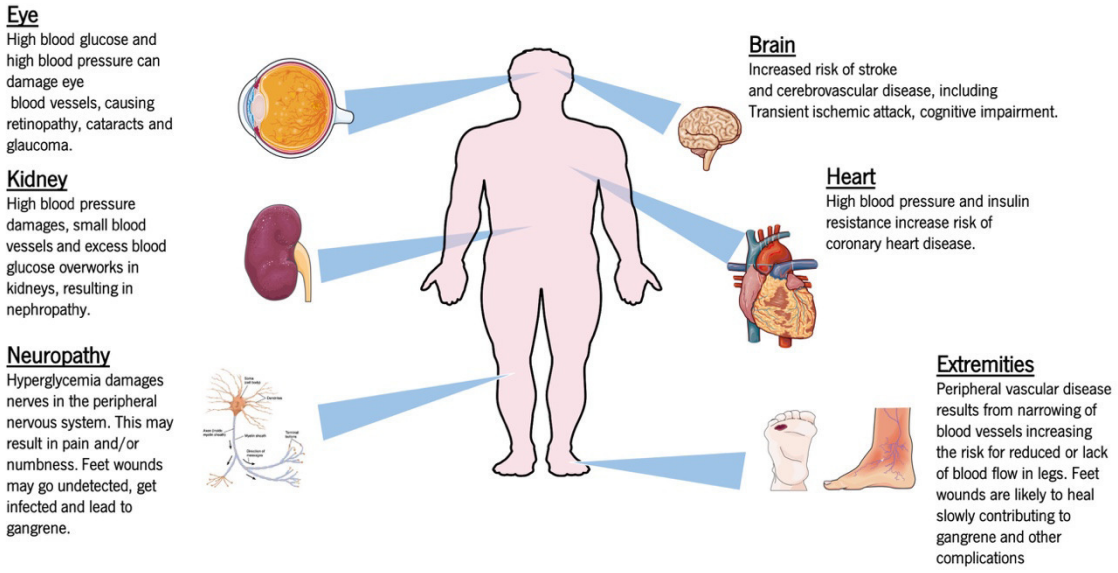


Figure II-2. Micro/macro vascular complications of diabetes mellitus.

II-2.1. Microvascular complications:

- Diabetic nephropathy: manifest as progressive albuminuria, increased blood pressure, and even end-stage renal disease. T2D leads to renal failure in 20-30% of patients, especially in patients with longer duration since diagnosis (usually ≥ 10 years) [15].
- Diabetic neuropathy: Diabetes affects the small vessels that supply the nerves, which leads to neuronal dysfunction, especially in the peripheral nerves and the autonomic nervous system. Adverse effects of diabetic neuropathy include diabetic ulceration of the foot and lower - limb amputation, diabetic gastropathy, and erectile dysfunction in men. It may also mask the signs of ischemic heart disease, resulting in the clinically ambiguous silent angina.
- Diabetic eye disease: A series of eye problems may occur as a complication of diabetes including diabetic retinopathy, which damages the small vessels in the retina and leads to poor vision or even blindness.

II-2.2. Macrovascular complications:

- Cardiovascular diseases are the most common cause of mortality in diabetic patients [15,16]. Associated with these diseases we have arteriosclerosis, which may lead to fatal myocardial infarction or cerebral stroke. One of the major causes is chronic hyperglycemia and dyslipidemia affecting the blood vessels; in people with diabetes the risk of having arteriosclerosis increases.

- Peripheral Arterial Disease: also referred to as peripheral vascular disease (PVD), is caused by the narrowing of blood vessels that carry blood to the arms, legs, stomach, and kidneys. In people with diabetes, the risk for PAD is increased by age, duration of diabetes, and the presence of neuropathy.

II-3. CURRENT TREATMENTS

The higher morbidity, the severity of the symptoms, and the drastic impact on the life quality of the patients are the main reasons for the research increases on diabetes type I (T1D) instead of diabetes type II (T2D). There is currently no definite and optimal cure available to treat DM patients and eradicate the condition. The most important breakthrough in diabetes research occurred in 1921 when insulin was discovered by Frederick G. Banting [4,12]. Since then, the most common method to control blood glucose levels in T1D patients is multiple daily administrations of exogenous insulin accompanied with regular blood glucose checks. However, insulin injections or using a pump only have a mitigation effect and do not provide an optimal long-term cure. Besides, these treatments have long term complications such as blindness, vascular damage, and kidney failure since the kidneys have to work harder to purify the urine.

Insulin pumps deliver insulin more efficiently than injections by providing constant, low-dose, insulin 24 hours a day [4,18]. Nevertheless, the pump itself is still directly connected to the skin, which can be bothersome for the patient and more expensive than injections of insulin. There is also a range of severe drawbacks for both insulin injections and insulin pumps, as e.g. hypoglycemia, which is the most common and serious side effect of insulin therapy, with an average of 1.9 episodes per patient per year [4,19]. Therefore, new treatments among patients with T1D without exogenous insulin injections are urgently needed.

Pancreatic transplantation is also used as a treatment for T1D. During this operation, the entire pancreas and a small part of the intestine are removed from a donor, usually deceased. The donor's intestine is then attached to either the recipient's small intestine or bladder, and the donor pancreas will

be connected through blood vessels. The recipient pancreas is usually not removed to avoid further digestion problems [4,20]. In more than 80 percent of patients, this therapy has shown promising but short-term results in terms of insulin control. The main advantage of this treatment is that patients become insulin-independent directly during surgery [4,21]. Nevertheless, it is a very complicated and invasive procedure with significant peri and post - operative morbidity and mortality [4,22]. Moreover, the availability of donor pancreas is very low, and only a small percentage of T1D patients are eligible for the operation. This is because this surgery is usually performed after 20 years of established diabetes, and only on patients with end-stage diabetes that also require a kidney transplant [4,23].

Another alternative to the administration of exogenous insulin is the transplantation of allogeneic islets, isolated from cadaveric sources. However, in this scenario, the number of islets recovered from a single donor is often insufficient for a full transplantation treatment [7,24]. During this procedure, only the functional units of the pancreas, known as islets of Langerhans (with five different types of cells, the most important being alpha and beta cells), are collected from a donor pancreas and transplanted to a recipient patient affected by T1D. **Figure II - 3** provides a visual representation of this process, in which pancreatic Islets are isolated from the donor, usually deceased, and then inserted with a tiny catheter into the recipient´s hepatic portal vein [4,25]. This method has shown promising results following the implementation of the "Edmonton Protocol," a procedure involving glucocorticoid-free immunosuppression combined with the optimal islet with more than 1,500 procedures performed worldwide. This procedure has shown promising results such as insulin independence in up to 80% of patients, with 50% insulin independence 5 years after receiving the islets transplant. These levels of glycemic stabilization have never been observed with exogenous insulin or glucose monitoring techniques.

However, major obstacles for the successful long-term efficacy of islet transplantation are the lack of vascularization and the patient's immune response. Pancreatic islets are highly metabolic cells that need to quickly produce insulin in response to rising levels of blood glucose, and this is why blood vessels within the pancreas are of a greater density than in many other tissues. Once removed from the donor pancreas, the connection to the blood vessels is lost, and compared to organ transplantation where perfusions are rapidly restored, the blood vessels of islets take several days and many angiogenic factors to be fully functional again, leaving the islets in extremely hypoxic conditions [22,26]. Clinical Islet transplantation has overall low morbidity and comparable results in terms of glucose homeostasis when compared to pancreatic transplantation. Nonetheless, only a limited number of patients are considered suitable for islet transplantation, including those affected by dysfunctional T1D, dispute of hypoglycemia, and severe hypoglycemic events that cannot be adequately controlled with exogenous insulin therapies

[4,26]. Moreover, to improve clinical islet transplantation, there are two current strategies, namely using a close immunoprotected device, and restoring the revascularization as fast as possible to ensure optimal islet survival.

For T2D, a variety of anti-diabetic drugs such as insulin sensitisers (e.g. thiazolidinediones; TZDs), insulin secretagogues (e.g. sulphonyreas (SUs) and meglitinides) and external insulin delivery (insulin analogues) are prescribed aiming to preserve or rejuvenate the β cells [7,27,28]. The biggest challenges in pancreas bioengineering is the delivery of oxygen and nutrients to β cells inside delivery devices.

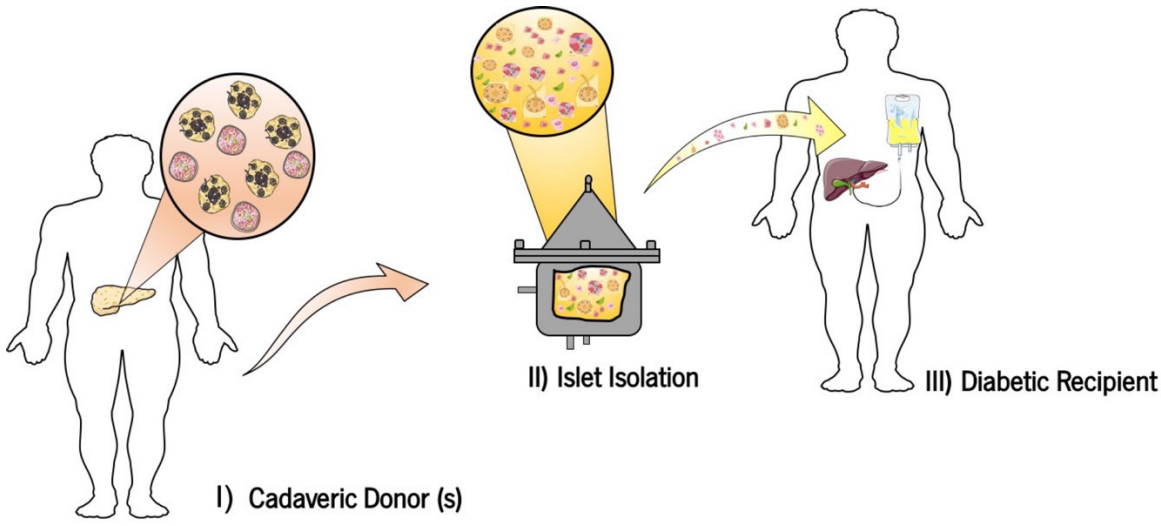


Figure II-3. Schematic illustration of clinical islet transplantation I: Cadaveric donor: pancreatic islets are isolated from donor, II: Ricordi chamber: the islets are isolated and III: Diabetic recipient: the islets are infused by gravity into the portal vein of liver (adapted from [29]).

II-4. BIOMATERIALS BASED MATRIX ARCHITECTURES FOR DIABETES TREATMENT

Biomaterials and regenerative medicine have been playing an increasing role in diabetes treatment, namely islet transplantation (T1D) and drug/hormone therapy (T2D). Several strategies are being developed based on delivery systems like polymeric based [30–32], lipid-based [33–36], and porous-based particulate delivery systems [37,38] for oral administration of incretins (hormones developed by intestinal cells). In this context, new tools for drug delivery systems have been obtained using biomaterials, nanomedicine, and specific surface functionalization strategies [39]. Besides, some of the more recent

and common examples of biomaterials and techniques used in the treatment of type I diabetes (T1D) will be discussed in this point.

For the treatment of T1D, there are two emerging methods that can be used to enhance the efficiency on transplantation of clinical islets: immunoprotective device and revascularization. During transplantation of the islets, some of them are destroyed because of several factors, such as the lack of vasculature resulting in reduced nutrient, oxygen supply, and subject to oxidative stress after transplantation. By placing the islets in a polymer-based device, graft survival could be greatly improved by allowing placement of the islets at some other site in the body, as well as providing a better base for revascularization. In that way, different strategies and a variety of natural (chitosan, alginate, hyaluronic acid, and gelatin), synthetic (poly (lactic-co-glycolic acid) (PLGA), poly (ε-caprolactone) (PCL) and poly (vinyl alcohol)) polymers and their combinations have been investigated for immunoprotective or no-immunoprotective strategies [40]. **Tables II – 1 and 2** shows some examples of these polymers or combinations used in diabetes treatment. **Figure II - 4** shows some extrahepatic beta-cell delivery strategies. These strategies can be divided into immunoprotective strategies (micro and nanoencapsulation) and non-immunoprotective strategies (macroencapsulation and deviceless). The encapsulation strategies used for non and immunoprotective approaches can be classified as microencapsulation, wherein single islet is enveloped in a micron-scale immunoisolating membrane, or macroencapsulation, wherein groups of cells are encased in a suitable membrane that could further be housed in a device. In the next sections, we describe the different materials used in microencapsulation or macroencapsulation systems, and their clinical status in diabetes treatment [41].

II - 4.1. Microencapsulation

Microencapsulation can be defined as single islet encapsulation or a small group of islets inside the semipermeable immunoprotective capsule of polymer gel coating. This technique can be achieved by polymerizing a precursor solution around islet surfaces, forming a gel shell around the islet [42–44]. The most commonly used form of microcapsules is the spherical shape; these microcapsules led to a higher surface-to-volume ratio than did the microcapsule tube or disk geometry, resulting in a higher diffusion rate [45,46]. In addition, microcapsules can be delivered in large quantities, are durable, and they are difficult to destroy mechanically [46–48]. Nevertheless, the biocompatibility of the encapsulation material is challenge that affects the clinical applicability of the microencapsulation technology for transplantation of pancreatic islets [49,50]. A large number of natural/synthetic biocompatible polymers have been used

in microencapsulation applications such as: agarose [40,52,53], collagen [52,54,55], cellulose [56,57], chitosan [40,58–60], polylactic-co-glycolide (PLGA) [61], 2-hydroxyethylmethacrylate [59,62] and polyethylene glycol (PEG)[40,63,64] [49,52,59] (see examples in **Table II -1)**. Among them, alginate is the most widely used biomaterial, as it displays high biocompatibility for both the implantation site cells in the microenvironment and the islets inside [65]. In the microencapsulation, there are two types of techniques, namely, the droplet generator if a random islet distribution is desired, and the microfluidics for a controlled islet distribution [39]. Microencapsulation has some advantages such as the reduced diameter and the large surface area to volume ratio of microcapsules, which improves diffusion, makes this encapsulation system preferable over the others, such as macroencapsulation, where longer distances may compromise oxygen and nutrients diffusion [49,59]. Higher diffusion distances induce a gradient of nutrients and oxygen from the cell encapsulation system surface to the center of the cells, which may affect cell function and survival [49,66]. This fact also has a direct impact on glucose changes in the bloodstream, which is faster and more effective with microencapsulation than with macroencapsulation systems [49]. Another advantage is the survival of islets that is potentially higher than with the macroencapsulation. In that way, when one microcapsule breaks or is attacked by the immune system, only the islet encapsulated in that particular microcapsule will be affected while the rest islets will remain viable [49,59]. Despite the described advantages, the lack of a large-scale system for microcapsules production is the major limitation to translate the microencapsulated islet to the clinics. In fact, the existing methodologies cannot encapsulate large numbers of islets in a reasonable amount of time, which can contribute to hypoxic stress causing the loss of islets function and reduce the viability [49,67]. Another drawback of microencapsulation is related to the large therapeutic graft volume that needs to be used, which enhances the host immune reaction after implantation. This disadvantage can be related with two factors: the very small volume of islets compared with a large volume of macroencapsulation, and the too elevated number of empty microcapsules without islets that are produced during the process [49,68,69]. Generally, the excessive volume of the graft and the large diameter of the microcapsules prevents the transplantation of microencapsulated islets into the liver, as this would presume a high risk of thrombosis. Alternatively, in most clinical trials, microcapsules containing islets were transplanted into the peritoneal cavity where large volumes of microcapsules can be transplanted without the obstruction of the vascular system [49,70–72]. Nevertheless, the indirect access to blood within the peritoneum, however, leads to lower nutritional and oxygen availability, which can threaten the survival of the islet and thus reduce the chance of success [49,73]

Table II-1. Microencapsulation systems based on natural/synthetic polymers or a combination thereof used in diabetes treatment.

Material	Cell type and *in vivo* model	Graft site	Description	Refs
Alginate	Porcine islet cell graft	Peritoneal cavity	Alginate-based radiopaque microcapsule	[41,53,74]
	Rat/Mice	Peritoneal cavity	Core-shell capsule, co-axial nozzle for a stable formation of uniform core-shell	[75,76]
PEG	Mice/Mice	Kidney	Capsule, conformal coating of islets through microfluidics	[76,77]
ECM	hESC/Mice	Subcutaneous	ECM composed of polysaccharides and proteins, mainly collagen and elastin	[76,78]
PLO-Alginate	Human islet cells	Peritoneal cavity	Microcapsules produced microdroplet generator Pilot clinical trial	[49,71]
PLL - alginate	Xeno-allo pancreatic islets	Epididymal fat pad	Alginate microcapsules with a coating of PLL electrostatic droplet generator	[41,79]
Alginate-AEMA	Mice/rat	Omentum	Alginate with 2-aminoethyl methacrylate hydrochloride, photocrosslinking	[76,80]
Organic polymers	Xeno-allo pancreatic islets	Peritoneal cavity	Encapsulife: develops technologies in biomedical field on proving a living cell/function cure for diabetes.	[41,81,82]
PFD-alginate	Mice/Mice	Peritoneal cavity	Suspension of islets in polymer solution, coaxial bead generator	[76,83]

CHT - coated alginate	Pig, dog/mice, dog	Intraperitoneal	Alginate capsules suspended in chitosan solution, air-driven droplet generator	[76,84]

Abbreviation: PEG - polyethylene glycol; **ECM** - extracellular matrix; **PLO** – poly-L-ornithine; **PLL** - poly-L-lysine; **AEMA** - 2-aminoethyl methacrylate hydrochloride**; EFP** - epididymal fat pad; **PFD** - perfluorodecalin; **CHT**- chitosan; **hESC** - human embryonic stem cell.

II-4.1. Macroencapsulation

Macroencapsulation can be defined as encapsulation of a large number of pancreatic islets or insulin-producing cells, thereby allowing the delivery of curative β-cell dose within only one or very few devices [49]. These systems are macroscopic encapsulation devices (> 1mm), and the shape of the devices can be a hollow fiber, planar membranes or macroparticles. In recent years, some developments in macroencapsulation have been made, such as the use of 3D printing and microfabrication technologies [76,85]. Some technologies such as particle leaching, phase separation and electrospinning have been used for random islet distribution, while thermoforming, pillar wafer, and 3D printing have been used for a control islet distribution [39]. The macroencapsulation provides immune isolation of islets within semi-permeable membranes [42,76,86]. One of the major focus on the research of macroencapsulation systems is the development of strategies and device configurations that can provide sufficient oxygen and nutrients to transplanted islets of insulin-producing cells. Macroencapsulation systems that use hydrogels are predominantly spheric or planar devices consisting of islets embedded in semi-permeable chamber hydrogels. This encapsulation system is designed to avoid the aggregation and clustering of the therapeutic cells inside the unit while preserving the cells after implantation from mechanical stress [76,87]. The company Islet Sheet Medical had designed a planar flat sheet device which involved a multilayered construct of alginate composed of a central alginate layer containing islets, and two external acellular alginate layers covering the central layer for immunoprotection. This device has been demonstrated to provide excellent graft survival in diabetic dogs, achieving normoglycemia for 12 weeks [76,88]. In 2010, Dufrane et al developed a planar flat sheet device, consisting in a monolayer of collagen matrix where pig islets are embedded, and two alginate layers covering both sides of the collagen matrix; this system was called a monolayer cellular device. This device was implanted in diabetic monkeys without immunosuppression and demonstrated to correct hyperglycemia for up to 6 months. Although a strong immune response was detected after transplantation, a total impermeability of alginate layers to IgG was demonstrated up to 20 weeks [54,76]. **Table II - 2** shows some macroencapsulation devices that have been commercialized, such as β-Air device, Encaptra [89], Nanogland [90], and Theracyte [76,91,92]. BetaO_2 Technologies have developed the β-Air device, which consists of three major compartments: (i) an islet compartment with islets embedded in a 500–600 μm thick alginate slab; (ii) a gas chamber pO_2 with inlet and outlet ports; and (iii) a 25 mm polytetrafluoroethylene

(PTFE) membrane separating the islet module from the host tissue. Newly active and successful xenotransplantation of porcine islets without immunosuppression in a diabetic NHP(non-human primate) has been achieved with favorable results [76,93]. Evron *et al* have recently determined a supraphysiological level of the gas chamber pO_2 to substantially increase islet surface density [76,94]. Viacyte company has developed the Encaptra, a planar macroencapsulation device containing a semipermeable barrier that can be engineered properly and loaded with hESCs [76,89]. Thomas Robert *et al* have published a new study that determines the biologic characteristics at which this combination product (VC-01™) establishes metabolic control in mouse models [76,95]. Omaima M. Sabek *et al* developed a macroencapsulation device for the autotransplantation of human islets called silicon Nanogland. This consists of a micro-fabricated membrane with parallel nanochannels for immunoprotection and perpendicular microchannels that facilitate neovascularization. Silicon Nanoglan enograft of human islets was subcutaneously implanted in mice and lasted for >120 days [76,90]. Theracyte device is another macroencapsulation system in the market, is a thin biocompatible membrane-bound polymeric chamber that has been tested in a large number of animal studies preventing hyperglycemia and allograft rejection [76,91,92].

This technology has some advantages over microencapsulation is the easy implantation of the islets in the precise location of the body in one single device and the possibility to simply retrieve the device in case of graft failure or some complications after transplantation [49,96,97]. Another benefit of macroencapsulation devices is when the islets are embedded in hydrogels, as this provides physical separation of islets that prevent aggregation, maintains a rounded morphology of the islet, improves the supply of oxygen and nutrients to all encapsulated islets, thereby improving their viability and survival [49,76,98]. Some limitations of this technology are, in most cases, islets are freely floating inside the encapsulation device, resulting in aggregation of islets that negatively affects the structure, limits the nutrients and oxygen diffusion, and leads to loss of islet function, apoptosis and death [49,73]. Another issues are the reduction of oxygen supply due to larger diffusional distances between the encapsulated islets and the outside of the device [46,49], and the other is the place where the device is implanted, which presents low vascularization that affects the islet viability and subsequently the glycemic control [49,99]. Additional problems limit the effectiveness of macroencapsulation devices such as cell adhesion and fibrotic reaction to the outer surface devices. In this regard, the success of the graft is determined by the way an implantable device interacts with the host´s biological environment and

immune system at the implantation site [49,100]. This fact depends on the size, geometry, and configuration of the device and, most importantly, depends on the physicochemical properties of the device's surface, such as chemical composition, degree of hydrophilicity, roughness, morphology, and pore size. But how they affect the inflammatory and fibrotic response is still not well known [49,101]. To achieve a successful and functional graft during the short and long term after implantation, it is essential to explore macro device designs and surface properties in that sense

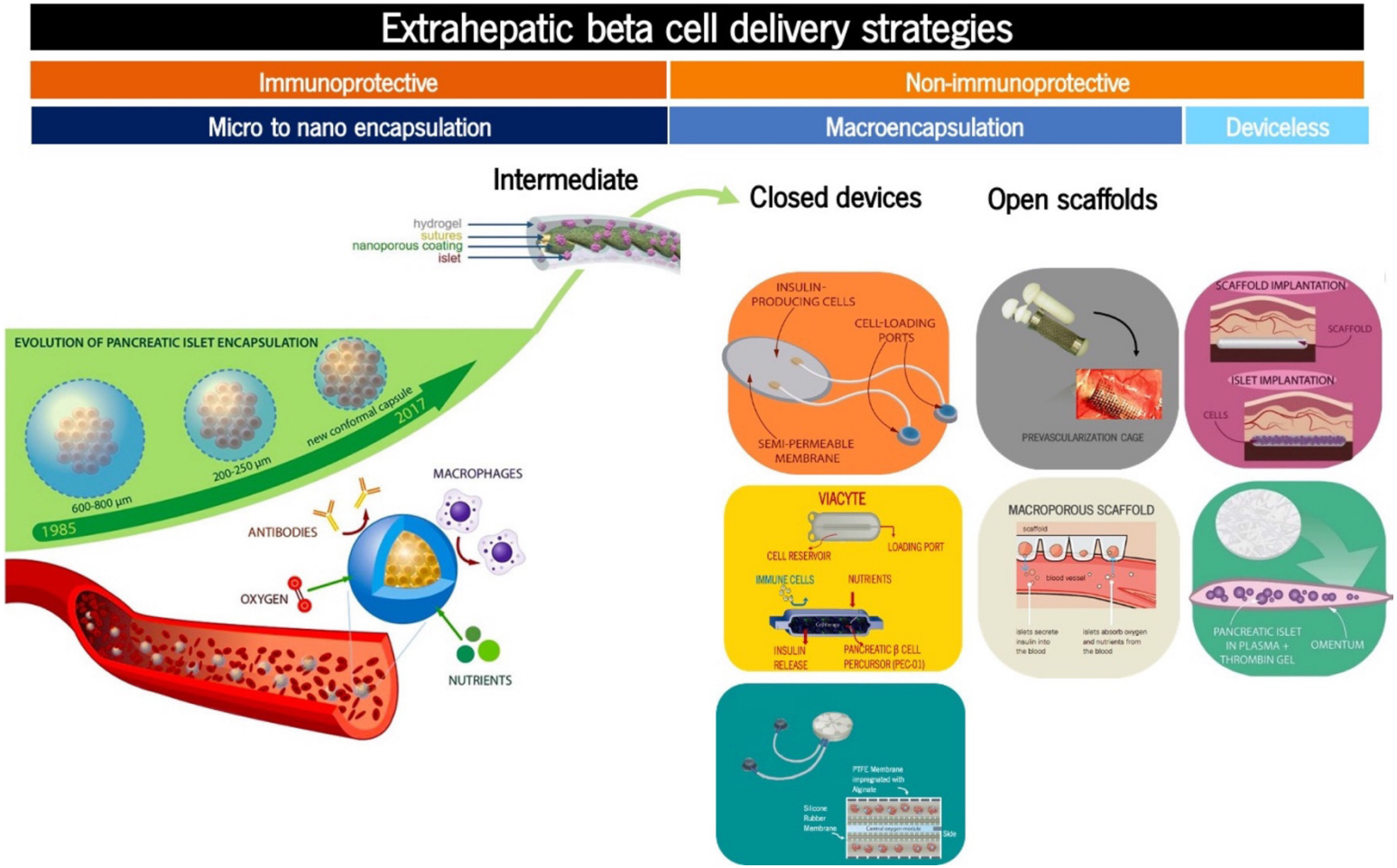


Figure II-4. Extrahepatic beta-cell delivery strategies , divided in I: Immunoprotective, through micro and macroencapsulation, and II: Non -immunoprotective through macroencapsulation or without using encapsulation devices (adapted from [41,102]).

Table II-2. Macroencapsulation systems based on natural/synthetic polymers or combination thereof used in diabetes treatment

Material	Cell type and *in vivo* model	Graft site	Description	Refs
PEG	Mice/mice	EFP- epididymal fat pad	Combines Encapsulation with biography techniques to generate PDMS molds 600mm thickness	[76,115]
PLA	hESC/mice	Subcutaneous	3D printed PLA scaffold microporous PLA with fibrin gel	[76,85]
Alginate/gelatin	Rat	Subcutaneous	3D-printed alginate scaffold	[76,108]
Collagen/Alginate	Islets	_____	In situ islet spheroid formation and encapsulation on a single platform. Minimizing damage to spheroids during encapsulation	[49,112]
PTFE-membrane (Theracyte)	Islet ESC - derived Islets from Lewis rats hESC/mice	Subcutaneous	Encapsulation of cells in bilaminar device. Thin bound polymeric chamber composed of 2 membranes	[41,76,92,103,104]
PTFE-membrane (Viacyte)	Human Embrionic stem cells	Subcutaneous	Nanofluidic membrane technology capable to achieving active and tunable control of molecular transport thought nanofluidic devices	[41,105–107]

Teflon-Alginate	Pig Islets Human pancreatic Islets	Subcutaneous	An oxygenated chamber system composed of immune isolating alginate and polymembrane covers that allows survival and function of islets without immosupression. The chamber is composed of 68mm in diameter and 18mm in thickness, composed of 600µm thick immobilized islets module attached to an oxygen module by a gas-permeable silicon- rubber membrane	[41,76,93]
Thrombin/patients own plasma biological scaffolds (BioHub)	Human Islets Allogeneic	Omentum	In situ generated adherent, resorbable plasma thrombin biological scaffolds evaluated in rat and nonhuman primate models	[41,46,49,109]
Medical-grade polymers	Human pancreatic islet/beta cells	Subcutaneous	Silicon device, the Nanogland for long-term islet viability and revascularization.	[90,110]
	Insulin secreting cell		Planar immune barrier membrane diffusion devices were used for syngeneic islet transplantation	[41,111]
VEGF-PEG-MAL	Mice/mice	Peritoneal cavity	Polymer and islets mixed and then crosslinked	[76,113]
Encaptra	hRSC/mice	Subcutaneous	Pec-01 cell population differentiated form hESC, contains pancreatic progenitors	[76,89]
Device- encapsulated hESC - PE	hESC/mice	Subcutaneous	hESC – derived pancreatic endodum, engineered Encaptra drug delivery system	[76,95]

Traffic Alginate	Rat/human mice	Peritoneal cavity	Ca^{2+}- releasing nanoporous polymer thread that promoted uniform in situ crosslinking and strong adhesion of a thin layer of alginate hydrogel around the thread	[76,97]
PDMS scaffold	Rodent, NHP, Human/rat	Omentum	Biostable macroporous scaffold fabricated using solvent casting and particle leaching technique	[76,114]
Biological scaffold	Rat, NHP, Human/Rat,	Intraomental	Plasma and recombinant human thrombin	[76,109]
PDLLCL scaffold	Rat/rat	Subcutaneous	Scaffold transplantation to initiate vascularization	[76,116]
SNM-based IBAP	Mice/Pig	Intravascular	Intravascular BAP with V10 and ~ 40mm pore size membranes	[76,117]

Abbreviation: PEG, polyethylene glycol; **PLA**, polylactic acid**; PTFE** politetrafluoretileno; **hESC-PE**, human embryonic stem cell-derived pancreatic endoderm; pancreas device; **NHP**, non-human primate; **PDLLCL**, poly(D,L-lactide-co-e-caprolactone); **EFP**, epididymal fat pad; **PDMS**, poly(dimethylsilox); **SNM**, silicon nanopore membranes; **IBAP**, intravascular bioartificial

II-5. FUTURE PERSPECTIVES

Worldwide the number of patients with diabetes is steadily increasing. The social burden of diabetes is, therefore, massive and needs urgent countermeasures. Diabetes is a condition that affects blood sugar levels and causes many serious health problems if left uncontrolled or untreated. There is no cure for any type of diabetes, but it can go into remission. It may be managed by people with changes in medication and lifestyle. Advancements in the development of biomaterials for diabetes treatment have been demonstrated as extraordinary opportunities for current and future clinical therapies. Future strategies include incorporating different types of biomaterials creating an unlimited supply of insulin-producing β cells to replace primary islet transplants and promoting revascularization with immune and inflammatory response alerts. One of the biggest challenges in bioengineering the pancreas for type I diabetes is the delivery of oxygen and nutrients in supply systems to β cells inside. For type II diabetes, the biggest hits are glucagon-like peptide (GLP)-1 receptor agonist, which stimulates insulin production in β-pancreatic cells while suppressing glucagon secretion, a hormone with the opposite effect of insulin.

There is now tremendous demand for new approaches (fabrication technologies, safer implantation strategies and angiogenesis inducement) and more suitable biomaterials to be used as drug delivery or bioartificial pancreas. Clearly, there is still a long way to go before this becomes a reality, but we believe this is the right path to take in the search for new and more successful diabetes therapies.

II-6. REFERENCES

[1] Silva LP. *Advance gellam gum-based hydrogels for the treatment of diabetic foot ulcerations*.University of Minho, Portugal, Doctroal Thesis; 2016.

[2] Wong TY, Sabanayagam C. *Strategies to Tackle the Global Burden of Diabetic Retinopathy: From Epidemiology to Artificial Intelligence*.Ophthalmologica 2020. 243(1):9–20.

[3] *World Health Organization*.https://www.who.int/health-topics/diabetes. 2017 [cited 2019 Nov].

[4] Oldrini I. *Design and study of an immuno-protective Islets encapsulating device for Type 1 Diabetes applications.*Maasstricht University, Bachelor thesis; 2019.

[5] Ribeiro D. *Pancreatic extracellular communication. Applications to beta cell cultures and islet amyloid polypeptide aggregation.*Chalmers University of technology, Doctoral Thesis; 2018.

[6] Amer LD, Mahoney MJ, Bryant SJ. *Tissue engineering approaches to cell-based type 1 diabetes therapy.*Tissue Eng Part B Rev 2014. 20(5):455–67.

[7] *Diabetes Care in the School and Day Care Setting.*Diabetes Care 2010. 33(Supplement 1):S70

LP-S74.

[8] Groot M de. *Immunoprotection of pancreatic islets: in vitro studies into causes of microencapsulated graft failure*.University of Groningen, Doctoral Thesis; 2004.

[9] *History of Diabetes*.https://www.news-medical.net/health/History-of-Diabetes.aspx. [cited 2019 Nov].

[10] Marchioli G. *A journey towards an extrahepatic islets delivery device with a tissue engineering toolbox in hand*.University of Twente, Doctoral thesis; 2017.

[11] Alberti KG, Zimmet PZ. *Definition, diagnosis and classification of diabetes mellitus and its complications. Part 1: diagnosis and classification of diabetes mellitus provisional report of a WHO consultation*.Diabet Med 1998. 15(7):539–53.

[12] Atkinson MA, Eisenbarth GS, Michels AW. *Type 1 diabetes*.Lancet (London, England) 2014. 383(9911):69–82.

[13] Crowther CA, Hiller JE, Moss JR, McPhee AJ, Jeffries WS, Robinson JS. *Effect of Treatment of Gestational Diabetes Mellitus on Pregnancy Outcomes*.N Engl J Med 2005. 352(24):2477–86.

[14] Papatheodorou K, Banach M, Bekiari E, Rizzo M, Edmonds M. *Complications of Diabetes 2017*.J Diabetes Res 2018. 2018:3086167.

[15] Elhendi MY. *Assessment of Type 2 Diabetes management practice: A study in public hospitals outpatient clinics, Khartoum and Gezira, Sudan*.University of Oslo, Masther thesis; 2015.

[16] *International Diabetes Federation. Complications of diabetes*.https://www.idf.org/aboutdiabetes/complications.html. 2015 [cited 2019 Nov].

[17] Pickup J, Keen H. *Continuous Subcutaneous Insulin Infusion at 25 Years*.Diabetes Care 2002. 25(3):593 LP – 598.

[18] DeWitt DE, Hirsch IB. *Outpatient Insulin Therapy in Type 1 and Type 2 Diabetes MellitusScientific Review*.JAMA 2003. 289(17):2254–64.

[19] *Pancreas transplantation. American Diabetes Association*.https://www.diabetes.org/search?keywords=pancreas+transplantation. 2018 [cited 2019 Dec].

[20] Ojo AO, Meier-Kriesche HU, Hanson JA, Leichtman A, Magee JC, Cibrik D, et al. *The impact of simultaneous pancreas-kidney transplantation on long-term patient survival*.Transplantation 2001. 71(1):82–90.

[21] Lakey JRT, Burridge PW, Shapiro AMJ. *Technical aspects of islet preparation and transplantation*.Transpl Int 2003. 16(9):613–32.

[22] Association AD, Drouin P, Blickle JF, Charbonnel B, Eschwege E, Guillausseau PJ, et al. *Diagnosis and classification of diabetes mellitus*.Diabetes Care 2013. 36 Suppl 1:S67-74.

[23] Croon A-C, Karlsson R, Bergström C, Björklund E, Möller C, Tydén L, et al. *Lack of donors limits the use of islet transplantation as treatment for diabetes*.Transplant Proc 2003. 35(2):764.

[24] Pepper AR, Gala-Lopez B, Ziff O, Shapiro AJ. *Current status of clinical islet transplantation*.World J Transplant 2013. 3(4):48–53.

[25] Shapiro AMJ, Pokrywczynska M, Ricordi C. *Clinical pancreatic islet transplantation*.Nat Rev Endocrinol 2016. 13(5):268–77.

[26] Wajchenberg BL. *β-Cell Failure in Diabetes and Preservation by Clinical Treatment*.Endocr Rev

2007. 28(2):187–218.

[27] He Z-X, Zhou Z-W, Yang Y, Yang T, Pan S-Y, Qiu J-X, et al. *Overview of clinically approved oral antidiabetic agents for the treatment of type 2 diabetes mellitus*.Clin Exp Pharmacol Physiol 2015. 42(2):125–38.

[28] Emamaullee JA, Pepper A, Shapiro AMJ. *Chapter 56 - Islet Cell Transplantation*.In: Atala A, Lanza R, Mikos AG, Nerem RBT-P of RM (Third E, editors. 2019. Boston: Academic Press; 2019. p. 987–1007.

[29] Attivi D, Wehrle P, Ubrich N, Damge C, Hoffman M, Maincent P. *Formulation of insulin-loaded polymeric nanoparticles using response surface methodology.*Drug Dev Ind Pharm 2005. 31(2):179–89.

[30] Ensign LM, Cone R, Hanes J. *Oral drug delivery with polymeric nanoparticles: the gastrointestinal mucus barriers*.Adv Drug Deliv Rev 2012. 64(6):557–70.

[31] Damgé C, Maincent P, Ubrich N. *Oral delivery of insulin associated to polymeric nanoparticles in diabetic rats*.J Control Release 2007. 117(2):163–70.

[32] Li X, Guo S, Zhu C, Zhu Q, Gan Y, Rantanen J, et al. *Intestinal mucosa permeability following oral insulin delivery using core shell corona nanolipoparticles*.Biomaterials 2013. 34(37):9678–87.

[33] Zhang N, Ping Q, Huang G, Han X, Cheng Y, Xu W. *Transport Characteristics of Wheat Germ Agglutinin-Modified Insulin-Liposomes and Solid Lipid Nanoparticles in a Perfused Rat Intestinal Model*.J Nanosci Nanotechnol 2006. 6:2959–66.

[34] Zhang Z-H, Zhang Y-L, Zhou J-P, Lv H-X. *Solid lipid nanoparticles modified with stearic acid-octaarginine for oral administration of insulin*.Int J Nanomedicine 2012. 7:3333–9.

[35] Zhang Z, Lv H, Zhou J. *Novel solid lipid nanoparticles as carriers for oral administration of insulin.*Pharmazie 2009. 64(9):574–8.

[36] Huotari A, Xu W, Mönkäre J, Kovalainen M, Herzig K-H, Lehto V-P, et al. *Effect of surface chemistry of porous silicon microparticles on glucagon-like peptide-1 (GLP-1) loading, release and biological activity.*Int J Pharm 2013. 454(1):67–73.

[37] Kilpeläinen M, Mönkäre J, Vlasova MA, Riikonen J, Lehto V-P, Salonen J, et al. *Nanostructured porous silicon microparticles enable sustained peptide (Melanotan II) delivery.*Eur J Pharm Biopharm 2011. 77(1):20—25.

[38] de Vries R, Stell A, Mohammed S, Hermanns C, Martinez AH, Jetten M, et al. *Chapter 33 - Bioengineering, biomaterials, and β-cell replacement therapy.*In: Orlando G, Piemonti L, Ricordi C, Stratta RJ, Gruessner Bioengineering, and Regeneration of the Endocrine Pancreas RWGBT-T, editors. 2020. Academic Press; 2020. p. 461–86.

[39] Ernst AU, Wang L-H, Ma M. *Islet encapsulation*.J Mater Chem B 2018. 6(42):6705–22.

[40] Farina M, Alexander JF, Thekkedath U, Ferrari M, Grattoni A. *Cell encapsulation: Overcoming barriers in cell transplantation in diabetes and beyond*.Adv Drug Deliv Rev 2019. 139:92–115.

[41] Kozlovskaya V. *Encapsulation and Surface Engineering of Pancreatic Islets: Advances and Challenges*.In: Zavgorodnya O, editor. 2012. Rijeka: IntechOpen; 2012. p. Ch. 1.

[42] Beck J, Angus R, Madsen B, Britt D, Vernon B, Nguyen KT. *Islet encapsulation: strategies to enhance islet cell functions.*Tissue Eng 2007. 13(3):589–99.

[43] Weber L, Cheung C, Anseth K. *Multifunctional Pancreatic Islet Encapsulation Barriers Achieved*

Via Multilayer PEG Hydrogels.Cell Transplant 2008. 16:1049–57.

[44] Schilfgaarde R, de Vos P. *Factors influencing the properties and performance of microcapsules for immunoprotection of panreatic islets*.J Mol Med (Berl) 1999. 77:199–205.

[45] Dufrane D, Gianello P. *Macro- or microencapsulation of pig islets to cure type 1 diabetes*.World J Gastroenterol 2012. 18(47):6885–93.

[46] Duvivier-Kali VF, Omer A, Lopez-Avalos MD, O'Neil JJ, Weir GC. *Survival of Microencapsulated Adult Pig Islets in Mice In Spite of an Antibody Response*.Am J Transplant 2004. 4(12):1991–2000.

[47] Omer A, Duvivier-Kali VF, Trivedi N, Wilmot K, Bonner-Weir S, Weir GC. *Survival and Maturation of Microencapsulated Porcine Neonatal Pancreatic Cell Clusters Transplanted into Immunocompetent Diabetic Mice*.Diabetes 2003. 52(1):69 LP – 75.

[48] Espona-Noguera A, Ciriza J, Cañibano-Hernández A, Orive G, Hernández RMM, Saenz Del Burgo L, et al. *Review of Advanced Hydrogel-Based Cell Encapsulation Systems for Insulin Delivery in Type 1 Diabetes Mellitus*.Pharmaceutics 2019. 11(11):597.

[49] Vaithilingam V, Tuch BE. *Islet transplantation and encapsulation: an update on recent developments*.Rev Diabet Stud 2011. 8(1):51–67.

[50] Gasperini L, Mano JF, Reis RL. *Natural polymers for the microencapsulation of cells*.J R Soc Interface 2014. 11(100):20140817.

[51] Iwata H, Takagi T, Amemiya H, Shimizu H, Yamashita K, Kobayashi K, et al. *Agarose for a bioartificial pancreas*.J Biomed Mater Res 1992. 26(7):967–77.

[52] Llacua LA, Hoek A, de Haan BJ, de Vos P. *Collagen type VI interaction improves human islet survival in immunoisolating microcapsules for treatment of diabetes*.Islets 2018. 10(2):60–8.

[53] Huang P-J, Qu J, Saha P, Muliana A, Kameoka J. *Microencapsulation of beta cells in collagen micro-disks via circular pneumatically actuated soft micro-mold ({cPASMO}) device*.Biomed Phys Eng Express 2018. 5(1):15004.

[54] Salmons B, Brandtner E, Dangerfield J, Günzburg W. *Encapsulation of Insulin Producing Cells for Diabetes Treatment Using Alginate and Cellulose Sulphate as Bioencapsulation Polymers*.Diabetes Res Treat 2014. 1:1–7.

[55] Schaffellner S, Stadlbauer V, Stiegler P, Hauser O, Halwachs G, Lackner C, et al. *Porcine islet cells microencapsulated in sodium cellulose sulfate*.Transplant Proc 2005. 37(1):248–52.

[56] A. Zielinski B, Aebischer P. *Chitosan as a matrix for mammalian cell encapsulation*.Biomaterials 1994. 15(13):1049–56.

[57] Krishnan R, Alexander M, Robles L, Foster 3rd CE, Lakey JRT. *Islet and stem cell encapsulation for clinical transplantation*.Rev Diabet Stud 2014. 11(1):84–101.

[58] Yang K-C, Qi Z, Wu C-C, Shirouza Y, Lin F-H, Yanai G, et al. *The cytoprotection of chitosan based hydrogels in xenogeneic islet transplantation: An in vivo study in streptozotocin-induced diabetic mouse*.Biochem Biophys Res Commun 2010. 393(4):818–23.

[59] Abalovich A, Jatimliansky C, Diegex E, Arias M, Altamirano A, Amorena C, et al. *Pancreatic islets microencapsulation with polylactide-co-glycolide.*Transplant Proc 2001. 33(1–2):1977–9.

[60] Klomp GF, Ronel SH, Hashiguchi H, D'Andrea M, Dobelle WH. *Hydrogels for encapsulation of pancreatic islet cells.*Trans Am Soc Artif Intern Organs 1979. 25:74–6.

[61] Cruise GM, Hegre OD, Lamberti F V, Hager SR, Hill R, Scharp DS, et al. *In Vitro and in Vivo Performance of Porcine Islets Encapsulated in Interfacially Photopolymerized Poly(Ethylene Glycol) Diacrylate Membranes*.Cell Transplant 1999. 8(3):293–306.

[62] Cheung CY, Anseth KS. *Synthesis of Immunoisolation Barriers That Provide Localized Immunosuppression for Encapsulated Pancreatic Islets*.Bioconjug Chem 2006. 17(4):1036–42.

[63] de Vos P, Faas MM, Strand B, Calafiore R. *Alginate-based microcapsules for immunoisolation of pancreatic islets*.Biomaterials 2006. 27(32):5603–17.

[64] Lovett M, Lee K, Edwards A, Kaplan DL. *Vascularization strategies for tissue engineering*.Tissue Eng Part B Rev 2009. 15(3):353–70.

[65] Jr WFK, Opara EC. *Immunoisolation techniques for islet cell transplantation*.Expert Opin Biol Ther 2002. 2(5):503–11.

[66] Buder B, Alexander M, Krishnan R, Chapman DW, Lakey JR. *Encapsulated islet transplantation: strategies and clinical trials*.Immune Netw 2013. 13(6):235–9.

[67] Lee KY, Mooney DJ. *Alginate: properties and biomedical applications*.Prog Polym Sci 2012. 37(1):106–26.

[68] Calafiore R, Basta G, Luca G, Lemmi A, Montanucci MP, Calabrese G, et al. *Microencapsulated Pancreatic Islet Allografts Into Nonimmunosuppressed Patients With Type 1 Diabetes*.Diabetes Care 2006. 29(1):137 LP – 138.

[69] Tuch BE, Keogh GW, Williams LJ, Wu W, Foster JL, Vaithilingam V, et al. *Safety and viability of microencapsulated human islets transplanted into diabetic humans*.Diabetes Care 2009. 32(10):1887–9.

[70] Tan PLJ. *Company Profile: Tissue regeneration for diabetes and neurological diseases at Living Cell Technologies*.Regen Med 2010. 5(2):181–7.

[71] Schweicher J, Nyitray C, Desai TA. *Membranes to achieve immunoprotection of transplanted islets*.Front Biosci (Landmark Ed 2014. 19:49–76.

[72] Barnett BP, Kraitchman DL, Lauzon C, Magee CA, Walczak P, Gilson WD, et al. *Radiopaque alginate microcapsules for X-ray visualization and immunoprotection of cellular therapeutics*.Mol Pharm 2006. 3(5):531–8.

[73] Ma M, Chiu A, Sahay G, Doloff JC, Dholakia N, Thakrar R, et al. *Core-shell hydrogel microcapsules for improved islets encapsulation*.Adv Healthc Mater 2013. 2(5):667–72.

[74] Dimitrioglou N, Kanelli M, Papageorgiou E, Karatzas T, Hatziavramidis D. *Paving the way for successful islet encapsulation*.Drug Discov Today 2019. 24(3):737–48.

[75] Tomei AA, Manzoli V, Fraker CA, Giraldo J, Velluto D, Najjar M, et al. *Device design and materials optimization of conformal coating for islets of Langerhans*.Proc Natl Acad Sci 2014. 111(29):10514 LP – 10519.

[76] Chaimov D, Baruch L, Krishtul S, Meivar-levy I, Ferber S, Machluf M. *Innovative encapsulation platform based on pancreatic extracellular matrix achieve substantial insulin delivery*.J Control Release 2017. 257:91–101.

[77] Strand BL, Ryan L, Veld PI, Kulseng B, Rokstad AM, Skjak-Braek G, et al. *Poly-L-Lysine Induces Fibrosis on Alginate Microcapsules via the Induction of Cytokines*.Cell Transplant 2001. 10(3):263–75.

[78] Somo SI, Langert K, Yang C-Y, Vaicik MK, Ibarra V, Appel AA, et al. *Synthesis and evaluation of dual crosslinked alginate microbeads*.Acta Biomater 2018. 65:53–65.

[79] Mitsuo M, Inoue K, Nakai I, Oda T, Gu Y, Shinohara S, et al. *Efficacy of mesh reinforced polyvinylalcohol tube as a novel device for bioartificial pancreas: a functional study of rat islets in vivo*.Transplant Proc 1992. 24(6):2939–40.

[80] Papas KK, Avgoustiniatos ES, Suszynski TM. *Effect of oxygen supply on the size of implantable islet-containing encapsulation devices*.Panminerva Med 2016. 58(1):72–7.

[81] Lee S-H, Park H-S, Yang Y, Lee E-Y, Kim J-W, Khang G, et al. *Improvement of islet function and survival by integration of perfluorodecalin into microcapsules in vivo and in vitro*.J Tissue Eng Regen Med 2018. 12(4):e2110–22.

[82] Yang HK, Ham D-S, Park H-S, Rhee M, You YH, Kim MJ, et al. *Long-term Efficacy and Biocompatibility of Encapsulated Islet Transplantation With Chitosan-Coated Alginate Capsules in Mice and Canine Models of Diabetes*.Transplantation 2016. 100(2):334–43.

[83] Song J, Millman JR. *Economic 3D-printing approach for transplantation of human stem cell-derived $\upbeta$ -like cells*.Biofabrication 2016. 9(1):15002.

[84] Nyitray CE, Chang R, Faleo G, Lance KD, Bernards DA, Tang Q, et al. *Polycaprolactone Thin-Film Micro- and Nanoporous Cell-Encapsulation Devices*.ACS Nano 2015. 9(6):5675–82.

[85] Pham TT, Nguyen TT, Pathak S, Regmi S, Nguyen HT, Tran TH, et al. *Tissue adhesive FK506–loaded polymeric nanoparticles for multi–layered nano–shielding of pancreatic islets to enhance xenograft survival in a diabetic mouse model*.Biomaterials 2018. 154:182–96.

[86] Azadi SA, Vasheghani-Farahani E, Hashemi-Najafbabadi S, Godini A. *Co-encapsulation of pancreatic islets and pentoxifylline in alginate-based microcapsules with enhanced immunosuppressive effects*.Prog Biomater 2016. 5(2):101–9.

[87] Agulnick AD, Ambruzs DM, Moorman MA, Bhoumik A, Cesario RM, Payne JK, et al. *Insulin-Producing Endocrine Cells Differentiated In Vitro From Human Embryonic Stem Cells Function in Macroencapsulation Devices In Vivo*.Stem Cells Transl Med 2015. 4(10):1214–22.

[88] Sabek OM, Ferrati S, Fraga DW, Sih J, Zabre E V, Fine DH, et al. *Characterization of a nanogland for the autotransplantation of human pancreatic islets*.Lab Chip 2013. 13(18):3675–88.

[89] Boettler T, Schneider D, Cheng Y, Kadoya K, Brandon EP, Martinson L, et al. *Pancreatic Tissue Transplanted in TheraCyte™ Encapsulation Devices Is Protected and Prevents Hyperglycemia in a Mouse Model of Immune-Mediated Diabetes*.Cell Transplant 2016. 25(3):609–14.

[90] Kumagai-Braesch M, Jacobson S, Mori H, Jia X, Takahashi T, Wernerson A, et al. *The TheraCyte™ Device Protects against Islet Allograft Rejection in Immunized Hosts*.Cell Transplant 2013. 22(7):1137–46.

[91] Ludwig B, Ludwig S, Steffen A, Knauf Y, Zimerman B, Heinke S, et al. *Favorable outcome of experimental islet xenotransplantation without immunosuppression in a nonhuman primate model of diabetes*.Proc Natl Acad Sci U S A 2017. 114(44):11745–50.

[92] Evron Y, Colton CK, Ludwig B, Weir GC, Zimermann B, Maimon S, et al. *Long-term viability and function of transplanted islets macroencapsulated at high density are achieved by enhanced oxygen supply*.Sci Rep 2018. 8(1):6508.

[93] Robert T, De Mesmaeker I, Stangé GM, Suenens KG, Ling Z, Kroon EJ, et al. *Functional Beta Cell Mass from Device-Encapsulated hESC-Derived Pancreatic Endoderm Achieving Metabolic*

Control.Stem Cell Reports 2018. 10(3):739–50.

[94] Ye Y, Yu J, Wang C, Nguyen N-Y, Walker GM, Buse JB, et al. *Microneedles Integrated with Pancreatic Cells and Synthetic Glucose-Signal Amplifiers for Smart Insulin Delivery*.Adv Mater 2016. 28(16):3115–21.

[95] An D, Chiu A, Flanders JA, Song W, Shou D, Lu Y-C, et al. *Designing a retrievable and scalable cell encapsulation device for potential treatment of type 1 diabetes*.Proc Natl Acad Sci U S A 2018. 115(2):E263–72.

[96] Silva AI, de Matos AN, Brons IG, Mateus M. *An overview on the development of a bio-artificial pancreas as a treatment of insulin-dependent diabetes mellitus*.Med Res Rev 2006. 26(2):181–222.

[97] Weaver JD, Headen DM, Aquart J, Johnson CT, Shea LD, Shirwan H, et al. *Vasculogenic hydrogel enhances islet survival, engraftment, and function in leading extrahepatic sites*.Sci Adv 2017. 3(6):e1700184–e1700184.

[98] Chandorkar Y, K R, Basu B. *The Foreign Body Response Demystified*.ACS Biomater Sci Eng 2019. 5(1):19–44.

[99] Thevenot P, Hu W, Tang L. *Surface chemistry influences implant biocompatibility*.Curr Top Med Chem 2008. 8(4):270–80.

[100] van Apeldoorn AA. *Challenges and opportunities in bioengineering, advanced microfabrication, 3D priting and beta cell replacement devices*.In: 2019. International pancreas & islet transplant association (IPITA) conference, Lyon; 2019.

[101] Rios PD, Zhang X, Luo X, Shea LD. *Mold-casted non-degradable, islet macro-encapsulating hydrogel devices for restoration of normoglycemia in diabetic mice*.Biotechnol Bioeng 2016. 113(11):2485–95.

[102] Marchioli G, van Gurp L, van Krieken PP, Stamatialis D, Engelse M, van Blitterswijk CA, et al. *Fabrication of three-dimensional bioplotted hydrogel scaffolds for islets of Langerhans transplantation*.Biofabrication 2015. 7(2):25009.

[103] Lee BR, Hwang JW, Choi YY, Wong SF, Hwang YH, Lee DY, et al. *In situ formation and collagen-alginate composite encapsulation of pancreatic islet spheroids*.Biomaterials 2012. 33(3):837–45.

[104] Krishnamurthy N V, Gimi B. *Encapsulated cell grafts to treat cellular deficiencies and dysfunction*.Crit Rev Biomed Eng 2011. 39(6):473–91.

[105] Kirk K, Hao E, Lahmy R, Itkin-Ansari P. *Human embryonic stem cell derived islet progenitors mature inside an encapsulation device without evidence of increased biomass or cell escape*.Stem Cell Res 2014. 12(3):807–14.

[106] Grattoni A, Fine D, Zabre E, Ziemys A, Gill J, Mackeyev Y, et al. *Gated and Near-Surface Diffusion of Charged Fullerenes in Nanochannels*.ACS Nano 2011. 5(12):9382–91.

[107] Bruno G, Geninatti T, Hood RL, Fine D, Scorrano G, Schmulen J, et al. *Leveraging electrokinetics for the active control of dendritic fullerene-1 release across a nanochannel membrane*.Nanoscale 2015. 7(12):5240–8.

[108] Ziemys A, Grattoni A, Fine D, Hussain F, Ferrari M. *Confinement Effects on Monosaccharide Transport in Nanochannels*.J Phys Chem B 2010. 114(34):11117–26.

[109] Berman DM, Molano RD, Fotino C, Ulissi U, Gimeno J, Mendez AJ, et al. *Bioengineering the Endocrine Pancreas: Intraomental Islet Transplantation Within a Biologic Resorbable*

Scaffold.Diabetes 2016. 65(5):1350–61.

[110] Orive G, Maria Hernández R, Rodríguez Gascón A, Calafiore R, Swi Chang TM, Vos P de, et al. *History, challenges and perspectives of cell microencapsulation*.Trends Biotechnol 2004. 22(2):87–92.

[111] Suzuki K, Bonner-Weir S, Trivedi N, Yoon KH, Hollister-Lock J, Colton CK, et al. *Function and survival of macroencapsulated syngeneic islets transplanted into streptozocin-diabetic mice.*Transplantation 1998. 66(1):21–8.

[112] Phelps EA, Headen DM, Taylor WR, Thulé PM, García AJ. *Vasculogenic bio-synthetic hydrogel for enhancement of pancreatic islet engraftment and function in type 1 diabetes*.Biomaterials 2013. 34(19):4602–11.

[113] Pedraza E, Brady A-C, Fraker CA, Molano RD, Sukert S, Berman DM, et al. *Macroporous three-dimensional PDMS scaffolds for extrahepatic islet transplantation*.Cell Transplant 2013. 22(7):1123–35.

[114] Smink AM, Hertsig DT, Schwab L, van Apeldoorn AA, de Koning E, Faas MM, et al. *A Retrievable, Efficacious Polymeric Scaffold for Subcutaneous Transplantation of Rat Pancreatic Islets*.Ann Surg 2017. 266(1):149–57.

[115] Song S, Blaha C, Moses W, Park J, Wright N, Groszek J, et al. *An intravascular bioartificial pancreas device (iBAP) with silicon nanopore membranes (SNM) for islet encapsulation under convective mass transport*.Lab Chip 2017. 17(10):1778–92.

SECTION 2

DETAILED DESCRIPTION OF EXPERIMENTAL MATERIALS AND METHODOLOGIES

Chapter III

Materials and Methods

Chapter III

Materials and Methods

OVERVIEW

Under the scope of this thesis, several methodologies were used to understand the mechanism behind the proposed system. This chapter aims to contextualize in more detail the information about the materials and techniques used under the scope of this thesis. Although the experimental procedure is described in the experimental section of each corresponding chapter, herein the objective is to give some general theoretical concepts and complement with more detailed information, as well as to justify the selection of the materials and methods employed to develop the systems proposed. **Figure III -1** presents an overview of the materials studied as well as the respective processing and characterization methodologies. It is important to highlight that information related to reagents suppliers and specifications of general equipment are described in each chapter of **Section 3** and will also be described here.

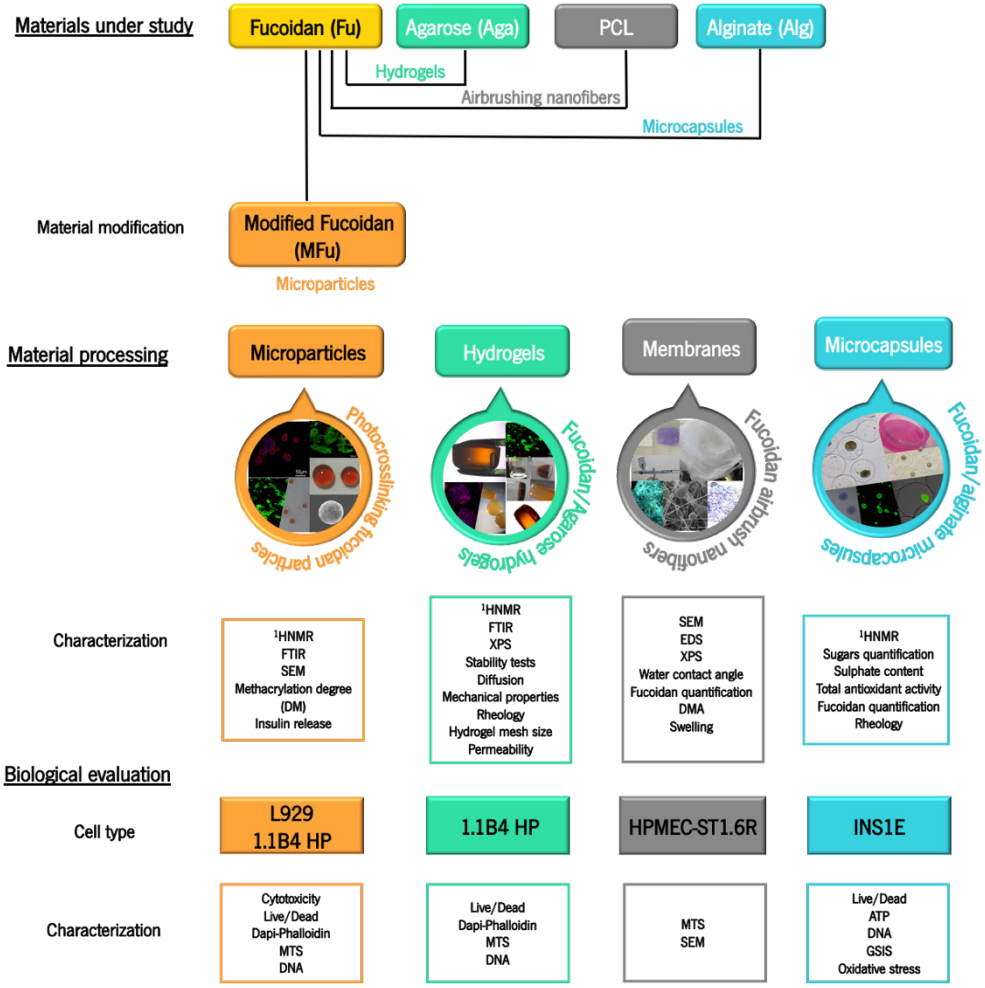


Figure III-1. Schematics overview of the materials studied and respective processing and characterization techniques. (Legend in alphabetic order: DMA - Dynamic mechanical analysis; Diffusion; DM- Methacrylation degree; EDS - Energy dispersive X-ray spectroscopy; FTIR - Fourier transform infrared spectroscopy; GSIS – Glucose-induced insulin secretion; ¹H-NMR - Proton nuclear magnetic resonance; 1.1B4HP – Human pancreatic cells; HPMEC-ST1.6R – Human pulmonary microvascular endothelial cells; INS1E – Rat insulinome cells; L929 - Mouse lung fibroblast cell line; PCL - Poly (ε - Caprolactone); SEM - Scanning electronic microscopy; TEAC - Total antioxidant activity; WCA - Water contact angle; XPS – X-ray photoelectron spectroscopy).

III-1. MATERIALS

III-1.1. Fucus vesiculosus and Ascophyllum nodosum

Algae are autotrophic, aerobic species that, like vascular plants, contain chlorophyll, being thus photosynthetic organisms. They grow in water or on shorelines and "seaweed" is a common name for marine algae [1]. Owing to adaptation to the extreme conditions in which they grow, marine algae contain unusual components as compared to plants. Marine algae can be grouped into three major classes based on the photosynthetic pigments displayed: red, brown and green. Botanists refer to these groups as Rhodophyceae, Phaeophyceae and Chlorophyceae, respectively [2,3]. The second most common type of algae, Brown Algae (Phaeophyte), contains a variety of active components. The structure of their cell walls is made up of an amorphous matrix of acid polysaccharides, bound by proteins. These acid polysaccharides are mainly composed of fucoidan and alginic acid, which confer structural toughness and flexibility to seaweed **(Figure III - 2)** [4]. Fucoidan usually constitutes about 5%–10 % of dry algal biomass, depending on the species, the part of the thallus being used and the harvesting period [2,3,5]. The sulfated polysaccharide, fucoidan, can be isolated from different species of brown algae such as *Fucus vesiculosus* [6], *Undaria pinnatifida* [7], *Ascophyllum nodosum* [6], *Bifurcaria bifurcata* [6,8], *Sargassum* [9] and *Kelp* [10]. Fucoidan isolated from *Fucus vesiculosus* and *Ascophyllum nodosum* were selected based on their bioactive properties namely anti-diabetic.

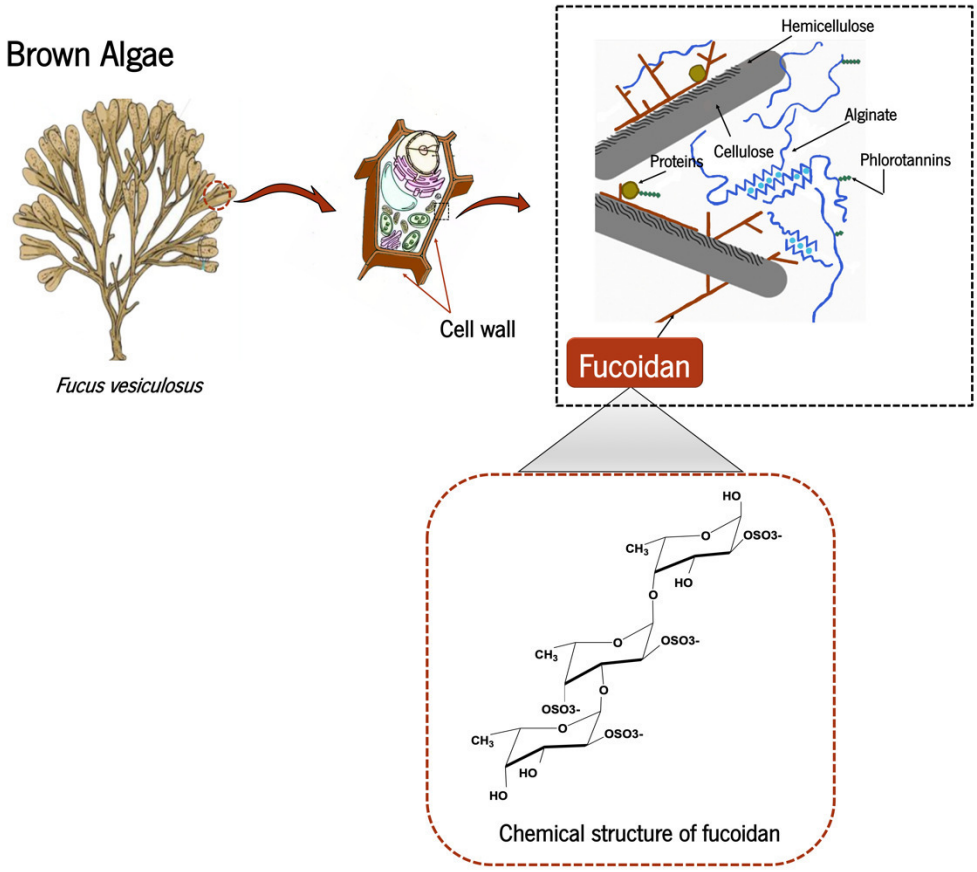


Figure III-2.Schematic representation of brown algae as well as the cell wall where fucoidan is present.

III-1.2. Fucoidan

Fucoidan is a sulfated polysaccharide present in the cell wall of brown seaweeds and some marine invertebrates, such as sea urchins and sea cucumbers **(Figure III - 3)** [11–13]. As mentioned before, fucoidan usually constitutes about 5-10 % of dry algae biomass [2]**.** The principal components of fucoidan are L-fucose and sulfated groups, together with varying amounts of other sugar residues, as glucuronic acid and xylose, with the composition varying with algae species [14,15]. Because of the presence of uronic acid in its structure, fucoidan has been compared with mammalian glycosaminoglycans (GAGs) that are composed of repeating disaccharide units of amino sugars and uronic acid [14]**.** The chemical structure of fucoidan is a polymer chain of (1⟶3)-linked α-l-fucopyranosyl residues, although it is possible to find alternating (1⟶3) and

(1→4)-linked α-l-fucopyranosyl residues [16]. In the **Figure III - 3** we can observe different chemical structures of fucoidan. However, some factors can be influencing the chemical composition of the polysaccharide, such as the season, geographic location, species, the maturity of the plant and also the process of extraction [3,16–19]. Fucoidan can be extracted using different methods such as ultrasonic or microwave-assisted extraction [20], ethanol/water [21,22]**,** and acidic solutions (classic chemical extraction) [23] and through enzymatic processes [9]. Although the different extraction methods have different methodologies, the initial part of the procedure is similar, since the granulated algae need a pre-treatment with ethanol to remove mannitol, lipids, salts, and color pigments [24]. The color of fucoidan is related to the amount of fucoidan present in the powder, from white or creamy (small amounts) to dark brown color (highest amounts). In the last decades, fucoidan has been extensively studied and isolated from different species of brown algae such as *Fucus vesiculosus*, *Ecklonia cava*, *Undaria pinnatifida,* and *Ascophyllum nodosum* [3,11]. Fucoidan exhibits a wide variety of biological properties. Among them are anticoagulant, antioxidant, antiviral, antithrombic, reducing blood sugar and anticancer activities [3,11]. In this work it was used fucoidan from two different species: from *Fucus vesiculosus* (Maritech® Fucoidan, Marinova, Australia, batch # FVF2011527) and *Ascophyllum nodosum* (Ascophycient, Algues & Mer, France, batch # ASPHY16241), herein known as FF and FA. Fucoidan from two different species were used to study the influence of chemical features, as molecular weight (FA < FF) and sulfation degree (FA < FF) on the performance of the derived biocomposites.

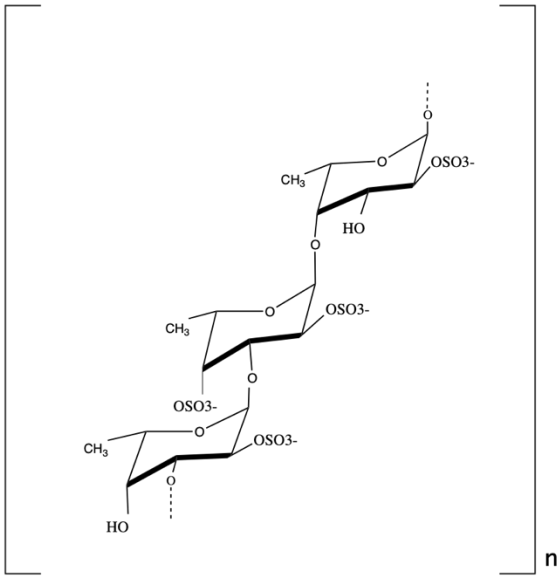


Figure III-3. Chemical structure of Fucoidan from species *Fucus vesiculosus and Ascophyllum nodosum*.

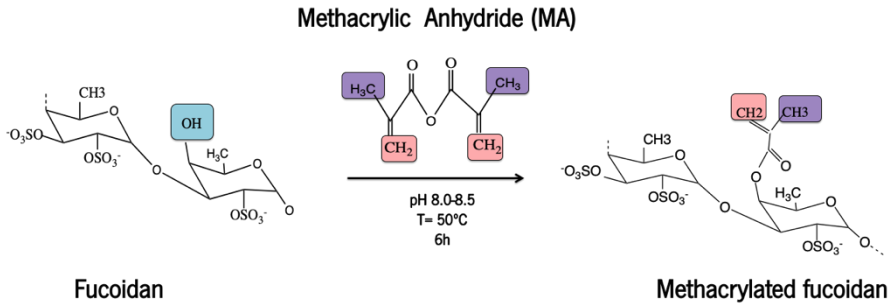
III-1.3. Purification of fucoidan

Due to their natural origin and non-standardized methods of purification, fucoidans form a complex family of polysaccharides varying in molecular weight, structure and composition. In order to minimize this natural heterogeneity, a purification method was used in fucoidan. Prior to any use, commercial fucoidan from Fucus vesiculosus (Maritech® Fucoidan, Marinova, Australia, Cat N FVF2011527) and Ascophyllum nodosum (Ascophycient, Algues & Mer, France, batch # ASPHY16241) were purified, based on the calcium ions methodology [25]. The purification with calcium ions was performed to remove the alginates contained in crude fucoidan. These alginates residues from complexes with calcium ions and precipitate [25]. The purification of fucoidan (PFu) was achieved after dissolution (160 mg/mL) of fucoidan (Fu) with calcium acetate aqueous solution (20 mM) (Sigma, USA, Cat N C1000) during 4 hours at 50 °C under magnetic stirring and the pH was constantly adjusted continuously between 6.6 and 7.5, to avoid acid hydrolysis of fucoidan. The solution was left at 4 °C overnight and then centrifuged 15 min at 8000 rpm (Allegra X-15R centrifuge, Beckman-Coulter France, Villepinte, France). The supernatant was dialyzed against

water using 12–14 kDa cutoff dialysis membranes (Sigma, USA, Cat N D9652) for 3 days at room temperature, frozen at -80 °C (Thermo scientific, Model VXE380, serial n° 50611005) and then lyophilized (Telstar, Model CryoDos-80, serial n° 1414) [25].

III-1.4. Methacrylated fucoidan (MFu)

Methacrylation reaction of fucoidan is described in this thesis **(Chapter IV)**, where ester bonds were introduced in the Fu backbone, enabling the formation of chemically crosslinked hydrogels upon exposure to visible light (VIS) [14]. The reaction of fucoidan methacrylation (MFu), with various degrees of methacrylation (DM), was synthesized by substituting the hydroxyl (-OH) groups of fucoidan (Fu) with methacrylic groups **(Figure III - 4)**. Briefly, Fu was dissolved in distilled water (DH_2O) at a final concentration of 4 % (wt/v) at 50 °C until the polymer was fully dissolved. Methacrylic anhydride (MA, Sigma, Germany, Cat N 276685) was added, at once, to the Fu at concentrations of 8 and 12 % (v/v) and allowed to react for 6 hours, under continuous stirring, at 50 °C. The pH of the reaction was periodically adjusted to pH 8.0 with 5.0 M sodium hydroxide solution (NaOH) (Panreac, Spain, Cat 131687). The modified fucoidan solutions were dialyzed against water using 12–14 kDa cutoff dialysis membranes (Sigma, USA, Cat N D9652) for 3 days at 4 °C to remove the excess of unreacted MA. MFu solutions were frozen at –80 °C (Thermo scientific, Model VXE380, serial n° 50611005) and then lyophilized (Telstar, Model CryoDos-80, serial n° 1414). MFu was further purified with acetone and lyophilized for 4 days. The obtained powder was stored at 4 °C, protecting from light until further use [14].



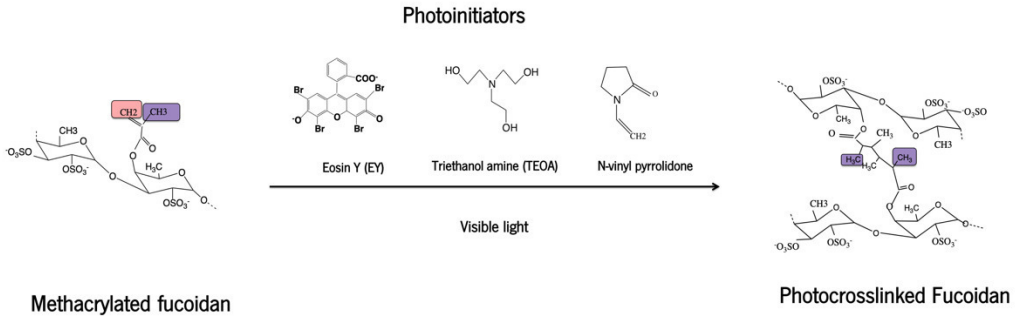


Figure III-4. Scheme–of the possible reaction mechanism of fucoidan and methacrylated anhydride and further crosslinking mediated by visible radiation (fucoidan (Fu), Methacrylated Anhydride (MA), and photoinitiators (Eosin Y (EY); Triethanol amine (TEOA); N-vinyl pyrrolidone).Reaction scheme adapted from [9,22,23].

III-1.5. Agarose

Agarose is a natural linear based polysaccharide extracted from red algae (Rhodophyceae), and it is the major component of agar, with the other component being agaropectin [28,29]. Agarose has a neutral charge and lower degree of chemical complexity when compared to agaropectin, which makes it less likely to interact with biomolecules, such as proteins [30]. This polysaccharide is a linear polymer consisting of alternating D-galactose, and 3,6-anhydro-L-galactose units (chemical structure schematized in **Figure III – 5**). Agarose is heated to 90 °C to form a polymeric solution by solving agarose powder with water or phosphate saline buffer. When the temperature is lowered to close to room temperature (fluctuations may take place considering the several commercially available agarose products), gelation occurs. Gels produced from agarose has been used in biomedical field, namely on cartilage, nervous system, cardiac, bone, corneal regeneration and diabetes treatment [31,32]. Despite the slow degradation profile, the soft and flexible structure provided by these gels recreates a 3D environment [33]. In this thesis, agarose hydrogels (3 and 5 %, Agarose of low temperature of gellification of analytic grade (Sigma-Aldrich, USA)) were used as encapsulating systems of 1.1B4 pancreatic Cell lines, as described in **Chapter VI**, by dissolving a 3 or 5 % of agarose solution in fucoidan solutions and transfer into molds to cool down at room temperature and form the hydrogels.

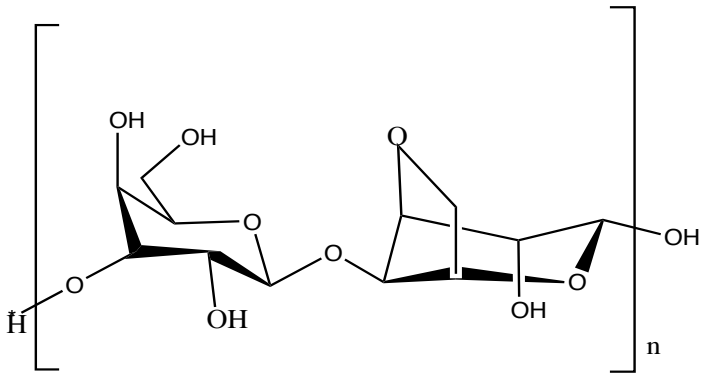


Figure III-5.Chemical structure of agarose.

III-1.6. Alginate

Alginate (ALG) is one of the most studied polysaccharides in tissue engineering (TE), being quite abundant in nature. It is found in the cell walls of brown algae or as a capsular polysaccharide in some soil bacteria [34–36]. Alginate is a linear unbranched copolymer that consists of residues of β-D-mannuronic acid (M) and α-L-guluronic acid (G) linked by 1,4-glycosidic bonds. Both residues are covalently linked in different sequences, namely, rearranged in homopolymer (GG blocks and MM blocks) or heteropolymer block structures (GM blocks) [37,38] **(Figure III - 6)**. The length and distribution of the M and G-blocks along the polymer chain varies depending on the source of the ALG. Additionally, the carboxyl groups from both blocks can be deprotonated above the pH values of 3.2 and 4, respectively, for G and M-blocks [36,39,40]. Thus, the stimuli-responsiveness toward pH makes ALG behaves as a polyanion in such media, being a polyacid ($pK_a \approx 3.4$ or 3.65 for glucuronic and mannuronic acid units, respectively). The sol transition of ALG is ionotropic, requiring the presence of ions for gelation [41–44]. The stability of the ionic cross-linking is highly dependent on the type of ions used, being stronger in the presence of divalent cations (such as calcium (Ca^{2+}), barium (Ba^{2+}) and magnesium (Mg^{2+})) than with monovalent ones (such as sodium (Na^{+}) and potassium (K^{+})). Thus, in the presence of divalent cations, ionic interactions are established with blocks of glucuronic acid residues, resulting in the formation of a three-dimensional (3D) network that is usually described by the "egg-box" model [36,39,40,42,43].

According to this model glucuronic chains in ALG form electronegative cavities to host divalent cations [36]. This polymer has been widely used, for example, for drug delivery, cell encapsulation and in the food industry, usually for gels preparation by ionotropic gelation with calcium ions. ALG are known to lack mammalian cell-adhesive ligands, which are important to promote and regulate cellular interactions, and support low protein adsorption being frequently combined with other materials or modified [45–48]. In the **Chapter VIII,** alginate microcapsules containing rat insulin cells (INS1E cells) or rat/pig islets were used as controls to evaluate the efficiency of the strategy used to encapsulate cells in Alginate/fucoidan microcapsules.

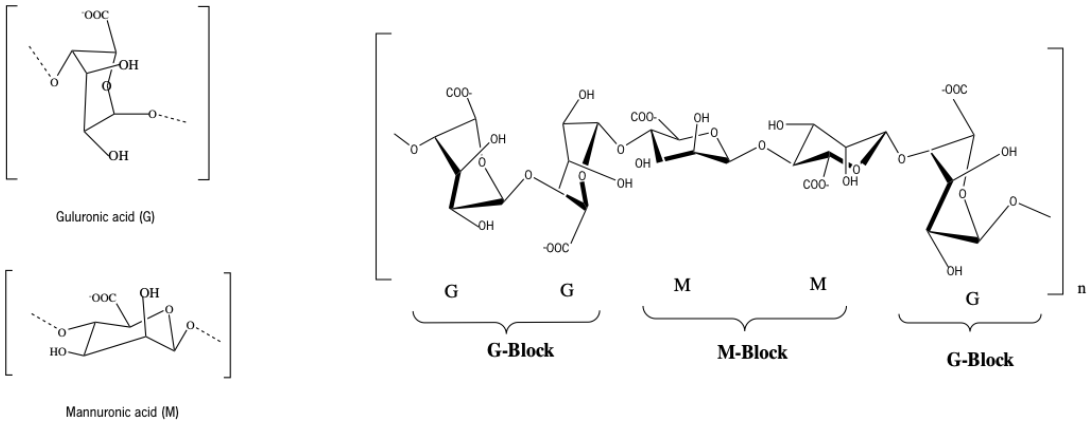


Figure III-6. Chemical structure of alginate (M-(1-4)-β-D-mannuronic acid and G-α-(1-4)-L-guluronic acid residues).

III-1.7. Poly (ε- caprolactone) PCL

Poly (ε-caprolactone) (PCL) is a synthetic biodegradable polyester obtained by ring-opening polymerization of ε-caprolactone, whose chemical structure is shown in **Figure III - 7**. It is a hydrophobic and semi-crystalline polymer whose crystallinity increases with increasing molecular weight, with a melting point around 60 °C and a glass transition temperature around -60 °C [49]. It has good solubility at room temperature in several organic solvents, which makes it suitable for both melt and solvent-based approaches in tissue engineering [50]. PCL is a Food and Drug Administration (FDA) approved material to be used in the human body like a drug delivery device,

suture, or adhesion preventing barrier [51,52]. In physiological conditions such as in the human body, PCL is degraded by hydrolysis of its ester bonds [53,54]. However, the degradation is slow, and its properties remain almost unchanged for at least 6 months, and its shape may not change over a few years [55,56]. Nevertheless, its degradation products do not accumulate in the body and are completely excreted and do not show adverse host tissue reactions but instead good biocompatibility [55,56]. The slow hydrolytic degradation of PCL is dependent on its crystallinity, molecular weight, hydrophobicity, and on the scaffold porosity and surface-to-volume ratio [57]. Additionally, the degradation rate may also be tuned by preparing blends with materials with higher degradation ratios, such as some calcium phosphates and starch. PCL (Mw 70,000 - 90,000 by GPC) purchase to Sigma was selected for the preparation of the 2D and 3D supports by airbrushing technique since it is a simple material to process, to modify and with promising good compatibility. PCL was used to prepare airbrush nanofibrous with and without fucoidan in the work reported in **Chapter VII.**

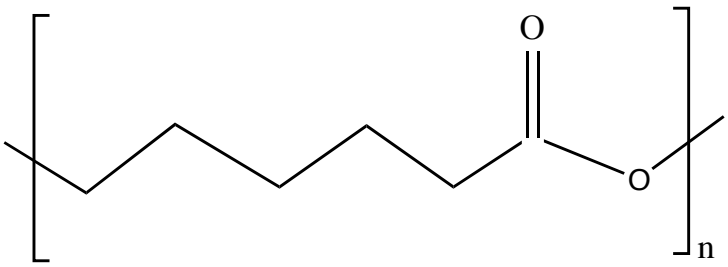


Figure III-7. Chemical structure of poly (ε- caprolactone) (PCL).

III-2. METHODOLOGIES FOR PROCESSING OF BIOMATERIALS

III-2.1. Superhydrophobic surfaces

The superhydrophobic methodology was used as a platform to produce hydrogel particles. This methodology was inspired in the water repellent properties of the lotus leaves, demonstrating

that the water droplets acquire an almost spherical shape when they are on the top of those natural surfaces due to the combination of micro/nano topographical features and low surface energy [37,58,59]. Superhydrophobic surfaces have been proposed for the preparation of polymeric spherical particles, under mild conditions and with 100% drug encapsulation efficiency [14,60–62]. This technology allows one to obtain barely spherical particles with controlled sizes, highly dependent on the volume of the liquid droplets deposited onto the superhydrophobic surfaces [14,63].

Microscope glass slide (Mgs) superhydrophobic surfaces were used in **Chapter IV** and were obtained by promoting a coating with candle soot, which is a simple, fast, and inexpensive method **(Figure III - 8)** [64]. Briefly, a microscope glass slide (Fisher scientific, USA, Cat n° 10149870) was held above the flame of a paraffin candle to form a thin carbon layer (soot). Afterward, the soot-coated substrates were further modified with a silica layer using chemical vapor deposition, by exposing it to vapors from 4 mL of tetraethyl orthosilicate (TEOS) (VWR, USA, Cat n° 8.00658.1000) and 4 mL of aqueous ammonium solution (Laborspirit, Portugal, cat n° 05002) (30–33 %) during 24 hours. The modified microscope glass slides were then heated at 600 °C for 2 h (EBA1350°C Ceramica, Fornoceramica, Portugal), to promote the calcination of hybrid carbon/silica coating. Further, the material was exposed (without immersion) to 1H, 1H, 2H,2 H-perfluorodecyl-trichlorosilane (PFDTS) (Sigma, USA, Cat n° 658758) for 3 days to form the desired superhydrophobic surfaces [14].

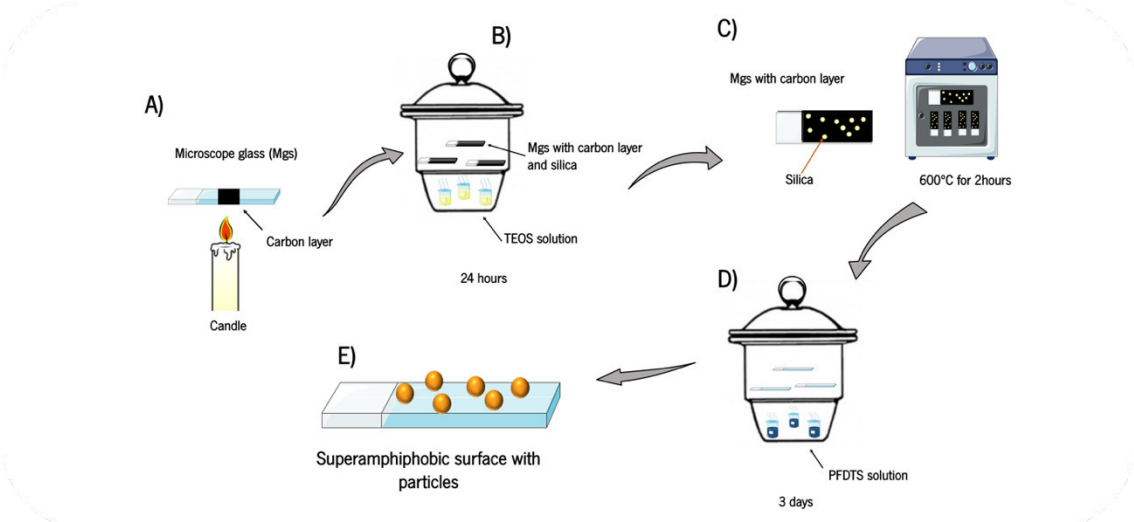


Figure III-8. Scheme representative of glass superhydrophobic surface (G-SHS). A) formation of carbon layer (soot) in microscope glass slide with flame of paraffin candle, B) modification of soot-coated substrates with silica layer,

C) calcination of hybrid carbon/silica coating, D) formation of desired superhydrophobic surfaces by exposed the materials with PFDTS and E) Superhydrophobic surface with particles.

III-2.2. Fucoidan-based particles

Some studies highlighted the benefits of photo-cross-linking with visible radiation over UV radiation [14,65], enlarging the applications in the biomedical area (e.g., light-sensitive organs). The exploitation of visible light instead of at UV light through the combined used of eosin-y and triethanolamine, although not new, represents a promising method to obtain biocompatible hydrogels since it significantly reduces the cytotoxic effects of UV light [14,66–69]. Fucoidan-based particles (MFu particles) were formed by photocrosslinking with visible light **(Figure III – 9)**. Briefly, freeze-dried MFu (5 % m/v) with different DM was added to a photoinitiator (PI) solution consisting of 0.3 % (m/v) eosin Y (Sigma, USA, Cat n° E4009) (photoinitiator) in N-vinylpyrrolidone (JMGS, Portugal, cat n°140925000) (comonomer) and 5 M triethanolamine (TEOA) (Sigma, USA, cat n° T58300) (co-initiator) in water, at room temperature until complete dissolution [14,67,70]. Drops of 1–5 μL of MFu and photoinitiators solution were dispensed onto the superhydrophobic surface, forming spherical particles with different sizes in a single step, benefiting from the high repellency of the surfaces that hinders the solution to spread, thus keeping the integrity of the spheroidal liquid particles. The drop-loaded surfaces were left below visible light (visible light, T5-8W-220–240 V/50–60 Hz) for 15 min to promote photo-cross-linking. Finally, the particles were removed and washed with Dulbecco's phosphate-buffered saline (DPBS) (Alfagene, Portugal, Cat n° 21600-044) and water to remove all residues of non-photo-cross-linked polymer and photoinitiators. Particles (wet state) with diameters ranging from 0.2 to 2 mm could be obtained, illustrating the versatility of this processing technology. Nevertheless, particles produced using 1 μL drops were used in further studies [14].

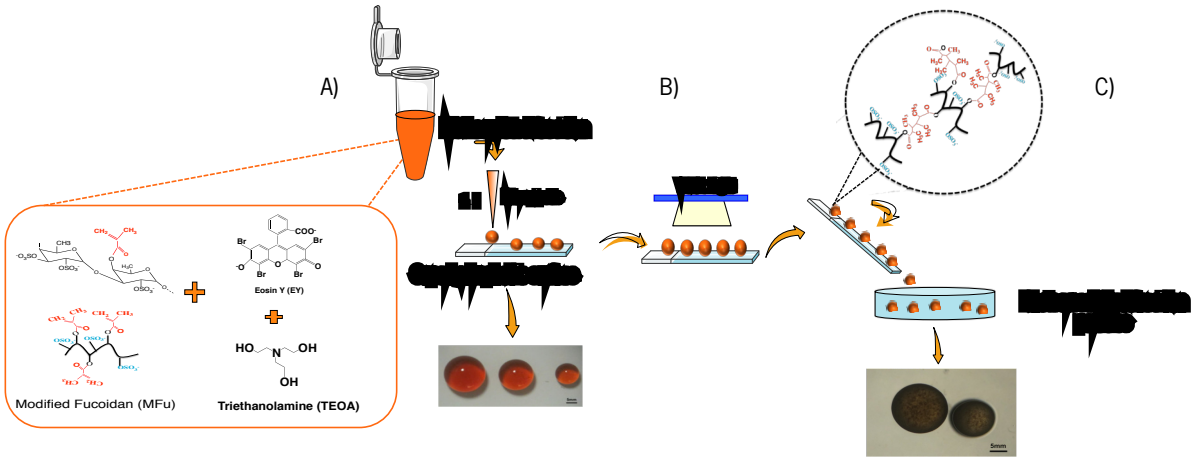


Figure III-9. Scheme depicting the methodology for the production of modified fucoidan particles (MFu). A) Pipetting volumes between 1 to 5 µL of the solution of methacrylated fucoidan with photoinitiators, B) Crosslinking of fucoidan-based particles with visible light, and C) Stable fucoidan hydrogel particles with or without encapsulated cells. Adapted from [14].

III-2.3. Agarose/fucoidan hydrogels (Aga and AgaFu hydrogels)

Hydrogels of agarose have been proved to be biologically compatible, and thus they have been widely used for cell encapsulation in numerous *in vitro* and *in vivo* studies, envisioning biomedical applications [71,72]. For this reason, agarose was selected to be used in **Chapter VI** as a gelling material. Agarose hydrogels (Aga hydrogels) were produced by dissolving 3 or 5 % (w/v) of agarose (low temperature of gellification) in powder (Sigma-Aldrich, USA) prepared in distilled water and heated to 75-80 °C for 15 min until complete homogenization was observed. The solution was then allowed to cool at room temperature in appropriated mold, thereby decreasing the temperature and promoting gelation; afterwards the hydrogels were removed from molds and used for different characterization tests **(Figure III - 10)**.

Agarose/fucoidan hydrogels (AgaFu) were formed by thermo gelation reaction, through the sol-gel transition of mixtures of agarose and fucoidan [73,74]. Purified fucoidan (Fu) was dissolved in distilled water at a concentration of 3 or 5 %(w/v) under stirring and at 75 °C, and then Agarose (Aga) powder was then added to the Fu solutions. The AgaFu hydrogels were prepared at different Aga/Fu proportions (4:10; 5:10 and 7:10 wt) and represented as AgaFu 3X or AgaFu 5X (where different letters in X represent different formulation), throughout the thesis. The obtained solution

was then transferred into appropriated molds, and the hydrogels were progressively formed until room temperature was reached. The hydrogels were removed from molds and replenished with DPBS to enable the complete gel formation **(Figure III - 10)**.

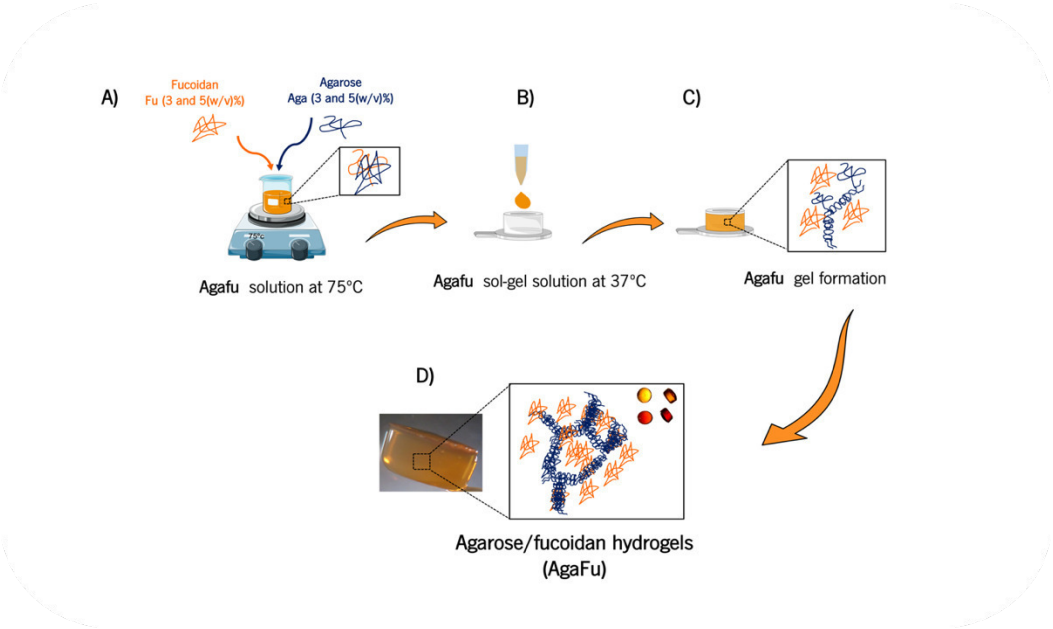


Figure III-10. Schematic representation for the production of agarose-fucoidan hydrogels (AgaFu). A) reparation of agarose (Aga) or agarose/fucoidan (AgaFu) solutions, B) transferring of Aga or AgaFu solutions to molds, C) Aga or AgaFu gel formation by cooling the solution at room temperature and D) AgaFu hydrogels.

III-2.4. Alginate/fucoidan beads produced by a droplet generator

Several methods, such as extrusion or emulsification, were used for the production of microcapsules with applicability in different contexts [75], including for cells encapsulation, as is the case of pancreatic islets. The extrusion method is the most popular method, where the islets mixed within a polymer solution are forced through a nozzle, and the microcapsules are formed under the influence of gravity, coaxial airflow or electrostatic potential [76]. Microcapsules are mechanically stable and are generally very simple to construct, encapsulating one or a few islets. These can be obtained in many different forms, sizes, compositions, and with different permeability [77]. An advantage over macrocapsules is that they have an optimal volume-to-surface ratio, which implies a faster exchange of glucose, insulin, and nutrients [78–81]. Nevertheless, the difficulty

associated with retrieving microcapsules from the recipient is a major disadvantage, particularly when there is pericapsular fibrotic overgrowth [76,82–84].

Microcapsules of alginate (ALG) and alginate/fucoidan (Fucocaps) were produced in the work developed in the context of this thesis for encapsulation of pancreatic cells and islets, by using an air-driven droplet generator (Nisco D-0038, Zurich, Switzeland, Nozzle from Biored, California, USA), as schematically represented in **Figure III - 11.** For that, alginate (ALG) and fucoidan (Fu) were dissolved overnight in an aqueous solution to obtain sodium alginate solution (2.2 % wt) and sodium alginate and fucoidan solutions (2.2 % and 0.5 % wt) (Fucogel). After complete dissolution and filtration, the prepared solutions were extruded using a droplet generator connected to a syringe pump (at rate 16 mL/min), with an air flow of 4 L/min. The ALG or Fucocaps droplets/beads were collected in a 145 mm petri dish, containing 50 mL of 20mM barium chloride ($BaCl_2$) as gelling solution, placed 16.5 cm from the tip of the nozzle of the generator. The ALG or Fucocaps microcapsules were incubated in this solution for 2 min and then washed three times with 0.9 % sodium chloride (NaCl) solution or with Dulbecó s phosphate buffered saline (DPBS) to remove excess $BaCl_2$. The microcapsules were allowed to settle between washings, and the supernatant discarded. Microcapsules were then placed in DPBS and maintained at 37 °C in air with 5 % CO_2 until further use [38]. $BaCl_2$ was selected to be used as gelling solution instead of the common calcium chloride ($CaCl_2$) solutions, as microcapsules gelation with Ba^{2+} ions has better strength and stability, according to the studies developed by *Morch et al* [85].

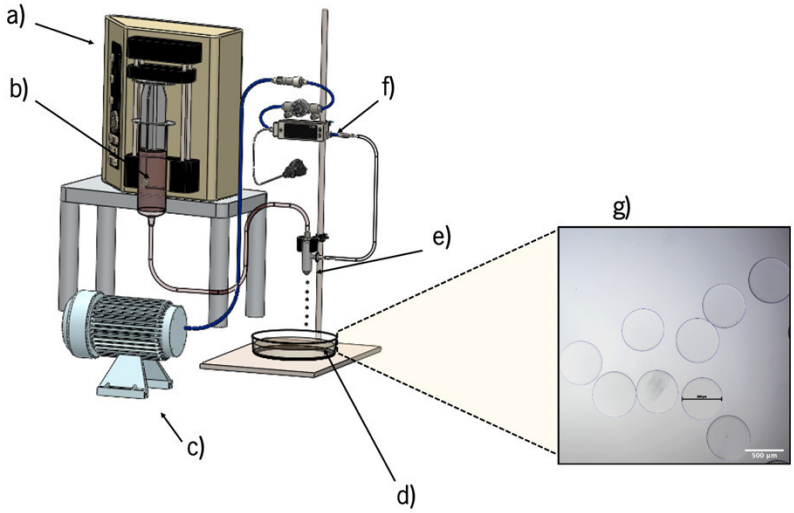


Figure III-11. Schematic representation of the methodology used for the production of alginate/fucoidan microcapsules (ALG or Fucocaps). a) Syringe pump, b) polymer solution (alginate or alginate/fucoidan (fucogel)), c) air compressor, d) precipitation bath, e) nozzle, f) flow meter, and g) microcapsules.

III-2.5. Production of PCL nanofibrous by airbrushing

III-2.5.1. Airbrushing

Nanofiber mats and scaffolds have been widely investigated for biomedical applications since they mimic the fibrous nanostructure of a native extra-cellular matrix (ECM) [86–88]. These mats can be used in different applications such as drug delivery, wound dressings [87], tissue engineering [88], and enzyme immobilization [89–91]. Electrospinning is the most common method for making nanofibrous for tissue engineering scaffolds [92,93], but compressed gas can also be used to blow polymer solutions as fibers into a collector, in a process that is called solution spraying, solution blow spinning (SBS) or airbrushing [91]. Airbrushing is a low cost technique that

can be used in a variety of applications, with biomedical engineering being highlighted, showing enhanced cell infiltration and proliferation [90]. Airbrushing is a fiber manufacturing process requiring two parallel concentrate fluid streams: a polymer dissolved in a volatile solvent and a pressurized gas flowing around the polymer solution, creating fibers that are deposited in the direction of gas flow **(Figure III - 12).** Generally, an airbrush setup consists of a compressed gas source for delivering the carrier gas and a commercially available airbrush (**Figure III - 12).** Airbrush also has the ability to deposit conformal fibers with a deposition rate approximately 10 times faster than traditional electrospinning on both planar and nonplanar substrates [94–96]. The unique attributes of airbrush provide a means to explore the utility of nonwoven fibrous materials in new fields. New opportunities for applications include rapid biological scaffold generation and custom *in situ* materials fabrication. Airbrush does not require an electric field and uses a simple apparatus. The method is, therefore, easily implemented using inexpensive, transportable, and hand-held equipment [94]. When deployed as a technique to deposit materials *in situ*, airbrush is capable of additive deposition of microfibers or nanofibrous in custom conformal geometries. Because the process is contained inside the spinning system, and the solvent usually evaporates within the working distance (typically 10–20 cm, but varies based on solvent volatility), polymers fibers are deposited without any further drying, cooling, or washing. The production of airbrush fiber depends on the molecular weight of the polymer, its concentration, viscosity, and process variables such as gas pressure and the flow rate of the polymer solution [90]. Airbrush has been used to easily create fibers conferred with unique morphologies, various microstructural features, and diverse mechanical properties. Fibers with diameters ranging from ~100 nm to greater than 1 μm can be fabricated by the airbrush technique [90]. The airbrush apparatus used in this PhD work comprises a commercially available airbrush designed for painting (Airbrush, DEXTER, Model DX-1839, Spain 0.3 mm. nozzle diameter), (**Figure III - 12).** The airbrush was connected to compressed air (Wuto, model: TC-20 series, Spain) and different distances from the nozzle to the target where tested until establishing the best condition. Different types of substrates (plastic, metal, aluminum foil and vegetable paper) were tested as a target.

III-2.5.2. Airbrushing nanofibrous meshes of PCL and PCL/fucoidan (PCLFu)

To produce polycaprolactone (PCL) airbrushed nanofibrous mesh, a PCL solution of 4 % (w/v) PCL solution in chloroform (Sigma Aldrich, Germany) was prepared and placed in the airbrush connected to compressed air. The distance from the nozzle to the target was held constant at 50 cm for all experiments, collecting the random nanofiber mesh on a plastic surface or the patterned nanofiber mesh on a metallic wire net. These were the optimized processing conditions of PCL nanofiber meshes, resulting from an optimization procedure where three variables/parameters were systematically studied: the distance to the target, polymer concentration, and air pressure. After being produced, the PCL airbrushed nanofibrous meshes were dried in a desiccator at room temperature for 1 day allowing for complete evaporation of the solvent. To produce PCL/fucoidan (PCLFu) airbrush nanofiber meshes, different quantities of fucoidan (FA and FF) dissolved in acetic acid were added to the PCL solution previously prepared and let to stir until homogenization (~ 3 hours) [97]. The airbrushing procedure was similar to the one just described but using an alternate layer by layer process: firstly, only PCL, then PCLFu, repeated until having deposited 6 layers of each and having PCLFu as the external layer. Then, PCLFu airbrushed nanofibrous meshes were dried for 3 days in a desiccator to evaporate the solvent and cut into samples of 1x1 cm^2 for further assays.

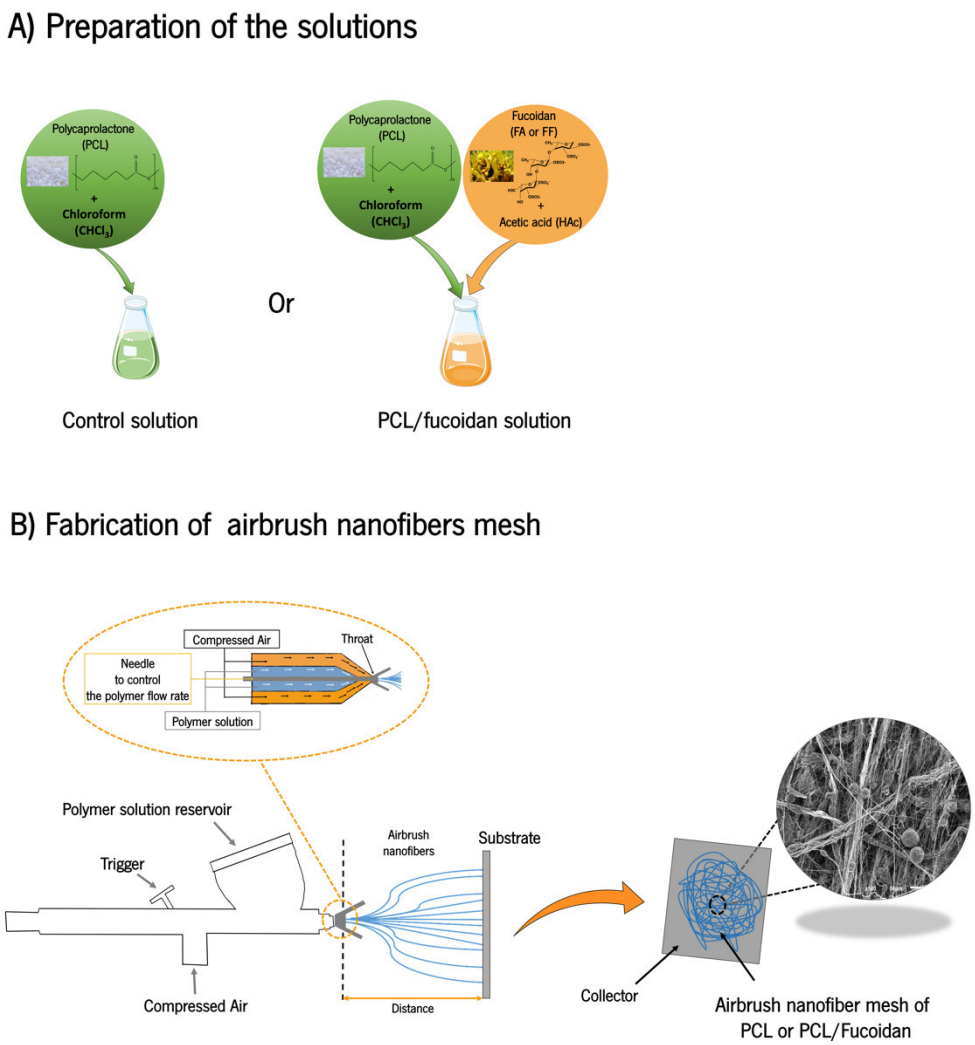


Figure III-12. Schematic overview of the experimental steps required to fabricate airbrushed nanofibrous of PCL and PCLFu. A- Preparation of PCL or PCLFu solutions and B - Fabrication of airbrushed nanofibrous mesh, evidencing the airbrushing equipment and the resulting nanofibrous mesh.

III-3. TECHNIQUES USED FOR CHARACTERIZING THE DEVELOPED MATERIALS/STRUCTURES

III-3.1. Morphological characterization: Scanning electron microscopy (SEM)

Scanning Electron Microscopy (SEM) is a commonly used technique to analyze the topography of the solid materials and structures that gives high-resolution 2D images of a sample [98]. This procedure consists of the use of a focused beam of high-energy electrons capable of generating signals at the surface of the solid sample. By scanning sample's surface with a focused beam of electrons that interact with the atoms of the sample at various depths, scattered electrons produce a diverse type of signals which are detectable by the SEM equipment and transformed into a 2D image. Samples can be scanned at low to a high vacuum, cryogenic to elevated temperatures, as well as moisture conditions. SEM provides qualitative information regarding the sample's surface morphology, including microstructure, lumen and wall thickness, topography, and composition. In this thesis, SEM was employed in **Chapters III, IV, and VI** for the assessment of the surface of the particles as well as surface morphology of airbrushing nanofibrous. The morphology of produced materials was analyzed on a scanning electron microscope (SEM) (Jeol, JSM-6010LV, Japan). Prior to analysis, all the samples were coated with a conductive material (gold) by sputtering using a sputter coater (Cressington, model 108A, United Kingdom), with the aim to increase the degree of magnification, avoiding the damage of the samples by the high-energy electron beam.

III-3.2. Chemical characterization

III-3.2.1. Fourier transform infrared spectroscopy (FTIR)

Fourier transform infrared spectroscopy (FTIR) is an analytical method used to obtain information about the sample's chemical structure and chemical bonding. FTIR spectrum is obtained through the determination of absorbed incident radiation at given energy and corresponds to the frequencies of vibrations between the bonds of the atoms present within the molecule [99,100]. Thus, one can identify the presence of chemical groups on the sample through the FTIR

spectrum. The attenuated total reflection (ATR) sampling mode can be used to increase the intensity of the surface signal because it analyses the region near the surface. However, FTIR-ATR is not truly surface sensitive, due to the high penetration depth of the IR beam (1-5 μm) [101], thus care should be taken while preparing the sample. Nevertheless, the rich structural information that the IR spectra provide makes the FITR-ATR a valuable technique to evaluate chemical changes, such as the grafting of polymers with functional groups. In the initial stage of the work presented in this thesis, FTIR analyses were applied to the study of fucoidan and modified fucoidan composition. The analyses were performed with a FTIR spectrophotometer (Shimadzu IRPrestige 21 A21004200704). The samples were prepared by pressing the powder with potassium bromide (KBr) into a small disc. The FTIR spectra were recorded from 400 to 4400 cm^{-1} with a resolution of 4 cm^{-1}. FTIR-ATR analysis was also used to study the composition of the airbrushing nanofibrous, but recording at least 100 scans with a resolution of 2 cm^{-1}.

III-3.2.2. Proton nuclear magnetic resonance (^{1}H-NMR)

Proton-Nuclear Magnetic Resonance (^{1}H-NMR) spectroscopy is a fundamental tool when studying the chemistry of polysaccharides as it allows identification and the study of their structure. This technique measures the magnetic resonance of protons, when materials are submitted to a significant magnetic field. Distribution of electrons in molecules, and hence their resonance frequencies, is distinct in different chemical groups but have proximal resonances in identical chemical groups, enabling the identification of the chemical groups of the polymer. The addition or alteration of a proton in a chemical group of a polymer, through chemical modification of the polymer, results in the alteration of the magnetic resonance of the polymer, and hence a chemical shift or a new peak is created in the ^{1}H-NMR spectrum [102–104]. Since ^{1}H NMR spectra are recorded in solution, protons from the solvent should not interfere in the analysis, thus, samples must be dissolved in a proton-free solvent, as deuterated solvents (e.g. deuterium oxide D_2O). The chemical groups of fucoidans (FA and FF) and methacrylated fucoidan (MFu) were assessed by ^{1}H NMR spectroscopy **(Chapters IV and VIII)**, by collecting the respective spectra in deuterated water (D_2O), at 5 mg/mL and 50 °C, being recorded on Bruker Avance III with the following spectral

conditions: 300 Hz spectra with 90° impulses, 4 s acquisition time. The methacrylation degree (DM, a fraction of modified hydroxyl groups per repeating unit) was determined by the relative integration of the methylene proton peak ($I_{methylene}$, iii) in **Figure III - 13**) of methacrylate groups to methyl protons of the initial standard (I_{CH3}, i) in **Figure III -13**), according to **Equation III -1**, as described elsewhere [14,105,106]. The $n_{methylene}$ and n_{CH3} standard correspond to the number of protons in the CH_2 from the methacrylic group and in methyl groups of fucose, respectively. The n_{OH} monomer corresponds to the number of reactive –OH sites per sugar residue in the Fu structure [14,105].

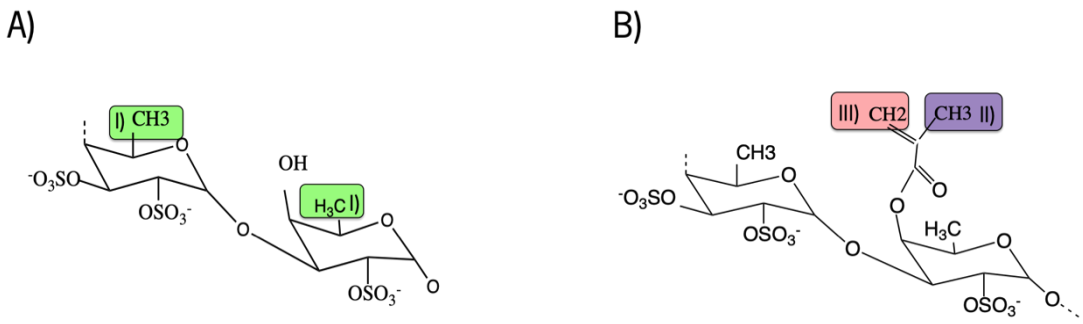


Figure III-13. Scheme of repeating units A) fucoidan, B) methacrylated fucoidan. i) methyl group of fucoidan, ii) methyl group of methacrylates, and iii) methylene groups from methacrylate.

Equation III-1- Methacrylation degree

$$DM = \left(\frac{I_{methylene} / n_{Hmethylene}}{I_{CH3\ standard} / n_{CH3\ standard}} \right) 100$$

III-3.2.3. Electrophoresis and Laser Doppler velocimetry: The Zeta (ζ)- potential

The Malvern Zetasizer device used the combination of electrophoresis and laser Doppler velocimetry techniques for the quantification of the electrical charge of particles, polymers or

proteins, associated to the zeta(ζ)-potential [107,108]. A relation is established between the speed of a particle moving in a liquid and the applied electrical field. These properties will be related to two other known constants of the samples, the viscosity and dielectric constant, to determine the final ζ-potential of the particles. The ζ-potential is calculated according to **Equation III - 2**, where UE-electrophoretic mobility, ζ - ζ-potential, ε - dielectric constant, η - viscosity and f(κa)= Henry's function. The units of κ, termed the Debye length, are the reciprocal length. The parameter 'a' refers to the radius of the particle, and therefore κa measures the ratio of the particle radius to the electrical double layer thickness [107,108]. ζ-potential can be used as an indicator of the tendency of aggregation between similarly charged particles. A value of 30 mV (rather positive or negative) indicates particle stability. A ζ-potential value lower than 30 mV indicates that the attraction forces are stronger than the repulsion ones, leading to the formation of aggregates [109–111]. In this thesis, ζ-potential of fucoidan was determined by dispersing 3 mg of a sample in 5 mL of filtered ultrapure water, pouring the resulting dispersion into a capillary cell with electrodes at either end to which potential was applied. Then, a laser provided a light source that illuminates the particles within the sample. This light source was splatted to provide an incident and reference beam. The incident laser beam passed through the center of the sample cell, and the scattered light was detected. When an electric field was applied to the cell, the particles moved towards the electrodes passing through the laser measurement volume and fluctuated the intensity of light with a frequency proportional to the particle speed. This information is passed to a digital signal processor and then to a computer that produces a frequency spectrum from which the electrophoretic mobility is calculated [108].

Equation III-2- Henry equation

$$U_E = \frac{2\varepsilon\zeta f(K_a)}{3\eta}$$

III-3.2.4. X-ray photoelectron spectroscopy (XPS)

X-ray Photoelectron Spectroscopy (XPS), also called ESCA (from Electron Spectroscopy for Chemical Analysis), is a technique for studying the chemical composition of a material's surface, by analysing the energy distribution of electrons ejected from such material when irradiated with a source of ionized radiation such as X-rays [112,113]. A focused beam of X-rays induces the emission of core-level electrons from the material surface (10-250 Å) with a certain kinetic energy, enabling the determination of bond energy of those electrons, characteristic of a specific chemical element within a specific chemical entity. A survey spectrum provides the elemental composition of the material and high-resolution spectrum of each of the detected elements gives information about their chemical and electronic state [114,115]. XPS was performed for further chemically characterization of agarose/fucoidan hydrogels **(Chapter VI),** fucoidan (FA and FF) in powder and airbrushed nanofibrous meshes of PCL and PCLFu **(Chapter VII).** The chemical analysis of the surfaces was performed by XPS analysis in regard to the carbon, oxygen, and sulfur content. Analyses were performed using a Kratos Axis-Supra instrument equipped with Al-Kα monochromatized radiation at 1486.6 eV X-ray source, using ESCApe software. Due to the no conducting nature of the samples, it was necessary to use a co-axial electron neutralizer to minimize surface charging, which performed the neutralization by itself. Photoelectrons were collected from a take-off angle of 90° relative to the sample surface. The measurement was done in a Constant Analyser Energy mode (CAE) with a 160 eV pass energy for survey spectra and 20 eV pass energy for high resolution spectra of the hydrogels and 20ev or 40 eV pass energy for the polymer powder and airbrushed nanofibrous meshes. Charge referencing was done by setting the lower binding energy of the C1s hydrocarbon peak at 285.0 eV.

III-3.2.5. Energy Dispersive X-ray spectrometry (EDS)

Energy-dispersive X-ray Spectroscopy (EDS) is an analytical technique used for the elemental analysis or chemical characterization of samples [116,117]. Basically, EDS consists of detecting the characteristic X-rays produced by each element after bombarding a sample with a high energy

beam of charged particles in an electron microscope. The number of X-rays emitted by each element present in a sample bears a direct relationship with the concentration of that element (mass or atomic fraction). This information allows converting the X-ray measurements into a final X-ray spectrum, assessing the concentrations of the various chemicals present in the sample [118]. EDS technique was applied in **Chapter VII,** to confirm the presence of fucoidan coating on the surface of airbrushing nanofibrous by tracing nitrogen (present in surface coating, but not in PCL) and sulfur element characteristic of fucoidan. Elemental analysis was carried out with an energy dispersive spectrometer (EDS/EDX; Incax-Act, PentaFet Precision, Oxford-Instruments), attached to the abovementioned SEM equipment**.** Therefore, the samples were analyzed as prepared for SEM. All observations/image acquisitions and measurements were made at an acceleration voltage of 15 kV.

III-3.2.6. Sugars content on fucoidan

Fucoidan represents a range of polymers characterized by a polymeric chain of fucose, often sulfated, with other sugars being also present, namely as substituents. Thus, to better characterize the used samples, it is important to assess molecular weight, sugars contents and sulfation degree. Monosaccharides present on fucoidan samples were determined as alditol acetates as described elsewhere [17,119–121]. Briefly, the pre-hydrolysis of fucoidans (FA, FF) was performed, with 72 % sulfuric acid for 3 h at room temperature. Afterward, the FA and FF extracts were submitted to hydrolysis with sulfuric acid 1 M at 100 °C for 2.5 h. 2-Deoxyglucose was used as an internal standard. Monosaccharides were reduced with sodium borohydride and acetylated by acetic anhydride using methylimidazole as a catalyst. The formed alditol acetate derivatives were analyzed by gas chromatography (GC) with a 30 m column DB-225 (J&W Scientific, Folsom, CA, USA), with internal diameter and film thickness of 0.25 and 0.15 mm, respectively, and using a flame ionization detector (Perkin Elmer, Clarus 400). The hydrolysis of all samples was performed in duplicate, and each one was injected twice. A third analysis was done for the few samples with higher variability. Uronic acids were quantified by a modification of the 3-phenylphenol colorimetric

method [17,119–121]. A calibration curve was made with d-galacturonic acid. The hydrolysis and analysis of the samples were done in triplicate.

III-3.2.7. Sulphate content

The quantification of sulfates in fucoidan was performed based on barium sulfate determination ($BaSO_4$) by turbidimetry following interaction with barium chloride ($BaCl_2$) [17]. Briefly, the conditioning reagent was prepared by mixing 10 mL glycerol, 6 mL concentrated hydrochloric acid (HCl), 60 mL deionized water, and 20 mL isopropyl alcohol, and sodium chloride, with stirring at room temperature overnight. Four replicate samples were prepared by weighing 10 mg/mL of dried fucoidan into separate closed test tubes containing 2 mL of 4 M hydrochloric acid (HCl), thus subjecting samples to acid hydrolysis for 2 hours at 100 °C. Barium chloride ($BaCl_2$) (0.3 g/mL) was added, stirred for exactly 1min, and then left standing for 4 - 6 minutes to allow the barium sulfate ($BaSO_4$) precipitate to form. Potassium sulfate standard solutions with concentrations ranging from 200 - 1000 μg/mL were prepared. Absorbance was measured at 420 nm using a microplate reader (SynergyHT, Biotek Instruments, microplate reader-Gen52.01).

III-3.2.8. Fucoidan quantification by toluidine blue assay

Toluidine blue (also known as tolonium chloride) (TBO) is a metachromatic acidophilic dye that selectively stains components of acidic tissue (sulfates, carboxylates, and radicals of phosphate) [122–124]. TBO stains tissues based on the principle of metachromasia, attributed to the stacking of dye cations at the sites of the high density of anionic groups in the tissue [122–124]. The dye interacts with scaffolds to create a different color from the original color; TBO´s color change is usually from blue to violet, which means that the color absorption shifts to shorter

wavelengths. It is expected to reflect the dye´s polymerization. Metachromasia is higher, the greater the degree of polymerization.

In **Chapter VII and VIII**, fucoidan in PCL and PCL/fucoidan airbrushed nanofibrous meshes, as well as alginate microcapsules and Fucocaps was quantified based on Toluidine blue assay. Briefly, 0.04 wt.% TBO solution was prepared by dissolving the TBO powder in aqueous 0.01 M HCl/0.2 wt.% NaCl, and then the samples were incubated in 5 mL TBO solution under static conditions at 37 °C for 4 hours and rinsed three times with distilled water. Subsequently, the fucoidan–TBO complex that formed on sample surface was eluted and dissolved in 5 mL of 80 % ethanol/0.1 M NaOH mixture (4/1 v/v) solution. Ultimately 150 µL of the supernatant was transferred to a 96-well plate, and the absorbance was measured at 530 nm by a microplate reader (Biotek, Synergy HT, USA) and the Fu density on the sample surface was evaluated using a calibration standard curve. There were six parallel samples in each group, and DPBS was set as blank control. For standard curve preparation, 2 mL 0.04 wt.% TBO has first added to 2 mL of a known concentration Fu solution and incubated at 37 °C with gentle shaking for 4 h, the Fucoidan–TBO complex spontaneously formed and precipitated in the mixture. Then the mixture was centrifuged at 3500 rpm for 10 min, the supernatant was removed, and the precipitate was carefully rinsed twice with 0.01M HCl/0.2 wt.% NaCl solution. Finally, 5 mL 80 % ethanol/0.1 M NaOH mixture (4/1 v/v) solution was added to dissolve the precipitate, and the absorbance was measured at 530 nm. For the quantitative characterization of the Fu release, the samples were immersed in DPBS at 37 °C and shaken (60 rpm) for 1, 7, 14, 21, and 28 days in an airtight centrifuge tube. The release medium at each time point was collected, and the amount of Fu released was measured by using the same procedure based on a standard curve preparation [125,126].

III-3.2.9. Antioxidant properties of fucoidans

Oxidants, such as reactive oxygen species (ROS) and reactive nitrogen species (RNS), can produce free radicals which can cause severe oxidative damage to cellular lipids, membranes, proteins, and DNA [127–129]. Antioxidants can scavenge these free radicals by enzymatic and

non-enzymatic mechanisms, thereby preventing cellular oxidative stress. Catalase and peroxidase include enzyme systems which act as antioxidants. Beta-carotene, tocopherols, carotenoids, vitamin A, lycopene, ubiquinols, and sulfated polysaccharides serve as lipid-soluble antioxidants; whereas, glutathione and ascorbate are among the water-soluble antioxidants [127,130]. In recent years, antioxidant activity has been demonstrated by marine sulfated polysaccharides such as fucoidan, ulvan and carragenan [131]. Seaweeds that emerge in shallow waters are constantly exposed to ultraviolet light and air, resulting in the formation of free radicals and other reactive oxygen species (ROS). Even though chronic exposure to ROS, healthy seaweeds are resilient to oxidative damage demonstrating the existence of potent antioxidant defense mechanisms within their cells, which is attributed to these sulfated polysaccharides [132].

III - 3.2.9.1. Antioxidant activity: Trolox equivalent antioxidant activity (TEAC)

The total non-enzymatic antioxidant capacity (TAC) of biological samples is indicative of their ability to counteract oxidative stress-induced damage in cells. TAC is used to provide insight into the development and treatment of disorders linked to oxidative stress [127]. Either the concentration of the combination of both small molecule and protein antioxidants, or the concentration of only small molecule antioxidants can be determined in this assay. Cupric ion (Cu^{2+}) ion is converted to cuprous ion (Cu^{+}) by both small molecules and proteins. Nevertheless, the use of the Protein Mask prevents Cu^{2+} reduction by protein, enabling the analysis of only the small molecule antioxidants. The reduced Cu^{+} ion chelates with a colorimetric probe, giving a broad absorbance peak at ~570 nm, which is proportional to the total antioxidant capacity **(Figure III - 14).** In **Chapter VIII**, the Total Equivalent Antioxidant Activity (TEAC) of the purified fucoidans and solutions of 2.2 % sodium alginate and 2.2 % sodium alginate with 0.5 % fucoidan was measured based on the method of Prieto *et al.* [133,134]. The TEAC was determined using a Total Antioxidant Capacity Assay kit (Sigma, USA) according to the manufacturer's instructions [135]. Briefly, 100 µL of sample or standards were added to the well of a 96-well white polystyrene plate, mixed with 100 µL of Cu^{2+} working solution and incubated for 90 min at RT, and the plate protected from the light. Absorbance was read at 570 nm in the microplate reader (SynergyHT, Biotek Instruments, microplate reader-Gen52.01). After confirming linearity in the graph of inhibition percentage *versus*

concentration (1-20 mg/mL), the antioxidant activity was calculated as a concentration of Trolox equivalent value (mg Trolox/g fucoidan) using the **Equation III - 3,** where Sa is Trolox equivalent of an unknown sample from a standard curve, Sv is sample volume, and C is the concentration of antioxidant in the sample.

Equation III-3 - Antioxidant activity

$$S_a/S_v = C$$

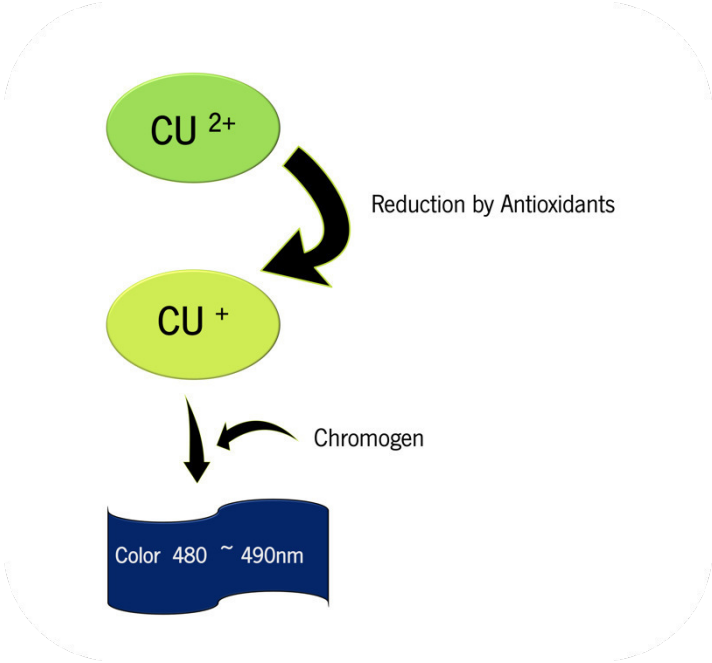


Figure III-14. Representative scheme of the principle of total antioxidant capacity. Reduction of cupric ion (Cu^{2+} to Cu^{+}). Cu^{2+} are reduced by antioxidants to form Cu^{+}. Reduced Cu^{+} react with chromatic solution and can be detected by absorbance at wavelength 480 to 490nm.

III - 3.2.9.2. Free radical scavenging assay

DPPH assay is used to determine the free radical scavenging ability of an antioxidant molecule. It is considered one of the normal and simple colorimetric methods for evaluating the antioxidant properties of pure compounds. This test measures the potential of an antioxidant (AH, generally phenolic compounds) to reduce the radical chemical DPPH (2,2-diphenyl-1-picrylhydrazyl) through

a hydrogen transfer resulting into reduction of DPPH to DPPH2. The DPPH°, which is initially violet, becomes DPPH-H, now pale yellow. The color change is monitored by spectrophotometry at 515 nm (λmax DPPH°) and used for the determination of parameters for antioxidant properties **(Figure III -15)** [136]. The reaction speed depends on the nature of the antioxidant, and the amount of DPPH-H formed depends on the concentration of the antioxidant [137].

The scavenging activity of FF and FA fucoidans against free radicals was measured using the DPPH (2, 2-diphenyl-1-picrylhydrazyl) assay. Briefly, Ascorbic acid, FF, and FA fucoidans were dissolved in water (1 mg/mL), and 200 µL of the above solution was added to each well of a 96-well plate. The samples were then serially diluted in water for varying concentrations ranging from 1000 µg/mL to 1.56 µg/mL. Freshly prepared DPPH solution (0.2 mM) in methanol was prepared, and 100 µL of the resulting solution was mixed thoroughly with 100 µL of FF and FA fucoidans of varied concentrations. The plate was then covered with aluminum foil (to protect DPPH radical degradation by light), and the reaction mixture was incubated for 1 h at room temperature. Absorbance was then measured at 515 nm using microplate reader (Clariostar). Ascorbic acid dissolved in water (1 mg/mL) was used as a standard, and solvent alone (methanol: water; 1:1) was used as a blank. DPPH solution alone (100 µL) mixed with water (100 µL) served as control. The percentage of radical scavenging was obtained using the equation:

Equation III-4 - Percentage of radical scavenging activity

$$\%\ \mathrm{DPPH}_{\mathrm{scavenging}} = \left[\left(\mathrm{Abs}_{\mathrm{sample}} + \mathrm{DPPH}\right) - \left(\mathrm{Abs}_{\mathrm{Sample\ blank}}\right)\right] / \left[\left(\mathrm{Abs}_{\mathrm{DPPH}}\right) - \left(\mathrm{Abs}_{\mathrm{solvent}}\right)\right] \mathrm{X}\ 100$$

and the IC50 values calculated using the Graph Prism software. Ascorbic acid was used a positive control in this study.

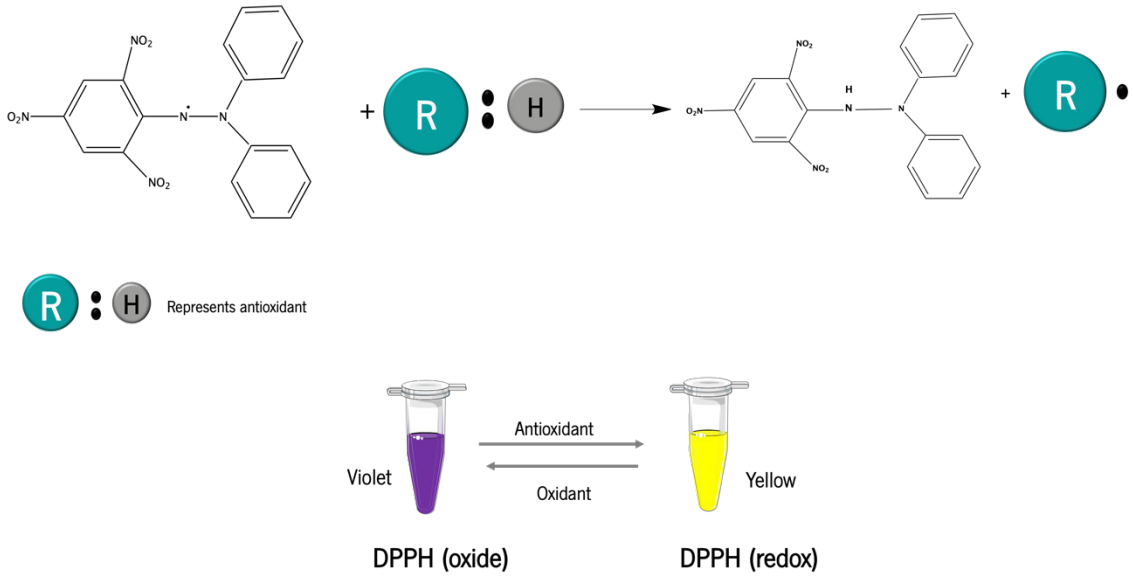


Figure III-15. Schematic representation of the principal of DPPH radical scavenging capacity assay. Reaction mechanism of DPPH with antioxidant. R:H= antioxidant radical scavenger, R= antioxidant radical.

III-3.3. Physical characterization

III-3.3.1. Contact angle

The wettability of a surface can be quantified by the measurement of contact angle (CA) of liquid drops deposited onto that surface, i.e., the angle at which a liquid/vapor interface meets a solid surface. The contact angle mainly depends on the balance of pressures between the drop´s liquid/vapor surface tension and the interfacial tension between the solid and the drop [36,138]. This methodology allows quantifying the wettability of a solid surface by a liquid via the Young equation. A hydrophobic surface repels water and forms a small surface with the water droplet giving a high-water contact angle. On the opposite, the solid surface was considered hydrophilic when the water droplet spread, giving a small water contact angle **(Figure III -16).**

In **Chapter VII** water contact angles (WCA) were measured for airbrushed nanofibrous meshes made of PCL and PCLFu, to evaluate the influence of the addition of fucoidan in their hydrophilicity. Static CA measurements were carried out by the sessile drop method, under ambient conditions

at RT. A drop (6 µL) of Milli-Q-water was added by a motor-driven syringe, and the CA was measured after the contact between the drop and the membrane's surface. Three different samples of each material were used, and at least five measurements were carried out for each sample.

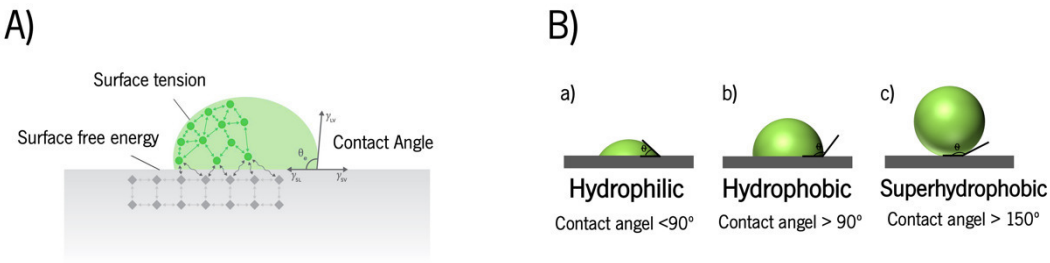


Figure III-16. Varying a water contact angle. Adapted from [139].

III-3.3.2. Mechanical Analysis

Biomaterials are subjected to different loads once implanted. The type and strength of those loads depend on the tissue they are being inserted into. Mechanical properties of different polymeric structures can be characterized by their deformation behavior, resulting in a stress-strain response. These properties are associated with the molecular arrangements of the processed materials (namely, polymers) and are crucial in evaluating the effectiveness of the processed structures to be selected for a particular biomedical application [104,140].

III - 3.3.2.1. Compression test

Compression tests are a destructive technique that measures the mechanical behavior of a material under compression loads [141,142]. This technique involves the use of a compressive

machine with two plates and material (with a defined morphology) set between the plates, in which a compressive force (stress) is applied to the material, and the deformation (strain) at different loads is recorded **(Figure III -17).** In the present thesis, the mechanical behavior of hydrogels was tested by the compression test. Compressive studies were performed with a Malvern Kinexus Rotational Rheometer, UK, using a parallel plate geometry of 8 mm diameter, with radial grooves to avoid hydrogel leakage. The Aga and AgaFu hydrogels were prepared in distilled water, as described in **Chapter VI,** and maintained in DPBS. The hydrogels were compressed in the direction normal to the circular face of the cylindrical samples at a rate of 1 mm per minute for a maximum strain of 85 % and at room temperature. The Young's modulus, defined as the initial slope of the linear region of the stress-strain curve, was determined using the tangent method. Each experiment was performed in quintupled.

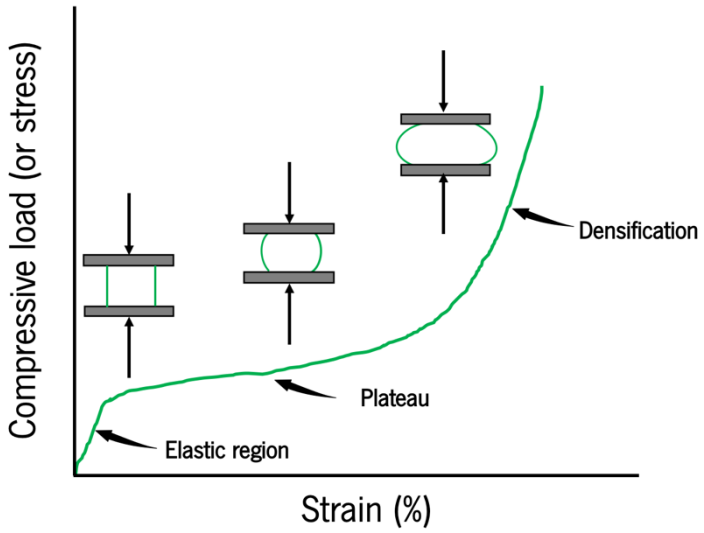


Figure III-17. Schematic representation of a compression-stress-strain curve for a polymer.

III-3.3.3. Dynamic mechanical analysis (DMA)

For proper physiological integration, a biomaterial needs to withstand cyclical thermal loads and be able to dissipate energy to be consistent with the mechanical properties of the biological

tissues [108,143]. Mechanical characterization of biomaterials is essential to understand their potential role in mechanosensing, which may drive cellular response [108,144–146]. Therefore, the combined study of the stiffness and damping properties of materials is valuable for the full characterization of the performance of biomaterials. Along with the thesis, the mechanical properties of developed constructs were evaluated with two major techniques: dynamic mechanical analysis (DMA) and universal mechanical testing. The main difference between the DMA and the universal mechanical test is that the load is applied cyclically in DMA [36,147], while a static load is applied in the universal mechanical test [36,148]. In DMA equipment, an oscillating force (stress) is applied, and an oscillating sample response is recorded. So, the modulus is calculated from the elastic response, i.e., sample response "in phase" with applied oscillatory stress. On the other side, the damping is calculated from the viscous response, e.g., sample response "out of phase" with applied oscillatory stress. DMA allows one to obtain the frequency dependence of the complex modulus **Equation III - 5**. The storage (elastic) modulus, E', is the real component of the complex modulus, being a measure of the sample's stiffness. The loss modulus, E'', is the imaginary component, being a measure of the energy loss in viscous mechanisms [36,147,149]. The loss factor (tan δ) gives the ratio between the amount of mechanical energy lost and stored during a cycle (**Equation III – 6**), measuring the damping capability of the sample [36,149,150]. The main advantage of this technique is the possibility to measure the mechanical properties in physiological-like environments, which have been reported to affect the mechanical behavior of materials that easily swell when exposed to aqueous solutions [36,151,152]. In **Chapter VII**, the mechanical properties were evaluated using a dynamic mechanical analyzer (DMA) (Tritec 2000B equipment, Triton Technology, UK). Airbrushed nanofibrous meshes (PCL, PCLFA, and PCLFF) previously soaked in a PBS solution were cut in regular stripes and clamped in the DMA apparatus with total immersion of the sample in a reservoir containing PBS solution at 37 °C. DMA spectra were obtained using a stress mode cycle of increasing frequency from 0.01 Hz to 20 Hz (5 points per decade), in order to simulate the physiological loading frequencies. Five samples for each condition have been tested, at least.

Equation III-5 - Frequency dependence of the complex modulus

$$E^* = E'' + iE''$$

Equation III-6 - Loss factor

$$\tan\delta = {}^{E''}/_{E'}$$

III - 3.3.3.3. Rheology

Rheology studies the relationship between deformation and flow in materials. This technique gives the elasticity, viscosity, and plasticity information of materials under changes of shear, strain, frequency, temperature or time [153]. It is also sensitive to any chemical reactions in the flows, such as gelation and polymerization. Measurement of rheological properties extends to all materials from fluids, such as dilute solutions of polymers and surfactants, to concentrated protein forms, such as semi-solids, pastes, and creams, to molten or solid polymers as well as asphalt [154,155]. Rheological or viscoelastic evaluation is done through flow measurements and dynamical mechanical tests. The first one investigates the flow viscosity, whereas the latter evaluates small periodic deformations that determine molecular-level mobility or rearrangement of structure. For example, the time sweep test provides a means of monitoring the time-dependent behavior of a material. It measures the storage modulus, G', which is an indicator of elastic behavior and reveals the ability of the polymer system to store elastic energy while the loss modulus, G'', is a measure of the dynamic viscous behavior. Additionally, loss tangent (tan δ) is a parameter that represents the ratio between the viscous and elastic components of the modulus of the polymer, being a good indicator of the overall viscoelastic nature of the samples and is dimensionless. The relationship between G', G'' and tan δ is calculated following **Equation III - 7** [153].

Equation III-7- Loss tangent

$$\tan\delta = {}^{G''}/_{G'}$$

In **Chapter V,** the rheological experiment was performed to characterize the Aga and AgaFu hydrogels using a Kinexus pro^{+} rheometer (Malvern Instruments, UK), equipped with the

acquisition software rSpace. All the oscillatory measurements were performed by using stainless steel parallel-plate geometry with a diameter of 20 mm, while for the rotational experiments a conic plate holder of 40 mm and 1 mm gap was used. The rheological tests were performed in the solutions used for the preparation of hydrogels and in the Aga and AgaFu hydrogels. In the rotational experiments, two different plots were obtained: a) the traditional shear viscosity (Pa.s) throughout shear rate (1/s) and b) the shear stress (Pa) as a function of shear rate (1/s). From these curves, it was possible to obtain information about the flow behavior of the samples. From the oscillatory experiments, those were preceded by strain sweep curves to determine the linear viscoelastic region (LVER) of the samples. Strain amplitude was thus performed in the shear rate range changing from 0.1 to 100 Hz in a 10/decade rate, a range of temperature between 80 °C and 37 °C and a constant 1 % strain. After this, the mechanical spectra of each sample were obtained, and the elastic modulus (G´) and viscous modulus (G″) were recorded over a frequencies sweep ranging from 0.1 Hz to 100 Hz at a constant temperature of 37 °C. The strain dependency measurements were performed using 1 mL of solution or one hydrogel (Aga and AgaFu hydrogels). All plots are the average of at least 3 samples.

In **Chapter VIII** the rheology experiments were performed with a Discovery HR-2 hybrid rheometer with conic geometry (20 mm diameter, 0.3 mm gap). Hydrogel precursor solution and 20 mM barium chloride solution $BaCl_2$ were mixed in a 1:2 ratio and directly loaded in the rheometer, making sure hydrogel crosslinking occurred in between the two rheometer plates. A solvent trap was placed around the sample and filled with distilled water to prevent solvent evaporation from the gel. Hydrogels were preconditioned with a flow peak hold with a shear rate of 1/s before each of the following steps. Initially, hydrogels were subjected to a strain sweep with strains ranging between 0.01-10 % and an arbitrary angular frequency to determine the linear viscoelastic region of the hydrogels. Secondly, hydrogels were exposed to a frequency sweep with a strain within the linear viscoelastic region and angular frequency ranging between 1-500 rad/s. Lastly, storage modulus G' was monitored during a strain sweep in which hydrogels were subjected to a strain sweep with strains ranging between 0.01-10 % and an angular frequency of 10 rad/s. Hydrogel mesh size (D_{mesh}) was then calculated based on **Equation III -8,** and the measured storage modulus G'. The classical theory of rubber elasticity relates the shear modulus (G') to the mesh size r_{mesh} **(Equation III -8)**, where R is the gas constant, T the absolute temperature and N_{av} is Avogadro's number. This allows estimation of the mesh size of a hydrogel-based on its shear

modulus [156,157]. The mesh size (D_{mesh}) represents the diameter of a hard sphere that fills the void in between hydrogel network strands.

Equation III-8 - Mesh size of hydrogels

$$D_{mesh} = \left(\frac{6\,RT}{\pi N_{av} G'}\right)^{\frac{1}{3}}$$

Equation III - 8 is based on the "equivalent network model" as proposed by Schurz *et al.* and the affine network model proposed by Rubinstein *et al.* [158,159]. These models cannot comprehend the complexity of actual hydrogel networks, and instead, make use of an idealized infinite network. The main assumption for the affine network model is that of affine deformation: the relative deformation of each network strand is the same as the macroscopic relative deformation imposed of the whole network. Within this model, stress and deformation are related due to the shear modulus G' **(Equation III - 9),** where the number of network strands per unit volume (number density of strands) is $v = \frac{n}{V}$, ρ is the network density (mass per unit volume), M_s is the number-average molar mass of a network strand and k the Boltzmann constant.

Equation III-9- Shear modulus G´

$$G' = \frac{n\,kT}{V} = vkT = \frac{\rho RT}{M_s}$$

The Boltzmann constant can be rewritten into $k = \frac{R}{N_{av}}$, resulting in:

$$G' = v\frac{R}{N_{av}}T$$

or, if making v the subject of the equation:

$$v = \frac{N_{av}\,G'}{RT}$$

Given that a hydrogel network is represented by a molecule junction diameter (D) and the average mesh width (M) (**Figure III -18),** and the assumption that D=M, the free volume in between the network is represented by $V = \frac{\pi D_{mesh}^3}{6}$. [160]. When evaluating a single network strand (n=1), v or $\frac{n}{V}$ can be rewritten into $\frac{6}{\pi r_{mesh}^3}$, resulting in:

$$\frac{6}{\pi D_{mesh}^3} = \frac{N_{av}\, G'}{RT}$$

which results in **Equation III - 8** when D_{mesh} is made the subject of the formula.

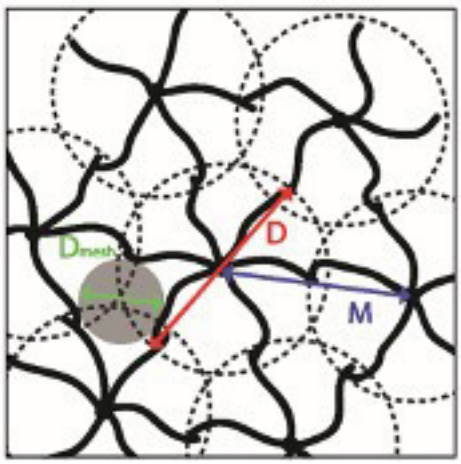


Figure III-18. Schematic representation of a hydrogel network with molecule junction diameter (D), average mesh width (M), and hydrogel mesh size (D_{mesh}) [160].

III-3.3.4. Swelling study

In the context of TE, it is important to expose the polymeric networks to conditions that mimic as much as possible the *in vivo* environment. A proper evaluation of their behavior within this setup will help to predict there *in vivo* performance [161,162]. Weight loss and water uptake and are important parameters in the evaluation of biodegradable materials. They translate the degradation behavior and the ability of the biomaterial to absorb water in their matrix (swelling), respectively.

The rate at which a fluid penetrates into material depends, mainly, on its surface area, the hydrophilic/hydrophobic character, and in some cases, its porosity [153,163,164]. Moreover, the swelling of polymeric networks is significantly influenced by water- material interactions. These affect the mass transport characteristics, determinant for nutrient and oxygen diffusion to encapsulated cells and their metabolic waste disposal, but also the mechanical properties as well as morphological features, such as shape and size, of a given hydrogel geometry or pattern. To study the swelling kinetics of the developed hydrogels **(Chapter VI and VII),** three solutions with different ionic content were used: distilled water (no ions); phosphate buffered saline (DPBS, Gibco, with monovalent ions); and media (Dulbecco's Modified Eagle's medium, DMEM, Gibco, with mono and divalent ions). For the determination of the water uptake and weight loss profiles, samples were weighted and immersed in a phosphate buffer saline solution at physiological pH (pH 7.4) and placed into a water bath at 37 °C [153,165]. Sodium azide (0.02 % w/v) was added to the buffer to prevent bacterial growth. After pre-determined time periods, the samples were removed from the vials, washed with distilled water, removed excess of solution using a filter paper and then weighted. Water uptake was determined using **Equation III - 10** where $W_S(t)$ and W_i represent the weight of the samples at time t and 0, respectively. Each experiment was repeated three times and the average value was considered as the water uptake value. After that, the samples were dried in an oven (60° C/24 h). The percentage weight loss of the materials was then calculated by **Equation III - 11** where W_i is the initial dry weight of the sample and W_f (t) denotes the dry weight of the sample after a certain time t of incubation. Each experiment was repeated three times. In the case of particles, water uptake assays were performed through immersion of the materials in buffer solutions at pH 3, 7.4 and 9 instead of PBS, and incubated at 37 °C under static conditions. The samples were left for 24 hours in each buffer solution prior to weight determination. The swelling ratio was determined using **Equation III - 10**.

Equation III-10- Water uptake

$$\text{Water uptake}(\%) = \left[{(W_s(t) - W_i)}/{W_i}\right] * 100$$

Equation III-11 - Weight loss

$$\text{Weight loss (t)} = \left[{(W_i - W_f(t))}/{W_i}\right] * 100$$

III-3.3.5. Stability tests

Stability is an important parameter for assessing the suitability of materials for a proposed biomedical application. Biodegradable materials should be designed to degrade overtime at the same rate as neo-tissue is formed. The products of the degradation should be non-toxic and be able to be removed from the organism. The biodegradation of materials requires the hydrolytic or enzymatic cleavage of polymeric bonds sensitive to those mechanisms. Biomaterials are known to be susceptible to these degradation mechanisms can be tuned in vitro, in an attempt to predict their behavior in vivo. The stability tests were carried out by immersion of the hydrogels (Ø 7 ±0.01 x 10±0.02 mm height, n=3) in either PBS, pH 7.4 or culturing medium (RPMI) supplemented with fetal bovine serum, FBS, Gibco, pH 7.4) at 37°C. The hydrogels were lyophilized and weighed (initial weight) before being transferred to 15 mL Falcon tubes and soaked in 10 mL PBS or RPMI medium under constant agitation (60 rpm). The degradation solutions were changed every 7 days to restore the original level of ions activity. After each selected degradation time point, namely 1, 7, 14, 21, and 28 days, the samples were washed thoroughly with PBS to remove traces of soluble degradation products, salts, or other impurities and then dried until a constant weight was achieved; the dried samples were weighed (final weight) for determination of weight loss. The extent of degradation is commonly determined by calculating the percentage of weight loss **(Equation III - 12).**

Equation III-12 - Weight loss

$$\text{Weight loss (\%)} = \left[{(m_i - m_f)}/{m_i}\right] * 100$$

Where mi is dry weight and mf the final weight.

III-3.3.6. Diffusion and Permeability tests

III-3.3.6.1. Diffusion of methylene blue

Diffusion of chemical compounds through Agarose (Aga) and Agarose/fucoidan (AgaFu) hydrogels was evaluated by using an assay based on Kirby Bauer method [166]. Briefly, purified fucoidan (Fu) was dissolved in distilled water at a concentration of 3 or 5% (w/v) under stirring and at 75°C, and then Agarose (Aga) powder was added to the Fu solutions. The AgaFu solutions were prepared at different Aga/Fu proportions (4:10; 5:10 and 7:10 wt). These solutions were disposed in petri dishes and gelation was enabled by cooling down to room temperature for 15-20 min. Afterwards, some holes (d=6 mm) were done in gel solution and a 100 mM methylene solution was dropped in holes. The diffusion of methylene blue is calculated considering the starting position of the dye and the diameter of dye spot at different time points.

III-3.3.6.2- Insulin release

To quantify the release of a drug from the produced structures (modified fucoidan particles (MFu)), a simple methodology was employed. We incubated these drug-charged particles in PBS; simulated gastric fluid (SGF) and simulated intestinal fluid (SIF). The SGF solution was prepared in aqueous solution, for 1liter of SGF we use 2g of sodium chloride (NaCl), 3.2g of pepsin derived from stomach mucosa and 7mL of concentrated hydrochloric acid (HCl), while SIF was prepared in aqueous solution, for 1liter of this buffer we use 6.8g of monobasic potassium phosphate, 77mL of 0.2N sodium hydroxide (NaOH) and 1g of pancreatin. MFu microparticles loaded with insulin were produced in the same way, but using MFu solutions with 5mg/mL of insulin. Ten MFu microparticles loaded with insulin were placed in 20mL of release PBS and incubated at 37°C under stirring. Ten MFu particles were incubated in SGF and SIF not in sequence, at 37°C under stirring. At appropriate time intervals (0.5 to 6h), 1mL of the solution was removed for analysis and replaced by fresh solution. The samples were analysed by UV- Vis spectrophotometry at 272 nm (Shimadzu, UV 1601, Japan). The insulin concentration of each sample was calculated using a

standard curve (concentrations ranging from 0 to 6 mg/mL), relating the quantity of insulin with the absorbance intensity. The results presented are an average of three measurements. Calculations of the amount of drug released took into account the replacement of aliquots with a fresh medium. Control modified fucoidan particles without insulin was considered as blanks in the performed quantification [113].

III-3.3.6.3 - Permeability to glucose

In **Chapter VI,** permeability studies on Aga and AgaFu hydrogels was evaluated using one model molecule: the glucose. The glucose permeability measurements were conducted using a glass Franz-type diffusion cell with 8 mL reactor compartment (effective mass transfer area of 1 cm^2) **(Figure III - 19)**. For this experiment, Aga and AgaFu hydrogel membranes were prepared (with same methodology used in the preparation of hydrogels but using a different mold) and previously equilibrated in a DPBS solution (overnight), then placed between the two compartments and held with a stainless-steel clamp. The receptor compartment was immediately filled with DPBS solution, and the air bubbles were removed. Finally, the donor compartment was filled with 16 mM of glucose (DPBS, pH 7.4). Aliquots of 1000 μL were withdrawn from the receptor compartment at predetermined time periods and replenished by fresh DPBS. The experiments were performed at 37 °C, and the receptor compartment was stirred to eliminate the boundary layer effect. The concentration of glucose in the aliquots removed from the receptor chamber in pre-determined periods of time was evaluated using the dinitrosalicylic acid (DNS) method. The DNS reacts with reducing sugars, and other reducing molecules, forming 3-amino-5-nitrosalicylic acid, an aromatic compound that strongly absorbs light at 540 nm, thus enabling the measurement of the amount of reducing sugars present in the solutions [36,167]. The amount of glucose was measured by absorbance at a wavelength of 540 nm using a microplate reader (Synergy HT, Bio-TEK, USA). The permeability (P) of glucose was calculated by the **Equation III - 13**.

Equation III-13 - Permeability (P) of glucose

$$-\ln\left(1-\frac{2C_t}{C_0}\right)=\frac{2A}{V}\times P\times t$$

where C_t is the concentration in receptor compartment at time t, C_0 is the initial concentration in the donor compartment, V is the solution volume in the two compartments, and A is the effective area of permeation.

The permeability can be calculated from the slope of the curve obtained by the following relation:

$$-\left({}^{V}/_{2A}\right).ln\left({}^{1-2C_t}/_{C_0}\right)\ versus\ t$$

The diffusion coefficient (D) of glucose across the membrane was calculated according to Fick's law of diffusion, as follows **(Equation III - 14)**

Equation III-14- Determination of the diffusion coefficient

$$D=\frac{V_1\ V_2}{V_1+V_2}\times\frac{h}{A}\times\frac{1}{t}\ln\left(\frac{C_f-C_i}{C_f-C_t}\right)$$

where D is the diffusion coefficient (cm^2/s); C_i and C_f are the initial and final concentrations, respectively, and C_t is the concentration at time t of solute in the receptor side (mol/L); V_1 and V_2 correspond to the volume of the liquid in the donor and receptor compartments (cm^3), respectively; h is the thickness of the membrane (cm); and A is the effective diffusion area of the membrane (cm^2). The partition coefficient (K_d) is defined as a measure of the solubility of glucose in the hydrogel and was calculated from **Equation III – 15**

Equation III-15 - Determination of partition coefficient

$$K_d=\frac{P\times h}{D}$$

where P is the permeability, h is the thickness of the membrane, and D is the diffusion coefficient.

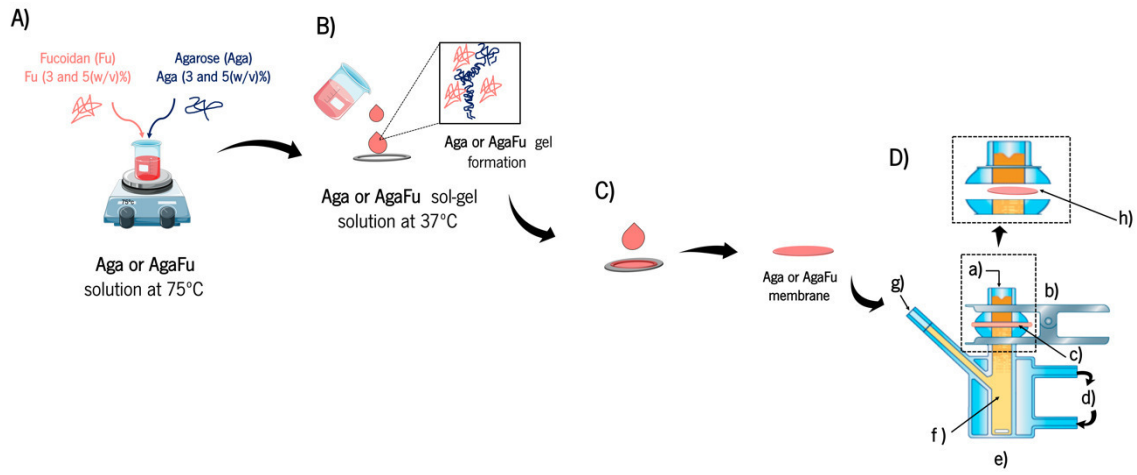


Figure III-19. Schematic representation of the experimental glucose diffusion systems used during the assay A) Preparation of agarose (Aga) or agarose/fucoidan (AgaFu) solutions, B) transferring of Aga or AgaFu solutions to molds, C) Aga or AgaFu membrane formation by cooling the solution at room temperature and D) Franz cell: a) glucose solution, b) cell clamp, c) and h) Aga or AgaFu membrane, d) water bath, e) Franz diffusion cell, f) PBS solution and g) sample port. (adapted from [168,169]).

III-4. BIOLOGICAL EVALUATION OF THE DEVELOPED MATERIALS/STRUCTURES

To evaluate the potential use of the developed structures as biomaterials in tissue engineering context, biological assays need to be performed. *In vitro* tests enable an initial screening of the biological performance of the structures. Regarding the chosen cell type used in the different chapters were based on the objective of the work namely study the biocompatibility of materials, treatment of diabetes and vascularization. Either cell line (mouse fibroblast-like L929 cell line, 1.1B4 human pancreatic cell line, insulinoma INS1E cell line, INS1E report oxidative cells and human pulmonary microvascular endothelial cells HPMEC-ST1.6R cell line) or primary cultures

(sheep islets and human islets) were used to these analyses. After seeding on developed polymeric structures, cell viability, proliferation, morphology and distribution were evaluated through a series of different methodologies. With the outcomes from these studies, different materials were selected or optimized for further biological evaluation. In the following section, it is described the cell sources, the seeding methodologies, and techniques used for the biological evaluation of the extracts and structures developed in the scope of this thesis [30].

III-4.1. Cell source

III-4.1.1. Mouse fibroblast-like cell line (L929 cells)

For the cytotoxicity assessment of the materials and for encapsulation into modified fucoidan particles and agarose/fucoidan hydrogels described in **Chapter IV, V and VII**, a mouse fibroblast-like cell line, L929 (ECACC- European Collection of Cell Cultures, UK), was used. L929 cell line is the usual choice in many standard tests such as material biocompatibility testing, drug cytotoxicity testing and cell biology studies. Cells were cultured with Dulbecco's modified Eagle's medium (DMEM, D5523, Sigma, USA), supplemented with 10 % fetal bovine serum (FBS, 10270-106, Invitrogen, USA) and 1 % antibiotic/antimycotic (A/B, 15240-062, Invitrogen, USA) solution. The cells were incubated at 37 °C in a humidified air atmosphere of 5 % CO_2 in 75 cm^2 flasks. At approximately 90 % of confluence, the cells were washed with PBS, and collected by adding 0.05 % trypsin-EDTA for 5 min at 37 °C. Trypsin-EDTA is a mixture of proteases derived from a porcine pancreas, and, due to its digestive strength, it is widely used for cell dissociation, routine cell culture passaging, and primary tissue dissociation. After the detachment of the cells, the trypsin was inactivated by adding fresh cell culture medium. The cell suspension obtained was then centrifuged at 300 g at 25 °C. The cell density of L929 cells used for the cytotoxicity tests was 2×10^4 cells/mL, which were seeded in 96-well cell culture plates ($4x10^3$ cells/well, 200 µl/well), in order to reach 70 % confluence for 24 hours of incubation at 37 °C, in a humidified atmosphere with 5 % CO_2 [55]. The supernatant was discarded, and the cell pellet was suspended in a modified fucoidan **(Chapter IV, V)** or fucoidan solutions **(Chapter VII)** in order to be encapsulated.

III-4.1.2. 1.1B4 Human pancreatic cells

One of the commonly used cell lines used in treatment of diabetes is 1.1 B4 human pancreatic cells.1.1B4 human pancreatic cells (Sigma, USA) were used in cytotoxicity test, encapsulated into hydrogels and used in the surface of microcapsules, as described in **Chapter V and VI**. These cells were cultured in RMPI 1640 (Gibco, USA) supplemented with 5 % (v/v) fetal bovine serum (FBS, Lonza, Switzerland), 100 U/mL penicillin and 100 mg/mL streptomycin (Gibco, USA) and incubated at 37 ℃ and in a humidified air atmosphere of 5 % CO_2. At approximately 90 % of confluence, the cells were washed with PBS, and collected by adding 0.05 % trypsin-EDTA for 5 min at 37 °C. After the detachment of the cells, the trypsin was inactivated by adding fresh cell culture medium. The cell density of 1.1B4HP cells used for the cytotoxicity tests was 10.000 cells/cm^2, which was seeded in 48-well cell culture plates, in order to reach 70 % confluence for 24 h of incubation at 37 °C, in a humidified atmosphere with 5 % CO_2. For encapsulation, the supernatant of cell suspension was discarded, and the cell pellet was suspended in a neutralized agarose or agarose/fucoidan **(Chapter VI)** solution in order to be encapsulated.

III-4.1.3. Rat insulinome cells (INS1E cells)

In **Chapter VIII,** INS1E cells were used in cytotoxicity assessment and were encapsulated into the developed microcapsules. Rat insulinoma beta cells are one of the most common used diabetes treatment cell line. INS1E rat insulinoma cells (AddexBio, USA) were cultured in RMPI 1640 medium (Gibco, USA) supplemented with 5 % (v/v) fetal bovine serum (FBS, Lonza, Switzerland), 100 U/mL penicillin and 100 mg/mL streptomycin (Gibco, USA), 10 mM HEPES, 1 mM sodium pyruvate, and 50 μM freshly added beta-mercaptoethanol (Gibco, USA) and incubated at 37℃ and in a humidified air atmosphere of 5 % CO_2. At approximately 90 % of confluence the cells were washed with PBS, and collected by adding 0.05 % trypsin-EDTA for 5 min at 37 °C. After the detachment of the cells, the trypsin was inactivated by adding fresh cell culture medium. The cell

suspension obtained was then centrifuged at 300 g at 25 °C. The cell density of INS1E cells used for the cytotoxicity tests were $2x10^4$ cells/mL, which were seeded in 96-well cell culture plates ($4x10^3$ cells/well, 200 µl/well), in order to reach 70 % confluence for 24 h of incubation at 37 °C, in a humidified atmosphere with 5 % CO_2. For encapsulation, the supernatant of cell suspension was discarded, and the cell pellet was suspended in a neutralized alginate or alginate/fucoidan (**Chapter VIII)** solution in order to be encapsulated.

III-4.1.4. Islets Isolation

III - 4.1.4.1. Rat islets isolation

Rat islets of Langerhans from male Lewis rats (>10 weeks) were isolated in MERLN laboratory (Maastricht, Netherlands). Animal usage and all experimental procedures were approved by the Institutional Animal Care and Ethics Committee of Maastricht University. The next points are the protocol used for rat islets isolation [129].

- **Animals**

Lewis rats (> 10 weeks), male, body mass 250~300 g was bought by MERLN Institute at Maastricht University in the Netherlands. All animal experimental procedures were approved by the Dutch ethical committee on animal experimentation (CCD) and the institute's Animal Care and Ethics Committee at Maastricht University (IVD).

- **Preparation solutions before islets isolation**

  - Krebs-Ringer bicarbonate (KRB) solution: It was as a base for quench and lysis buffer. For 1liter of KRB solution it was used 500 ml of KRB, 2 ml of glucose 1 M, 10 ml of 100 U/ml penicillin and 100 mg/ml streptomycin, 1 ml of calcium chloride ($CaCl_2$) aqueous solution 1 M and 10 ml of HEPES 1 M. Bubble with air 1X KRB 15 min and pH 7.4.

- Make perfusion solution (liberase): for perfuse one pancreas it was used ~ 2.5 – 3 ml of liberase. It was taken out 15 ml of the 1 x KRB and filtered (0.2 µm) this into a separate falcon tube. It was added to this 150 µl of liberase (T-flex from Roche) (100 x, 25 mg/ml) and 150 µl of thermolysis (100 x, 0.75 mg/ml). Kept on ice.
- Make quench buffer: to the remaining 1x KRB was added heat inactivated neonatal calf serum (NCS) (to give 10 % NCS). This was the quench buffer. The quench buffer was filtered and stored at 4 °C until required.

- **Pancreas removal**

Rats were euthanasia with anaesthetize and neck break. Pancreas and common bile ducts were fully exposed. Then, common bile duct was intubated with a self-made catheter and ligation fixed **(Figure III –20).** Two and half ml of perfusion solution was sucked into a 5 ml syringe and the syringe was attached to the end of cannula. A small amount of perfusion solution was injected to the common bile duct to move the bile into the intestine and ligate the distal common bile duct. Then the pancreas was removed rapidly and completely. After removing the fat and connective tissue from, tweezers were used and carefully torn the pancreas up on ice, 5ml of pre-warmed collagenase solution was transfered into 50 ml conical flask.

- **Islet isolation:**

Once incubation was completed it was added 15 ml quench buffer to each falcon tube and shaken vigorously for 15-17 seconds. Then it was poured through net well filter into the new tube. More quench buffered was added, the falcon was shaken, and that material passed through net well. All procedure was performed in ice. The solution was transferred to a centrifuge tube and homogenized by pipetting, before centrifuged at 1000 rpm for 1.5 min at 4 °C. Centrifugation was performed 3 times, pouring off the supernatant and gently resuspending in 20 ml quench between centrifugations.

- **Islets purification:**

The supernatant was discarded, and the pellet was purified by the discontinuous Ficoll density gradient centrifugation. First, the pellet was suspended in 15 ml Ficoll solution and added 10 ml of quench buffer carefully on top of Ficoll. Then the tubes were centrifuged at 1360 g for 22 min at 10 °C. After the centrifugation the islets were carefully pipette (from the interface) all of Ficoll and quench, and then trapped on top of the filter. The islets were washed 3 times with quench buffered and then completed with RPMI 1640 medium. Islets were incubated for 48 hours in RPMI 1640 medium (Life Technologies, The Netherlands), supplemented with penicillin and streptomycin and 10 % fetal bovine serum (FBS) in an incubator at 37 °C supplied with 5 % CO_2 in air before being encapsulated. The purity of the islets was assessed by dithizone (Sigma, St Luois, MO) staining and found to be > 95 %.

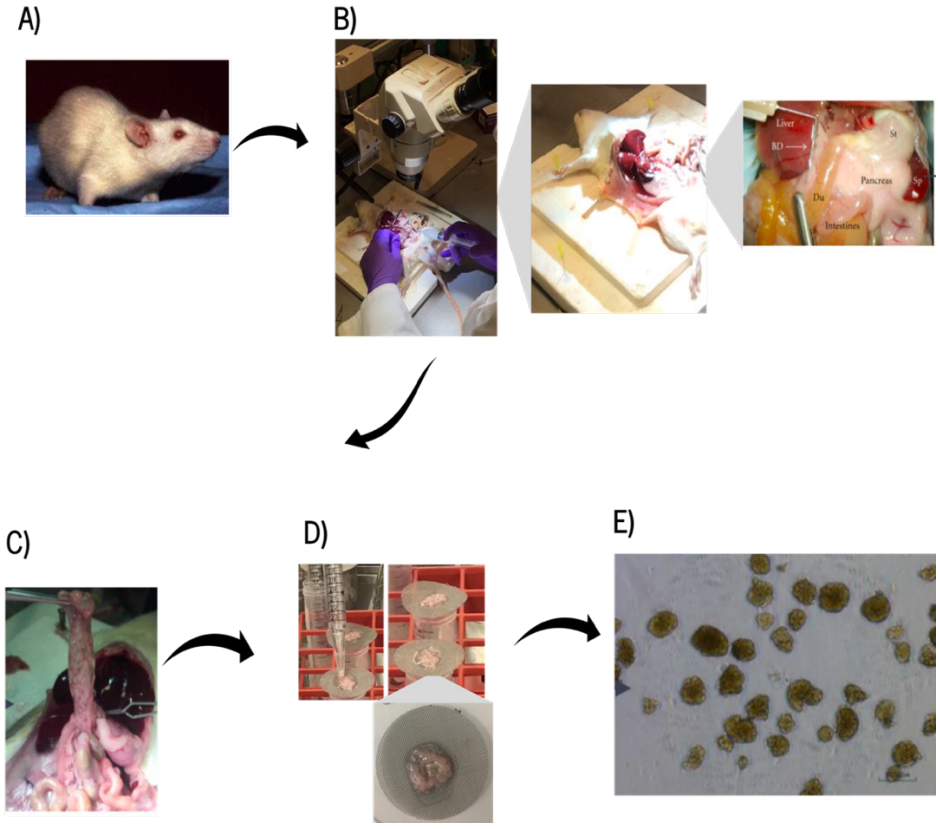


Figure III-20. Schematic representation of rat islet isolation. A) Lewis rats (> 10 weeks); B) pancreas removal; C) perfused pancreas D) Islet isolation by shaking the pancreas in falcons and pass the material through net well and E) Islets isolated from rats.

III - 4.1.4.2. Neonatal pig islet isolation

All experiments were conducted in accordance with the local ethical committee and with EU Directive 2010/63/EU for animal experiments. Piglets (Belgian landrace; 3-8 kg) were directly delivered to the islet isolation facility in Brussels. Neonatal pancreatic islet isolation was carried out as previously described [164]. Briefly, the harvested neonatal pig pancreas was cut into small pieces and transferred to a 50 ml tube. The pancreas was then washed twice with 30 ml of ice-cold supplemented HBSS (10 mM Hepes, 100 U/mL Penicillin-streptomycin, 10 mM Glucose, 0.075 % Amphotericin B, 0.25 % BSA) with each time allowing the pancreatic tissue to sediment and removing the supernatant with debris and fatty tissues. After washing, collagenase V (Sigma) (10 mg dissolved in 5 ml HBSS) was added and the pancreas digested by manual shaking for 20 min at 37 °C followed by addition of 40 ml of cold HBSS to stop the digestion process. The pancreas was washed 3 times by filtering the preparation on a sterile 500 μM mesh and the filtered pancreas was suspended in supplemented HAM F10 medium. Neonatal pig islets (NPI) were cultured in HAM-F10 culture medium supplemented with 0.5% BSA, 50 μmol/L IBMX (3-isobutyl-1-methylxanthine), 10 mmol/L glucose, 2 mmol/L glutamine, 10 mmol/L nicotinamide, 1 % penicillin, and 1 % streptomycin during a period of 8 days to allow maturation of islet cells and removal of exocrine tissue as previously described before encapsulation [164].

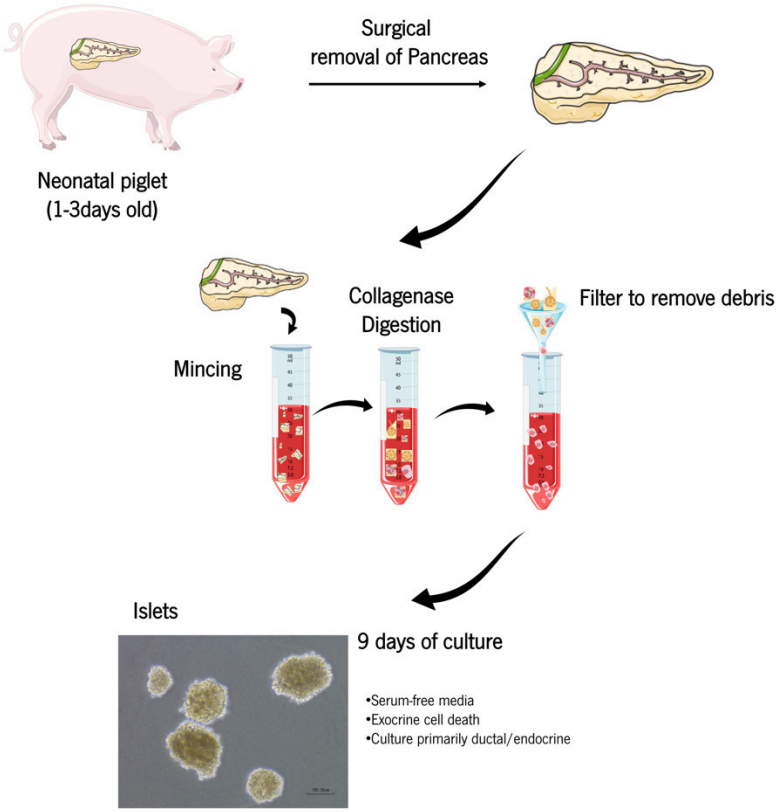


Figure III-21. Scheme representative of protocol for the isolation of neonatal porcine islets and islet progenitor cells. Pancreas are surgically removed from 1-3 days old pigs, minced, enzymatically dissociated (collagenase), and filtered before culture. After nine days of culture of this digest in serum-free media results in exocrine cell death and the derivation of a primarily ductal/endocrine population. Adapted from *[171]*.

III-4.1.5. Human pulmonary microvascular endothelial cells (HPMEC-ST1.6R)

Human pulmonary microvascular endothelial cells (HPMEC-ST1.6R cell line) was used to study the angiogenic potential of airbrush nanofibrous are described in **Chapter VII.** This cell line is commonly used to study the angiogenic process *in vitro* [166]. These cells were cultured in M199 medium (Sigma Aldrich, USA), supplemented with 20 % fetal bovine serum (FBS) (Gibco, USA), 2 mM Glutamax (Alfagene, Portugal), 100 U/mL penicillin, and 100 mg/mL streptomycin (Pen/Strep 100 U/100 g mL^{-1}) (Alfagene, Portugal), endothelial cell growth supplement (ECGS)

(25 μg mL $^{-1}$) (VWR, Batch 8135001, USA). Cells were used at passages 38–40 and incubated at 37℃ and in a humidified air atmosphere of 5 % CO_2. At approximately 90 % of confluence the cells were washed with PBS, and collected by adding 0.05 % trypsin-EDTA for 5 min at 37 °C. After the detachment of the cells, the trypsin was inactivated by adding fresh cell culture medium. The cells were seeded in 50000 cells/sample using the drop method. After 4 hours of adherence, 450 μm of the medium with ECGS supplement (1 μl/ml) was added at each sample. Tissue culture polystyrene (TCP) was used as a control for all the assays. Each experimental condition was tested in triplicate, and three independent assays were performed.

III-4.2. Cell culture

III-4.2.1. Assessment of cytotoxicity of extracts of fucoidan

Materials in contact with human tissues should not release any toxic agent or adverse effect to the host [147]. To establish the possible toxic effects of leachable eventually released from the material or scaffolds developed, indirect cytotoxicity tests were performed. The cytotoxicity procedure described in this thesis follows the ISO International Standards Organization (ISO/EN 10993) guidelines [147,167] for testing biomedical materials [147]. Cytotoxicity assays were carried out using latex rubber and standard culture medium as positive and negative controls, respectively. Latex rubber is commonly used as a positive control for standard toxicological assays, as it is known to have a cytotoxic effect inducing cell death and lysis [98,168]. Possible toxic leachable might be released when scaffolds or material (concentrations between 0 and 30 mg/ml) are incubated in a culture medium diluted to the final test concentrations [98]. Thus, incubate at 37 °C for a period of 24 hours, leachable is filtered and placed in contact with cells. This method allows to quantify the effect of material over the viability of cell culture and thus deduces about the cytotoxic behavior (or lack of) in contact to a material. In the studies, mouse fibroblast-like cells (L929) and rat insulinoma cells (INS1E) were used to perform the cytotoxicity tests on leachable products of fucoidan powder and modified fucoidan particles **(Chapter IV and VIII)** respectively. L929 cells were cultured and expanded in basic medium: Dulbecco's Modified Eagle's Medium

(DMEM, Sigma-Aldrich, USA) with phenol red and supplemented with 10 % fetal bovine serum, (FBS, Gibco, UK) and 1 % antibiotic/antimycotic (A/B, Gibco, UK) solution. L929 cells were incubated at 37 °C in an atmosphere containing 5 % of CO_2 until achieving 90 % of confluence. INS1E cells were culture RMPI 1640 medium (Gibco, USA) supplemented with 5 % (v/v) fetal bovine serum (FBS, Lonza, Switzerland), 100 U/mL penicillin and 100 mg/mL streptomycin (Gibco, USA), 10 mM HEPES, 1 mM sodium pyruvate, and 50 μM freshly added beta-mercaptoethanol (Gibco, USA) and incubated at 37 ℃ and in a humidified air atmosphere of 5 % CO_2 [169]. Then, L929 cells and INS1E were seeded onto adherent 24 well plates at a concentration of $2x10^5$ cells/well. After 24hours leachable (fucoidan in powder and MFu microparticles dissolved on DMEM medium for 24hours) were placed in contact with cells and a MTS ((3-(4,5-dimethylthiazol-2-yl)-5-(3-carboxymethoxyphenyl)-2-(4-sulfophenyl)-2H-tetrazolium)) assay and Cell-Titer Glo assay were performed to screen the cellular viability after 24, 48 and 72 hours [147].

III-4.2.2. Seeding L929 cells in surface of the particles

To evaluate the biological performance of the modified fucoidan particles, an *in vitro* cell adhesion test was performed using L929 fibroblast-like cells **(Chapter IV and V)**. For these experiments, L929 cells were cultured in Dulbecco's modified Eagle's medium (DMEM) supplemented by 10 % (v/v) fetal bovine serum (FBS) and 1 % (v/v) antibiotic- antimycotic [9,170–172]. L929 were seeded on the surface of the materials (10 particles/well) and TCPS at a density of 3.5×10^5 cells/mL (500 μL/well) and cultured for 1, 7 and 14 days **(Figure III – 22)**. Triplicates were made for each sample formulation. The samples were incubated at 37 °C in a humidified 95 % air/5 % CO_2 atmosphere. Culture medium was replaced twice a week. After each culture time, the medium was removed, and the samples were washed with a PBS solution. After each time point, the cell viability, proliferation, total protein quantification and morphology of the samples was evaluated, as described below.

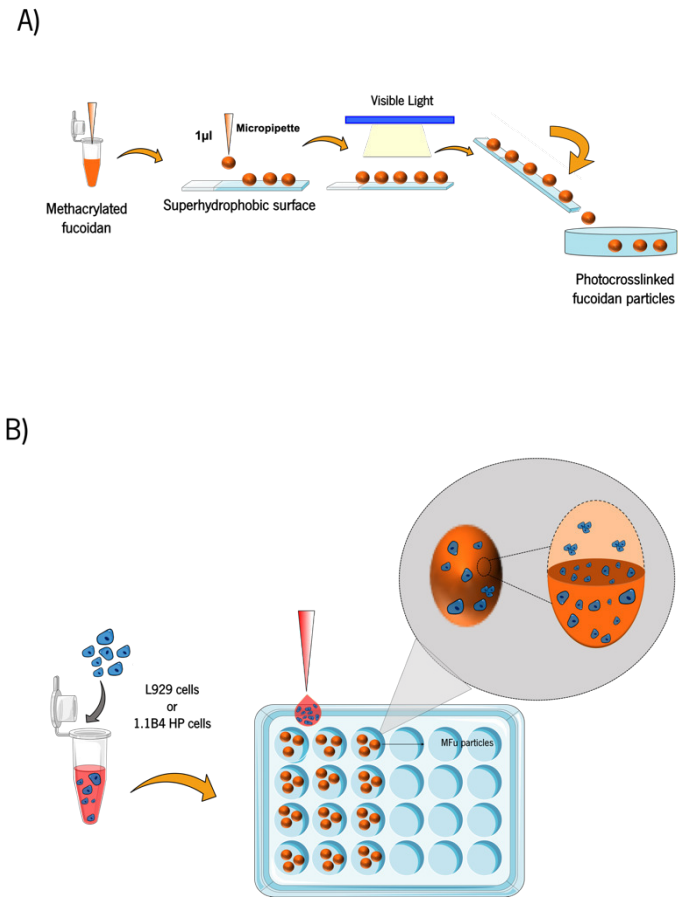


Figure III-22. Scheme depicting of modified fucoidan particles (MFu) and direct contact with cells (L929 and 1.1B4 cells). A) Pipetting the solution of methacrylated fucoidan (MFu) with photoinitiators and crosslinking of fucoidan-based particles with visible light and B) Seeding of cells (L929 and 1.1B4 cells) in the surface of fucoidan-based microparticles.

III-4.2.3. Encapsulation 1.1B4 in Hydrogels

The effect of methacrylation and photocrosslinking on cell viability, adhesion and proliferation was assessed by direct contact of 1.1B4 human pancreatic cells in MFu microparticles **(Figure III - 22) (Chapter V).** These cells were also encapsulated within the Agarose/Fucoidan (AgaFu) hydrogels in **Chapter VI** to demonstrate the ability of the system to support the encapsulation of viable cells. A cell suspension of 1.1B4HP cells (1.5 x 10^6 cells/mL) was prepared by trypsinization (trypsin/EDTA solution, Gibco) and mixed with the Aga and AgaFu polymer solution at 37 °C. The

protocol for generating hydrogels laden with 1.1B4 HP cells was similar to that described for obtaining the simple Aga and AgaFu hydrogels **(Figure III - 23)**. The viability of the encapsulated cells in the hydrogels was assessed by using the live/dead assay, was performed for 1, 3, and 7 days. After each culture time, the medium was removed, and the samples were washed with a PBS solution for a posterior characterization.

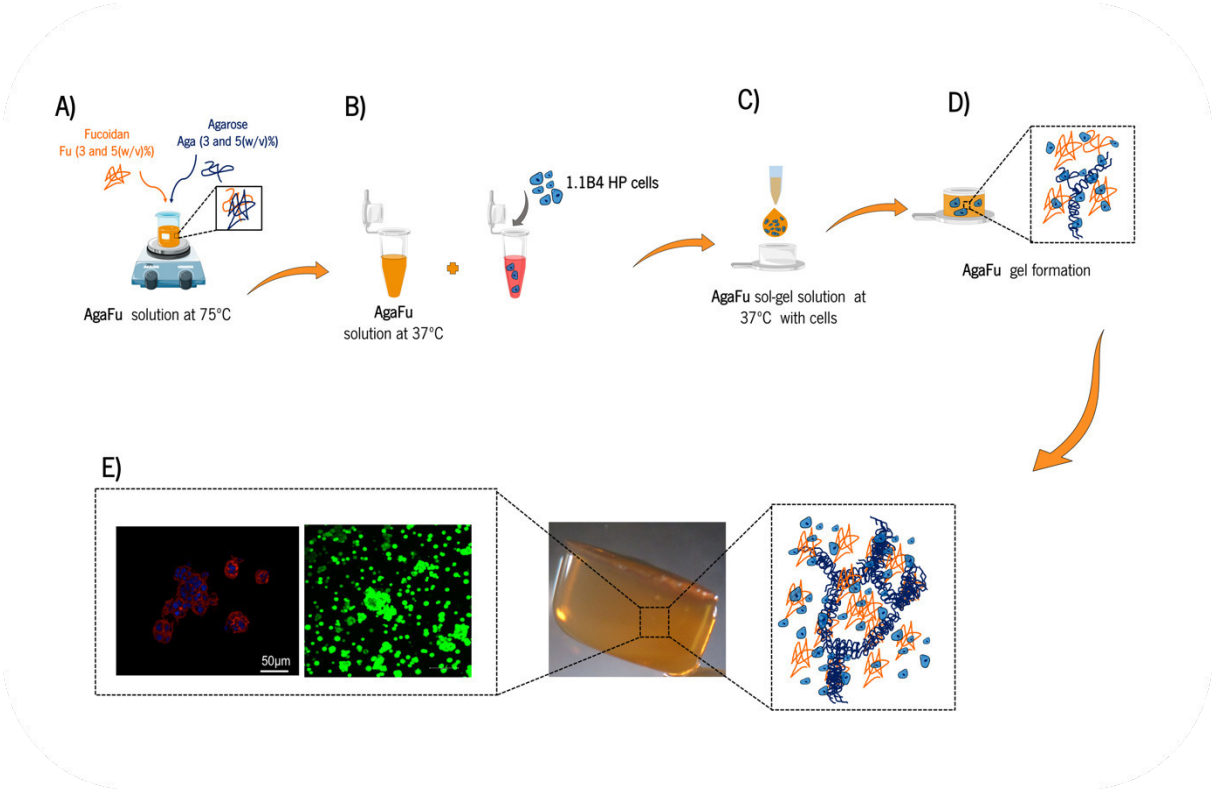


Figure III-23. Schematic representation for production of agarose-fucoidan hydrogels (AgaFu). A) Preparation of agarose (Aga) or agarose/fucoidan (AgaFu) solutions, B) Preparation of the pellet of 1.1B4HP cells and adding to Aga or AgaFu solutions, C) transferring of Aga or AgaFu solutions with cells to molds D) formation of Aga and AgaFu gel with encapsulated cells by cooling the solution at room temperature and E) AgaFu hydrogels with cells.

III-4.2.4. Formation of aggregates of single cells islets

Aiming to mimic a pancreatic islet, cell aggregates can be made from single beta cells in agarose chips. Non-adherent agarose microwell chips were aseptically fabricated by replica molding as described previously [173–175]. Briefly, negative replicates of patterned poly-

dimethylsiloxane (PDMS, Sylgard 184, Dow Corning, Midland, USA) stamps, each containing 1585 microwells with a diameter of 400 µm, were prepared using 3 % agarose solution (Ultra-pure agarose, Invitrogen, Bleiswijk, The Netherlands) [175]. After agarose solidification, the molds were removed, covered with PBS, and stored at 4 °C until usage **(Figure III - 24A)**. Before cell seeding, the agarose chips were pre-incubated in culture medium overnight at 37 °C. For cell aggregate formation, single cells were resuspended in fresh medium and 800'000 INS1E cells were seeded per agarose chip **(Figure III -24B)**. Immediately after seeding, agarose chips were briefly centrifuged at 200 g during 1 min to allow the cells to settle down in the microwells. Medium was refreshed every 1-2 days **(Figure III -24 B-C)**. Cell aggregates were cultured up to 4 days after which they were removed from the chips by upside down for further use. To measure the average aggregate diameter, microscopic images were taken, and the aggregate diameter was quantified using Image J [176].

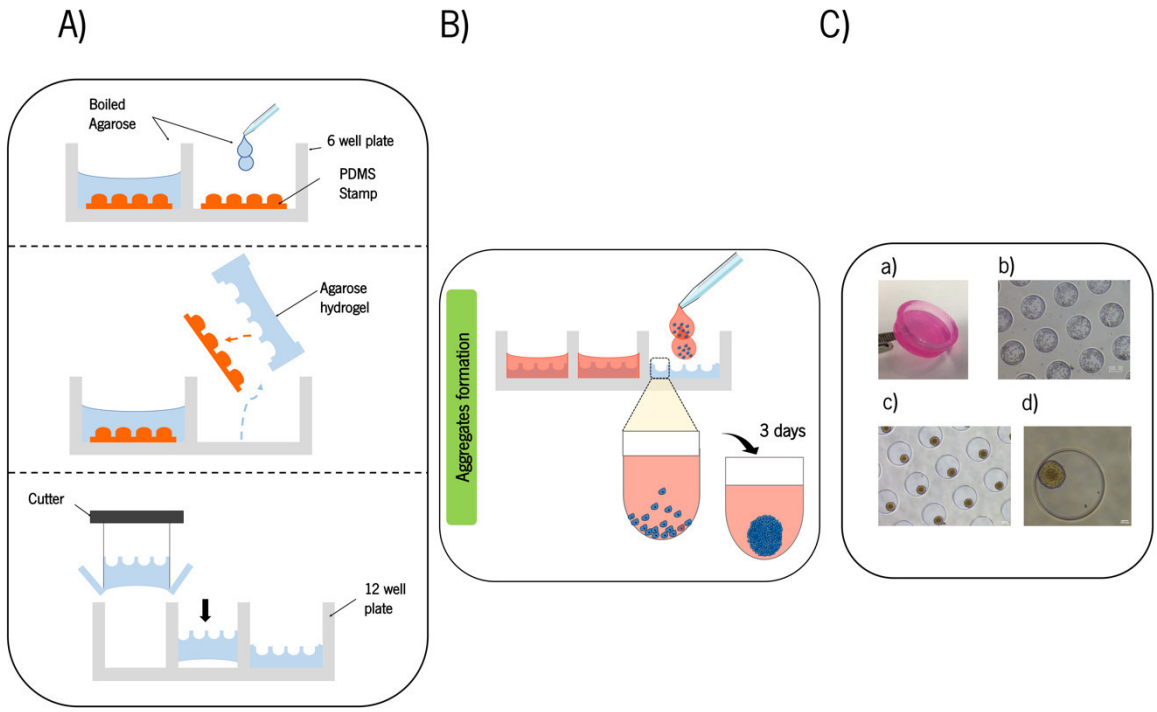


Figure III-24. Schematic representation of agarose microwell fabrication and cell aggregation. A) Agarose microwell fabrication 1) PDMS stamp that contains positive microwells. By pouring a 3% agarose solution on top of negative microwells. 2) Removing PDMS stamps and production of agarose microwells 3) Cut the agarose

hydrogel and placed in a new 12 well plate. B) Cell Aggregation a) Seed single cells in solidified agarose microwells and b) aggregation of the cells over the time. C) Microwells with cells over the time.

III-4.2.5. Encapsulation of INS1E aggregates and rat/pig islets in microcapsules

In **Chapter VII** INS1E aggregates were used in the encapsulation into microcapsules. The encapsulation into microcapsules was carried out using the air-driven droplet generator (Nisco D-0038, Zurich, Switzeland, Nozzle from Biored, California, USA). Before the encapsulation procedure, INS1E aggregates or rat/pig islet cells were removed from agarose chips and pooled together in 50 ml falcon tube. The INS1E aggregates were divided by the volume for each solution. Normally, 800 µl of alginate (2.2 %) or alginate/fucoidan (2.5 %) solutions were added to 100 µl of INS1E aggregates suspension (1:8). Around 0.8 ml of alginate or alginate/fucoidan cell suspension was drawn into 1 ml syringe and loaded onto the encapsulation machine. The principle of microencapsulation using air-driven droplet is shown in **Figure III - 26**. The syringe containing the alginate or alginate/fucoidan (Fucogel) cell suspension was fixed securely onto the encapsulation device, using velocity 16 ml/min and the airflow set at 4 L/min. Once the syringe driver was turned on, the plunger in the driver pushes the syringe downwards, thereby forcing the alginate or alginate/fucoidan cell suspension through the encapsulation device to produce alginate beads (called microcapsules). The beads that formed were collected in a sterile 145 mm petri dish containing 30 ml of $BaCl_2$ coagulation bath (for 1 liter of coagulation bath: 4.89 g barium chloride ($BaCl_2$) solution; 2.093 g MOPS [(3-N-Mopholino)-propanesulfonic acid] (10 mM); 6.43 g sodium chloride (1109 mM) dissolved in 1 L of milliQ water; after dissolution, it was filtered and sterilized) placed at a distance of 16.5 cm from tip of the nozzle of the encapsulation device. Subsequently, the cell-laden alginate or alginate/fucoidan beads were incubated in a 20 mM $BaCl_2$ solution for 2 min, and then washed five times with phosphate buffer solution (PBS) to remove excess $BaCl_2$. The microcapsules were allowed to settle after repeated washings, and the supernatant was discarded. The microencapsulated INS1E aggregates were then incubated in supplemented RPMI 1640 medium at 37 °C, 5 % CO_2 until used for *in vitro* studies.

To explore the potential of fucoidan to alleviate oxidative stress post-encapsulation, we encapsulated genetically encoded redox probe mt-roGFP2-Orp1 transduced INS1E beta cells (INS1E report cells) were used. The probe is a fusion protein consisting of redox-active green fluorescent protein 2 (roGFP2) genetically fused to the redox enzyme Orp1 that is oxidized by H_2O_2 [177]. A major advantage of roGFPs over other fluorescent probes is their ratiometric fluorescence excitation behavior. When measuring fluorescence emission at 510 nm, roGFP2 exhibits excitation maxima at both 400 and 490 nm; oxidation increases the intensity of the 400 nm peak while decreasing the intensity of the 490 nm peak and vice versa for reduction **(Figures III- 25)**. The procedure used for encapsulation of INS1Es report cells was the same used for the encapsulation of INS1Es aggregates. Briefly, we used a genetically encoded redox probe mt-roGFP2-Orp1 transduced INS1E beta cells (passage 93). Stably expressing mito-roGFP2-Orp1 INS1E cells were obtained from Leticia Prates Roma (Saarland University). INS1E cells were retrovirally transduced with pLPCX mito roGFP2-Orp1 as previously described for H1975 cells [178,179]. The stably transduced mito-roGFP2-Orp1 INS1E cells were cultured in RPMI (Gibco 61870) supplemented with 5% (v/v) fetal bovine serum, 10 mM HEPES, 1 mM sodium pyruvate, 100 U/ mL penicillin, 100 mg/mL streptomycin and 0.05 mM 2-mercaptoethanol at 5% CO_2 at 37°C. For these experiments INS1Es report cells were cultured as previously described. Report INS1Es cells were encapsulated in ALG and fucocaps at a density of 1 x 10^6 cells/ml described before for 24hours. In the following day the encapsulated cells were washed with PBS and exposed to H_2O_2 (1 mM) for 1 hr to induce oxidative stress. To induce reduction and oxidation, DTT (5 mM) and Diamide (0.5 mM) were added respectively as controls and the OxDmtroGFP2 was calculated as previously described [180].

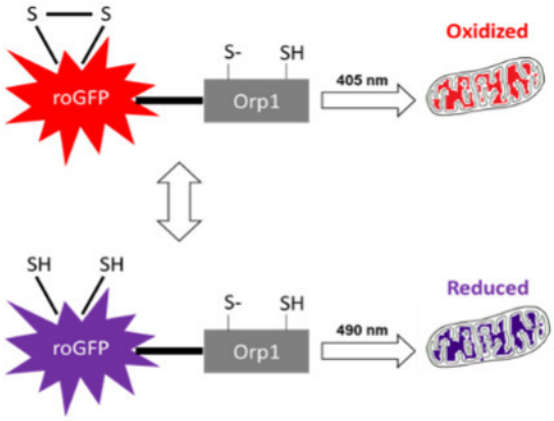


Figure III-25. Schematic illustration of the mitochondrial ROS sensor mt-roGFP2-Orp1

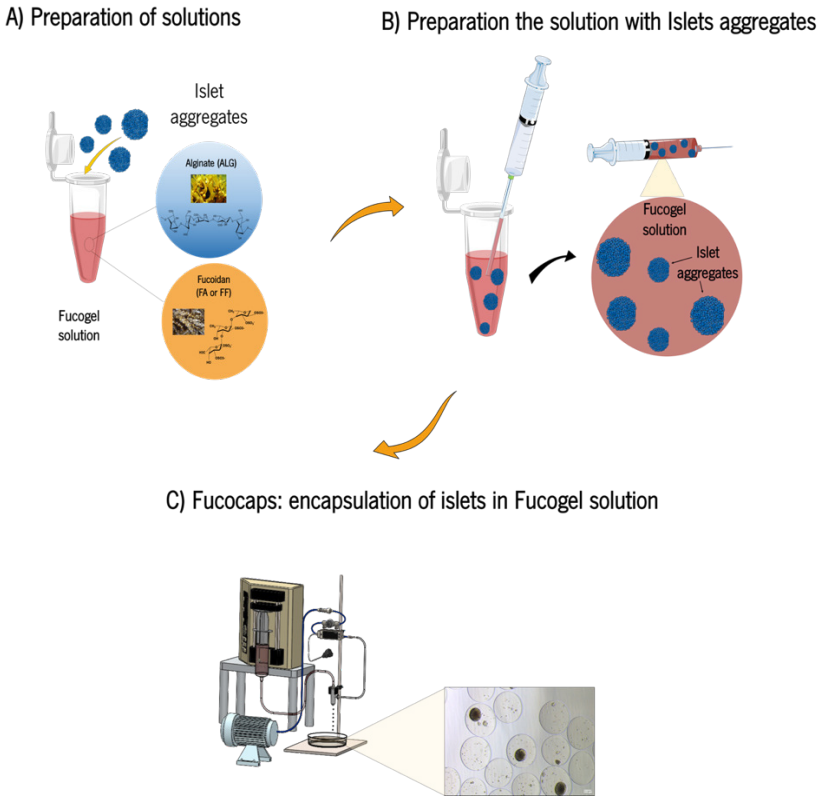


Figure III-26. Schematic representation of cell encapsulation in ALG or ALGFu. A) Preparation the solutions of alginate or alginate/fucoidan (FA or FF) and pellet of islet aggregates, B) Added the islet aggregates and transfer for a syringe and C) Production of microcapsules with islets encapsulated using droplet generator.

III-4.3. Evaluation of cell culture

In vitro cell culture studies performed under the scope of this thesis include experiments/assays designed to evaluate the *in vitro* viability of the cells in both 2D and 3D cultures. In this section it is described the experimental procedure, namely reagent volumes, concentrations, incubation times and temperatures, while other measurement details are extensively described in each respective chapter of **Section 3.** These details varied slightly according to the brand of the kit used and they were always adapted and optimized for each system.

III-4.3.1. Metabolic activity and cell viability examination

III - 4.3.1.1. MTS assay

MTS is commonly used for the analysis of cell metabolic activity and provides an indication of cell viability. This particular assay determines if cells exposed to the different polymers are metabolically active. It is based on reduction of the substrate 3-(4,5-dimethylthiazol-2-yl)-5(3-carboxymethoxyphenyl)-2(4-sulfofenyl)-2H-tetrazolium, MTS, in a mitochondria-dependent reaction to yield a brown formazan product. This conversion is accomplished via NADPH or NADH produced by mitochondrial dehydrogenase enzymes in metabolically active cells. In this sense, only viable cells, undamaged by a foreign agent, can express this enzymatic activity [98,181]. The different systems studied, namely (i) fucoidan in powder and microparticles assessed by direct contact with L929 fibroblast-like cells and 1.1B4 HP cells **(Chapter IV and VI)**, (ii) hydrogels encapsulating 1.1B4HP cells **(Chapters VI),** and (iii) microcapsules encapsulating INS1E and rat/pig islets **(Chapter VIII)** were placed in cell culture plate and incubated at 37 °C and 5 % CO_2. At different pre-determined periods (1, 7, 14, 21 and 28 days), MTS assay was performed protected from light. Briefly, culture medium was removed and 1 mL of culture medium without FBS and without phenol red was mixed with MTS reagent at ratio of 1:5 and added to each well (samples/cells constructs).

Samples were then incubated in the dark at 37 °C and 5 % CO_2. After 3 hours, 100 µL of each well (in triplicate) was transferred to a 96- well plate. The amount of formazan product was measured by absorbance at a wavelength of 490 nm using a multiwell spectrophotometer (Biotek, Synergy HT, USA).

III – 4.3.1.2. ATP bioluminescence assay

ATP bioluminescence is a homogeneous and reproducible method for the determination of cell viability based on the quantification of the existing Adenosine Triphospate (ATP), which directly quantifies the metabolic activity of cells. This assay was designed for direct use in multi-well culture plates, making it ideal for an automated screening of cells cytotoxicity, and highly reproducible. This assay involves adding a single reagent (CellTiter-Glo® Reagent) directly to the cultured cells/hydrogels, prepared in the corresponding serum-free culture medium. The contact with this reagent induces cell lysis and generation of a luminescent signal proportional to the amount of the present ATP. The amount of ATP is directly proportional to the number of cells in culture [182].

In **Chapter VIII**, to quantify the metabolic activity of the cells seeded inside the microcapsules, a Cell-Titer Glo assay was performed. CellTiter-Glo 3D reagent was added to the cell culture media with a 1:1 ratio. The Petri dish was then closed with Parafilm and mixed vigorously for 5 minutes on a plate shaker in order to induce cell lysis, next the plate was left 25 minutes at room temperature to equilibrate the signal. After this, the luminescent signal was recorder with a CLARIOstar microplate reader.

III - 4.3.1.3. Live/dead staining assay for cell viability

Live/Dead assay was used to evaluate the viability of cells cultured on the processed materials **(Chapter V, VI and VIII)**. This test provides a two colors fluorescence simultaneous visualization of the live and dead cells. The live cells were identified using Calcein AM. Despite not being fluorescent, this hydrophobic molecule easily permeates intact live cells. Upon hydrolysis by intracellular esterases, the Calcein AM is converted into Calcein, which is a hydrophilic fluorescent

dye. The Calcein retained in the cell cytoplasm allowed the visualization of the live cells through adequate methods (fluorescent/confocal microscopy, excitation ≈ 495 nm, and emission ≈ 515 nm), as cells will appear bright green and recorded as live cells. The dead cells were labeled by propidium iodide (PI), which binds to nuclear DNA by intercalating between the bases, with little or no sequence preference, after crossing the damaged cell membrane of dead cells (that is not permeant in live cells). Thus, by using a rhodamine filter (fluorescence excitation of 535 nm and emission of 617 nm), cells will appear bright red and recorded as dead cells [31].

Cell viability was assessed after each time point using live/dead assay (n= 3 samples per well, in triplicate). Briefly, the samples (hydrogels) were incubated for 10 min with 2 µL calcein-AM (1 mg mL-1) and 1 µL PI (1 mg mL-1) in 1 mL of PBS protected from light. Afterward, the samples were washed with PBS to remove residual fluorescent and visualized by optical or confocal microscope.

In **Chapter VIII**, this staining was performed in order to determine the viability of cells inside a closed device. The first step of this staining is to prepare a calcein-AM (2.5 µM)/ethidium homodimer-1 (4 µM) solution in PBS. This was obtained by mixing 2.5 µL calcein-AM (1 vial) and 5 µL ethidium bromide in 4 mL of PBS. The sealed device containing cells was washed with 5 mL of PBS, and then 2.5 mL of LIVE/DEAD® assay reagent was added to the sample. The cells were left to incubate for 45 minutes at room temperature, after which they were ready to be observed under a fluorescent microscope.

III-4.3.2. DNA content

DNA assay is one of the most used measurements to evaluate cell proliferation by quantifying the double strand DNA (dsDNA) content of cells cultured on the developed devices. Double stranded DNA quantification is based on fluorescence enhancement of a dye, PicoGreen, upon binding to dsDNA. The relative fluorescence units measured correlate with the total number of cells [98,183]. In this sense, measurements of DNA are frequently taken to be representative and indicative of cell proliferation [98,184]. The DNA content for different systems, namely (i)

microparticles in direct contact with L929 cells **(Chapter IV)** and (ii) hydrogels in direct contact with, or encapsulating, 1.1B4 cells **(Chapters V and VI)** were analysed for different time points. At different pre-determined periods, each well was washed with PBS and 1 mL of ultrapure sterile water was added. Upon mixing, contents were transferred to eppendorf tubes, which were then placed in a shaking water bath at 37 °C for 1 h. Ultimately, the tubes were immediately stored at -80°C until use [185]. Prior to DNA quantification, samples were defrosted at room temperature and sonicated for 15 min. Samples and controls were vortexed and 28.7 μL of each, plus 71.3 μL of PicoGreen solution and 100 μL of TE (200 mM Tris-HCl and 20 mM EDTA) solution were transferred into an opaque 96-well plate. Triplicates were made for each sample or standard. The plate was incubated for 10 min in the dark and the fluorescence was measured, using an excitation of 485 nm (excitation of the dye) and an emission wavelength of 528 nm (when the dye is bounded to the dsDNA). A standard curve was created (concentration of DNA ranging between 0 and 2 μg mL^{-1}) and the DNA values of the samples were read off from the standard graph [30].

In **Chapter VIII**, this assay was used to detect and quantify the amount of DNA present in the samples. It's important to perform this experiment after the cells of the sample have been lysed, so either after the CellTiter Glo assay or a separate buffer. 10 μL of the lysed CellTiter-Glo samples were taken and 90 μL of PicoGreen solution was added. The plate is left to incubate for 2-5 minute at room temperature covered with aluminium foil. Fluorescent can then be read with a Plate Reader. The values of the samples were compared to the standard curve to calculate the amount of DNA.

III-4.3.3. Cell morphology and distribution study

Confocal laser scanning microscopy (CLSM) is an optical imaging technique used to increase contrast and optical resolution, overcoming the limitations of conventional widefield microscopy. Simultaneously, CLSM facilitates the generation of high-resolution 3D images from a relatively thick sample [135,186,187]. In some cases, the 3D reconstruction allows a better understanding of the distribution, organization or morphology of cells, or molecules of interest. Confocal microscopy was

a very useful technique to assess cellular viability by Calcein AM in 1.1B4 human pancreatic encapsulated in fucoidan microparticles, fucoidan based hydrogels, described in **Chapters IV, V, VI and VIII**. CLSM was also used for the detection of specific formation of pseudo islets. Samples were prepared accordingly to Calcein AM and immunofluorescence protocols above mentioned before analyzed under a confocal microscope (Leica, TCS SP8, Germany) equipped with argon/He-Ne laser sources. Briefly, the samples (microparticles and hydrogels) were incubated for 10 min with 2 μL calcein AM (1 mg mL^{-1}) and 1 μL PI (1 mg mL^{-1}) in 1 mL of PBS protected from light. Afterward, the samples were washed with PBS to remove residual fluorescent and visualized by confocal. For the immunofluorescence, before staining, at each time point, the culture medium was removed, and 10 % formalin was added to each well (n = 5 particles or capsules per well, in triplicate). After 1 h at RT, formalin was removed and replaced by 0.1 % Triton X for 5 min to permeabilize cells. Upon PBS washing, 1 mL of PBS containing 1 μL of DAPI and 10 μL of Phalloidin was added to each well. After 1 hour at RT protected from light, samples were washed three times with PBS and immediately visualized in the dark by confocal. Cell nuclei appeared bright blue, and F-actin filaments appeared on bright red, respectively, due to DAPI and phalloidin dyes.

III-4.3.4. Micro BCA

Micro Bicinchoninic Acid Protein assay (Micro BCA™) is a colorimetric method that quantifies protein content in a sample [188]. The test combines the protein induced biuret reaction with the highly sensitive and selective colorimetric detection of the resulting cuprous cation (Cu^{1+}) by BCA [183]. This assay is based in the reduction of Cu^{+2} to Cu^{+1} by protein in an alkaline environment. The chelation of Cu^{+1} by two molecules of BCA creates a purple color that is linear with increasing protein concentrations. Micro-BCA assay was used to determine the amount of protein present in MFu particles, according to manufacturers' instructions (Fisher Scientific, USA). Working Reagent was prepared by mixing Micro BCA Reagent MA, MB and MC at the proportion of 25:24:1. Following, 150 μL of the sample (including blank, control and standards) and Working Reagent were mixed in a multi-well plate and incubated at 37 °C for 2 h. After, the plate was cooled to RT and the absorbance was read at 562 nm in a Synergy HT multi-mode microplate reader (BioTek,

Synergy HT, USA). A standard curve, using albumin as a standard (0 to 200 μg/ml), was created and sample protein values were read off from the standard graph. Plotting the measured absorbance against albumin concentration allowed the calculation of protein concentration.

III-4.3.5. *In vitro* insulin secretion assays

III - 4.3.5.1 Glucose induced insulin secretion test (GSIS)

To test the insulin secretion of rat insulinoma cells (INS1E) and INS1E aggregates, a glucose-stimulated insulin secretion (GSIS) assay were performed at day 1 and 5. Each sample was pre-incubated for 1 hour in a glucose-free incubation buffer consisting of a modified Krebs-Ringer bicarbonate buffer with (115 mM of sodium chloride (NaCl), 5 mM potassium chloride (KCl), 24 mM sodium bicarbonate ($NaHCO_3$) and 2.2 mM calcium chloride ($CaCl_2$)) at pH 7.4 supplemented with 20 mM (4-(2-hydroxyethyl)-1-piperazineethanesulfonic acid) (HEPES), and 2 mg/ml human serum albumin (Sanquin, Amsterdam, The Netherlands). Subsequently, samples were incubated with three consecutive steps of 1.5 h consisting of low glucose (1.8 mM), high glucose (20 mM), and another low glucose (1.8 mM) in KRBH buffer at 37 °C. The media samples were collected after each incubation step and concentrations of secreted insulin were determined by ELISA assay according to the manufacturers´ protocol (Mercodia, Uppsala, Sweden). Secreted insulin was normalized to the total insulin amount. Stimulation index (SI) was calculated as a ratio of released insulin after high glucose stimulation divided by released after low glucose stimulation [176].

III - 4.3.5.2. Effect of fucoidan on insulin secretion (dose - and time- response)

To assess rat insulinoma functionality, a glucose-induced insulin secretion test was performed at different time points (3, 6, 12 and 24h) [175]. The INS1E cells were seeded into 24-well plates at a density of 2 x 10^5 cells/well in RPMI 1640 medium, supplemented with penicillin streptomycin 5 % (v/v) fetal bovine serum (FBS), 1 % sodium pyruvate and 1 % HEPES 1 M, and incubated at

37℃ in an atmosphere of 5 % CO_2 for 24 hours. The cells were then treated with various doses of fucoidan (0, 0.1, 0.5, 1, 5, and 10 mg/ml) for 3 hours; and with 5 mg/ml fucoidan for various durations (6, 12 and 24 hours), in the presence of a 20 mM high glucose condition. As controls, cells were exposed to low glucose (2.8 mM) concentrations. Aliquots of the media were removed from each of the wells and centrifuged (1.175 x g, for 5 min at 4 °C) to remove the cells and stored at -20 °C. For insulin content, cells were exposed to 600µl of acid ethanol (2.0 ml 37 % HCl+13 ml dH20+35 ml 100 % ethanol), incubated overnight at 4 °C, followed by vortexing and centrifugation to collect the supernatant. Secreted insulin was normalized to the total insulin amount. The concentration of insulin in the supernatants was determined using an insulin ELISA kit (Mercodia, Uppsala, Sweden). The absorbance was measured at 450 nm using a CLARIOstar microplate reader (BMG Labtech, Cary, North Carolina, United States).

III - 4.3.5.3. Quantification of insulin secretion

In **Chapter VIII**, the possible mechanism of action for fucoidan induced insulin secretion was studied. For insulin secretion assay using rat islets, 20 rat islets were hand-picked and seeded in a non-adherent 24 wells plate equipped with a 24 well culture insert containing 1 ml RPMI 1640 medium, supplemented with penicillin, streptomycin, and 10 % FBS, and incubated at 37 °C in an atmosphere of 5 % CO_2 for 24 h. After 24 hours, the insert with islets were taken out of the wells plate and blot dry on paper wipe. Then were washed 3 x 5 min with 600 µl of low glucose solution (1.7 mM) and equilibrated the samples for at least 1.5 h at 37 °C in low glucose solution. The inserts with islets were taken out of the wells plate and blot dry on paper wipe. The islets were then exposed to different test conditions namely i) low glucose (1.7 mM); ii) high glucose (17 mM); high glucose + fucoidan (5 mg/ml); high glucose + 50 µM phosphodiesterase inhibitor (IBMX) + 5 mg/ml fucoidan; high glucose + 50 µM MDL 12330A hydrochloride + 5 mg/ml fucoidan for 1 h at 37°C. After 1 hour, aliquots of the media were removed from each of the wells and stored at -20°C. For insulin content, islets were exposed to 600 µl of acid ethanol (2.0 ml 37 % HCl+13 ml dH_2O+35 ml 100 % Ethanol), incubated overnight at 4 °C, followed by vortexing and centrifugation to collect supernatant. The concentration of insulin in the supernatants was determined using an

insulin ELISA kit (Mercodia). The absorbance was measured at 450 nm using the Clariostar microplate reader.

III-4.3.6. Antioxidant properties of fucoidan in the presence of pancreatic cells

III - 4.3.6.1. DCFH test for determination of intracellular oxidative stress

DCFH-DA probe (Intracellular ROS assay) is a fluorescence-based and quantitative method used to measure intracellular generation of H_2O_2 and other oxidants or monitor redox signaling changes in cells in response to intra or extracellular activation with oxidative stimulus. This probe is cell-permeable and is hydrolyzed intracellularly to the DCFH carboxylate anion, which is retained in the cell. Two-electron oxidation of DCFH results in the formation of a fluorescent product called dichlorofluorescein (DCF) **(Figure III - 28).** Consequently, DCF can be monitored by several fluorescence-based techniques. In **Chapter VIII,** the intracellular oxidative stress studies on fucoidan extracts and after cell encapsulation were performed using this assay, that results in a fluorescent signal after oxidation by a wide range of Reactive Oxygen Species (ROS) [189,190]. Despite several limitations like its limited specificity to measure H_2O_2, the DCFH assay is still appropriate to measure general oxidative stress [190–193]. A stock solution of 10 mM DCFH-Diacetate was made in DMSO, dilutions were made in exposure medium comprising minimal essential Dulbbecco´s modified eagle medium (Gibco 1180-028) supplemented with 10 mM HEPES, 1 mM sodium pyruvate, 200 g/L glucose and 200 mM L-glutamine. For direct measurements, INS1E were seeded at a density of 140,000 cells/well in a black 96 well plate with clear bottom cultured overnight. Next, cells were incubated for 45 minutes, with 20 μM DCFH-Diacetate at 37 °C and 5 % CO_2. Then, cells were washed using PBS. Cells were incubated with or without fucoidans (FA or FF) extracts (10 mg/ml), the extracts were prepared in an exposure medium. Afterward, cells were incubated with 10 mg/ml fucoidan extracts or a combination of 10 mg/ml fucoidan extracts and 2 mM H_2O_2. Every 5 minutes, the fluorescence was determined for a period of 60 minutes on CLARIOstar microplate reader (BMG Labtech, Cary, North Carolina, United States) using an excitation wavelength of λ= 485 nm and measuring emission at λ= 538 nm and the level of

oxidative stress was determined [194]. The area under the kinetic curve was considered the total oxidative stress experienced by cells and was normalized to the number of viable cells and a reference sample of cells on tissue culture polystyrene after 1 day.

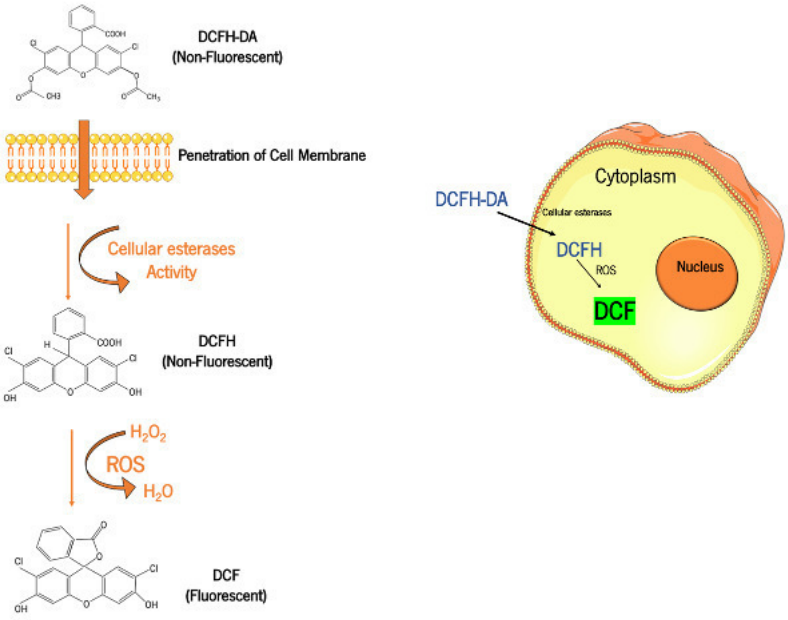


Figure III - 28- Schematic representation of DCFH-DA probe action inside the cells A) mechanism of DCFH-DA probe. DFH-DA is cleaved by intracellular esterases to DCFH and oxidized by ROS to highly florescent molecule DCF. B)possible mechanism of DCFH-DA inside the cell (adapted from [198]).

III-4.3.7. RNA sequencing

Transcriptome sequencing is used to reveal the presence, quantity and structure of RNA in a biological sample under specific conditions. Compared to hybridization-based RNA quantification methods such as microarray analysis, sequencing-based transcriptome detection can quantify gene expression with low background, high accuracy and high levels of reproducibility within a large dynamic range. In addition, transcriptome sequencing does not require an existing genome sequence and can detect mutations, splice variants and fusion genes that cannot be detected by microarrays [196,197].

The experimental work on the **Chapter VIII** involved the use of molecular approaches (RNA-seq) to understand the effect of fucoidan treatment on the varied cellular pathways in INS1E cells in the presence or absence of H_2O_2.

For RNA Isolation, INS1E cells ($1x10^6$/well) were seeded onto 6 well plates and the cells exposed to H_2O_2 (1mM) for 1hour in the presence or absence of fucoidan (5mg/ml). Following incubation, the cells were washed in PBS, lysed and RNA isolation performed according to the RNeasy Mini Kit (Qiagen, Netherlands) and quantified using the BioDrop (BioChrom, United Kingdom).

The RNA-sequencing sample was prepared using a KAPA Stranded mRNA-Seq Kit, with KAPA mRNA Capture Beads (Roche, cat# 07962207001) protocol being performed on 500ng of initial RNA from bulk material. RNA size selection was performed for 300pb fragments. RNA-seq libraries were amplified with 8 cycles. The purified libraries were quantified using Qubit (ThermoFisher) and the fragment distribution analyzed using TapeStation (Agilent). Complete libraries were sequenced (paired-end) on Illumina HiSeqTM4000, with 151bp from each end.

The transcriptomic analysis was performed by RNA-seq reads, aligned to the reference genome (rat rn6) using HISAT2 (version 0.1.6) with default parameters. Read counts representing gene expression levels were calculated with featureCounts (version 2.0.0) using default parameters. Only genes with counts above zero were retained for the downstream analyses. Differential expression analyses were performed using EdgeR (version 3.12) with adjusted p-value < 0.05 as the cutoff. Factor normalization was done using the CPM method. Dimension reduction and clustering analysis were performed on EdgeR. All Gene Ontology (GO) analyses were performed with ToppGene method (https://toppgene.cchmc.org/), and only Biological Process terms were kept for downstream analyses. Enrichment score was calculated from the as -log10 of the p-value. Plots were created using GraphPad Prism7.

III-4.4. *In ovo* assement of the angiogenic potential of fucoidan

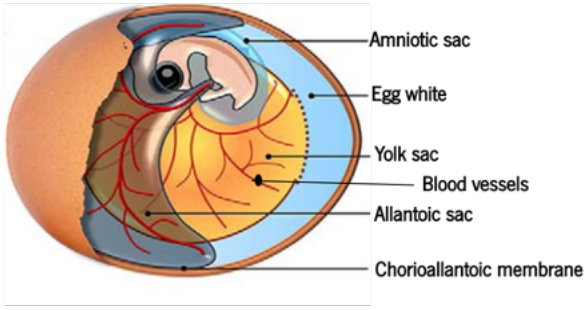
III-4.4.1. Chick chorioallantoic membrane assay (CAM)

The chick embryo chorioallantoic membrane (CAM) is an extraembryonic membrane that is highly vascularized. Its principal function is to exchange gases and nutrients between the growing embryo and environment and is assisted by a dense capillary network [198–200]. Due to its extensive vascularization and its ease of use and cost-effectiveness, the CAM is a widely utilized research tool **(Figure III - 28 A)** to study morpho-functional characteristics of angiogenesis *in vivo* as well as the efficacy and mechanisms of action of pro- and anti-angiogenic molecules [198–200]. We focused on the use of the CAM as an assay for the study of angiogenic potential of system/platform to be used in the treatment of diabetes mellitus. In their native state, islets of Langerhans are characterized by extensive vascularization, with this being important for proper glucose sensing and consequent insulin secretion, thus assuring their correct functionality [201]. In this perspective, the islet transplantation involving encapsulated pancreatic cells require competent vascularization, promoted by the encapsulation material or other supports [202]. In this thesis it was proposed the use of a membrane inducing angiogenesis, which would support the integration of hydrogels or capsules encapsulating pancreatic islets with patient tissues through a vast vascular network.

In **Chapter VII**, CAM assay was conducted to evaluate the effectiveness of the PCL and PCL/fucoidan airbrushed nanofibers meshes to promote angiogenesis. This method was conducted as described in the referred chapter. White fertilized chicken eggs from Pintobar (n=150, Pintobar, Amares, Portugal) were incubated at 37°C for 3 days (model B8420, Termarks; Bergen, Norway). In the longitudinal extremities of the egg, two small holes were created to promote dissociation of CAM from the membrane of the eggshell. A circular window was open into the eggshell to assess CAM and embryo viability. The window in the eggshell was then sealed with transparent tape (~50 x 30 mm, AXTON 50 mm) to avoid dehydration and the eggs were incubated again at 37°C until day 10th of embryonic development. At day 10 of embryonic development, the sterile PCL and PCLFF airbrushed nanofibrous meshes, prepared as previously described, and controls (without membranes) were implanted on the CAM.

Following implantation, shell opening windows were protected again with transparent tape, and the eggs returned to the incubator at 37°C until day 15th of embryonic development **(Figure III – 28 B)**. All these procedures were performed in a laminar flow hood to minimize contamination. At the 15th day, the chicken embryos were sacrificed by adding paraformaldehyde (PFA, Merck, Berlin, Germany) solution at 4% (v/v), followed by its incubation at -80°C for 10 min in an ultra-low freezer. The implanted materials with underlying CAM portions were cut and fixed with 4% paraformaldehyde. *Ex ovo* images were acquired with camera (Nikon D5100) with tripod in constant distance and manual mode, for each condition; the photos were taken in both sides of the CAM (i.e. chorinic and allantoic ephithelium). A minimum of 5 eggs/samples were used for each condition.

A)



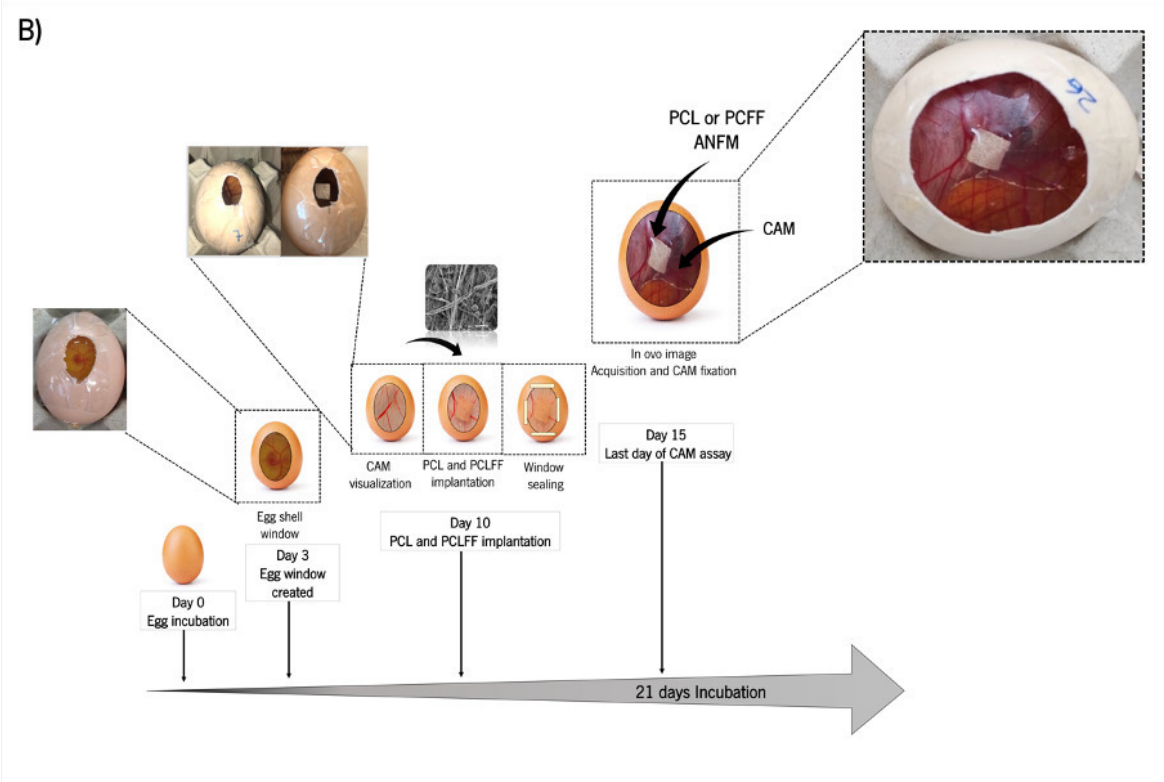


Figure III - 29 - A) Diagram illustrating a chicken egg in its 10th day with all extraembryonic membranes, B) Schematic representation of the optimized chorioallantoic membrane (CAM) assay. Fertile eggs were incubated for 3 days before creating the window. At 10th day PCL and PCLFF ANFM were placed on the CAM and the eggshell was sealed to prevent infection. The assay proceeded until day 15 (adapted from [203,204]).

III-5. STATISTICAL ANALYSIS

GraphPad Prism 7.00 software (San Diego, USA) was used to perform statistical analysis. Statistical significances (*$p<0.05$, **$p<0.01$; ***$p<0.001$) were determined using specifical statistical test. Data was analyzed by Shapiro-Wilk test to assess data normality. Data with normal distribution was analyzed using one-way analysis of variance, followed by Turkey post-test or Dunnett's post-test, when more than two groups were compared. Data that did not follow a normal distribution was analyzed by the Kruskal-Wallis test, followed by Dunn's multiple comparison test, when more than two groups were compared. The quantitative results are as mean ± standard deviation.

III-6. REFERENCES

[1] Kim K-T. *Seasonal Variation of seaweed components and novel biological function of Fucoidan extracted from Brown Alage in Quebec*.Departement Des Sciences des Aliments et de Nutrition. FACULTÉ DES SCIENCES DE L'AGRICULTURE ET DE L'ALIMENTATION UNIVERSITÉ LAVAL QUÉBEC; 2012.

[2] Cunha L, Grenha A. *Sulfated Seaweed Polysaccharides as Multifunctional Materials in Drug Delivery Applications*.Mar Drugs 2016. 14(3):42.

[3] Ferreira LFG. *Extração de fucoidana a partir da alga marinha Bifurcaria bifurcata*.Instituto Politécnico de Viana; 2016.

[4] Wijesinghe WAJP, Jeon Y-J. *Biological activities and potential industrial applications of fucose rich sulfated polysaccharides and fucoidans isolated from brown seaweeds: A review*.Carbohydr Polym 2012. 88(1):13–20.

[5] Usov AI, Zelinsky ND. *2 - Chemical structures of algal polysaccharides A2 - Domínguez, Herminia*.In: 2013. Woodhead Publishing; 2013. p. 23–86.

[6] Li B, Lu F, Wei X, Zhao R. *Fucoidan: Structure and bioactivity*.Molecules 2008. 13:1671–95.

[7] Chizhov AO, Dell A, Morris HR, Haslam SM, McDowell RA, Shashkov AS, et al. *A study of fucoidan from the brown seaweed Chorda filum*.Carbohydr Res 1999. 320:108–19.

[8] Bilan MI, Grachev AA, Ustuzhanina NE, Shashkov AS, Nifantiev NE, Usov AI. *Structure of a fucoidan from the brown seaweed Fucus evanescens C.Ag*.Carbohydr Res 2002. 337(8):719–30.

[9] Reys LL, Silva SS, Soares da Costa D, Oliveira NM, Mano JF, Reis RL, et al. *Fucoidan Hydrogels Photo-Cross-Linked with Visible Radiation As Matrices for Cell Culture*.ACS Biomater Sci Eng 2016. 2(7):1151–61.

[10] Silva TH, Alves A, Popa EG, Reys LL, Gomes ME, Sousa RA, et al. *Marine algae sulfated polysaccharides for tissue engineering and drug delivery approaches*.Biomatter 2012. 2(4):278–89.

[11] Cardoso J., Costa, R, R., Mano, J, F., C. *Polissacarídeos de origem marinha aplicados à libertação controlada de agentes bioativos.*Valorização dos recursos marinhos: Biomateriais em regeneração de tecidos e libertação de fármacos.: Tórculo Comunicación Gráfica,; 2015.

[12] Wilfred Fung, Mak W, White Nazimah LH. *Extraction, Characterization and Antioxidant Activity of Fucoidan from New Zealand Undaria pinnatifida (Harvey) Suringar.*Vol. Masther of, Faculty of Health and Environmental Scinces . Auckland University; 2012.

[13] Rioux LE, Turgeon SL, Beaulieu M. *Characterization of polysaccharides extracted from brown seaweeds*.Carbohydr Polym 2007. 69(3):530–7.

[14] Yuan Y, Macquarrie D. *Microwave assisted extraction of sulfated polysaccharides (fucoidan) from Ascophyllum nodosum and its antioxidant activity*.Carbohydr Polym 2015. 129:101–7.

[15] Hahn T, Lang S, Ulber R, Muffler K. *Novel procedures for the extraction of fucoidan from brown algae*.Vol. 47, Process Biochemistry. 2012. p. 1691–8.

[16] Pomin VH, Valente AP, Pereira MS, Mourão PAS. *Mild acid hydrolysis of sulfated fucans: A selective 2-desulfation reaction and an alternative approach for preparing tailored sulfated oligosaccharides*.Glycobiology 2005. 15:1376–85.

[17] Balboa EM, Rivas S, Moure A, Dominguez H, Parajo JC. *Simultaneous extraction and depolymerization of fucoidan from Sargassum muticum in aqueous media*.Mar Drugs 2013. 11(11):4612–27.

[18] Rodriguez-Jasso RM, Mussatto SI, Pastrana L, Aguilar CN, Teixeira JA. *Microwave-assisted extraction of sulfated polysaccharides (fucoidan) from brown seaweed*.Carbohydr Polym 2011. 86:1137–44.

[19] Ale MT, Meyer AS. *Fucoidans from brown seaweeds: an update on structures, extraction techniques and use of enzymes as tools for structural elucidation*.RSC Adv 2013. 3(22):8131–41.

[20] Mak WF. *Extraction, characterization and antioxidant activity of Fucoidan from New Zealand Undaria pinnatifida (Harvey) Suringar*.Auckland University of Technology; 2012.

[21] Sabboural P, Chaubet F, Rouzet F, Al-Shoukr F, Azzouna R Ben, Bouchemal N, et al. *Purification of a low molecular weight fucoidan for SPECT molecular imaging of myocardial infarction*.Mar Drugs 2014. 12(9):4851–67.

[22] Mihaila Gaharwar Akhilesh K.; Reis, Rui L.; Marques, Alexandra P.; Gomes, Manuela E.; Khademhosseini, Ali SM, Mihaila SM, Gaharwar AK, Reis RL, Marques AP, Gomes ME, et al. *Photocrosslinkable Kappa-Carrageenan Hydrogels for Tissue Engineering Applications*.Adv Healthc Mater 2013. 2(6):895–907.

[23] Rose JB, Pacelli S, Haj AJ El, Dua HS, Hopkinson A, White LJ, et al. *Gelatin-Based Materials in Ocular Tissue Engineering*.Mater (Basel, Switzerland) 2014. 7(4):3106–35.

[24] Cuatrecasas P. *Protein purification by affinity chromatography. Derivatizations of agarose and polyacrylamide beads*.J Biol Chem 1970. 245(12):3059–65.

[25] Sparks DL, Phillips MC. *Quantitative measurement of lipoprotein surface charge by agarose gel electrophoresis*.J Lipid Res 1992. 33(1):123–30.

[26] Oliveira JMT de. *New 3D scaffolds and adequate mesenchymal stem cells culture methodologies for engineering an articular cartilage transplant*.University of Minho; 2009.

[27] Gasperini L, Mano JF, Reis RL. *Natural polymers for the microencapsulation of cells*.J R Soc Interface 2014. 11(100):20140817.

[28] Malafaya PB, Silva GA, Reis RL. *Natural–origin polymers as carriers and scaffolds for biomolecules and cell delivery in tissue engineering applications*.Adv Drug Deliv Rev 2007. 59(4):207–33.

[29] Rinaudo M. *Main properties and current applications of some polysaccharides as biomaterials*.Polym Int 2008. 57:397–430.

[30] Silva J, Reis R, Mano JF. *Natural origin polymer- based multilayers as a tool for tissue engineering strategies*.2016.

[31] Lima ACC. *Development of natural-based hydrogel particles using a biomimetic methodology*.University of Minho;

[32] Vaithilingam V, Vaithilingam Medical Sciences, Faculty of Medicine, UNSW V, Vaithilingam V. *Microencapsulated Human Islets as a Therapy for Type 1 Diabetes*.Guillemin Medical Sciences, Faculty of Medicine, UNSW G, editor. The University of New South Wales; 2010.

[33] Lee KY, Mooney DJ. *Alginate: properties and biomedical applications*.Prog Polym Sci 2012. 37(1):106–26.

[34] Augst AD, Kong HJ, Mooney DJ. *Alginate hydrogels as biomaterials*.Macromol Biosci 2006. 6:623–33.

[35] Breger JC, Fisher B, Samy R, Pollack S, Wang NS, Isayeva I. *Synthesis of "click" alginate hydrogel capsules and comparison of their stability, water swelling, and diffusion properties with that of Ca(+2) crosslinked alginate capsules*.J Biomed Mater Res B Appl Biomater 2015. 103(5):1120–32.

[36] Delaney JT, Liberski AR, Perelaer J, Schubert US. *Reactive inkjet printing of calcium alginate hydrogel porogens—a new strategy to open-pore structured matrices with controlled geometry*.Soft Matter 2010. 6(5):866–9.

[37] Jeon O, Bouhadir KH, Mansour JM, Alsberg E. *Photocrosslinked alginate hydrogels with tunable biodegradation rates and mechanical properties*.Biomaterials 2009. 30:2724–34.

[38] Pillay V, Dangor CM, Govender T, Moopanar KR, Hurbans N. *Ionotropic gelation: encapsulation of indomethacin in calcium alginate gel discs*.J Microencapsul 1998. 15(2):215–26.

[39] Oliveira SM. *Novel 3D scaffolds modified with nanostructured polymeric coatings or micro/nanofibers for tissue engineering applications*.University of Minho; 2014.

[40] Mano JF, Hungerford G, Gómez Ribelles JL. *Bioactive poly(L-lactic acid)-chitosan hybrid scaffolds*.Mater Sci Eng C 2008. 28(8):1356–65.

[41] Antunes JC, Oliveira JM, Reis RL, Soria JM, Gómez-Ribelles JL, Mano JF. *Novel poly(L-lactic acid)/hyaluronic acid macroporous hybrid scaffolds: characterization and assessment of*

cytotoxicity.J Biomed Mater Res A 2010. 94(3):856–869.

[42] Decher G, Hong JD, Schmitt J. *Buildup of ultrathin multilayer films by a self-assembly process: III. Consecutively alternating adsorption of anionic and cationic polyelectrolytes on charged surfaces*.Thin Solid Films 1992. 210–211:831–5.

[43] Labet M, Thielemans W. *Synthesis of polycaprolactone: a review*.Chem Soc Rev 2009. 38(12):3484–504.

[44] Woodruff MA, Hutmacher DW. *The return of a forgotten polymer—Polycaprolactone in the 21st century*.Prog Polym Sci 2010. 35(10):1217–56.

[45] Bezwada RS, Jamiolkowski DD, Lee IY, Agarwal V, Persivale J, Trenka-Benthin S, et al. *Monocryl suture, a new ultra-pliable absorbable monofilament suture*.Biomaterials 1995. 16(15):1141–8.

[46] Allen C, Han J, Yu Y, Maysinger D, Eisenberg A. *Polycaprolactone-b-poly(ethylene oxide) copolymer micelles as a delivery vehicle for dihydrotestosterone*.J Control Release 2000. 63(3):275–86.

[47] Pitt CG, Gratzl MM, Kimmel GL, Surles J, Schindler A. *Aliphatic polyesters II. The degradation of poly (DL-lactide), poly (epsilon-caprolactone), and their copolymers in vivo*.Biomaterials 1981. 2(4):215–20.

[48] Tsuji H, Ikada Y. *Blends of aliphatic polyesters. II. Hydrolysis of solution-cast blends from poly(L-lactide) and poly(E-caprolactone) in phosphate-buffered solution*.J Appl Polym Sci 1998. 67(3):405–15.

[49] Lam CX, Hutmacher DW, Schantz JT, Woodruff MA, Teoh SH. *Evaluation of polycaprolactone scaffold degradation for 6 months in vitro and in vivo*.J Biomed Mater Res A 2009. 90(3):906–19.

[50] Sun H, Mei L, Song C, Cui X, Wang P. *The in vivo degradation, absorption and excretion of PCL-based implant*.Biomaterials 2006. 27(9):1735–40.

[51] Lam Christopher XF, Teoh Swee H, Hutmacher Dietmar W. *Comparison of the degradation of polycaprolactone and polycaprolactone–(β-tricalcium phosphate) scaffolds in alkaline medium*.Polym Int 2007. 56(6):718–28.

[52] Lima A, Mano JF. *Micro/nano-structured superhydrophobic surfaces in the biomedical field: Part II: Applications overview*.Nanomedicine 2015. 10:271.

[53] Lima A, Mano JF. *Micro-/nano-structured superhydrophobic surfaces in the biomedical field: Part I: Basic concepts and biomimetic approaches*.Nanomedicine (Lond) 2015. 10:103–19.

[54] Song W, Lima AC, Mano JF. *Bioinspired methodology to fabricate hydrogel spheres for multi-applications using superhydrophobic substrates*.Soft Matter 2010. 6(23):5868–71.

[55] Lima AC, Custodio CA, Alvarez-Lorenzo C, Mano JF. *Biomimetic methodology to produce*

polymeric multilayered particles for biotechnological and biomedical applications.Small 2013. 9(15):2486,2487-2492.

[56] Rial-Hermida MI, Oliveira NM, Concheiro A, Alvarez-Lorenzo C, Mano JF. *Bioinspired superamphiphobic surfaces as a tool for polymer- and solvent-independent preparation of drug-loaded spherical particles*.Acta Biomater 2014. (10):4314.

[57] Li Wang Jingfeng, Cai Yaopio, Xien Mei. ZJXCHLH. *The hypolipidemic effects and antioxidative activity of sulfate fucan on the experimental hyperlipidemia in rats*.Acta Nutr Sin 1999. 21:280–3.

[58] Deng X, Mammen L, Butt H-J, Vollmer D. *Candle Soot as a Template for a Transparent Robust Superamphiphobic Coating*.Science (80-) 2012. 335(6064):67–70.

[59] Kim S, Chu C-C. *Visible light induced dextran-methacrylate hydrogel formation using (–)-riboflavin vitamin B2 as a photoinitiator and L-arginine as a co-initiator*.Fibers Polym 2009. 10(1):14–20.

[60] Bahney Lujan, T. J., Hsu, C. W., Bottlang, M., West, J. L., Johnstone, B. CS. *Visible light photoinitiation of mesenchymal stem cell-laden bioresponsive hydrogels*.Eur Cell Mater 2011. 22:43–55; discussion 55.

[61] Shih Lin, C. C. H. *Visible-light-mediated thiol-ene hydrogelation using eosin-Y as the only photoinitiator*.Macromol Rapid Commun 2013. 34(3):269–73.

[62] Kirschner Anseth, Kristi S. CM. *Hydrogels in healthcare: From static to dynamic material microenvironments*.Acta Mater 2013. 61(3):931–44.

[63] Schweller RM, West JL. *Encoding Hydrogel Mechanics via Network Cross-Linking Structure*.ACS Biomater Sci Eng 2015. 1(5):335–44.

[64] Ki CS, Shih H, Lin C-C, Ki Han; Lin, Chien-Chi CSS. *Facile preparation of photodegradable hydrogels by photopolymerization*.Polymer (Guildf) 2013. 54(8):2115–22.

[65] Bougault C, Paumier A, Aubert-Foucher E, Mallein-Gerin F. *Molecular analysis of chondrocytes cultured in agarose in response to dynamic compression*.BMC Biotechnol 2008. 8:71.

[66] Huang CY, Reuben PM, D'Ippolito G, Schiller PC, Cheung HS. *Chondrogenesis of human bone marrow-derived mesenchymal stem cells in agarose culture*.Anat Rec A Discov Mol Cell Evol Biol 2004. 278(1):428–36.

[67] Indovina PL, Tettamanti E, Micciancio-Giammarinaro MS, Palma MU. *Thermal hysteresis and reversibility of gel–sol transition in agarose–water systemsa)*.J Chem Phys 1979. 70(6):2841–7.

[68] Lahaye M, Rochas C. *Chemical structure and physico-chemical properties of agar*.Hydrobiologia 1991. 221:137–48.

[69] Silva PT da, Fries LLM, Menezes CR de, Holkem AT, Schwan CL, Wigmann ÃF, et al.

*Microencapsulation: concepts, mechanisms, methods and some applications in food technology.*CiÃ\textordfemeninencia Rural 2014. 44:1304–11.

[70] Vaithilingam V. *Microencapsulated Human Islets as a Therapy for Type 1 Diabetes.*The University of New South Wales; 2010.

[71] de Vos P, Lazarjani HA, Poncelet D, Faas MM. *Polymers in cell encapsulation from an enveloped cell perspective.*Adv Drug Deliv Rev 2014. :15–34.

[72] Uludag H, De Vos P, Tresco PA. *Technology of mammalian cell encapsulation.*Adv Drug Deliv Rev 2000. 42(1–2):29–64.

[73] Krishnamurthy N V, Gimi B. *Encapsulated cell grafts to treat cellular deficiencies and dysfunction.*Crit Rev Biomed Eng 2011. 39(6):473–91.

[74] Vaithilingam V, Tuch BE. *Islet transplantation and encapsulation: an update on recent developments.*Rev Diabet Stud 2011. 8(1):51–67.

[75] Paredes-Juarez G, Spasojevic M, Faas M, de Vos P. *Immunological and Technical Considerations in Application of Alginate-Based Microencapsulation Systems.*Front Bioeng Biotechnol 2014. 2:1–15.

[76] Narang AS, Mahato RI. *Biological and biomaterial approaches for improved islet transplantation.*Pharmacol Rev 2006. 58(2):194–243.

[77] de Vos P, Spasojevic M, Faas MM. *Treatment of diabetes with encapsulated islets.*Adv Exp Med Biol 2010. 670:38–53.

[78] Beck J, Angus R, Madsen B, Britt D, Vernon B, Nguyen KT. *Islet encapsulation: strategies to enhance islet cell functions.*Tissue Eng 2007. 13(3):589–99.

[79] Mørch ÝA, Donati I, Strand BL, Skjåk-Bræk G. *Effect of Ca2+, Ba2+, and Sr2+ on Alginate Microbeads.*Biomacromolecules 2006. 7(5):1471–80.

[80] Zeng J, Xu X, Chen X, Liang Q, Bian X, Yang L, et al. *Biodegradable electrospun fibers for drug delivery.*J Control Release 2003. 92(3):227–31.

[81] Khil MS, Cha D Il, Kim HY, Kim IS, Bhattarai N. *Electrospun nanofibrous polyurethane membrane as wound dressing.*J Biomed Mater Res Part B Appl Biomater 2003. 67B(2):675–9.

[82] Li WJ, Laurencin CT, Caterson EJ, Tuan RS, Ko FK. *Electrospun nanofibrous structure: a novel scaffold for tissue engineering.*J Biomed Mater Res 2002. 60(4):613–21.

[83] Wang ZG, Wan LS, Liu ZM, Huang XJ, Xu ZK. *Enzyme immobilization on electrospun polymer nanofibers: An overview.*J Mol Catal B Enzym 2009. 56(4):189–95.

[84] Daristotle JL, Behrens AM, Sandler AD, Kofinas P. *A Review of the Fundamental Principles and Applications of Solution Blow Spinning.*ACS Appl Mater Interfaces 2016. 8(51):34951–63.

[85] Behrens AM, Casey BJ, Sikorski MJ, Wu KL, Tutak W, Sandler AD, et al. *In Situ Deposition of PLGA Nanofibers via Solution Blow Spinning*.ACS Macro Lett 2014. 3(3):249–54.

[86] Agarwal S, Wendorff JH, Greiner A. *Use of electrospinning technique for biomedical applications*.Polymer (Guildf) 2008. 49(26):5603–21.

[87] Yarin AL, Koombhongse S, Reneker DH. *Taylor cone and jetting from liquid droplets in electrospinning of nanofibers*.J Appl Phys 2001. 90(9):4836–46.

[88] Tutak W, Sarkar S, Lin-Gibson S, Farooque TM, Jyotsnendu G, Wang D, et al. *The support of bone marrow stromal cell differentiation by airbrushed nanofiber scaffolds*.Biomaterials 2013. 34(10):2389–98.

[89] Medeiros ES, Glenn GM, Klamczynski AP, Orts WJ, Mattoso LHC. *Solution blow spinning: A new method to produce micro- and nanofibers from polymer solutions*.J Appl Polym Sci 2009. 113(4):2322–30.

[90] Polat Y, Pampal Esra S, Stojanovska E, Simsek R, Hassanin A, Kilic A, et al. *Solution blowing of thermoplastic polyurethane nanofibers: A facile method to produce flexible porous materials*.J Appl Polym Sci 2015. 133(9).

[91] S. Uday Kumar, Kumar U. *Electrospun fucoidan loaded PCL/PEO nanofiber scaffolds for small diameter vascular grafts*.Masther Thesis, Indian Institute of Technology Roorkee, India; 2012.

[92] McMullan D. *Scanning electron microscopy 1928–1965*.Scanning 2006. 17(3):175–85.

[93] Hsu C-PS. *Infrared Spectroscopy. In Handbook of Instrumental Techniques for Analytical Chemistry*.Infrared Spectroscopy. Settle, F. A., Ed. Prentice Hall PTR; 1997.

[94] Stuart BH. *Infrared Spectroscopy: Fundamentals and Applications*.Wiley; 2004. 244 p.

[95] Coviello T, Matricardi P, Marianecci C, Alhaique F. *Polysaccharide hydrogels for modified release formulations*.J Control Release 2007. 119(1):5–24.

[96] Mcgregor. *Nuclear Magnetic Resonance Spectroscopy. In handbook of Instrumental Techniques for Analytical Chemistry*.J Liq Chromatogr Relat Technol 1997. 21(19):3072–6.

[97] Duus JØ, Gotfredsen CH, Bock K. *Carbohydrate Structural Determination by NMR Spectroscopy: Modern Methods and Limitations*.Chem Rev 2000. 100(12):4589–614.

[98] Pinto AA. *Exploring the biomedical potential of a novel algae origin polysaccharide*.University of <minho; 2012.

[99] Coutinho DF, Sant S V, Shin H, Oliveira JT, Gomes ME, Neves NM, et al. *Modified Gellan Gum hydrogels with tunable physical and mechanical properties*.Biomaterials 2010. 31(29):7494–502.

[100] Hamcerencu J.; Khoukh, A.; Popa, M.; Riess, G. MD, Hamcerencu M, Desbrieres J, Khoukh

A, Popa M, Riess G. *Synthesis and characterization of new unsaturated esters of Gellan Gum*.Carbohydr Polym 2008. 71(1):92–100.

[101] Smith BA, Ware BR. *Apparatus and Methods for Laser Doppler Electrophoresis*.In: Hercules DM, Hieftje GM, Snyder LR, Evenson MA, editors. 1978. Boston, MA: Springer US; 1978. p. 29–54.

[102] Leite AJM. *Advanced Nanocomposites Based on Bioactive Glass Nanoparticles for Biomedical Applications*.Unversity of Minho; 2019.

[103] Luz GAM da. *Bioactive Glass Nanoparticles combined with natural-based polymers for biomedical applications*.University of Minho; 2012.

[104] Schultz N, Metreveli G, Franzreb M, Frimmel FH, Syldatk C. *Zeta potential measurement as a diagnostic tool in enzyme immobilisation*.Colloids Surfaces B Biointerfaces 2008. 66(1):39–44.

[105] Doostmohammadi A, Monshi A, Salehi R, Fathi MH, Golniya Z, Daniels AU. *Bioactive glass nanoparticles with negative zeta potential*.Ceram Int 2011. 37(7):2311–6.

[106] Vadgama P, editor. *Surfaces and interfaces for biomaterials*.In: 2005. Woodhead Publishing; 2005. p. ii. (Woodhead Publishing Series in Biomaterials).

[107] Martins AMP. *Development of electrospun nanofibrous-based scaffolds for bone regeneration*.University of Minho; 2009.

[108] McArthur SL. *Applications of XPS in bioengineering*.Surf Interface Anal 2006. 38(11):1380–5.

[109] Coutinho DF. *Micro/nano-scale strategies for engineering in vitro the cellular microenvironment using biodegradable biomaterials*.University of Minho; 2011.

[110] Notthoff C, Winterer M, Beckel A, Geller M, Heindl J. *Spatial high resolution energy dispersive X-ray spectroscopy on thin lamellas*.Ultramicroscopy 2013. 129:30–5.

[111] Moore KT. *X-ray and electron microscopy of actinide materials*.Micron 2010. 41(4):336–58.

[112] Meyer E. *Atomic force microscopy*.Prog Surf Sci 1992. 41(1):3–49.

[113] Selvendran RR, March JF, Ring SG. *Determination of aldoses and uronic acid content of vegetable fiber*.Anal Biochem 1979. 96(2):282–92.

[114] Coimbra MA, Waldron KW, Selvendran RR. *Isolation and characterisation of cell wall polymers from olive pulp (Olea europaea L.)*.Carbohydr Res 1994. 252:245–62.

[115] Oliveira C, Ferreira AS, Novoa-Carballal R, Nunes C, Pashkuleva I, Neves NM, et al. *The Key Role of Sulfation and Branching on Fucoidan Antitumor Activity*.Macromol Biosci 2017. 17(5):1600340-n/a.

[116] Sridharan G, Shankar A. *Toluidine blue: A review of its chemistry and clinical utility*.J Oral

Maxillofac Pathol 2012. 16:251–5.

[117] Epstein JB, Scully C, Spinelli J. *Toluidine blue and Lugol's iodine application in the assessment of oral malignant disease and lesions at risk of malignancy.*J Oral Pathol Med 1992. 21(4):160–3.

[118] Carleton HM (Harry M. *Carleton's Histological technique*.Drury RAB (Roger AB, Wallington EA, editors. Oxford ; New York: Oxford University Press; 1980.

[119] Liu T, Liu Y, Chen Y, Liu S, Maitz MF, Wang X, et al. *Immobilization of heparin/poly-l-lysine nanoparticles on dopamine-coated surface to create a heparin density gradient for selective direction of platelet and vascular cells behavior.*Acta Biomater 2014. 10(5):1940–54.

[120] Smith PK, Mallia AK, Hermanson GT. *Colorimetric method for the assay of heparin content in immobilized heparin preparations.*Anal Biochem 1980. 109(2):466–73.

[121] *Total Antioxidant Capacity Assay Kit*. [cited 2020 Feb].

[122] Sayed AE-DH, Soliman HAM. *Developmental toxicity and DNA damaging properties of silver nanoparticles in the catfish (Clarias gariepinus).*Mutat Res Toxicol Environ Mutagen 2017. 822:34–40.

[123] Abdel-Magied N, Abdel-Aziz N, Shedid SM, Ahmed AG. *Modulating effect of tiron on the capability of mitochondrial oxidative phosphorylation in the brain of rats exposed to radiation or manganese toxicity.*Environ Sci Pollut Res Int 2019. 26(12):12550–62.

[124] Pal M, Misra K, Dhillon G, Brar S, Verma M. *Antioxidants*.In: 2014. 2014. p. 117–38.

[125] Balakrishnan D, Kandasamy D, Nithyanand P. *A review on Antioxidant activity of marine organisms*.Int J ChemTech Res 2014. 6:974–4290.

[126] Mallick N, Mohn FH. *Reactive oxygen species: response of algal cells*.J Plant Physiol 2000. 157(2):183–93.

[127] Hemalatha A, Karthik G, Chermapandi P, Saranya C, Anantharaman P. *Antioxidant properties and total phenolic content of a marine diatom, Navicula clavata and green microalgae, Chlorella marina and Dunaliella salina*.Adv Appl Sci Res 2013. 4:151–7.

[128] Ajisaka K, Yokoyama T, Matsuo K. *Structural Characteristics and Antioxidant Activities of Fucoidans from Five Brown Seaweeds*.J Appl Glycosci 2016.

[129] Vaithilingam V, Evans MDM, Lewy DM, Bean PA, Bal S, Tuch BE. *Co-encapsulation and co-transplantation of mesenchymal stem cells reduces pericapsular fibrosis and improves encapsulated islet survival and function when allografted.*Sci Rep 2017. 7(1):10059.

[130] Mishra K, Ojha H, Chaudhury NK. *Estimation of antiradical properties of antioxidants using DPPH assay: A critical review and results*.Food Chem 2012. 130(4):1036–43.

[131] *DPPH assay*. [cited 2020 Mar].

[132] Kwok DY, Neumann AW. *Contact angle measurement and contact angle interpretation*.Adv

Colloid Interface Sci 1999. 81(3):167–249.

[133] Lauren S. *White Paper: Surface free energy – what is it and how to measure it?*2018.

[134] Ratner, B. D., Hoffman, A. S., Schoen, F. J., and Lemons, J. E. *Biomaterials Science- An introduction to materials in medicine,*.In: 2004. 2004.

[135] Silva LP. *Advance gellam gum-based hydrogels for the treatment of diabetic foot ulcerations*.University of Minho, Portugal, Doctroal Thesis; 2016.

[136] Oyen ML. *Mechanical characterisation of hydrogel materials*.Int Mater Rev 2014. 59(1):44–59.

[137] Fan J, Shang Y, Yuan Y, Yang J. *Preparation and characterization of chitosan/galactosylated hyaluronic acid scaffolds for primary hepatocytes culture*.J Mater Sci Mater Med 2010. 21(1):319–27.

[138] Lin S, Sangaj N, Razafiarison T, Zhang C, Varghese S. *Influence of physical properties of biomaterials on cellular behavior*.Pharm Res 2011. 28(6):1422–30.

[139] Correlo VM, Boesel LF, Pinho E, Costa-Pinto AR, Alves da Silva ML, Bhattacharya M, et al. *Melt-based compression-molded scaffolds from chitosan-polyester blends and composites: Morphology and mechanical properties*.J Biomed Mater Res A 2009. 91(2):489–504.

[140] Engler AJ, Sen S, Sweeney HL, Discher DE. *Matrix Elasticity Directs Stem Cell Lineage Specification*.Cell 2006. 126(4):677–89.

[141] Gaisford S, Kett V, Haines P, editors. *Principles of Thermal Analysis and Calorimetry*.The Royal Society of Chemistry; 2016.

[142] Grellmann W, Langer B. *Deformation and fracture behaviour of polymers materials*.Springer Science & Business Media; 2013.

[143] Menard K. *Dynamic Mechanical Analysis. Boca Raton: CRC Press,*.2008.

[144] Mano JF. *Viscoelastic properties of bone: Mechanical spectroscopy studies on a chicken model*.Mater Sci Eng C 2005. 25(2):145–52.

[145] Caridade SG, da Silva RMP, Reis RL, Mano JF. *Effect of solvent-dependent viscoelastic properties of chitosan membranes on the permeation of 2-phenylethanol*.Carbohydr Polym 2009. 75(4):651–9.

[146] Silva RM, Silva GA, Coutinho OP, Mano JF, Reis RL. *Preparation and characterisation in simulated body conditions of glutaraldehyde crosslinked chitosan membranes*.J Mater Sci Mater Med 2004. 15(10):1105–12.

[147] Silva SS. *Processing and surface modification of novel natural- origin architectures aimed for biomedical applications*.Unioversity of Minho; 2008.

[148] Spaull AJB. *An Introduction to Rheology By H. A. Barnes, J. F. Hutton and K. Walters, Elsevier Science Publishers, Amsterdam, 1989. 200 pp, price US$92.00/Dfl. 175.00*

*(Hardcover), US$60.50/Dfl. 115.00 (Paperback). ISBN 0 444 87140 3 (Hardcover), ISBN 0–444–87469-0 (P.*J Chem Technol Biotechnol 1991. 50(3):437.

[149] Carvalho MR de. *Tissue Engineered In Vitro Models on a Chip for Cancer Research.*University of Minho; 2019.

[150] Kuijpers AJ, Engbers GHM, Feijen J, De Smedt SC, Meyvis TKL, Demeester J, et al. *Characterization of the Network Structure of Carbodiimide Cross-Linked Gelatin Gels.*Macromolecules 1999. 32(10):3325–33.

[151] Li J, Mooney DJ. *Designing hydrogels for controlled drug delivery.*Nat Rev Mater 2016. 1(12):16071.

[152] Schurz J. *Rheology of polymer solutions of the network type.*Prog Polym Sci 1991. 16(1):1–53.

[153] Rubinstein M and RHC. *Polymer Physics.*. Oxford Uni.2003.

[154] Schurz J. *Lösungen und Schmelzen von Hochpolymeren.*Rheol Acta 1966. 5(2):75–8.

[155] Slaughter B V, Khurshid SS, Fisher OZ, Khademhosseini A, Peppas NA. *Hydrogels in regenerative medicine.*Adv Mater 2009. 21(32–33):3307–29.

[156] Mihaila SM. *Routes to Advance Vascularized Bone Tissue Engineering Constructs.*University of Minho; 2014.

[157] Ratner BD, Hoffman AS, Schoen FJ, Lemons J. *Biomaterials Science : A Multidisciplinary Endeavor.*In: 2004. 2004. p. 1–20.

[158] Ratner B. *A history of biomaterials.*Biomater Sci 2nd Ed ... 2004. :10–9.

[159] Silverman RP, Passaretti D, Huang W, Randolph MA, Yaremchuk MJ. *Injectable tissue-engineered cartilage using a fibrin glue polymer.*Plast Reconstr Surg 1999. 103(7):1809–1818.

[160] Jan H. *Kirby-Bauer Disk Diffusion Susceptibility Test Protocol.*American Society for Microbiology. 2016.

[161] Gonçalves C, Rodriguez-Jasso RM, Gomes N, Teixeira JA, Belo I. *Adaptation of dinitrosalicylic acid method to microtiter plates.*Anal Methods 2010. 2(12):2046–8.

[162] *Franz cell*. [cited 2020 Mar].

[163] Chen M-C, Huang S-F, Lai K-Y, Ling M-H. *Fully embeddable chitosan microneedles as a sustained release depot for intradermal vaccination.*Biomaterials 2013. 34(12):3077–86.

[164] Korbutt GS, Elliott JF, Ao Z, Smith DK, Warnock GL, Rajotte R V. *Large scale isolation, growth, and function of porcine neonatal islet cells.*J Clin Invest 1996. 97(9):2119–29.

[165] Street CN, Sipione S, Helms L, Binette T, Rajotte R V, Bleackley RC, et al. *Stem cell-based approaches to solving the problem of tissue supply for islet transplantation in type 1 diabetes.*Int J Biochem Cell Biol 2004. 36(4):667–83.

[166] Krump-Konvalinkova V, Bittinger F, Unger RE, Peters K, Lehr H-A, Kirkpatrick CJ. *Generation of Human Pulmonary Microvascular Endothelial Cell Lines*.Lab Investig 2001. 81(12):1717–27.

[167] ISO2009. *Biological evaluation of medical devices part 5.Test for in vitro cytotoxicity*.ISO10993-5.

[168] Salgado AJ, Coutinho OP, Reis RL. *Novel starch-based scaffolds for bone tissue engineering: cytotoxicity, cell culture, and protein expression.*Tissue Eng 2004. 10(3–4):465–74.

[169] Marchioli G. *A journey towards an extrahepatic islets delivery device with a tissue engineering toolbox in hand.*University of Twente, Doctoral thesis; 2017.

[170] Gomes Reis, R. L., Cunha, A. M., Blitterswijk, C. A.,de Bruijn, J. D. ME, Gomes ME, Reis RL, Cunha AM, Blitterswijk CA, de Bruijn JD. *Cytocompatibility and response of osteoblastic-like cells to starch-based polymers: effect of several additives and processing conditions*.Biomaterials 2001. 22(13):1911–7.

[171] Miranda ES, Silva TH, Reis RL, Mano JF. *Nanostructured natural-based polyelectrolyte multilayers to agglomerate chitosan particles into scaffolds for tissue engineering.*Tissue Eng Part A 2011. 17(21–22):2663–74.

[172] Silva SS, Caridade SG, Mano JF, Reis RL. *Effect of crosslinking in chitosan/aloe vera-based membranes for biomedical applications*.Carbohydr Polym 2013. 98:581–8.

[173] Hilderink J, Spijker S, Carlotti F, Lange L, Engelse M, van Blitterswijk C, et al. *Controlled aggregation of primary human pancreatic islet cells leads to glucose-responsive pseudoislets comparable to native islets*.J Cell Mol Med 2015. 19(8):1836–46.

[174] Rivron NC, Vrij EJ, Rouwkema J, Le Gac S, van den Berg A, Truckenmuller RK, et al. *Tissue deformation spatially modulates VEGF signaling and angiogenesis*.Proc Natl Acad Sci U S A 2012. 109(18):6886–91.

[175] Buitinga M. *Plan-β: a bioengineering approach against type 1 diabetes*.University of Twente; 2015.

[176] Hilderink J. *Beating diabetes: strategies to improve pancreatic islet transplantation*.2013.

[177] Pathak S, Regmi S, Gupta B, Poudel B, Pham Thanh T, Kim J-R, et al. *Hybrid Congregation of Islet Single Cells and Curcumin-Loaded Polymeric Microspheres as an Interventional Strategy to Overcome Apoptosis Associated with Pancreatic Islets Transplantation*.ACS Appl Mater Interfaces 2016. 8.

[178] Merglen A, Theander S, Rubi B, Chaffard G, Wollheim CB, Maechler P. *Glucose Sensitivity and Metabolism-Secretion Coupling Studied during Two-Year Continuous Culture in INS-1E Insulinoma Cells*.Endocrinology 2004. 145(2):667–78.

[179] Fujikawa Y, Roma LP, Sobotta MC, Rose AJ, Diaz MB, Locatelli G, et al. *Mouse redox histology using genetically encoded probes*.Sci Signal 2016. 9(419):rs1 LP-rs1.

[180] Morgan B, Sobotta MC, Dick TP. *Measuring E(GSH) and H2O2 with roGFP2-based redox probes*.Free Radic Biol Med 2011. 51(11):1943–51.

[181] Pizzoferrato A, Ciapetti G, Stea S, Cenni E, Arciola CR, Granchi D, et al. *Cell culture methods for testing Biocompatibility*.Clin Mater 1994. 15(3):173–90.

[182] Crouch SPM, Kozlowski R, Slater KJ, Fletcher J. *The use of ATP bioluminescence as a measure of cell proliferation and cytotoxicity*.J Immunol Methods 1993. 160(1):81–8.

[183] Wiegand C, Hipler U-C. *Methods for the measurement of cell and tissue compatibility including tissue regeneration processes*.GMS Krankenhhyg Interdiszip 2008. 3(1):Doc12.

[184] Freshney RI. *Cytotoxicity*.In: 2005. American Cancer Society; 2005.

[185] Correia MCR da S. *Multifunctional and Liquified Capsules for Tissue Regeneration*.University of Minho; 2016.

[186] Matsumoto B. *Cell Biological Applications of Confocal Microscopy*.2003. 38.

[187] Jones C, Smolinski D, Keogh A, Kirk T, Zheng M-H. *Confocal laser scanning microscopy in orthopaedic research*.Prog Histochem Cytochem 2005. 40:1–71.

[188] Smith PK, Krohn RI, Hermanson GT, Mallia AK, Gartner FH, Provenzano MD, et al. *Measurement of protein using bicinchoninic acid*.Anal Biochem 1985. 150(1):76–85.

[189] Winterbourn CC. *The challenges of using fluorescent probes to detect and quantify specific reactive oxygen species in living cells*.Biochim Biophys Acta - Gen Subj 2014. 1840(2):730–8.

[190] Sthijns MMJPE. *Protection, adaptation or cell death as response to toxins: Dependence of time and dose*.Maastricht University; 2017.

[191] Kalyanaraman B, Darley-Usmar V, Davies KJA, Dennery PA, Forman HJ, Grisham MB, et al. *Measuring reactive oxygen and nitrogen species with fluorescent probes: challenges and limitations*.Free Radic Biol Med 2012. 52(1):1–6.

[192] Aziza SAH, Azab ME-S, El-Shall SK. *Ameliorating role of rutin on oxidative stress induced by iron overload in hepatic tissue of rats*.Pakistan J Biol Sci PJBS 2014. 17(8):964–77.

[193] Lemmens KJA, van de Wier B, Vaes N, Ghosh M, van Zandvoort MAMJ, van der Vijgh WJF, et al. *The flavonoid 7-mono-O-(β-hydroxyethyl)-rutoside is able to protect endothelial cells by a direct antioxidant effect*.Toxicol Vitr 2014. 28(4):538–43.

[194] Sthijns MMJPE, Schiffers PM, Janssen GM, Lemmens KJA, Ides B, Vangrieken P, et al. *Rutin protects against H2O2-triggered impaired relaxation of placental arterioles and induces Nrf2-mediated adaptation in Human Umbilical Vein Endothelial Cells exposed to oxidative stress*.Biochim Biophys Acta - Gen Subj 2017. 1861(5, Part A):1177–89.

[195] Criel H. *Intracellular accumulation of quercetin and its impact on cellular stress an In vitro study*.Univesity of Ghent; 2019.

[196] *Transcriptome sequencing, BGi company*.https://www.bgi.com/global/sequencing-services/rna-sequencing-solutions/transcriptome-sequencing/.

[197] Wang Z, Gerstein M, Snyder M. *RNA-Seq: a revolutionary tool for transcriptomics*.Nat Rev Genet 2009. 10(1):57–63.

[198] Lokman NA, Elder ASF, Ricciardelli C, Oehler MK. *Chick chorioallantoic membrane (CAM) assay as an in vivo model to study the effect of newly identified molecules on ovarian cancer invasion and metastasis*.Int J Mol Sci 2012. 13(8):9959–70.

[199] Yuan Y-J, Xu K, Wu W, Luo Q, Yu J-L. *Application of the chick embryo chorioallantoic membrane in neurosurgery disease*.Int J Med Sci 2014. 11(12):1275–81.

[200] Ribatti D. *The Chick Embryo Chorioallantoic Membrane as an In Vivo Assay to Study Antiangiogenesis*.Pharmaceuticals (Basel) 2010. 3(3):482–513.

[201] Marchioli G, van Gurp L, van Krieken PP, Stamatialis D, Engelse M, van Blitterswijk CA, et al. *Fabrication of three-dimensional bioplotted hydrogel scaffolds for islets of Langerhans transplantation*.Biofabrication 2015. 7(2):25009.

[202] Marchioli G, Di Luca A, Koning E, Engelse M, Blitterswijk C, Karperien M, et al. *Hybrid Polycaprolactone/Alginate Scaffolds Functionalized with VEGF to Promote de Novo Vessel Formation for the Transplantation of Islets of Langerhans*.Adv Healthc Mater 2016. 5.

[203] Da Silva M, Dombre C, Brionne A, Monget P, Chessé M, De Pauw M, et al. *The Unique Features of Proteins Depicting the Chicken Amniotic Fluid*.Mol & Cell Proteomics 2019. 18(Supplement 1):S174 LP-S190.

[204] Moreno-Jiménez I, Hulsart-Billstrom G, Lanham SA, Janeczek AA, Kontouli N, Kanczler JM, et al. *The chorioallantoic membrane (CAM) assay for the study of human bone regeneration: a refinement animal model for tissue engineering*.Sci Rep 2016. 6(1):32168.

SECTION 3

EXPERIMENTAL SECTION

Chapter IV

Fucoidan hydrogels photo-cross-linked with visible light radiation as matrices for cell culture

Chapter IV

Fucoidan hydrogels photo-cross-linked with visible radiation as matrices for cell culture[2]

ABSTRACT

Algae are abundant sources of bioactive components with extensive therapeutic properties, receiving much interest in recent years. The research on marine brown algae, namely one of its polysaccharide-fucoidan, has increased exponentially. Fucoidan is a sulfated cell-wall polysaccharide with several reported biological properties including anticancer, antivirus, anticoagulant, antioxidant and anti-inflammatory effects. In this study, fucoidan was functionalized by grafting methacrylic groups in the chain backbone, photocrosslinkable under visible light to obtain biodegradable structures for tissue engineering. The functionalization reaction was carried out by using different concentrations of methacrylic anhydride (MA), namely 8 and 12%(v/v). The modified fucoidan (MFu) was characterized by FTIR and ^{1}HNMR spectroscopy to confirm the functionalization. Further, modified fucoidan was photocrosslinked under visible light and using superhydrophobic surfaces, in order to obtain spherical particles with controlled geometries benefiting from the high repellence of the surfaces. When using higher concentrations of MA, the particles were observed to exhibit a smaller average diameter. Moreover, the viability of L929 mouse fibroblast-like cells cultured in the photocrosslinked particles was investigated, being observed up to 14 days in culture. The photocrosslinking of MFu under visible light enables thus

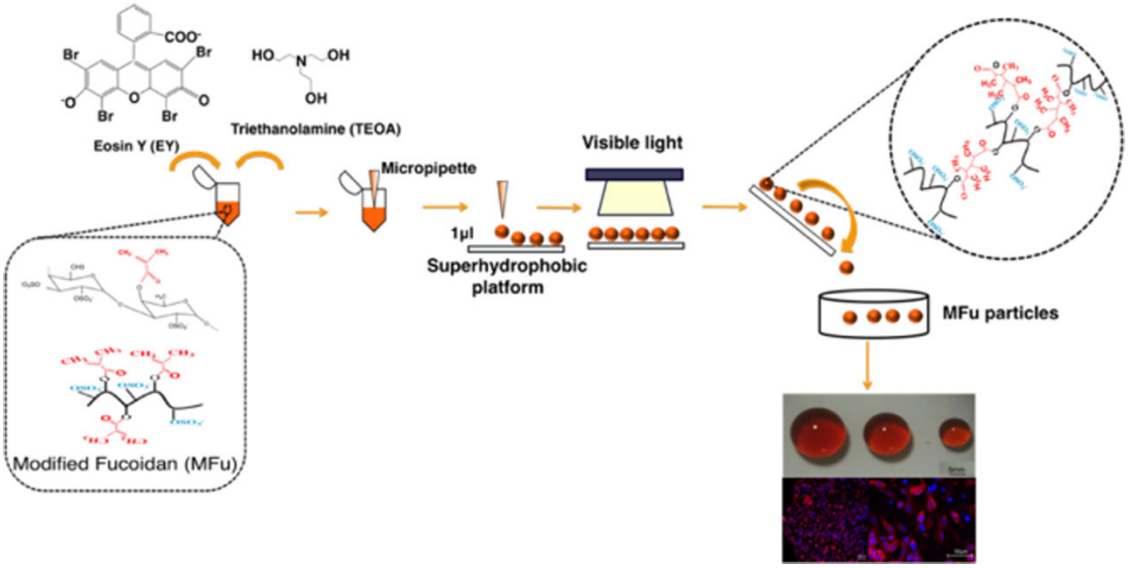
[2] This chapter is based on the following publication:

Reys L. L., Silva S. S., Soares da Costa D., Oliveira N.M., Mano J.F., Reis R.L. and Silva T.H. Silva *" Fucoidan hydrogels photo - cross – linked with visible radiation as matrices for cell culture"*, ACS Biomaterials Science& Engineering, Vol.2, issue7, pp1151-1161,doi:10.1021/acsbiomaterials.6b00180, 2016.

the formation of particles here suggested as a good candidate for a high range of biomedical applications.

Keywords: fucoidan, methacrylation, photocrosslinking, marine biomaterials, tissue engineering, hydrogel.

IV-1. GRAPHICAL ABSTRACT



IV-2. INTRODUCTION

Oceans are a rich environment containing a wide range of organisms, with representatives from all taxonomic kingdoms. Marine algae are a renewable source of different compounds with economic, environmental and biological interest [1,2]. In particular, brown algae contain a range of different polysaccharides, namely fucoidan, laminarans, and alginates. Fucoidan is a heterogeneous and anionic polysaccharide that contains L-fucose, sulfate groups and varying amounts of other sugar residues, as glucuronic acid and xylose, with composition differing with algae species and season [3–5]. Due to the presence of uronic acid in its structure, fucoidan has been compared with mammalian glycosaminoglycans (GAGs) that are composed by repeating

disaccharide units of an amino sugar and uronic acid [5–7]. The fucoidan has interesting bioactive properties, such as anti-inflammatory [3], anti-oxidative [4], anticoagulant [8], antithrombotic [8], anti-tumor [9], and reducing blood glucose [10]. The increasing number of reports supporting the bioactivity and promising properties of this molecule will foster the future application of fucoidan in the treatment of some diseases. Nevertheless, in some cases the bioactivity mechanism or the structure–function relation still needs to be enlighten [5,11]. This fact gains importance when we think of this polysaccharide for pharmaceutical and biomedical applications. Despite the promising properties, the biomedical use of fucoidan as a structural and support material has some limitations, mainly due to difficulties in the processing of matrices stable in aqueous medium. In fact, fucoidan is highly soluble in water but a crosslinking strategy needs to be followed. For that reason, most of the studies reporting the use of fucoidan have suggested the use of blends and composites with chitosan [12–14], silk [15–17], gelatin [18], polycaprolactone [19,20] and hydroxyapatite [21]. These combinations resulted in different structures, namely, gels [14,22], microspheres [18], fibers and films [14,15,17,23], with these matrices being proposed as drug and gene delivery systems, diagnostic microparticles and burn wound-healing membranes [24–28]. To the best of our knowledge, there are no reports in literature on methods for preparation of structures based only in fucoidan for tissue engineering (TE).

The aim of this work was to investigate the possibility of preparing fucoidan photocrosslinkable structures for biomedical application. The crosslinking of natural polymers promoted by photons offers considerable advantages such as ease, fast, safety, low pollution, low energy consumption and low-cost method over conventional chemical ways, which generally involve different reactive species, initiators and catalysts [18,29,30]. For visible light photocrosslinking, polymeric materials need to be conjugated with radically polymerizable groups. In this context, methacrylic groups, when grafted in the chain backbone via oxygen or nitrogen atom, could represent a good candidate for this function, as they work as degradable crosslinks sensitive to either hydrolysis or cell mediated proteolysis [30–32]. Recently, some natural polymers, such as kappa-carrageenan [29], gellan gum [33,34], alginate [35], gelatin [36,37], hyaluronic acid [38], mucin [39] and chondroitin sulfate [40], were modified by methacrylation in order to form 3D structures via photocrosslinking processes for further use in biomedical applications. The methodology for polymer modification needs to be adjusted to each polysaccharide, namely addressing the methacrylate initial compound (methacrylic acid and methacrylic anhydride are the most common), temperature of reaction,

purification steps, among others. To the best of our knowledge, there are no previous reports in the literature on the modification of fucoidan alone by different crosslinking agents (only when combined with chitosan [41,42]) or by methacrylation for further photocrosslinking. In preliminary studies, different crosslinking agents were tested to crosslink fucoidan, but no stable structures were produced; besides some loosen flake-like structures obtained could not be further processed in aqueous or organic solutions. To overcome this limitation, and based on the research group expertise on the modification of natural polymers, namely k-carragenan and gellan gum, using methacrylation reaction, we propose the fucoidan modification by this technique [43–45]. This approach can also be useful in the incorporation of bioactive agents and drugs into fucoidan formulations, increasing their broaden application. In this work, fucoidan from *Fucus vesiculosus* was functionalized using methacrylation reaction with methacrylic anhydride. In this context, methacrylate groups grafted to fucoidan backbone will allow their further photocrosslinking, which will result in the production of fucoidan structures (particles) stable in aqueous media. For that purpose, modified fucoidan was photocrosslinked in the presence of small amounts of co-initiators, namely eosin-y (photoinitiator) and triethanolamine [29,46–49]. Modified fucoidan (MFu) was characterized by Fourier-transform infrared spectroscopy (FTIR) and Nuclear magnetic resonance (^{1}HNMR) spectroscopy. Furthermore, morphology of fucoidan-based particles and cellular viability within them were evaluated as an assessment of their biocompatibility, potentiating their use in TE applications.

IV-3. Materials and Methods

IV-3.1. Materials

Fucoidan (Fu) in powder from brown algae *Fucus vesiculosus* (Maritech® Fucoidan, Marinova, FVF2011527) was used as raw material. Methacrylic Anhydride (MA), Triethanol amine (TEOA), Eosin-y, N-vinyl pyrrolidone (NVP), Tetraethyl Orthosilicate (TEOS) and 1H, 1H, 2H, 2H-perfluorodecyl-trichlorosilane (PFDTS) of analytic grade (Sigma Aldrich) were used as received.

IV-3.2. Synthesis of methacrylated fucoidan (MFu)

MFu was synthesized by reacting Fu with MA: Fu was dissolved at 4% (wt/v) into distilled water at 50°C and MA was added at a ratio of 8% v/v (MFu1) or 12% v/v (MFu2), allowing to react for 6 hours at 50°C. The pH (8.0) of the reaction was periodically adjusted with 5.0 M sodium hydroxide aqueous solution. The modified fucoidan solutions were dialyzed against water using 12-14 kDa cutoff dialysis tubing for 3 days at 4°C to remove the excess of unreacted MA. MFu solutions were frozen at -80°C and then lyophilized. MFu was further purified with acetone and lyophilized for 4 days. The obtained powder was stored at 4°C, protecting from light until further use [29].

IV-3.3. Characterization of methacrylated fucoidan

IV-3.3.1. ^{1}HNMR spectroscopy

The methacrylation of fucoidan was quantified by ^{1}HNMR spectroscopy. The ^{1}HNMR spectra of Fu and MFu were collected in deuterated water (D_2O), at 5mg/ml and 50°C, being recorded on Burker Avance III spectral conditions: 300Hz spectra with 90° impulses, 4s acquisition time. The methacrylation degree (DM, fraction of modified hydroxyl groups per repeating unit) was determined by the relative integration of the methylene proton peak ($I_{methylene}$, *iii* in **Figure IV - 1**) of methacrylated groups to methyl protons of the initial standard (I_{CH3}, *i* in **Figure IV - 1**), according to **Equation IV - 1**, as described elsewhere [33,50]. The $n_{methylene}$ and n_{CH3} standard correspond to the number of protons in the CH_2= from the methacrylic group and in methyl groups of fucose, respectively. The n_{OH} monomer corresponds to the number of reactive -OH sites per sugar residue in the Fu structure [33].

Equation IV-1. Methacrylation degree.

$$\mathrm{DM} = \left(\frac{I_{methylene}/n_{H_{methylene}}}{I_{CH_3\ standard.}/n_{CH_3 standard}} \right) * 100$$

IV-3.3.2. Fourier transform infrared spectroscopy (FTIR)

The FTIR analysis was performed on a Shimadzu IR Prestige 21 spectrometer. The samples were powdered, mixed with potassium bromide (KBr) and processed into pellets. The spectra were recorded at region of 4000-400cm^{-1} with resolution of 16 cm^{-1} and each spectrum resulted from 32 scans.

IV-3.4. Preparation of modified fucoidan-based particles

Freeze-dried MFu (5% m/v) with different DM was added to a photoinitiator (PI) solution consisting of 0.3%(m/v) eosin Y (photoinitiator) in N-vinylpirrolidone (comonomer) and 5M triethanolamine (TEOA) (co-initiator) in water, at room temperature until complete dissolution [51]. To obtain modified fucoidan particles, a technology based in superhydrophobic surfaces developed in our research group was used [43,44]. The surfaces were prepared following a method based on that described by *Deng et al* [52]. Briefly, glass slides were held above the flame of a paraffin candle until the surface was coated with carbon layer. Then, the glass slides were placed inside a desiccator containing, at the bottom, a Petri dish with 4ml of ammonium aqueous solution (30-33%) and another dish with 4ml of TEOS for 24h (StbÖer reaction) in order to trigger the formation of a silica layer on the surface of the glass slides by means of chemical vapour deposition. Next, the glass slides were placed inside ceramic furnace (EBA 1350°C Ceramica, Fornocerâmica, Portugal) at 600°C for 2h, and finally placed into a desiccator on a tray above PFDTS (1H, 1H, 2H, 2H- perfluorodecyl-trichlorosilane) (without immersion) for 3 days in order to reach the repellence necessary for hydrophilic and hydrophobic solvents [44,53]. Drops of 1 to 5µl of MFu and photoinitiator solution were dispensed onto the superhydrophobic surface in order to form spherical particles with different sizes in one step, benefiting from the high repellence of the surfaces that hinders the solution to spread on the surface and thus keeps the integrity of the spheroidal liquid particles. The drop-loaded surfaces were left below visible light (visible light, T5-8W-220-240V/50-60Hz) for 15 minutes to promote photocrosslinking. Finally, the particles were removed and washed with Dulbecco´s Phosphate-Buffered Saline (DPBS) and water to remove all residues of non photocrosslinked polymer and photoinitiators.

IV-3.5. Scanning electron microscopy (SEM)

The morphology of the photocrosslinked fucoidan particles was observed using a NanoSEM-FEI Nova 200 (FEG/SEM) scanning electron microscope. Prior to SEM analysis, samples were freeze-dried and further coated with gold using a Quorum/Polaron model E 6700 equipment and the analysis was performed with an acceleration voltage of 5.00 kV and magnification from 150X to 4000X.

IV-3.6. Cytotoxicity assay

In order to assess the possible cytotoxicity of the samples, extracts (leachables) of all particles and polymer powder were evaluated following MEM extraction tests (72h) according to ANSI/AAMI/ISO-10993-5 guidelines [54]. For these tests a L929 mouse fibroblast-like cell line (L929 cells, ECACC, UK) was employed and cell metabolic activity was assessed by using MTS (3-(4,5-dimethythiazol-2y)-5-(3-carboxymethoxyphenyl) assay. In MEM extraction tests, the materials and the control (latex as a positive control) were extracted by incubation in complete medium (the same used for cell culture) for 24h at 37 °C and 60rpm (in thermostatic bath) [55]. After the defined period of incubation, the resulting solution was removed, thus obtaining the extraction fluid. L929 cells were cultured in basic medium: Dulbecco´s Modified Eagle´s Medium (DMEM, Sigma Aldrich, USA) with phenol red and supplemented with 10% fetal bovine serum (FBS, Gibco, UK) and 1% antibiotic/antimycotic (A/B Gibco, UK) solution and incubated at 37 °C in an atmosphere containing 5% CO_2. A cell suspension was prepared with a concentration of $0.2x10^5$ cell/ml and seeded in 24-well plates. After 24h, extracts were added to the cell monolayer and incubated for 24, 48 and 72h. The L929 cell´s relative viability (%) was determined for each extract and compared to tissue culture polystyrene (TCPS), used as a negative control of cell death. Latex extracts were considered as a positive control of cellular death. After each time point, extracts of the solutions were removed and the plates were evaluated microscopically (in an inverted phase contrast optical microscope) to assess the confluence of the monolayer and changes in cellular morphology. At each time point MTS assay was performed to assess L929 metabolic activity according to the suppliers' instructions. The optical density (OD) was read on a multiwell microplate

reader (SynergyHT, Biotek Instruments, microplate reader-Gen 5 2.01) at 490 nm. All cytotoxicity-screening tests were performed using three replicates (n=3).

IV-3.7. Direct contact test with L929 mouse fibroblast-like cells

To study the potential of the MFu particles to support cell adhesion and proliferation, a cell suspension of L929 cells was seeded on MFu1 particles for different culture periods. For these experiments L929 cells were cultured as previously described. L929 were seeded on the materials surface (10 particles/well) and TCPS at a density of $3.5x10^5$ cells/ml (500µL/well) for 1, 7 and 14 days. After each one of these periods of time, the samples were washed with PBS and MTS assay, DNA quantification, total protein quantification and confocal laser scanning microscopy (CLSM) were performed. Cell proliferation was evaluated using fluorimetric Picogreen double-stranded DNA assay according to the manufactures instructions (Quanti-it™, picogreen dsDNA kit P7589, Invitrogen). The total protein content of MFu1 particles was assessed up to 14 days using Micro-BCA kit (Thermo Fisher Scientific, USA) and following the manufacturer's instructions. The absorbance was read at 562 nm on a multiwell microplate reader (SynergyHT, Biotek Instruments, microplate reader-Gen 5 2.01). Adhesion, morphology and distribution of L929 cells on MFu1 particles were analysed by CLSM. The particles were fixed with 10% formalin for 30 min. and then samples were incubated with 3% bovine serum albumin (BSA) for 30 min. The structures were permeabilized using 0.1% Triton X-100 for 5 min., incubated with phalloidin-TRITC for 20 min. at room temperature, followed by washing with PBS and staining with 5 µg/mL DAPI (2-(4-amidinophenyl)-1H -indole-6-carboxamidine) for 30 min. Fluorescence images from the stained constructs were obtained by CLSM (Inverted Confocal Microscope with incubation, TCS SP8, Leica).

IV-3.8. Statistical analysis

Statistical analysis of the data was performed by non-parametric Kruskal-Wallis followed by Tukey´s multiple comparison test, using Graph Pad Prism ® 5.0. Differences between the groups with $p<0.001$ were considered statistically significant.

IV-4. RESULTS

IV-4.1. Characterization of methacrylated fucoidan

Fucoidan was functionalized with methacrylic anhydride to confer it photocrosslinkable feature. The methacrylation of fucoidan was confirmed by ^{1}HNMR by the presence of two groups of peaks; one, at δ = 5.5-6ppm, is due to methylene (=CH_2) in the double bond region **(Figure IV -1 B, C (iii))** and the other, at δ = 1.9-2ppm peak corresponds to the methyl (CH_3) **(Figure IV - 1B, C (ii))**, both from the incorporated methacrylate groups [29] . The degree of methacrylation (DM) was calculated by the relative integration of the double bond proton peak ($I_{methylene}$) of the methacrylate groups to the methyl protons of the internal standard ($I_{CH3\ fucose}$), using the equation 1. The results obtained for DM are in the range between 8% and 11%.

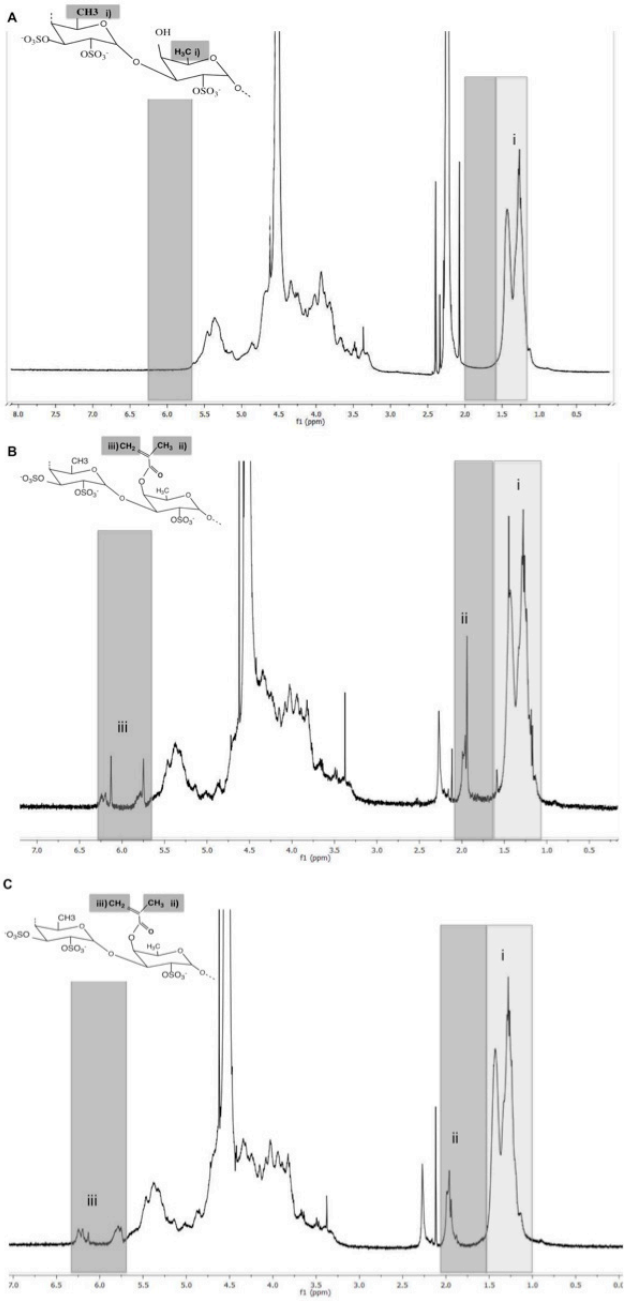


Figure IV-1. ^{1}H-NMR spectra (T=50°C) of A) Fucoidan (Fu), B) Modified fucoidan prepared with lower methacrylic anhydride concentration (MFu1), C) Modified fucoidan prepared with higher methacrylic anhydride concentration (MFu2). i) signal corresponding to H from methyl group of the fucoidan, ii) signal corresponding to H from methyl group from methacrylate; iii) signal corresponding to H from methylene groups from methacrylate.

The functionalization of fucoidan was also assessed by FTIR spectroscopy. The infrared spectrum of fucoidan in **Figure IV - 2A**, exhibits the signals in the range of 1315-1220 cm^{-1} and 1140-1020cm^{-1}, assigned to the symmetric and asymmetric stretching of ether sulfate groups ($RO\text{-}SO_3$)[56] . FTIR spectra of modified fucoidan revealed the appearance of carbon-carbon double bond characteristic peak (C=C) at 1400-1550 cm^{-1}, accompanied by the occurrence of characteristic ester peak (C=O) at 1680-1750 cm^{-1}, existent in the methacrylate groups but not present in fucoidan (Fu), thus confirming the methacrylation of fucoidan. Moreover, all spectra showed an absorbance peak at 1000-1270 cm^{-1} corresponding to the stretching vibration of sulphur-oxygen double bond (S=O) of sulfate group [57], with different intensity, which means that although some acidic hydrolysis during the methacrylation reaction may occur removing some sulfate groups, these are still abundant also in MFu1 and MFu2 [29,30,33].

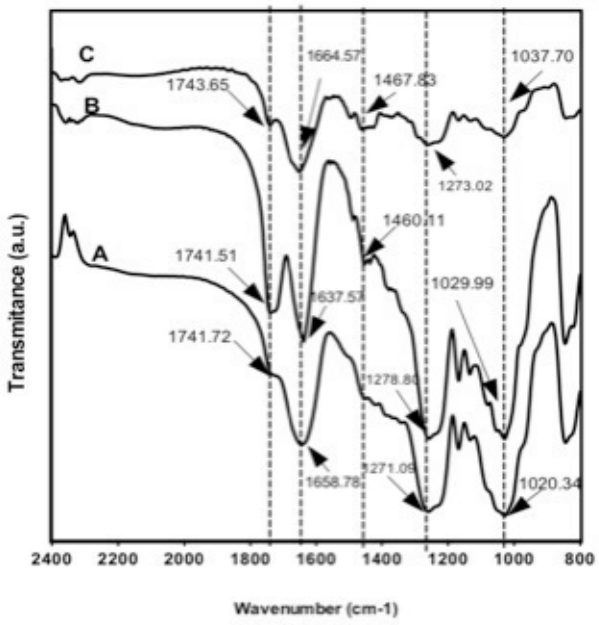
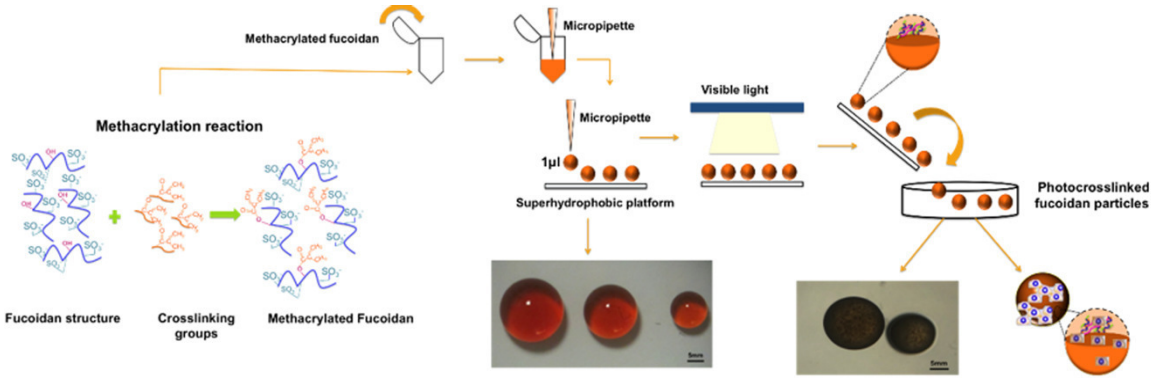


Figure IV-2. FTIR spectra of fucoidan and modified fucoidan : A) fucoidan, B) MFu1 and C) MFu2.

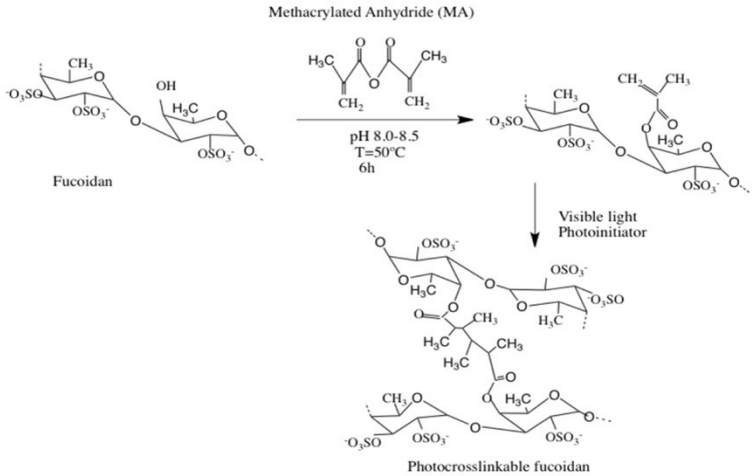
IV-4.2. Preparation of modified fucoidan-based particles

Modified fucoidan-based particles were successfully formed onto superhydrophobic surfaces and photocrosslinked using eosin-y as photoinitiator, triethanolamine (TEOA) as a co-initiator and 1-vynil-2-pyrolidone (NVP) as comonomer upon the irradiation with visible light [51,58]. Superhydrophobic surfaces have been proposed in a variety of biomedical applications [59,60],

being used as substrates for particle formation [61–63], open microfluidic devices [61,64], production of arrays for high-throughput analysis [61,64,65] among other applications [43–45,61,66]. Scheme 1 shows the methodology proposed for the preparation of the fucoidan-based particles, while the Scheme 2 illustrates the possible chemical reactions leading to fucoidan methacrylation and further photocrosslinking, supporting the formation of stable hydrogel structures with or without cells.



Scheme IV - 1. Scheme depicting MFu particles production A) pipetting, B) crosslinking fucoidan particles with visible light and C) stable hydrogel particles with or without cells.



Scheme IV - 2. Scheme of possible reaction mechanism of fucoidan and methacrylated anhydride and further crosslinking mediated by visible radiation. Reaction scheme based on [29,67].

Due to the superhydrophobicity of the substrate's surface, the drops of methacrylated fucoidan do not spread, keeping their spheroidal shape. Upon irradiation with visible light, in the presence of the photoinitiators, the photocrosslinking reaction is promoted, rendering fucoidan-based particles that can be washed is aqueous solutions without structural desegregation. The morphology of modified fucoidan-based particles after freeze-drying was evaluated using scanning electron microscopy. The particles have a porous structure and round shape. The diameter of the particles is different, depending on the DM, where the MFu1 has ≅ 1330 μm **(Figure IV - 3A)**, while MFu2 has ≅ 903 μm **(Figure IV - 3B)**.

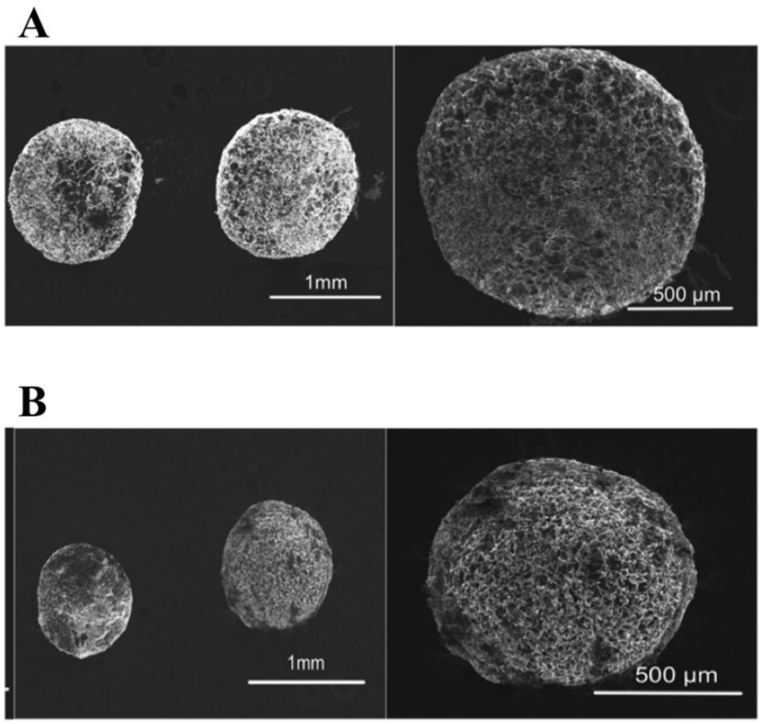


Figure IV-3. SEM images of methacrylated fucoidan photocrosslinked particles after freeze-drying: A) MFu1 and B) MFu2.

IV-4.3. Biological Characterization

A cytotoxicity assessment of Fu and extracts of both MFu particles was carried out as a preliminary approach to assess their potential cytocompatibility envisaging their use on the development of cell culture matrices in TE strategies. Results indicate that L929 cells have good metabolic activity

(Figure IV - 4) in the presence of particles extracts, thus proving their non cytotoxic behaviour. Statistical analysis of data showed some significant differences in metabolic activity of cells cultured in the presence of Fu when compared with the other samples, but no significant differences were observed between extracts of MFu particles and the control (TCPS), indicating that cells performed as good as in the control surfaces. Moreover, extracts of MFu1 particles seem to promote higher metabolic activity ($p<0.01$) than the one observed in TCPS and in the presence of extracts of MFu2 particles, but this difference is no longer observed after 3 days in culture. Nevertheless, MFu1 particles were selected for further studies due to the results of cell performance and also due to the lower methacrylation degree. The cytocompatibility of the developed structures was then evaluated by culturing L929 cells in direct contact with the methacrylated fucoidan photocrosslinked particles (MFu1) and evaluating cell metabolic activity (MTS assay), proliferation (DNA quantification), adhesion and morphology (CLSM).

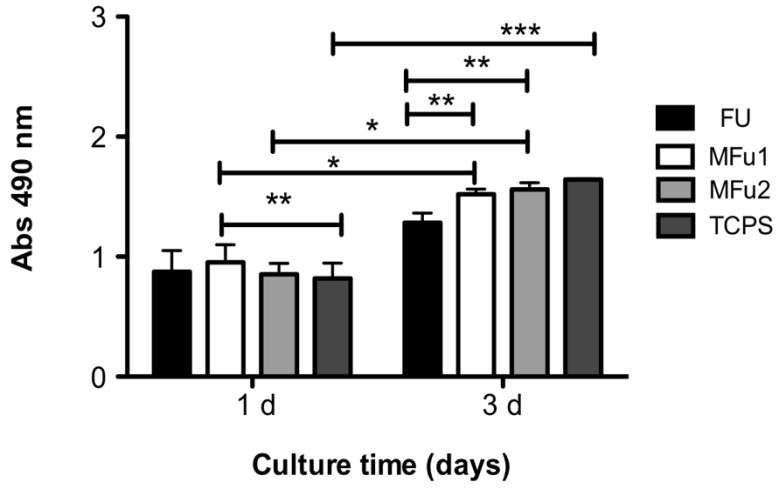


Figure IV-4. Metabolic activity (MTS) of L929 cells cultured in the presence of fucoidan (Fu) and methacrylated fucoidan (MFu). Data represent means ± sd (* $p<0.05$, ** $p<0.01$ and *** $p<0.0001$, one way ANOVA).

The metabolic activity of L929 cells cultured in the MFu1 particles **(Figure IV - 5A)** increased up to 7 days of culture, decreasing afterwards, on the measurement after 14 days in culture. Statistical analysis of the data showed significant differences ($p<0.001$) in metabolic activity between 1 and 7 days and between 7 and 14 days. However, no significant statistical differences were registered in metabolic activity between 1 and 14 days **(Figure IV - 5A)**.

By its turn, the results of DNA quantification showed that L929 cells in MFu1 particles were able to proliferate from the initial time point up to 14 days in culture **(Figure IV - 5B)**. Furthermore, significant statistical differences ($p<0.001$) between all the conditions were observed **(Figure IV - 5B)**.

The total protein content expressed by the cells after 1, 7 and 14 days of culture was also evaluated to better understand cell viability with results being represented in **Figure IV - 5C**. The results demonstrate an apparent increase of total protein between 1 and 7 days, being then constant up to 14 days **(Figure IV - 5C)**.

Cell adhesion to MFu1 particles and morphology of L929 cells were evaluated by CLSM after actin and nuclei staining **(Figure IV - 6 A-D)**, with actin filaments being represented in red and nuclei in blue. After 7 days in culture, CLSM confirmed cell attachment to the MFu1 particles and L929 cells show a spindle-like shape characteristic of fibroblastic cells. Moreover, images acquired from cross sections of the MFu particles show that L929 cells were able to migrate into particle core and proliferate within the developed hydrogel structures **(Figure IV - 6B)**.

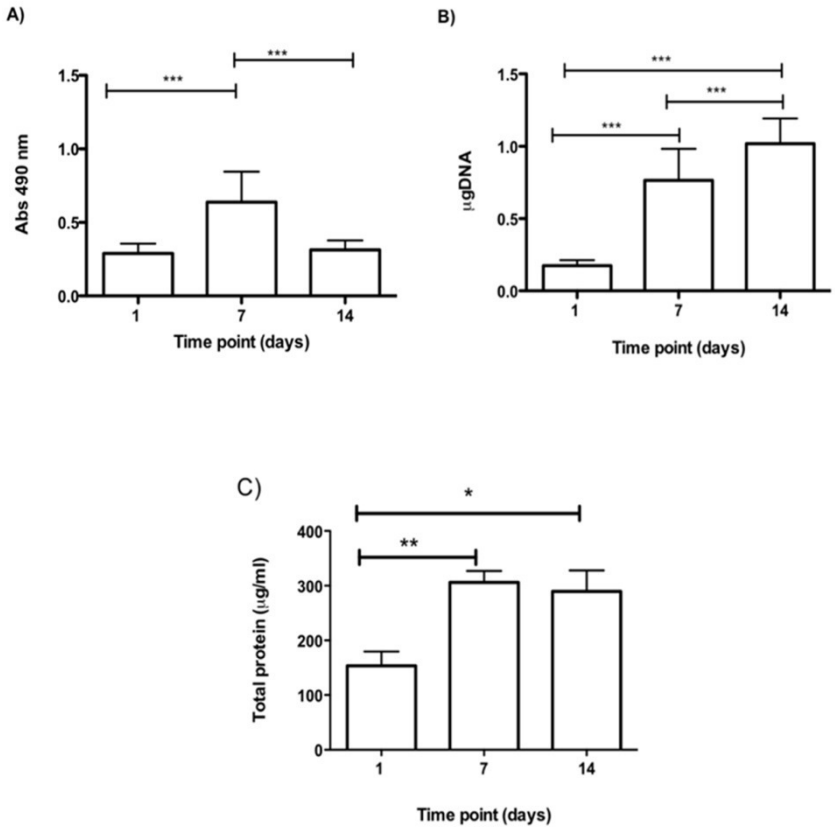


Figure IV-5. Metabolic activity (MTS) results, B) dsDNA content and C) total protein quantified by MicroBCA, of L929-cells seeded and cultured up to 14 days on MFu1 particles. Data represent means ± sd (* $p<0.05$, ** $p<0.01$ and *** $p<0.001$, non-parametric Kruskal-Wallis).

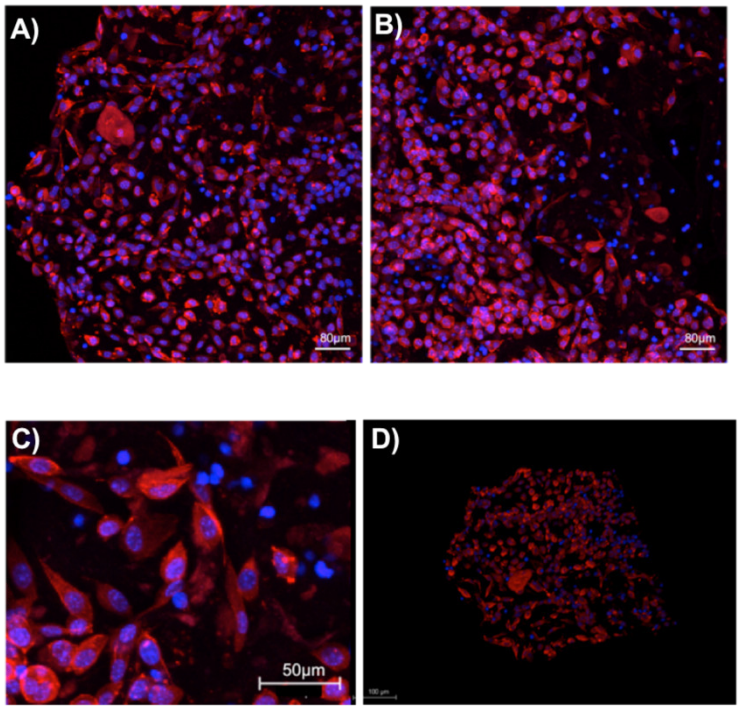


Figure IV-6. Confocal laser micrographs of L929 cells cultured on MFu1 particles during 7 days. A) Surface of the particle, B) cross-section, C) magnification of surface section and D) 3D-image. The cells were stained with phalloidin-TRITC for actin filaments (red) and Hoechst 33342 for nuclei (blue), (scale bars 80µm for A and B, 50µm for C and 100µm for D).

IV-5. DISCUSSION

Fucoidan is an underexploited sulfated polymer, although very promising polysaccharide of alga origin, which has a wide range of interesting bioactive properties that could be used in biomedical field [68,69]. Concerning the fucoidan biomedical application with a support role, the major obstacle for obtaining 2D or 3D structures is very difficult the processability because it is very soluble in water [19]. In order to control the processability of fucoidan and stability of structures in water, we propose the modification of fucoidan using different modifying agents. Initially, the crosslinking reaction onto fucoidan was addressed using different crosslinking agents already known for the chemical crosslink of polysaccharides, namely epichlorohydrin [70] and 1,4 Butanediol diglycidyl ether (BDDE) [71]. The results demonstrated that crosslinked fucoidan formed flake-like agglomerates insoluble in water and in different organic solvents (supporting information), hindering their processability to form 2D and 3D fucoidan structures. In our group the modification

of natural polymers (namely gellan gum [33,34] and k-carragenan [29]) by methacrylation reaction was successfully obtained. In view of these promising findings, we propose an equivalent concept for the chemical functionalization of fucoidan by methacrylation reaction. To achieve this purpose, an adequacy of the reaction parameters to fucoidan is required, namely considering temperature of reaction, concentrations of polymer and methacrylic anhydride and purification steps. Methacrylated-fucoidan (MFu), with different degrees of methacrylation, was synthesized by converting the hydroxyl groups of fucoidan (Fu) in methacrylate groups. The number and location of hydroxyl substitution was considered equivalent to the degree of methacrylation DM and was dependent on the quantity of MA that was used in reaction (8% and 12% (v/v) of MA to obtain a DM of 8 and 11%, respectively). The obtained results are consistent with those reported in literature for other sulfated polymers namely for chondroitin sulfate [30,72,73]. In fact, Mihaila *et al* and Coutinho *et al* have shown to be possible to synthesize a polymer with different degrees of methacrylation by changing the amount of methacrylic anhydride used during the reaction [29,33].

The potential of modified fucoidan for biomedical application, particularly on the development of cell culture matrices for tissue engineering strategies, was assessed through the production of stable MFu particles by photocrosslinking with visible light of polymer solutions droplets supported onto superhydrophobic surfaces [44]. Some studies highlighted the benefits of photocrosslinking with visible radiation over UV radiation [74], enlarging the applications in the biomedical area (e.g. eyes and other light sensitive organs). The exploitation of visible light instead at UV light through the combined used of eosin-y and triethanolamine reported before, although not new, represents a promising method to obtain biocompatible hydrogels since it significantly reduces the cytotoxic effects of UV light. Although the use of potentially cytotoxic co-initiators has been limiting the application of this technology for cell encapsulation, this disadvantage can be overcome by thoroughly washing the samples with water or buffer solutions before setting in contact with cells, using small concentrations of photoinitiator eosin-y (between 0.01mM and 0.1mM) and reduced exposure time [48,51,75,76]. Superhydrophobic surfaces have been proposed for the preparation of spherical particles from polymers and solvents of diverse nature, under mild conditions and with 100% drug encapsulation yield [43–45]. We were able to obtain nearly perfect spherical particles with controlled sizes, highly dependent on the volume of the liquid droplets deposited onto the superhydrophobic surfaces [43–45].

From the combination of the two above mentioned technologies (photocrosslinking with visible radiation and superhydrophobic surfaces) MFu particles with a spherical shape and porous structure were obtained. The microscopic observations of the particles by SEM analysis **(Figure IV - 3)** showed that both MFu1 and MFu2 particles have a similar morphology, with the latter exhibiting a slightly smaller diameter, due to the higher methacrylation degree, resulting in a more extended crosslinking and thus a more compact structure.

When considering a material for biomedical application, it is mandatory to assess its cytocompatibility. In this perspective, eventual cytotoxicity of developed MFu, MFu particles and Fu itself were evaluated through MTS assay after L929 cells being in contact with extracts from those materials during 24, 48 and 72 hours, following established protocols [54,55]. The obtained results demonstrate that besides Fu, both MFu and developed MFu particles are not cytotoxic, presenting cell metabolic activity equivalent to the one observed with negative control (TCPS). Moreover, it is important to highlight that those results show that non-cytotoxic behaviour is independent on the type of modified fucoidan and methacrylation degree. In order to assess if L929-like cells were able to adhere and proliferate maintaining viability in MFu particles, direct contact tests were performed. In this way, L929 cells were analysed after 1, 7 and 14 days of culture into the MFu1 particles by MTS assay, DNA quantification, total protein quantification and CLSM. MFu1, selected for biological assay, has lower DM than MFu2 that in the case of fucoidan particles could facilitate the migration of the cells into particle core. The overall results suggest that in the beginning cells are actively proliferating **(Figure IV - 5 A-B)** and protein synthesis is associated with this proliferation **(Figure IV - 5 C)**. In fact, after 7 days of culture, cells were able to join together two or more MFu particles due to extensive proliferation around them. After this initial boom, and probably before 14 days of culture, we can observe a proliferation arrest by a reduction in the metabolic activity and maintenance of protein content **(Figure IV - 5 A, C)**. Although we could not observe a decrease in the DNA quantification **(Figure IV - 5B)**, by CLSM we could observe several nuclei, particularly in the particle core, that did not stain for actin indicating that probably these cells were dead after 14 days of culture due to space limitation (data not shown). In fact, by DNA quantification, we could be accounting for cells that were already dead and only by comparison of metabolic activity and protein content we could hypothesize the effect of space limitation in the proliferation of cells. The results suggest that the small space in the particle supports cell proliferation until a certain period of time after which the cells start to die.

By reducing initial cell seeding, we could overcome this space limitation and prolong the culturing period. On the other hand, one could explore the ability of these particles to form a tissue-like structure by confining them to a smaller space and allowing cells to interconnect them via cell sheet. The cell morphology was evaluated by CLSM, and images show that cells have a spindle-like shape after 7 days of culture **(Figure IV -6C)**, which is characteristic of fibroblastic cells. Furthermore, we could clearly find that cells migrated from the surface of MFu1 particles towards the particle core during the culture period studied **(Figure IV - 6B)**.

All together, these results demonstrate that by modifying fucoidan by methacrylation it is possible to obtain structures that are stable in aqueous solutions. In this way, we have provided a simple methodology to foster the development of new fucoidan-based structures envisaging its biomedical application as cell culture matrices or for cell encapsulation in TE strategies.

IV-6. CONCLUSION

Modified fucoidan polymeric chains containing unsaturated groups sensitive to visible light were successfully prepared by reacting fucoidan with various amount of methacrylic anhydride. The reaction between Fu and MA under controlled basic conditions proved to render MFu with different degrees of methacrylation. Moreover, the photocrosslinking of fucoidan droplets onto superhydrophobic surfaces with visible light led to the formation of particles with uniform size, structurally stable in aqueous solution and exhibiting meaningful biological performance. Furthermore, the present approach could greatly improve the processability of fucoidan, allowing the production of high-added value fucoidan structures, and then enhancing the biomedical value of this marine biopolymer. The findings also suggested that the developed fucoidan particles could be good candidates as cell culture matrices or drug delivery vehicles for biomedical applications.

IV-7. ACKNOWLEDGEMENTS

This work was partially funded by ERDF through Atlantic Area Project 2011-1/164 MARMED, POCTEP Project 0687_NOVOMAR_1_P, by Portuguese Foundation for Science and Technology through of project CarbPol_μ_Algae (EXPL/MAR-BIO/0165/2013) and by European Union Seventh Framework programme for Research and development through project POLARIS (FP7-REGPOT_CT2012-316331). FCT is also gratefully acknowledged for doctoral grant of N. Oliveira (SFRH/BD/73172/2010) of L. Reys (SFRH/BD/112139/2015) and post-doctoral grants of S.S. Silva (SFRH/BPD/112140/2015) and D. Soares da Costa (SFRH/BPD/85790/2012). The authors would like to acknowledge to Dr. Silvia Mihaila, Dr. Ramon Novoa-Carballal and Pedro Babo from 3B´s Research Group for the assistance provided in the methacrylation and photocrosslinking reactions.

IV-8. ABBREVIATIONS

MA, Methacrylic anhydride; Fu, Fucoidan; MFu, modified fucoidan; MFu1, modified fucoidan using 8% of methacrylic anhydride; MFu2, modified fucoidan using 12% of methacrylic anhydride; FTIR, Fourier transform infrared spectroscopy; ^{1}HNMR, Nuclear magnetic resonance; SEM, Scanning electron microscopy; GAG´s, Glycosaminoglycans; TE, tissue engineering; TEOA, triethanolamine; NVP, N-vinylpyrrolidone; TEOS, Tetraethyl orthosilicate; PFDTS, 1H, 1H, 2H, 2H-perfluorodryl-triclorosilane; D_2O, deuterated water; DM, methacrylation degree; PI, photoinitiator; DPBS, Dulbecco´s phosphate buffered saline; DMEM, Dulbecco´s modified eagle´s medium; FBS, fetal bovine serum; TCPS, tissue culture polystyrene; CLSM, confocal laser scanning microscopy; BSA, bovine serum albumin.

IV-9. REFERENCES

[1] Michel C, Macfarlane GT, Michel Macfarlane, G. T. C. Digestive fates of soluble polysaccharides from marine macroalgae: involvement of the colonic microflora and physiological consequences for the host. 1996;80(4):349–69.

[2] Cardoso MJ, Costa RR, Mano JF. Marine Origin Polysaccharides in Drug Delivery Systems. 2016;14(2).

[3] Cumashi Ushakova, N. A.; Preobrazhenskaya, M. E.; D'Incecco, A.; Piccoli, A.; Totani, L.; Tinari, N.; Morozevich, G. E.; Berman, A. E.; Bilan, M. I.; Usov, A. I.; Ustyuzhanina, N. E.; Grachev, A. A.; Sanderson, C. J.; Kelly, M.; Rabinovich, G. A.; Iacobe A, Cumashi A, Ushakova NA, Preobrazhenskaya ME, D'Incecco A, Piccoli A, et al. A comparative study of the anti-inflammatory, anticoagulant, antiangiogenic, and antiadhesive activities of nine different fucoidans from brown seaweeds. 2007;17(5):541–52.

[4] Li Wang Jingfeng, Cai Yaopio, Xien Mei. ZJXCHLH, Li Jie; Xue, Changhu. H.; Lin Hong; Wang, Jingfeng; Cai, Yaopio; Xin, Mei Zh. The hypolipidemic effects and antioxidative activity of sulfated fucan on the experimental hyperlipidemia in rats. 1999;21:280–3.

[5] Li B, Lu F, Wei X, Zhao R. Fucoidan: Structure and bioactivity. 2008;13:1671–95.

[6] Alberts B Lewis J, et al. JA. The Extracellular Matrix of Animals. 2002. New York: Garland Science; 2002. p. http://www.ncbi.nlm.nih.gov/books/NBK26810/.

[7] Noti C, Seeberger PH. Chemical Approaches to Define the Structure-Activity Relationship of Heparin-like Glycosaminoglycans. 2005;12(7):731–56.

[8] Mourao PAS. Use of sulfated fucans as anticoagulant and antithrombotic agents: future perspectives. 2004;10(9):967–81.

[9] Xue Ge, Yinlin, Zhang, Jinyu, Wang, Qing, Hou, Lin, Liu, Yongchao, Sun, Lingling, Li, Quan M, Xue M, Ge Y, Zhang J, Wang Q, Hou L, et al. Anticancer Properties and Mechanisms of Fucoidan on Mouse Breast Cancer In Vitro and In Vivo. 2012;7(8):e43483.

[10] Wang J, Jin W, Zhang W, Hou Y, Zhang H, Zhang Q, et al. Hypoglycemic property of acidic polysaccharide extracted from Saccharina japonica and its potential mechanism. 2013;95(1):143–7.

[11] Morya Kim, Jungeun, Kim, Eun-Ki VK, Morya VK, Kim J, Kim E-KK. Algal fucoidan: structural and size-dependent bioactivities and their perspectives. 2012;93(1):71–82.

[12] Sezer D.; Cevher, E.; Hatipoğlu, F.; Oğurtan, Z.; Baş, A. L.; Akbuğa, J. A, Sezer AD, Cevher E, Hatipoğlu F, Oğurtan Z, Baş AL, et al. The use of fucosphere in the treatment of dermal burns in rabbits. 2008;69(1):189–98.

[13] Huang Lam, U. Ian, Y-C, Huang Y-C, Lam UI. Chitosan/Fucoidan pH Sensitive Nanoparticles for Oral Delivery System. 2011;58(6):779–85.

[14] Sezer AD, Cevher E, Hatıpoğlu F, Oğurtan Z, Baş AL, Akbuğa J, et al. Preparation of Fucoidan-Chitosan Hydrogel and Its Application as Burn Healing Accelerator on Rabbits. 2008;31(12):2326–33.

[15] Gao Song; Zhu, He-sun; Zhao, Dong-xu; Xu, Jia-chao ZW, Gao Z, Wang S, Zhu H, Zhao D,

Xu J. Improvements of anticoagulant activities of silk fibroin films with fucoidan. 2008;2(2):221–7.

[16] Cheng ZL. Physical and chemical characteristics of silk fibroin/fucoidan composite films. 2009;13(8):1589–92.

[17] Cheng Z, Wang S, Zhu H, Cheng S.; Zhu, H. Z. W, Cheng Z, Wang S, et al. Structural and thermal characteristics of silk fibroin/fucoidan blend films. 2004;(3):446–9.

[18] Ko J-A, Oh Y-S, Park H-J, Ko A.,Oh, Y., S., Park, H., J. J. Preparation and characterization of aminated gelatin-fucoidan microparticles. 2012;44(2):191–5.

[19] Ji Seok Lee Myung Gu Yeo, Chul Ho Jang, Haeongnam Lee, Geun Hyung Kim GHJ, Lee JS, Jin GH, Yeo MG, Jang CH, Lee H, et al. Fabrication of electrospun biocomposites comprising polycaprolactone/fucoidan for tissue regeneration. 2012;90:181–8.

[20] Kim GJ and GH, Gyuhyun Hyung, Kim; JG. Rapid-prototyped PCL/fucoidan composite scaffolds for bone tissue regeneration: design, fabrication, and physical/biological properties. 2011;21(1):17710–8.

[21] Jeong H-SS, Venkatesan J, Kim S-K, Jeong Venkatesan; Jayachandran; Kim, Se-Kwon H-S, Jeong H-SS, Venkatesan J, et al. Hydroxyapatite-fucoidan nanocomposites for bone tissue engineering. 2013;57(0):138–41.

[22] Murakami K, Aoki H, Nakamura S ichiro, Nakamura S ichiro, Takikawa M, Hanzawa M, et al. Hydrogel blends of chitin/chitosan, fucoidan and alginate as healing-impaired wound dressings. 2010;31(1):83–90.

[23] Sezer AD, Hatipoğlu F, Cevher E, Oğurtan Z, Baş AL, Akbuğa J, et al. Chitosan film containing fucoidan as a wound dressing for dermal burn healing: Preparation and in vitro/in vivo evaluation. 2007;8(2):E94–101.

[24] Sezer A, Cevher E, Sezer Erdal AC, Sezer A, Cevher E, Sezer Erdal AC. Fucoidan: A Versatile Biopolymer for Biomedical Applications. Springer Berlin Heidelberg; 2011. p. 377–406.

[25] Wu Don, Trong-Ming, Lin Cheng-Wei, Mi Fwu-Long S-J. Delivery of Berberine Using Chitosan/Fucoidan-Taurine Conjugate Nanoparticles for Treatment of Defective Intestinal Epithelial Tight Junction Barrier. 2014;12(11):5677–97.

[26] Huang Rou-Ying Y-CL. Preparation and Characterization of Antioxidant Nanoparticles Composed of Chitosan and Fucoidan for Antibiotics Delivery. 2014;12(8):4379–98.

[27] Tengdelius M, Lee C-J, Grenegård M, Griffith M, Påhlsson P, Konradsson P. Synthesis and Biological Evaluation of Fucoidan-Mimetic Glycopolymers through Cyanoxyl-Mediated Free-Radical Polymerization. 2014;15(7):2359–68.

[28] Baroli B. Photopolymerization of biomaterials: issues and potentialities in drug delivery, tissue engineering, and cell encapsulation applications. 2006;81(4):491–9.

[29] Mihaila Gaharwar Akhilesh K.; Reis, Rui L.; Marques, Alexandra P.; Gomes, Manuela E.; Khademhosseini, Ali SM, Mihaila SM, Gaharwar AK, Reis RL, Marques AP, Gomes ME, et al. Photocrosslinkable Kappa-Carrageenan Hydrogels for Tissue Engineering Applications. 2013;2(6):895–907.

[30] Morelli A, Chiellini F, Morelli Federica AC. Ulvan as a New Type of Biomaterial from

Renewable Resources: Functionalization and Hydrogel Preparation. 2010;211(7):821–32.

[31] Mahoney MJ, Anseth KS. Three-dimensional growth and function of neural tissue in degradable polyethylene glycol hydrogels. 2006;27(10):2265–74.

[32] Benoit DSW, Durney AR, Anseth KS, Benoit Durney, A. R.;Anseth, K. S. DS. Manipulations in hydrogel degradation behavior enhance osteoblast function and mineralized tissue formation. 2006;12(6):1663–73.

[33] Coutinho DF, Sant S V, Shin H, Oliveira JT, Gomes ME, Neves NM, et al. Modified Gellan Gum hydrogels with tunable physical and mechanical properties. 2010;31(29):7494–502.

[34] Silva-Correia J, Oliveira JM, Caridade SG, Oliveira JT, Sousa RA, Mano JF, et al. Gellan gum-based hydrogels for intervertebral disc tissue-engineering applications. 2011;5(6):e97-107.

[35] Jeon O, Bouhadir KH, Mansour JM, Alsberg E. Photocrosslinked alginate hydrogels with tunable biodegradation rates and mechanical properties. 2009;30:2724–34.

[36] Nichol JW, Koshy ST, Bae H, Hwang CM, Yamanlar S, Khademhosseini A, et al. Cell-laden microengineered gelatin methacrylate hydrogels. 2010;31(21):5536–44.

[37] Nguyen AH, McKinney J, Miller T, Bongiorno T, McDevitt TC. Gelatin methacrylate microspheres for controlled growth factor release. 2015;13:101–10.

[38] Baier Leach J, Bivens KA, Patrick Jr CW, Schmidt CE. Photocrosslinked hyaluronic acid hydrogels: Natural, biodegradable tissue engineering scaffolds. 2003;82(5):578–89.

[39] Duffy C V, David L, Crouzier T. Covalently-crosslinked mucin biopolymer hydrogels for sustained drug delivery. 2015;20:51–9.

[40] Wang D-A, Varghese S, Sharma B, Strehin I, Fermanian S, Gorham J, et al. Multifunctional chondroitin sulphate for cartilage tissue-biomaterial integration. 2007;6(5):385–92.

[41] Yu S-H, Wu S-J, Wu J-Y, Wen D-Y, Mi F-L. Preparation of fucoidan-shelled and genipin-crosslinked chitosan beads for antibacterial application. 2015;126:97–107.

[42] SEZER AD& JA, Akbuga J. Fucosphere—New microsphere carriers for peptide and protein delivery: Preparation and in vitro characterization. 2006;23(5):513–22.

[43] Song W, Lima AC, Mano JF. Bioinspired methodology to fabricate hydrogel spheres for multi-applications using superhydrophobic substrates. 2010;6(23):5868–71.

[44] Rial-Hermida MII, Oliveira NMM, Concheiro A, Alvarez-Lorenzo C, Mano JFF, Rial-Hermida N. M.; Concheiro, A.; Alvarez-Lorenzo C.; Mano, J. F. MI. O, et al. Bioinspired superamphiphobic surfaces as a tool for polymer- and solvent-independent preparation of drug-loaded spherical particles. 2014;10(10):4314–22.

[45] Lima AC, Custodio CA, Alvarez-Lorenzo C, Mano JF. Biomimetic methodology to produce polymeric multilayered particles for biotechnological and biomedical applications. 2013;9(15):2486,2487-2492.

[46] Nguyen KT, West JL. Photopolymerizable hydrogels for tissue engineering applications. 2002;23:4307–14.

[47] Sant S, Hancock MJ, Donnelly JP, Iyer D, Khademhosseini A. Biomimetic gradient hydrogels for tissue engineering. 2010;88:899–911.

[48] Bahney Lujan, T. J., Hsu, C. W., Bottlang, M., West, J. L., Johnstone, B. CS. Visible light photoinitiation of mesenchymal stem cell-laden bioresponsive hydrogels. 2011;22:43–55; discussion 55.

[49] Nettles DL, Vail TP, Morgan MT, Grinstaff MW, Setton LA. Photocrosslinkable hyaluronan as a scaffold for articular cartilage repair. 2004;32(3):391–7.

[50] Hamcerencu J.; Khoukh, A.; Popa, M.; Riess, G. MD, Hamcerencu M, Desbrieres J, Khoukh A, Popa M, Riess G. Synthesis and characterization of new unsaturated esters of Gellan Gum. 2008;71(1):92–100.

[51] Shih H, Lin CC, Shih Lin, C. C. H. Visible-light-mediated thiol-ene hydrogelation using eosin-Y as the only photoinitiator. 2013;34(3):269–73.

[52] Deng Xu Butt Hans-Jürgen, Vollmer Doris ML, Deng X, Mammen L, Butt H-J, Vollmer D. Candle Soot as a Template for a Transparent Robust Superamphiphobic Coating. 2012;335(6064):67–70.

[53] Costa A. M. S.; Alatorre-Meda Manuel Oliveira Nuno M.; Mano JF, Costa AMS, Alatorre-Meda M, Oliveira NM, Mano JF. Biocompatible Polymeric Microparticles Produced by a Simple Biomimetic Approach. 2014;30(16):4535–9.

[54] ISO2009. Biological evaluation of medical devices part 5.Test for in vitro cytotoxicity.

[55] Gomes Reis, R. L., Cunha, A. M., Blitterswijk, C. A.,de Bruijn, J. D. ME, Gomes ME, Reis RL, Cunha AM, Blitterswijk CA, de Bruijn JD. Cytocompatibility and response of osteoblastic-like cells to starch-based polymers: effect of several additives and processing conditions. 2001;22(13):1911–7.

[56] Saboural P, Chaubet F, Rouzet F, Al-Shoukr F, Azzouna R Ben, Bouchemal N, et al. Purification of a low molecular weight fucoidan for SPECT molecular imaging of myocardial infarction. 2014;12(9):4851–67.

[57] Pengzhan Y, Ning L, Xiguang L, Gefei Z, Quanbin Z, Pengcheng L. Antihyperlipidemic effects of different molecular weight sulfated polysaccharides from Ulva pertusa (Chlorophyta). 2003;48(6):543–9.

[58] Fu A, Gwon K, Kim M, Tae G, Kornfield JA. Visible-Light-Initiated Thiol–Acrylate Photopolymerization of Heparin-Based Hydrogels. 2015;16(2):497–506.

[59] Lima A, Mano JF. Micro-/nano-structured superhydrophobic surfaces in the biomedical field: Part I: Basic concepts and biomimetic approaches. 2015;10:103–19.

[60] Lima A, Mano JF. Micro/nano-structured superhydrophobic surfaces in the biomedical field: Part II: Applications overview. 2015;10:271.

[61] Lourenco BN, Marchioli G, Song W, Reis RL, van Blitterswijk CA, Karperien M, et al. Wettability influences cell behavior on superhydrophobic surfaces with different topographies. 2012;7(1–4):46.

[62] Lima AC, Song W, Blanco-Fernandez B, Alvarez-Lorenzo C, Mano JF. Synthesis of temperature-responsive dextran-MA/PNIPAAm particles for controlled drug delivery using superhydrophobic surfaces. 2011;28(6):1294–305.

[63] Oliveira MB, Song W, Martin L, Oliveira SM, Caridade SG, Alonso M, et al. Development of

an injectable system based on elastin-like recombinamer particles for tissue engineering applications. 2011;7(14):6426–34.

[64] Nuno MO, Ana IN, Wenlong S, João FM. Two-Dimensional Open Microfluidic Devices by Tuning the Wettability on Patterned Superhydrophobic Polymeric Surface. 2010;3(8):85205.

[65] Neto AI, Custodio CA, Song W, Mano JF. High-throughput evaluation of interactions between biomaterials, proteins and cells using patterned superhydrophobic substrates. 2011;7(9):4147–51.

[66] Langer R, Tirrell DA. Designing materials for biology and medicine. 2004;428(6982):487–92.

[67] Rose Settimio; Haj, Alicia; Dua, Harminder; Hopkinson, Andrew; White, Lisa; Rose, Felicity JP, Rose JB, Pacelli S, Haj AJ El, Dua HS, Hopkinson A, et al. Gelatin-Based Materials in Ocular Tissue Engineering. 2014;7(4):3106–35.

[68] Silva TH, Alves A, Popa EG, Reys LL, Gomes ME, Sousa RA, et al. Marine algae sulfated polysaccharides for tissue engineering and drug delivery approaches. 2012;2(4):278–89.

[69] Fitton JH. Therapies from fucoidan; multifunctional marine polymers. 2011;9(10):1731–60.

[70] Pirraco RP, Melo-Ferreira B, Santos TC, Frias AM, Marques AP, Reis RL. Adipose stem cell-derived osteoblasts sustain the functionality of endothelial progenitors from the mononuclear fraction of umbilical cord blood. 2013;9(2):5234–42.

[71] Alves A, Pinho ED, Neves NM, Sousa RA, Reis RL. Processing ulvan into 2D structures: Cross-linked ulvan membranes as new biomaterials for drug delivery applications. 2012;426(1–2):76–81.

[72] Li Q, Wang D, Elisseeff JH, Li Qiang Dongan Elisseeff, Jennifer H. W. Heterogeneous-Phase Reaction of Glycidyl Methacrylate and Chondroitin Sulfate: Mechanism of Ring-Opening–Transesterification Competition. 2003;36(7):2556–62.

[73] Bryant Kelly A. Luo, Ning, Shoemaker, Richard K., Arthur, Jeffrey A., Anseth, Kristi S. SJ. D-A. Synthesis and Characterization of Photopolymerized Multifunctional Hydrogels: Water-Soluble Poly(Vinyl Alcohol) and Chondroitin Sulfate Macromers for Chondrocyte Encapsulation. 2004;37(18):6726–33.

[74] Kim Sin-hee;Chu C-C, Kim S, Chu C-C. Visible light induced dextran-methacrylate hydrogel formation using (–)-riboflavin vitamin B2 as a photoinitiator and L-arginine as a co-initiator. 2009;10(1):14–20.

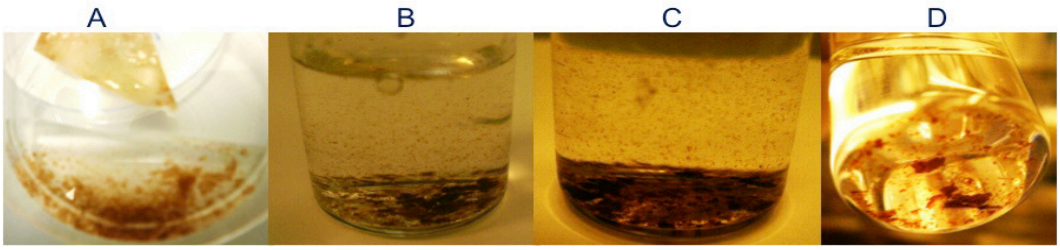
[75] Kirschner Anseth, Kristi S. CM. Hydrogels in healthcare: From static to dynamic material microenvironments. 2013;61(3):931–44.

[76] Schweller RM, West JL. Encoding Hydrogel Mechanics via Network Cross-Linking Structure. 2015;1(5):335–44.

IV-10. SUPPLEMENTARY PART

IV-10.1. Classical strategies for chemical crosslinking of fucoidan

The high solubility of fucoidan in aqueous solution hinders the formation of polymeric matrices structurally stable in such media, from which crosslinking strategies are deemed as necessary. Reaction of fucoidan with different crosslinking agents, namely epichlorohydrin or 1,4 Butanediol diglycidyl ether (BDDE) to address polymer crosslinking, was assessed, similar to what have been successfully accomplished with other sulfated polysaccharides, namely carrageenan and ulvan, respectively. Fucoidan was combined with epichlorohydrin at 4.63 mM in water solution of 50% (v/v) 2-propanol, 0.32M KOH at 37°C, 100 rpm for 24h and the crosslinking reaction resulted in the formation of flake-like agglomerates. Such precipitate could not be dissolved in water and other solvents, namely DMSO (1%v/v), NaOH 1M and acetic acid 2%(v/v) **(Figure IV -S1)**, neither be processed into polymeric structures with defined morphology. Fucoidan (4 and 8% w/v) was also combined with BDDE in different concentrations from 0.20 to 2.00 (w/w) in proportion of crosslinker relatively to fucoidan at room temperature at 100rpm in period of time between 15 minutes to 24hours, but the crosslinking reaction was not effective, with the resulting precipitate being still highly soluble in water.

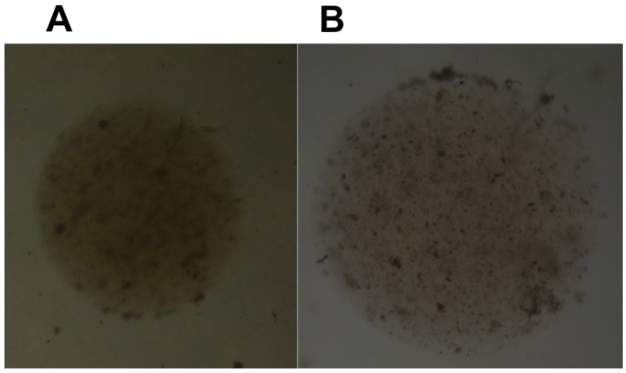


Supplementary Figure IV-1. Immersion of fucoidan cross-linked with epichlorohydrin in water (A) and different solvents (B- in NaOH 2M, C- in acetic acid and D- in DMSO).

IV-10.2. Evaluation of the structural stability of fucoidan-based particles in aqueous solution

Modified fucoidan-based particles were successfully formed **(Figure IV - S2 A)** onto superhydrophobic surfaces and photocrosslinked using eosin-y and triethanolamine (TEOA) as photoiniciators upon the irradiation with visible light, following the procedure described in the

experimental section of the manuscript. The structural stability of the produced fucoidan-based particles in aqueous solution was assessed by incubation in Dulbecco´s phosphate buffered saline (DPBS), at 37°C and 60rpm, during fifteen days **(Figure IV - S2 B)**. The produced particles revealed to be stable, with their structure remaining constant all long the period of study.



Supplementary Figure IV-2. Immersion of fucoidan based particles in DPBS in different time point's A) After immersion (day 0) and B) after 15 days of immersion.

Chapter V

Fucoidan - based hydrogel particles as biomaterials for diabetes treatment strategies

Chapter V

Fucoidan-based hydrogel particles as biomaterials for diabetes treatment strategies[3]

ABSTRACT

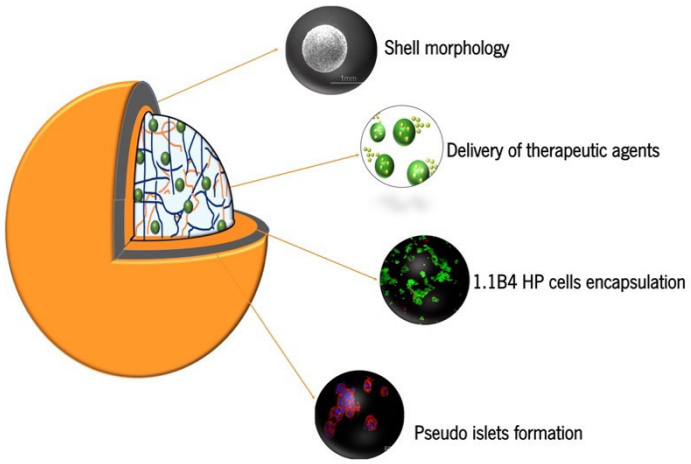
There is a current lack of fully efficient therapies for diabetes mellitus, a chronic disease where the metabolism of blood glucose is severely hindered by a deficit in insulin or cell resistance to this hormone. We developed fucoidan-based hydrogels particles and assess their potential for the sustained delivery of insulin, as well as for the encapsulation of insulin-producing pancreatic beta-cells. The sustained release profile of insulin, the uniform shape was characterized by UV spectroscopy, and the capacity for cells to adhere to the surface, to be able to migrate into particle core and proliferate are characterized by and optical microscopy. These results suggest that fucoidan hydrogel particles may be a good candidate biomaterial for diabetes treatment.

Keywords: fucoidan, diabetes mellitus, marine biomaterials, photo-crosslinking, insulin, pancreatic cells.

[3] This chapter is based on the following publication:

Reys L. L., Silva S. S., Soares da Costa D., Reis R. L., Silva T.H., *"Fucoidan-based microparticles as biomaterials for diabetes treatment strategies"* (submitted for publication).

V-1. GRAPHICAL ABSTRACT



V-2. INTRODUCTION

Diabetes mellitus is a life-threating disease that affects 450 million of people in the world, being the seventh most common cause of death. Diabetes is a metabolic disease characterized by hyperglycaemia resulting from defects in insulin secretion, insulin action or both [1]. Aetiologically, diabetes can be subdivided into two different types: type I and II. Type I diabetes occurs because the cells that produce insulin, β-cells, are damaged. In this type, the pancreas makes little or no insulin, so sugar cannot get into the body´s cells to be metabolized for the production of energy. Type II diabetes is characterized by the development of resistance to insulin by cells and, over time, insulin production by β-cells becomes insufficient to sustain a proper glucose metabolism [2,3]. Therefore, in the last decades new therapeutic strategies to treat this disease, as well as models to better understand it, have been developed. In this perspective, insulin sustained delivery systems have been proposed as a therapeutic approach [4–9], as well as encapsulation of insulin-producing pancreatic cells and islets of Langerhans to be further implanted near the patient liver [10,11]. Other implantation sites for these constructs are also being studied, such as kidney capsule, spleen, intraperitoneal transplantation and omentum pouch, gastrointestinal wall intramuscular and subcutaneous site, but the rational is the same, with the device being designed to support cell viability and reestablish the physiological secretion of insulin, while protecting the encapsulated cells from the host immune system [10,12]. Other strategies also involve the use of bioactive

compounds from marine resources as potential anti-diabetic drugs [13], such as fucoidan (Fu) a marine polysaccharide which has been reported as capable to regulate blood glucose homeostasis [14], besides several other biological activities [15]. Moreover, being a polysaccharide found in the cell wall of brown macroalgae, its role as a structural component for the development of biomaterials is being also addressed [16]. Fucoidan (Fu) is a heterogeneous and anionic polysaccharide that contains L-fucose and sulfate groups, together with other sugars, as xylose and glucuronic acid [17,18]. The diversity of biological activities being reported in the literature may vary depending on the composition and structural traits, the content (charge density) distribution and bonding of the sulfate substitutions and the purity of the extract. These characteristics are a direct result of the seaweeds used as raw-material and the extraction methodologies employed, among others [18]. Fucoidan has a high solubility in water, which is interesting for its delivery as a bioactive compound, however it could be a problem for the production of stable structures in aqueous media using fucoidan alone [19,20]. In fact, most of the reported studies involve fucoidan composites with natural or synthetic macromolecules, namely fucoidan with collagen [21], chitosan [22–24],chondroitin sulphate [25], poly (caprolactone) (PCL) [21,26], and hydroxyapatite [27,28], have been reported as 2D (films) [21,22], or 3D structures (hydrogels [22,29], microspheres [30], and fibers [20]). However, there is an absence of studies using pure fucoidan matrices. Nevertheless, our group has recently shown a process to obtain structures of fucoidan alone using functionalization by methacrylation and further photocrosslinking with visible light [11,19].

Herein in this new work was used the established methodology to produce fucoidan based hydrogel particles and explored their potential as biomaterial for new diabetes therapies, addressing twofold strategies: from one side, as insulin delivery system by studying drug encapsulation and further release in phosphate buffer solution (PBS) simulated gastric fluid (SGF) and simulated intestinal fluid (SIF); on the other side, as pancreatic cells scaffold by assessing the ability of the developed materials to support adhesion and proliferation of human pancreatic cells (1.1B4HPC).

V-3. EXPERIMENTAL

V-3.1. Materials

Fucoidan (Fu) in powder from brown algae *Fucus vesiculosus* (Maritech Fucoidan, Marinova, FVF2011527), methacrylic anhydride (MA), triethanol amine (TEOA), eosin-y, N-vinylpyrrolidone (NVP), tetraethyl orthosilicate (TEOS), and 1H, 1H, 2H, 2H-perfluorodecyl-trichlorosilane (PFDTS), of analytic grade (Sigma-Aldrich), were used as received.

V-3.2. Functionalization of Fucoidan

Details of the full modification are given elsewhere [19], but briefly, fucoidan was modified by methacrylation reaction: 4% (w/v) of Fu aqueous solution was mixed with methacrylate anhydride (MA) in two concentrations, 8% (MFu1) or 12% (MFu2), at 50 °C, allowing to react for 6h. After purification by dialysis and by washing with acetone, to remove the unreacted material, the obtained material was lyophilized for 4 days and stored at 4°C, protecting from light until further use.

V-3.3. Characterization of fucoidan and modified fucoidan (MFu)

V-3.3.1. Fourier Transform Infrared Spectroscopy (FTIR)

The FTIR were performed on Shimadzu IR Prestige 21 Spectrometer. The samples were powdered, mixed with potassium bromide (KBr) and processed into pellets. The spectra were recovered at region 4000-400 cm^{-1} with a resolution of 16 cm^{-1} and each spectrum resulted from the average of 32 scans.

V- 3.3.2. Nuclear magnetic resonance (^{1}HNMR)

The methacrylation of fucoidan was quantified by ^{1}HNRM spectroscopy. The ^{1}HNRM spectra of Fu and MFu were collected in deuterated water (D_2O) at 5 mg/ml and 50 °C, being recorded on Bruker Avance III spectral conditions: 300 Hz spectra with 90° impulses and 4 s acquisition time.

V-3.3.2. Zeta potential

The zeta potentials of fucoidan (Fu) and modified fucoidan (MFu1, MFu2) samples in powder were measured by laser Doppler anemometry using a Malvern Zeta sizer 3000 HS (Malvern Instruments, UK). The samples powders were prepared by dispersing 3 mg in 5 ml of filtrated ultrapure water. Each analysis was made at 25 °C for 60 s. Independent triplicate experiments were performed for obtaining statistical significance.

V-3.4. Preparation of fucoidan-based hydrogel particles (MFu hydrogel particles)

The preparation of fucoidan-based hydrogel particles (MFu hydrogel particles) is shown schematically in **Figure V- 1**, where the tube is composed by the solution of modified fucoidan (methacrylation) in the presence of photoinitiators (eosin-Y and triethanolamine) before photocrosslinking with visible radiation [31,32]. MFu hydrogel particles were produced by pipetting volumes between 1 and 5 µL of 5% MFu solution with triethanolamine and eosin-y (photoinitiators) onto a superamphiphobic surface and then photocrosslinking using visible light. MFu hydrogel particles loaded with insulin were produced in the same way but using MFu solutions with 5 mg/ml of insulin. The superamphiphobic surfaces have high repellence that hinders the solution to spread, thus keeping the integrity of the liquid droplets, resulting in spheroidal particles [33–35]. Moreover, it assures that all the drug is encapsulated in particle [33].

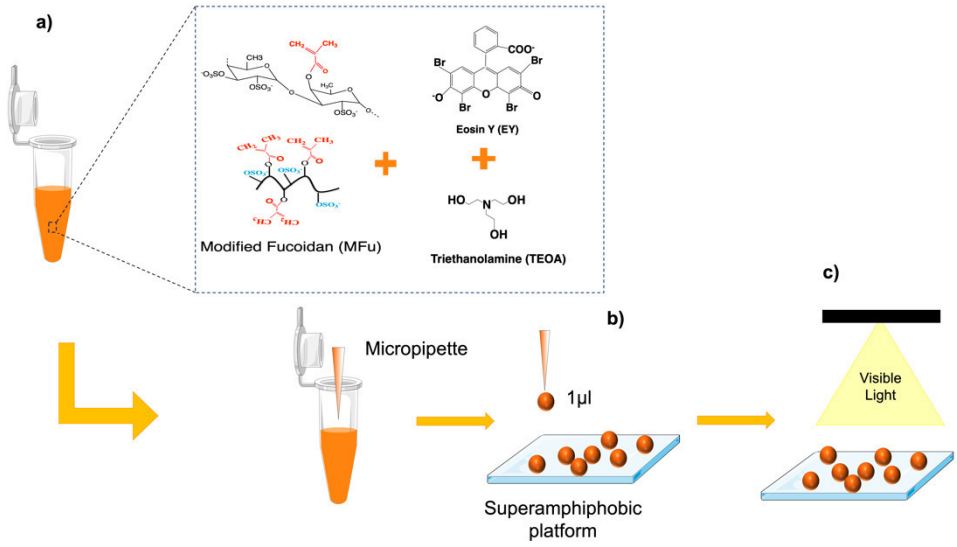


Figure V-1. Scheme to illustrate the formation of the fucoidan-based hydrogels particles using visible light and superamphiphobic surface : a) solution of modified fucoidan (MFu) and photoinitiators b) pipetting volumes between 1 to 5 µL of the solution to superamphiphobic surface and c) exposure the MFu hydrogel particles to visible light.

V-3.5. Morphology of MFu hydrogel particles

The MFu hydrogel particles morphology was observed using a NanoSEM- 194 FEI Nova 200 (FEG/SEM) scanning electron microscope. Before SEM analysis, samples were freeze-dried and further gold-sputtered by using a Quorum/Polaron model E 6700 equipment and the analysis was performed with an acceleration voltage of 15.00 kV and magnification from 30x to 60x.

V - 3.6. Assessment of in vitro insulin release

To quantify the insulin release and predict the bioavailability of insulin encapsulation in MFu hydrogel particles, we incubated these drug-charged particles in a simulated gastric fluid (SGF) and in a simulated intestinal fluid (SIF). The SGF solution was prepared in aqueous solution, for 1 liter of SGF we use 2 g of sodium chloride (NaCl), 3.2g of pepsin derived from stomach mucosa and 7ml of concentrated hydrochloric acid (HCl), while SIF was prepared in aqueous solution, for 1liter

of this buffer we use 6.8g of monobasic potassium phosphate, 77 ml of 0.2 N sodium hydroxide (NaOH) and 1 g of pancreatin. Ten MFu hydrogel particles loaded with insulin were placed in 20 ml of release PBS and incubated at 37 ° C under stirring. The release media was SIF (pH 6.5) for 4 h [36]. At appropriate time intervals (0.5 to 6 hours), 1 ml of the solution was removed for analysis and replaced by fresh solution. The absorbance at 272 nm was measured on a multiwell microplate reader (SynergyHT, Biotek Instruments, microplate reader-Gen 5 2.01) and the amount of insulin released from the particles was determined from a previously obtained calibration curve (0 to 6 mg/ml) [36]. All the samples were analyzed in triplicate.

V-3.6. Biological characterization by culturing human pancreatic cells

The ability of the developed materials to sustain the viability of human pancreatic cells (1.1B4HPC) was assessed by direct contact of 1.1B4 HPC cell line in MFu hydrogel particles for 1, 5 and 7 days.

- *Cell culture*

For these experiments, 1.1B4 HPC was cultured in Roswell Park Memorial Institute (RPMI 1640) medium (Invitrogen, USA) supplemented with 10 % fetal bovine serum (FBS) (Invitrogen, USA) and 1 % antibiotic/antimycotic (A/B) (Invitrogen, USA) at a temperature of 37 °C and 5 % of CO_2 until achieving 90 % confluence. The medium was refreshed every 2 - 3 days.

- *Direct contact*

These cells were seeded on the surface of the materials (10 particles/well) and TCPs at density of ($3.5x10^5$cells/ml) using 500 µL/well and cultured for 1, 5 and 7 days. The samples were incubated at 37° C in humidified 95% air and 5% CO_2 atmosphere. After each time point, the samples were washed with PBS and metabolic activity (MTS assay), proliferation (DNA quantification), viability and cell morphology by confocal laser scanning microscopy (CLSM) was performed.

- *Metabolic activity assay*

Metabolic activity was evaluated by MTS (3-(4,5-dimethythiazol-2y)-5-(3-carboxymethoxyphenyl) assay. The metabolic activity of 1.1B4 HPC cells in MFu hydrogel particles

was determined using MTS assay. Samples were incubated with an MTS solution prepared using a 1:5 ratio of MTS reagent and DMEM without phenol red and 1 % ATB solution for 3 h at 37 °C. The optical density (O.D.) was read at 490 nm on a multiwell microplate reader (Bio-Tek Instruments, US).

- *dsDNA quantification*

Cell proliferation was evaluated using fluorimetric Picogreen double stranded DNA assay according to the manufacture's instructions (Quanti-it, pico green dsDNA kit P7589, Invitrogen). Briefly, samples were collected at 1, 5 and 7 days washed with PBS and transferred into 1.5 ml tubes containing 1ml of ultra-pure water and stored at -80 °C until testing. Before the dsDNA quantification, the structures were thawed and sonicated for 20 min. The quantification was performed in triplicate according to supplier instructions. All quantitative experiments were run in triplicate, and the results are expressed as a mean standard deviation for n=3.

- *Live/dead assay*

To evaluate the viability living cells were stained with calcein AM (green) and dead cells red with propidium iodine (PI, red). The cellular viability was assessed using the live/dead assay (calcein AM/propidium iodide (PI) staining). Briefly, the cell-laden MFu hydrogel particles were incubated for 10 min with 2 μL calcein-AM (1 mg/mL, Molecular Probes, Invitrogen, USA) and 1 μL PI (1 mg/mL, Molecular Probes, Invitrogen, USA) in 1 mL of Dulbecco´s phosphate buffered saline (DPBS) protected from light. The MFu hydrogel particles were washed with DPBS to remove residual staining and visualized by confocal laser scanning microscopy (CLSM) (Inverted Confocal Microscope with incubation, TCS SP8, Leica).

- *Cell morphology*

Adhesion, morphology and distribution of 1.1B4HPC cells on MFu2 particles were analyzed by CLSM. To evaluate cell morphology, cells nuclei were stained with Dapi (blue) and F-actin filaments with phalloidin (red). The particles were fixated with 10% formalin for 30 min and then blocked with 3% bovine serum albumin (BSA) for 30 min. The structures were permeabilized with 0.1% Triton X-100 for 5 min, incubated with phalloidin-TRITC for 20 min at room temperature, followed by washing with PBS and staining with 5 μg/mL DAPI (2-(4-amidinophenyl)-1H -indole-6-

carboxamidine) for 30 min. Fluorescence images from the stained constructs were obtained by CLSM (Inverted Confocal Microscope with incubation, TCS SP8, Leica).

V-3.7. Statistical Analysis.

Statistical analysis of the data was performed using nonparametric Kruskal–Wallis test and the posthoc Tukeýs multiple comparison tests, by Graph Pad Prism 5.0. Differences between the groups with $p < 0.05$ were considered statistically significant.

V-4. RESULTS AND DISCUSSION

V-4.1. Characterization of fucoidan (Fu) and modified fucoidan (MFu)

The chemical modification of fucoidan by methacrylation was assessed by FTIR, ^{1}H NMR and Zeta potential measurements and the results are shown in Table 1. In the FTIR **(Figure V- 2A)** the two spectra show an absorbance peak at 1000-1270 cm^{-1} corresponding to the stretching vibration of the sulfur-oxygen double bond (S=O) of sulfate group with different intensity [37]. This means that some acidic hydrolysis could occur during the methacrylation reaction removing some sulphate groups. The spectra of modified fucoidan revealed the appearance of carbon-carbon double bond characteristic peak (C=C) at 1400-1550cm^{-1}, accompanied by the occurrence of characteristic ester peak (C=O) at 1680-1750 cm^{-1}, existent in MFU but not in Fu, thus confirming the methacrylation of fucoidan [19,38,39]. The functionalization of fucoidan with methacrylic groups was confirmed by ^{1}HNMR with the presence two peaks referent to methylene ($=CH_2$) characteristic signal, at δ= 5.5-6 ppm **(Figure V- 2 Ca)** and the other at δ= 1.9 -2ppm peak corresponds to methyl (CH_3) **(Figure V-2C b)** both from incorporated methacrylated groups, in the NMR spectra of MFu **(Figure V- 2C)**. Different methacrylation degrees (MD) were obtained, which depended on the concentration of methacrylated anhydride (MA) used for functionalization. In addition, the zeta potential measurement confirmed the anionic potential of both Fu, MFu1 and MFu2, with values varying between -30 and -62 mV.

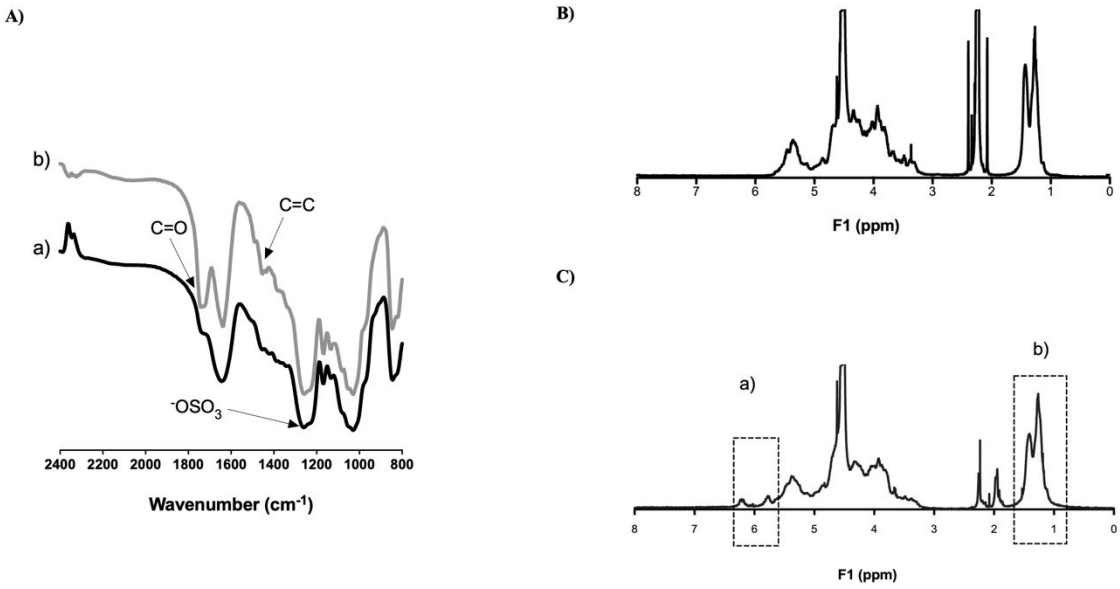


Figure V-2. Characterization of fucoidan (Fu) and modified fucoidan (MFu). A) FTIR spectra a) fucoidan (Fu) and b) modified fucoidan (MFu).^{1}HNMR spectra of B) fucoidan (Fu) and C) modified fucoidan (MFu), a) methylene groups (=CH2) and b) methyl group (CH3).

Table V-1. Methacrylation degree (MD) and zeta potential of bare and modified fucoidan, as determined by ^{1}HNMR and laser Doppler anemometry, respectively.

Methods	Fu[a)]	MFu1[b)]	MFu2[b)]
Ma[c)] concentration [v/v]	—	8%	12%
MD [d)] [%]	—	2.78	6.50
Zeta potential (mv)	-30.40	-32.98	-62.10

[a)] (Fu: fucoidan), [b)] (MFU modified fucoidan) and [c)] (Ma methacrylate anhydride) [d)] (Methacrylation degree

V- 4.2. Characterization of MFu microparticles

V – 4.2.1. Scanning electron microscopy (SEM)

The morphology of MFu hydrogel particles, prepared by photocrosslinking of MFu solution drops deposited on superamphiphobic surfaces, in dry state, depicted in **Figure V- 3**, was evaluated using scanning electron microscopy (SEM). The SEM images show that the produced fucoidan particles have a round shape and varying size, with diameters ranging from 0.63 to 1.30 mm and minimal roughness **(Figure V- 3 a)** and b)). This same photochemical methodology could be used to obtain hydrogels with different shapes, as discs, cylinders or cubes, if adequate molds were employed.

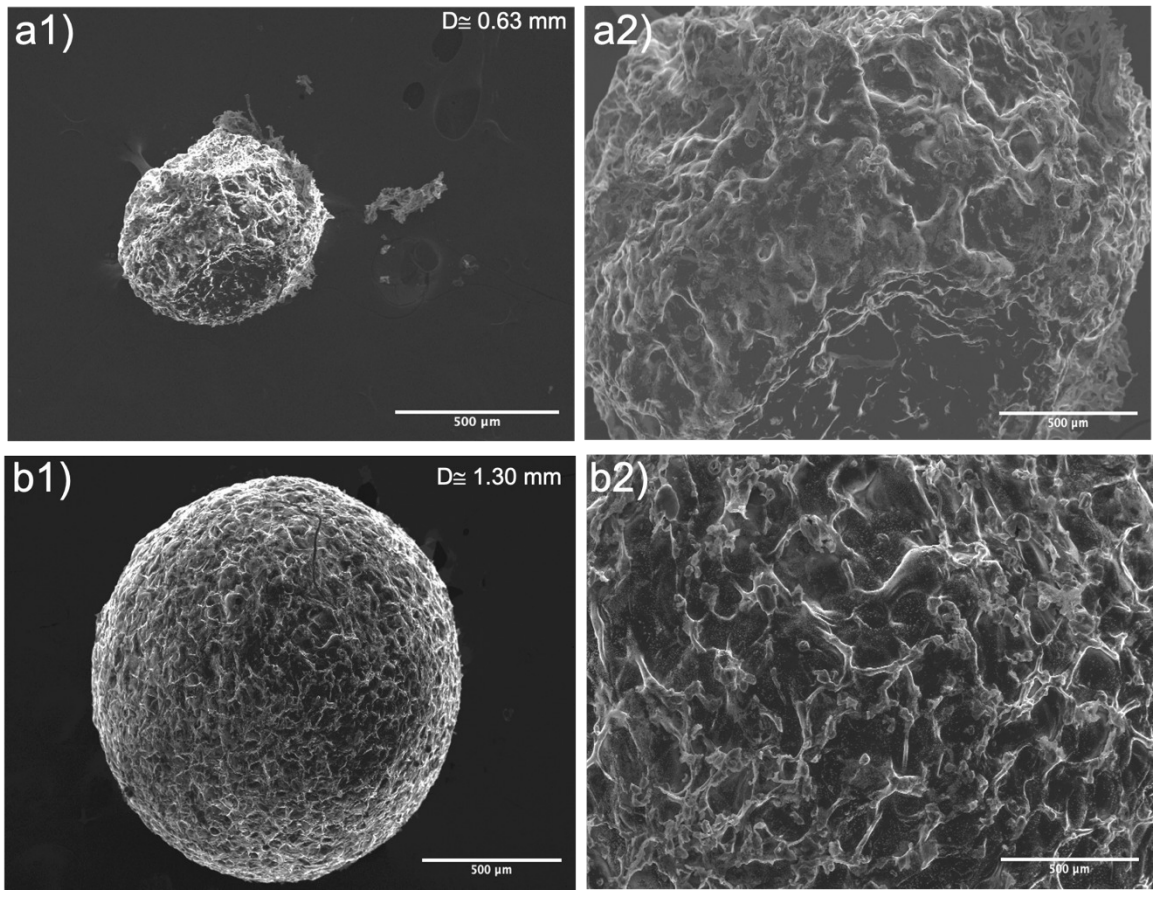


Figure V-3. SEM images of MFu microparticles : (a) MFu1, (b) MFu2; (a2) and (b2) higher magnification of MFu1 and MFu2, scale bar: 500µm.

V- 4.2.2. Release of insulin in vitro

Hydrogel particles encapsulating insulin may protect the drug against the proteolytic attack and further release it at or near the cellular membrane to optimize the driving force for passive permeation [40,41]. As first assessment of the release profile of insulin, we incubated MFu hydrogel particles loaded insulin in phosphate buffer saline (PBS), using as well MFu hydrogel particles without insulin in the assay as a control group (CTRL), and quantifying the released insulin over time. MFu 1 particles (lower methacrylation degree) allow a higher release of insulin in PBS, when compared with the release from MFu2 (higher methacrylation degree), as shown in **Figure V-4.** We hypothesized that the mesh size in MFu2 could be smaller than MFu1, probably due to the higher methacrylation degree and consequently a higher crosslinking degree, which implies hampering the diffusion of the encapsulated insulin. The behavior of insulin release in PBS is in agreement with previous studies with other polysaccharide systems [41,42].

The oral route is considered an acceptable and convenient route of insulin administration for treatment of diabetes. One major problem associated with the oral delivery of insulin is its low bioavailability (due to the proteolytic activity of the acidic juice in the stomach and susceptibility to enzymatic attack) and physical instability [40,41]. To predict the bioavailability of insulin encapsulated in MFu hydrogel particles, we selected MFu2 for this assay, as it rendered a lower insulin release in PBS. These MFu hydrogel particles loaded with insulin were incubated in simulated gastric fluid (SGF) and simulated intestinal fluid (SIF), not in sequence, and the insulin release quantified. It was observed a higher release in SGF in PBS, and in the latter higher than in SIF, which seems to indicate that lower pH facilitates insulin diffusion to the media. Nevertheless, considering a gastrointestinal time in stomach of 1h [43], we would observe that insulin was only partially release from MFu2 hydrogel particles in SGF after this time, which means that a significant amount of insulin would still be loaded in the MFu2 for later release in intestine. In this media, the higher pH values would support the insulin release from MFu2 which was lower in SIF when compared with the sustained release of the drug.

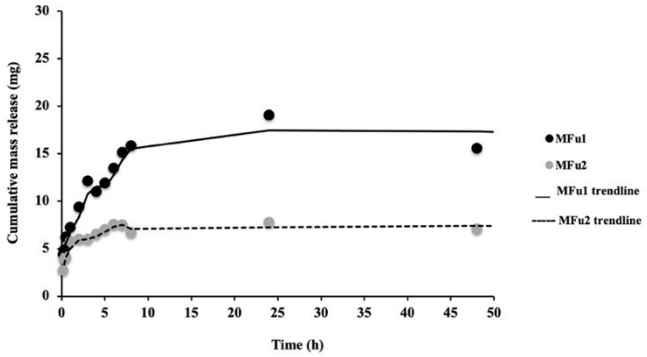


Figure V-4. Insulin release from MFu1 and MFu2 hydrogel particles in PBS , assessing the effect of fucoidan with different methacrylation degree.

V- 4.3. Biological characterization

The potential of the developed MFu hydrogel particles to support the culture of pancreatic beta cells (ultimately aiming to mimic the pancreatic islets microenvironment) was addressed by evaluation of cytocompatibility upon culturing 1.1B4 human pancreatic beta cells (1.1B4-HPC). Based on the findings namely insulin release, morphology (roughness) and methacrylate degree, we select MFu2 for direct contact with 1.1B4HPC. The metabolic activity (MTS assay), cell proliferation (DNA quantification) and cell morphology (CLSM) were assessed up to 7 days of culture. The direct contact assay on MFu2 hydrogel particles demonstrated that 1.1B4HPC cells were effectively able to proliferate from the initial time point up to 7 days in culture, as shown by the results of DNA quantification **(Figure V- 5 a)**. Moreover, cell adhesion on MFu hydrogel particles, as well as cell viability and morphology, were evaluated by CLSM. The MFu hydrogel particles shown a good cytocompatibility, with viability above 80% and almost no dead cells observed after 7 days of culture and seem to support cell proliferation **(Figure V- 5 b)**. Moreover, cells shown round-like shape **(Figure V- 5 c1- c2)** and tended to agglomerate after 7 days in culture to form pseudo-islets **(Figure V- 5 c3)**, characteristic of pancreatic cells during the culture period of study. Moreover, images acquired from cross-sections of MFu2 hydrogel particles **(Figure V- 5 c2)** show that 1.1B4HP cells were able to migrate into particle core and proliferate within the developed structures.

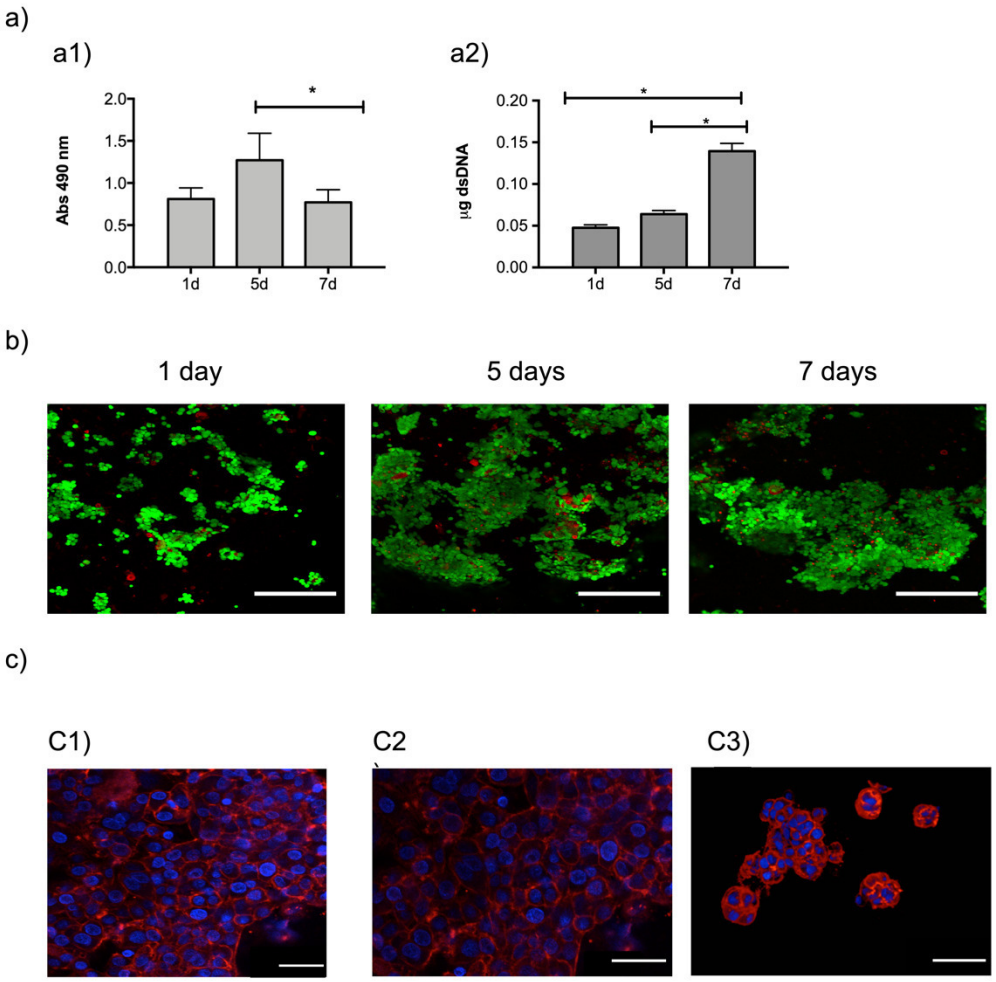


Figure V-5. Biological performance of 1.1B4HP cells in MFu microparticles. a) a1) MTS assay and a2) dsDNA content of 1.1B4HP cells, seeded and cultured up to 7 days on MFu2 microparticles. Data means ± sd (* $p<0.05$, nonparametric Kruskal-Wallis). b) cell viability demonstrated by live (green)/dead (red) staining for 1.1B4HP cells after 1, 5 and 7 days in direct contact with MFu2 microparticles, scale bar: 100µm. c) confocal laser micrographs of 1.1B4HP cells cultured on MFu2 microparticles during 7 days: c1) surface of the particles, c2) cross-section and c3) detail of pseudo-islets, scale bar: 50µm. The cells were stained with phalloidin-TRITC for actin filaments (red) and Hoechst 33342 for nuclei (blue), (scale bars 70 µm for c1) and 50 µm for c2) and c3).

V-5. CONCLUSIONS

We demonstrated that fucoidan hydrogel particles loaded insulin can be produced by methacrylation of fucoidan following by photocrosslinking and further incorporation of insulin. These MFu hydrogel particles revealed to be able to release insulin in a sustained fashion in SIF. Moreover, particles produced by photocrosslinking of MFu were also able to support the culture and encapsulation of human pancreatic cells (1.1B4HPC). These cells were able to proliferate and migrate into the particles core and further agglomerate into pseudo-islets. The results suggested that MFu hydrogel particles may be a good candidate for drug delivery vehicle or immuno-protectant for insulin-producing pancreatic cells, opening the doors for future assessment of their potential as a component of advanced therapeutic solutions for diabetes mellitus treatment.

V-6. ACKNOWLEDGEMENTS

We acknowledge ERDF for the financial support through POCTEP Project 0687_NOVOMAR_1_P, under the scope of INTERREG 2007-2013, and project 0302_CVMAR_I_1_P, under the scope of INTERREG España-Portugal 2014-2020, and Structured Projects NORTE-01-0145-FEDER-000021 and NORTE-01-0145-FEDER-000023, under the scope of Programa Operacional Regional do Norte (Norte 2020). Funding from the Portuguese Foundation for Science and Technology for doctoral grant of L.L. Reys (SFRH/BD/112139/2015) and post-doctoral grant of D. Soares da Costa (SFRH/BPD/85790/2012) is also acknowledged.

V-7. REFERENCES

[1] A.D. Association, Diagnosis and classification of diabetes mellitus., Diabetes Care. 33 Suppl 1 (2010) S62–S69. https://doi.org/10.2337/dc10-S062.

[2] K.G. Alberti, P.Z. Zimmet, Definition, diagnosis and classification of diabetes mellitus and its complications. Part 1: diagnosis and classification of diabetes mellitus provisional report of a WHO consultation, Diabet Med. 15 (1998) 539–553. https://doi.org/10.1002/(sici)1096-9136(199807)15:7.

[3] B.O. Roep, M. Peakman, Antigen Targets of Type 1 Diabetes Autoimmunity, Cold Spring Harb. Perspect. Med. 2 (2012) a007781. https://doi.org/10.1101/cshperspect.a007781.

[4] J. Xie, A. Li, J. Li, Advances in pH-Sensitive Polymers for Smart Insulin Delivery, Macromol. Rapid Commun. 38 (2017) 1700413. https://doi.org/10.1002/marc.201700413.

[5] T. Elshaarani, H. Yu, L. Wang, L. Lin, N. Wang, K. ur Rahman Naveed, L. Zhang, Y. Han, S. Fahad, Z. Ni, Dextran-crosslinked glucose responsive nanogels with a self-regulated insulin release at physiological conditions, Eur. Polym. J. 125 (2020) 109505. https://doi.org/https://doi.org/10.1016/j.eurpolymj.2020.109505.

[6] C. Cubayachi, C.N. Lemos, F. Pereira, K. Dias, R.D. Herculano, O. de Freitas, R.F. V Lopez, Silk fibroin films stabilizes and releases bioactive insulin for the treatment of corneal wounds, Eur. Polym. J. 118 (2019) 502–513. https://doi.org/https://doi.org/10.1016/j.eurpolymj.2019.06.022.

[7] B.Z. Chen, M. Ashfaq, D.D. Zhu, X.P. Zhang, X.D. Guo, Controlled Delivery of Insulin Using Rapidly Separating Microneedles Fabricated from Genipin-Crosslinked Gelatin, Macromol. Rapid Commun. 39 (2018) 1800075 (1–6). https://doi.org/10.1002/marc.201800075.

[8] A. Bhattacharyya, D. Mukherjee, R. Mishra, P.P. Kundu, Preparation of polyurethane–alginate/chitosan core shell nanoparticles for the purpose of oral insulin delivery, Eur. Polym. J. 92 (2017) 294–313. https://doi.org/https://doi.org/10.1016/j.eurpolymj.2017.05.015.

[9] S. Merani, C. Toso, J. Emamaullee, A.M. Shapiro, Optimal implantation site for pancreatic islet transplantation, Br J Surg. 95 (2008) 1449–1461. https://doi.org/10.1002/bjs.6391.

[10] H. Shih Lin, C. C., H. Shih, C.C. Lin, H. Shih Lin, C. C., Visible-light-mediated thiol-ene hydrogelation using eosin-Y as the only photoinitiator, Macromol Rapid Commun. 34 (2013) 269–273. https://doi.org/10.1002/marc.201200605.

[11] N. Fotino, C. Fotino, A. Pileggi, Re-engineering islet cell transplantation, Pharmacol. Res. 98 (2015) 76–85. https://doi.org/https://doi.org/10.1016/j.phrs.2015.02.010.

[12] C. Lauritano, A. Ianora, Marine Organisms with Anti-Diabetes Properties, Mar. Drugs. 14 (2016) 220. https://doi.org/10.3390/md14120220.

[13] K.J. Kim, K.Y. Yoon, B.Y. Lee, Fucoidan regulate blood glucose homeostasis in C57BL/KSJ m+/+db and C57BL/KSJ db/db mice, Fitoterapia. 83 (2012) 1105–1109. https://doi.org/10.1016/j.fitote.2012.04.027.

[14] B. Li, F. Lu, X. Wei, R. Zhao, Fucoidan: Structure and bioactivity, Molecules. 13 (2008) 1671–1695. https://doi.org/10.3390/molecules13081671.

[15] T.H. Silva, A. Alves, E.G. Popa, L.L. Reys, M.E. Gomes, R.A. Sousa, S.S. Silva, J.F. Mano, R.L. Reis, Marine algae sulfated polysaccharides for tissue engineering and drug delivery approaches, Biomatter. 2 (2012) 278–289.

[16] A. Sezer, E. Cevher, Fucoidan: A Versatile Biopolymer for Biomedical Applications, in: M. Zilberman (Ed.), Act. Implant. Scaffolds Tissue Regen., Springer Berlin Heidelberg, 2011: p. 377. https://doi.org/10.1007/8415_2011_67.

[17] M.T. Ale, J.D. Mikkelsen, A.S. Meyer, Important Determinants for Fucoidan Bioactivity: A Critical Review of Structure-Function Relations and Extraction Methods for Fucose-Containing Sulfated Polysaccharides from Brown Seaweeds, Mar. Drugs. 9 (2011) 2106.

[18] L.L. Reys, S.S. Silva, D. Soares da Costa, N.M. Oliveira, J.F. Mano, R.L. Reis, T.H. Silva, Fucoidan Hydrogels Photo-Cross-Linked with Visible Radiation As Matrices for Cell Culture, ACS Biomater. Sci. Eng. 2 (2016) 1151–1161. https://doi.org/10.1021/acsbiomaterials.6b00180.

[19] J.S. Lee, G.H. Jin, M.G. Yeo, C.H. Jang, H. Lee, G.H. Kim, Fabrication of electrospun biocomposites comprising polycaprolactone/ fucoidan for tissue regeneration, Carbohydr. Polym. 90 (2012) 181–188. https://doi.org/10.1016/j.carbpol.2012.05.012.

[20] R.K. Perumal, S. Perumal, R. Thangam, A. Gopinath, S.K. Ramadass, B. Madhan, S. Sivasubramanian, Collagen-fucoidan blend film with the potential to induce fibroblast proliferation for regenerative applications, Int J Biol Macromol. 106 (2018) 1032–1040. https://doi.org/https://doi.org/10.1016/j.ijbiomac.2017.08.111.

[21] A.D. Sezer, E. Cevher, F. Hatipoğlu, Z. Oğurtan, A.L. Baş, J. Akbuğa, Preparation of fucoidan-chitosan hydrogel and its application as burn healing accelerator on rabbits., Biol. Pharm. Bull. 31 (2008) 2326–2333. https://doi.org/10.1248/bpb.31.2326.

[22] A.D. Sezer, E. Cevher, F. Hatipoğlu, Z. Oğurtan, A.L. Baş, J. Akbuğa, The use of fucosphere in the treatment of dermal burns in rabbits, Eur. J. Pharm. Biopharm. 69 (2008) 189–198. https://doi.org/http://dx.doi.org/10.1016/j.ejpb.2007.09.004.

[23] K. Murakami, M. Ishihara, H. Aoki, S. Nakamura, S.I. Nakamura, S. Yanagibayashi, M. Takikawa, S. Kishimoto, H. Yokoe, T. Kiyosawa, Y. Sato, Enhanced healing of mitomycin C-treated healing-impaired wounds in rats with hydrosheets composed of chitin/chitosan, fucoidan, and alginate as wound dressings, Wound Repair Regen. 18 (2010) 478–485. https://doi.org/Doi 10.1111/J.1524-475x.2010.00606.X.

[24] V.R.A. Ferreira, M.A. Azenha, A.G. Bustamante, M.T. Mêna, C. Moura, C.M. Pereira, A.F. Silva, Metal cation sorption ability of immobilized and reticulated chondroitin sulfate or fucoidan through a sol-gel crosslinking scheme, Mater. Today Commun. 8 (2016) 172–182. https://doi.org/https://doi.org/10.1016/j.mtcomm.2016.08.003.

[25] G.J. and G.H. Kim, Rapid-prototyped PCL/fucoidan composite scaffolds for bone tissue regeneration: design, fabrication, and physical/biological properties, J. Mater. Chem. 21 (2011) 17710–17718.

[26] H.S. Jeong, J. Venkatesan, S.-K. Kim, Hydroxyapatite-fucoidan nanocomposites for bone tissue engineering, Int. J. Biol. Macromol. 57 (2013) 138–141. https://doi.org/http://dx.doi.org/10.1016/j.ijbiomac.2013.03.011.

[27] B. Lowe, J. Venkatesan, S. Anil, M.S. Shim, S.-K. Kim, Preparation and characterization of chitosan-natural nano hydroxyapatite-fucoidan nanocomposites for bone tissue engineering, Int. J. Biol. Macromol. 93 (2016) 1479–1487. https://doi.org/https://doi.org/10.1016/j.ijbiomac.2016.02.054.

[28] K. Murakami, H. Aoki, S. Nakamura, S. ichiro Nakamura, M. Takikawa, M. Hanzawa, S. Kishimoto, H. Hattori, Y. Tanaka, T. Kiyosawa, Y. Sato, M. Ishihara, Hydrogel blends of chitin/chitosan, fucoidan and alginate as healing-impaired wound dressings, Biomaterials. 31 (2010) 83–90. https://doi.org/10.1016/j.biomaterials.2009.09.031.

[29] A.D.& J.A. SEZER, Fucosphere—New microsphere carriers for peptide and protein delivery: Preparation and in vitro characterization, J. Microencapsul. 23 (2006) 513–522.

https://doi.org/doi:10.1080/02652040600687563.

[30] K.T. Nguyen, J.L. West, Photopolymerizable hydrogels for tissue engineering applications, Biomaterials. 23 (2002) 4307–4314. https://doi.org/10.1016/S0142-9612(02)00175-8.

[31] H. Shih Lin, C. C., Visible-light-mediated thiol-ene hydrogelation using eosin-Y as the only photoinitiator, Macromol Rapid Commun. 34 (2013) 269–273.

[32] M.I. Rial-Hermida, N.M. Oliveira, A. Concheiro, C. Alvarez-Lorenzo, J.F. Mano, Bioinspired superamphiphobic surfaces as a tool for polymer- and solvent-independent preparation of drug-loaded spherical particles, Acta Biomater. (2014) 4314. https://doi.org/http://dx.doi.org/10.1016/j.actbio.2014.06.009.

[33] X. Deng, L. Mammen, H.-J. Butt, D. Vollmer, Candle Soot as a Template for a Transparent Robust Superamphiphobic Coating, Science (80-.). 335 (2012) 67–70. https://doi.org/10.1126/science.1207115.

[34] H. Shih, R.G. Mirmira, C.C. Lin, Visible light-initiated interfacial thiol-norbornene photopolymerization for forming an islet surface conformal coating, J. Mater. Chem. B. 3 (2015) 170–175. https://doi.org/10.1039/C4TB01593B.

[35] D. Tahtat, M. Mahlous, S. Benamer, A.N. Khodja, H. Oussedik-Oumehdi, F. Laraba-Djebari, Oral delivery of insulin from alginate/chitosan crosslinked by glutaraldehyde, Int. J. Biol. Macromol. 58 (2013) 160–168. https://doi.org/https://doi.org/10.1016/j.ijbiomac.2013.03.064.

[36] A. Sood, R. Panchagnula, Peroral route: an opportunity for protein and peptide drug delivery, Chem. Rev. 101 (2001) 3275–3303. https://doi.org/10.1021/cr000700m.

[37] C.M. Silva, A.J. Ribeiro, D. Ferreira, F. Veiga, Insulin encapsulation in reinforced alginate microspheres prepared by internal gelation, Eur. J. Pharm. Sci. 29 (2006) 148–159. https://doi.org/https://doi.org/10.1016/j.ejps.2006.06.008.

[38] P. Mukhopadhyay, K. Sarkar, M. Chakraborty, S. Bhattacharya, R. Mishra, P.P. Kundu, Oral insulin delivery by self-assembled chitosan nanoparticles: In vitro and in vivo studies in diabetic animal model, Mater. Sci. Eng. C. 33 (2013) 376–382. https://doi.org/https://doi.org/10.1016/j.msec.2012.09.001.

[39] M.-A. Shahbazi, H.A. Santos, Improving oral absorption via drug-loaded nanocarriers: absorption mechanisms, intestinal models and rational fabrication., Curr. Drug Metab. 14 (2013) 28–56. https://doi.org/10.2174/1389200211309010028.

Chapter VI

Building fucoidan/agarose - based hydrogels as a platform for the development of therapeutic approaches diabetes

Chapter VI

Building fucoidan/agarose-based hydrogels as a platform for the development of therapeutic approaches diabetes[4]

ABSTRACT

Recent achievements in diabetes have enabled the development of versatile three-dimensional (3D) hydrogels as *in vitro* platforms that monitor high blood glucose levels and release insulin, serving as well as support for encapsulation of pancreatic cells and islets of Langerhans. Hydrogels, like scaffolds, can potentially increase islet viability and functionality compared to conventional intra-portal vein transplantations by reducing the receptor immune response. In this work, we aimed to create agarose/fucoidan hydrogels to encapsulate pancreatic cells as a potential new biomaterial for diabetes therapeutics. The hydrogels were produced combining fucoidan (Fu) with agarose (Aga), marine polysaccharides derived from the cell wall of brown and red seaweeds, respectively, and a thermal gelation process. The agarose/fucoidan (AgaFu) blended hydrogels were obtained by dissolving Aga in 3 or 5 wt % Fu aqueous solutions to obtain different proportions (4:10; 5:10 and 7:10 wt). Mechanical and chemical characterization of the produced hydrogels were addressed by rheology, FTIR, ^{1}H NMR, and XPS. Further, the ability of the developed materials to sustain the viability of human pancreatic cells was assessed by encapsulation of 1.1B4 HP cell line up to 7 days. The chemical characterization confirmed the presence of the two polymers into the structure of hydrogels. Rheological tests on hydrogels revealed a non-newtonian, viscoelastic behavior, while the assessment of mechanical behavior showed that increasing Aga concentrations resulted in hydrogels with higher Young modulus. Additionally, the biological assessment of the

[4] This chapter is based on the following publication:

Reys L. L., Silva S. S., Soares da Costa D., Rodrigues L. C., Reis R. L. and Silva T.H., "*Building fucoidan/agarose - based hydrogels as a platform for the development of therapeutic approaches against diabetes*" (submitted for publication).

hydrogels demonstrated that cultured pancreatic beta cells tended to self-organize and form pseudo-islets during the period studied.

Keywords: Fucoidan, agarose, hydrogels, diabetes mellitus, tissue engineering, cell encapsulation, pancreatic beta cells, marine biomaterials

VI-1. GRAPHICAL ABSTRACT



VI-2. INTRODUCTION

One of the most promising areas of biomaterial development is the use of hydrogels as scaffolds for tissue engineering [1]. In this area, the application of hydrogels is very popular as these can act as a matrix for delivery and retention of cells and growth factors within the site of injury, or as particles for encapsulation and sustained release of drugs, among others [2–5]. In that way, different hydrogels have been proposed as versatile platforms for the engineering of bone, cartilage, vascular and cornea tissue, as well as for the treatment of some diseases, namely diabetes mellitus [4]. Diabetes is a metabolic disorder characterized by high levels of plasma glucose and can be classified as type I or type II (insulin-dependent and non-insulin-dependent, respectively). Pancreatic beta cells replacement therapy by clinical islet transplantation (CIT) has

shown to be a promising alternative to conventional insulin treatment used for type I diabetes. However, CIT is limited by the significant risks involved in the use of immunosuppressive drugs to prevent rejection of allogeneic donor islets. In the context of diabetes monitoring and therapy, there are important cues that have to be further explored, as so advanced hydrogels are being developed to monitor high glucose levels, releasing insulin, or encapsulate pancreatic cells [6].

Hydrogels are insoluble 3D networks containing a high amount of water (at least 10% of the total weight or volume) [4,7], that may be produced using natural (i.e. agarose [8], collagen [9], gelatin [10] and chitosan [11]) and/or synthetic (i.e. poly (ethylene glycol) (PEG) [12,13], polyacrylamide (PAA) [13], polydimethylsiloxane (PDMS) [13]) polymers. Hydrogels can be produced by physical gelation like thermo-gelation, ionic-crosslinking, pH-sensitivity, and host-guest interaction or by chemical crosslinking like photopolymerization, click chemistry, enzyme-mediated crosslinking and through the use of a crosslinking agent establishing covalent bonds between polymeric chains to form an intricated network [14–18].

In this work, fucoidan and agarose were combined using thermo-gelation methods to produce hydrogels as a platform with potential to be applied in diabetes treatment. Fucoidan is a marine origin sulfated anionic polysaccharide that can be extracted and isolated from different brown algae species and marine invertebrates (such as sea urchin and sea cucumber (echinoderms)) [19–21]. Generally, the chemical structure of fucoidan is composed of L-fucose and sulfate groups and different amounts of other sugars as glucuronic acid, xylose, galactose, and mannose [19,21,22]. Fucoidan may present diversified bioactive properties, such as anti-inflammatory [19,23], anticoagulant [19,23], anti-fibrotic [24,25], antibacterial, antitumor [21,26–28], reducing the blood glucose [29] and antioxidant [19,22,30]. However, despite the promising biological properties, the biomedical use of fucoidan as component of scaffolds faces some limitations, mainly due to difficulties in the processing of matrices able to remain stable in aqueous medium. Agarose, a neutral polysaccharide, is the main component of Agar, which is derived from the cell wall of the red algae group [31,32]. The structure of agarose consists of a basic repeat unit consisting of 1,3-linked-d-galactopyranose and 1,4-linked 3,6-anhydro-α-l-galactopyranose [33,34]. The agarose gel is called 'physical gel' due to its thermo-reversible nature, suggesting its use as gelling agent. Agarose gels can be obtained by heating-cooling cycles, being observed a wide gap between the two processes – hysteresis – which makes it suitable for many applications, including in the

biomedical field, namely on cartilage, nervous system, cardiac, bone, corneal regeneration and diabetes treatment [35,36]. For more than two decades that islets encapsulation in hydrogels have been studied as a treatment of type I diabetes mellitus, with the intent of keeping the implanted cells away from the recipient´s immune system [6,37]. Indeed, this type of scaffolds can potentially provide an alternative to extra-hepatic transplantation site for islets by improving nutrient diffusion and blood supply to the scaffold, while preventing contact of the encapsulated cells with the host immune cells [37–40]. Moreover, several strategies have been explored, from simple hydrogel systems, with variable performance regarding diffusion of oxygen and insulin depending on gelling process, to functionalized systems incorporating growth factors promoting new vessels formation or smart responsiveness to external stimuli with impact on permeability.

This work aims to create an innovative approach that associates marine biopolymers, agarose/fucoidan (AgaFu), using thermo-gelation. This innovative approach would promote the design of hydrogels with distinct features for future applications in diabetes treatment. To our knowledge, there are no reports in the literature suggesting the use of agarose/fucoidan blends for biomedical applications, and naturally neither on the specific area of diabetes treatments. With this purpose, both marine biopolymers and the developed AgaFu hydrogels were extensively characterized regarding their structural changes, rheology behavior, and polymer distribution. The *in vitro* cytocompatibility evaluation of the developed AgaFu hydrogels was performed by encapsulation of human pancreatic cells (1.1B4HP) and proliferation, morphology and viability were investigated to potentiate their further use in diabetes treatment.

VI-3. EXPERIMENTAL

VI-3.1. Materials

Fucoidan (Fu) in powder from brown algae *Fucus vesiculosus* (Maritech® Fucoidan, Marinova, FVF2011527, Australia) was used after a purification process as described below. Agarose low gelling temperature for molecular biology (Sigma-Aldrich, USA) was used as received. All other reagents were of analytical grade and used as received.

VI-3.2. Purification of fucoidan (PFu)

A purification process was applied on fucoidan (Fu) powder, based on the calcium ions methodology [41]. The purification with calcium ions was performed to remove the alginates contained in the crude fucoidan. These alginates residues form complexes with calcium ions and precipitate [41]. Briefly, Fu was dissolved (160 mg mL^{-1}) in (20 mM) calcium acetate aqueous solution, during 4 h at 50 °C under stirring, and pH was adjusted continuously between 6.6 and 7.5, to avoid acid hydrolysis of fucoidan. Afterward, the solution was left at 4 °C overnight and then centrifuged for 15 min at 5,000 g (Centrifuge 5810, Eppendorf, Germany). The supernatant was dialyzed against water using 12-14 KDa cut-off dialysis membranes for 3 days and freeze-dried (CryoDos-80, Telstar, Spain) for 4 days [41].

VI-3.3. Preparation of fucoidan-based hydrogels

Agarose/fucoidan (AgaFu) hydrogels were prepared by thermo-gelation [32,42]. Purified fucoidan (Fu) was dissolved in ultrapure water at a concentration of 3 or 5 % (w/v) under stirring, at 75 °C, and then Agarose (Aga) powder was added to the solutions **(Figure VI - 1A)**. The AgaFu hydrogels were prepared at different Aga/Fu proportions (4:10; 5:10 and 7:10 wt) and represented as AgaFu 3X or AgaFu 5X (where different letters in X represent different formulations), throughout the manuscript **(Table VI - 1)**. The obtained solution was then casted into eppendorf caps (circular plastic with size 9.73 ± 0.09 mm width and 5.38 ± 0.09 mm height), that were used as molds, and the hydrogels were progressively formed until room temperature was reached **(Figure VI - 1B, C)**. The hydrogels were removed from molds and replenished with Dulbecco´s phosphate buffered saline (DPBS) solution to stabilize the gel formation **(Figure VI - 1D)**. Aga hydrogels were used as control material rather than Fu alone, as Fu does not form structures (without the use of chemical crosslinking) due to its high-water solubility [19,43]. The Aga hydrogels were produced with the same procedure but without fucoidan addition.

Table VI-1. Summary of formulations used in the preparation of Aga and AgaFu hydrogels.

	Polymer solutions concentration (%)		Hydrogels
	Agarose	Fucoidan	Agarose (Aga): Fucoidan (Fu) ratio (wt)
Aga 3	3	——	——
Aga 5	5	——	——
Fu 3	——	3	——
Fu 5	——	5	——
AgaFu 3a	1.2	3	4:10
AgaFu 3b	1.5		5:10
AgaFu 3c	2.1		7:10
AgaFu 5a	2	5	4:10
AgaFu 5b	2.5		5:10
AgaFu 5c	3.5		7:10

VI-3.4. Physical-chemical characterization of AgaFu hydrogels

VI-3.4.1. Rheology

Rheological assays were performed using the rheometer Kinexus pro+ (Malvern Instruments, UK), with the software of acquisition rSpace (Malvern Instruments, UK).

Oscillatory measurements: All the oscillatory measurements were performed by using stainless steel parallel-plate geometry with a diameter of 8 mm and for the rotational experiments, a conic plate holder of 40 mm and 1 mm gap. The rheological tests were performed with solutions prepared using the same conditions as the ones used for the preparation of hydrogels and with Aga and AgaFu formed hydrogels. In the rotational experiments, two different plots were obtained: a) the traditional shear viscosity (Pa.s) throughout shear rate (1/s) and b) the shear stress (Pa) as

a function of shear rate (1/s). From these curves, it was possible to obtain information about the flow behavior of the samples. The oscillatory experiments were preceded by strain sweep curves to determine the linear viscoelastic region (LVER) of the samples. Strain amplitude was thus performed in the shear rate range changing from 0.1 to 100 Hz in a 10/decade rate, at a range of cooling temperature between 80 °C and 37 °C and a constant 1 % strain. After this, the mechanical spectra of each sample were obtained, and the elastic modulus (G') and viscous modulus (G'') were recorded over a frequency sweep ranging from 0.1 Hz to 100 Hz at constant temperature of 37 °C. The strain dependency measurements were performed using 1 mL of the solution or a Aga or a AgaFu hydrogel (8.91 ± 0.09 mm width and 5.38 ± 0.09 mm height) in the sample holder [44,45]. All plots are the average of measurements with at least 3 different samples.

Compressive studies: These tests were performed using a parallel plate geometry of 8 mm diameter, with radial grooves to avoid hydrogel leakage. Aga and AgaFu hydrogels were prepared in distilled water as previously described and maintained in DPBS. Hydrogels were compressed in the direction normal to the circular face of the cylindrical samples at a rate of 1 mm/min for a maximum strain of 85 % and at room temperature. The Young's modulus was determined by the initial slope of the linear region of the stress-strain curve. Each experiment was performed in quintuplicate [46].

Hydrogel mesh size: The mesh size is often described by a structural parameter, (D_{mesh}), which represents the diameter of a hard sphere that fills the void in between hydrogel network strands. Hydrogel mesh size was calculated based on the classical theory of rubber elasticity, which relates the shear modulus (G') to the mesh size D_{mesh} **(Equation VI - 1)**, where R is the gas constant, T the absolute temperature and N_{av} is Avogadro's number. This allows to estimate the mesh size of a hydrogel based on its shear modulus [47–49].

Equation VI-1. Mesh size Dmesh

$$D_{mesh} = \left(\frac{6\,RT}{\pi N_{av} G'}\right)^{\frac{1}{3}}$$

VI-3.4.2. ^{1}H NMR spectroscopy

Aga, Fu powders and AgaFu freeze-dried hydrogel powder were analysed by ^{1}H NMR spectroscopy, after being dispersed/dissolved in deuterated water (D_2O), at 5 mg/mL. The ^{1}H NMR assay was made at 50 °C, being recorded on Burker Avance III according to the following spectral conditions: 300 Hz spectra with 90° impulses, 4 s acquisition time. Spectra were processed by using Mestre Nova Software.

VI-3.4.3. Fourier transform infrared spectroscopy (FTIR)

The FTIR analysis of the samples was performed on a Shimadzu IR Prestige 21 spectrometer. Samples were prepared using potassium bromide (KBr) pellets at room temperature. Each sample spectrum was collected by averaging 32 scans with a resolution of 16 cm^{-1}, within the 4000 – 400 cm^{-1} spectrum regions.

VI-3.4.4. X - ray photoelectron spectroscopy (XPS)

Analysis of the Aga, Fu, and AgaFu samples was performed using a Kratos Axis-Supra instrument equipped with aluminum Kα monochromatized radiation X-ray source (1486.6 eV) and ESCApe software. Due to the non-conducting nature of the samples, it was necessary to use a co-axial electron neutralizer to minimize surface charging, which performed the neutralization by itself. Photoelectrons were collected from a take-off angle of 90° relative to the sample surface. The measurement was done in a Constant Analyser Energy mode (CAE) with a 160 eV pass energy for survey spectra, 20 eV pass energy for high-resolution spectra of the hydrogels and 40 eV pass energy for the polymer's powders. Charge referencing was done by setting the lower binding energy C1s peak at 285.0 eV related to C1s hydrocarbon peak [44,50].

VI-3.4.5. Stability tests

Stability tests of the Aga and AgaFu hydrogels were performed by immersion in DPBS and in Roswell Park Memorial Institute (RPMI) 1640 medium supplemented with 10 % fetal bovine serum (FBS) (Invitrogen, USA) and 1 % antibiotic/antimycotic (A/B) (Invitrogen, USA), for 28 days, at 37 °C. The medium was replaced every 3 days. The swollen samples weight was measured after removing the excess of surface water by gently tapping the surface with filter paper. The swelling ratio was given by the ratio: W_s/W_d, where W_s is the swollen sample weight under specified environmental conditions, and W_d is dry sample weight.

VI-3.4.6. Diffusion within hydrogels

Diffusion of a model compound within Aga and AgaFu hydrogels was assessed based on Kirby Bauer method [51]. The AgaFu solutions were prepared as previous mentioned **(section VI - 3.3).** These solutions were dropped in a petri dish, and gelation occurred at room temperature for 15 - 20 min. Afterwards some holes (d= 6 mm) were done in the formed AgaFu gels and a 100 mM methylene solution was dropped into those holes. The diffusion of methylene blue is calculated by difference of starting position of the dye and the diameter of dye spot at different time points.

VI-3.4.7. Permeability to glucose

The permeability to glucose was determined using a glass Franz-type diffusion cell (PermeGear) with an 8 mL reactor compartment (using an effective mass transfer area of 1 cm^2) [52]. Aga and AgaFu hydrogels were previously equilibrated in a DPBS solution (overnight), placed between the two compartments, and held with a stainless-steel clamp. The receptor compartment was immediately filled with DPBS solution, and air bubbles were removed. Finally, the donor compartment was filled with 16 mM of glucose (DPBS, pH 7.4). Aliquots of 1 mL were removed from the receptor compartment at pre-stablished time points being further restored with the same quantity of fresh DPBS. The experiments were performed at 37 °C, and the receptor compartment was stirred using a magnetic bar to eliminate the boundary layer effect. The concentration of glucose in the receptor chamber was evaluated using the dinitrosalicylic acid (DNS) method. The

DNS reacts with reducing sugars, and other reducing molecules, forming 3-amino-5-nitrosalicylic acid, an aromatic compound that strongly absorbs light at 540 nm, enabling the determination of the amount of reducing sugar present in the solutions. The amount of glucose was calculated by measuring the absorbance at a wavelength of 540 nm using a microplate reader (Synergy HT, Bio-TEK, USA) and regression using an adequate calibration curve. The permeability (P) of glucose was calculated by the following **Equation VI - 2:**

Equation VI-2. Permeability (P) of glucose

$$-\ln\left(1-\frac{2C_t}{C_0}\right)=\frac{2A}{V}\times P\times t$$

where C_t is the concentration in the receptor compartment at time t, C_0 is the initial concentration in the donor compartment, V is the solution volume in the two compartments, and A is the effective area of permeation.

The diffusion coefficient (D) of glucose across the membrane was calculated according to Fick's law of diffusion, as follows **(Equation VI - 3):**

Equation VI-3. Diffusion coefficient of glucose across the membrane.

$$D=\frac{V_1\,V_2}{V_1+V_2}\times\frac{h}{A}\times\frac{1}{t}\ln\left(\frac{C_f-C_i}{C_f-C_t}\right)$$

where D is the diffusion coefficient (cm^2/s); C_i and C_f are the initial and final concentrations, and C_t is the concentration of solute in the receptor side at time t, respectively (mol/L); V_1 and V_2 correspond to the volume of the liquid in the donor compartment and in the receptor compartment (cm^3), respectively; h is the thickness of the membrane (cm); and A is the effective diffusion area of the membrane (cm^2).

The partition coefficient (K_d) is defined as a measure of the solubility of glucose in the hydrogel. The partition coefficient for the system was calculated as follows **(Equation VI - 4)**:

Equation VI-4. Partition coefficient

$$K_d = \frac{P \times h}{D}$$

where P is the permeability, h is the thickness of the membrane, and D is the diffusion coefficient.

VI-3.5. Biological assessment of developed fucoidan - based hydrogels

VI-3.5.1. Cell culture

Human pancreatic cell line (1.1B4 HP) was cultured in RPMI 1640 medium (Invitrogen, USA) supplemented with 10 % fetal bovine serum (FBS) (Invitrogen, USA) and 1 % antibiotic/antimycotic (A/B) (Invitrogen, USA) at a temperature of 37 °C and 5 % of CO_2 until achieving 90 % confluence. The medium was refreshed every 2 - 3 days.

VI-3.5.2. Cell encapsulation

Before encapsulation procedure, the 1.1B4 HP cells (passage 36) were washed with sterile DPBS followed by centrifugation at 300 g for 5 mins to form a pellet and the supernatant discarded. The suspension of 1.1B4 HP cells at a concentration of 1.5 x 10^6 cells/mL were added to Aga and AgaFu solutions and gently mixed at 37°C. The obtained suspension (cells: Aga/AgaFu solution) was then cast into appropriated molds, and the hydrogels were progressively formed until room temperature was reached. Subsequently, the hydrogels were removed from molds and replenished with DPBS to enable the complete gel formation. After repeated washings, the cell-laden hydrogels were cultured in RPMI 1640 medium for further *in vitro* studies.

VI-3.5.3. Metabolic activity, proliferation, and morphology

After each of the pre-determinated periods (1, 3 and 7 days), the samples were washed with DPBS and MTS (3-(4,5-dimethylthiazol-2-yl)-5-(3-carboxymethoxyphenyl)-2-(4-sulfophenyl)-2H-tetrazolium) assay, DNA quantification, live/dead assay, and assessment of cell morphology, adhesion and distribution were performed, as described below:

- **Metabolic activity assay**

The metabolic activity of 1.1B4 HP encapsulated cells in hydrogels was determined using MTS assay. Samples were incubated with an MTS solution prepared using a 1:5 ratio of MTS reagent and DMEM without phenol red, 10 % FBS and 1 % ATB solution for 3 h at 37 °C. The optical density (O.D.) was read at 490 nm on a multiwell microplate reader (Bio-Tek Instruments, US).

- **dsDNA quantification**

dsDNA quantification was performed after each experimental time point using the PicoGreen Quantification Kit (Invitrogen Corporation, USA), according to the manufacturer instructions in a lysed cell suspension obtained after osmotic and thermal shocks. Fluorescence was read in a microplate reader (Bio-Tek Instruments, US) at an excitation of 485/20 nm and emission of 528/20 nm.

- **Live/dead assay**

The cellular viability was assessed using the live/dead assay (calcein AM/propidium iodide (PI) staining). Briefly, the cell-laden Aga and AgaFu hydrogels were incubated for 10 min with 2 µL calcein AM (1 mg/mL, Molecular Probes, Invitrogen, USA) and 1 µL PI (1 mg/mL, Molecular Probes, Invitrogen, USA) in 1 mL of DPBS protected from light. The hydrogels were washed with DPBS to remove residual staining and visualized by confocal laser scanning microscopy (CLSM) (Axio Imager Z1m, Zeiss, Germany). Image J was used to count the number of live and dead cells and **Equation VI - 5** was used to calculate the percentage of viable cells.

Equation VI-5. Viability of cells

$$\text{Viability} = \frac{\%\ \text{Live cells}}{\%\ \text{Live cells} + \%\ \text{Dead cells}} \times 100$$

- **Cell morphology**

Adhesion, morphology, and distribution of 1.1B4HP cells encapsulated into AgaFu hydrogels were analysed by confocal laser scanning microscopy (CLSM). The Aga and AgaFu hydrogels were fixed with 10 % formalin for 30 min and then blocked with 3 % bovine serum albumin (BSA) for 30 min. The structures were permeabilized with 0.1 % Triton X-100 for 5 min, incubated with phalloidin-TRITC for 20 min at room temperature, followed by washing with DPBS and staining with 5 µg/mL DAPI (2-(4-amidinophenyl)-1H-indole-6-carboxamidine) for 30 min. Fluorescence images from the stained constructs were obtained by CLSM (Inverted Confocal Microscope with incubation, TCS SP8, Leica).

VI-3.6. Statistical analysis

Statistical analysis of the data was performed by Shapiro-Wilk normality test, One-way ANOVA and non-parametric Kruskal-Wallis and Dunn´s multiple comparison tests, using Graph Pad Prism ® 7.0. Results are presented as mean ± standard deviation (SD) and significance level between groups was set for $*p < 0.1$, $**p < 0.01$, and $***p < 0.001$.

VI-4. RESULTS AND DISCUSSION

Functional hydrogels envisioning diabetes treatment were developed by combining two marine origin polymers. agarose (Aga), a gelling polymer, with fucoidan (Fu), a biologically active polymer. The gel formation was obtained according to the representative scheme in **Figure VI - 1 A - D**. Blended hydrogels composed of AgaFu 3 and AgaFu 5 have a yellowish-brown color, good homogeneity and mechanical stability **(Figure VI - 1 A-C).** Aga hydrogels **(Figure VI-1 D1)** were used as control material rather than Fu alone; Fu does not form biomechanically stable structures (unless extensive crosslinking strategies are employed) due to its high-water solubility [19,43].

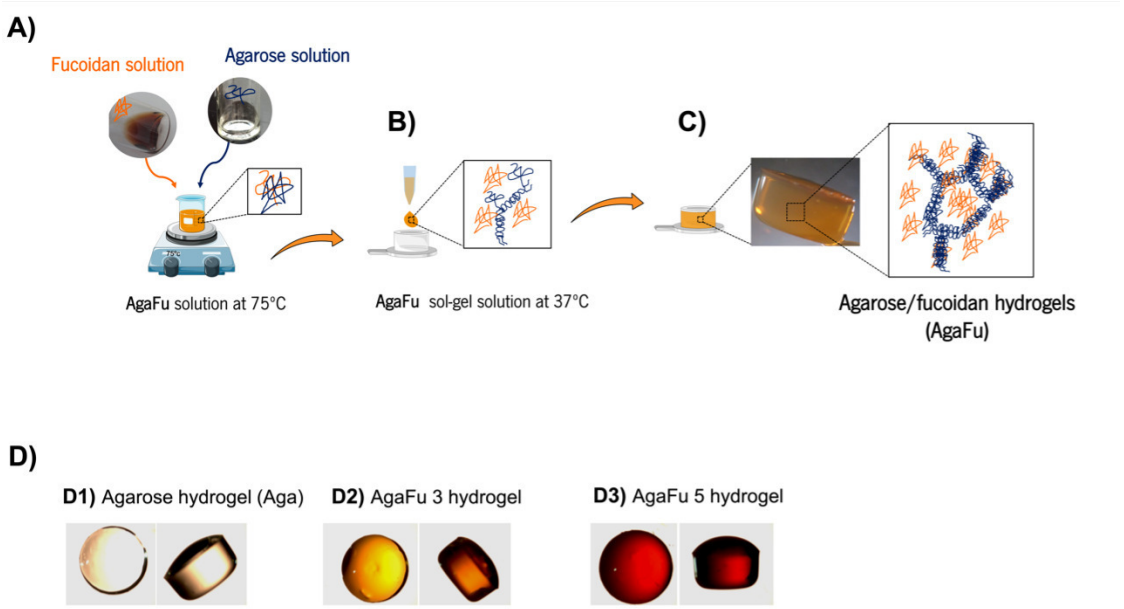


Figure VI-1.Schematic representation for production of agarose-fucoidan hydrogels (AgaFu). A) preparation of agarose (Aga) or agarose/fucoidan (AgaFu) solutions, B) transferring of Aga or AgaFu solutions to molds, C) Aga or AgaFu gel formation by cooling the solution on air until room temperature and AgaFu hydrogels and D) Photographs of the agarose/fucoidan based hydrogels D1) Agarose hydrogel, D2) AgaFu 3 hydrogel and D3) AgaFu 5 hydrogel.

VI-4.1. Physico-chemical characterization of Fu, Aga and AgaFu

To evaluate the influence of the composition of hydrogels on their physical-chemical properties, several characterization procedures were employed, and the obtained results were as follows.

- **Rheology**

The viscosity of the solutions of Fu and Aga at 3 and 5 % and the blended solutions (AgaFu 3 and AgaFu 5 at proportions: a (4:10), b (5:10), and c (7:10) were evaluated as a function of the applied shear rate **(Figure VI- 2 A1-A3)**. As expected, the Fu solution presented lower viscosity when compared with Aga solutions, where differences in viscosity are directly correlated to the gelling property of Aga and its concentration. This reveals that the gel formation was fundamentally governed by gelation of Aga, which can confine the fucoidan in the network established due to

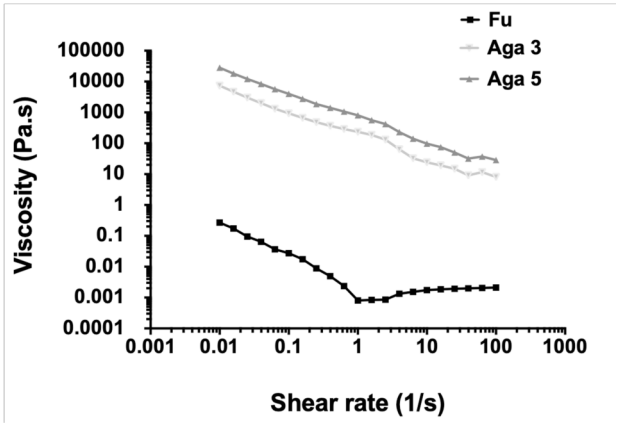
polymers chains rearrangement. Both blended (AgaFu 3 and AgaFu 5) solutions displayed shear thinning behavior, in which the viscosity decreased with increasing shear rate **(Figure VI - 2 A2 - A3).** This behavior was explained as the shearing of the polymer chains disrupts the three-dimensional structure through the breaking of primary and secondary bonds [53].

The prepared polysaccharide solutions performed as viscoelastic materials that exhibit solid and liquid characteristics. The storage (G′) and loss (G″) modulus refer to the elastic and viscous response of a given material to shear stress, respectively [54,55]. In Figure 2 B1-B2, the evaluation of the storage modulus as a function of temperature is shown for Aga hydrogels of different concentrations (3 and 5%) and AgaFu 3 and AgaFu 5 at different proportions a (4:10), b (5:10) and c (7:10). All the curves show almost the same behavior. For the AgaFu3 hydrogels, higher ratio of Fu, promoted a decrease on G´, with the storage modulus being roughly independent of temperature (pseudo-equilibrium modulus), but the increase of Aga proportion into the blend increased the storage modulus, more evidently at lower temperatures [53]. Furthermore, for the AgaFu5 formulation the same tendency was not so evident. The use of more concentrated polymeric solution, with increased viscosities, particularly for the Aga solution, leaded to a more difficult interaction between the polymeric chains, through a reduction of the chain mobility, reducing also the incidence of the intermolecular interaction. This is particularly noted for the AgaFu5b, where a significant decrease on G' was observed compared with AgaFu5a. This difficulty was overcome for the AgaFu5c, where the significant increase of the number of Aga molecules to pair and able to form the network of super-helices linked at their ends suppressed the influence of the reduction of the intermolecular interaction into the network [56].

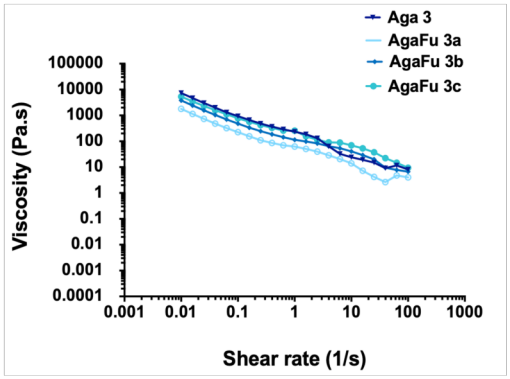
The fitting of the experimental data (shear stress-shear rate) is presented in **Figure VI - 2 C1-C3** based in the power law model: $y=k\,x^{n}$, where y is the shear stress (Pa), x is the shear rate (1/s), k is the consistency coefficient (Pa. s^{n}), and n is the flow behavior index, which describes the flow behavior of each solution [44,57]. In the literature, the flow behavior is classified according to this flow behavior index, and a Newtonian liquid present n=1, a pseudoplastic fluid n<1 and a swelling plastic fluid n>1. The Fu solutions, Fu 3 % (n=1.06 ± 0.03) and Fu 5 % (n=1.09 ± 0.06) solutions, presented a flow behavior index closest to 1, which is characteristic of Newtonian fluids, while Aga solutions, as well as most of the blended solutions, exhibited lower index values: AgaFu 3b (n=0.826 ± 0.04); AgaFu 3c (n=0.839 ± 0.04) and AgaFu 5a (n=0.955 ± 0.04), suggesting a

shear-thinning (pseudoplastic) flow behavior [46,58]. The results suggest that the shear-thinning behavior is governed by agarose [59]. The shear-thinning behavior, i.e., when viscosity significantly decreases with increasing shear rate, suggests that the gel mixture of agarose and fucoidan could be injected by applying high shear rate during injection with minimal effect over encapsulated cells and quickly self-healing after removal of shear. Most significantly, these gels could be used to deliver biological molecules and cells during injection process [17,59].

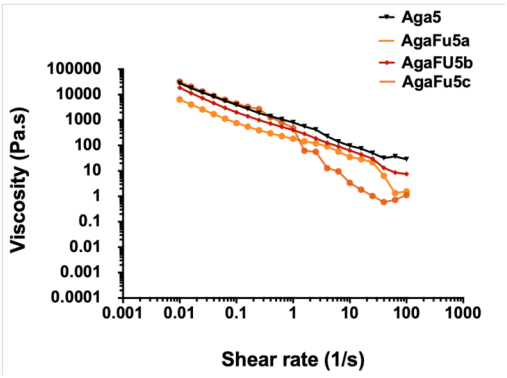
A1)



A2)



A3)



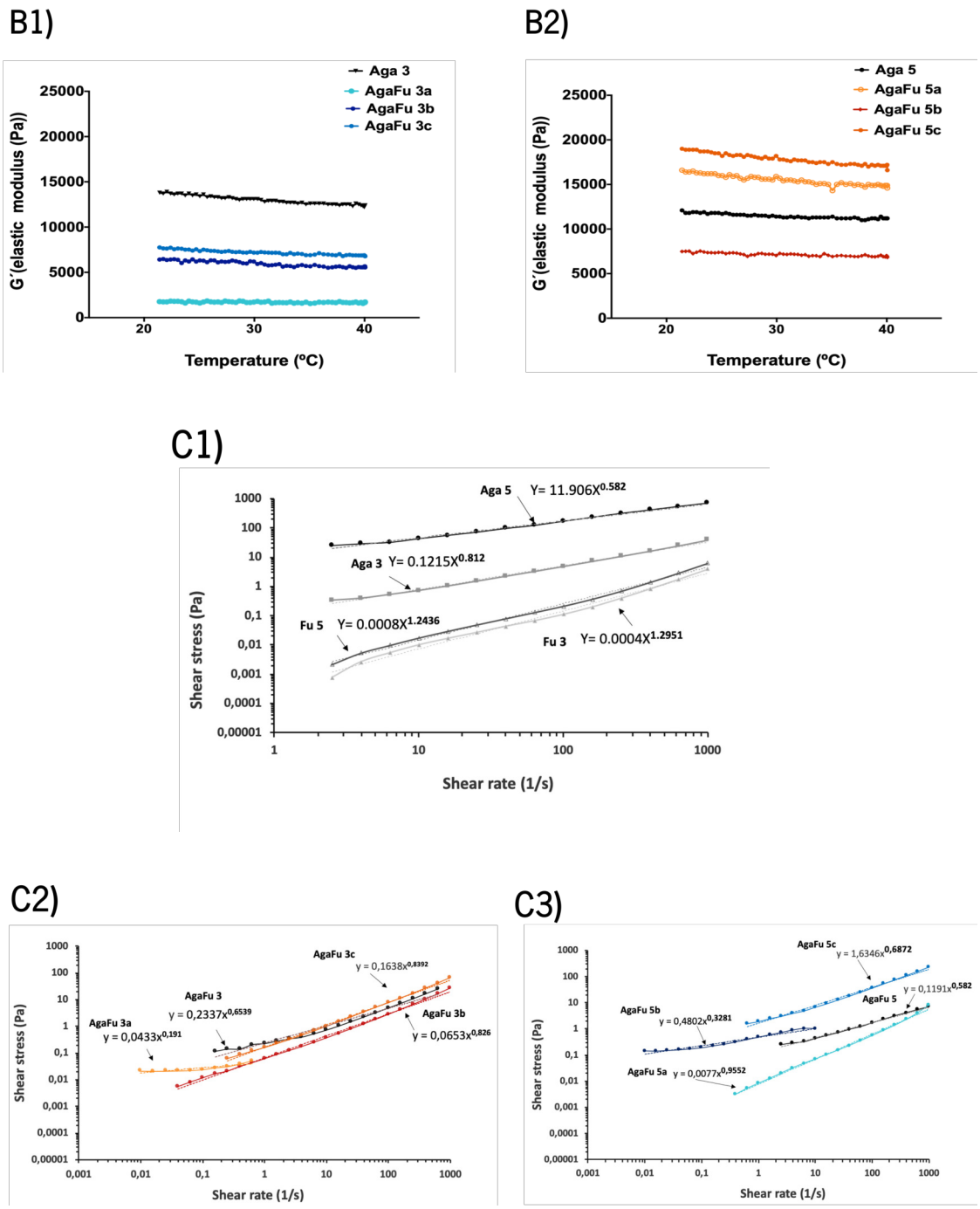


Figure VI-2. Rheological characterization of Aga, Fu and AgaFu hydrogels. A1, A2, A3) Viscosity curves as a function of shear rate, B1, B2) Oscillatory curves as a function of temperature and C1, C2, C3) Shear stress curves as a function of shear rate with adjusted power-law equations.

- **Chemical characterization**

The chemical structures of the samples were examined by Fourier transform infrared spectroscopy (FTIR) **(Figure VI- 3 A1, A2)** and with Proton nuclear magnetic resonance (^{1}H NMR) spectroscopy **(Figure VI- 3 B1-B3)**. On the FTIR spectra presented in **Figure VI - 3 A1**, the main characteristic peaks of Aga and Fu could be observed. At the Aga spectra the region located between 900 - 1200 cm^{-1} contained the characteristic saccharide peaks of Aga that are representative of the skeletal vibrations associated with C–O–C glycosidic bonds. The region 890 - 940 cm^{-1} also contains a characteristic signal of Aga that represents vibration associated with C-O-C bridge on 3,6 anhydrogalactose unit [58,60]. FTIR spectra of fucoidan showed an absorbance peak at 1000 – 1270 cm^{-1}, corresponding to the stretching vibration of the sulfur–oxygen double bond (S=O) of sulfate group. The spectra also showed signals in the range of 1315–1220 cm^{-1} and 1140–1020 cm^{-1}, assigned to the symmetric and asymmetric stretching of ether sulfate groups ($RO–SO_3^-$) [19,41]. A broad band around 3200–3500 cm^{-1} also appears, which is due to the stretching of –OH groups, a characteristic of carbohydrate monomers [19,58,61]. The characteristic peak of C-O-S stretching at 845 cm^{-1} was also attributed to the presence of sulfate groups from fucoidan[62]. For the further chemical characterization of AgaFu hydrogels it was used composition b (AgaFu3b and AgaFu5b) with intermediate (wt) ratio of Agarose (Aga): Fucoidan (Fu).

Moreover, all spectra of AgaFu hydrogels presented in **Figure VI- 3 A2** showed an absorbance band at 1220 cm^{-1}, corresponding to the sulfate groups characteristic of Fu [19,61]. This indicates that the intrinsic sulfate group of Fu is also present in the AgaFu 3 and AgaFu 5 formulations after the blending with Aga, confirming the presence of fucoidan on the final hydrogels, which is in accordance with the already suggested by their brownish color. In FTIR spectra of both AgaFu 3 and AgaFu 5, we observed bands characteristic of Aga and Fu, confirming the presence of the respective component on the hydrogel, but also suggesting that interactions between the polymers could occur, as discussed in the rheological characterization.

Furthermore, proton nuclear magnetic resonance (^{1}H NMR) spectroscopy of Aga shown two groups of peaks, one at δ= 5.15 - 5.25 ppm corresponding to protons C1 and C1´ from Aga skeleton and the other at δ= 3.45 - 4.61 ppm, attributed to protons C2 - 6 and C2´-6´in Aga

skeleton **(Figure VI- 3 B1).** Fu ^{1}H NMR spectra shown different peaks at δ= 1.20 - 1.30 and 1.95 - 2.26 ppm corresponding to methyl groups of fucose and L-fucopyranose; at δ= 3.35 - 4.55 ppm confirming the presence of different types of fucose groups with changes in glycosidic linkage positions and monosaccharides patterns; at δ= 5.29 - 5.40 ppm corresponding to anomeric protons of L-fucopyranosyl unit **(Figure VI - 3 B2)** [41,63]. The spectra corresponding to AgaFu 3 and AgaFu 5 solutions **(Figure VI - 3 B3)** shown peaks characteristic of Aga and Fu suggesting the existence of interactions between the polysaccharides. Additionally, the results obtained were compared in the literature with other systems that use these polymers, such as fucoidan, and it is verified that peaks appear in the same chemical shift (δ) values [62,64].

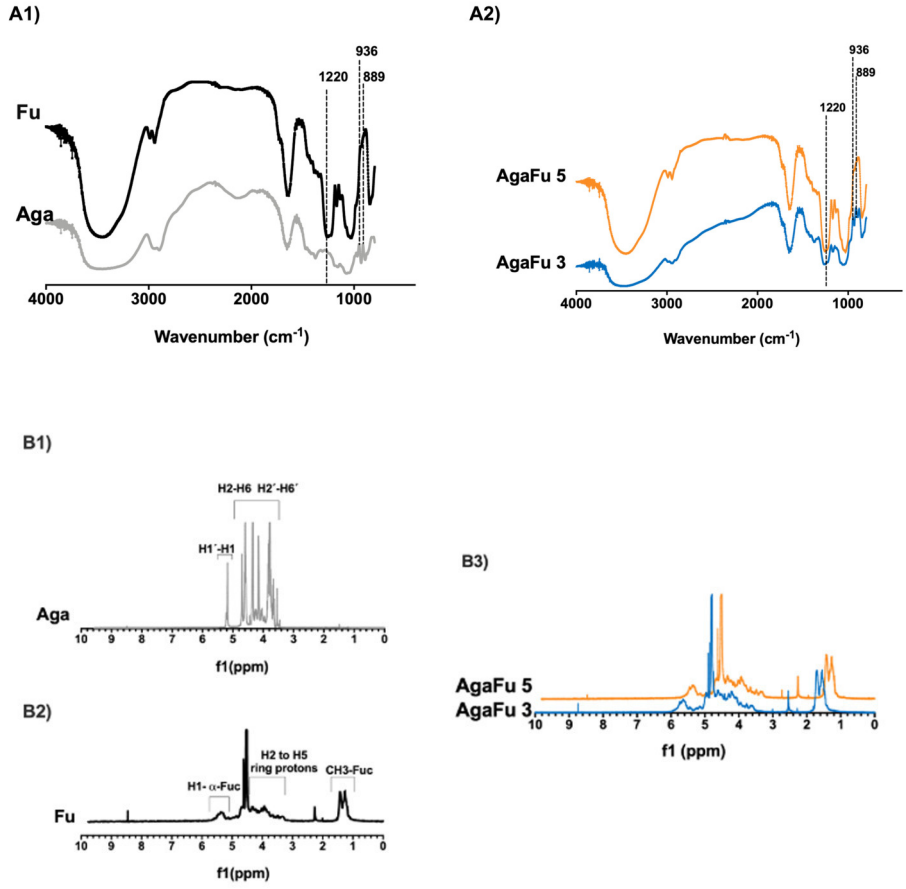


Figure VI-3.Chemical characterization of Aga, Fu and AgaFu hydrogels A1) Agarose and fucoidan A2) AgaFu 3 and AgaFu 5 hydrogels. B) ^{1}HNMR spectra of B1) Agarose (Aga), B2) Fucoidan (Fu) and B3) AgaFu 3/AgaFu 5 hydrogels.

- **X-ray photoelectron spectroscopy (XPS)**

The superficial chemical composition of the AgaFu hydrogels was also examined by XPS surface measurements **(Figure VI - 4 A, B)**. The XPS data are in accordance with the data obtained by ^{1}H NMR and FTIR. The XPS wide spectra of Fu, Aga, and the different proportions AgaFu 3 and AgaFu 5 prepared hydrogels displayed the presence of the expected peaks of carbon (C), oxygen (O), calcium (Ca), sodium (Na) and sulfur (S) **(Figure VI - 4 A, B)**. Besides, the surface atomic ratios of the main components (S2p, O1s, and C1s) and the respective ratio of O/C and S/C of all samples analyzed is represented in **Table VI - 2**. As expected, the amount of sulfur is higher in the samples with Fu, because fucoidan contains it in its atomic composition, namely in sulfate groups. No obvious differences were noted in the C1s and O1s region spectra of the AgaFu hydrogels **(Figure VI - 4 B2, B3)** when compared with the same regions for the isolated Aga and Fu separately. The increase of Aga concentration into hydrogel formulation led to a decrease in the presence of sulfur (S) in the sample, as the ratio of fucoidan decreased. Similar behavior was observed when Fu concentration increases on the blended hydrogel, when is evident an increase of the S/C ratio.

Table VI-2. Relative atomic composition (O, C and S) of the samples obtained by XPS data quantification and their ratio as a function of Carbon.

Composition %	O	C	S	O/C	S/C
Fu	35.29 ± 0.20	61.52 ± 0.21	3.19 ± 0.05	0.57	0.052
Aga 3	42.95 ± 0.57	56.88 ± 0.06	0.16 ± 0.05	0.75	0.002
Aga 5	47.14 ± 1.04	52.49 ± 1.05	0.38 ± 0.09	0.90	0.007
AgaFu 3a	40.66 ± 0.49	55.06 ± 0.54	4.28 ± 0.12	0.74	0.081
AgaFu 3b	42.77 ± 0.49	53.43 ± 0.52	3.79 ± 0.08	0.80	0.070
AgaFu 3c	45.70 ± 0.59	51.39 ± 0.62	2.91 ± 0.09	0.89	0.057
AgaFu 5a	46.06 ± 0.84	52.26 ± 0.86	1.68 ± 0.13	0.88	0.032
AgaFu 5b	31.93 ± 0.65	66.96 ± 0.67	1.09 ± 0.08	0.48	0.016
AgaFu 5c	54.22 ± 0.84	45.13 ± 0.85	0.65 ± 0.10	1.20	0.014

Symbols: O- Oxygen, C- Carbon and S-Sulfur

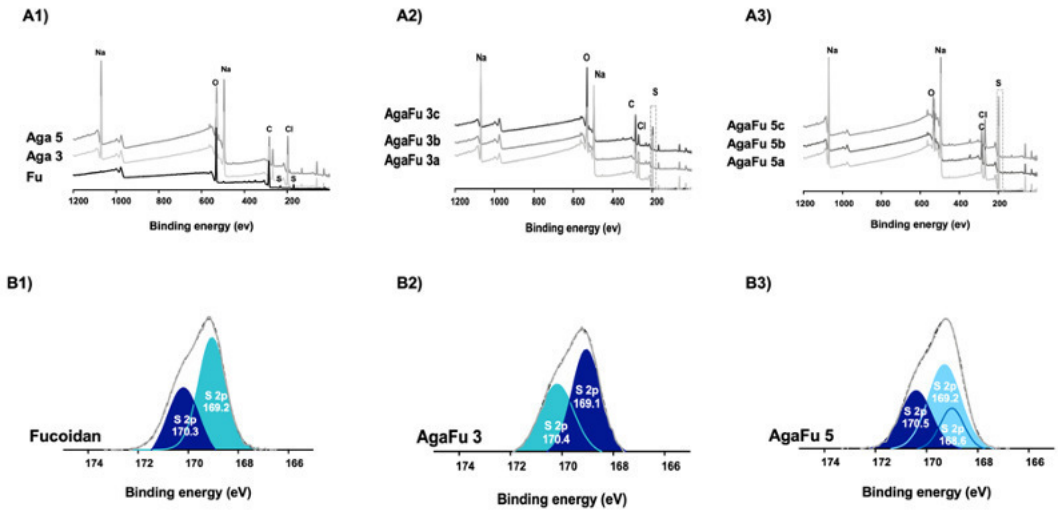


Figure VI-4.Characterization of fucoidan powder, Aga and AgaFu hydrogels by XPS analysis . XPS wide scan of A1) Fu (powder) and Aga 3 and Aga 5 hydrogels, A2) AgaFu 3a, AgaFu 3b and AgaFu 3c and A3) AgaFu 5a, AgaFu 5b and AgaFu 5c. B) XPS images of elements distribution, particularly sulfur region, of B1) Fu (powder), B2) AgaFu 3 hydrogels and B3) AgaFu 5 hydrogels.

- **Mechanical properties and hydrogel mesh size**

The mesh size of the hydrogel was calculated based on the equivalent network model **Equation1**. The **Figure VI - 5B** shows that when Aga concentration increased, there was a decrease in the mesh size, attributed to a tightly packed Aga polymeric chains [32,65] **(Figure VI - 5A).** The agarose is soluble in water at temperatures 85°C to 100°C [35]. So, in this work Aga solution was heated up to 85-95°C, which provided sufficient energy to break the hydrogen bonds, and the Aga chains are oriented with no long-range order, thus enabling the solubilization of this polysaccharide [32,42,66]. However, as the temperature decreases and hydrogen bonds started to be formed, Aga molecules pair up into double helices. The double helices themselves aggregate with other double helices to form thicker fibers. The gel is formed due to this network of Aga super-helices linked at their ends [32,42,66]. The results have also shown that the mesh size of hydrogel blends decreases with the increase of concentration of Aga in the solution from 3 to 5%. This may be related to an increase of the density of the initial solution and consequently of the produced

hydrogel. Moreover, independently of the polymeric proportion studied is possible to note that the combination of Aga with Fu promoted a reduction of mesh size of the produced hydrogel. This fact should be related to the intermolecular interactions stablished between Aga and Fu polymeric chains (e.g., electrostatic bonds, hydrogen bonds, ion-dipole and London forces), that allow the formation and maintenance of the blended network overcoming the natural non-gelling ability of Fu. Considering the blended hydrogels prepared using lower initial concentration of Aga (3a, 3b and 3c) it is observed a decrease of the mesh size with the reduction of the Fu proportion into the blended mixture or increase of Aga proportion. Besides the existent intermolecular interactions, the increasing number of Aga molecules to pair promote an increase in the hydrogel density, which leads to more tightly packed helices, promoting consequently a decrease on the mesh size [32,42]. Furthermore, when comparing the hydrogels prepared using the same polymeric ratio and different concentrations of Fu solution, is noted a decrease of mesh size for the hydrogels prepared with the highest concentration of Fu, however without significant differences.

Young's modulus of AgaFu hydrogels seemed to increase by increasing Aga and Fu concentration, although statistically significant differences between formulations have been identified only for samples AgaFu 3a, AgaFu 3c, AgaFu 5a and AgaFu 5c (***$p<0.001$) **(Figure VI - 5C)**. This result correlates well with the mesh size results, with the decreasing of the mesh size being associated with an increase of the stiffness of the hydrogels as represented schematically in **Figure VI - 5A** [46].

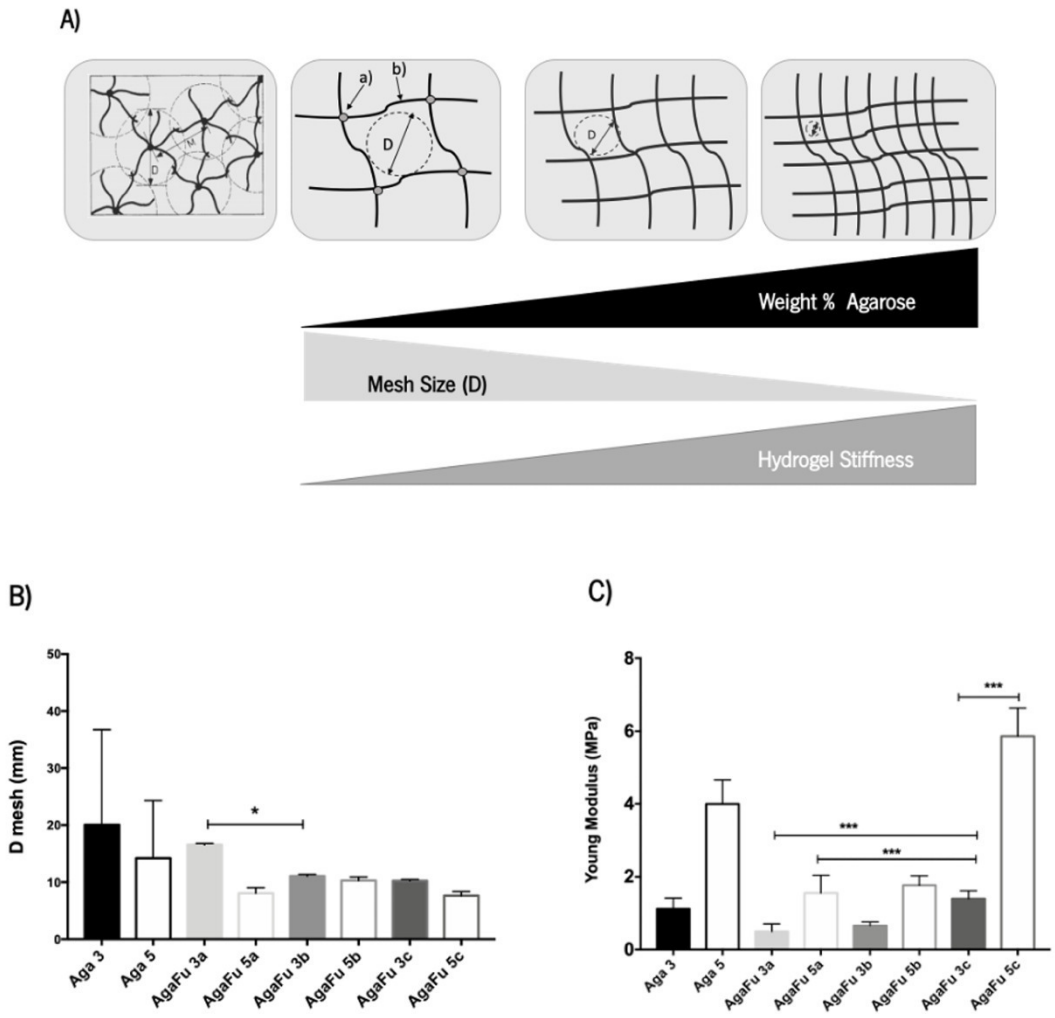


Figure VI-5. Schematic representation of a hydrogel network consist of a) cross-links connecting and b) polymer chains with molecule junction diameter (D) and average mesh width (M), as adapted from Schurz et al. [43] B) Mesh size of Aga and AgaFu hydrogels. C) Young Modulus of Aga and AgaFu hydrogels (Data represent means ± standard deviation *** $p<0.001$, one-way ANOVA).

- Diffusion tests and Permeability to glucose

Methylene blue assay was carried out to assess the diffusion of compounds within the developed hydrogels [67]. The diffusion of methylene blue through the Aga and AgaFu hydrogels, as illustrated by images available as supporting information **(Figure VI - S1 and S2)**, showed that samples with a higher concentration of agarose have a slower diffusion of methylene blue, caused

by a denser matrix as suggested by the reduced mesh size**.** However, the diffusion of methylene blue on the hydrogel blends, AgaFu, seems to be hampered when compared with pure Aga hydrogels, which may suggest a stronger interaction between the polymers and consequently a more cohesive and compact systems, particularly the samples AgaFu3/5c where methylene blue seemed to exhibit the slowest diffusion **(Figure VI - S2 B1 - B2)** [67].

To complement the information obtained from the evaluation of the diffusion of methylene blue, the permeability of AgaFu hydrogels to nutrients was also assessed using glucose as a model molecule for permeation. Diffusion profiles showed an initial lag phase in the receptor cell due to the time required for solute to traverse the membranes [52,68] **(Figure VI - 6)**. After this phase, the bulk liquid reached equilibrium after approximately 1 h. The higher water content of native membranes facilitates the permeation of water-soluble molecules such as glucose, which is related to the mesh size of hydrogel [52,69]. The permeability coefficient (P) was determined with Equation 3 and the obtained values increased when the fucoidan ratio increased **Table VI - 3.** These results could be related with charge of the compounds, its hydrophobicity and mesh size of hydrogel. The permeability tends to increase with anionic compounds and the ones that have higher affinity with water [70]. The hydrogels that have less mesh size and are more cohesive and compact systems tend to have reduced permeability, as just discussed and demonstrated with methylene blue. The diffusion coefficients (D) were deduced from Equation 4 and the partition coefficients from Equation 5. The diffusion coefficient is a crucial parameter to estimate the mass of a solute diffusing in time through the gel [52]. The obtained data showed that the increase in the Aga concentration resulted in lower diffusion coefficients, in accordance with the permeability observations and the more cohesive and compact systems obtained in these conditions. These observations are in accordance with the results reported by Marchioli *et al.* [37], when seeing an impact of scaffold porosity on performance, with porous alginate scaffolds showing a better permeability to nutrients than bulk hydrogels due to a higher surface to volume ratio. Moreover, Farina *et al*also highlighted the impact of the thickness of capsules on the transport of oxygen, and consequently on cell viability, in cell encapsulating devices [38]. Furthermore, it is known that permeability is also directly related with immune protection, associated to the interaction and diffusion of antibodies, besides the need to avoid contact between graft and host cells [40]. The partition coefficients (K_d) are a measure of solubility in the hydrogels [68] and increased with increasing fucoidan concentration, which is

attributed to a higher water uptake capacity, and, consequently, the solutes have higher ability to remain trapped within the hydrogel [52].

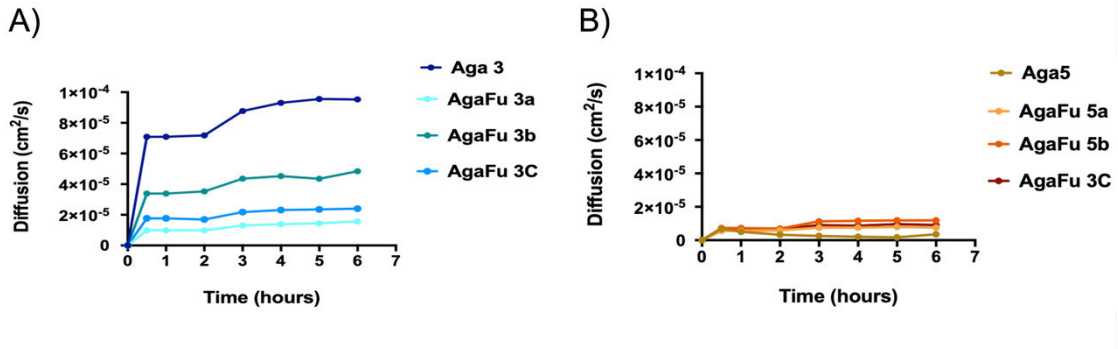


Figure VI-6. Diffusion of glucose across A) AgaFu 3 and B) AgaFu 5 hydrogels.

Table VI-3. Permeability (P), Partition (Kd) and diffusion (D) Coefficients of glucose on AgaFu hydrogels.

Samples	P (10^{-6} cm/s)	D (10^{-5} cm^2/s)	K_d
AgaFu 3a	24.36	1.24	0.45
AgaFu 3b	9.91	4.05	0.05
AgaFu 3c	9.94	2.07	0.11
AgaFu 5a	9.90	0.68	0.32
AgaFu 5b	3.99	1.14	0.10
AgaFu 5c	10.61	0.82	0.28

VI-4.2. Biological characterization

The biological performance of the Aga and AgaFu hydrogels was tested using human pancreatic beta cells-line 1.1B4HP. The 1.1B4HP cells have been used in several studies focusing pancreatic beta-cell biology, representing a source of cellular therapy for type 1 diabetes [71]. To evaluate the effect of using fucoidan, we have compared the performance of AgaFu hydrogels with

Aga hydrogels rather than Fu alone, as Fu does not form 3D-based structures alone due to its high water solubility [19,72]. To assess if 1.1B4HP encapsulated cells were able to proliferate maintaining viability in Aga and AgaFu hydrogels, cell-laden samples were analyzed after 1, 3, and 7 days of culture by MTS assay, DNA quantification, live/dead assay and evaluation of cell morphology by CLSM. The MTS results showed, in general, an increase in 1.1B4HP cells metabolic activity during the culture time in both Aga and AgaFu hydrogels **(Figure VI - 7A)**. Moreover, comparing the results obtained for hydrogels prepared with different polymeric concentrations (3 and 5%), we observed that in the samples with higher Aga concentration 1.1B4HP cells had lower metabolic activity. However, results obtained from dsDNA quantification did not show relevant differences on the proliferation of 1.1B4HP cells encapsulated into Aga and AgaFu hydrogels **(Figure VI - 7 B).** These results are correlated with the mesh size of the hydrogel, as the increase of Aga and Fu concentrations would reduce the mesh size of the hydrogel and the cells would be much more space constrained and potentially facing a lower nutrients diffusion causing slower metabolic activity. In fact, Strand *et al* have pointed to the variation in oxygen concentration through the encapsulation devices, depending on the shape and surface to volume ratio, and its impact in cell viability [40]. Moreover, the ability of hydrogels to support cell viability was evaluated by a live/dead assay. Confocal images obtained after 1, 3 and 7 days of culture **(Figure VI - 8)** allowed to conclude that all the formulations (Aga 3, Aga 5 and AgaFu 3 a, b, c, AgaFu 5 a, b, c) shown viable cells, demonstrating that the biomaterials proposed in this work are generally not cytotoxic **(Figure VI - 8 A, B).** Results obtained with hydrogels produced with lower polymer concentrations (3% of agarose or 3% of fucoidan and different ratios of agarose) showed higher rates of cell viability, while hydrogels produced with the highest polymeric content presented the lowest number and ratio of live cells (~ 45%), potentially translating the effect of more cohesive and compact hydrogels and consequently on the space confinement of the cells, with a negative impact on cell viability. These results are in agreement with diffusion coefficient values, where increase in the Aga concentration resulted in lower diffusion coefficients, which can lead to increase of dead cells and decreased metabolic activity. The effect of hydrogel formulation is more evident than the one observed by Marchioli *et al* with alginate-based materials [37], as they detected impact of the components of the hydrogel but, surprisingly, not on the shape as this would affect the surface to volume ratio and consequently the transport of oxygen and nutrients. Indeed, those authors

attribute the observed limitations on cell viability to hampered nutrients transport, given the viscous and highly concentrated gel used in their work, thus suggesting the relevance of hydrogel mesh size on cell fate. Furthermore, the cell morphology was evaluated by CLSM after staining of actin and nuclei with phalloidin and DAPI, respectively, and images show that cells had a round like shape and tend to self-organize, forming pseudo-islets after 3 days of culture **(Figure VI - 9 A, B).** This pseudo-islet morphology was maintained up to 7 days of culture, which is characteristic of human pancreatic cells **(Figure VI - 9)** [73]. The noted behavior suggested that the formulated hydrogels with 3% fucoidan supported the encapsulation of 1.1B4HP cells that remained viable for at least 7 days **(Figure VI - 7, 8).** Moreover, the presence of fucoidan seemed to allow higher number of cells encapsulated in the hydrogels, also enabling the self-organization of larger pseudo-islets.

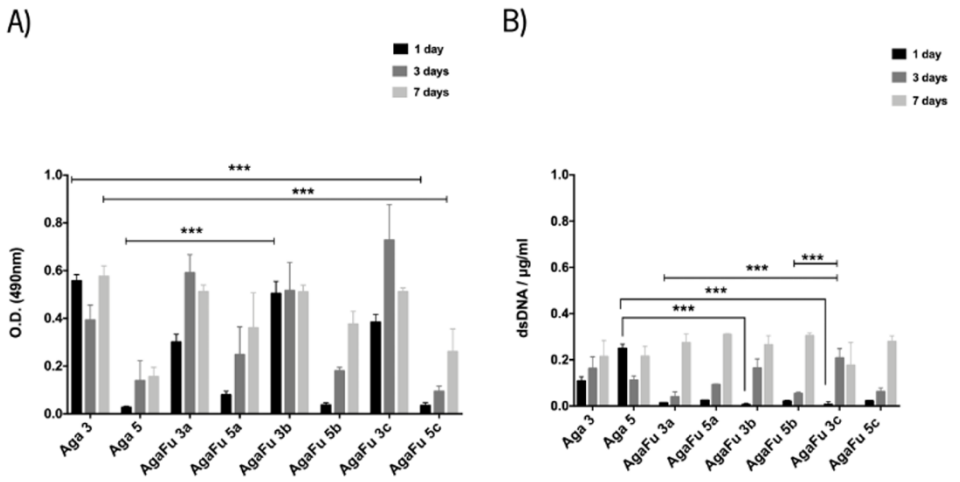
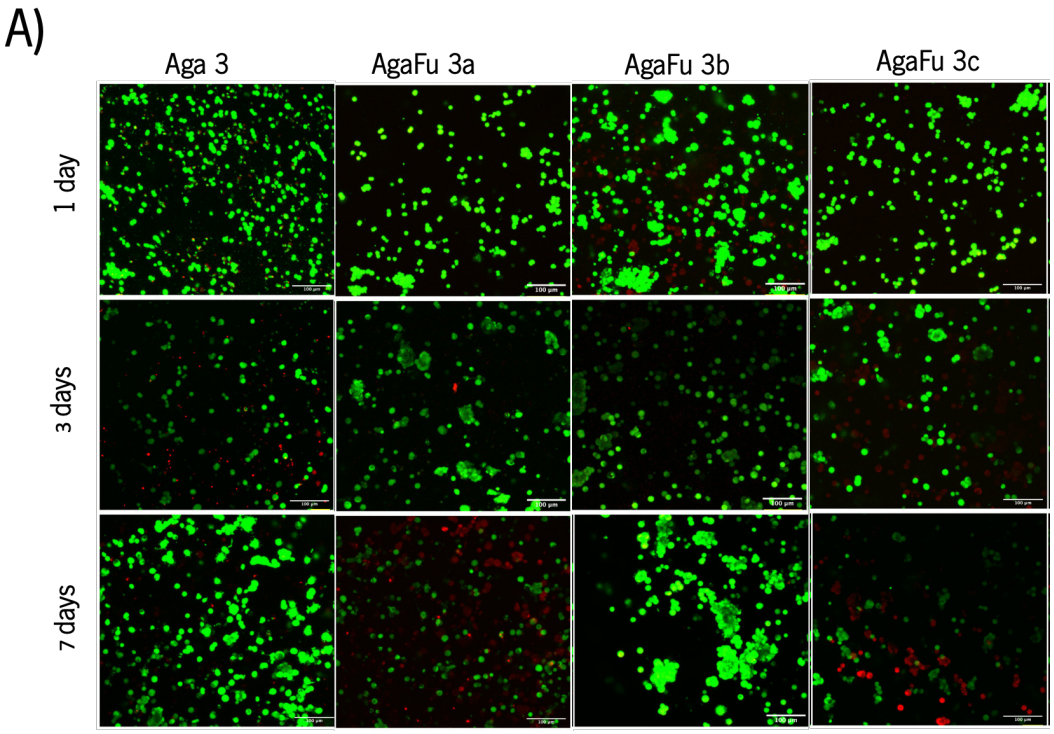


Figure VI-7. A) MTS results, B) dsDNA content of 1.1B4 human pancreatic cells encapsulated in Aga 3, 5 and AgaFu 3 and AgaFu 5 at different proportions (a (4/10), b (5/10) and c (7/10)) hydrogels (Data represent means ± standard deviation; *** $p<0.001$, Kruskal-wallis test, other data are in supplementary information).



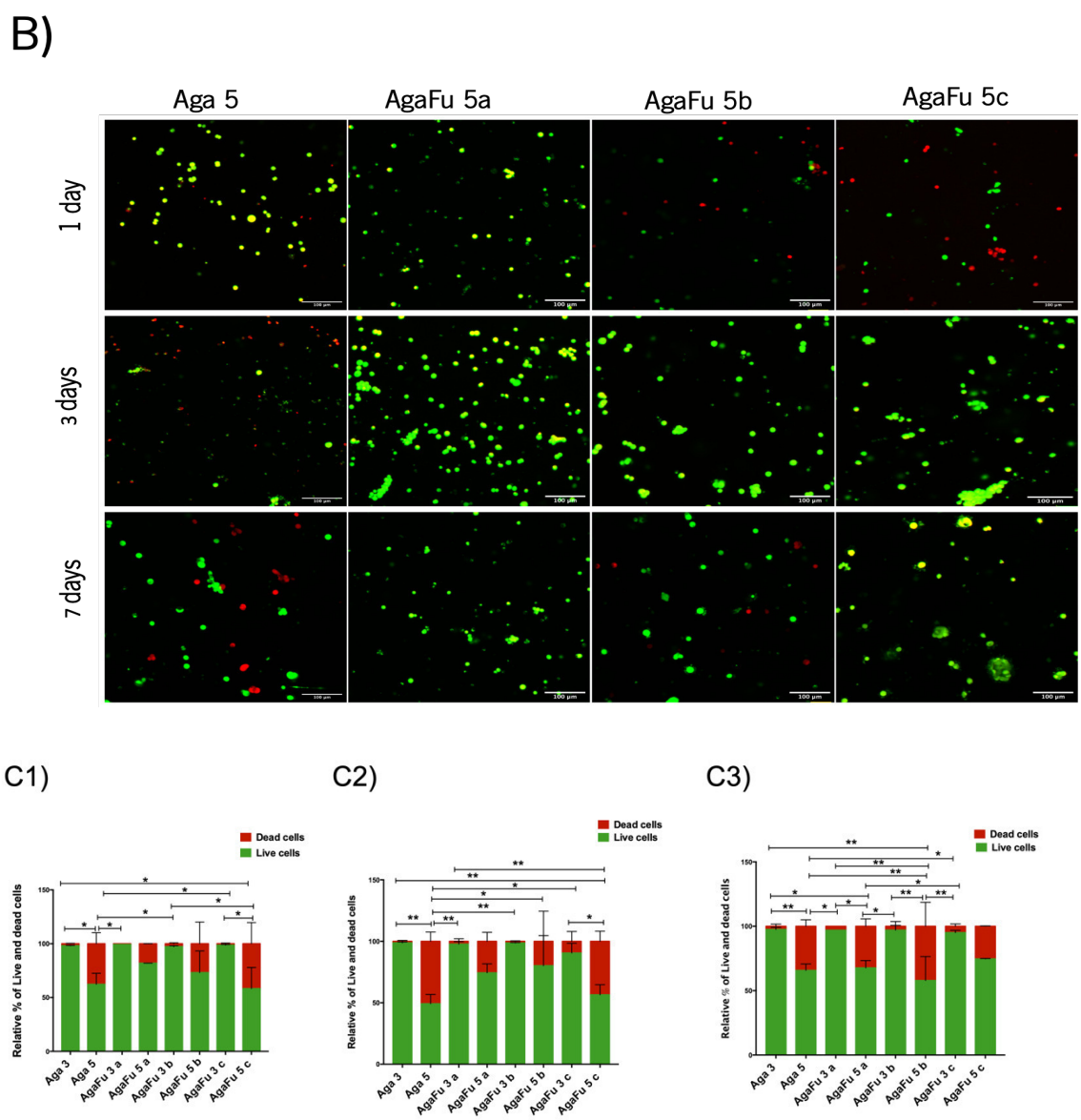


Figure VI-8. Live/dead microscopy images of 1.1B4 HP cells encapsulated into A) Aga and AgaFu 3 and B) Aga and AgaFu 5 hydrogels after 1, 3 and 7 days in culture. The cells were stained with calcein/ethidium solutions, being live cells (green) calcein positive and dead cells (red) ethidium-homodimer positive, scale bar: 100µm.

C) Quantification of cell viability in Aga 3,5, AgaFu 3 and AgaFu 5 at different proportions (a (4/10), b (5/10) and c (7/10)) hydrogels for different time points (C1) 1 day, C2) 3 days and C3) 7 days).

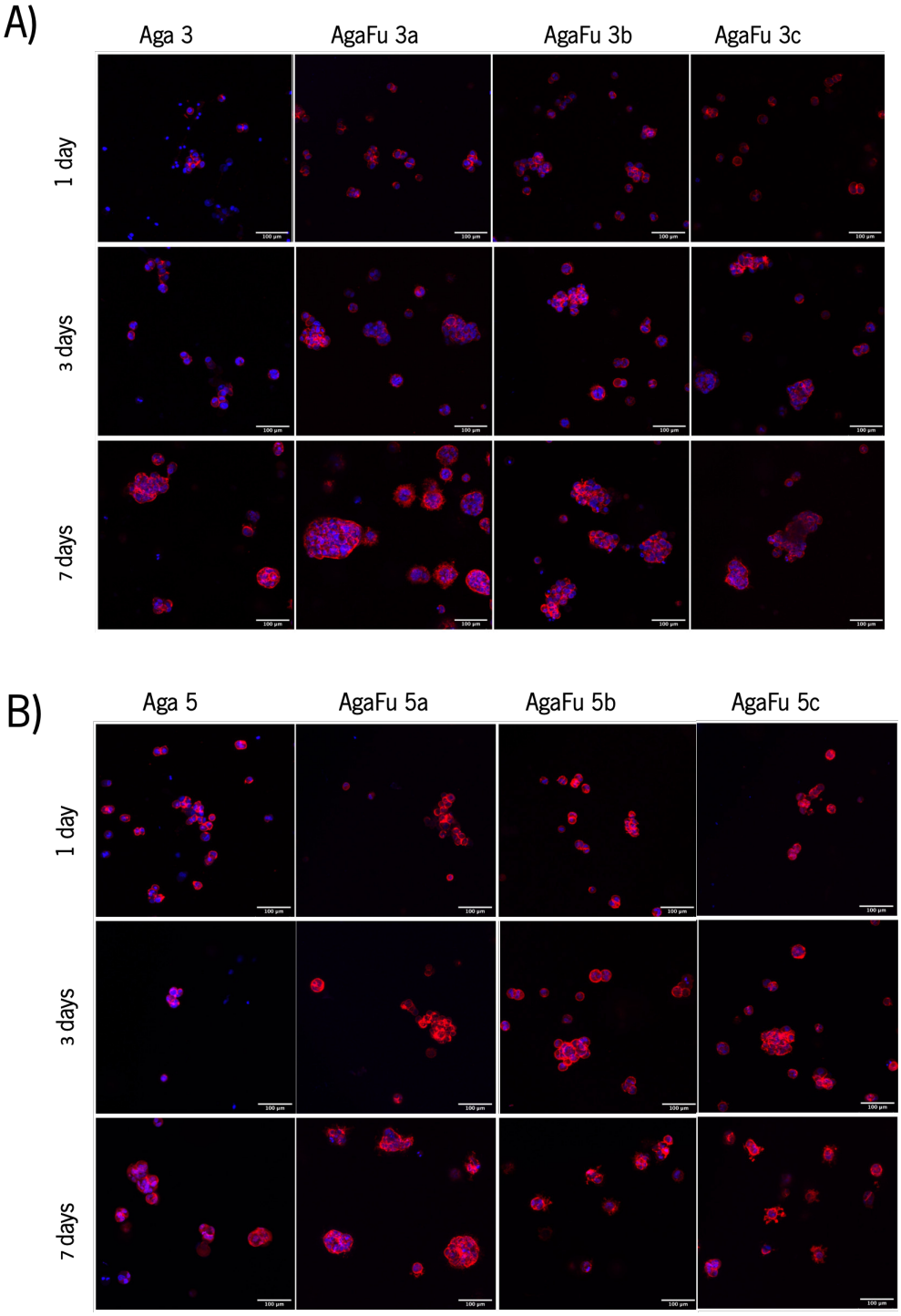


Figure VI-9. Confocal images of 1.1B4HP cells encapsulated in A1) Aga3 and AgaFu 3 and A2) Aga5, AgaFu 5 hydrogels for 1, 3 and 7 days in culture. Staining of actin (red) and nuclei (blue), scale bar: 100 µm.

VI-5. CONCLUSIONS

In this work, AgaFu hydrogels were successfully obtained through the combination of agarose and fucoidan, two well-known natural origin polymers, using the thermo-gelation technique at 37° C. Combining agarose and fucoidan at different concentrations using temperature variations, we have obtained hydrogels with tunable mechanical properties, stability, and diffusion coefficients. Moreover, we were also able to modulate cell viability and to promote the organization of HP cells into pseudo-islets. Comparing all the conditions, we concluded that AgaFu 3b hydrogel formulation presented a suitable mesh size of the gel that contributed to a good diffusion of molecules, suggesting higher nutrients permeability. These AgaFu3 hydrogels revealed as well sustained viability of encapsulated 1.1B4 HP pancreatic cells during the studied culture time (up to 7 days), which seemed to self-organize towards the formation of pseudo-islets.

Overall, we have provided a simple methodology to foster the development of new fucoidan-based structures envisaging its biomedical application as cell culture matrices in diabetes treatment strategies.

VI-6. ACKNOWLEDGMENTS

This work has received financial support from Portuguese Foundation for Science and Technology (FCT) (SFRH/BD/112139/2015, SFRH/BPD/93697/2013, PTDC/CTM-CTM//29813/2017 and PTDC/BII-BIO/31570/2017), from Northern Portugal Regional Operational Programme (NORTE 2020), under the Portugal 2020 Partnership Agreement, through Structured projects NORTE-01-0145-FEDER-000021 and NORTE-01-0145-FEDER-000023 and from European Union Transborder Cooperation Program Interreg España-Portugal 2014-2020 (POCTEP) under project 0302_CVMAR_I_1_P.

VI-7. REFERENCES

[1] Hoffman AS. *Hydrogels for biomedical applications*.Vol. 64, Advanced Drug Delivery Reviews. 2012. p. 18–23.

[2] Fan C, Wang D-A. *Macroporous Hydrogel Scaffolds for Three-Dimensional Cell Culture and Tissue Engineering*.Tissue Eng Part B Rev 2017. 23(5):451–61.

[3] Jabbari E. *Bioconjugation of hydrogels for tissue engineering*.Vol. 22, Current Opinion in Biotechnology. 2011. p. 655–60.

[4] Mantha S, Pillai S, Khayambashi P, Upadhyay A, Zhang Y, Tao O, et al. *Smart Hydrogels in Tissue Engineering and Regenerative Medicine*.Mater (Basel, Switzerland) 2019. 12(20):3323.

[5] Wilson AN, Guiseppi-Elie A. *Bioresponsive hydrogels*.Adv Healthc Mater 2013. 2:520–32.

[6] Reyes Martínez JE, Ruiz-Pacheco J, Flores-Valdéz M, Elsawy M, Vallejo AA, Castillo Díaz L. *Advanced hydrogels for treatment of diabetes*.J Tissue Eng Regen Med 2019. 13:1375–93.

[7] Bahram M, Mohseni N, Moghtader M. *An Introduction to Hydrogels and Some Recent Applications*.In: 2016. 2016.

[8] Roach BL, Nover AB, Ateshian GA, Hung CT. *Agarose Hydrogel Characterization for Regenerative Medicine Applications: Focus on Engineering Cartilage*.In: 2016. John Wiley & Sons, Ltd; 2016. p. 258–73.

[9] Choi J, Park H, Kim T, Jeong Y, Oh MH, Hyeon T, et al. *Engineered collagen hydrogels for the sustained release of biomolecules and imaging agents: promoting the growth of human gingival cells*.Int J Nanomedicine 2014. 9:5189–201.

[10] Nichol JW, Koshy ST, Bae H, Hwang CM, Yamanlar S, Khademhosseini A. *Cell-laden microengineered gelatin methacrylate hydrogels*.Biomaterials 2010. 31:5536–44.

[11] Ahmadi F, Oveisi Z, Samani SM, Amoozgar Z. *Chitosan based hydrogels: characteristics and pharmaceutical applications*.Res Pharm Sci 2015. 10(1):1–16.

[12] Lensen M, Schulte V, Diez M. *Cell Adhesion and Spreading on an Intrinsically Anti-Adhesive PEG Biomaterial*.In: Rosario Pignatello I, editor. 2011. 2011. p. 397–414.

[13] Gibas I, Janik H. *Review: Synthetic polymer hydrogels for biomedical applications*.Chem Chem Technol 2010. 4:297–304.

[14] Nam S, Hu KH, Butte MJ, Chaudhuri O. *Strain-enhanced stress relaxation impacts nonlinear elasticity in collagen gels*.Proc Natl Acad Sci U S A 2016. 113(20):5492–7.

[15] Chaudhuri O, Gu L, Klumpers D, Darnell M, Bencherif SA, Weaver JC, et al. *Hydrogels with tunable stress relaxation regulate stem cell fate and activity*.Nat Mater 2016. 15(3):326–34.

[16] Chaudhuri O, Gu L, Darnell M, Klumpers D, Bencherif SA, Weaver JC, et al. *Substrate stress relaxation regulates cell spreading*.Nat Commun 2015. 6:6364.

[17] Guvendiren M, Lu HD, Burdick JA. *Shear-thinning hydrogels for biomedical applications*.Vol. 8, Soft Matter. 2012. p. 260.

[18] Trappmann B, Baker BM, Polacheck WJ, Choi CK, Burdick JA, Chen CS. *Matrix degradability controls multicellularity of 3D cell migration*.Nat Commun 2017. 8(1):371.

[19] Reys LL, Silva SS, Soares da Costa D, Oliveira NM, Mano JF, Reis RL, et al. *Fucoidan Hydrogels Photo-Cross-Linked with Visible Radiation As Matrices for Cell Culture*.ACS Biomater Sci Eng 2016. 2(7):1151–61.

[20] Oliveira C, Ferreira AS, Novoa-Carballal R, Nunes C, Pashkuleva I, Neves NM, et al. *The Key Role of Sulfation and Branching on Fucoidan Antitumor Activity*.Macromol Biosci 2017. 17(5):1600340-n/a.

[21] Isnansetyo A, Lutfia F, Nursid M, Trijoko T. *Cytotoxicity of Fucoidan from three tropical brown algae Sargassum cristaefolium, Turbinaria conoides and Padina fraseri against breast and colon cell lines*.Pharmacogn J 2017. 9(1):14–20.

[22] Ale MT, Mikkelsen JD, Meyer AS. *Important determinants for fucoidan bioactivity: A critical review of structure-function relations and extraction methods for fucose-containing sulfated polysaccharides from brown seaweeds*.Mar Drugs 2011. 9(10):2106–30.

[23] Cumashi Ushakova, N. A.; Preobrazhenskaya, M. E.; D'Incecco, A.; Piccoli, A.; Totani, L.; Tinari, N.; Morozevich, G. E.; Berman, A. E.; Bilan, M. I.; Usov, A. I.; Ustyuzhanina, N. E.; Grachev, A. A.; Sanderson, C. J.; Kelly, M.; Rabinovich, G. A.; Iacobe A, Cumashi A, Ushakova NA, Preobrazhenskaya ME, D'Incecco A, Piccoli A, et al. *A comparative study of the anti-inflammatory, anticoagulant, antiangiogenic, and antiadhesive activities of nine different fucoidans from brown seaweeds*.Glycobiology 2007. 17(5):541–52.

[24] El-Boshy M, Abdelhamidb F, Richab E, Ashshia A, Ghaith M, Qustya N. *Attenuation of CCl4 Induced Oxidative Stress, Immunosuppressive, Hepatorenal Damage by Fucoidan in Rats*.Ferment Technol 2017. 07.

[25] Gauldie J, Sime PJ, Xing Z, Marr B, Tremblay GM. *Transforming Growth Factor-$β$ Gene Transfer to the Lung Induces Myofibroblast Presence and Pulmonary Fibrosis*.In: Desmoulière A, Tuchweber B, editors. 1999. Berlin, Heidelberg: Springer Berlin Heidelberg; 1999. p. 35–45.

[26] Kim EJ, Park SY, Lee J-Y, Park JHY. *Fucoidan present in brown algae induces apoptosis of human colon cancer cells.*BMC Gastroenterol 2010. 10:96.

[27] Kawamoto H, Miki Y, Kimura T, Tanaka K, Nakagawa T, Kawamukai M, et al. *Effects of Fucoidan from Mozuku on Human Stomach Cell Lines*.Vol. 12, Food Science and Technology Research. 2006. p. 218–22.

[28] Synytsya AA, Kim WJ, Kim SM, Pohl R, Synytsya AA, Kvasnička F, et al. *Structure and antitumour activity of fucoidan isolated from sporophyll of Korean brown seaweed Undaria pinnatifida*.Carbohydr Polym 2010. 81:41–8.

[29] Wang J, Jin W, Zhang W, Hou Y, Zhang H, Zhang Q. *Hypoglycemic property of acidic polysaccharide extracted from Saccharina japonica and its potential mechanism*.Carbohydr Polym 2013. 95(1):143–7.

[30] Fitton HJ, Stringer DS, Park AY, Karpiniec SN. *Therapies from Fucoidan: New Developments*.Mar Drugs 2019. 17(10):571.

[31] Fu XT, Kim SM. *Agarase: review of major sources, categories, purification method, enzyme characteristics and applications*.Mar Drugs 2010. 8(1):200–18.

[32] Gasperini L, Mano JF, Reis RL. *Natural polymers for the microencapsulation of cells*.J R Soc Interface 2014. 11(100):20140817.

[33] Roberts JJ, Martens PJ. *Engineering biosynthetic cell encapsulation systems*.In: Poole-Warren L, Martens P, Green RBT-BP for MA, editors. 2016. Woodhead Publishing; 2016. p. 205–39.

[34] Normand V, Lootens DL, Amici E, Plucknett KP, Aymard P. *New Insight into Agarose Gel Mechanical Properties*.Biomacromolecules 2000. 1(4):730–8.

[35] Zarrintaj P, Manouchehri S, Ahmadi Z, Saeb MR, Urbanska AM, Kaplan DL, et al. *Agarose-based biomaterials for tissue engineering*.Carbohydr Polym 2018. 187:66–84.

[36] Garcia F, Solis J, Luque E, Neyra L, Manrique H, Cancino R, et al. *Prevalencia de diabetes mellitus y factores de riesgo relacionados en una población urbana*.Rev Soc Peru Med Interna 2007. 20:90–4.

[37] Marchioli G, van Gurp L, van Krieken PP, Stamatialis D, Engelse M, van Blitterswijk CA, et al. *Fabrication of three-dimensional bioplotted hydrogel scaffolds for islets of Langerhans transplantation*.Biofabrication 2015. 7(2):25009.

[38] Farina M, Alexander JF, Thekkedath U, Ferrari M, Grattoni A. *Cell encapsulation: Overcoming barriers in cell transplantation in diabetes and beyond*.Adv Drug Deliv Rev 2019. 139:92–115.

[39] Paez-Mayorga J, Capuani S, Hernandez N, Farina M, Chua CYX, Blanchard R, et al. *Neovascularized implantable cell homing encapsulation platform with tunable local immunosuppressant delivery for allogeneic cell transplantation*.Biomaterials 2020. 257:120232.

[40] Strand BL, Coron AE, Skjak-Braek G. *Current and Future Perspectives on Alginate Encapsulated Pancreatic Islet*.Stem Cells Transl Med 2017. 6(4):1053–8.

[41] Saboural P, Chaubet F, Rouzet F, Al-Shoukr F, Azzouna R Ben, Bouchemal N, et al. *Purification of a low molecular weight fucoidan for SPECT molecular imaging of myocardial infarction*.Mar Drugs 2014. 12(9):4851–67.

[42] Indovina PL, Tettamanti E, Micciancio-Giammarinaro MS, Palma MU. *Thermal hysteresis and reversibility of gel–sol transition in agarose–water systemsa)*.J Chem Phys 1979. 70(6):2841–7.

[43] Ji Seok Lee Myung Gu Yeo, Chul Ho Jang, Haeongnam Lee, Geun Hyung Kim GHJ, Lee JSS, Jin GHH, Yeo MGGG, Jang CHHH, Lee H, et al. *Fabrication of electrospun biocomposites comprising polycaprolactone/fucoidan for tissue regeneration*.Carbohydr Polym 2012. 90:181–8.

[44] Rodrigues LC, Silva SS, Reis RL. *Acemannan-based films: an improved approach envisioning biomedical applications*.Mater Res Express 2019. 6(9):95406.

[45] Radhouani H, Bicho D, Gonçalves C, Maia FR, Reis RL, Oliveira JM. *Kefiran cryogels as potential scaffolds for drug delivery and tissue engineering applications*.Mater Today Commun 2019. 20:100554.

[46] Agnello S, Gasperini L, Mano JF, Pitarresi G, Palumbo FS, Reis RL, et al. *Synthesis, mechanical and thermal rheological properties of new gellan gum derivatives*.Int J Biol Macromol 2017. 98:646–53.

[47] Kuijpers AJ, Engbers GHM, Feijen J, De Smedt SC, Meyvis TKL, Demeester J, et al. *Characterization of the Network Structure of Carbodiimide Cross-Linked Gelatin Gels*.Macromolecules 1999. 32(10):3325–33.

[48] Li J, Mooney DJ. *Designing hydrogels for controlled drug delivery*.Nat Rev Mater 2016. 1(12):16071.

[49] Schurz J. *Lösungen und Schmelzen von Hochpolymeren*.Rheol Acta 1966. 5(2):75–8.

[50] Castle JE. *Practical surface analysis by Auger and X-ray photoelectron spectroscopy. D. Briggs and M. P. Seah (Editors). John Wiley and Sons Ltd, Chichester, 1983, 533 pp., £44.50*.Surf Interface Anal 1984. 6(6):302.

[51] Jan H. *Kirby-Bauer Disk Diffusion Susceptibility Test Protocol*.American Society for Microbiology. 2016.

[52] Silva JM, Duarte ARC, Caridade SG, Picart C, Reis RL, Mano JF. *Tailored Freestanding Multilayered Membranes Based on Chitosan and Alginate*.Biomacromolecules 2014. 15(10):3817–26.

[53] Fernández E, López D, Mijangos C, Duskova-Smrckova M, Ilavsky M, Dusek K. *Rheological and thermal properties of agarose aqueous solutions and hydrogels*.J Polym Sci Part B Polym Phys 2008. 46(3):322–8.

[54] Bartnikowski M, Wellard M, Woodruff M, Klein T. *Tailoring Hydrogel Viscoelasticity with Physical and Chemical Crosslinking*.Polymers (Basel) 2015. 7:2650–69.

[55] Silva SS, Rodrigues LC, Reis RL. *An alternative approach to prepare alginate/acemannan 3D architectures*.SN Appl Sci 2019. 1(7):684.

[56] Karoyo AH, Wilson LD. *Physicochemical Properties and the Gelation Process of Supramolecular Hydrogels: A Review*.Gels (Basel, Switzerland) 2017. 3(1):1.

[57] Schurz J. *Rheology of polymer solutions of the network type*.Prog Polym Sci 1991. 16(1):1–53.

[58] Trivedi T, Kumar A. *Efficient Extraction of Agarose from Red Algae Using Ionic Liquids*.Green Sustain Chem 2014. 04:190–201.

[59] Kandemir N, Xia Y, Duan P, Yang W, Chen J. *Rheological Characterization of Agarose and Poloxamer 407 (P407) Based Hydrogels*.MRS Adv 2018. 3(30):1719–24.

[60] Duarte MER, Cardoso MA, Noseda MD, Cerezo AS. *Structural studies on fucoidans from the brown seaweed Sargassum stenophyllum*.Carbohydr Res 2001. 333:281–93.

[61] Sinurat E, Peranginangin R, Saepudin E. *Purification and Characterization of Fucoidan from the Brown Seaweed Sargassum binderi Sonder*.Squalen Bull Mar Fish Postharvest

Biotechnol 2016. 10(2):79.

[62] Huang Y-C, Yang Y-T. *Effect of basic fibroblast growth factor released from chitosan–fucoidan nanoparticles on neurite extension*.J Tissue Eng Regen Med 2016. 10(5):418–27.

[63] Alwarsamy M, Gooneratne R, Ravichandran R. *Effect of fucoidan from Turbinaria conoides on human lung adenocarcinoma epithelial (A549) cells*.Carbohydr Polym 2016. 152:207–13.

[64] Hao Y, Zhao W, Zhang L, Zeng X, Sun Z, Zhang D, et al. *Bio-multifunctional alginate/chitosan/fucoidan sponges with enhanced angiogenesis and hair follicle regeneration for promoting full-thickness wound healing*.Mater Des 2020. 193:108863.

[65] Pernodet N, Maaloum M, Tinland B. *Pore size of agarose gels by atomic force microscopy*.Electrophoresis 1997. 18(1):55–8.

[66] Lahaye M, Rochas C. *Chemical structure and physico-chemical properties of agar*.Hydrobiologia 1991. 221:137–48.

[67] You K, Kim D, Kwon B-J, Vagaska B, Kang J, Seo H, et al. *Methods for Evaluation of the Chemotactic Migration of the Cells in 3D Biomimetic Matrix*.Biomater Res 2012. 16:129–34.

[68] Matsuyama H, Tamura T, Kitamura Y. *Permeability of ionic solutes in a polyamphoteric membrane*.Sep Purif Technol 1999. 16(2):181–7.

[69] Singh NK, Lee DS. *In situ gelling pH- and temperature-sensitive biodegradable block copolymer hydrogels for drug delivery*.J Control Release 2014. 193:214–27.

[70] *What is the permeability of the cell membrane?*2015 [cited 2020 Jun].

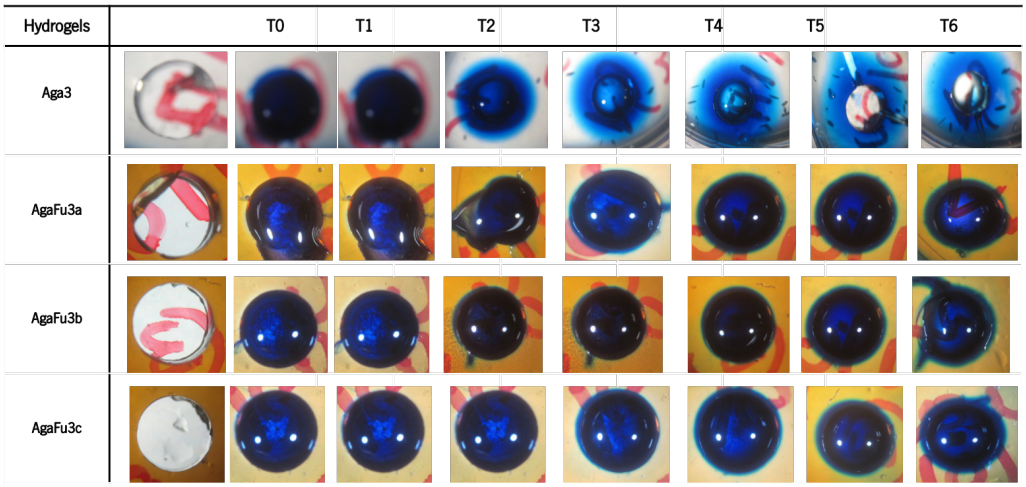
[71] McCluskey JT, Hamid M, Guo-Parke H, McClenaghan NH, Gomis R, Flatt PR. *Development and functional characterization of insulin-releasing human pancreatic beta cell lines produced by electrofusion*.J Biol Chem 2011. 286(25):21982–92.

[72] Lee JS, Jin GH, Yeo MG, Jang CH, Lee H, Kim GH. *Fabrication of electrospun biocomposites comprising polycaprolactone/ fucoidan for tissue regeneration*.Carbohydr Polym 2012. 90:181–8.

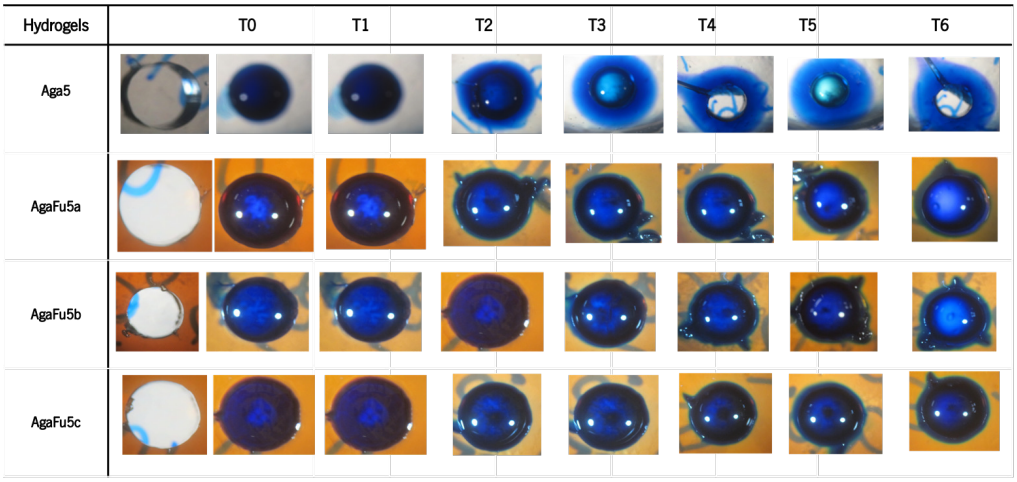
[73] Guo-Parke H, McCluskey JT, Kelly C, Hamid M, McClenaghan NH, Flatt PR. *Configuration of electrofusion-derived human insulin-secreting cell line as pseudoislets enhances functionality and therapeutic utility*.J Endocrinol 2012. 214(3):257–65.

VI-8. SUPPLEMENTARY PART

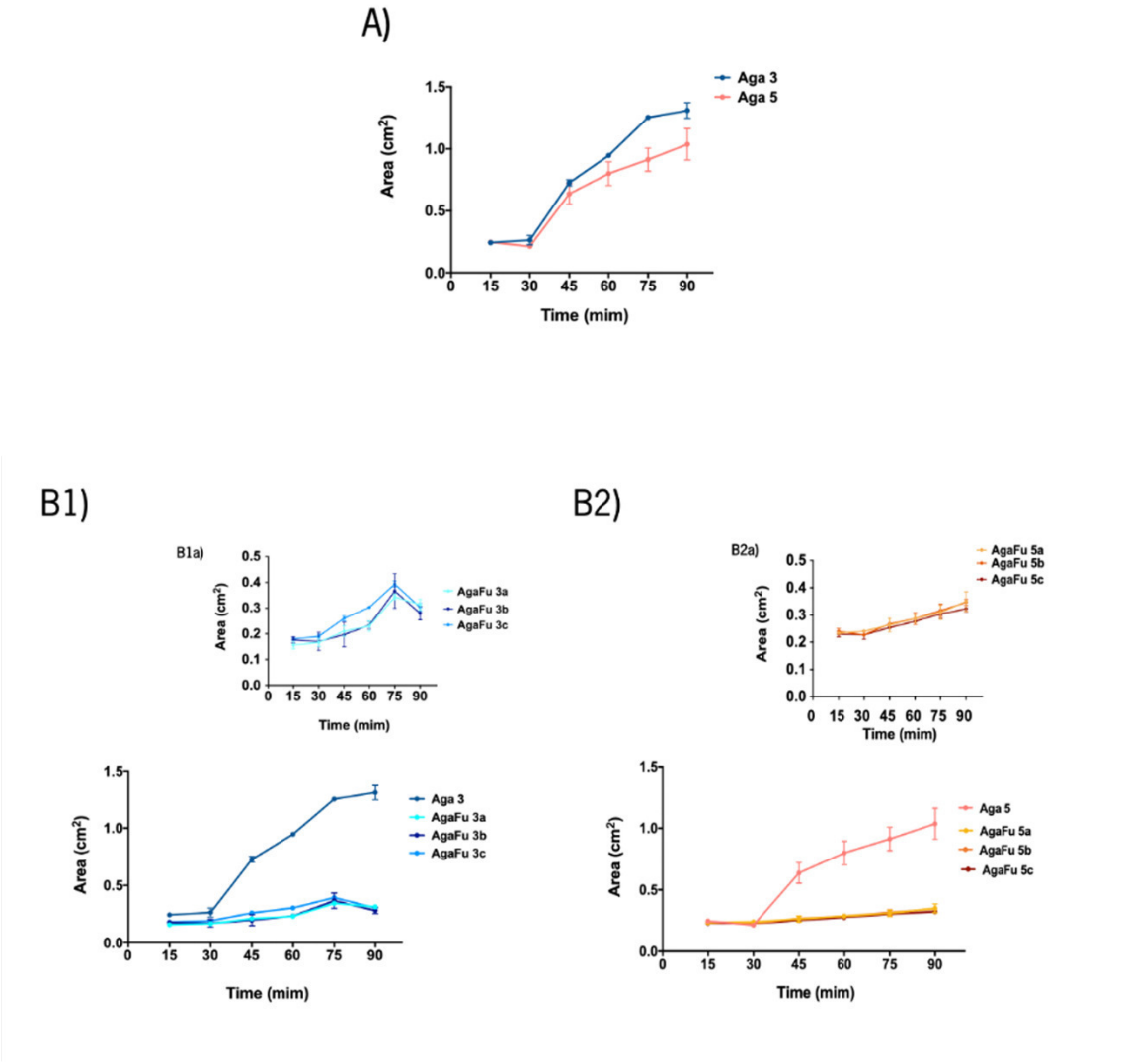
A)



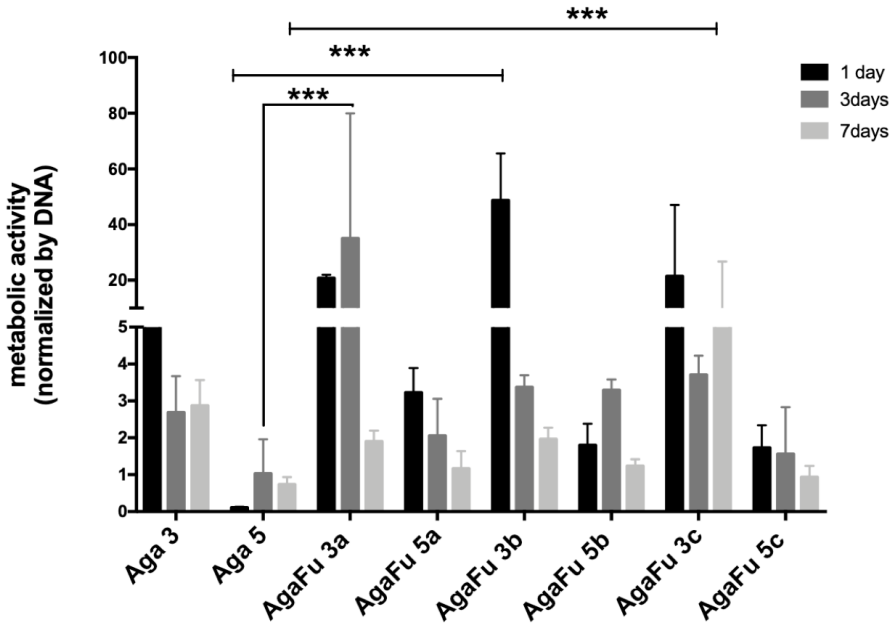
B)



Supplementary Figure VI-1. Images of Agarose (Aga) and Agarose/fucoidan (AgaFu) hydrogels (3% A) and (5% B) evidencing the diffusion of methylene blue for different time points (0 (T0), 15 (T1),30 (T2),45 (T3), 60 (T4), 75 (T5) and 90 (T6) minutes.



Supplementary Figure VI-2. Diffusion of methylene blue through the different hydrogels formulations A) Aga 3 and Aga5 hydrogels B1) Aga 3 and AgaFu 3 a, b, c hydrogels (b1a) and B2) Aga 5 and AgaFu 5 a, b, c hydrogels (b1a).



Supplementary Figure VI-3. MTS/dsDNA as indication of normalized metabolic activity of 1.1B4 human pancreatic cells encapsulated in Aga 3, 5 and AgaFu 3 and AgaFu 5 at different proportions (a (4/10), b (5/10) and c (7/10)) hydrogels (Data represent means ± standard deviation; *** $p<0.001$, Kruskal-wallis test).

Chapter VII

Angiogenic potential of airbrush fucoidan/polycaprolactone nanofibrous meshes

Chapter VII

Angiogenic potential of airbrush fucoidan/polycaprolactone nanofibrous meshes[¨]

ABSTRACT

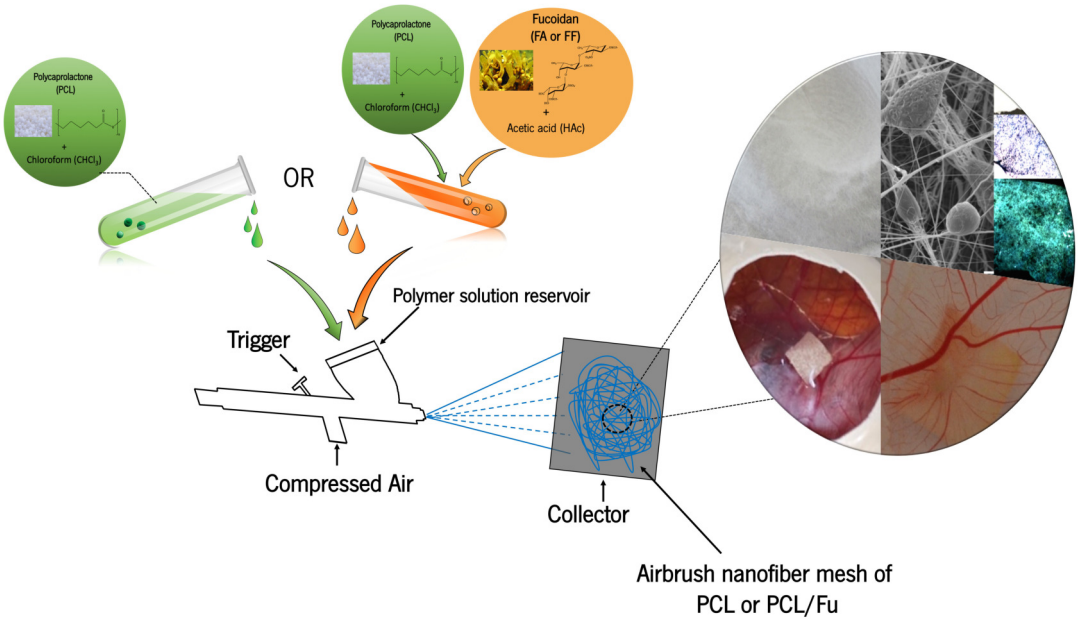
Implantation of biomaterials and hybrid constructs in tissue engineering approaches presents major limitations such as inflammatory reaction and the lack of vasculature integration. Therefore, new strategies are needed to enhance implants function, immune protection, and revascularization. In this work, we developed fibrous meshes composed by fucoidan (Fu), a sulfated polysaccharide extracted from brown algae, and polycaprolactone (PCL), a synthetic biodegradable polymer, using the airbrush technique. The chemical characterization by FTIR, EDS and XPS confirmed the presence of the two polymers in the structure of airbrushed nanofibrous meshes (ANFM). Moreover, these nanofibrous exhibited good wettability and mechanical properties envisaging their application as templates for biomaterials and cell culture. The developed ANFM were directly cultured with human pulmonary microvascular endothelial (HPMEC-ST1.6R) cells for up to 7 days. Biological results demonstrated that ANFM comprising Fu promoted cellular attachment, spreading, and proliferation of human endothelial cells. The angiogenic potential of ANFM was further evaluated by onplantation of PCL and PCL/Fu ANFM in chick chorioallantoic membrane (CAM). *In ovo* and *ex ovo* results showed that the incorporation of Fu increased the pro-angiogenic potential of ANFM. Altogether, the results suggest that airbrush biocomposite meshes could be used as a biomaterial substrate to promote vascularization.

Keywords: airbrushing, nanofibrous meshes, fucoidan, poly(ε-caprolactone), endothelial cells, tissue engineering, angiogenesis, vascularization.

¨ This chapter is based on the following publication:

Reys L. L., Silva S. S., Oliveira C., Martins A., Reis R. L. and Silva T H., *"Airbrush biocomposite nanofibers of polycaprolactone/fucoidan for diabetes treatment"*. (submitted for publication)

VII-1. GRAPHICAL ABSTRACT



VII-2. INTRODUCTION

Nanofibrous meshes are effective scaffolds for tissue engineering (TE) since they can mimic the fibrous structure of the native extracellular matrix (ECM). These have been widely investigated for biomedical applications, including drug delivery [1,2], wound dressings [1,2], enzyme immobilization [1,3], and as a substrate to support cells culture [4–6]. Electrospinning has been the most common technique for fabricating nanofibrous mats [7–10]. However, the airbrush is also a useful technique to produce nanofibrous meshes, less expensive to set up than electrospinning [11]. Airbrush requires i) a simple apparatus like commercial airbrushes, typically used for painting; ii) a concentrated polymer solution in a volatile solvent; iii) and high-pressure gas source to successfully generate nanofibrous onto a broad range of targets [1,11–13]. A large number of polymers/solvent systems and deposition conditions have been demonstrated with this technique [1,14–18]. Airbrush technique has the possibility for *in-situ* fabrication, by rapidly nanofiber deposition and increased number of new applications in the biomedical field have been suggested, with good-performed airbrushed nanofibrous meshes and structures allowing precise and tissue-specific reconstruction [1,11]. Applications of this technique are

largely analogous to electrospinning, including enzyme immobilization, drug delivery [1,15], microfiltration, and as a sealant for surgeries in surgery [1]. The variety of natural and synthetic polymers that can be airbrushed provide ample opportunities to tailor the mechanical and biological properties of fibers [19,20]. Synthetic polymers such as polylactic acid (PLA) [1,11], poly(ethylene oxide) (PEO) [19,21], polyvinyl alcohol (PVA) [22] and poly(ε-caprolactone) (PCL) [11,21,23–25] have been widely used in production of nanofibrous meshes. Particularly, PCL has been widely used in the manufacture of nanofibrous meshes due to its controllable biodegradability, easy processing, and good mechanical properties. However, it has low initial cell attachment and proliferation due to its hydrophobicity and low inclusion of growth factors [23,24,26].

Natural polymers are often used in biomedical arena due to their unique properties, namely their biocompatibility, hydrophilicity, and biodegradability [19,27]. Among them, marine sulfated polysaccharides demonstrate a wide range of bioactivities, making them ideal for the development of bio-based functional systems for tissue engineering scaffolds and drug delivery systems. Furthermore, in the literature, a small number of fibers structures based on marine sulfated polysaccharides have been developed by electrospinning [19,28]. Fucoidan (Fu) is a complex anionic sulfated polysaccharide extracted from the cell walls of brown seaweeds [29–31]. In the literature, many studies have demonstrated that Fu possesses anticoagulant [31,32] antitumor [7,29,33], reducing blood sugar [31,34], antihyperlipidemic [31,35], antioxidant activities [31,36] and pro-angiogenic activity [37,38]. These biological activities can be related with different physicochemical properties, such as molecular weight, carbohydrates composition, sulfation degree and pattern along the fucoidan backbone [7,33,39,40]. Based on these features, Fu-based systems, namely nanoparticles, liposomes, hydrogels, films, and microspheres, have been developed envisaging different biomedical applications [30,39]. In most of those studies, Fu was combined with other polymers, mainly due to difficulties in processing of stable matrices in an aqueous medium, since Fu is highly soluble in water [24,30]. Then, the association of synthetic polymers, such as PCL, with Fu could improve rheological properties and processability, which is crucial for fiber formation [23,24]. Furthermore, the successful combination of Fu with PCL could contribute to its known benefits in biomedical properties [24,40,41]. Some studies have already developed electrospun meshes using PCL/Fu and PCL/PEO/Fu for bone regeneration and vascular graft. The incorporation of Fu increased the total protein content, alkaline phosphatase activity, and calcium mineralization [24], while Fu loaded PCL/PEO mesh c was proposed as a potential solution for long term patency of small-diameter vascular graft [40,41].

In this work, we developed airbrushed meshes made of PCL and Fu. We hypothesize that the incorporation of Fu will have a positive impact on the hydrophobicity, mechanical properties, and angiogenic properties of PCL ANFM. Fucoidan from two different species, namely *Ascophyllum nodosum* (FA) and *Fucus vesiculosus* (FF), was blended with PCL and further processed into nanofibrous meshes using an airbrush technique. Fucoidan quantification, mechanical properties, and morphological features of ANFM, as well as their capability to support human endothelial cells culture were investigated, complemented by assessment of vascularization enhancement using the chick chorioallantoic membrane (CAM) assay.

VII-3. MATERIALS AND METHODS

VII-3.1. Materials

Powder of fucoidan from brown algae *Fucus vesiculosus* (FF) (Maritech® Fucoidan, Marinova, batch #FVF2011527, Australia) and from *Ascophyllum nodosum* (FA) (Ascophycient, Algues & Mer, batch # ASPHY16241, France), were used after purification with calcium ions, as described below. Poly(ε-caprolactone) (PCL) and calcium acetate were obtained from Sigma Aldrich. All other reagents, of analytical grade, were used as received.

VII-3.2. Purification of fucoidan

A purification process was required to obtain pure fucoidan, needed for the production of airbrush nanofibrous. The purification of fucoidan (PFu) was based on the calcium ions method [42], which relies on the complexation of alginates eventually present in the crude fucoidan sample with calcium ions and further precipitation. Briefly, fucoidan (160 mg/mL) was dissolved in 20 mM calcium acetate aqueous solution, during 4h at 50 °C under stirring, and pH was adjusted continuously between 6.6 and 7.5. The solution was cooled down, left at 4 °C overnight and centrifuged during 15 min at 5 000 g (Centrifuge 5810, Eppendorf, Germany). The supernatant was dialyzed against water for 5 days using 12-14 KDa cut-off dialysis membranes and freeze-dried for 4 days (CryoDOS-80, Telstar, Spain).

VII-3.3. Airbrushing nanofibrous mesh

A commercially available airbrush designed for painting (Airbrush, DEXTER, model DX-1839, Spain), with a 0.3 mm nozzle diameter, was used to fabricate nanofibrous mesh (ANFM). The airbrush was connected to pressurized compress air (Wuto, model: TC-20 series, Spain) with constant pressure between 4-6bar and the distance from the nozzle to the target was held constant at 50 cm for all experiments, using a plastic surface as collector. PCL ANFM were produced by airbrushing 6 consecutive layers (about 30 s each layer) of 4% (w/v) f poly (ε-caprolactone) (PCL) solution prepared in chloroform. PCL/Fu ANFM were produced using a similar procedure, but alternating PCL and PCL/Fu layers. **(Figure VII - 1)**. To produce the latter, 10 mg/ml fucoidan (purified FA or FF) dissolved in pure acetic acid was added to the PCL solution previously prepared, left under stirring to complete dissolution (~3 hours) at room temperature, with the resulting mixture being used for airbrushing. After the complete processing, all the ANFM were dried in a desiccator at room temperature for 3 days to evaporate the solvent, and were cut in 1x1 cm^2 samples for further assays. Throughout the paper, the PCL/Fu ANFM produced from FA and FF are referred to as PCLFA and PCLFF, respectively.

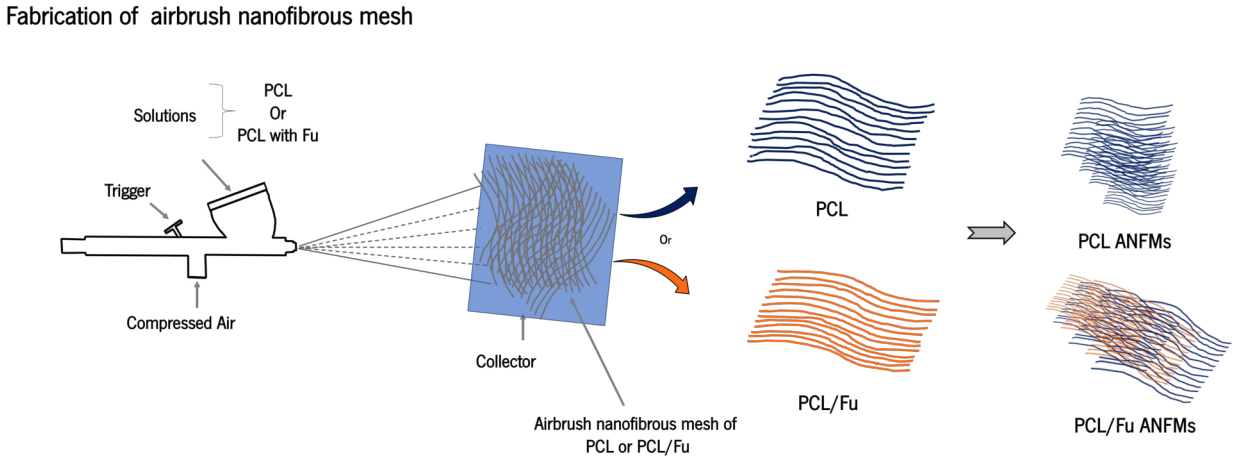


Figure VII-1. Schematic overview of the experimental steps required to fabricate ANFM of PCL and PCL/Fu , each composed by 6 consecutive airbrushed polymeric layers.

VII-3.4. Physicochemical characterization of ANFMs

VII-3.4.1. ANFM morphology and chemical composition

The morphology of ANFMs was analyzed in a scanning electron microscope (SEM) (JSM-6010 LV, JEOL, Japan). Before SEM analysis, samples were gold-palladium coated using a sputter coater (Cressington,108A, US), and the analysis was made at an accelerating voltage of 10 keV and magnifications from 100x to 10 000x. Chemical analyses of samples were made by Energy Dispersive Spectroscopy (EDS) (INCAx-Act, PentaFET Precision, Oxford Instruments), using an acceleration voltage of 1 keV. The nanofibres diameters were measured by ImageJ software using the SEM pictures at the magnification 2 000x.

VII-3.4.2. X-ray photoelectron spectroscopy (XPS)

Analysis of the samples (FA and FF powders, and PCL, PCLFA and PCLFF ANFM) was performed using a Kratos Axis-Supra instrument equipped with aluminum Kα monochromatized radiation at 1486.6 eV X-ray source, within ESCApe software. Due to the non-conducting nature of the samples, it was necessary to use a co-axial electron neutralizer to minimize surface charging, which performed the neutralization by itself. Photoelectrons were obtained from a take-off angle of 90° relative to the surface of the sample. The measurement was done in a Constant Analyser Energy mode (CAE) with a 160 eV pass energy for survey spectra and 20 eV or 40 eV pass energy for high-resolution spectra of the ANFMs and polymer powders, respectively. Charge referencing was done by setting the lower binding energy C1s peak at 285.0 eV C1s hydrocarbon peak [43,44].

VII-3.4.3. Water contact angle

The static contact angles on ANFMs were determined at room temperature with a Contact Angle Equipment (DataPhysics Instruments, model OCA 15plus; Germany and SCA-20 software). Sesile drop method was used to obtain the values. The water droplets are applied by a motor-driven syringe at different zones of each sample, and the measurement time was extended until 5 min. At least three measurements were carried to each sample (PCL, PCLFA, and PCLFF), and the presented data are averaged values for those measurements.

VII-3.4.4. Fucoidan quantification by toluidine blue assay

The amount of fucoidan into the nanofiber was quantified via toluidine blue assay (TBO) [7,45,46]. Each sample (PCL, PCLFA, and PCLFF) was immersed in 1ml of TBO solution, previously prepared using 0.1 M HCl, 0.2% NaCl, and 0.04% toluidine blue O chloride, for 4h at room temperature. Further, the samples were washed with distilled water (DW) for 24 h to remove the unreacted TBO. Afterwards, ANFMs were immersed in a mixture of 0.1 M NaOH/80% ethanol (1:4, v/v) until complete decolourization and the TBO released to that solution, proportional to the amount of fucoidan on the ANFM, was quantified by measuring the absorbance at 530 nm using a microplate reader (Bio-Tek Instruments, US) and a calibration curve. For the calibration curve preparation, 2 ml 0.04 wt.% TBO solution was first added to 2 ml of a fucoidan solution with known concentration and incubated at 37 °C with gentle shaking for 4 h. Then the mixture was centrifuged at 350 g for 10 min, the supernatant was removed, and the precipitate was carefully rinsed twice with aqueous 0.01 M HCl/0.2 wt.% NaCl. Finally, 5 ml 0.1 M NaOH/80% ethanol mixture (1:4, v/v) solution was added to dissolve the precipitate, and the absorbance was measured at 530 nm.

VII-3.4.5. Mechanical Tests

Mechanical properties were evaluated using a dynamic mechanical analyzer (DMA) (Tritec 2000B equipment, Triton Technology, UK). Samples (PCL, PCLFA, and PCLFF) were cut in regular stripes (width 5.31 $\pm$ 0.46 mm and thickness 0.19 $\pm$ 0.013 mm) and soaked in a PBS solution for equilibration. Samples were then clamped in the DMA apparatus with the total immersion of samples in a reservoir containing PBS solution at 37°C. DMA plot was obtained using a stress mode cycle of increasing frequency from 0.01 to 20 Hz (5 points per decade), to simulate the physiological loading frequencies. At least five samples were tested for each condition.

VII-3.4.6. Swelling

The swelling behavior of the nanofibrous mesh was determined after immersion in solutions such as PBS, for 28 days, at 37 °C. The weight of the swollen samples was measured by gently tapping the surface of samples in filter paper to remove the excess of water from the surface. The degree of swelling (Q) for each sample was calculated using **Equation VII - 1.**

Equation VII-1. Degree of swelling

$$Q = \left[{(W_s - W_d)}/{W_d}\right] * 100\%$$

where W_S is the swollen sample weight under specified environmental conditions, and W_d is dry sample weight after swollen.

VII-3.5. Biological tests

- **CELL CULTURE**

Human pulmonary microvascular endothelial cells (HPMEC-ST1.6R cell line) were cultured in M199 medium supplemented with 20% fetal bovine serum (FBS), 2 mM Glutamax, 100 U/mL penicillin and 100 mg/mL streptomycin (Pen/Strep 100 U/100 g mL^{-1}) and endothelial cell growth supplement (ECGS) (25 μg mL^{-1}). Cells were used at passages 38–40.

- **Cell seeding**

Before the biological assays, the samples were sterilized with ethylene oxide. Then, endothelial cells were seeded on ANFM at a density of 50000 cells/sample using the drop method. After 4 h of adherence, 450 μL of the culture medium was added at each sample. Tissue culture polystyrene (TCP) was used as a control for all the assays. Each experimental condition was tested in triplicate, and three independent assays were performed.

- **Cell viability**

The metabolic activity of endothelial cells was determined by the MTS assay. After 1, 3, and 7 days, the culture medium was removed, and the testing conditions were rinsed with sterile PBS. A mixture of culture medium (without FBS and phenol red) and [3-(4,5-dimethylthiazol-2-yl)−5-(3-carboxymethoxyphenyl)−2-(4-sulfophenyl)-2H-tetrazolium] MTS reagent (5:1 ratio) was added to each well and left to incubate for 3 h, at 37 °C with a 5% CO_2 atmosphere. After that, the absorbance of the MTS reaction medium from each sample was read at 490 nm in a microplate reader (Bio-Tek Instruments, USA).

- CELL MORPHOLOGY

To evaluate the cell adhesion and morphology, the constructs (PCL, PCLFA and PCLFF) were fixed with 2.5 % glutaraldehyde (Sigma; USA) in PBS (Sigma; USA) solution, for 1 h at 4 °C. The samples were further dehydrated through a graded series of ethanol and gold-palladium coated in a sputter coating equipment (Cressington,108A, USA) for 2 min, and analyzed by SEM (JSM-6010 LV, JEOL, Japan) using magnifications from 100x to 10000x.

VII-3.6. *In vivo* angiogenesis evaluation

VII-3.6.1. Chick chorioallantoic membrane (CAM) assay

White fertilized chicken eggs (*n*=150; Pintobar, Portugal) were incubated at 37 °C (Laboratory Incubator, model B8420; Termarks) for 3 days. After this period of time, a small hole was created in the pointed end of the egg to allow dissociation of the chick chorioallantoic membrane (CAM) from the eggshell membrane. In addition, a window was open into the eggshell, with dissecting scissors, to evaluate embryo viability and allow access to the CAM **(Figure VII - 2).** The window was then sealed with transparent tape (~50 x 30 mm, AXTON 50 mm) to prevent dehydration, and the eggs were returned to the incubator at 37 °C until day 10 of embryonic development. The sterile PCL and PCLFF ANFM (*n* = 22) were implanted on the CAM at day 10 of embryonic development under sterile conditions. The shell windows were then protected again with transparent tape, and the eggs were returned to the incubator at 37 °C until day 15 of embryonic development. On that day, the chicken embryos were sacrificed by adding a paraformaldehyde (PFA, Merck) solution at 4% (v/v), followed by its incubation at -80° C for 10 min. The implanted specimens and the immediately adjacent CAM portions were cut and fixed with 4% PFA. The specimens implanted and the adjacent portions of CAM were cut and fixed with a PFA solution at 4% (v/v). The implants and immediately adjacent portions of CAM were dissected. Chorionic epithelium (*ex ovo)* images were then captured for each CAM implant directly from the plate. A minimum of 5 eggs/samples were used for each condition.

VII-3.6.2. Analysis of blood vessels convergence

The macroscopic evaluation of the angiogenic response was carried out using a semiquantitative method by analyzing the convergence of blood vessels toward the implanted ANFM, both a allantoic epithelium (*in ovo*) and chorionic epithelium (*ex ovo*), as previously described by Ribatti and co-workers [47,48]. The *ex ovo* and *in ovo* images obtained at day 15 of embryonic development were processed using the ImageJ 1.52a software program (National Institutes of Health, USA). For quantification purposes, the magnification of the stereomicroscope images was kept constant, as well as the image-processed area (500 x 500 pixels). The total number of macroscopic microvessels that converged toward the graft was counted blindly for each egg. An automated angiogenesis quantification method was also conducted by using the Vessel Analysis plugin with Fiji (ImageJ 1.52i) to perform in a reliable and repeatable way a sequence of operations leading to a robust segmentation of EC images and a reproducible extraction of the skeleton representing the microvascular network [8,49]. Measurements of vascular density (i.e. ratio of vasculature area to total selection area) and vascular length density (i.e. ratio of skeletonized vasculature area to total area) are expressed as % area.

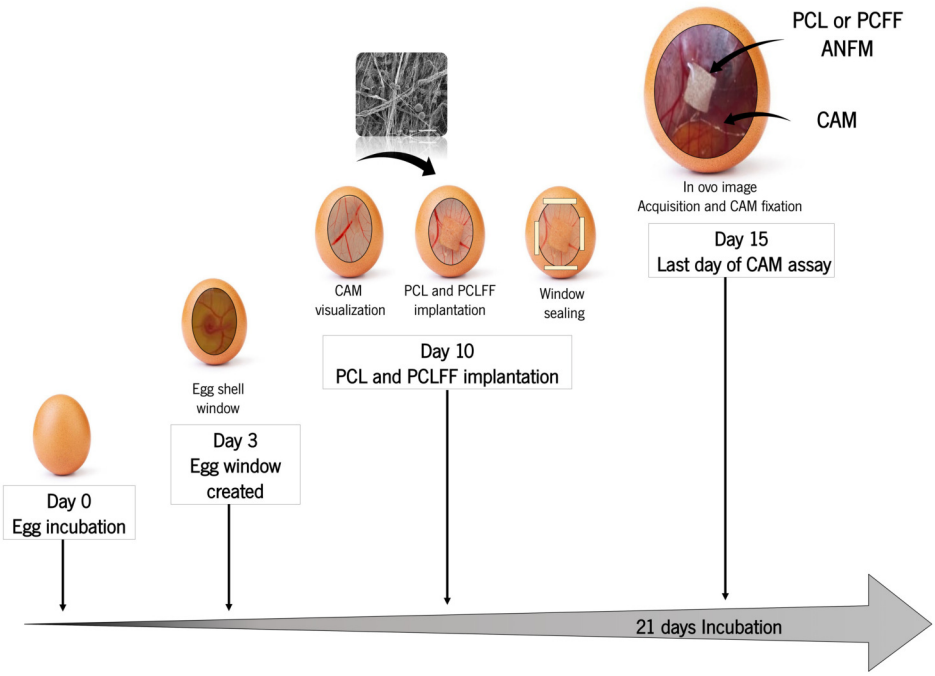


Figure VII-2. Schematic representation of the optimized chick chorioallantoic membrane (CAM) assay. Fertile eggs were incubated for 3 days before creating the window. At 10th day PCL and PCLFF ANFM were placed on the CAM and the eggshell was sealed to prevent dehydration and infection. The assay proceeded until day 15 (adapted from [50]).

VII-3.7. Statistical analysis

Statistical analysis of the data was performed by Graph Pad Prism ® 7.0. First, a Shapiro Wilk test was performed to ascertain the data normality. When data follow a normal distribution, parametric test was used (one-way ANOVA test followed by Tukey´s HSD test). When the normality was rejected, a non-parametric test was used (Kruskal-Wallis followed by Dunn´s multiple comparisons test), and $p<0.05$ was considered significant. Data are presented as mean ± standard deviation.

VII-4. RESULTS AND DISCUSSION

- **Fucoidan quantification by toluidine blue assay**

To confirm the presence of fucoidan on the airbrushed meshes and thus show the effectiveness of the production technology, a quantitative toluidine blue O (TBO) assay was conducted [7,45,46]. TBO is used in histological analysis as it stains tissues based on the metachromasia concept attributed to stacking dye cations at sites of high-density of anionic groups, with a change in color from blue to violet [60,61]. Following the same concept, in the present work TBO cations would interact with the negatively charged sulfate groups from fucoidan. As shown in **Figure VII - 3A**, whereas PCL ANFM did not change in color, the PCLFA and PCLFF ANFM were stained with violet and blue, with different intensities due to the different chemical structure. This test was also performed for 28 days in PBS solution (data not shown), and fucoidan was also detected, indicating that the fucoidan was not released from ANFM, at least over one month. The two types of PCL/Fu ANFM presented similar fucoidan contents, as the solutions resulting from the release of bonded dye from the respective ANFM, during TBO assay, had similar concentration: ≅ 0.37 mg/ml for PCLFA and 0.38 mg/ml for PCLFF.

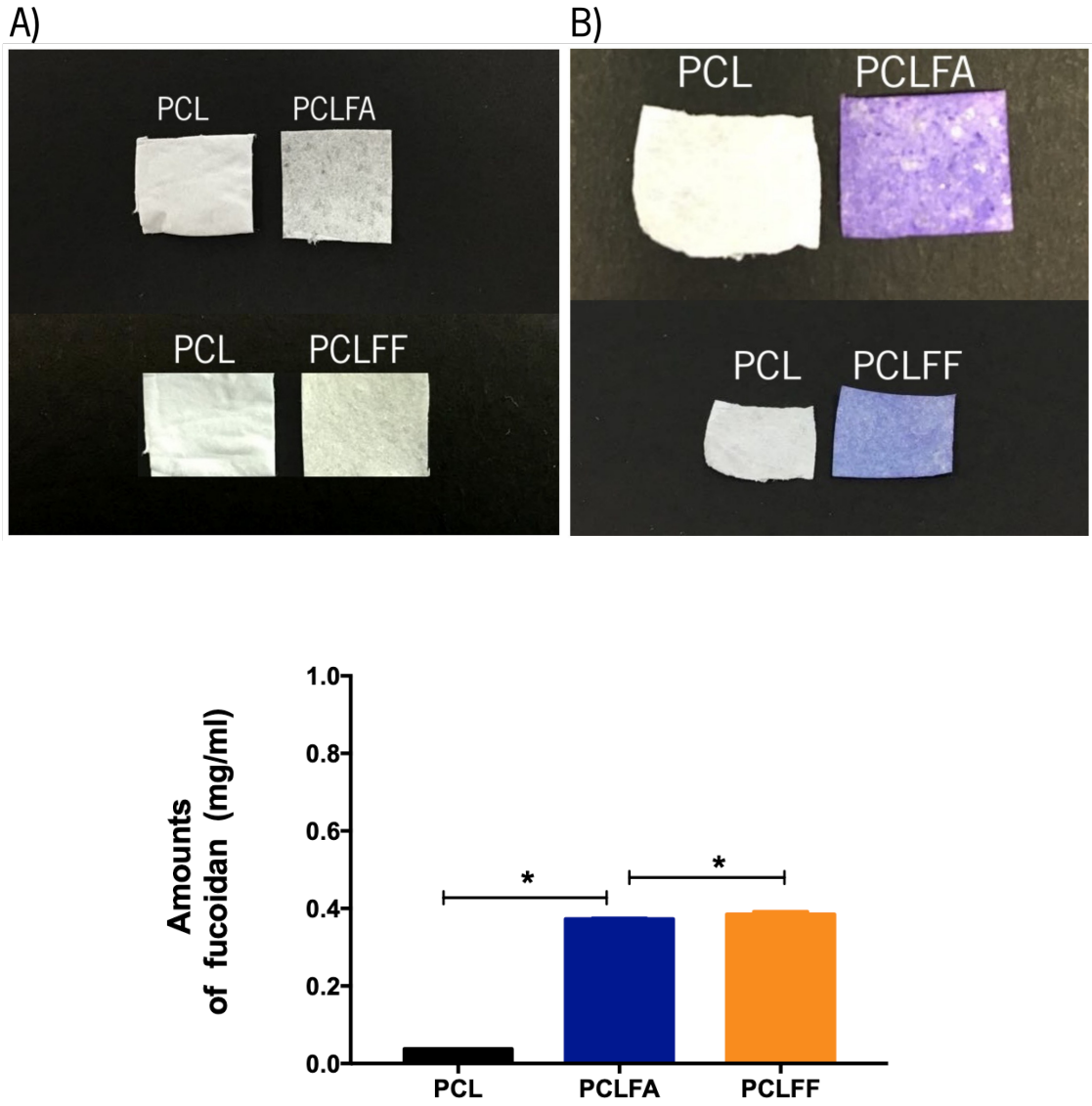


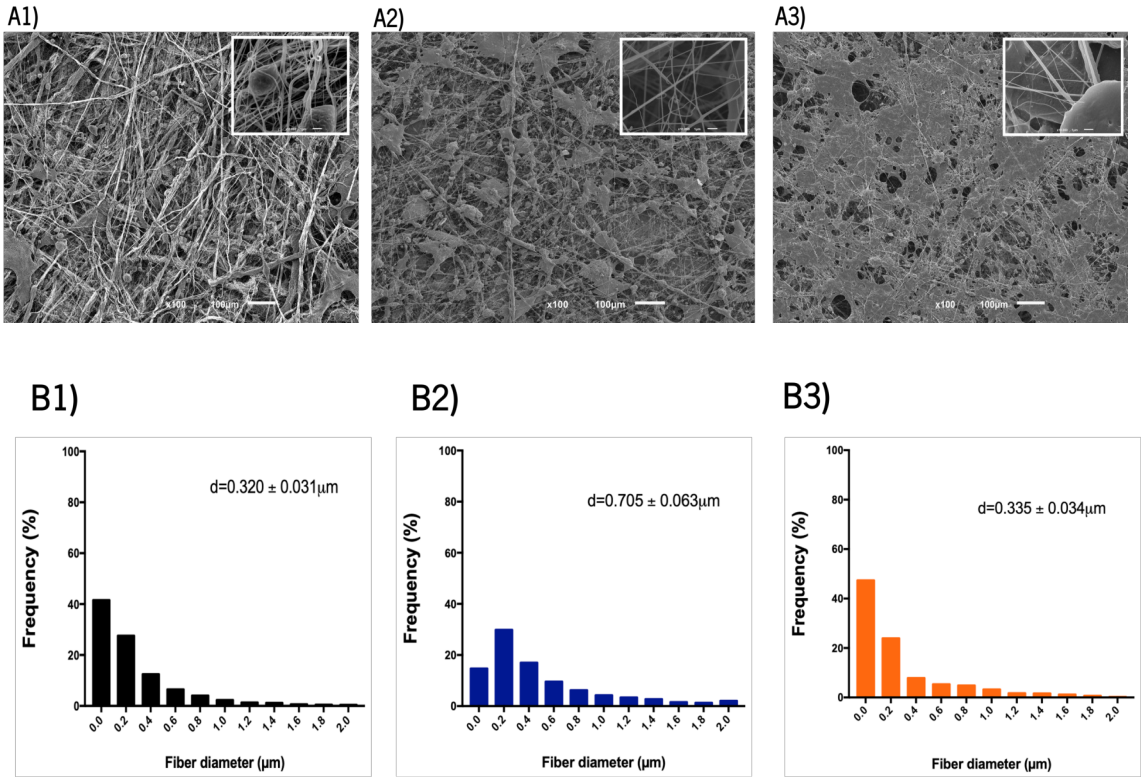
Figure VII-3. Toluidine blue (TBO) assay in ANFM A) PCLFA and PCLFF before and B) after TBO assay. C) Quantification of fucoidan into the ANFM. Data were considered statistically different (*) $p \leq 0.05$.

- **Morphology and composition of PCL and PCL/Fu ANFM**

PCL and PCL/Fu solutions were airbrushed into a plastic collector, rendering the production of polymeric meshes. Two different fucoidan samples, obtained from distinct brown seaweed species, *Ascophyllum nodosum* (FA) and *Fucus vesiculosus* (FF), were used to study the influence of different chemical features, as molecular weight (FA < FF) and sulfate contents (FA < FF), on the properties of the produced ANFM. Scanning electron microscope observation of PCL and PCL/Fu ANFM **(Figure VII – 4**

A1-A3) indicated a similar nanofiber diameter and different morphological aspect that could suggest a controlled production of nanofibres **(Figure VII - 4 A1-A3)**. Furthermore, porous fibrous mesh with a diameter ranges from 0.30 to 0.72 µm was also observed. PCL and PCLFF showed to be similar and tendentially higher for PCLFA, although not having differences. These results demonstrated that the airbrush technique was reproducible and have uniform outcomes **(Figure VII - 4 B1-B3).** The incorporation of fucoidan increases the fiber diameter for FA (0.705 ± 0.063) and for FF (0.335 ± 0.034 µm) in comparison with PCL (0.320 ± 0.031 µm) alone. The incorporation of fucoidan induced the production of less straight fibers, less orientation, and more lumps. This can be related to the fact that chloroform, being less volatile than acetic acid, moves out of the polymer fiber in the latter phase of polymer solidification, thereby rendering roughness to the mesh surface [46]. On the other hand, PCL meshes were free of lumps, straighter, and deposited randomly.

Energy-dispersive X-ray spectroscopy (EDS) was performed to confirm that fucoidan has been incorporated in ANFM. This technique allowed determining the presence of sulphur (S) element, only present in the chemical structure of fucoidan, in both PCL/Fu ANFM **(Figure VII - 4 C1- C3)**, thus showing that both fucoidans (FA, FF) were well embedded in ANFMs.



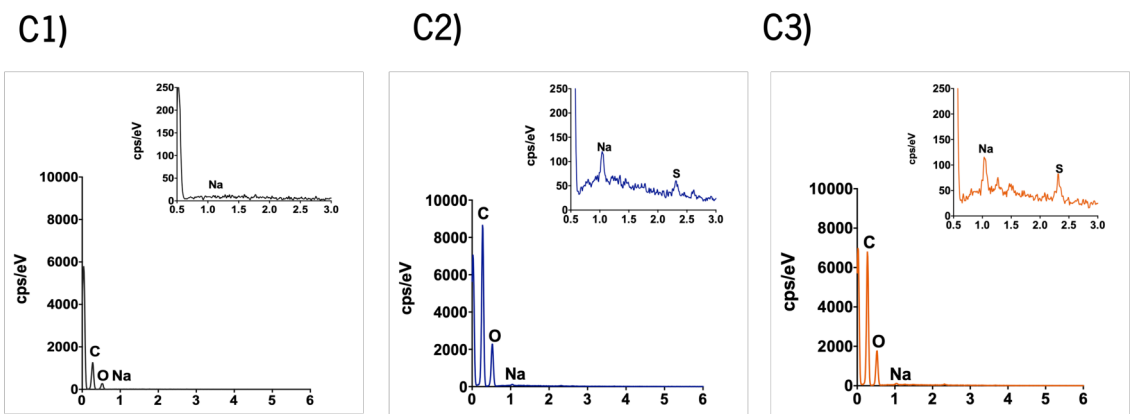


Figure VII-4. Morphology and composition of PCL and PCLFu ANFM. SEM images of A1) PCL, A2) PCLFA, and A3) PCLFF airbrush nanofibrous (ANFM) samples. Scale bar: 100 µm for the background images, 1 µm for the insert images. Fiber diameter distribution profile B1) PCL, B2) PCLFA, and B3) PCLFF ANFM airbrush nanofibrous. EDS spectra of C1) PCL, C2) PCLFA, and C3) PCLFF ANFM samples. The peaks of carbon (C), oxygen (O), sodium (Na), and sulphur (S) elements are labeled in the spectra.

The surface composition of ANFMs was assessed by XPS, as shown in **Figure VII – 5 A – C and Table VII -1**, aiming to complement the information obtained by EDS for bulk elemental analysis. The XPS wide spectra **(Figure VII - 5 A - C)** displayed the presence of the expected peaks of carbon (C) and oxygen (O) on all samples, while only the ones containing fucoidan presented the sulphur peak, being thus in accordance with the data obtained by EDS. No apparent changes were noted in the C1s and O1s region spectra of the samples with fucoidan when compared with the raw material. The XPS quantification procedure, obtained using the spectra of the regions of the high-resolution scan (C1s, O1s, and S2p) of the fucoidans and ANFM, resulted in values depicted in **Table VII - 1**, considering the homogeneous distribution of the elements in all the samples. The elements quantification of PCL/Fu ANFM showed that PCLFA had about 0.08 % and PCLFF 0.65 % of sulphur (S) in its composition **(Table VII - 1 and Figure VII - 5 B_1 - C_1)**. These results are in agreement with the sulfur values presented by fucoidan powders: 0.31% for FA and 3.19% for FF, with difference in contents being of about one order of magnitude, thus suggesting that fucoidans were well embedded during the airbrush process. Regarding the high-resolution scan **(Table VII-1)** and the chemical elements identified by EDS analysis of the PCL/Fu **(Figure VII- 5 iii and iv)** ANFMs, it is observed the presence of sulphur in the surface of these nanofibrous, being in a higher quantity for PCLFF **(Table VII-1)**.

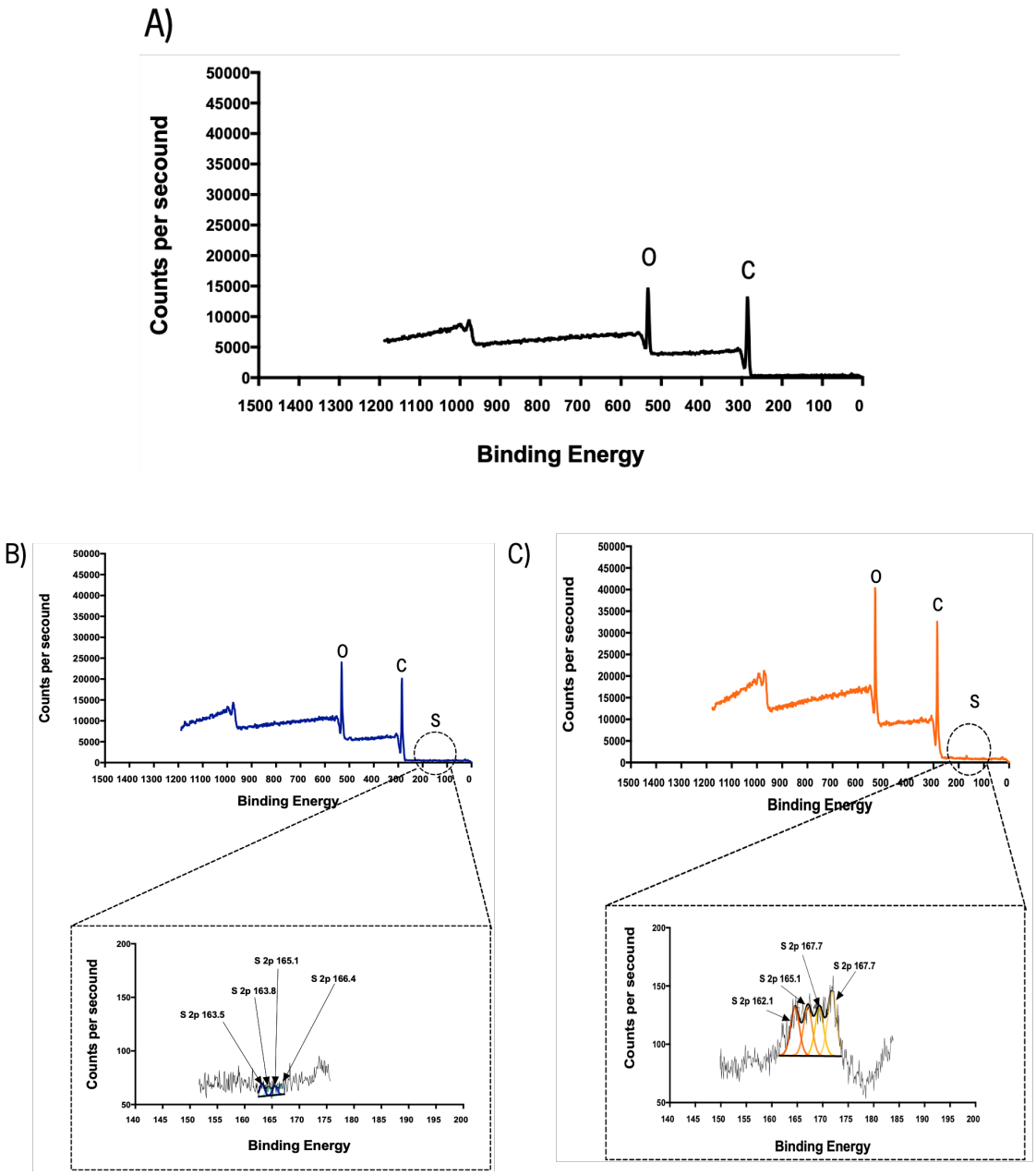


Figure VII-5. Characterization of PCL and PCLFu ANFM by XPS analysis : A) survey spectrum of PCL, B) general spectra of PCLFA ANFMs, he insert is sulphur spectra of PCLFA ANFMs C) general spectra of PCLFF ANFMs and the isnert is sulphur spectra of PCLFF ANFMs.

Table VII-1. XPS surface atomic ratios of the main components (O1s, C1s, and S2p) and the respective ratio of O/C and S/C of the controls (fucoidan FA, FF, PCL, PCLFA, and PCLFF) and ANFM.

		Atomic concentration (%)			Ratios	
		O 1s	C 1s	S 2p	O/C	S/C
Fu	FA	26.10 ± 1.15	73.59 ± 1.15	0.31 ± 0.14	0.354	0.004
	FF	35.29 ± 0.20	61.52 ± 0.21	3.19 ± 0.05	0.574	0.052
ANFMs	PCL	23.39 ± 0.44	76.61 ± 0.44	——	0.305	——
	PCLFA	26.62 ± 0.56	73.30 ± 0.56	0.08 ± 0.04	0.363	0.001
	PCLFF	29.28 ± 0.71	70.07 ± 0.71	0.65 ± 0.09	0.417	0.010

Note: Oxygen (O), Carbon (C) and Sulphur (S).

- **Water contact angle**

The surface properties of ANFM, namely their wettability, are important for the interaction with cells, immune system, and biocompatibility [51]. In this regard, the hydrophilicity of PCL and PCL/Fu ANFM was examined using water contact angle (WCA) analysis. The obtained data (**Figure VII - 6** and **Table VII – 2)** confirmed that PCL ANFM had a highly hydrophobic character, with a WCA close to 150°, thus near the limit to superhydrophobicity, due to the nature of its chemical composition, and it can cause a low rate of water absorption within the nanofibrous [23,51]. However, the hydrophobicity of the ANFM decreased with the addition of fucoidan **(Table VII - 2)**, more evidently in PCLFF than in PCLFA. Previous investigation [23,52] has shown that blend/composite systems using synthetic and natural polymers have improved hydrophilic properties compared to synthetic polymers alone [52,53]. This effect is due to the various functional groups such as hydroxyl, carboxyl, amine, and sulfate groups that are commonly present in natural polymers [23,52]. In the case of fucoidan, the hydrophilicity is provided by the presence of sulfate and hydroxyl groups [54]. FA has lower sulfate groups in comparison with FF, which could explain the higher hydrophilicity for PCLFF ANFM.

The swelling results **(Figure VII-7)** showed that PCL ANFMs had lower water uptake in comparison with ANFMs comprising fucoidan, which is in accordance with the hydrophilicity grade of those systems.

From a biological perspective, the ability to absorb water is an important factor affecting the adhesion of proteins and cells in the scaffolds and, consequently, their performance towards tissue regeneration and integration [53,55].

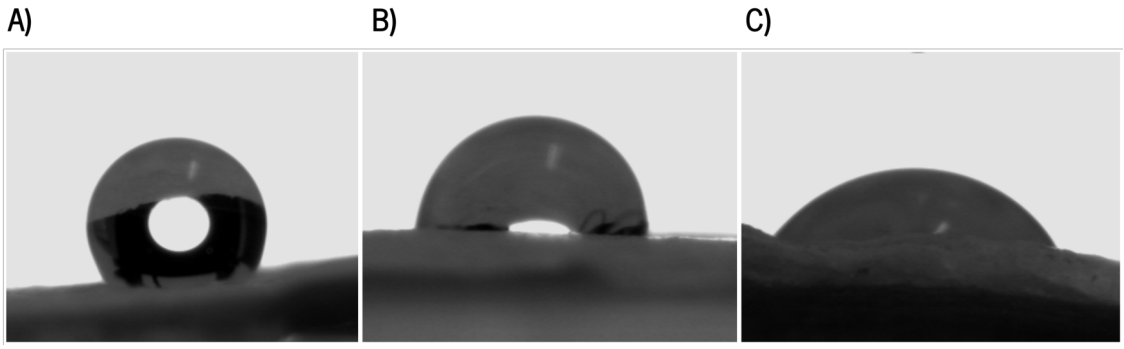


Figure VII-6. Contact angle measurements of A) PCL, B) PCLFA, and C) PCLFF ANFM.

Table VII-2. Contact angle in water for the ANFM nanofibrous

Condition	PCL	PCLFA	PCLFF
Contact angle	146.5 ± 6.3°	96.3 ± 10.0°	69.0 ± 10.0°

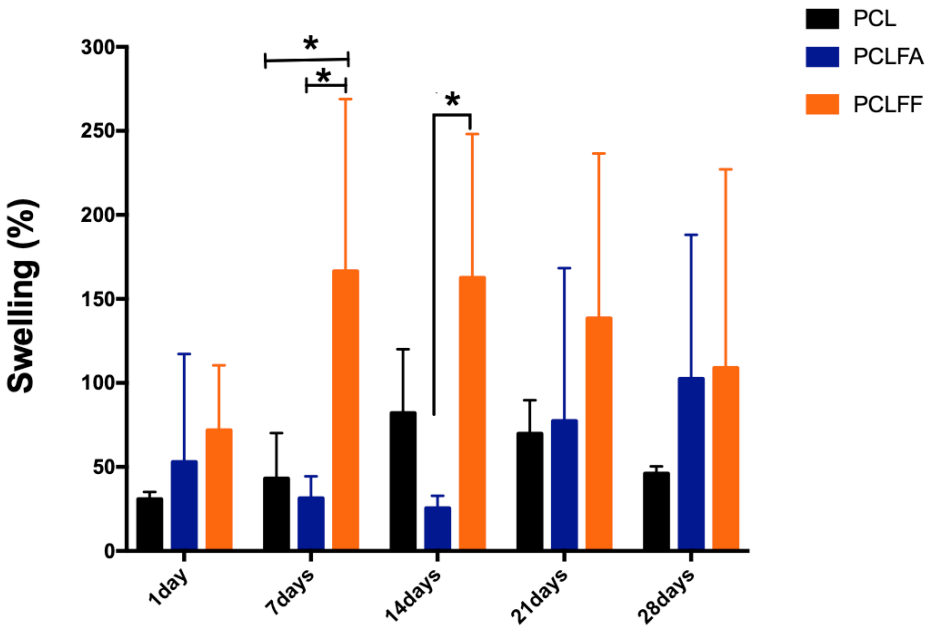


Figure VII-7. Swelling of ANFMs after immersion in PBS under stirring at 37°C.

- **Mechanical properties**

The mechanical and viscoelastic properties of ANFM (PCL and PCL/Fu) were evaluated by a dynamic mechanical analysis (DMA). These assays were performed in a hydrated environment, in PBS at 37 °C, allowing the assessment of the mechanical properties in conditions closer to physiological environment [56,57]. Variations of both storage modulus (E'), loss modulus (E'') and loss factor ($tan\ \delta = E''/E'$) as a function of the frequency (from 0.01 to 20Hz) are shown in **(Figure VII- 8)** [58,59]. Besides, **Table VII - 3** summarizes the viscoelastic properties obtained at a physiological frequency (1 Hz). The ANFM exhibited little frequency dependence for all samples. The E' values for all samples were much higher than the E'' values (**Figure VII- 8, Table VII- 3**). Furthermore, the incorporation of fucoidan significantly increased E' for ANFMs as compared to PCL mesh. It is presumed that, due to fucoidan incorporation, the increased hydrophilicity and, therefore, higher swelling of nanofibrous mesh resulted in such a change in modulus values. Although the fucoidan alone makes the PCL polymer network much stiffer, the increased volume (thus the distance between polymer chains) in water and the interspaced water molecules should compensate such rigidity. Altogether, the results show the effective stiffening of the

nanofibrous due to the incorporation of fucoidan. The *tan δ* values of all the formulations, ranging from 0.06 and 0.10 confirm the clear viscoelastic nature of all the formulations analysed.

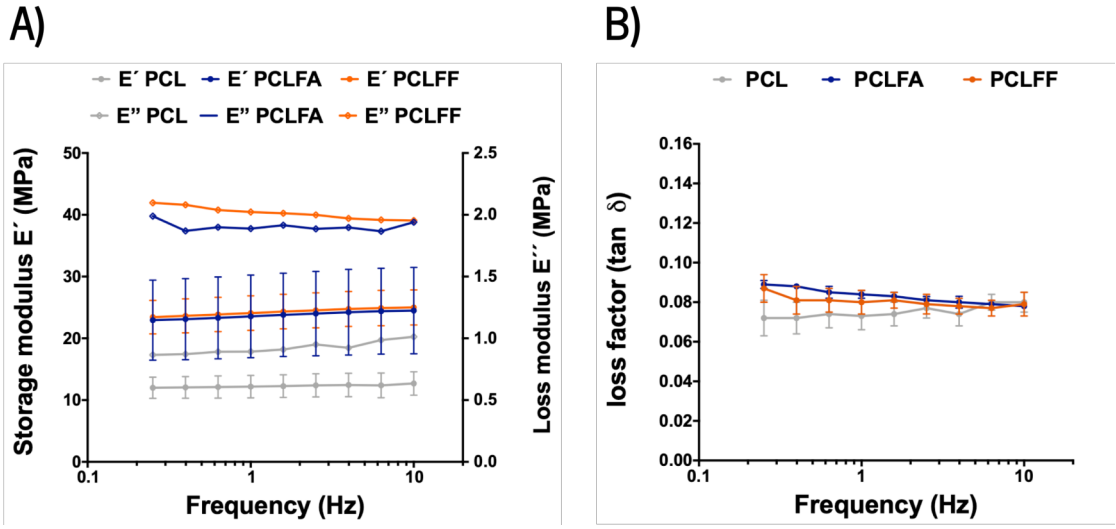


Figure VII-8. Mechanical properties : A) Frequency dependence of storage modulus (*E'*), loss modulus (*E"*) and B) loss factor (*tan δ*) of the PCL and PCL/Fu ANFM at 37°C with samples immersed in PBS.

Table VII-3. Viscoelastic properties of ANFM at a physiological frequency (1Hz).

Sample	Storage modulus, *E´* (MPa)	Loss modulus, *E´´* (MPa)	*tan δ*
PCL	12.18 ± 0.82	0.89 ± 0.01	0.07 ± 0.01
PCLFA	23.56 ± 6.69	1.89 ± 0.04	0.08 ± 0.01
PCLFF	24.08 ± 2.79	2.02 ± 0.01	0.08 ± 0.01

VII-4.1. . Biological performance

It is hypothesized that incorporation of fucoidan into PCL ANFM can enhance cell-scaffold interactions. To evaluate cell metabolic activity and morphology on the PCL and PCL/Fu, endothelial cells were cultured on the ANFM up to 7 days. Biological experiments were also performed in TCPS coverslips used as a control for comparative purposes. Human pulmonary microvascular endothelial cells (HPMEC-

ST1.6R was) were used as a model for angiogenesis [48]. To quantify the metabolic activity up to 7 days of endothelial cells in the ANFMs, an MTS assay was performed **(Figure VII - 9).** At 1 day following cell seeding, higher cell metabolic activity was observed on PCLFF as compared to PCL alone, indicative of greater cell viability **(Figure VII - 9)**, consistent with better cell adhesion to these substrates. At day seven, the cell viability on PCLFF scaffolds was significantly higher than either PCL or PCLFA, suggesting the presence of a higher number of cells on the former and consequently that the PCLFF surfaces supported the highest rate of proliferation. These results could be related to the increase of fiber diameter and water absorption of the PCL/Fu ANFM. These MTS assay results supported the hypothesis that the addition of FF provided a favorable matrix for endothelial cells attachment and growth, in agreement with other studies showing that the incorporation of marine polymers on PCL mats could increase the viability and proliferation of cells [19,62]. The morphology of the seeded endothelial cells on the PCL and PCL/Fu ANFM was observed by SEM, with the obtained micrographs being illustrated by the images in **Figure VII - 9B.** The endothelial cells were well spread onto the ANFM after 1 day of seeding, where PCLFF showed a higher cell density in the surface in all time points. This behavior could be related to higher hydrophilicity and water uptake, as well as to the FF chemical features.

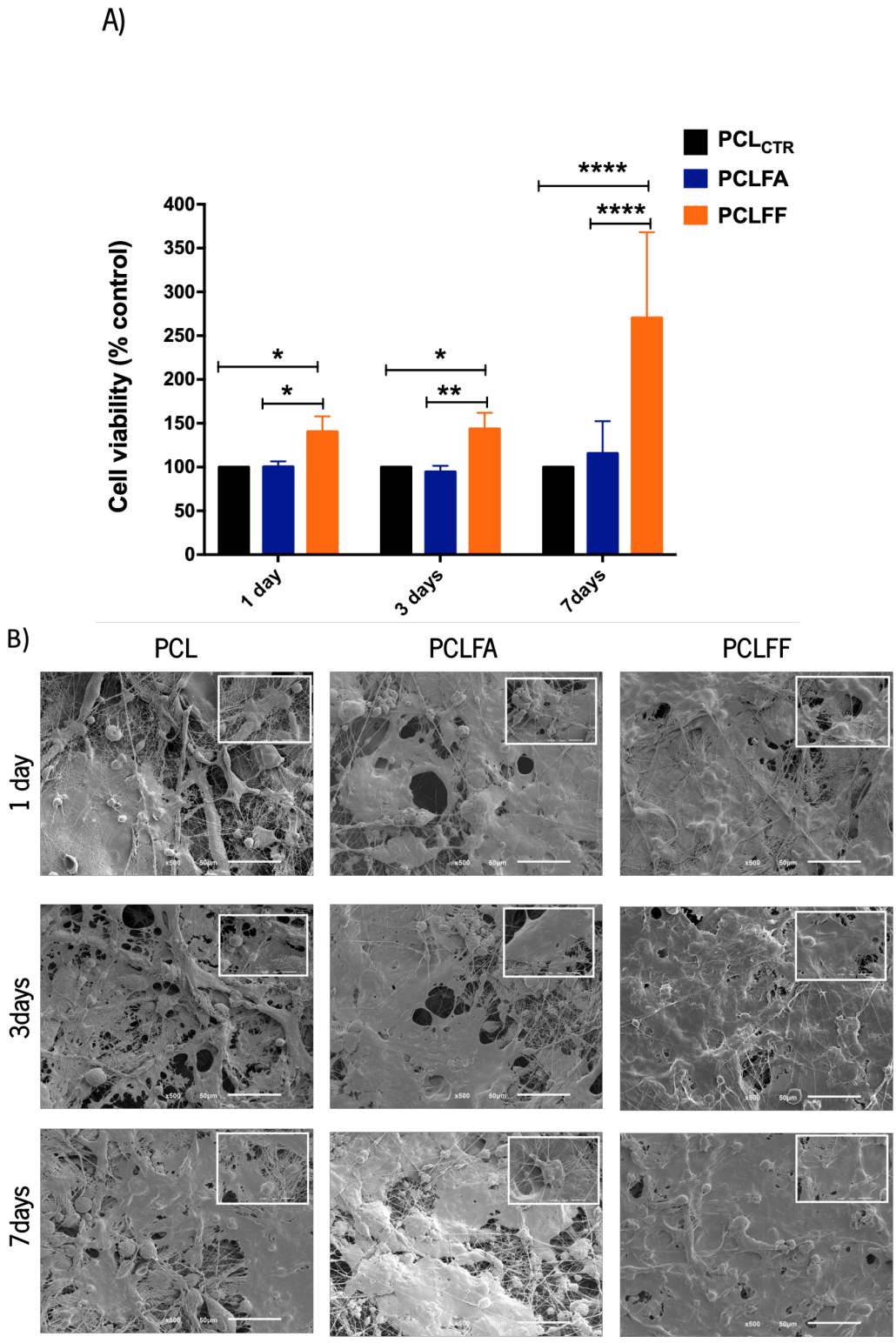


Figure VII-9. Cell viability and morphology of PCL and PCLFu ANFM . A) Viability of endothelial cells on ANFMs over 1, 3 and 7 days, as the percentage of methabolic activity in respect to control (cells in PCL ANFM). Data were considered statistically different if: (*) $p \leq 0.05$, (**) $p \leq 0.01$ and (****) $p \leq 0.0001$. B) SEM observations of endothelial cells

cultured onto PCL, PCLFA, and PCLFF nanofibrous meshes. Scale bar: 50µm for the main images and 10 µm for the insert images

VII-4.2. Angiogenic potential of airbrush nanofibrous using CAM assay

CAM assay has been proposed to evaluate the biocompatibility of biomaterials and, in particular, their angiogenic potential [63]. Based on the cell viability results, the PCLFF was selected for the angiogenesis test, as was the one in which endothelial cells showed higher viability and proliferation. The CAM assay was herein conducted to evaluate *in vivo* ability of PCL and PCLFF to induce angiogenesis. **Figure VII - 10A** shows the photographs of the chorionic and allantoic epithelium of the excised CAM sections after 5 days of implantation. Eggs without ANFM were used as control. The pro-angiogenic response of ANFM was evaluated by micro vascularity formation at adjacent tissues to the samples onplantation, which is higher for PCLFF as compared to PCL **(Figure VII - 10A)**. To quantify the convergence of blood vessels towards the onplanted ANFM, the vascular length density and vascular density were investigated by analyzing the *ex ovo* chorionic epithelium **Figure VII - 10B**. The maximum growth of blood vessels around and inside the ANFM was estimated by counting the total number of macroscopic microvascular that converge toward the graft in PCLFF **(Figure VII – 10 b1).** There was not a significant difference between samples. *In ovo* allantoic epithelium **(Figure VII - 10 b2 and b3)** was used to quantify the blood vessels, the vascular length density, and vascular density. PCLFF showed a higher number of blood vessels, vascular length, vascular density, and statistically significant pro-angiogenic property compared to the PCL and the control CAM. Furthermore, there was no statistical significance between PCL and control CAM. Considering those results, it is clear that the PCLFF was the most pro-angiogenic one. In the literature, some studies report the pro-angiogenic property of fucoidan [37,38]. Some authors reported that pro-angiogenic property of fucoidan is related to structural factors such as Mw, sulfation degree, and its ability to modulate heparin-binding growth factors such as FGF-2, but the relationship between fucoidan chemical structure and effect on the formation of new vessels is not yet established [37,38,64]. We have shown, by using the CAM assay, that the developed PCLFF can promote pro-angiogenesis, which could help support implants' integration and vascularization. Both are critical factors in transplantation, avoiding delays on blood supply and oxygenation/nutrients and overcoming the rejection of the transplant.

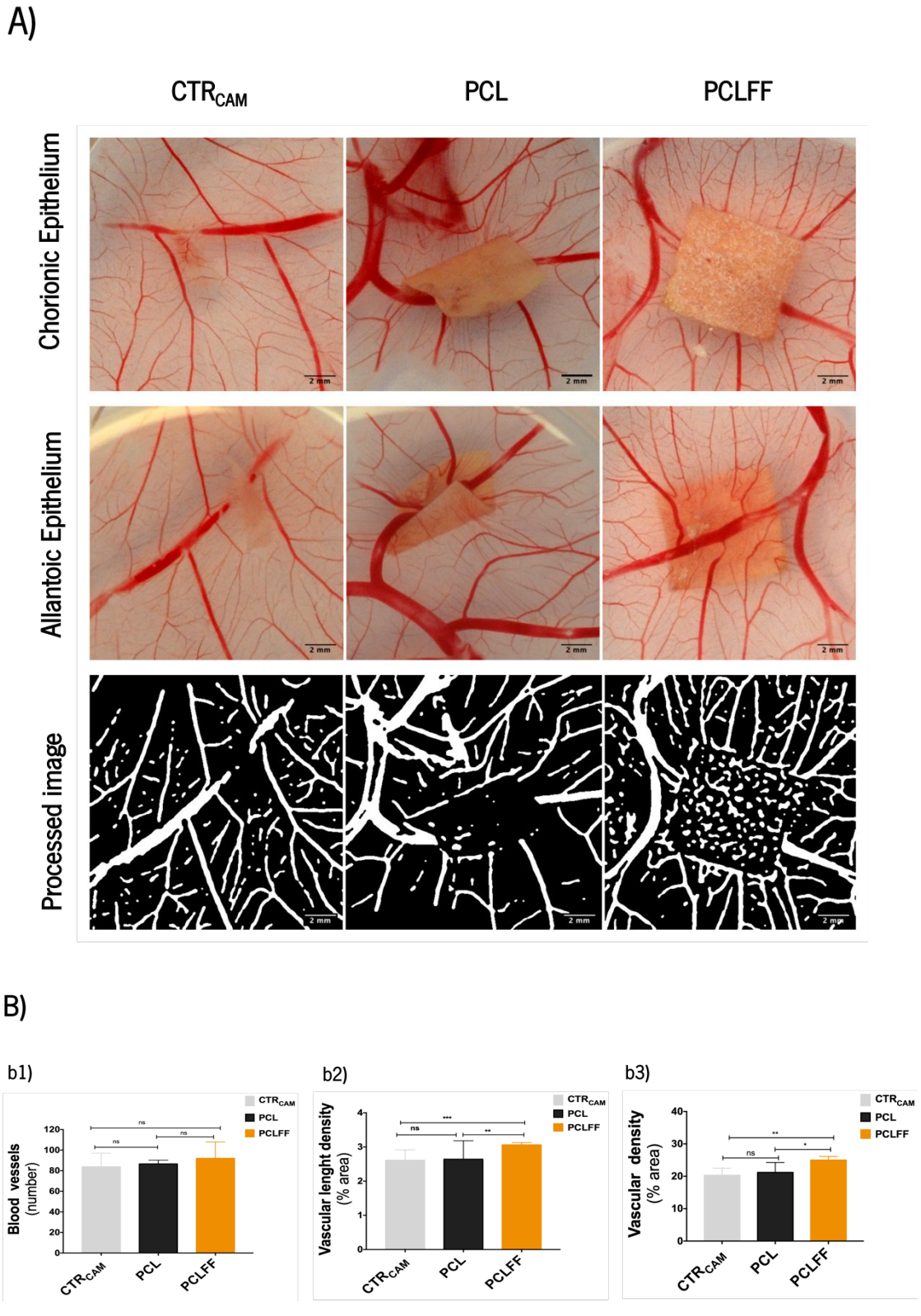


Figure VII-10. Characterization of angiogenic potential of ANFM using CAM assay. A) Stereomicroscope photographs of ex ovo ANFM after incubation on the chorioallantoic membrane of the chick embryo, scale bar: 2 mm. B) Macroscopic quantification of blood vessels converging towards implanted structures (b1). Vascular Length Density (i. e. ratio of

skeletonized vasculature area to total area) (b2), and Vascular Density (i.e. ratio of vasculature area to total selection area) (b3). Data was considered statistically different if: (*) $p \leq 0.05$, (**) $p \leq 0.01$ and (***) $p \leq 0.001$.

VII-5. CONCLUSION

Fucoidan, a marine sulfated polysaccharide, blended with the biodegradable polymer PCL, was successfully airbrushed into a nanofibrous mesh, as illustrated by EDS and XPS analysis. The incorporation of fucoidan had clear impact on the properties of the meshes, namely an increase in the average fiber diameter and increased hydrophilicity of ANFM. We also showed that PCL and PCL/Fu could support endothelial cells adherence and growth, from which PCLFF stands out as the one with better results. Moreover, in vivo test of PCLFF exhibited higher pro-angiogenic properties comparing with PCL ANFM. Altogether, the results support our hypothesis that the incorporation of a marine polysaccharide, fucoidan (Fu), would have a positive impact on the hydrophobicity and mechanical properties, of the developed membranes. Moreover, the use of a higher sulfated fucoidan (FF) with larger molecular weight resulted in a functional ANFM exhibiting pro-angiogenic effect. This suggests the further testing of the airbrushed PCLFF nanofibrous mesh as a biomaterial substrate to promote vascularization, namely aiming to improve integration of the so developed implant in host tissue.

VII-6. ACKNOWLEDGEMENTS

This work is partially funded by Northern Portugal Regional Operational Programme (NORTE 2020), under the Portugal 2020 Partnership Agreement, through Structured projects NORTE-01-0145-FEDER-000021 and NORTE-01-0145-FEDER-000023. Financial support from Portuguese Foundation for Science and Technology (FCT) is also acknowledged through PhD fellowship SFRH/BD/112139/2015 and R&D&I projects PTDC/CTM-CTM/29813/2017 and PTDC/BII-BIO/31570/2017. The authors are thankfull to Dr Luisa Rodrigues for the XPS analysis and Dr Catarina Vale for the DMA analysis.

VII-7. REFERENCES

[1] Behrens AM, Casey BJ, Sikorski MJ, Wu KL, Tutak W, Sandler AD, et al. *In Situ Deposition of PLGA Nanofibers via Solution Blow Spinning*.ACS Macro Lett 2014. 3(3):249–54.

[2] Khil M-S, Cha D-I, Kim H-Y, Kim I-S, Bhattarai N. *Electrospun nanofibrous polyurethane membrane as wound dressing*.J Biomed Mater Res Part B Appl Biomater 2003. 67B(2):675–9.

[3] Wang Z-G, Wan L-S, Liu Z-M, Huang X-J, Xu Z-K. *Enzyme immobilization on electrospun polymer nanofibers: An overview*.J Mol Catal B Enzym 2009. 56(4):189–95.

[4] Hwang PTJ, Lim D-J, Fee T, Alexander GC, Tambralli A, Andukuri A, et al. *A bio-inspired hybrid nanosack for graft vascularization at the omentum*.Acta Biomater 2016. 41:224–34.

[5] Buitinga M, Truckenmüller R, Engelse MA, Moroni L, Ten Hoopen HWM, van Blitterswijk CA, et al. *Microwell Scaffolds for the Extrahepatic Transplantation of Islets of Langerhans*.PLoS One 2013. 8(5):e64772.

[6] Wang K, Wang X, Han C, Hou W, Wang J, Chen L, et al. *From Micro to Macro: The Hierarchical Design in a Micropatterned Scaffold for Cell Assembling and Transplantation*.Adv Mater 2017. 29(2):1604600.

[7] Oliveira C, Soares AI, Neves NM, Reis RL, Marques AP, Silva TH, et al. *Fucoidan Immobilized at the Surface of a Fibrous Mesh Presents Toxic Effects over Melanoma Cells, But Not over Noncancer Skin Cells*.Biomacromolecules 2020. 21(7):2745–54.

[8] Casanova MR, Oliveira C, Fernandes EM, Reis RL, Silva TH, Martins A, et al. *Spatial immobilization of endogenous growth factors to control vascularization in bone tissue engineering*.Biomater Sci 2020. 8(9):2577–89.

[9] Sobreiro-Almeida R, Fonseca DR, Neves NM. *Extracellular matrix electrospun membranes for mimicking natural renal filtration barriers*.Mater Sci Eng C 2019. 103:109866.

[10] Bacelo E, Alves da Silva M, Cunha C, Faria S, Carvalho A, Reis RL, et al. *Biofunctional Nanofibrous Substrate for Local TNF-Capturing as a Strategy to Control Inflammation in Arthritic Joints*.Vol. 9, Nanomaterials . 2019.

[11] Tutak W, Sarkar S, Lin-Gibson S, Farooque TM, Jyotsnendu G, Wang D, et al. *The support of bone marrow stromal cell differentiation by airbrushed nanofiber scaffolds*.Biomaterials 2013.

34(10):2389–98.

[12] Srinivasan S, Chhatre S, Mabry J, Cohen R, Mckinley G. *Solution Spraying of Poly(methyl methacrylate) Blends to Fabricate Micro-textured, Superoleophobic Surfaces (PREPRINT)*.Polymer (Guildf) 2011. 52:3209–18.

[13] Medeiros ES, Glenn GM, Klamczynski AP, Orts WJ, Mattoso LHC. *Solution blow spinning: A new method to produce micro- and nanofibers from polymer solutions*.J Appl Polym Sci 2009. 113(4):2322–30.

[14] Oliveira JE, Moraes EA, Costa RGF, Afonso AS, Mattoso LHC, Orts WJ, et al. *Nano and submicrometric fibers of poly(D,L-lactide) obtained by solution blow spinning: Process and solution variables*.J Appl Polym Sci 2011. 122(5):3396–405.

[15] Oliveira JE, Mattoso LHC, Orts WJ, Medeiros ES. *Structural and Morphological Characterization of Micro and Nanofibers Produced by Electrospinning and Solution Blow Spinning: A Comparative Study*.Lejcek P, editor. Adv Mater Sci Eng 2013. 2013:409572.

[16] Sinha-Ray S, Yarin AL, Pourdeyhimi B. *The production of 100/400nm inner/outer diameter carbon tubes by solution blowing and carbonization of core–shell nanofibers*.Carbon N Y 2010. 48(12):3575–8.

[17] Sinha-Ray S, Zhang Y, Yarin AL, Davis SC, Pourdeyhimi B. *Solution Blowing of Soy Protein Fibers*.Biomacromolecules 2011. 12(6):2357–63.

[18] Zhuang X, Yang X, Shi L, Cheng B, Guan K, Kang W. *Solution blowing of submicron-scale cellulose fibers*.Carbohydr Polym 2012. 90(2):982–7.

[19] Kikionis S, Ioannou E, Toskas G, Roussis V. *Electrospun biocomposite nanofibers of ulvan/PCL and ulvan/PEO*.J Appl Polym Sci 2015. 132(26).

[20] Agarwal S, Wendorff JH, Greiner A. *Use of electrospinning technique for biomedical applications*.Polymer (Guildf) 2008. 49(26):5603–21.

[21] Singh R, Ahmed F, Polley P, Giri J. *Fabrication and Characterization of Core–Shell Nanofibers Using a Next-Generation Airbrush for Biomedical Applications*.ACS Appl Mater Interfaces 2018. 10(49):41924–34.

[22] Santos AMC, Medeiros ELG, Blaker JJ, Medeiros ES. *Aqueous solution blow spinning of poly(vinyl alcohol) micro- and nanofibers*.Mater Lett 2016. 176:122–6.

[23] Kim GJ and GH. *Rapid-prototyped PCL/fucoidan composite scaffolds for bone tissue regeneration: design, fabrication, and physical/biological properties*.J Mater Chem 2011. 21(1):17710–8.

[24] Lee JS, Jin GH, Yeo MG, Jang CH, Lee H, Kim GH. *Fabrication of electrospun biocomposites comprising polycaprolactone/ fucoidan for tissue regeneration*.Carbohydr Polym 2012. 90:181–8.

[25] Li R, Li Z, Yang R, Yin X, Lv J, Zhu L, et al. *Polycaprolactone/poly(L-lactic acid) composite micro/nanofibrous membrane prepared through solution blow spinning for oil adsorption*.Mater Chem Phys 2020. 241:122338.

[26] Glowacki J, Mizuno S. *Collagen scaffolds for tissue engineering*.Biopolymers 2008. 89(5):338–44.

[27] Chakraborty S, Liao I-C, Adler A, Leong KW. *Electrohydrodynamics: A facile technique to fabricate drug delivery systems*.Adv Drug Deliv Rev 2009. 61(12):1043–54.

[28] Yu C-C, Chang J-J, Lee Y-H, Lin Y-C, Wu M-H, Yang M-C, et al. *Electrospun scaffolds composing of alginate, chitosan, collagen and hydroxyapatite for applying in bone tissue engineering*.Mater Lett 2013. 93:133–136.

[29] Oliveira C, Neves NM, Reis RL, Martins A, Silva TH. *A review on fucoidan antitumor strategies: from a biological active agent to a structural component of fucoidan-based systems*.Carbohydr Polym 2020. :116131.

[30] Reys LL, Silva SS, Soares da Costa D, Oliveira NM, Mano JF, Reis RL, et al. *Fucoidan Hydrogels Photo-Cross-Linked with Visible Radiation As Matrices for Cell Culture*.ACS Biomater Sci Eng 2016. 2(7):1151–61.

[31] Sezer A, Cevher E. *Fucoidan: A Versatile Biopolymer for Biomedical Applications*.In: Zilberman M, editor. 2011. Springer Berlin Heidelberg; 2011. p. 377–406.

[32] Mourão A., S. P. *Use of sulfated fucans as anticoagulant and antithrombotic agents: future perspectives*.Curr Pharm Des 2004. (10):967–81.

[33] Oliveira C, Ferreira AS, Novoa-Carballal R, Nunes C, Pashkuleva I, Neves NM, et al. *The Key Role of Sulfation and Branching on Fucoidan Antitumor Activity*.Macromol Biosci 2017. 17(5):1600340-n/a.

[34] Wang J, Jin W, Zhang W, Hou Y, Zhang H, Zhang Q. *Hypoglycemic property of acidic polysaccharide extracted from Saccharina japonica and its potential mechanism*.Carbohydr Polym 2013. 95(1):143–7.

[35] Huang L, Wen K, Gao X, Liu Y. *Hypolipidemic effect of fucoidan from Laminaria japonica in hyperlipidemic rats*.Pharm Biol 2010. 48(4):422–6.

[36] Wang J, Zhang Q, Zhang Z, Li Z. *Antioxidant activity of sulfated polysaccharide fractions extracted from Laminaria japonica*.Int J Biol Macromol 2008. 42(2):127–32.

[37] Ustyuzhanina NE, Bilan MI, Ushakova NA, Usov AI, Kiselevskiy M V, Nifantiev NE. *Fucoidans: Pro- or antiangiogenic agents?*Glycobiology 2014. 24(12):1265–74.

[38] Wang Y, Xing M, Cao Q, Ji A, Liang H, Song S. *Biological Activities of Fucoidan and the Factors Mediating Its Therapeutic Effects: A Review of Recent Studies*.Mar Drugs 2019. 17(3):183.

[39] Ale MT, Mikkelsen JD, Meyer AS. *Important Determinants for Fucoidan Bioactivity: A Critical Review of Structure-Function Relations and Extraction Methods for Fucose-Containing Sulfated Polysaccharides from Brown Seaweeds*.Mar Drugs 2011. 9(10):2106.

[40] Li B, Lu F, Wei X, Zhao R. *Fucoidan: Structure and bioactivity.*Molecules 2008. 13:1671–95.

[41] Silva TH, Alves A, Popa EG, Reys LL, Gomes ME, Sousa RA, et al. *Marine algae sulfated polysaccharides for tissue engineering and drug delivery approaches*.Biomatter 2012. 2(4):278–89.

[42] S. Uday Kumar, Kumar U. *Electrospun fucoidan loaded PCL/PEO nanofiber scaffolds for small diameter vascular grafts*.Masther Thesis, Indian Institute of Technology Roorkee, India; 2012.

[43] Mishra NC, Kumar SU, Jayaganthan R. *Fucoidan Loaded PCL-PEO Nanofibrous Scaffold for Small Diameter Vascular Graft - a Solution to Intimal Hyperplasia*.In: 2012. 2012.

[44] Saboural P, Chaubet F, Rouzet F, Al-Shoukr F, Azzouna R Ben, Bouchemal N, et al. *Purification of a low molecular weight fucoidan for SPECT molecular imaging of myocardial infarction.*Mar Drugs 2014. 12(9):4851–67.

[45] Castle JE. *Practical surface analysis by Auger and X-ray photoelectron spectroscopy. D. Briggs and M. P. Seah (Editors). John Wiley and Sons Ltd, Chichester, 1983, 533 pp., £44.50*.Surf Interface Anal 1984. 6(6):302.

[46] Rodrigues LC, Silva SS, Reis RL. *Acemannan-based films: an improved approach envisioning biomedical applications*.Mater Res Express 2019. 6(9):95406.

[47] Jeong J-O, Jeong SI, Park J-S, Gwon H-J, Ahn S-J, Shin H, et al. *Development and characterization of heparin-immobilized polycaprolactone nanofibrous scaffolds for tissue engineering using gamma-irradiation*.RSC Adv 2017. 7(15):8963–72.

[48] Yao Y, Zaw AM, Anderson DEJ, Hinds MT, Yim EKF. *Fucoidan functionalization on poly(vinyl alcohol) hydrogels for improved endothelialization and hemocompatibility.*Biomaterials 2020. 249:120011.

[49] Ribatti D, Nico B, Vacca A, Presta M. *The gelatin sponge-chorioallantoic membrane assay.*Nat Protoc 2006. 1(1):85–91.

[50] Oliveira C, Granja S, Neves NM, Reis RL, Baltazar F, Silva TH, et al. *Fucoidan from Fucus vesiculosus inhibits new blood vessel formation and breast tumor growth in vivo.*Carbohydr Polym 2019. 223:115034.

[51] Nowak-Sliwinska P, Ballini J-P, Wagnières G, van den Bergh H. *Processing of fluorescence angiograms for the quantification of vascular effects induced by anti-angiogenic agents in the CAM model.*Microvasc Res 2009. 79(1):21–8.

[52] Moreno-Jiménez I, Hulsart-Billstrom G, Lanham SA, Janeczek AA, Kontouli N, Kanczler JM, et al. *The chorioallantoic membrane (CAM) assay for the study of human bone regeneration: a refinement animal model for tissue engineering.*Sci Rep 2016. 6(1):32168.

[53] Li L, Qian Y, Jiang C, Lv Y, Liu W, Zhong L, et al. *The use of hyaluronan to regulate protein adsorption and cell infiltration in nanofibrous scaffolds.*Biomaterials 2012. 33(12):3428–45.

[54] Chandrasekaran AR, Venugopal J, Sundarrajan S. *Fabrication of nanofibrous scaffold with improved bioactivity for cultured of human dermal fibroblast for skin regeneration.*Biomed Mater 2011. 6:15001.

[55] Kim GJ and GH, Gyuhyun Hyung, Kim; JG. *Rapid-prototyped PCL/fucoidan composite scaffolds for bone tissue regeneration: design, fabrication, and physical/biological properties.*J Mater Chem 2011. 21(1):17710–8.

[56] Cunha L, Grenha A. *Sulfated Seaweed Polysaccharides as Multifunctional Materials in Drug Delivery Applications.*Mar Drugs 2016. 14(3):42.

[57] Roosa SMM, Kemppainen JM, Moffitt EN, Krebsbach PH, Hollister SJ. *The pore size of polycaprolactone scaffolds has limited influence on bone regeneration in an in vivo model.*J Biomed Mater Res Part A 2010. 92A(1):359–68.

[58] Silva JM, Duarte ARC, Caridade SG, Picart C, Reis RL, Mano JF. *Tailored Freestanding Multilayered Membranes Based on Chitosan and Alginate.*Biomacromolecules 2014. 15(10):3817–26.

[59] Caridade S, Merino E, Alves N, Mano JF. *Bioactivity and Viscoelastic Characterization of Chitosan/Bioglass® Composite Membranes.*Macromol Biosci 2012. 12:1106–13.

[60] Kim J-J, Singh RK, Seo S-J, Kim T-H, Kim J-H, Lee E-J, et al. *Magnetic scaffolds of polycaprolactone with functionalized magnetite nanoparticles: physicochemical, mechanical, and biological properties effective for bone regeneration.*RSC Adv 2014. 4(33):17325–36.

[61] Wu LC, Yang J, Kopeček J. *Hybrid hydrogels self-assembled from graft copolymers containing complementary β-sheets as hydroxyapatite nucleation scaffolds*.Biomaterials 2011. 32(23):5341–53.

[62] Sridharan G, Shankar A. *Toluidine blue: A review of its chemistry and clinical utility*.J Oral Maxillofac Pathol 2012. 16:251–5.

[63] Carleton HM (Harry M. *Carleton's Histological technique*.Drury RAB (Roger AB, Wallington EA, editors. Oxford ; New York: Oxford University Press; 1980.

[64] Phipps MC, Clem WC, Catledge SA, Xu Y, Hennessy KM, Thomas V, et al. *Mesenchymal stem cell responses to bone-mimetic electrospun matrices composed of polycaprolactone, collagen I and nanoparticulate hydroxyapatite*.PLoS One 2011. 6(2):e16813–e16813.

[65] Aldemir Dikici B, Dikici S, Reilly GC, MacNeil S, Claeyssens F. *A Novel Bilayer Polycaprolactone Membrane for Guided Bone Regeneration: Combining Electrospinning and Emulsion Templating*.Mater (Basel, Switzerland) 2019. 12(16):2643.

[66] Matou S, Helley D, Chabut D, Bros A, Fischer AM. *Effect of fucoidan on fibroblast growth factor-2-induced angiogenesis in vitro*.Thromb Res 2002. 106:213–21.

Chapter VIII

Fucoidan hydrogels significantly alleviated oxidative stress and enhance the endocrine function of encapsulated beta cells

Chapter VIII

Fucoidan hydrogels significantly alleviate oxidative stress and enhance the endocrine function of encapsulated beta cells[6]

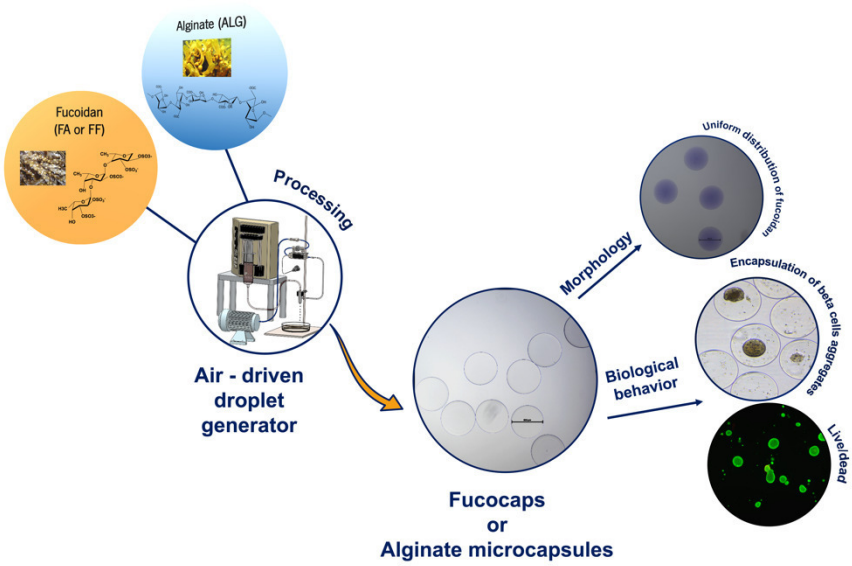
ABSTRACT

Microencapsulating pancreatic islets in immunoprotective alginate hydrogels is a promising strategy for treatment of type 1 diabetes. However, this strategy is limited by inflammation and hypoxia mediated oxidative stress, due to encapsulation and the hydrogel itself, leading to impaired insulin secretion and limited short and long term cell survival. We report on the anti-oxidant effect of fucoidan, an algae derived polysaccharide, on beta cells, and how it positively affects encapsulated beta cell viability and function. Fucoidan from *Fucus vesiculosus* (FF) exhibits a high total antioxidant capacity, and free radical scavenging activity, and is able to significantly alleviate intracellular oxidative stress in INS1E beta cells. In addition, FF significantly increases insulin secretion in a dose- and time-dependent manner. When FF is incorporated in ultrapure alginate used for microencapsulation of primary rat islets, both viability and glucose responsiveness of rat islets in these socalled Fucogel microcapsules (Fucocaps) were found to be significantly higher compared to islets encapsulated in alginate alone. Similar results were obtained with INS1E pseudo-islets and neonatal pig islets. Fucocaps can provide a redox-modulatory niche and an immune barrier for islets and beta cells in the same time leading to significantly improved survival and endocrine function by mitigating oxidative stress.

[6] This chapter is based on the following publication:

Reys. L. L., Vaithilingam V., Sthijns M.M.J.P.E. , Soares E., de Vries R. , Mohammed S., de Bont D., Jetten M., Hermanns C., Paulino da Silva Filho O., Stell A. , Mourad NI, Gianello P, LaPointe V. L.S., Silva S. S., Reis R. L., Silva T.H. and van Apeldoorn A. A., *"Fucoidan hydrogels significantly alleviate oxidative stress and enhance the endocrine function of encapsulated beta cells"* accepted for publication on Advanced Functional Materials, 2021.

VIII-1. GRAPHICAL ABSTRACT



VIII-2. INTRODUCTION

Type 1 diabetes (T1D) is an autoimmune disorder, hallmarked by specific destruction of the insulin producing beta cells in the pancreatic islets leading to poor glycemic control. Type 1 diabetes is typically treated by exogenous insulin administration (either through injections or pumps), accompanied with regular blood glucose checks via fingerpricks multiple times a day. Although most patients can cope relatively well with their diabetes, exogenous insulin can not fully compensate for the natural blood glucose regulation by beta cells, wich ultimately leads to long term complications, such as vascular damage, neuropathy, loss of sight and kidney failure [1]. The best way to prevent these complications, and restore the natural blood glucose homeostasis is by replacing the patient's lost beta cell mass. Pancreatic islet transplantation, or clinical islet transplantation, is an interesting treatment option for patients with severe type 1 diabetes, involving the infusion of human donor islets into the hepatic portal vein accompanied with immunosuppresive therapy [2]. Although effective, the intervention is not very efficient, ~ 60% of the islets are lost in the first two weeks after transplantation. This is caused by multifactorial reaction, such as impaired revacularisation, high concentrations of lipids and glucose, an immediate blood mediated inflammatory response, allo- and auto-immune rejection, and high concentrations of immunosuppressive

drugs causing stress in beta cells [2]. Commonly patients need to be transplanted multiple times before insulin independence is achieved.

The use of immunospressive drugs can potentially be omitted by encapsulating the islets in an immunoprotective envelope to block the recipent's immune cells from directly interacting with the donor cells. The envelope typically consists of a nanoporous polymer membrane or a hydrogel, such as alginate, in which the pancreatic islets are embedded prior to transplantation. Alginate microcapsules allow for the diffusion of nutrients, oxygen and metabolites to and from the encapsulated cells while acting as an immunoprotective barrier to prevent the interaction of immune cells and limit diffusion of large molecular weight antibodies [3]. In most preclinical studies microencapsulated islets are transplanted into the peritoneal cavity and have been shown to reverse diabetes in various small and large *in vivo*, allo- and xeno- transplantation models with variable success rates [4]. Phase 1 clinical trials demonstrated that the use of microencapsulated human islets was safe but, could only provide a minor clinical benefit due to poor graft survival [5,6]. The most important factor contributing to encapsulated islet graft failure are, a hindered oxygen and nutrient supply due to the barrier function of the capsule, sometimes aggravated by foreign body response to the implant causing fibrosis, a combined effect leading to hypoxia mediated cell damage and long term graft failure [3]. Native islets residing within the pancreas are highly vascularized microtissues and receive ample oxygen (pO_2 of 40 mmHg) and nutrient supply [7]. During the isolation process this dense vascular network is destroyed and the islets are removed from their pancreatic niche leading to significant post-isolation cell stress. The encapsulation process further enhances this effect since it prevents revascularization, while biomaterials used for encapsulation can potentially induce significant amounts of oxidative stress in both beta and alpha cells [8]. The absence of revascularization and a limited mass transport lead to ultimately to irreversible chronic hypoxia induced oxidative stress. Although microencapsulation is able to block immune cells and large antibodies, smaller molecules such as chemokines, cytokines, and reactive oxygen species (ROS), can easily permeate through the microcapsule's hydrogel network [9]. Some of these small molecules are also produced by islets themselves in response to various stress stimuli further aggrevating the unfavorable conditions [10]. It has been shown that ROS such as H_2O_2 and superoxide radicals, can not only negatively impact insulin secretion, but also activate beta cell specific autoreactive T cell subsets, which play an important role in beta cell destruction [11–14]. Oxidative stress occurs when there is an imbalance between the production of reactive oxygen species and antioxidant defences in the cell leading to tissue damage [15]. It has been

shown that beta cells are highly susceptible to oxidative stress and vulnerable to ROS mediated damage, due to their low intrinsic intracellular levels of antioxidant enzymes such as superoxide dismutase (SOD), catalase, and glutathione peroxidase (Gpx-1) [16]. Strategies to mitigate oxidative stress potentially improve encapsulated islet function and survival leading to better *in vivo* outcomes.

Several strategies have been investigated to protect encapsulated islets from oxidative stress induced cell death. It has been shown that entrapping a natural antioxidant curcumin within a polymer matrix can reduce oxidative stress and support insulin secretion in encapsulated rat islets [17]. Studies have demonstrated the benefit of incorporating tannic acid in microcapsules to scavenge ROS and suppress the production of pro-inflammatory cytokines leading to improved encapsulated islet survival and function [18,19]. In the last decade a number of different brown seaweed derived sufated polysaccharides called fucoidan have been described to posses high antioxidant capacity [20]. The molecular weight of fucoidan influences its hydroxyl radical scavenging activity and reduction potential [21]. Apart from their anti-oxidant activity, fucoidan also possesses anti-inflammatory properties, and is known to suppress mechanistic events of inflammation via activation of NF-kβ, generation of reactive oxygen species (ROS), and upregulation of proinflammatory cytokines and associated cell adhesion molecules [22].

Here we report about the effect of fucoidan on islets and beta cells when used in an alginate based microencapsulation strategy. We compared fucoidan obtained from two different algae species *Fucus vesiculosus* (FF) and *Ascophylum nodosum* (FA) (with varying molecular weights), and determined their potency to alleviate oxidative stress *in vitro*. We show that fucoidan obtained from FF has not only very high antioxidant capacity, but is also able to significantly decrease oxidative stress in islets and beta cells exposed to oxidative stress conditions. In addition, incorporation of FF fucoidan in alginate microcapsules has no detrimental effect on mass transport, nor the mesh size of ultrapure alginate hydrogels, and leads to a significant increase in cell survival and insulin secretion in primary islets and beta cells from different species.

VIII-3. MATERIALS AND METHODS

VIII-3.1. Fucoidans

Commercially sourced fucoidan extracts isolated from two species of brown algae *Fucus vesiculosus* (*FF*) (Maritech Fucoidan, Marinova, batch # FVF2011527, Australia) and *Ascophyllum nodosum (FA)* (Ascophycient, Algues & Mer, batch # ASPHY16241, France), were purified using calcium acetate in order to reduce the natural heterogeneity and to get a more purified fucoidan fraction [23].

VIII-3.2. Purification of fucoidans

Fucoidan was purified using calcium acetate in order to reduce the natural heterogeneity and to get a more purified fraction [23]. Briefly, both FA and FF extracts were dissolved (160 mg ml^{-1}) in 20mM calcium acetate, maintained and stirred for 4h at 55°C with constant pH adjustment between 6.6 and 7.5; followed by overnight cooling at 4°C and centrifugation for 15 min at 5000 rpm (Centrifuge 5810, Eppendorf, Germany). The resulting supernatant was dialyzed against water using 12-14 kDa cut-off dialysis membranes and freeze-dried (CryoDos-80, Telstar, Spain). The purified fractions of both FF and FA were used for subsequent characterization and encapsulation studies.

VIII-3.3. Cell Culture

a) Rat β-cell (INS1E) culture

INS1E β-cells, derived from rat insulinoma (AddexBio, USA) were cultured in RPMI 1640 (Gibco) supplemented with 5% (v/v) fetal bovine serum, 100 U mL^{-1} penicillin and 100 mg mL^{-1} streptomycin, 1mM sodium pyruvate and 10 mM HEPES. For cell expansion, 2-mercaptoethanol was added fresh to the culture to a final concentration of 1 µl mL^{-1} medium. Medium was refreshed every 2–3 days.

b) INS1E pseudoislet generation and culture

Non-adherent agarose microwell chips were aseptically fabricated as described previously [24]. Briefly, microwell chips containing 1585 microwells with a diameter of 400 µm were fabricated by pouring a 3% (w/v) Ultrapure™ agarose (Invitrogen, Bleiswijk, The Netherlands) solution on negative molds of polydimethylsiloxane (PDMS) on 6 well plates. After agarose solidification, the molds were removed and chips transferred to 12 well plates, covered with PBS and stored at 4 °C until usage. Before cell seeding, the agarose chips were pre-incubated in culture medium overnight at 37 °C. For cell aggregate formation, single cells were resuspended in fresh medium and seeded onto agarose chips at a concentration of 800,000 cells per agarose chip. Immediately after seeding, agarose chips were briefly centrifuged for 1 min at 200 rpm to allow the cells to settle down in the microwells. The medium was refreshed every 1–2 days. The pseudoislets were cultured up to 4 days after which they were harvested from the chips by upside down centrifugation (1 min @ 200rpm) and gently rinsing with medium and collected for further studies. The average pseudoislet diameter, was measured using light microscopy and ImageJ software [24]

c) Primary rat islet isolation and culture

Pancreatic islets from male Lewis rats (> 10 weeks) were isolated by ductal perfusion of collagenase (0.25 mg ml^{-1}) (Liberase TL Research grade, Roche Diagnostics GmbH, Germany) as described previously [25], followed by purification on Ficoll-Paque Plus (GE Healthcare, Merck, Netherlands) and separated from unwanted tissue debris using a stereomicroscope. The isolated islets were then cultured for 48 h in RPMI 1640 medium (Life Technologies, The Netherlands) supplemented with penicillin and streptomycin and 10% foetal bovine serum (FBS) in an incubator at 37°C supplied with 5% CO2 in air before being encapsulated. The purity of the islets was assessed by dithizone (Sigma-Aldrich, The Netherlands) staining and found to be >95%. All animal experimental procedures were approved by the Dutch ethical committee on animal experimentation (CCD) and the institute's Animal Care and Ethics Committee at Maastricht University (IVD).

d) Neonatal pig islet isolation and culture

All neonatal pig studies were conducted in accordance with the local ethical committee and with EU Directive 2010/63/EU for animal experiments. Piglets (Belgian landrace; 3-8 kg) were directly delivered to the islet isolation facility in Brussels. Neonatal pancreatic islet isolation was carried out as previously described [26]. Briefly, the harvested neonatal pig pancreas was cut into small pieces and transferred to a 50 ml tube. The pancreas was then washed twice with 30 ml of ice cold supplemented HBSS (10 mM Hepes, 100 U/mL Penicillin-streptomycin, 10 mM Glucose, 0.075% Amphotericin B, 0.25% BSA) with each time allowing the pancreatic tissue to sediment and removing the supernatant with debris and fatty tissues. After washing, collagenase V (Sigma-Aldrich, Belgium) (10 mg dissolved in 5 ml HBSS) was added, and the pancreas digested by manual shaking for 20 min at 37°C followed by addition of 40 ml of cold HBSS to stop the digestion process. Wash the pancreas 3 times by filtering the preparation on a sterile 500 μM mesh and suspend the filtered pancreas in supplemented HAM F10 medium. Neonatal pig islets (NPI) were cultured in HAM-F10 culture medium supplemented with 0.5% BSA, 50 μmol/L IBMX (3-isobutyl-1-methylxanthine), 10 mmol/L glucose, 2 mmol L^{-1} glutamine, 10 mmol L^{-1} nicotinamide, 1% penicillin, and 1% streptomycin during a period of 8 days to allow maturation of islet cells and removal of exocrine tissue as previously described before encapsulation [26].

VIII-3.4. Cytotoxicity assay

INS1E cells were seeded at 2×10^4 cells/well (96-well plate) for 24 hr at 37 °C in RPMI media (supplemented with 5% fetal bovine serum, 100 U mL^{-1} penicillin and 100 mg mL^{-1} streptomycin, 1mM sodium pyruvate and 10 mM HEPES). Thereafter, the media was removed, cells washed twice in serum free medium (SFM) before the addition of test samples FF and FA fucoidan in SFM in concentrations ranging from 0.15–100 mg ml^{-1}. Solutions of 5% PBS and 5% DMSO were prepared in SFM and used as negative and positive controls respectively. Test samples and controls were incubated with INS1E cells (100 μl/well in triplicates) for 24 hr, and cell viability measured by MTT (0.5 mg ml^{-1}) for the final 4 hr of the culture period. The resultant insoluble formazan product was solubilised with DMSO and absorbance measured at 540 nm. Cell viability was expressed as a percentage of SFM incubated cells. A reduction of cell viability to < 70% as compared to SFM control medium alone was regarded as cytotoxic. The

cytotoxicity assay was carried out as per ISO10993-5 "Biological evaluation of medical devices – Part 5: Tests for in vitro cytotoxicity".

VIII-3.5. Physico-chemical characterization of fucoidans

a) NMR Spectroscopy

Purified fucoidan fractions from both FF and FA were characterized by ^{1}HNMR spectroscopy. ^{1}HNMR spectra of FA and FF fucoidan dissolved (5 mg ml^{-1}) in deuterated water (D_2O), were recorded with a Burker Avance III 300 Hz at 90° impulses and 4s acquisition time. The resulting spectra were processed and analysed using Mnova v 14.1.0 software (Mestrelab research).

b) Quantification of carbohydrates

Total carbohydrate analysis in purified FF and FA fucoidan was determined as described elsewhere [27,28]. Briefly, a pre-hydrolysis of fucoidan was performed with 72% sulfuric acid for 3 h at room temperature followed by complete hydrolysis with sulfuric acid 1M at 100°C for 2.5 h. Monosaccharides in the hydrolysates were reduced with sodium borohydride and acetylated by acetic anhydride using methylimidazole as a catalyst. The formed alditol acetate derivatives were analyzed by gas chromatography (GC) using a 30 m column DB-225 (J&W Scientific, Folsom, CA, USA), internal diameter, and film thickness of 0.25 and 0.15 mm, and a flame ionization detector (Perkin Elmer, Clarus 400). The hydrolysis of all samples was performed in duplicate, and each sample was injected twice. 2-Deoxyglucose (Alfagene, Portugal) was used as an internal standard. Uronic acids were quantified by a modification of the 3-phenylphenol colorimetric method [27,28]. A calibration curve was made with d-galacturonic acid. The hydrolysis and analysis of the samples was done in triplicates.

c) Quantification of sulphate content

The quantification of sulphates in purified fucoidan was performed as described previously [29]. Briefly, conditioning reagent composed by a mixing of 10 mL glycerol, 6 mL concentrated hydrochloric acid (HCl), 60 mL deionized water, and 20 mL isopropyl alcohol, and sodium chloride was prepared (Sigma-Aldrich, Portugal). The conditioning reagent was stirred at room temperature overnight. Four

replicate samples were prepared by weighing 10 mg ml^{-1} of dried fucoidan into separate closed test tubes containing 2 mL 4 M hydrochloric acid (HCl). Samples were subjected to acid hydrolysis for 2 hours at 100°C. A solution of potassium sulphate standards with concentrations ranging from 200-1000 µg mL^{-1} was prepared. Barium chloride ($BaCl_2$) (0.3 g ml^{-1}) (Sigma -Aldrich, Portugal) was added, stirred for exactly 1 min and then left standing for 4-6 minutes to allow the barium sulphate ($BaSO_4$) precipitate to form. Absorbance was measured at 420 nm using a microplate reader (SynergyHT, Biotek Instruments, Portugal).

VIII-3.6. Antioxidant properties of fucoidans

a) Total antioxidant capacity assay

Measurement of the total non-enzymatic antioxidant capacity of biological samples provide us with some insight of their ability to counteract oxidative stress-induced damage in cells. The total antioxidant capacity of purified FF and FA fucoidan were expressed as the Trolox equivalent antioxidant capacity (TEAC) was determined using a Total Antioxidant Capacity Assay kit (Sigma-Aldrich, The Netherlands) according to the manufacturer's instructions. Briefly, small molecule anti-oxidants convert Cu^{2+} ions to Cu^{+}, after which reduced Cu^{+} ions chelate with a colorimetric probe resulting in a absorbance peak at 570 nm. The height of the absorbance peak is proportional to the total antioxidant capacity expressed as TEAC. Trolox, a water-soluble vitamin E analogue is used as an antioxidant standard in all conditions. Purified FF and FA fucoidan samples ranging from 4-20 nmoles/well were prepared in a protein mask solution (to prevent the Cu^{2+} reduction by protein) followed by addition of a Cu^{2+} working solution and incubation for 90 min at room temperature after which the absorbance at 570 nm was measured using a CLARIOstar microplate reader. The amount of antioxidant in fucoidans can subsequently be determined using the Trolox reference curve and is expressed as TEAC; nmole, from which the antioxidant concentration in Trolox equivalents (nmole $µl^{-1}$), can be calculated.

b) Free radical scavenging assay

The scavenging activity of FF and FA fucoidan against free radicals was measured using the DPPH (2, 2-diphenyl-1-picrylhydrazyl) (Sigma-Aldrich, The Netherlands) assay. Briefly, Ascorbic acid, FF and FA fucoidan were dissolved in water (1 mg ml^{-1}) and 200 µl of the above solution added to each well of a 96-

well plate. The samples were then serially diluted in water for varied concentrations ranging from 1000 µg ml^{-1} to 1.56 µg ml^{-1}. Freshly prepared DPPH solution (0.2 mM) in methanol was prepared and 100 µl of the resulting solution was mixed thoroughly with 100 µl of FF and FA fucoidan of varied concentrations. The plate was then covered with aluminium foil (to protect DPPH radical degradation by light) and the reaction mixture was incubated for 1 h at room temperature. Absorbance was then measured at 515 nm using microplate reader (Clariostar). Ascorbic acid dissolved in water (1 mg ml^{-1}) was used as a standard and solvent alone (methanol: water; 1:1) was used as a blank. DPPH solution alone (100 µl) mixed with water (100 µl) served as control. The percentage of radical scavenging was obtained using the **equation VIII-1**:

Equation VIII-1. The percentage of radical scavenging:

$$\%\ DPPH_{scavenging} = 100 \times \left[\left(Abs_{sample} + DPPH\right) - \left(Abs_{Sample\ blank}\right)\right] / \left[\left(Abs_{DPPH}\right) - \left(Abs_{solvent}\right)\right]$$

and the IC_{50} values calculated using the GraphPrism software (GraphPad Software, USA). Ascorbic acid was used a positive control in this study.

c) Intracellular oxidative stress assay

Intracellular oxidative stress levels were determined using the 2´,7´-dichlorodihydrofluorescein-diacetate (DCFH-DA) (Sigma-Aldrich, The Netherlands) [30]. A stock solution of 10 mM DCFH-DA was made in DMSO; dilutions were made in exposure medium comprising RPMI supplemented with 10 mM HEPES, 1 mM sodium pyruvate, 200 g L^{-1} glucose and 200 mM L-glutamine. For direct measurements, INS1E cells were seeded at a density of 140,000 cells/well in a black 96 well imaging plate with clear bottom and cultured overnight. Cells were then incubated for 45 min with 20 µM DCFH-DA at 37°C and 5% CO_2 after which cells were washed using PBS. After DCFH-DA exposure, cells were incubated with fucoidan containing media (FA & FF; 10 mg ml^{-1}) in the presence or absence of 2 mM H_2O_2. Fluorescence was measured at 5 min interval over a period of 60 min in a microplate reader (CLARIOstar) at an excitation wavelength of λ = 485 nm, and emission wavelength at λ = 538 nm. The area under the curve was considered the total oxidative stress experienced by cells and was normalized to the number of viable cells in each sample, and compared to reference sample of non-treated cells cultured for 24 h in tissue

culture polysterene. Viability in each condition was calculated as percentage relative to non-treated controls.

VIII-3.7. Effect of fucoidan on insulin secretion

To determine the direct effects of fucoidan on insulin secretion, INS1E cells were seeded into 24-well plates at a density of 200,000 cells/well in supplemented RPMI 1640 medium and incubated at 37°C for 24 h. The cells were then washed in PBS and exposed to low glucose (2.8 mM), high glucose (20 mM), high glucose in the presence of varied FF fucoidan concentrations (0.01, 0.1, 0.5, 1, 5, and 10 mg ml^{-1}) for 3 h and high glucose in the presence of 5 mg ml^{-1} FF fucoidan for varied time points (6, 12 and 24 h). Aliquots of the media were removed from each of the wells and centrifuged (1,175 x g, for 5 min at 4°C) to remove the cells and stored at -20°C. The cells were exposed to 600 µl of acid ethanol, incubated overnight at 4°C, and the supernatant collected the following day for measuring insulin content. The concentration of insulin in the supernatants was determined using a rat insulin ELISA kit (Mercodia, Uppsala, Sweden).

VIII-3.8. Characterization of fucoidan alginate hydrogels and fucoidan alginate microcapsules

a) Antioxidant capacity of fucoidan containing alginate hydrogels (Fucogels)

The total antioxidant capacity of ultrapure sodium alginate (> 60% G sodium alginate Pronova™, UPMVG, Novamatrix, FMC Biopolymer, Norway) hydrogel and ultrapure sodium alginate hydrogel with fucoidan was determined using the Total Antioxidant Capacity Assay kit (Sigma-Aldrich). For this study, 2.5% w/v of alginate solution was made in protein mask solution. For the alginate/fucoidan hydrogel (Fucogel), 0.5% w/v purified FF fucoidan was mixed with 2% w/v ultrapure sodium alginate to obtain a 2.5% w/v Fucogel in protein mask solution. Both alginate and fucogel were diluted further in protein mask solution to provide final concentrations of 0.5%, 1%, 1.5%, 2% and 2.5% w/v and from each sample the TEAC and antioxidant concentration was determined.

b) Rheology and viscoelastic properties of fucogel

Rheology experiments were performed with a Discovery HR-2 hybrid rheometer (TA instruments, The Netherlands) with a 8 mm flat plate geometry (TA instruments, serial number 109413). A total of 175 µl hydrogel precursor solution was casted in a 12 mm silicon mold and crosslinked in an excess of 20 mM $BaCl_2$ for 5 minutes. A solvent trap was placed around the sample and filled with distilled water to prevent solvent evaporation from the gel. Hydrogels were preconditioned with a time sweep hold with a 1% strain at an angular frequency of 10 rad/s. Initially, hydrogels were subjected to a frequency sweep with a strain of 1% and frequencies ranging between 1-500 rad s^{-1} to determine a suitable frequency for the strain sweep. Next, hydrogels were exposed to a strain sweep with strains ranging between 0.01-10% and an angular frequency of 10 rad s^{-1} to determine the linear viscoelastic region of the hydrogels. The storage modulus (G') was monitored during the strain sweep and used to calculate the hydrogel mesh size (D_{mesh}) based on the **equation VIII-2**:

Equation VIII-2. The hydrogel mesh size

$$D_{mesh} = \left(\frac{6\,RT}{\pi N_{av} G'}\right)^{\frac{1}{3}}$$

The classical theory of rubber elasticity relates the shear modulus (G') to the mesh size r_{mesh} (equation VIII-2), where R is the gas constant, T the absolute temperature and Nav is Avogadro's number. This allows estimation of the mesh size of a hydrogel based on its shear modulus [31,32]. The mesh size (D_{mesh}) represents the diameter of a hard sphere that fills the void in between hydrogel network strands.

c) Generation of alginate and alginate/fucoidan microcapsules (Fucocaps)

The formation of both alginate and alginate/fucoidan (Fucocaps) microcapsules were carried out using an air-driven droplet generator (Nisco D-0038, Zurich, Switzeland, Nozzle from Biored, California, USA) as described previously [25]. Briefly, for microcapsule formation, 2.2% w/v sodium alginate and 2.5% w/v fucogel polymer solutions were injected through the droplet generator with a steady airflow rate of 5 L/min. The microcapsules were collected on a sterile 145 mm petri dish containing 50 ml $BaCl_2$ (20 mM) working as a gelling solution, which was placed at a distance of 16.5 cm from the tip of the

encapsulation device to bath. The microcapsules formed were then incubated in $BaCl_2$ solution for 2 min, followed by five-time washings with Dulbeco´s phosphate buffered saline (DPBS) (Sigma-Aldrich) to remove excess $BaCl_2$. After repeated washings, the microcapsules were stored in DPBS and microcapsule size determined by optical microscopy (Nikon TiS microscope, Nikon, The Netherlands).

e) Toluidine blue staining

The presence of fucoidan in microcapsules was visualized using a toluidine blue O (TBO) staining. Briefly, alginate microcapsules and fucocaps were randomly collected and immersed in 1 ml of TBO solution (0.1 M HCl, 20 mg NaCl, and 4 mg toluidine blue O chloride) for 30 min at room temperature. The microcapsules were then washed in DPBS to remove excess TBO solution and incubated further for 24 h. After 24 h incubation, the microcapsules were washed again, stored in DPBS and aliquots of microcapsules were randomly chosen at different time points for imaging using optical microscopy (Nikon TiS microscope).

VIII-3.9. Encapsulation

a) Encapsulation of insulin producing cells

Before the microencapsulation procedure, INS1E pseudoislets, primary rat islets and neonatal pig islets were pooled and mixed thoroughly with either 2.2% w/v ultrapure sodium alginate, or a 2.5% w/v ultrapure alginate fucoidan solution in a 1:8 ratio (cells: alginate) in a 50 ml falcon tube. Subsequently, the alginate cell mixture was then extruded through the nozzle of the droplet generator with an airflow of 5 L min^{-1} leading to the formation of uniform droplets. The droplets were collected in a sterile 145 mm petri dish containing 50 ml $BaCl_2$ (20 mM) gelling solution to crosslink the alginate molecules after which cell containing microcapsules were formed. The microcapsules were left to incubate in the $BaCl_2$ solution for 2 min after which they were collected, and washed five times with DPBS to remove any excess $BaCl_2$. After washing, the microcapsules were allowed to settle down, and the remaining supernatant was discarded. The microencapsulated cells and islets were then cultured for a 24 h in appropriate media before being used for further *in vitro* studies.

b) Encapsulation of INS1E reporter cells

To explore the potential of fucoidan to alleviate oxidative stress post-encapsulation, we used a genetically encoded redox probe mt-roGFP2-Orp1 transduced INS1E beta cells (passage 93). Stably expressing mito-roGFP2-Orp1 INS1E cells were obtained from Leticia Prates Roma (Saarland University). INS1E cells were retrovirally transduced with pLPCX mito roGFP2-Orp1 as previously described for H1975 cells [33,34]. The stably transduced mito-roGFP2-Orp1 INS1E cells were cultured in RPMI (Gibco 61870) supplemented with 5% (v/v) fetal bovine serum, 10 mM HEPES, 1 mM sodium pyruvate, 100 U/ mL penicillin, 100 mg mL^{-1} streptomycin and 0.05 mM 2-mercaptoethanol at 5% CO2 at 37°C. INS1E reporter cells (1 x 10^6) were encapsulated in alginate and fucocaps as described above and cultured for 24 hr. The following day the encapsulated cells were washed in PBS and exposed to H_2O_2 (1 mM) for 1 hr to induce oxidative stress. To induce reduction and oxidation DTT (5 mM) and Diamide (0.5 mM) were added respectively as controls and the OxDmtroGFP2 was calculated as previously described [35].

VIII-3.10. Cell viability and ATP measurements

The viability of non-encapsulated and encapsulated cells was assessed using the fluorescent dyes Calcein AM (for live cells) and Ethidium homodimer-1 (for dead cells) (Thermo Fisher Scientific, The Netherlands). Briefly, aliquots of non-encapsulated and encapsulated cells were randomly collected from the tissue culture dishes with a Gilson P 1000 µl pipette under sterile conditions. They were washed twice by suspending them in 0.5 ml PBS followed by careful removal of the supernatant and discarded. Subsequently, a solution of 4 ml of PBS and 2.5 µl of calcein AM and 5 µl of ethidium homodimer-1 were prepared and 1 ml of this solution added to each sample and incubated for 30 mim in darkness. The non-encapsulated and encapsulated cells were then visualized under a fluorescence microscope (Nikon Eclipse E600), and the percentage of green (live cells) to red (dead cells) was estimated in 25 microcapsules. For ATP measurements, aliquots of encapsulated cells were washed twice by suspending them in 0.5 ml PBS, discarding the supernatant and suspending again in 100 µl of PBS followed by addition of 100 µl of CellTiter-Glo® 3D Reagent (Promega). The contents were mixed vigorously for 5 min to induce cell lysis and the plates allowed to incubate at room temperature for a further 25 min to stabilize the luminescent signal. After 30 min of incubation, luminescence was measured on a microplate reader (CLARIOstar) and the amount of ATP measured which signals the presence of metabolically active cells.

VIII-3.11. Glucose stimulated insulin secretion (GSIS) assay

For GSIS assay, different concentrations of exposure solutions were made in Kreb's buffer containing 0.2% bovine serum albumin. Accordingly, for non-encapsulated rat islets, encapsulated rat and neonatal pig islets low glucose (LG) solution (1.7 mM) and high glucose (HG) solution (16.7 mM) were prepared and sterile filtered. For encapsulated pseudoislet derived from INS1E cells low and high glucose exposure solutions of 2.8 mM and 20 mM were prepared respectively. On the day of GSIS, aliquots of non-encapsulated and encapsulated islet/pseudoislet were handpicked and placed on inserts in 24 wells and washed thrice in low glucose solution (1.7 mM or 2.8 mM) followed by equilibration for 1.5 h at 37°C in low glucose solution. After equilibration, the cells were sequentially exposed to low (1.7 mM or 2.8 mM), high (16.7 mM or 20 mM) and low (1.7 mM or 2.8 mM) glucose concentrations with a 1.5 h incubation at 37°C for each exposure condition. Non-encapsulated rat islets and encapsulated neonatal pig islets were exposed to only low (1.7 mM) and high (16.7 mM) glucose concentrations for 1 hr. After each incubation, the supernatant was collected and stored for insulin measurements. After the final incubation step, the encapsulated cells were washed in PBS followed by addition of cold acid ethanol and vortexed vigorously to enhance cell lysis. The extracts were kept at 4°C overnight and the supernatant collected the following day for measuring insulin content. Insulin secretion was quantified by using a rat and pig insulin ELISA kit (Mercodia, Uppsala, Sweden) according to the manufacturer´s instructions. Results were presented as low–high–low profiles normalized to total insulin content and as stimulation index, which is the ratio of insulin secretion between the high and low glucose conditions.

VIII-3.12. RNA-sequencing

a) RNA isolation

INS1E cells (1 x 10^6/well) were seeded onto 6 well plates and the cells exposed to H_2O_2 (1 mM) for 1 hr in the presence or absence of fucoidan (5 mg ml^{-1}). Following incubation, the cells are washed in PBS, lysed and RNA isolation performed according to the RNeasy Mini Kit (Qiagen, Netherlands) and quantified using the BioDrop (Biochrom, United Kingdom).

b) RNA-seq sample preparation

The KAPA Stranded mRNA-Seq Kit, with KAPA mRNA Capture Beads (Roche, cat# 07962207001) protocol was performed on 500ng of initial RNA from bulk material. RNA size selection was performed for 300pb fragments. RNA-seq libraries were amplified with 8 cycles. The purified libraries were quantified using Qubit (ThermoFisher) and the fragment distribution analyzed using TapeStation (Agilent). Complete libraries were sequenced (paired-end) on Illumina HiSeqTM4000, with 151bp from each end.

c) Transcriptomic analysis

RNA-seq reads were aligned to the reference genome (rat rn6) using HISAT2 (version 0.1.6) with default parameters. Read counts representing gene expression levels were calculated with feature Counts (version 2.0.0) using default parameters. Only genes with counts above zero were retained for the downstream analyses. Differential expression analyses were performed using EdgeR (version 3.12) with adjusted p-value < 0.05 as the cut-off. Factor normalization was done using the CPM method. Dimension reduction and clustering analysis were performed on EdgeR. All Gene Ontology (GO) analyses were performed with ToppGene method (https://toppgene.cchmc.org/), and only Biological Process terms were kept for downstream analyses. Enrichment score was calculated from the as -log10 of the p-value. Plots were created using GraphPad Prism7.

VIII-3.13. Statistical analysis

All data are presented as mean ± standard error of mean (SEM). Differences between two groups were analysed by the two-tailed Student's t-test and more than two groups by one-way analysis of variance (ANOVA) with post-hoc Multiple-Comparison test using GraphPad Prism software (GraphPad Software, USA). Significant differences among data groups were assigned when $p < 0.05$.

VIII-4. RESULTS & DISCUSSION

VIII-4.1. Characterization and antioxidant properties of fucoidans

Seaweeds growing in shallow waters are continuously exposed to ultraviolet light and air, which leads to the formation of free radicals and other reactive oxygen species (ROS). Despite chronic exposure to ROS, healthy seaweeds are resilient to oxidative damage demonstrating the existence of potent antioxidant defense mechanisms within their cells that is attributed to sulphated polysaccharides namely fucoidan [21]. Fucoidan constitutes the cell walls of these brown seaweeds and have a very complex chemical composition of which sulphated-l-fucose is the major component [36]. The biological activity of fucoidan is largely determined by these sulphate groups and is highly variable between the different genera of brown seaweeds influenced by the extraction procedure [36]. In this study, we characterized fucoidan extracted from two brown seaweed genera *Fucus vesiculosus* (FF) and *Ascophyllum nodosum* (FA) and determined their antioxidant potential.

NMR spectra of both FA and FF fucoidan show similar general bands **(Figure VIII - S1)**. NMR spectral bands typical of anomeric protons H-1 from α-L-fucose residues and uronic acid residues can be observed between 5.6 and 5.20 ppm. H-2, H-3 and H-4 of sulfated fucose can be found between 4.66 and 4.10 ppm, and bands between 4.20 to 3 ppm typical for H-2, H-3, H-4 and H-5 of unsulfated fucose and uronic acid [23]. The two peaks, appearing around 1.2 and 1.35 ppm were assigned to the methyl group belonging to fucose. We also observed an individual peak at 2.2 ppm, which can be ascribed to acetyl groups.

Monosaccharide analysis of the purified fucoidan (FF and FA) **(Figure VIII - 1A)** showed that the predominant sugar moiety present in both batches was fucose (18% - 38% w/w) followed by xylose (4-5% w/w), galactose, mannose rhamnose (1-2% w/w) and traces of glucose and arabinose (< 1% w/w). The fucose content was found to be significantly higher in FF compared to FA fucoidan, while other carbohydrate species showed similar amounts. Similar to fucose, sulfate quantification analysis demonstrated that FF fucoidan has a significantly higher sulfate content (30 ± 4.4%) compared to FA fucoidan (20 ± 3.7%) **(Figure VIII - 1B).** Chemical characterization of both FF and FA fucoidan demonstrated the presence of various sugar moieties (rhamnose, fucose, ribose, arabinose, xylose, mannose, galactose and glucose) and as well uronic acid and sulfate groups as reported in the literature

[37–39]. However, in this study, we found that the fucose sugar and sulfate content is significantly higher in FF compared to FA fucoidan. The difference in the fucose sugars and sulfate composition determine the antioxidant capacity of fucoidan and it varies according to the algal species, the season when they are collected and the method used for the extraction procedure [40,41].

The antioxidant potential of purified FF and FA fucoidan was determined using the total antioxidant capacity assay kit and expressed as TEAC with Trolox serving as an antioxidant standard. As seen from **Figure VIII - 1C**, both FA and FF fucoidan demonstrated a dose-response increase in their antioxidant capacity (measured as TEAC) with FF fucoidan always possessing significantly higher amount of antioxidants than FA fucoidan at all tested concentrations. Subsequently, the concentration of antioxidant (measured as Trolox equivalents) in FF fucoidan (17.97±1.06 nmoles/µl Trolox equivalents) was ~ 33-fold higher compared to FA fucoidan (0.55±0.06 nmoles/µl Trolox equivalents) **(Figure VIII - 1D)**. The high antioxidant capacity of FF fucoidan compared to FA may be attributed to its high fucose and sulphate content [40,41].

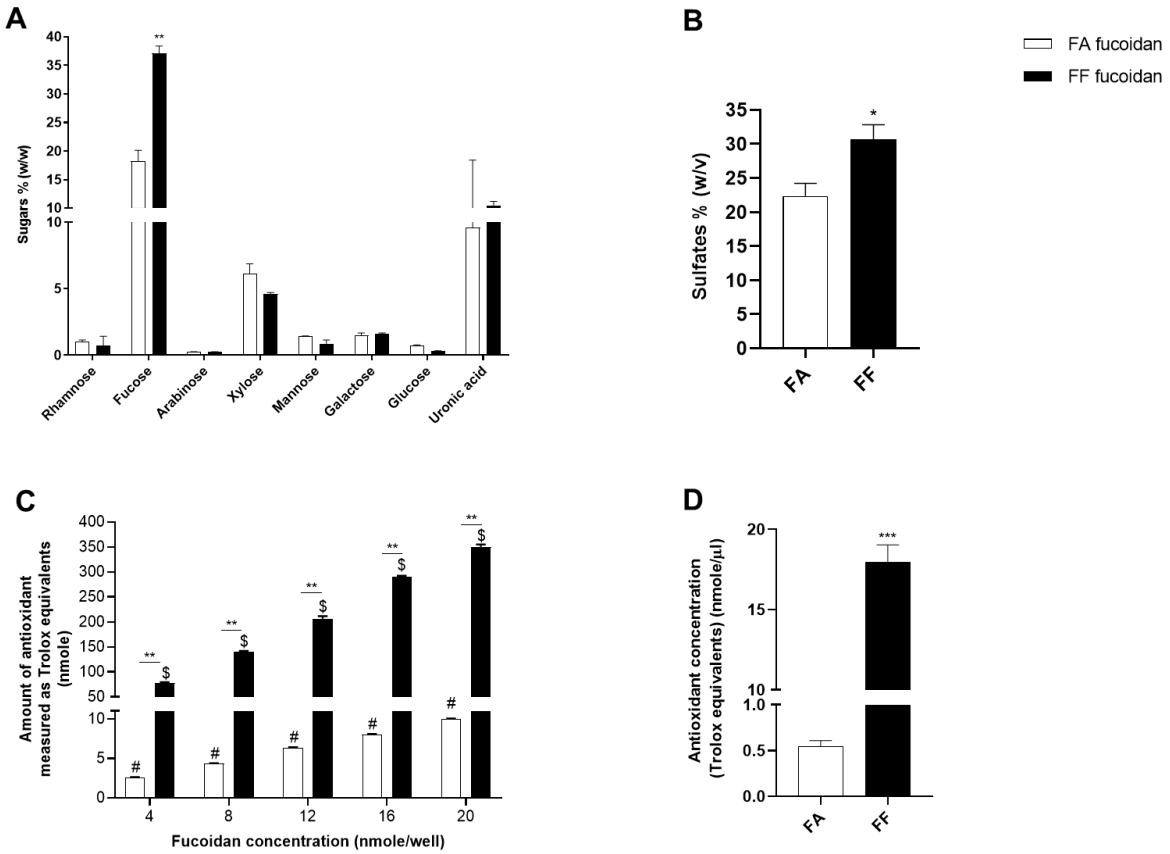


Figure VIII-1. Chemical characterization and antioxidant properties of purified fucoidans. Sugar composition of purified FF and FA fucoidan; Values: mean ± SEM; $^{**}p < 0.01$ comparing FA and FF fucoidan (Student's t-test) (A). Sulfation degree (%) of purified FF and FA fucoidan (B); Values: mean ± SEM; $^{*}p < 0.05$ comparing FF and FA fucoidan (Student's t-test). Measurement of the total antioxidant capacity of both FF and FA fucoidan measured as Trolox equivalents (C). Trolox, a vitamin E analogue was used as a standard. Values: mean ± SEM (n=6); $^{****}p < 0.0001$ for the amount of antioxidant at different concentrations for both FF and FA fucoidan (ANOVA with posthoc Dunnett's T3 multiple comparisons test and $^{**}p < 0.01$ for the amount of antioxidant when compared between FF and FA fucoidan at different concentration (Student's t-test). Concentration of antioxidant measured as Trolox equivalents between FF and FA fucoidan (D). Values: mean ± SEM (n=6); $^{***}p < 0.0001$ comparing FF and FA fucoidan (Student's t-test).

VIII-4.2. Cytotoxicity and free radical scavenging activity of fucoidans and its potential to alleviate oxidative stress

INS1E cells were used to evaluate the cytotoxicity of two different types of fucoidan. using a direct contact cytotoxicity assay. INS1E cells were seeded into 96-well plates, treated with a range of different concentrations of FF or FA fucoidan for 24 h after which an MTT assay was performed. Both FF and FA fucoidan were found to be nontoxic with a cell viability of ≥ 90% similar to the control cells at concentrations ranging from 2.5 mg ml^{-1} to 0.15 mg ml^{-1} **(Figure VIII - 2A)**. However, at concentrations of 5 and 10 mg ml^{-1}, both FF and FA fucoidan demonstrated a slight decrease in cell viability. Regardless, both FF and FA fucoidan were found to be non-cytotoxic and did not elicit an adverse response with cell viabilities well above = 70%, which is considered to be the cytotoxicity value cut off, for all dilutions tested **(Figure VIII - 2A)**.

To determine the free radical scavenging activity and the ability of fucoidan to scavenge DPPH free radicals, a DPPH free radical assay was carried out. Generally, a high percentage of DPPH free radical inhibition at low IC_{50} values indicates a high antioxidant activity. As seen from **Figure VIII - 2B**, FF fucoidan above 7.8 µg ml^{-1} exhibits a dose response increase in its free radical scavenging activity with a maximum inhibition of 78.6 ± 0.66%, seen at 1000 µg ml^{-1}, with an IC_{50} of 362.2 µg ml^{-1}. Ascorbic acid, used as a positive control, at the same concentration exhibits a maximum inhibition of 94.7 ± 0.21%, with a low IC_{50} of 6.2 µg ml^{-1} **(Figure VIII - 2B)**. In contrast, FA fucoidan showed very poor free radical scavenging activity compared to FA fucoidan with a maximum inhibition of only 8.7 ± 0.8%, seen at 1000

μg ml^{-1}. This clearly shows that FF fucoidan exhibits a significant higher free radical scavenging capacity compared to FA fucoidan. One factor that largely determines the reducing ability of fucoidan is its molecular weight. It has been reported that low molecular weight fucoidan possesses significantly higher antioxidant and radical scavenging properties compared to high molecular weight fucoidan, as it easily crosses the lipid bilayer to exert its biological effect [23,42]. In contrast, we found that the high molecular weight FF fucoidan (91 kDa) exhibits a superior free radical DPPH scavenging activity, compared to the lower molecular weight FA fucoidan (5-15 kDa), suggesting that lower uptake of FF can lead to a much stronger decrease in oxidative stress. This discrepancy can further be explained by the degree of substitution of molecular groups in FF fucoidan, their position, and glycosidation branching, which are known to positively influence the reducing properties of fucoidan [43,44].

In order to study the effect of fucoidan on alleviating oxidative stress in depth, an intracellular oxidative stress assay was carried out in INS1E beta cells using 2′,7′-dichlorodihydrofluorescin diacetate (DCFH-DA) which can de-esterify intracellularly and turn into highly fluorescent 2′,7′-dichlorofluorescein upon oxidation by a wide range of reactive oxygen species (ROS) including H_2O_2 [30]. The amount of fluorescence signal is directly proportional to the intracellular oxidative stress levels and can be used to determine the effect on ROS in cells influenced by either FF or FA fucoidan. Pre-treatment with FF or FA fucoidan reduced the basal oxidative stress levels in INS1E cells compared to control conditions albeit not significantly **(Figure VIII - 2C).** We found that in the presence of H_2O_2, the intracellular oxidative stress level in INS1E cells was significantly decreased in cells pre-treated with FF fucoidan compared to H_2O_2 treated cells alone, while oxidative stress was also lower compared to N-acetyl cysteine (NAC) treated cells, serving as a positive control, suggesting a strong ROS mitigating activity. Quite the reverse, FA fucoidan did not exhibit any ROS mitigating activity to alleviate oxidative stress, and intracellular oxidative stress levels were found to be similar to control cells treated with H_2O_2 alone **(Figure VIII - 2C)**. Based on these outcomes, we show that FF fucoidan significantly reduces intracellular oxidative stress levels in beta cells exposed to H_2O_2 compared to FA fucoidan. This beneficial effect may be attributed to the redox modulating property of FF fucoidan and the induction of antioxidant enzymes leading to the protection of beta cells from free radical induced cell toxicity [45]. We concluded that a combination of the significantly higher antioxidant concentration and free radical scavenging activity of FF compared to FA fucoidan, clearly leads to a superior antioxidant capacity and alleviation of oxidative stress.

Subsequently, FF fucoidan was used in a number of follow up tests using primary islets, and in combination with alginate microcapsules.

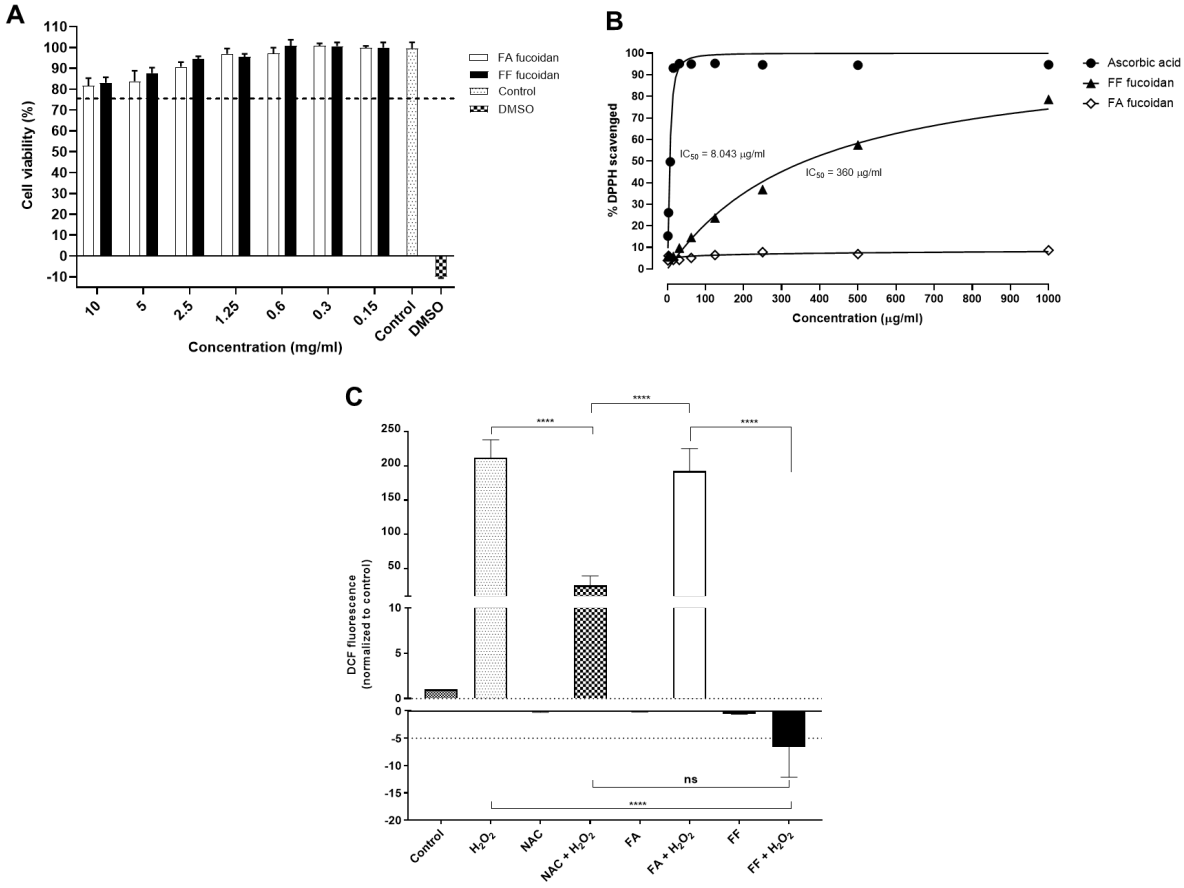


Figure VIII-2. Cytotoxicity and free radical scavenging properties of fucoidan and its ability to alleviate oxidative stress. Cytotoxicity and free radical scavenging properties of fucoidan and its ability to alleviate oxidative stress: The cytotoxicity of fucoidan was determined in a MTT assay using INS1E cells (A). Values: mean ± SEM (n=3); $p > 0.05$ (ANOVA with posthoc Dunn's multiple comparisons test). DPPH free radical scavenging activity of FF and FA fucoidan (B). Values: mean ± SEM (n=3). Effect of FF and FA fucoidan to alleviate intracellular oxidative stress in INS1E cells using the DCFH-DA probe (C). In the presence of H_2O_2, FF fucoidan significantly alleviated oxidative stress compared to FA fucoidan. Values: mean ± SEM (n=3); ****$p<0.0001$ when compared FF and FA with control NAC in the presence of H_2O_2 (ANOVA with posthoc Dunnett's multiple comparisons test).

VIII-4.3. Effect of fucoidan on beta cell viability and function

Apart from its antioxidant properties, fucoidan has been shown to possess anti-diabetic properties by inducing insulin secretion, and reducing blood glucose levels, stimulating glucose uptake and improving insulin sensitivity [46–48]. To explore the direct effect of FF fucoidan on insulin secretion, INS1E cells were treated with varying doses of fucoidan and for different time intervals. **Figure VIII - 3A**, shows that incubation of INS1E cells with different FF fucoidan concentrations (0.01, 0.1, 0.5, 1, 5 and 10 mg ml^{-1}) for 3 hr induced insulin secretion in a dose-dependent manner with a significant increase seen with 5 and 10 mg ml^{-1} compared to high glucose. However, there was no significant difference in the insulin induction between 5 and 10 mg ml^{-1} FF fucoidan. Therefore, for time-response studies, we chose 5 mg ml^{-1} of FF fucoidan and treated the INS1E cells with this concentration for 6, 12 and 24 hr respectively. At all time intervals tested, FF fucoidan significantly increased insulin secretion in a time-dependent manner in the presence of high glucose **(Figure VIII - 3B)**. This data demonstrates the insulinogenic properties of FF fucoidan, and that FF induced insulin secretion is both dose- and time-dependent.

In order to determine the effect of fucoidan on primary beta cells, rat islets were treated with FF fucoidan (1 mg ml^{-1}) for 24 hr while their viability and function was assessed. Pre-treatment with FF fucoidan significantly improved rat islet viability and function. Live/dead analysis revealed that the viability of islets treated with FF fucoidan was significantly higher compared to non-treated controls (Control vs FF treated: 84.5 ± 1.6% vs 93.1 ± 1.9%; $p < 0.05$) **(Figure VIII - 3C).** Primary rat islets treated with FF fucoidan showed a significantly better insulin secretory behaviour, with a higher insulin release in response to glucose stimulation compared to non-treated controls **(Figure VIII - 3D)**. This improved function resulted in a significantly higher stimulation index (20.1 ± 2.8) which is ~ 1.8 fold higher in FF treated islets compared to non-treated controls (11.1 ± 0.7) **(Figure VIII - 3D)**.

The above data suggest that when islets are pre-treated with FF fucoidan they respond better to changes in glucose with significantly higher insulin secretion and improved stimulation indices. We also showed that in high glucose conditions, FF fucoidan supports the increase of insulin secretion in a dose- and time- dependent manner in comparison to controls. FF fucoidan assisted insulin secretion may be attributed to an increase in cAMP concentrations which has shown to be significantly elevated in fucoidan treated insulin producing RIN-5F cells [48]. Elevation in cAMP levels has been shown to stimulate insulin

exocytosis both in a Ca^{2+} dependent and independent mechanisms and supports membrane depolarization by directly inhibiting K_{ATP} channels [49–51].

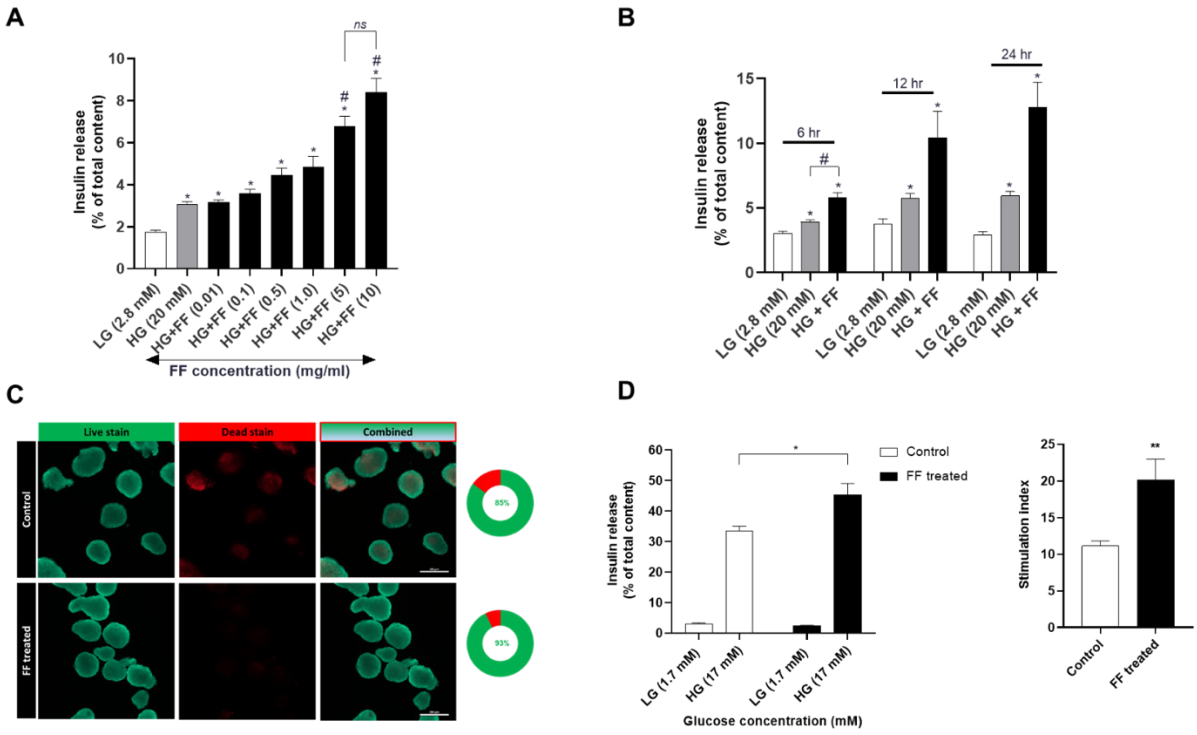


Figure VIII-3. Effect of fucoidan on beta cell viability and function.Measurement of insulin secretion in INS1E cells exposed to varied concentrations of FF fucoidan in the presence of high glucose (HG) for 3 hr (A). Incubation of INS1E cells with different FF fucoidan concentrations (0.01, 0.1, 0.5, 1, 5 and 10 mg ml^{-1}) induced insulin secretion in a dose-dependent manner compared to low glucose (LG) (*p<0.0001) and with a significant increase seen with 5 and 10 mg ml^{-1} compared to high glucose (#p<0.001) (ANOVA with posthoc Dunnett's T3 multiple comparisons test). Measurement of insulin secretion in INS1E cells exposed to 5 mg ml^{-1} of FF fucoidan in the presence of high glucose (HG) for 6, 12 and 24 hr (B). Values: mean ± SEM (n=3). In the presence of high glucose (HG), at all-time points tested, FF fucoidan treatment significantly increased insulin secretion in a time-dependent manner compared to low glucose (LG) (*p<0.05) and with a significant increase seen with high glucose (HG) at 6 hr time point (#p<0.05) (ANOVA with posthoc Dunnett's T3 multiple comparisons test). Viability of primary rat islets pretreated with FF fucoidan for 24 hr (C). Pretreatment with FF fucoidan significantly improved islet viability (93.1 ± 1.9%) compared to the non-treated controls (84.5 ± 1.6%) (p<0.05) (Student's t-test). Values: mean ± SEM (n=25 islets). Assessment of primary rat islet function in glucose

stimulated insulin secretion (GSIS) (D). Pretreatment with FF fucoidan significantly improved islet function (*p<0.05) which resulted in a significantly higher stimulation index (p<0.01) compared to non-treated controls.**

VIII-4.4. Characterization of fucoidan hydrogels and fucoidan microcapsules

Based on the above positive findings we explored the possibility of incorporating FF fucoidan in ultra-pure alginate microcapsules as a carrier for beta cells and islets. We chose ultrapure alginate due to its long term use as an immunoprotective carrier in the field of type 1 diabetes and its frequent use in microencapsulation of islets [3]. Fucoidan is a water-soluble molecule with low viscosity and cannot be used by itself for cell microencapsulation purposes. However, by mixing fucoidan with alginate we were able to obtain a suitable hydrogel for microencapsulation of cells using an air driven microdroplet generator. In brief, FF fucoidan (0.5% w/v) was mixed with ultrapure sodium alginate (2% w/v) to obtain a 2.5% w/v alginate/fucoidan polymer solution which is then cross-linked with barium chloride (20 mM) to form stable alginate/fucoidan hydrogels. The alginate/fucoidan hydrogel will hereafter be referred to as "Fucogel" and alginate/fucoidan microcapsules as "Fucocaps". The antioxidant potential of fucogel, and alginate alone, was determined using a total antioxidant capacity assay kit. Both alginate and fucogel demonstrated a dose-response increase in their antioxidant capacity (measured as TEAC), with fucogel always exhibiting significantly higher amount of antioxidant capacity than alginate alone **(Figure VIII - 4A)**. We found that the antioxidant concentration (measured as Trolox equivalents) in fucogel was ~35- fold higher compared to alginate polymer (4.2 ± 0.2 nmoles μl^{-1} Trolox equivalents vs 0.12 ±0 .04 nmoles μl^{-1} Trolox equivalents) **(Figure VIII - 4B)**. The high antioxidant activity of fucogel is due to the FF fucoidan molecules that can be attributed to the high fucose and sulphate content **(Figures VIII - 1 A&B)**.

Next, we determined the viscoelastic properties of fucogel using a rheometer. Mechanical testing revealed that both alginate and fucogel have similar viscoelastic properties and show similar strain-dependent behaviour for G' **(Figure VIII - 4C)**. Both hydrogels showed a linear viscoelastic region until 0.5% strain. The G' at 0.1% strain was used to calculate their respective hydrogel mesh sizes. There were no significant differences in hydrogel mesh sizes between alginate, 8.15 ± 0.92 nm, and fucogel, 8.05 ± 0.64 nm **(Figure VIII - 4D)**. Strain sweep experiments for both hydrogels displayed a stable G' within the linear viscoelastic region (LVR) (until 0.5% strain) **(Figure VIII - 4C)**, which is in agreement with literature [52]. Decrease in G' outside of the linear viscoelastic region (LVR), indicates structural breakdown and yielding of the hydrogel microstructure. The G' value within the LVR was subsequently used to calculate

the hydrogel mesh size (D_{mesh}) which represents the diameter of a hard sphere that fills the void in between hydrogel network strands, and is an important indication for hydrogel diffusion properties. The D_{mesh} of alginate hydrogels has been described to range between 5-90 nm, which seems to be in agreement with our data with a mesh size of 8.15 ± 0.92 nm **(Figure VIII - 4D)** [53–56]. The D_{mesh} of alginate hydrogels depends on its molecular weight, guluronic acid/mannuronic acid (G/M ratio) and purity and as well the crosslinker concentration. The dimensions of insulin ranges between 2.7 and 5.5 nm and should be capable to diffuse through these alginate hydrogels given that the mesh size is around 8 nm [57]. The ultrapure alginate used in this study has a molecular weight > 200 kDa, while FF fucoidan has a molecular weight of ~ 91 kDa. Hence, the relatively small fucoidan moieties did not hinder the formation of an alginate network, depicted by the similar G' values with D_{mesh} of 8.05 ± 0.64 nm compared to alginate alone hydrogel. This data suggests that fucoidan moieties can be easily blended with alginate hydrogels without compromising the viscoelastic and diffusion properties to form stable fucogels suitable for encapsulation studies.

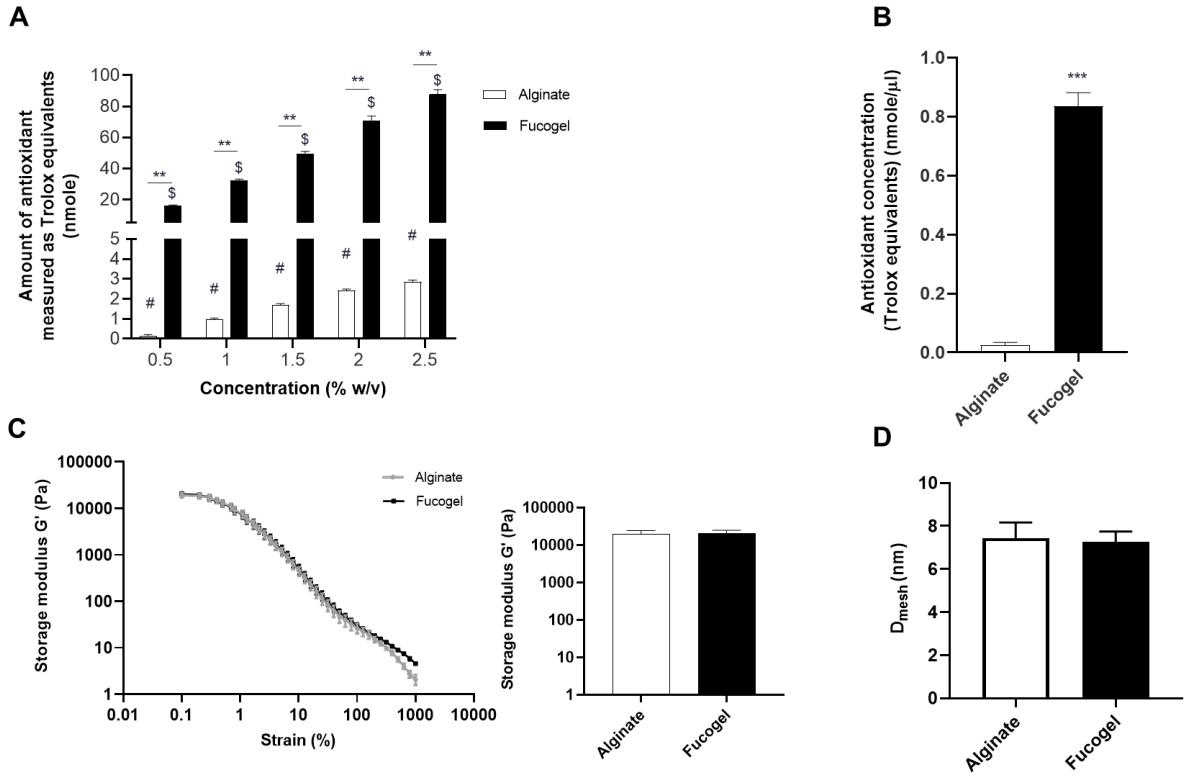


Figure VIII-4. Characterization of fucogels. Measurement of the total antioxidant capacity of fucogel measured as Trolox equivalents (A). Trolox, a vitamin E analogue was used as a standard. Values = mean ± SEM (n=6); *,\$ p<0.0001 for

the amount of antioxidant capacity seen with different concentrations for both fucogel and alginate (ANOVA with posthoc Dunnett's T3 multiple comparisons test) and ¨p<0.01 for the amount of antioxidant when compared between fucogel and alginate at different concentrations (Student's t-test). Concentration of antioxidant measured as Trolox equivalents between fucogel and alginate (B). Values = mean ± SEM (n=6); ¨¨p<0.0001 when compared between fucogel and alginate (Student's t-test). Rheological properties of fucogel and alginate: Strain sweep alginate (grey) and fucogel (black) (C) and measurement of hydrogel mesh size based on the storage moduli at 0.1% strain (D) and calculated using formula 1: D_{mesh}= ((6 RT)/(πN_av G'))^(1/3). Values = mean ± SEM (n=5).

Alginate microcapsules and fucocaps were produced using an air-driven droplet generator and their size was determined by phase contrast light microscopy. Light micrographs of alginate and fucocaps show that for both hydrogels the microcapsules are homogenous in size and equal in appearance. Both alginate and fucogel microcapsules have similar dimensions and are composed of uniform spheres of approximately 500 µm (500 ± 24.2 µm) diameter **(Figure VIII - 5A)**. The droplet sizes were reproducibly made and the polydispersity in the microcapsule diameter is close to the range typically seen for microcapsules prepared by the air-stripping technique. In order to visualize the presence of fucoidan in fucocaps, microcapsules were stained with TBO and imaged at subsequent regular time intervals for 40 days. After removing excess TBO staining, a clear blue coloration of fucocaps could be seen which persisted during 40 days. In **Figure VIII - 4A**, clear toluidine blue staining can be seen after 40 days indicative of the long term presence of fucoidan in fucocaps. These data suggest that the fucocaps remained stable, while toluidine blue staining confirmed the presence of fucoidan within these microcapsules for at least 40 days suggesting the entrapment of small fucoidan moieties within the crosslinked alginate network. We have previously demonstrated the permeability of barium alginate microcapsules by Inverse Size Exclusion Chromatography (ISCE) for the determination of the molecular weight cut-off of microcapsules (MWCO) [58]. We showed that the MWCO for these barium alginate microcapsules correspond to ~ 50 kDa suggesting that any molecules > 50 kDa cannot permeate through the microcapsule pores. The fucoidan molecules used in this study is quite bigger with a molecular weight of ~ 91 kDa and hence will not be able to permeate easily through the alginate hydrogel network in the Fucocaps. However, the release kinetics of fucoidan from fucocaps needs to be evaluated in future studies.

Native islets residing within the pancreas are highly vascularized microtissues that are destroyed during the islet isolation process leading to post-isolation cell stress [15]. This is further aggravated by the encapsulation process which prevents revascularization, and moreover, we have recently shown that

different biomaterials can induce significant amounts of oxidative stress in both beta and alpha cells [16]. The absence of revascularization and limited mass transport caused by the immunoprotective barrier subject the encapsulated islets to chronic oxidative stress. Oxidative stress occurs when there is an imbalance between the production of reactive oxygen species (ROS) and antioxidant defenses, and islets are particularly prone to ROS due to their relatively low antioxidant enzymes [2]. Therefore, in this study, we explored the potential of FF fucoidan to alleviate oxidative stress post-encapsulation using a genetically encoded redox probe mt-roGFP2-Orp1 transduced INS1E beta cells. The probe is a fusion protein consisting of redox-active green fluorescent protein 2 (roGFP2) genetically fused to the redox enzyme Orp1 that is oxidized by H_2O_2 [17]. A major advantage of roGFPs over other fluorescent probes is their ratiometric fluorescence excitation behavior. When measuring fluorescence emission at 510 nm, roGFP2 exhibits excitation maxima at both 400 and 490 nm; oxidation increases the intensity of the 400 nm peak while decreasing the intensity of the 490 nm peak and vice versa for reduction **(Figures VIII - 5 B&C)**. Using the ratiometric fluorescence, we found that INS1E beta cells in fucocaps experienced significantly less oxidative stress compared to alginate microcapsules **(Figure VIII - 5D)**. Further, exposure of encapsulated INS1E beta cells to H_2O_2 (1 mM) for 1 hr, suggested the oxidative stress is significantly reduced in Fucocaps compared to those in alginate microcapsules **(Figure VIII - 4D)**. These data again confirm the free radical scavenging capacity of fucoidan and its ability to alleviate oxidative stress post-encapsulation and in the presence of an external stress stimulus.

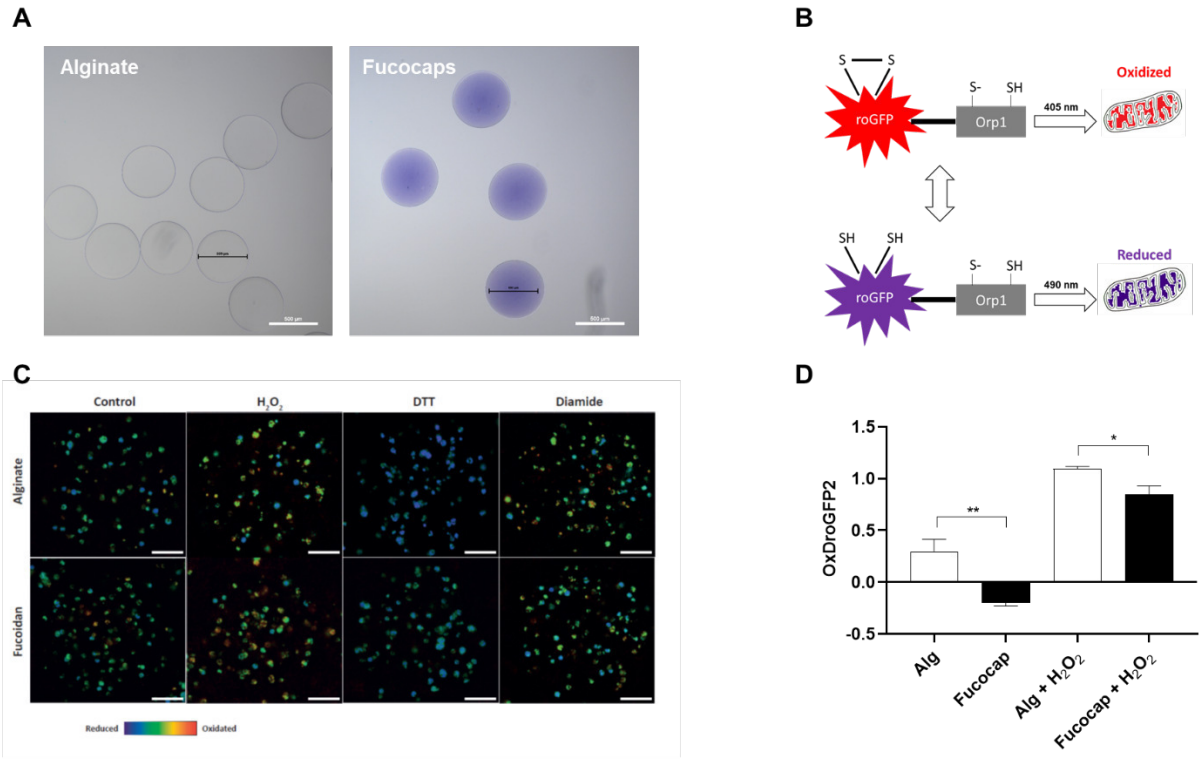


Figure VIII-5. Characterization of fucocaps. Optical microscopy images of alginate and fucocaps generated by an air-droplet generator with size of ~500 µm and toluidine blue staining to demonstrate the presence of fucoidan within the fucocaps (A). Schematic illustration of the mitochondrial ROS sensor mt-roGFP2-Orp1 (B). To explore the potential of fucoidan to alleviate oxidative stress post-encapsulation a genetically encoded redox probe mt-roGFP2-Orp1 transduced INS1E beta cells were used. The fluorescence maximum of this sensor shifts from 490 to 400 nm with increasing mitochondrial H_2O_2 levels, as shown by representative fluorescence images (C). Ratiometric fluorescence demonstrated that mt-roGFP2-Orp1 transduced INS1E beta cells encapsulated in Fucocaps experienced significantly less oxidative stress compared to alginate microcapsules (**p<0.01). Further, exposure of encapsulated mt-roGFP2-Orp1 transduced INS1E beta cells to H_2O_2 suggested the oxidative stress is significantly reduced in Fucocaps compared to those in alginate microcapsules (D) (*p<0.05) (ANOVA with posthoc Dunnett's T3 multiple comparisons test). Values = mean ± SEM (n=3).

VIII-4.5. Encapsulation of insulin producing cells in fucocaps

To determine the effect of fucoidan encapsulation on beta cell survival and function both primary rat islets and pseudoislets (generated from rat insulin producing INS1E cell line) were encapsulated in fucocaps, cultured and evaluated at different time points for cell viability, ATP content, and beta cell function by glucose stimulated insulin secretion. Live/dead analysis revealed that the viability of primary rat islets encapsulated in fucocaps was always higher compared to those encapsulated in alginate microcapsules. Viability of islets in fucocaps was significantly higher both on days 1 (95.2 ± 1.4%) and 5 (91.3 ± 2.1%) respectively compared to those in alginate microcapsules (Day 1 vs Day 5: 86.2 ± 3.6 vs 83.5 ± 2.3%) **(Figure VIII - 6A)**. This is further confirmed by ATP measurements, whereby the ATP levels of rat islets encapsulated in fucocaps was significantly higher on day 1 and 5, ~ 1.2- fold, compared to islets in alginate microcapsules **(Figure VIII - 6B).** Regarding islet function, rat islets encapsulated in fucocaps showed a better insulin secretory behaviour, including a significantly higher stimulation index at days 1 (59.6 ± 2.4) and 5 (53.3 ± 9.5) compared to alginate controls (Day 1 vs Day 5: 32.6 ± 2.8 vs 28.4 ± 2.1) **(Figure VIII - 5C)**. Similar results were found for pseudoislets, whereby INS1E pseudoislets encapsulated in fucocaps demonstrated a significantly higher viability both on days 1 (90.2 ± 4.5%) and 5 (95.5 ± 0.01%) respectively compared to alginate microcapsules (Day 1 vs Day 5: 80.1 ± 0.01% vs 90.2 ± 3.2%) **(Figure VIII - S2A)**. The ATP levels of pseudoislets encapsulated in fucocaps was significantly higher on day 1 and 5, 1.5- and 1.4- fold, compared to those embedded in alginate microcapsules **(Figure VIII - S2B)**. Further, pseudoislets encapsulated in fucocaps responded better to high glucose stimuli, and with a significantly higher stimulation index on day 5 (2.4 ± 0.2) compared to those encapsulated in alginate microcapsules (1.6 ± 0.1) **(Figures VIII - S2 C&D)**.

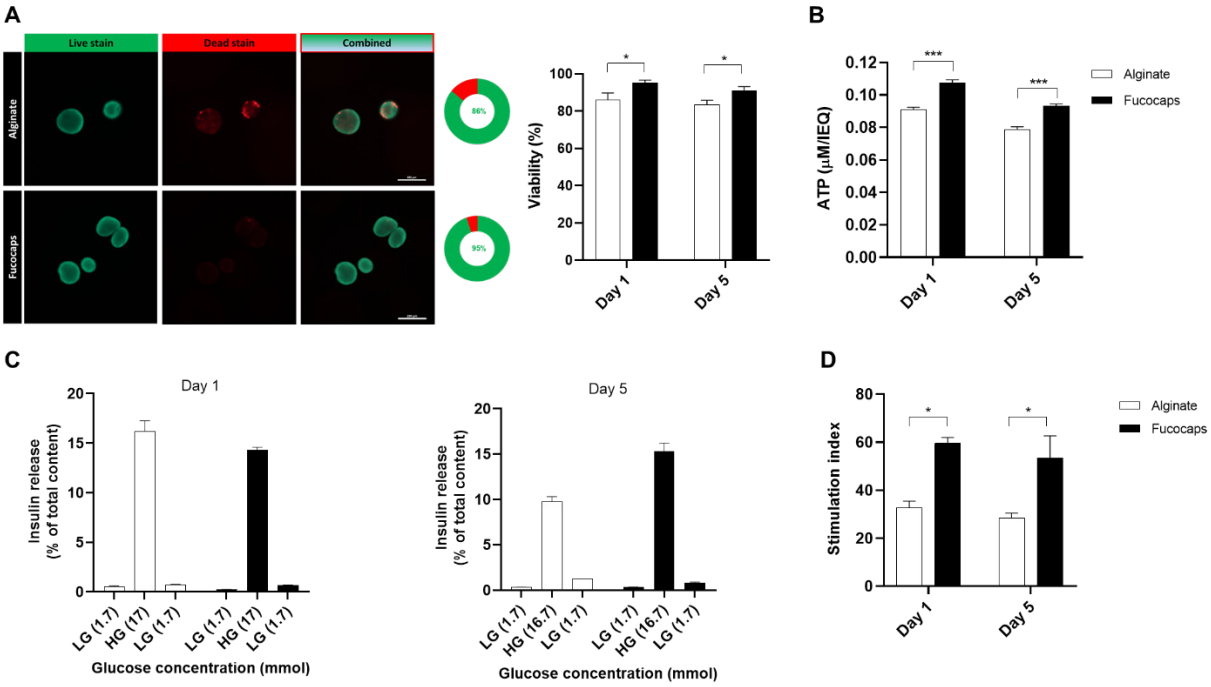


Figure VIII-6. Encapsulation of rat islets in fucocaps. Representative viability images of rat islets encapsulated in alginate microcapsules and fucocaps at day 1 and 5 post-encapsulation (A) (Scale bar = 500 μm). Viability of islets in fucocaps was significantly higher on both days compared to those in alginate microcapsules. Values = mean ± SEM (n=25 islets); *p<0.05 for viability when compared between alginate microcapsules and fucocaps both on days 1 and 5 (Student's t-test). (B). The relative ATP amount in both conditions are depicted as per islet equivalent to compensate for variability in islet size indicative of the average number of metabolically active cells in both alginate microcapsules and fucocaps. Values are depicted as mean ± SEM (n=5-6); ***p<0.001 for ATP of alginate microcapsules and fucocaps per encapsulated IEQ on day 1 and 5 (Student's t-test). (C) Glucose stimulated insulin secretion (GSIS) of islets in alginate microcapsules and fucocaps at day 1 and 5 post-encapsulation, and the corresponding stimulation indices (SI) (D). Stimulation indices are depicted as mean ± SEM (n=3-4); *p<0.05 for both alginate microcapsules and fucocaps at day 1 and 5 (Student's t-test).

In order to verify whether the positive effect of FF fucoidan on insulin secretion in primary rat islets and pseudoislets is consistent between different species, a pilot study was carried out using neonatal porcine islets. The viability of neonatal porcine islets following isolation dropped drastically during the 8 day culture period to produce mature beta cells. Despite the poor survival, encapsulation of neonatal porcine islets in fucocaps had higher viability compared to those in alginate microcapsules 48 hr post-

encapsulation. Live/dead analysis demonstrated that viability of neonatal porcine islets in fucocaps (54.2 ± 0.7%) was significantly higher than those in alginate microcapsules (35.6 ± 1.5%) **(Figure VIII - 7B)**. As expected, there was a marginal but significant increase in the ATP levels in neonatal porcine islets encapsulated in fucocaps (0.042 ± 0.001 μM/IEQ) compared to those embedded in alginate capsules (0.04 ± 0.0002 μM/IEQ) **(Figure VIII - 7C)**. As seen with rat islets, neonatal pig islets encapsulated in fucocaps functioned better with an increase in insulin release in response to high glucose with a significantly higher stimulation index (3.1 ± 0.4) compared to those in alginate microcapsules (1.4 ± 0.1) **(Figures VIII - 7 D&E)**. Further, in the presence of forskolin (1 μM), which mimics the effect of GLP-1 by activating adenylate cyclase, thus raising intracellular cAMP and activating protein kinase A (PKA) [59], insulin secretion was increased 1.7 fold for neonatal islets encapsulated in fucocaps compared to those in alginate microcapsules **(Figure VIII - 7D)**. These data suggest that encapsulation of islets in fucocaps proved beneficial in the short term by improving cell survival and function and the benefit observed could be translated across islets obtained from different species.

To our knowledge, this is the first study exploring the potential of fucoidan in the context of islet encapsulation. We used pseudoislets (from INS1E cells) as a model, and primary islets from rats and neonatal pigs for fucocaps microencapsulation and assessed cell viability and the insulin secretion. In all cases, and across the different species used in this study, we found that islets encapsulated within fucocaps demonstrated significantly improved viability and function. This beneficial effect may be attributed to the redox modulating property of fucoidan by induction of the antioxidant enzyme superoxide dismutase and glutathione activity [46]. The encapsulation process by itself induces some degree of oxidative stress and we have shown that fucoidan can indeed significantly alleviate oxidative stress in encapsulated cells **(Figure VIII - 5D)**. Apart from its antioxidant properties, fucoidan has been shown to possess anti-diabetic properties by inducing insulin secretion, and reducing blood glucose levels, stimulating glucose uptake and improving insulin sensitivity [46–48]. We found that islets encapsulated within fucocaps responded better to changes in glucose with significantly higher insulin secretion and improved stimulation indices. Further, we have also shown that in high glucose conditions, fucoidan support the increase of insulin secretion in a dose- and time- dependent manner in comparison to controls **(Figures VIII - 3 A&B)**. Fucoidan assisted insulin secretion may be attributed to an increase in cAMP concentration which was shown to be significantly elevated in fucoidan treated insulin producing RIN-5F cells [48]. Elevation in cAMP levels has been shown to stimulate insulin exocytosis both in Ca^{2+} dependent

and independent manner, and supports membrane depolarization by directly inhibiting K_{ATP} channels [49–51]. This is in concurrent with our findings in neonatal porcine islets where addition of forskolin, a cAMP stimulator, significantly increased insulin secretion in fucoidan containing microcapsules than those in alginate microcapsules alone suggesting a possible synergistic effect. However, the role of cAMP signalling pathways in mediating fucoidan induced insulin secretion needs to be fully elucidated.

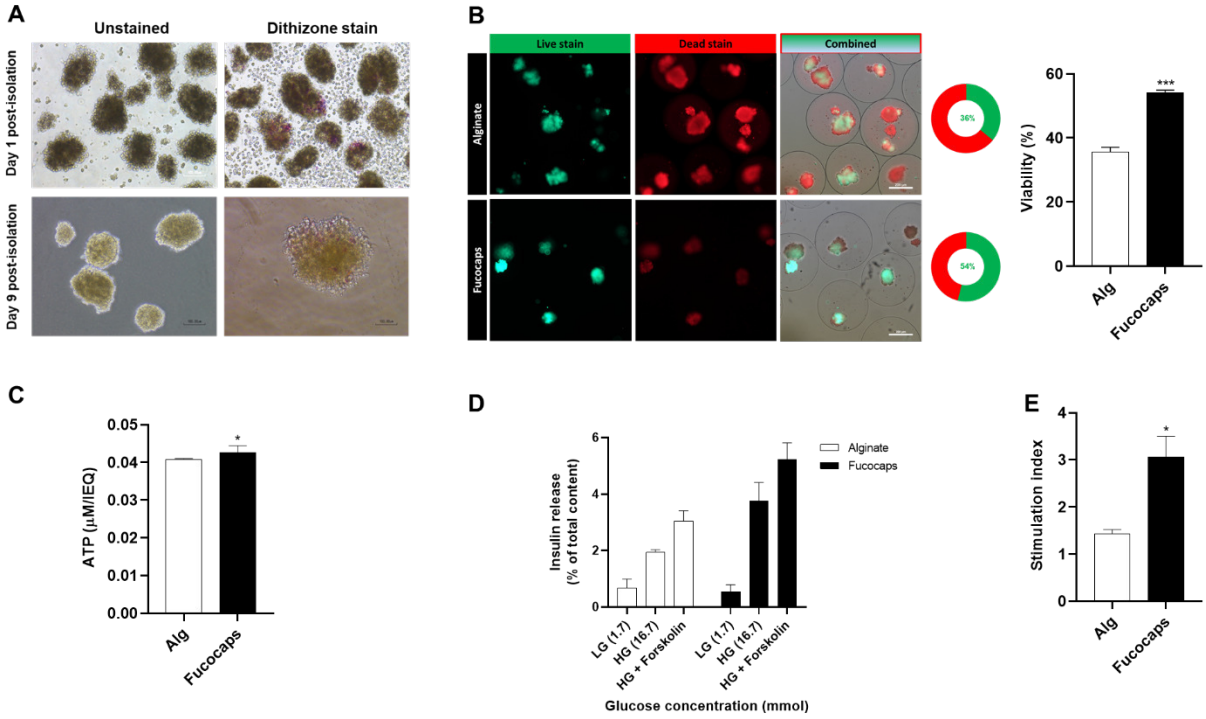


Figure VIII-7. Encapsulation of neonatal pig islets in fucocaps. Representative optical microscopy images of neonatal pig islets immediately after isolation and day 9 post-isolation for maturation and their corresponding dithizone staining (A). Representative viability images of neonatal pig islets encapsulated in alginate microcapsules and fucocaps at day 2 post-encapsulation (B) (Scale bar = 500 µm). Viability of neonatal islets in fucocaps was significantly higher compared to those in alginate microcapsules. Values: mean ± SEM (n=25 neonatal islets); ***p<0.001 for viability when compared between alginate microcapsules and fucocaps (Student's t-test). Measurement of ATP levels, a marker of metabolically active cells both in alginate microcapsules and fucocaps (C). Values: mean ± SEM (n=3); *p<0.05 for ATP levels when compared between alginate microcapsules and fucocaps (Student's t-test). Glucose stimulated insulin secretion (GSIS) on neonatal islets encapsulated in alginate microcapsules and fucocaps for day 2 post-encapsulation (D) and the corresponding stimulation index (SI) (E). Values: mean ± SEM (n=3-4); *p<0.05 for stimulation index (SI) when compared between alginate microcapsules and fucocaps (Student's t-test).

VIII-4.6. Effect of fucoidan on the cellular response pathway in pancreatic beta cells

RNA-seq was carried out to understand the effect of fucoidan treatment on the varied cellular pathways in INS1E cells in the presence or absence of H_2O_2. Dimension reduction followed by CPM (counts per million) normalization demonstrated that controls and fucoidan treated biological duplicates are consistent and clustered together. H_2O_2 duplicates, however, exhibited very different transcriptional response with one sample clustering closer to the fucoidan group while another one being isolated in the dimension reduction **(Figure VIII - S3A)**. The distance between the global pseudo-counts was confirmed in a heatmap generated from the mixOmics package **(Figure VIII - S3B)**.

Differential gene expression analysis shows the presence of three main clusters **(Figure VIII - 8A)**. Cluster I is composed of genes that are lowly expressed in the controls but slightly expressed in the control samples. Among these genes, Fos and Fosb, have been described to be important for pancreatic β-cell proliferation[60]. Other genes such as Nr4a1 and Nr43 are associated with hormone stimulus and pancreatic β-cell proliferation. These results could indicate that alginate encapsulation with fucoidan might reduce β-cell proliferation.

Cluster II contain genes related to biosynthetic processes, and they are lowly expressed in all the groups but, slightly higher in the control group. Among these genes, regulators of cell cycle progression, such as Rgs2 and Atf3 are differentially regulated between the groups. These results reflect induction of H_2O_2-induced oxidative stress, in which cell cycle progression seems highly affected.

Cluster III contains genes that are highly expressed in both groups but, mostly more induced in the control group. These genes are involved in metabolic processes, such as response to reactive oxygen species and oxidative stress, as TXNIP and HIPK2 [61–63], and to carbohydrates, which might reflect the functionality of the pseudo-islets in processing sugars. These results indicate that the pseudo-islets are still functional in the present culturing conditions, supporting the protective role of fucoidan on alleviating oxidative stress observed in this report.

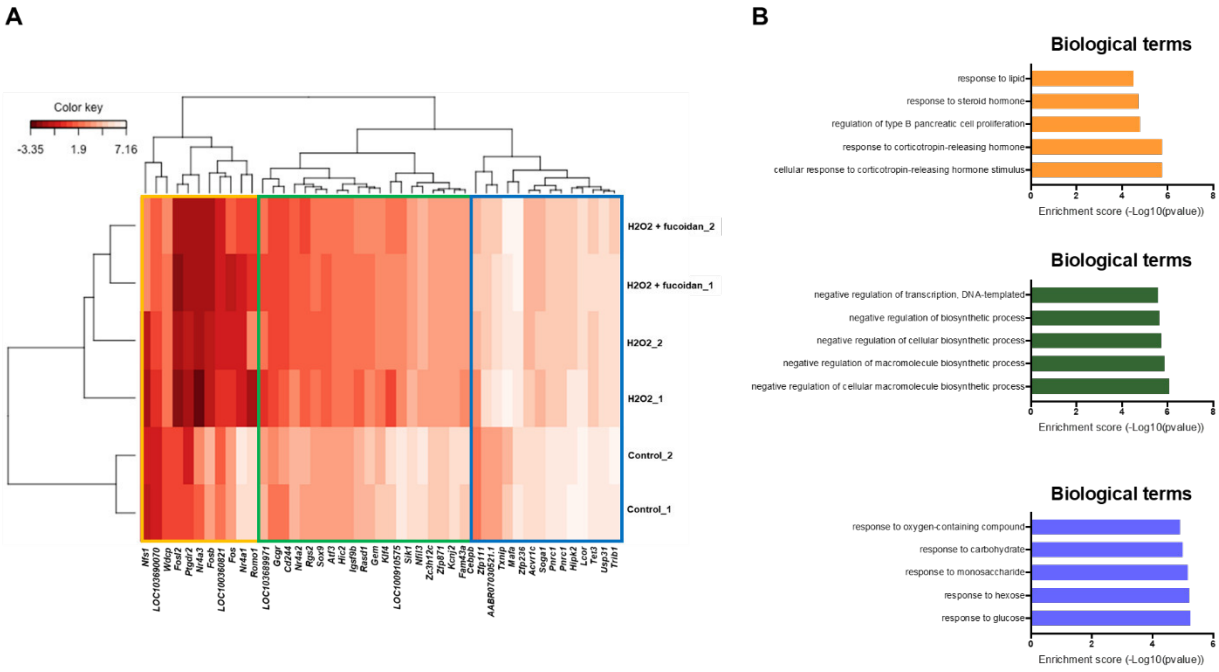


Figure VIII-8. Gene expression clustering in INS1E cells. RNA-seq reads were aligned to the reference genome (rat rn6) using HISAT2 (version 0.1.6). Differential expression analyses were performed using EdgeR (version 3.12) with adjusted p-value < 0.05 as the cut-off. The expression data were grouped, and clustering analysis were performed on EdgeR (A). All Gene Ontology (GO) analyses were performed with ToppGene method (https://toppgene.cchmc.org/), and only Biological Process terms were kept for downstream analyses (B). Enrichment score was calculated from the as -log10 of the p-value.

VIII-5. CONCLUSION

To the best of our knowledge, the present study is the first to explore the potential of fucoidan for islet encapsulation. Our results showed that fucoidan from *Fucus vesiculosus* (FF) possess high fucose & sulfate content, exhibiting potent antioxidant capacity, and is able to significantly alleviates oxidative stress, while enhancing the viability and function of INS1E pancreatic beta cells. Interestingly, this protective and enriching effect of fucoidan was also observed on rat and pig pancreatic islets, and pseudo-islets formed from INS1E cells, encapsulated in FF-containing ultrapure alginate (Fucogel) microcapsules. The fucoidan containing alginate microcapsules (Fucocaps) may also act as an immune barrier, which together with the positive effects on mitigating oxidative stress and enhancing cell survival and beta cell

function, results in an easy applicable biomaterial which can potentially lead to improved long term delivery of islets and beta cells to patients.

VIII-6. ACKNOWLEDGMENTS

Lara L. Reys and Vijayaganapathy Vaithilingam contribute equally to this work. The authors especially acknowledge financial support from Portuguese FCT (SFRH/BD/112139/ 2015) and PTDC/CTM-CTM//29813/2017. This work is partially funded by Northern Portugal Regional Operational Programme (NORTE 2020), under the Portugal 2020 Partnership Agreement, through Structured projects NORTE-01-0145-FEDER-000021 and NORTE-01-0145-FEDER-000023. The authors would like to acknowledge Marinova company for the supply of fucoidan extracted from *Fucus vesiculosus* species.

VIII-7. REFERENCES

[1] Amer LD, Mahoney MJ, Bryant SJ. *Tissue engineering approaches to cell-based type 1 diabetes therapy.*Tissue Eng Part B Rev 2014. 20(5):455–67.

[2] Shapiro AMJ, Pokrywczynska M, Ricordi C. *Clinical pancreatic islet transplantation*.Nat Rev Endocrinol 2016. 13(5):268–77.

[3] Vaithilingam V, Bal S, Tuch BE. *Encapsulated Islet Transplantation: Where Do We Stand?*Rev Diabet Stud 2017. 14(1):51–78.

[4] Silva AI, de Matos AN, Brons IG, Mateus M. *An overview on the development of a bio-artificial pancreas as a treatment of insulin-dependent diabetes mellitus*.Med Res Rev 2006. 26(2):181–222.

[5] Tuch BE, Keogh GW, Williams LJ, Wu W, Foster JL, Vaithilingam V, et al. *Safety and viability of microencapsulated human islets transplanted into diabetic humans*.Diabetes Care 2009. 32(10):1887–9.

[6] Jacobs-Tulleneers-Thevissen D, Chintinne M, Ling Z, Gillard P, Schoonjans L, Delvaux G, et al. *Sustained function of alginate-encapsulated human islet cell implants in the peritoneal cavity of mice leading to a pilot study in a type 1 diabetic patient.*Diabetologia 2013. 56(7):1605–14.

[7] Carlsson PO, Palm F, Andersson A, Liss P. *Markedly decreased oxygen tension in transplanted rat pancreatic islets irrespective of the implantation site.*Diabetes 2001. 50(3):489–95.

[8] Sthijns MMJPE, Jetten MJ, Mohammed SG, Claessen SMH, de Vries R, Stell A, et al. *Oxidative stress in alpha and beta cells as a selection criterion for biocompatible biomaterials.*bioRxiv 2019. :728683.

[9] de Vos P, Spasojevic M, Faas MM. *Treatment of diabetes with encapsulated islets.*Adv Exp Med Biol 2010. 670:38–53.

[10] Siebers U, Horcher A, Brandhorst H, Brandhorst D, Hering B, Federlin K, et al. *Analysis of the cellular reaction towards microencapsulated xenogeneic islets after intraperitoneal transplantation.*J Mol Med 1999. 77(1):215–8.

[11] Newsholme P, Cruzat V, Arfuso F, Keane K. *Nutrient regulation of insulin secretion and action.*J Endocrinol 2014. 221(3):R105-20.

[12] Sklavos MM, Tse HM, Piganelli JD. *Redox modulation inhibits CD8 T cell effector function.*Free Radic Biol Med 2008. 45(10):1477–86.

[13] Padgett LE, Tse HM. *NADPH Oxidase-Derived Superoxide Provides a Third Signal for CD4 T Cell Effector Responses.*J Immunol 2016. 197(5):1733–42.

[14] Chen J, Gusdon AM, Thayer TC, Mathews CE. *Role of increased ROS dissipation in prevention of T1D.*Ann N Y Acad Sci 2008. 1150:157–66.

[15] Betteridge DJ. *What is oxidative stress?*Metab - Clin Exp 2000. 49(2):3–8.

[16] Tiedge M, Lortz S, Drinkgern J, Lenzen S. *Relation between antioxidant enzyme gene expression and antioxidative defense status of insulin-producing cells.*Diabetes 1997. 46(11):1733–42.

[17] Pathak S, Regmi S, Gupta B, Poudel B, Pham Thanh T, Kim J-R, et al. *Hybrid Congregation of Islet Single Cells and Curcumin-Loaded Polymeric Microspheres as an Interventional Strategy to Overcome Apoptosis Associated with Pancreatic Islets Transplantation.*ACS Appl Mater Interfaces 2016. 8.

[18] Kozlovskaya V, Xue B, Lei W, Padgett LE, Tse HM, Kharlampieva E. *Hydrogen-bonded multilayers of tannic acid as mediators of T-cell immunity.*Adv Healthc Mater 2015. 4(5):686–94.

[19] Pham-Hua D, Padgett LE, Xue B, Anderson B, Zeiger M, Barra JM, et al. *Islet encapsulation with polyphenol coatings decreases pro-inflammatory chemokine synthesis and T cell trafficking.*Biomaterials 2017. 128:19–32.

[20] Husni A. *Therapeutic Potential of Seaweed Polysaccharides for Diabetes Mellitus.*In: 2018. 2018.

[21] Mallick N, Mohn FH. *Reactive oxygen species: response of algal cells.*J Plant Physiol 2000. 157(2):183–93.

[22] Zhang Z, Zhang Q, Wang J, Song H, Zhang H, Niu X. *Chemical modification and influence of function groups on the in vitro-antioxidant activities of porphyran from Porphyra haitanensis.*Carbohydr Polym 2010. 79(2):290–5.

[23] Phull AR, Kim SJ. *Fucoidan as bio-functional molecule: Insights into the anti-inflammatory potential and associated molecular mechanisms*.J Funct Foods 2017. 38:415–26.

[24] Hilderink J, Spijker S, Carlotti F, Lange L, Engelse M, van Blitterswijk C, et al. *Controlled aggregation of primary human pancreatic islet cells leads to glucose-responsive pseudoislets comparable to native islets*.J Cell Mol Med 2015. 19(8):1836–46.

[25] Vaithilingam V, Evans MDM, Lewy DM, Bean PA, Bal S, Tuch BE. *Co-encapsulation and co-transplantation of mesenchymal stem cells reduces pericapsular fibrosis and improves encapsulated islet survival and function when allografted*.Sci Rep 2017. 7(1):10059.

[26] Korbutt GS, Elliott JF, Ao Z, Smith DK, Warnock GL, Rajotte R V. *Large scale isolation, growth, and function of porcine neonatal islet cells*.J Clin Invest 1996. 97(9):2119–29.

[27] Selvendran RR, March JF, Ring SG. *Determination of aldoses and uronic acid content of vegetable fiber.*Anal Biochem 1979. 96(2):282–92.

[28] Oliveira C, Ferreira AS, Novoa-Carballal R, Nunes C, Pashkuleva I, Neves NM, et al. *The Key Role of Sulfation and Branching on Fucoidan Antitumor Activity.*Macromol Biosci 2017. 17(5):1600340-n/a.

[29] Mak WF. *Extraction, characterization and antioxidant activity of Fucoidan from New Zealand Undaria pinnatifida (Harvey) Suringar*.Auckland University of Technology; 2012.

[30] Saboural P, Chaubet F, Rouzet F, Al-Shoukr F, Azzouna R Ben, Bouchemal N, et al. *Purification of a low molecular weight fucoidan for SPECT molecular imaging of myocardial infarction.*Mar Drugs 2014. 12(9):4851–67.

[31] Sthijns MMJPE, Schiffers PM, Janssen GM, Lemmens KJA, Ides B, Vangrieken P, et al. *Rutin protects against H2O2-triggered impaired relaxation of placental arterioles and induces Nrf2-mediated adaptation in Human Umbilical Vein Endothelial Cells exposed to oxidative stress*.Biochim Biophys Acta - Gen Subj 2017. 1861(5, Part A):1177–89.

[32] Kuijpers AJ, Engbers GHM, Feijen J, De Smedt SC, Meyvis TKL, Demeester J, et al. *Characterization of the Network Structure of Carbodiimide Cross-Linked Gelatin Gels*.Macromolecules 1999. 32(10):3325–33.

[33] Merglen A, Theander S, Rubi B, Chaffard G, Wollheim CB, Maechler P. *Glucose Sensitivity and Metabolism-Secretion Coupling Studied during Two-Year Continuous Culture in INS-1E Insulinoma Cells*.Endocrinology 2004. 145(2):667–78.

[34] Fujikawa Y, Roma LP, Sobotta MC, Rose AJ, Diaz MB, Locatelli G, et al. *Mouse redox histology using genetically encoded probes*.Sci Signal 2016. 9(419):rs1 LP-rs1.

[35] Morgan B, Sobotta MC, Dick TP. *Measuring E(GSH) and H2O2 with roGFP2-based redox probes.*Free Radic Biol Med 2011. 51(11):1943–51.

[36] Silva TH, Alves A, Popa EG, Reys LL, Gomes MEME, Sousa RA, et al. *Marine algae sulfated*

polysaccharides for tissue engineering and drug delivery approaches.Biomatter 2012. 2(4):278–89.

[37] Wang C-Y, Chen Y-C. *Extraction and characterization of fucoidan from six brown macroalgae*.J Mar Sci Technol 2016. 24:319–28.

[38] Bilan MI, Grachev AA, Shashkov AS, Nifantiev NE, Usov AI. *Structure of a fucoidan from the brown seaweed Fucus serratus L*.Carbohydr Res 2006. 341:238–45.

[39] Holtkamp AD, Kelly S, Ulber R, Lang S. *Fucoidans and fucoidanases–focus on techniques for molecular structure elucidation and modification of marine polysaccharides*.Appl Microbiol Biotechnol 2009. 82(1):1–11.

[40] Ale MT, Mikkelsen JD, Meyer AS. *Important determinants for fucoidan bioactivity: A critical review of structure-function relations and extraction methods for fucose-containing sulfated polysaccharides from brown seaweeds*.Mar Drugs 2011. 9(10):2106–30.

[41] Skriptsova A V., Shevchenko NM, Zvyagintseva TN, Imbs TI. *Monthly changes in the content and monosaccharide composition of fucoidan from Undaria pinnatifida (Laminariales, Phaeophyta)*.J Appl Phycol 2010. 22:79–86.

[42] Zhao X, Xue C-H, Li Z-J, Cai Y-P, Liu H-Y, Qi H-T. *Antioxidant and hepatoprotective activities of low molecular weight sulfated polysaccharide from Laminaria japonica*.J Appl Phycol 2004. 16(2):111–5.

[43] Wang J, Liu L, Zhang Q, Zhang Z, Qi H, Li P. *Synthesized oversulphated, acetylated and benzoylated derivatives of fucoidan extracted from Laminaria japonica and their potential antioxidant activity in vitro*.Food Chem 2009. 114:1285–90.

[44] Wang J, Wang F, Zhang Q, Zhang Z, Shi X, Li P. *Synthesized different derivatives of low molecular fucoidan extracted from Laminaria japonica and their potential antioxidant activity in vitro*.Int J Biol Macromol 2009. 44:379–84.

[45] Park M-J, Han J-S. *Protective Effects of the Fermented Laminaria japonica Extract on Oxidative Damage in LLC-PK1 Cells*.Prev Nutr food Sci 2013. 18(4):227–33.

[46] Kim KJ, Yoon KY, Lee BY. *Fucoidan regulate blood glucose homeostasis in C57BL/KSJ m+/+db and C57BL/KSJ db/db mice*.Fitoterapia 2012. 83:1105–9.

[47] Sim S-Y, Shin Y-E, Kim H-K. *Fucoidan from Undaria pinnatifida has anti-diabetic effects by stimulation of glucose uptake and reduction of basal lipolysis in 3T3-L1 adipocytes*.Nutr Res 2019. 65:54–62.

[48] Jiang X, Yu J, Ma Z, Zhang H, Xie F. *Effects of fucoidan on insulin stimulation and pancreatic protection via the cAMP signaling pathway in vivo and in vitro*.Mol Med Rep 2015. 12(3):4501–7.

[49] Damdindorj B, Dezaki K, Kurashina T, Sone H, Rita R, Kakei M, et al. *Exogenous and endogenous ghrelin counteracts GLP-1 action to stimulate cAMP signaling and insulin secretion in islet beta-*

*cells.*FEBS Lett 2012. 586(16):2555–62.

[50] Furman B, Ong WK, Pyne NJ. *Cyclic AMP signaling in pancreatic islets.*Adv Exp Med Biol 2010. 654:281–304.

[51] Tengholm A. *Cyclic AMP dynamics in the pancreatic β-cell.*Ups J Med Sci 2012. 117(4):355–69.

[52] Cuomo F, Cofelice M, Lopez F. *Rheological Characterization of Hydrogels from Alginate-Based Nanodispersion.*Polymers (Basel) 2019. 11:259.

[53] Somo SI, Langert K, Yang C-Y, Vaicik MK, Ibarra V, Appel AA, et al. *Synthesis and evaluation of dual crosslinked alginate microbeads.*Acta Biomater 2018. 65:53–65.

[54] Grassi M, Sandolo C, Perin D, Coviello T, Lapasin R, Grassi G. *Structural characterization of calcium alginate matrices by means of mechanical and release tests.*Molecules 2009. 14(8):3003–17.

[55] Baumberger T, Ronsin O. *From thermally activated to viscosity controlled fracture of biopolymer hydrogels.*J Chem Phys 2009. 130(6):61102.

[56] Kaklamani G, Cheneler D, Grover LM, Adams MJ, Bowen J. *Mechanical properties of alginate hydrogels manufactured using external gelation.*J Mech Behav Biomed Mater 2014. 36:135–42.

[57] Oliva A, Fariña J, Llabrés M. *Development of two high-performance liquid chromatographic methods for the analysis and characterization of insulin and its degradation products in pharmaceutical preparations.*J Chromatogr B Biomed Sci Appl 2000. 749(1):25–34.

[58] Vaithilingam V, Kollarikova G, Qi M, Lacik I, Oberholzer J, Guillemin G, et al. *Effect of prolonged gelling time on the intrinsic properties of barium alginate microcapsules and its biocompatibility.*J Microencapsul 2011. 28:499–507.

[59] Ramos LS, Zippin JH, Kamenetsky M, Buck J, Levin LR. *Glucose and GLP-1 stimulate cAMP production via distinct adenylyl cyclases in INS-1E insulinoma cells.*J Gen Physiol 2008. 132(3):329–38.

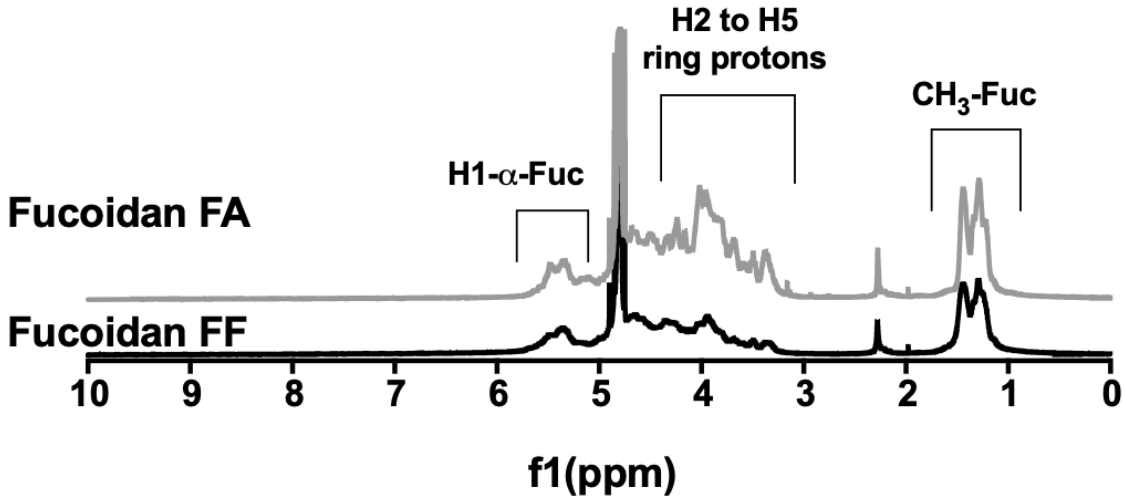
[60] Ray JD, Kener KB, Bitner BF, Wright BJ, Ballard MS, Barrett EJ, et al. *Nkx6.1-mediated insulin secretion and β-cell proliferation is dependent on upregulation of c-Fos.*FEBS Lett 2016. 590(12):1791–803.

[61] Zhou J, Chng W-J. *Roles of thioredoxin binding protein (TXNIP) in oxidative stress, apoptosis and cancer.*Mitochondrion 2013. 13(3):163–9.

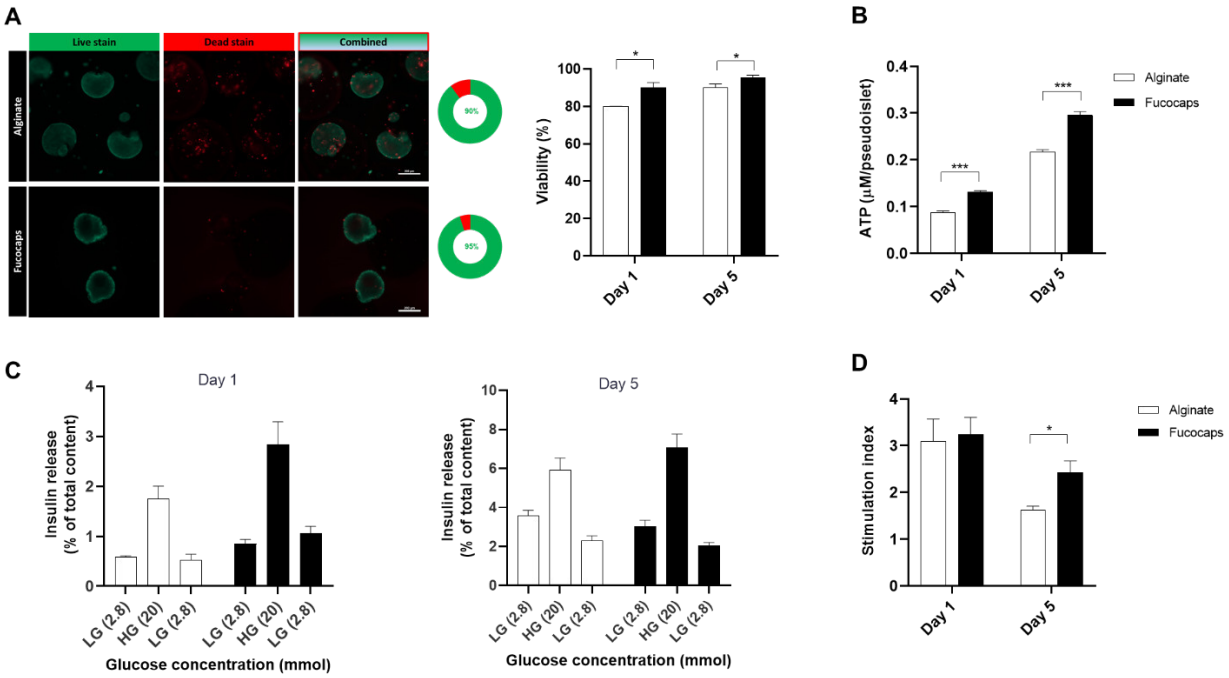
[62] Tian Y, Su Y, Ye Q, Chen L, Yuan F, Wang Z. *Silencing of TXNIP Alleviated Oxidative Stress Injury by Regulating MAPK–Nrf2 Axis in Ischemic Stroke.*Neurochem Res 2020. 45(2):428–36.

[63] de la Vega L, Grishina I, Moreno R, Krüger M, Braun T, Schmitz ML. *A Redox-Regulated SUMO/Acetylation Switch of HIPK2 Controls the Survival Threshold to Oxidative Stress.*Mol Cell 2012. 46(4):472–83.

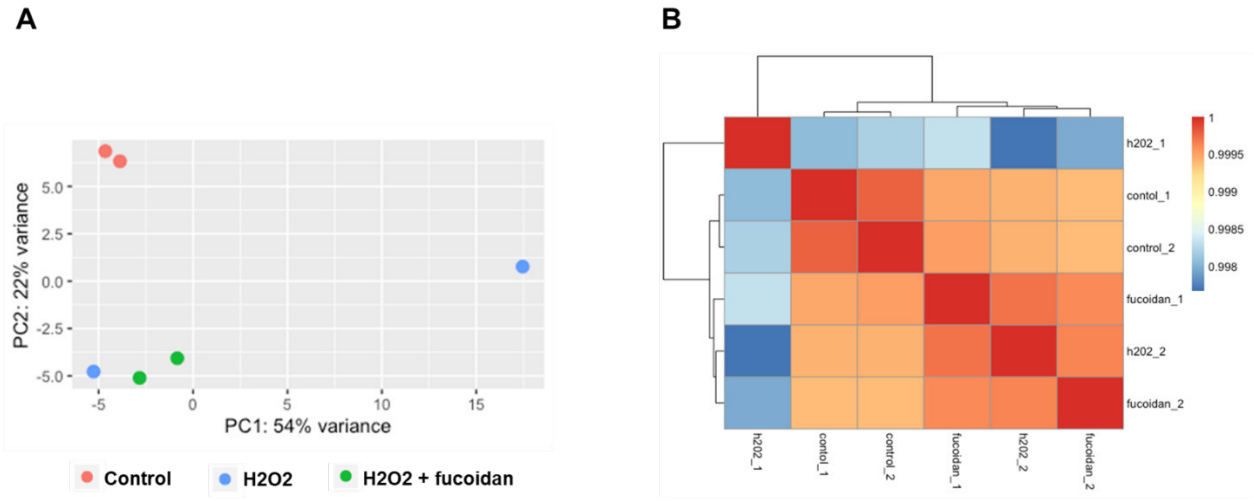
VIII-8. SUPPLEMENTARY PART



Supplementary Figure VIII-1. NMR spectra of purified fucoidans. ^{1}HNMR of purified FF and FA fucoidan, spectra show different peaks δ = 1.20-1.30 and 1.95-2.26 ppm corresponding to methyl groups of fucose and L-fucopyranose; δ = 3.35-4.55 ppm confirmed the presence of different types of fucose groups with changes in glycosidic linkage positions and monosaccharides patterns, δ = 5.29-5.40 ppm corresponding to anomeric protons of L-fucopyranosyl unit.



Supplementary Figure VIII-2. Encapsulation of pseudoislets in fucocaps. Representative viability images of pseudoislets encapsulated in alginate microcapsules and fucocaps at day 1 and 5 post-encapsulation (A) (Scale bar = 500 µm). Viability of islets in fucocaps was significantly higher on both days compared to those in alginate microcapsules. Values = mean ± SEM (n=25 pseudoislets); *p<0.05 for viability when compared between alginate microcapsules and fucocaps both on days 1 and 5 (Student's t-test). Measurement of ATP levels, a marker of metabolically active cells both in alginate microcapsules and fucocaps (B). Values = mean ± SEM (n=5-6); ***p<0.001 for ATP levels when compared between alginate microcapsules and fucocaps both on days 1 and 5 (Student's t-test). Glucose stimulated insulin secretion (GSIS) on pseudoislets encapsulated in alginate microcapsules and fucocaps for days 1 and 5 post-encapsulation (C) and the corresponding stimulation indices (SI) (D). Values = mean ± SEM (n=3-4); *p<0.05 for stimulation index (SI) when compared between alginate microcapsules and fucocaps on day 5 (Student's t-test).



Supplementary Figure VIII-3. Differential expression analysis of the RNA-seq data. Dimension reduction followed by CPM (counts per million) normalization demonstrated that controls and fucoidan treated biological duplicates are consistent and clustered together (A). H_2O_2 duplicates did not cluster together and exhibited very different transcriptional response with one sample clustering closer to the fucoidan group and another one being isolated in the dimension reduction (A). Heatmap generated using the mixOmics package confirm the distance between the global pseudo-counts (B).

SECTION 4

Conclusions and Future Perspectives

Chapter IX

General Conclusions and Future Perspectives

Chapter IX

General Conclusions and Future Perspectives

IX-1. GENERAL CONCLUSIONS AND FUTURE PERSPECTIVES

A considerable number of people suffer from diabetes mellitus all around the world. Diabetes mellitus is a metabolic disorder caused by inherited and/or acquired deficiency in the production of insulin by the pancreas. In type 1 diabetes, the insulin-producing beta cells are destroyed by the immune system. Therefore, it is crucial to develop new therapeutic strategies and models to treat this disease. Approaches as devices for oral delivery of insulin or electronic pumps for controlled and responsive injection have been explored but are mitigation routes. The full treatment requires the reestablishment of insulin-producing cells, which involves transplantation of pancreatic islets of Langerhans or other approaches restoring that physiologic function of pancreas. Such a β-cell replacement device should lead to improved islet viability, reducing the number of donor organs needed for transplantation. Nevertheless, the success of this therapy is limited by a decrease of islet mass caused by mechanical stress, a lack of oxygen flow toward the islets due to lack of vascularization, an immediate blood-mediated immune response that requires the permanent use of a relatively high concentration of immunosuppressive drugs. Thus, two main issues need to be addressed to improve clinical islet transplantation: one is the development of a close immunoprotective device, while the second is to restore the vascularization as fast as possible to ensure optimal islet survival. This is currently being addressed through the development of different devices to encapsulate pancreatic islets or β-cells. In addition, these devices can offer enhanced glycemia maintenance, with the reduction or even absence of the need to use exogenous insulin, resulting in a lower risk of long-term complications linked to type I diabetes. There are several requirements for devices used in extrahepatic transplantation sites, including the ability to house a sufficient number of islets, or β cells, the presence of a dense vascular network in close proximity, or the capacity to initiate the formation of one, allowing for swift revascularization ensuring an efficient exchange of nutrients, metabolites, and hormones, and maintenance of adequate oxygen tension. Other preferred characteristics should be a minimal or no inflammatory response against the materials used in the device

(that could potentially lead to islet loss), easy surgical accessibility with minimal operative risks, the ability for graft recovery and noninvasive monitoring.

The main goal of the work developed under the context of the present thesis was to develop alternative systems for diabetes treatment, with a strong strategy supported in marine natural polymers-based structures, namely composed by fucoidan. Fucoidan is a sulfated polysaccharide extracted from brown algae, which has interesting chemical and biological properties. The use of fucoidan on a medical device for tissue engineering, particularly in diabetes treatment, is still in its early stages, particularly on what concerns polysaccharide modification, processing, and biomaterial design. Nevertheless, it is possible to envisage the use of this polysaccharide in a diabetes area, where it can act as a support to encapsulate islets of Langerhans/pancreatic cells or as a drug delivery system. On the other hand, it is known to possess various distinctive biochemical properties, such as antioxidant, anti-inflammatory, reducing blood glucose, anti-obesity, and blood lipids reducing that may enhance and define its applicability in this context. To achieve these objectives, fucoidan was physically or chemically modified and further combined with other natural and/or synthetic polymers, insulin, and cells to develop 2D/3D matrices (microparticles, hydrogels, membranes, and capsules) based on fucoidan envisaged to be used for diabetes treatment.

In particular, the main goals of the experimental work performed under the scope of this PhD thesis, presented and discussed in Section 3, include: i) to increase the processability of fucoidan (chemical modification of fucoidan by methacrylation reaction and further photocrosslinking using visible light) (Chapter IV); ii) production of fucoidan microparticles for insulin encapsulation and its subsequent sustained release, and evaluation of biocompatibility of fucoidan microparticles with human pancreatic cells (Chapter V); iii) development of fucoidan-based hydrogels envisaging its further use on the encapsulation of pancreatic cells (Chapter VI); iv) evaluation of the angiogenic potential of airbrushed nanofibrous mesh comprising fucoidan, envisaging its further use as support biomaterial to improve vascularization on transplanted islets-laden systems (Chapter VII) and v) assessment of the antioxidant effect of fucoidan on β-cells and its effect on encapsulated islet viability and function (Chapter VIII). All the strategies and technologies studied and proposed were developed to balance the most significant drawbacks found in the literature and address them, recurring to creative and accurate approaches.

The principal limitation of fucoidan in the processing of matrices stable in an aqueous medium is its high solubility in water. To overcome it, fucoidan has been combined with other polymers, resulting in multicomponent matrices, but single component systems were never described before. Chemical modification on fucoidan, namely a methacrylation reaction, was performed to control fucoidan stability in water and increase its processability. Although an effective methacrylated fucoidan (MFu) was obtained and further photocrosslinked using visible light, the methacrylation process still needs to be adjusted to achieve better control of matrices, namely a narrower range of methacrylation degree. In fact, limited reproducibility of methacrylation and photocrosslinking approach with other polymers have been described by others, limiting its widespread use until current efforts succeed to solve this bottleneck. Hydrogel MFu particles were produced using superamphiphobic surfaces and visible light. This methodology has enabled spherical particles' production in one step, using the benefit of the high repellency of the surfaces and tuning particle diameter by playing with the size of solution droplets displayed in these surfaces. Another advantage of this methodology was the use of visible light irradiation, which would be beneficial regarding their use with cell-laden systems since visible light is a benign light source and readily available when compared with other light sources such as UV.

The present approach could greatly improve the processability of fucoidan, allowing the production of high-added-value fucoidan structures with good morphology and biological performance and then enhancing the biomedical value of this marine biopolymer. The findings suggested that the developed MFu particles may also be used on the design of devices for the sustained insulin release and templates supporting the culture of pancreatic cells. To explore this hypothesis, MFu particles were produced using fucoidan functionalized with different methacrylation degrees, and insulin was incorporated into them. The experiments addressing the release of insulin in PBS demonstrated that the particles could release insulin until 28 days, in a sustained manner, and the insulin release profile was controlled by the methacrylation degree of fucoidan. The methacrylation degree is correlated to cross-link density, and higher methacrylation degree results in the formation of hydrogels with a denser network. Therefore, an increasing amount of methacrylate groups in the feed composition is expected to enhance the density of the network and subsequently reduce the diffusion of insulin. Moreover, biological assays on MFu particles using pancreatic cells (1.1B4 HP cells) demonstrated that the produced hydrogels were not cytotoxic, with cells revealing good adhesion, viability, and proliferation. Besides, the 1.1B4HP cells tend to aggregate, forming pseudo-islets (cells configuration as three-dimensional islet-like structures) during the culture period studied. The findings indicate that β-cell lines retained the ability to self-organize into

anatomically appropriate islet-like structures, important for their physiological function, which propose such an *in vitro* approach as alternative to the use of islets. The results suggest that MFu microparticles may be a good candidate for drug delivery vehicles or aiming to achieve an immuno-protectant device for insulin-producing pancreatic cells in the scope of advanced therapeutic solutions for diabetes mellitus treatment. Moreover, further assays should be focus on: i) extend the culture period for longer times (21 or 28 days) and assess cell viability within the structures, which would request appropriated oxygen and nutrients supply, ii) study the glucose-induced insulin secretion, iii) study the encapsulation of islets of Langerhans, and later on iv) evaluate the capacity of the devices to protect encapsulated cells from host immune system upon implantation.

The development of versatile three-dimensional (3D) hydrogels as platforms for encapsulation of pancreatic cells and islets of Langerhans has been explored by several groups, studying the combination of different materials, as natural and synthetic macromolecules. In the scope of Chapter VI, we aimed an alternative strategy for the production of 3D hydrogels, combining two marine polysaccharides: agarose (Aga), a gelling polymer, with fucoidan. After reacting agarose with fucoidan, hydrogels were formed by thermal gelation, with tunable mechanical properties and stability. Their use, combined with model molecules and cells, has shown that diffusion of nutrients or other compounds (including secreted insulin or cell waste products), as well as cell adhesion, could be clearly modulated. In fact, the high viscosity of agarose solution used (5%) resulted in reduced mesh size, translated as a dense polymeric matrix, which impairs glucose or nutrients diffusion that would limit pancreatic cell functionality. Comparing all the formulations, we conclude that AgaFu 3b hydrogel formulation, prepared with 3% agarose blended with fucoidan in a 2:5 weight ratio, presented a good size of gel fiber mesh, which is a major key for good diffusion of molecules, thus suggesting higher nutrients permeability, but also enhanced cell adhesion and proliferation. Moreover, these AgaFu3 hydrogels supported the viability and functionality of encapsulated pancreatic cells during culture, enabling their use as a support platform for pancreatic cells. Overall, our results represent a promising strategy to be explored as a cell-laden biomaterial for extra-hepatic transplantation to be used to treat diabetes mellitus. In addition, further assays such as i) co-encapsulation of alpha and beta cells, ii) to study how the construct/device material reacts in the presence of excessively high or low glucose values, and iii) to study the immune response of these materials upon implantation would give important cues on the performance of these devices on type I diabetes therapeutics.

One of the biggest challenges to improve the effectiveness of the currently applied clinical islet transplantation is to convert a low vascularized site into an integrated implanted tissue. Besides the possible inflammatory reaction, pancreatic islet transplantation presents a major limitation associated with the limited number of blood vessels providing the required nutrients and oxygen supply to feed the implanted cells. Therefore, new strategies are needed to enhance islet function by triggering a rapid vascularization after transplantation, as the connection to systematic circulation will ultimately lead to an increase in the viability of transplanted islets. With this aim in perspective, in this thesis, we proposed to study the angiogenic potential of nanofibrous meshes comprising fucoidan that could be used as a support for revascularization of constructs – namely, biomaterials with encapsulated cells or islets – on therapeutic approaches for diabetes treatment (Chapter VII). To reach this, fucoidan from two different species and with distinct chemical features, blended with a biodegradable polymer PCL, was successfully airbrushed into nanofibrous meshes (ANFM). Fucoidans from *Ascophyllum nodosum* (FA) and *Fucus vesiculosus* (FF) were used to study the influence of chemical features, as molecular weight (FA < FF) and sulfation degree (FA < FF), on the performance of the derived biocomposites. The incorporation of fucoidan had clear impact on the properties of the meshes, namely an increase in the average fiber diameter and increased hydrophilicity of airbrush nanofibrous meshes. This fact could be related to intrinsic properties of fucoidan such as sulfate groups, the presence of some sugars such as fucose, and molecular weight. This work demonstrates the successful production of PCL and PCLFu airbrush nanofibers with a versatile mechanical, physical, and biological performance. Moreover, the *in vivo* test of the effect of PCL/fucoidan ANFM (PCLFF) over the vascularization of the chicken embryo chorioallantoic membrane (CAM) shown higher pro-angiogenic properties of this system compared with PCL ANFM. The incorporation of fucoidan improved the physicochemical properties of airbrush nanofibrous mesh and promoted angiogenesis, which could help support implants' integration and vascularization. In addition, further studies like i) microthermoforming for islet accommodation or to envelope cell-laded hydrogels, ii) assessment of islet survival on airbrush nanofibers, iii) vascularization test in the presence of islets or hydrogels, and in vivo accommodation and revascularization would add important information. This fibrous mesh could represent a new promising biomaterial, as support of immunoprotecting devices laden with pancreatic islets useful in revascularization upon implantation, representing an innovative and multi efficient therapeutic approach for diabetes treatment.

Relying on the several biological activities being described for fucoidan, namely antioxidant activity, regulation of blood glucose level, among others, the development of a functional biomaterial, where fucoidan would be not only a support component (building block) but also elicit a biological effect, appeared as the logic following step. The first goal was to evaluate the antioxidant properties of fucoidan and determine its potency to alleviate oxidative stress *in vitro*, which is known to severely affect encapsulated islets. Further, the possibility of making fucoidan-based hydrogels by blending with alginate (Fucogel) to generate novel fucoidan microcapsules (Fucocaps) for islet encapsulation was explored, assessing their biological performance regarding cell survival and function *in vitro*. Beta cells are highly susceptible to oxidative stress because they contain lower endogenous antioxidant levels than many other cell types. Several strategies have been investigated to protect encapsulated islets from oxidative stress induced cell death. It has been shown that entrapping a natural antioxidant within a polymer matrix can reduce oxidative stress and support insulin secretion in encapsulated rat islets. In the perspective of using fucoidan as a material antioxidant, we compared two fucoidans from different species (*Ascophyllum nodosum* (FA) and *Fucus vesiculosus* (FF)), characterized by differences in molecular weight (FA < FF) and sulfation degree (FA < FF), regarding its antioxidant action (total antioxidant capacity and free radical scavenging activity). It is well known that the chemical features of sulfated polysaccharides, as molecular weight and sulfation degree, but also sulfation pattern, sugars profile, and polymer branching, are determined by the algae species, the harvest season, environmental conditions, and extraction methodology. Although the fucoidan's structure-activity relationship has not yet been fully established, the influence of chemical properties on the biological performance of fucoidans was remarked by several authors in literature, and it has just been addressed in the previous paragraph regarding pro-angiogenic effect. Likewise, the obtained results discussed in Chapter VIII showed that FF exhibited potent antioxidant capacity, associated with high fucose and sulfate content, further significantly alleviating oxidative stress and enhancing the viability and function of encapsulated beta cells. Based on the obtained results, the inclusion of fucoidan FF in alginate/fucoidan-based microcapsules (Fucocaps) provided beneficial effects regarding the high antioxidant activity, with viability increment of encapsulated cells, and enhanced insulin secretion ability and glucose responsiveness. FF fucoidan solution containing alginate hydrogel (Fucogel) provided a redox-modulatory niche and could be an immune barrier at the same time. Moreover, further studies like: i) study the mechanism as fucoidan acts in insulin stimulation and islets protection, ii) study the immune response to these materials (Fucogel and Fucocaps) in the presence of macrophages, and iii) *in vivo* studies of these constructs using rats as a model, would definitely add important information

to help to elucidate the potential performance of Fucogel as biomaterial for bioengineered immunoprotective beta cell replacement devices within the context of type I diabetes treatment procedures.

Overall, the work performed and described in the scope of this PhD thesis demonstrates the feasibility of increasing the processability of fucoidan and transforming it into different structures envisaged for diabetes mellitus treatment. The exploitation of this marine polysaccharide in this context and considering the diversity of developed structures may lead to novel research opportunities. The cumulative data generated from the work described in this thesis presents and scientifically demonstrates that intrinsic properties of fucoidan and fucoidan-based microparticles, hydrogels, microcapsules, and nanofiber mesh can be valid alternatives for the treatment of diabetes type I and II and may have a distinct important role in the biomedical field. This is the main innovation coming from this thesis. While numerous tests have been made within this dissertation, those efforts were mainly limited to the laboratory *in vitro* studies. *In vivo* experiments using diabetic models to restore the function of beta cells would help to elucidate the validity of the results obtained *in vitro*.

Although this sulfated polysaccharide has been known and researched for several decades, the knowledge about its biological activities and biomedical potential is still far from being fully accomplished. The author would like to think that this scenario is changing and, hopefully, the current thesis could contribute to a better understanding of fucoidan, its processability, and beneficial potential for human health. Ultimately, she foresees this thesis serving as a stepping stone for future work on fucoidan (and other sulfated polysaccharides) and its applicability, particularly in highly demanding diabetes treatment.